

# WAKEN THE SILENT MAJORITY: PRINCIPLES AND PATHOGENIC SIGNIFICANCE OF NON-ACETYL ACYLATION AND OTHER UNDERSTUDIED POST-TRANSLATIONAL MODIFICATIONS

EDITED BY: Yong Liu, Lianjun Zhang and Fangliang Zhang  
PUBLISHED IN: Frontiers in Cell and Developmental Biology



# frontiers

## Frontiers eBook Copyright Statement

The copyright in the text of individual articles in this eBook is the property of their respective authors or their respective institutions or funders. The copyright in graphics and images within each article may be subject to copyright of other parties. In both cases this is subject to a license granted to Frontiers.

The compilation of articles constituting this eBook is the property of Frontiers.

Each article within this eBook, and the eBook itself, are published under the most recent version of the Creative Commons CC-BY licence.

The version current at the date of publication of this eBook is CC-BY 4.0. If the CC-BY licence is updated, the licence granted by Frontiers is automatically updated to the new version.

When exercising any right under the CC-BY licence, Frontiers must be attributed as the original publisher of the article or eBook, as applicable.

Authors have the responsibility of ensuring that any graphics or other materials which are the property of others may be included in the CC-BY licence, but this should be checked before relying on the CC-BY licence to reproduce those materials. Any copyright notices relating to those materials must be complied with.

Copyright and source acknowledgement notices may not be removed and must be displayed in any copy, derivative work or partial copy which includes the elements in question.

All copyright, and all rights therein, are protected by national and international copyright laws. The above represents a summary only. For further information please read Frontiers' Conditions for Website Use and Copyright Statement, and the applicable CC-BY licence.

ISSN 1664-8714

ISBN 978-2-88976-089-3

DOI 10.3389/978-2-88976-089-3

## About Frontiers

Frontiers is more than just an open-access publisher of scholarly articles: it is a pioneering approach to the world of academia, radically improving the way scholarly research is managed. The grand vision of Frontiers is a world where all people have an equal opportunity to seek, share and generate knowledge. Frontiers provides immediate and permanent online open access to all its publications, but this alone is not enough to realize our grand goals.

## Frontiers Journal Series

The Frontiers Journal Series is a multi-tier and interdisciplinary set of open-access, online journals, promising a paradigm shift from the current review, selection and dissemination processes in academic publishing. All Frontiers journals are driven by researchers for researchers; therefore, they constitute a service to the scholarly community. At the same time, the Frontiers Journal Series operates on a revolutionary invention, the tiered publishing system, initially addressing specific communities of scholars, and gradually climbing up to broader public understanding, thus serving the interests of the lay society, too.

## Dedication to Quality

Each Frontiers article is a landmark of the highest quality, thanks to genuinely collaborative interactions between authors and review editors, who include some of the world's best academicians. Research must be certified by peers before entering a stream of knowledge that may eventually reach the public - and shape society; therefore, Frontiers only applies the most rigorous and unbiased reviews.

Frontiers revolutionizes research publishing by freely delivering the most outstanding research, evaluated with no bias from both the academic and social point of view. By applying the most advanced information technologies, Frontiers is catapulting scholarly publishing into a new generation.

## What are Frontiers Research Topics?

Frontiers Research Topics are very popular trademarks of the Frontiers Journals Series: they are collections of at least ten articles, all centered on a particular subject. With their unique mix of varied contributions from Original Research to Review Articles, Frontiers Research Topics unify the most influential researchers, the latest key findings and historical advances in a hot research area! Find out more on how to host your own Frontiers Research Topic or contribute to one as an author by contacting the Frontiers Editorial Office: [frontiersin.org/about/contact](http://frontiersin.org/about/contact)

# WAKEN THE SILENT MAJORITY: PRINCIPLES AND PATHOGENIC SIGNIFICANCE OF NON-ACETYL ACYLATION AND OTHER UNDERSTUDIED POST-TRANSLATIONAL MODIFICATIONS

Topic Editors:

**Yong Liu**, Xuzhou Medical University, China

**Lianjun Zhang**, Center of Systems Medicine, Chinese Academy of Medical Sciences, Suzhou Institute of Systems Medicine (ISM), China

**Fangliang Zhang**, University of Miami, United States

**Citation:** Liu, Y., Zhang, L., Zhang, F., eds. (2022). Waken the Silent Majority: Principles and Pathogenic Significance of Non-Acetyl Acylation and Other Understudied Post-Translational Modifications.

Lausanne: Frontiers Media SA. doi: 10.3389/978-2-88976-089-3

# Table of Contents

- 04 Editorial: Waken the Silent Majority: Principles and Pathogenic Significance of Non-Acetyl Acylation and Other Understudied Post-Translational Modifications**  
Fangliang Zhang
- 06 Regulation of Mitochondrial Respiratory Chain Complex Levels, Organization, and Function by Arginyltransferase 1**  
Chunhua Jiang, Balaji T. Moorthy, Devang M. Patel, Akhilesh Kumar, William M. Morgan, Belkis Alfonso, Jingyu Huang, Theodore J. Lampidis, Daniel G. Isom, Antoni Barrientos, Flavia Fontanesi and Fangliang Zhang
- 22 Roles of Lipid Peroxidation-Derived Electrophiles in Pathogenesis of Colonic Inflammation and Colon Cancer**  
Lei Lei, Jianan Zhang, Eric A. Decker and Guodong Zhang
- 32 Protein Lipidation by Palmitoylation and Myristoylation in Cancer**  
Chee Wai Fhu and Azhar Ali
- 47 Functions and Mechanisms of Lysine Glutarylation in Eukaryotes**  
Longxiang Xie, Yafei Xiao, Fucheng Meng, Yongqiang Li, Zhenyu Shi and Keli Qian
- 59 Lysine Fatty Acylation: Regulatory Enzymes, Research Tools, and Biological Function**  
Garrison Komaniecki and Hening Lin
- 77 Cardioprotective Role of SIRT5 in Response to Acute Ischemia Through a Novel Liver-Cardiac Crosstalk Mechanism**  
Boda Zhou, Min Xiao, Hao Hu, Xiaoxia Pei, Yajun Xue, Guobin Miao, Jifeng Wang, Wanqi Li, Yipeng Du, Ping Zhang and Taotao Wei
- 85 Post-translational Modifications of the Protein Termini**  
Li Chen and Anna Kashina
- 99 Sirtuin 5 is Dispensable for CD8<sup>+</sup> T Cell Effector and Memory Differentiation**  
Qianqian Duan, Jiying Ding, Fangfang Li, Xiaowei Liu, Yunan Zhao, Hongxiu Yu, Yong Liu and Lianjun Zhang
- 112 Arginylation Regulates G-protein Signaling in the Retina**  
Marie E. Fina, Junling Wang, Pavan Vedula, Hsin-Yao Tang, Anna Kashina and Dawei W. Dong
- 126 Protein Posttranslational Signatures Identified in COVID-19 Patient Plasma**  
Pavan Vedula, Hsin-Yao Tang, David W. Speicher and Anna Kashina  
The UPenn COVID Processing Unit





# Editorial: Waken the Silent Majority: Principles and Pathogenic Significance of Non-Acetyl Acylation and Other Understudied Post-Translational Modifications

Fangliang Zhang<sup>1,2\*</sup>

<sup>1</sup>Department of Molecular and Cellular Pharmacology, University of Miami Miller School of Medicine, Miami, FL, United States,

<sup>2</sup>Sylvester Comprehensive Cancer Center, University of Miami Health System, Miami, FL, United States

**Keywords:** posttranslational modification, arginylation, arginyltransferase, Ate1, terminal modification, evolution

## Editorial on the Research Topic

### Waken the Silent Majority: Principles and Pathogenic Significance of Non-Acetyl Acylation and Other Understudied Post-Translational Modifications

## OPEN ACCESS

### Edited and reviewed by:

Cecilia Giulivi,  
University of California, Davis,  
United States

### \*Correspondence:

Fangliang Zhang  
fzhang2@miami.edu

### Specialty section:

This article was submitted to  
Cellular Biochemistry,  
a section of the journal  
Frontiers in Cell and Developmental  
Biology

**Received:** 14 March 2022

**Accepted:** 22 March 2022

**Published:** 13 April 2022

### Citation:

Zhang F (2022) Editorial: Waken the  
Silent Majority: Principles and  
Pathogenic Significance of Non-Acetyl  
Acylation and Other Understudied  
Post-Translational Modifications.  
Front. Cell Dev. Biol. 10:896324.  
doi: 10.3389/fcell.2022.896324

Arginylation, the ribosome-independent transfer of arginine to protein/peptide, was discovered nearly six decades ago (Kaji et al., 1963; Kaji, 1968). Despite the long history, this posttranslational modification (PTM) remains underexplored. This is hindered by the fact that the study of arginylation is currently only conducted by a few dozen of research groups with a limited number of relevant publications each year.

In a certain sense, the lack of understanding of arginylation even leads to a false impression that this phenomenon may be unimportant. However, arginylation is an exceptionally widespread process that has been found in all eukaryotes examined (Graciet et al., 2006; Graciet et al., 2009; Licausi et al., 2011; Van and Smith, 2020). Such a conservation would be unimaginable if this PTM did does not play some important physiological role.

In this Research Topic “Waken the Silent Majority: Principles and Pathogenic Significance of Non-Acetyl Acylation and other Understudied Post-Translational Modifications,” several papers directly relevant to the intriguing phenomenon of arginylation are included to showcase the diverse functions of this PTM and the evolutionary root of arginyltransferase1 (ATE1) (Balzi et al., 1990), the main enzyme catalyzing arginylation in most eukaryotes (Kato and Nozawa, 1984).

In the review paper “Post-translational Modifications of the Protein Termini” by Chen and Kashina, a concise and balanced summary of many different types of PTMs on both the N- and C-termini of proteins are presented for their biochemical mechanisms and potential physiological roles. These include arginylation, which is mostly an N-terminal modification. In the original research paper “Arginylation regulates G-protein signaling present in the retina” by Fina et al., the researchers found that several components in the G-protein signaling complexes in retina are subjected to arginylation, which may in turn affect the retinal function. In another research paper “Protein Posttranslational Signatures Identified in COVID-19 Patient Plasma” by Vedula et al., researchers used comprehensive proteomic approaches and identified significant alterations of arginylation (and several other PTM) signatures in the plasma of COVID-19 patients. While the exact physiological meaning of these changes still awaits further clarification, this finding nevertheless highlights the potential involvement of arginylation in virus-induced pathological

conditions. Finally, new clues for interpreting the role of the arginylation enzyme ATE1 was provided in the original research “Regulation of Mitochondrial Respiratory Chain Complex Levels, Organization, and Function by Arginyltransferase 1” by Jiang et al. (contributed by my own research group). In this study, a small fraction of ATE1 was found located inside mitochondria and is essential for the proper function of mitochondria in respiration. Intriguingly, homologues of eukaryotic ATE1 can be traced back to alpha-proteobacteria, relatives of the ancient ancestor of mitochondria. This connection between ATE1 and mitochondria may constitute a new angle for understanding the diverse functions of ATE1 in cellular metabolism (Brower and Varshavsky, 2009; Zhang et al., 2015),

stress response (Wiley et al., 2020; Kumar et al., 2016; Deka et al., 2016), and oxygen sensing (Moorthy et al., 2022).

Overall, while arginylation is still a poorly understood process, the papers presented in this Research Topic will help to shorten the gap. Hopefully with more research and further advancements of techniques including proteomic study tools, a more comprehensive picture of arginylation will soon be on the horizon.

## AUTHOR CONTRIBUTIONS

FZ wrote this manuscript.

## REFERENCES

- Balzi, E., Choder, M., Chen, W. N., Varshavsky, A., and Goffeau, A. (1990). Cloning and Functional Analysis of the Arginyl-tRNA-Protein Transferase Gene ATE1 of *Saccharomyces cerevisiae*. *J. Biol. Chem.* 265, 7464–7471. doi:10.1016/s0021-9258(19)39136-7
- Brower, C. S., and Varshavsky, A. (2009). Ablation of Arginylation in the Mouse N-End Rule Pathway: Loss of Fat, Higher Metabolic Rate, Damaged Spermatogenesis, and Neurological Perturbations. *PLoS One* 4, e7757. doi:10.1371/journal.pone.0007757
- Deka, K., Singh, A., Chakraborty, S., Mukhopadhyay, R., and Saha, S. (2016). Protein Arginylation Regulates Cellular Stress Response by Stabilizing HSP70 and HSP40 Transcripts. *Cel Death Discov.* 2, 16074. doi:10.1038/cddiscovery.2016.74
- Graciet, E., Hu, R.-G., Piatkov, K., Rhee, J. H., Schwarz, E. M., and Varshavsky, A. (2006). Aminoacyl-transferases and the N-End Rule Pathway of Prokaryotic/eukaryotic Specificity in a Human Pathogen. *Proc. Natl. Acad. Sci. U.S.A.* 103, 3078–3083. doi:10.1073/pnas.0511224103
- Graciet, E., Walter, F., Maoiléidigh, D. Ó., Pollmann, S., Meyerowitz, E. M., Varshavsky, A., et al. (2009). The N-End Rule Pathway Controls Multiple Functions during Arabidopsis Shoot and Leaf Development. *Proc. Natl. Acad. Sci. U.S.A.* 106, 13618–13623. doi:10.1073/pnas.0906404106
- Kaji, H., Novelli, G. D., and Kaji, A. (1963). A Soluble Amino Acid-Incorporating System from Rat Liver. *Biochim. Biophys. Acta (Bba) - Specialized Section Nucleic Acids Relat. Subjects* 76, 474–477. doi:10.1016/0926-6550(63)90070-7
- Kaji, H. (1968). Soluble Amino Acid Incorporating System from Rat Liver. *Biochemistry* 7, 3844–3850. doi:10.1021/bi00851a009
- Kato, M., and Nozawa, Y. (1984). Complete Purification of arginyl-tRNA: Protein Arginyltransferase from Hog Kidney and Production of its Antibody. *Anal. Biochem.* 143, 361–367. doi:10.1016/0003-2697(84)90675-4
- Kumar, A., Birnbaum, M. D., Patel, D. M., Morgan, W. M., Singh, J., Barrientos, A., et al. (2016). Posttranslational Arginylation Enzyme Ate1 Affects DNA Mutagenesis by Regulating Stress Response. *Cell Death Dis* 7, e2378. doi:10.1038/cddis.2016.284
- Licausi, F., Kosmacz, M., Weits, D. A., Giuntoli, B., Giorgi, F. M., Voesenek, L. A. C. J., et al. (2011). Oxygen Sensing in Plants Is Mediated by an N-End Rule Pathway for Protein Destabilization. *Nature* 479, 419–422. doi:10.1038/nature10536
- Moorthy, B. T., Jiang, C., Patel, D. M., Ban, Y., O'Shea, C. R., Kumar, A., et al. (2022). The Evolutionarily Conserved Arginyltransferase 1 Mediates a pVHL-independent Oxygen-Sensing Pathway in Mammalian Cells. *Dev. Cel.* doi:10.1016/j.devcel.2022.02.010
- Van, V., and Smith, A. T. (2020). ATE1-Mediated Post-Translational Arginylation Is an Essential Regulator of Eukaryotic Cellular Homeostasis. *ACS Chem. Biol.* 15, 3073–3085. doi:10.1021/acscchembio.0c00677
- Wiley, D. J., D'Urso, G., and Zhang, F. (2020). Posttranslational Arginylation Enzyme Arginyltransferase1 Shows Genetic Interactions with Specific Cellular Pathways *In Vivo*. *Front. Physiol.* 11, 427. doi:10.3389/fphys.2020.00427
- Zhang, F., Patel, D. M., Colavita, K., Rodionova, I., Buckley, B., Scott, D. A., et al. (2015). Arginylation Regulates Purine Nucleotide Biosynthesis by Enhancing the Activity of Phosphoribosyl Pyrophosphate Synthase. *Nat. Commun.* 6, 7517. doi:10.1038/ncomms8517

**Conflict of Interest:** The author declares that the research was conducted in the absence of any commercial or financial relationships that could be construed as a potential conflict of interest.

**Publisher's Note:** All claims expressed in this article are solely those of the authors and do not necessarily represent those of their affiliated organizations, or those of the publisher, the editors and the reviewers. Any product that may be evaluated in this article, or claim that may be made by its manufacturer, is not guaranteed or endorsed by the publisher.

Copyright © 2022 Zhang. This is an open-access article distributed under the terms of the Creative Commons Attribution License (CC BY). The use, distribution or reproduction in other forums is permitted, provided the original author(s) and the copyright owner(s) are credited and that the original publication in this journal is cited, in accordance with accepted academic practice. No use, distribution or reproduction is permitted which does not comply with these terms.



## OPEN ACCESS

### Edited by:

Cesare Indiveri,  
University of Calabria, Italy

### Reviewed by:

Brijesh Kumar Singh,  
Duke-NUS Medical School, Singapore  
Steven Michael Claypool,  
Johns Hopkins University,  
United States

### \*Correspondence:

Flavia Fontanesi  
ffontanesi@med.miami.edu  
Fangliang Zhang  
fzhang2@miami.edu

### †Present address:

Chunhua Jiang,  
Pharmacology Center, Zhongqi  
Pharmaceutical Technology  
(Shijiazhuang) Co., Ltd., China  
Shijiazhuang Pharmaceutical  
Company, Shijiazhuang, China  
Devang M. Patel,  
Department of Diabetes, Monash  
University, Melbourne, VIC, Australia  
Akhilesh Kumar,  
Department of Botany, Banaras Hindu  
University, Varanasi, India

### Specialty section:

This article was submitted to  
Cellular Biochemistry,  
a section of the journal  
*Frontiers in Cell and Developmental  
Biology*

**Received:** 07 September 2020

**Accepted:** 23 November 2020

**Published:** 21 December 2020

### Citation:

Jiang C, Moorthy BT, Patel DM,  
Kumar A, Morgan WM, Alfonso B,  
Huang J, Lampidis TJ, Isom DG,  
Barrientos A, Fontanesi F and Zhang F  
(2020) Regulation of Mitochondrial  
Respiratory Chain Complex Levels,  
Organization, and Function by  
Arginyltransferase 1.  
*Front. Cell Dev. Biol.* 8:603688.  
doi: 10.3389/fcell.2020.603688

# Regulation of Mitochondrial Respiratory Chain Complex Levels, Organization, and Function by Arginyltransferase 1

Chunhua Jiang<sup>1†</sup>, Balaji T. Moorthy<sup>1</sup>, Devang M. Patel<sup>1†</sup>, Akhilesh Kumar<sup>1†</sup>, William M. Morgan<sup>1</sup>, Belkis Alfonso<sup>2</sup>, Jingyu Huang<sup>2</sup>, Theodore J. Lampidis<sup>3,4</sup>, Daniel G. Isom<sup>1,4,5</sup>, Antoni Barrientos<sup>6,7</sup>, Flavia Fontanesi<sup>7\*</sup> and Fangliang Zhang<sup>1,4\*</sup>

<sup>1</sup> Department of Molecular & Cellular Pharmacology, University of Miami Leonard M. Miller School of Medicine, Miami, FL, United States, <sup>2</sup> Department of Human Genetics, University of Miami Leonard M. Miller School of Medicine, Miami, FL, United States, <sup>3</sup> Department of Cell Biology, University of Miami Leonard M. Miller School of Medicine, Miami, FL, United States, <sup>4</sup> Sylvester Comprehensive Cancer Center, University of Miami Leonard M. Miller School of Medicine, Miami, FL, United States, <sup>5</sup> Institute for Data Science and Computing, University of Miami, Coral Gables, FL, United States, <sup>6</sup> Department of Neurology, University of Miami Leonard M. Miller School of Medicine, Miami, FL, United States, <sup>7</sup> Department of Biochemistry & Molecular Biology, University of Miami Leonard M. Miller School of Medicine, Miami, FL, United States

Arginyltransferase 1 (ATE1) is an evolutionary-conserved eukaryotic protein that localizes to the cytosol and nucleus. It is the only known enzyme in metazoans and fungi that catalyzes posttranslational arginylation. Lack of arginylation has been linked to an array of human disorders, including cancer, by altering the response to stress and the regulation of metabolism and apoptosis. Although mitochondria play relevant roles in these processes in health and disease, a causal relationship between ATE1 activity and mitochondrial biology has yet to be established. Here, we report a phylogenetic analysis that traces the roots of ATE1 to alpha-proteobacteria, the mitochondrion microbial ancestor. We then demonstrate that a small fraction of ATE1 localizes within mitochondria. Furthermore, the absence of ATE1 influences the levels, organization, and function of respiratory chain complexes in mouse cells. Specifically, *ATE1*-KO mouse embryonic fibroblasts have increased levels of respiratory supercomplexes I+III<sub>2</sub>+IV<sub>n</sub>. However, they have decreased mitochondrial respiration owing to severely lowered complex II levels, which leads to accumulation of succinate and downstream metabolic effects. Taken together, our findings establish a novel pathway for mitochondrial function regulation that might explain ATE1-dependent effects in various disease conditions, including cancer and aging, in which metabolic shifts are part of the pathogenic or deleterious underlying mechanism.

**Keywords:** arginylation, arginyltransferase, mitochondria, biogenesis, respiration, respiratory chain complexes

## INTRODUCTION

Mitochondria are the eukaryotic organelles responsible for oxidative phosphorylation (OXPHOS). They originated from an endosymbiotic event between a respiratory-competent alpha-proteobacteria and an ancient archaea host cell (Bock, 2017). Through evolution, regulatory mechanisms coordinating mitochondrial catabolism have been adjusted to meet the energy and biomass requirements of the eukaryotic cell. At the same time, most of the original bacterial genes have been transferred to the nucleus of the host cell. Currently, the mitochondrial genome (mtDNA) only encodes for a handful of protein-coding genes (8 in yeast, 13 in mammals). The remaining mitochondrial proteome is encoded by the nuclear genome, synthesized in the cytoplasm, and then imported into mitochondria. Therefore, mitochondrial functions are under nuclear control, which involves regulatory processes that are not fully understood.

Arginyltransferase 1 (ATE1) is an evolutionarily conserved enzyme existing in nearly all eukaryotes, with the exception of a few protists (Balzi et al., 1990; Rai and Kashina, 2005; Hu et al., 2006; Rai et al., 2006). Sequence homologs of ATE1 are also found in prokaryotes, although their biological significance is unknown (Graciet et al., 2006). In eukaryotes, ATE1 mediates posttranslational arginylation, the addition of one extra arginine to the target protein. In many cases, arginylation leads to hyper-ubiquitination and rapid degradation of the modified protein, as summarized by the N-end rule theory (Varshavsky, 2011). Mounting evidence suggests that arginylation may act as a response to oxidative stress (Decca et al., 2007; Carpio et al., 2010, 2013; Deka et al., 2016; Kumar et al., 2016). For example, global arginylation activity in cells or tissues is activated by stress caused by reactive oxygen species (ROS), as evidenced by the preferential arginylation of oxidized or misfolded proteins (Ingoglia et al., 2000; Hu et al., 2005). Since mitochondria are a major source of ROS in eukaryotic cells, ATE1 could be an important regulator of mitochondrial redox functions. However, this possibility has yet to be explored.

Several lines of evidence support the idea that the effects of ATE1 activity may be linked to ROS. Cellular phenotypes induced by ATE1 dysregulation often resemble those caused by mitochondrial abnormalities (Saha and Kashina, 2011). Additionally, systematic knockout (KO) of the only gene coding for ATE1 (*ATE1*) leads to embryonic lethality in mouse (Kwon et al., 2002), and postnatal deletion causes rapid weight loss, neurological perturbation, early lethality, and infertility (Brower and Varshavsky, 2009; Kurosaka et al., 2010). Furthermore, tissue-specific knockout (KO) of *ATE1* in mice heart, testis, and central neural system (CNS) leads to cardiomyopathy, infertility, or neural development retardation, respectively (Leu et al., 2009; Kurosaka et al., 2010, 2012; Saha and Kashina, 2011; Wang et al., 2017). Many of these pathological outcomes are consistent with those derived from mitochondrial and metabolic dysregulation and might be explained at the molecular/cellular level by Ate1

activities. For example, *ATE1*-KO leads to multiple metabolic defects, including increased demand for purine supplies and elevated synthesis rate of glycine and alanine, which are often signs of perturbed balance between glycolysis and mitochondrial respiration (Zhang et al., 2015). This hypothesis is further supported by the observation that *ATE1* downregulation is commonly seen in many types of cancer associated with mitochondrial dysfunction (Zhong et al., 2005; Rai et al., 2015).

Recently, we began exploring the genetic interactions between ATE1 and thousands of other genes in the fission yeast model system (*Schizosaccharomyces pombe*) (Wiley et al., 2020). In this study, we observed that ATE1 interacts with only 5% of other yeast genes in a screening library covering 75% of the predicted open reading frames (ORF). Remarkably, more than 10% of those ATE1-interacting genes were related to mitochondria.

This observation motivated us to directly examine the relationship between ATE1 activity, localization, and mitochondrial function. Here, we first analyzed *ATE1* sequences from multiple organisms and determined that eukaryotic *ATE1* may have arisen by gene transfer from alpha-proteobacteria and co-evolved with the function of mitochondria in respiration. Moreover, we show that a small fraction of ATE1 localizes within mitochondria and that ATE1 is required for optimal mitochondrial respiration in both mammalian and budding yeast (*Saccharomyces cerevisiae*) cells. Lastly, we demonstrate that lack of ATE1 in murine cells differentially affects the levels, organization, and function of mitochondrial respiratory complexes. Overall, our finding suggests a hitherto unknown role of ATE1 in the regulation of mitochondrial and cellular energy metabolism.

## RESULTS

### The Alpha-Proteobacterial Origin of ATE1 Links the Protein to Mitochondria

While a nuclear gene encoded ATE1 in eukaryotes, our search of ATE1 homologs in archaea, where most of the nuclear genome originated (Williams et al., 2013), returned no matches (Figure 1). However, sequence homologs of ATE1 are present in a large population of bacteria, including modern alpha-proteobacteria (Buffet et al., 2020), a close relative to the ancient alpha-proteobacteria that became mitochondria (Figures 1A–C). As such, it is likely that the *ATE1* gene, like many mitochondria-associated genes, was transferred to the nuclear genome during mitochondrial domestication (Janeway and Medzhitov, 2002; Buffet et al., 2020). To gain further insight into the relationship between ATE1 and mitochondria from the perspective of molecular evolution, we examined the status of mitochondrial development and the presence of the *ATE1* gene in several branches of eukaryotes. While almost all eukaryotes contain the *ATE1* gene, two exceptions exist. One is the family of giardia, and the other is the superfamily of dinoflagellates and apicomplexan. Intriguingly, both families lack respiratory-active mitochondria. Instead, they possess mitosomes, a reduced form of mitochondria with minimal functions that cannot perform oxidative phosphorylation (Figure 1D). Since these two families

**Abbreviations:** ATE1, arginyltransferase 1; GFP, green-fluorescence protein; HFF, human foreskin fibroblasts; KD, knockdown; KO, knock-out; MEF, mouse embryonic fibroblasts; WT, wild-type.



are distally related and separated by many other families that possess ATE1, their loss of ATE1 is unlikely to derive from the same ancestor. For the same reason, their lack of respiratory-competent mitochondria is likely the result of convergent evolution. These data suggest that the presence of ATE1 may be essential for maintaining fully functional mitochondria.

## A Subpopulation of ATE1 Localizes to Mitochondria

Several studies have used fluorescent protein fusions to show the localization of ATE1 in the nucleus or the cytoplasm (Rai and Kashina, 2005; Hu et al., 2006; Rai et al., 2006; Wang et al., 2011). However, the potential localization of ATE1 to mitochondria was not examined directly. To investigate this question, we first utilized a budding yeast (*Saccharomyces cerevisiae*) strain with a genomically-integrated green fluorescent protein (GFP) fused to the C-terminus of the endogenous Ate1 (Ate1-GFP), which showed that a subfraction of the GFP-fused Ate1 colocalizes with Mitotracker red-stained mitochondria (Figure 2A). Next, to test if the mitochondrial localization of ATE1 was organism-specific, we fused a C-terminal GFP to the mouse ATE1, transcript variant 1, a ubiquitously-expressed isoform (Rai and Kashina, 2005; Wang et al., 2011). To avoid the competition of the endogenous protein, this recombinant ATE1 was expressed in ATE1-knockout (KO) mouse embryonic fibroblasts (MEF). We detected a fraction of the fluorescent ATE1 colocalizing with the Mitotracker red-stained branched mitochondrial network surrounding the nucleus (Figure 2B). In mice, there are six ATE1 transcript variants, four of which (transcript variants 1, 2, 3, and 4) are known to be translated into protein isoforms that are >90% identical in sequences (Rai and Kashina, 2005; Hu et al., 2006). We found that the mitochondrial localization of ATE1 is not isoform-specific, because the other three known protein isoforms also appear to localize to mitochondria (Figure 2B; see also Supplementary Figure 1A for the expression level of the tested isoforms).

To further assess the mitochondrial localization of endogenous ATE1, we purified mitochondria from MEF by differential centrifugation and probed for endogenous ATE1 by immunoblotting. We were able to detect a fraction of ATE1 associated with purified mitochondria from wildtype (WT) MEF, while the specificity of the anti-ATE1 antibody was validated by the absence of signals in mitochondria from ATE1-KO cells (Figure 2C; see also the purity of the mitochondrial fraction in Figure 2D). Furthermore, a proteinase K protection assay in purified mitochondria showed that the mitochondrion-associated ATE1 is resistant to proteinase K digestion, except when the mitochondrial membranes are disrupted by sonication (Figure 2E). These data indicated that a fraction of ATE1 localizes within mitochondria. To estimate the percentage of ATE1 that is associated with mitochondria, we used a dilution assay of the whole cell and isolated mitochondria to compare the ratios of ATE1 over Voltage-dependent anion channel (VDAC), an established mitochondrial marker. We found that only about 0.5% of total endogenous ATE1 in the cell is associated with mitochondria (Supplemental Figure 1B).

## ATE1 Is Essential for Maintenance of Mitochondrial Morphology and Respiratory Function

We next examined in whole cells the steady-state levels of VDAC and TOM20, two mitochondrial markers, and did not find a significant difference between WT and ATE1-KO MEF (Figure 3A). This suggested that the ATE1 does not directly affect cellular mitochondrial mass. However, when we examined mitochondrial morphology by electron microscopy, we found significant differences between WT and ATE1-KO cells (Figure 3B). Remarkably, mitochondrial filaments in ATE1-KO cells were significantly shorter and wider (Figure 3C), reminiscent of the swollen mitochondria often observed in respiratory-deficient cells, as well as typical cancer cells with a glycolytic metabolic profile (Alirol and Martinou, 2006).

To assess whether any mitochondrial functional difference accompanies the observed morphological changes, we measured cellular respiration in ATE1-KO and WT MEF. Our data showed that ATE1-KO cells had a ~30% reduction in endogenous oxygen consumption rate compared to WT MEF (Figure 3D). As an essential control, we reconstituted ATE1-KO MEF with a recombinant ATE1 (transcript variant 3, which was shown to have the most potent anti-tumor growth effect) at a level comparable to the endogenous protein. Recombinant ATE1 rescued the ATE1-KO respiratory defects (Figure 3E). Consistent with the observations in mammalian cells, we found that the deletion of *ate1* in budding yeast also lead to slower growth in respiratory media (Figure 3F), reduced endogenous cell respiration by nearly 30%, and attenuated the mitochondrial membrane potential by more than 50% (Figures 3G,H).

## ATE1 Is Essential for the Proper Assembly, Organization, and Function of Mitochondrial Respiratory Complexes

The mitochondrial respiratory chain (MRC) is formed by four multimeric complexes (complex I to IV, CI-CIV) and two mobile electron carriers (coenzyme Q and cytochrome *c*). Electrons from the reducing equivalents NADH and FADH<sub>2</sub> enter the MRC at the level of CI and CII, respectively, and are sequentially transferred until CIV, where the final electron acceptor, molecular oxygen, is reduced to water. Additionally, MRC CI, CIII, and CIV dynamically associate in supramolecular structures known as supercomplexes. To further dissect the respiratory defect observed in the ATE1-KO cells, we first measured oxygen consumption rates in digitonin-permeabilized cells following the addition of substrates specific for CI (glutamate-malate) or CII (succinate). When we examined the overall impact of ATE1 on mitochondrial respiration, we found that the combined rate of CI- and CII substrate-driven respiration, and the maximum respiratory capacity measured in the presence of the uncoupler FCCP, are both reduced in KO cells (Figure 4A). CI does not contribute to the deleterious effect on cellular respiration since the glutamate-malate oxidation rate is slightly but significantly higher in ATE1-KO cells than in control. In contrast, the oxygen consumption rate in the presence of succinate was lowered by nearly 50% in ATE1-KO

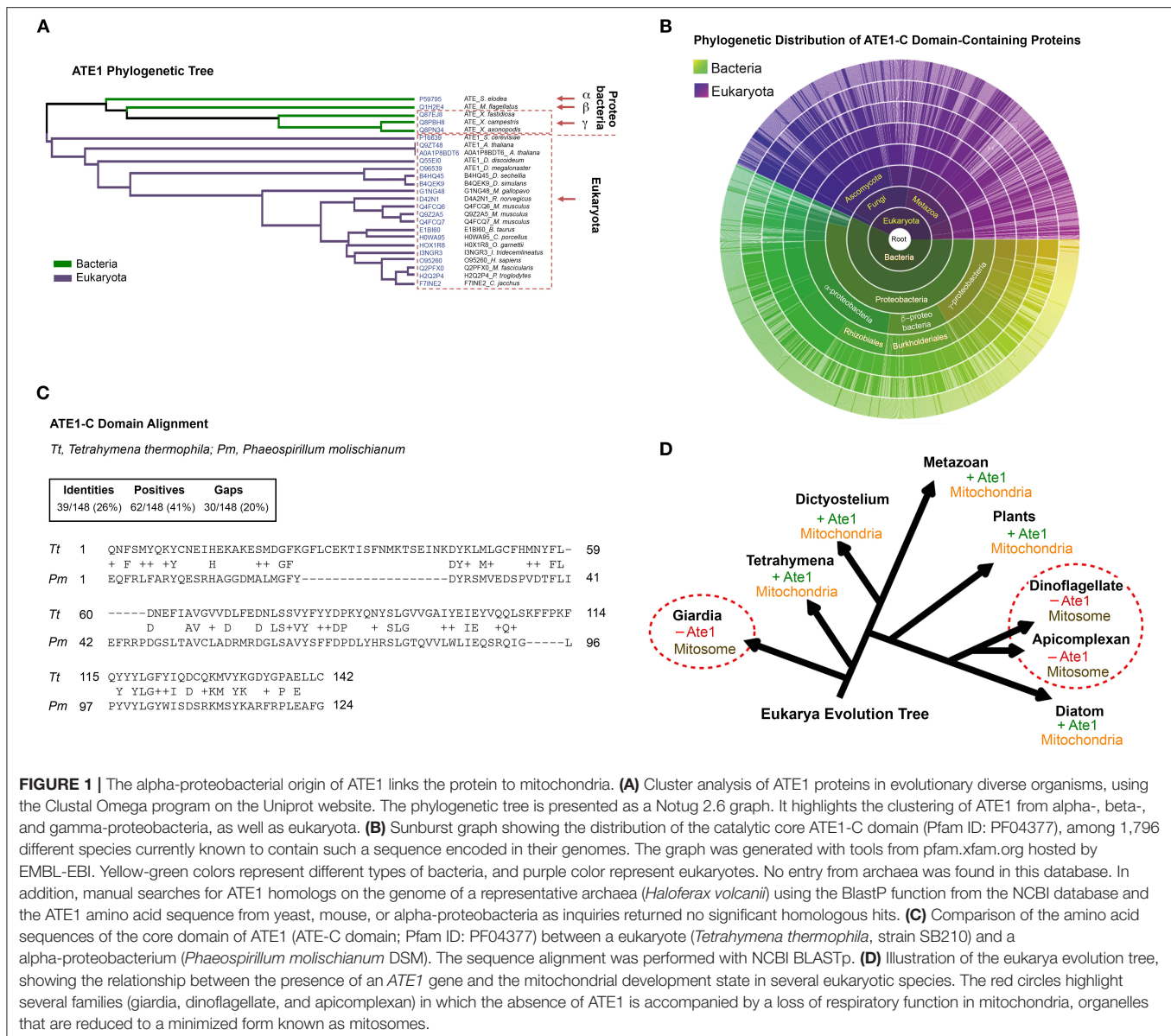


**FIGURE 1 |** The alpha-proteobacterial origin of ATE1 links the protein to mitochondria. **(A)** Cluster analysis of ATE1 proteins in evolutionary diverse organisms, using the Clustal Omega program on the Uniprot website. The phylogenetic tree is presented as a Notug 2.6 graph. It highlights the clustering of ATE1 from alpha-, beta-, and gamma-proteobacteria, as well as eukaryota. **(B)** Sunburst graph showing the distribution of the catalytic core ATE1-C domain (Pfam ID: PF04377), among 1,796 different species currently known to contain such a sequence encoded in their genomes. The graph was generated with tools from pfam.xfam.org hosted by EMBL-EBI. Yellow-green colors represent different types of bacteria, and purple color represent eukaryotes. No entry from archaea was found in this database. In addition, manual searches for ATE1 homologs on the genome of a representative archaea (*Haloferax volcanii*) using the BlastP function from the NCBI database and the ATE1 amino acid sequence from yeast, mouse, or alpha-proteobacteria as inquiries returned no significant homologous hits. **(C)** Comparison of the amino acid sequences of the core domain of ATE1 (ATE-C domain; Pfam ID: PF04377) between a eukaryote (*Tetrahymena thermophila*, strain SB210) and a alpha-proteobacterium (*Phaeosporillum molischianum* DSM). The sequence alignment was performed with NCBI BLASTp. **(D)** Illustration of the eukarya evolution tree, showing the relationship between the presence of an ATE1 gene and the mitochondrial development state in several eukaryotic species. The red circles highlight several families (giardia, dinoflagellate, and apicomplexan) in which the absence of ATE1 is accompanied by a loss of respiratory function in mitochondria, organelles that are reduced to a minimized form known as mitosomes.

cells (Figures 4A,B and Supplementary Figure 2), indicating a specific CII activity defect.

To determine the cause of the respiratory alteration, we examined the levels of individual mitochondrial respiratory complexes and supercomplexes by Blue Native-PAGE followed by immunoblotting. Consistent with the respiratory data, the steady-state levels of mitochondrial CII in ATE1-KO cells were found to be ~50% than in WT MEFs (Figure 4C). However, we also observed a decrease in dimeric complex III (CIII<sub>2</sub>) accumulation, while CIV was unaffected (Figure 4C). Moreover, an evident remodeling of the MRC organization was detected. In ATE1-KO cells, the levels of CI-containing supercomplexes (I+III<sub>2</sub> and I+III<sub>2</sub>+IV<sub>1-n</sub>) were increased, whereas the amount of CIII that accumulated in CIII<sub>2</sub> and the III<sub>2</sub>+IV supercomplex

was attenuated (Figures 4D,E). This remodeling facilitates an increase in CI stability, presumably in an attempt to compensate for the lower levels of CII.

MRC CII or succinate dehydrogenase (SDH) is also an enzyme of the TCA cycle, in which it catalyzes the conversion of succinate to fumarate. Succinate, when in excess, promotes glycolysis and therefore acts as a critical signaling component connecting the TCA cycle to glycolysis. When we measured the enzymatic activity of SDH, we found it significantly reduced in ATE1-KO cells (Figure 5A). Correspondingly, the level of succinate in ATE1-KO MEF was nearly 2-fold higher than in WT (Figure 5B). To test if this would change the balance between mitochondrial OXPHOS and glycolysis, we measured the viability of ATE1-KO MEF under glucose starvation and found that they are

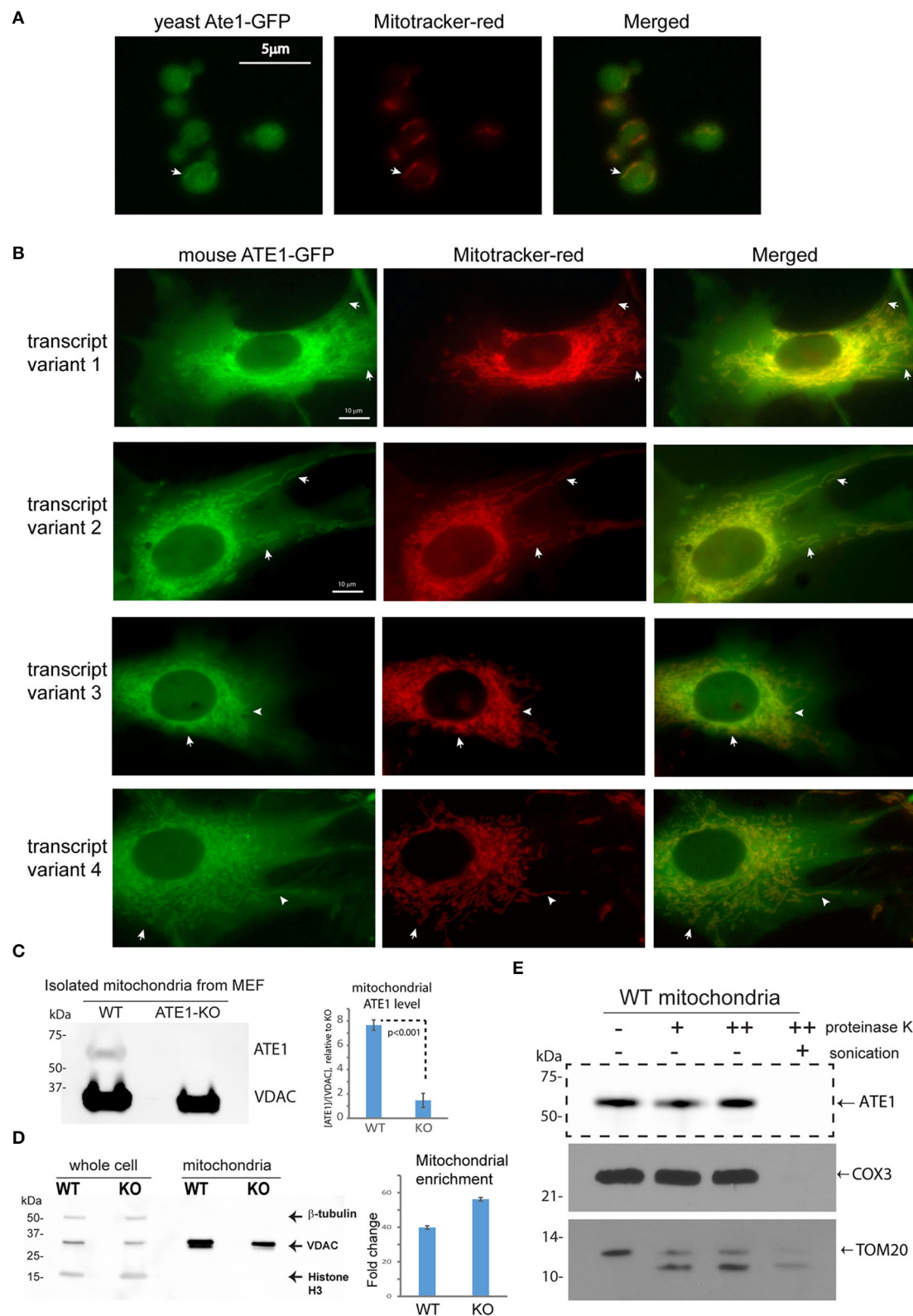


**FIGURE 2 |** ATE1 locates inside mitochondria. **(A)** The location of yeast Ate1 is traced by a GFP fused to the C-terminus of the endogenous Ate1 on the chromosome of *S. cerevisiae*. The location of Ate1 (shown in green) is then compared to the mitochondria-specific dye, Mitotracker-Red (shown in red). White arrows point to locations where colocalization of Ate1 and mitochondrial structure can be seen. Scale bar indicates 5 micrometers. **(B)** A recombinant mouse ATE1 is fused a  
(Continued)



**FIGURE 2** | C-terminal GFP and stably expressed in mouse embryonic fibroblasts (MEF) with *ATE1*-knockout (referred as “KO” in figure labeling hereon). All four known protein isoforms from splice variants (1, 2, 3, and 4) of the *ATE1* gene were examined. The location of GFP-fused *ATE1* (shown in green) is compared to mitochondria stained with Mitotracker-Red (shown in red). White arrows point to locations where discrete mitochondrial structures are seen. See also **Supplementary Figure 1A** for the expression levels of the different *ATE1* isoforms. Scale bar indicates 10 micrometers. **(C)** Representative Western blot using a monoclonal antibody that recognizes all four *ATE1* isoforms showing a detectable band of endogenous *ATE1* in mitochondria from WT MEF, but not from *ATE1*-KO (KO) cells. Antibody for VDAC was used as a loading control on the same blot for mitochondria mass. The experiment was repeated 3 times ( $n = 3$ ). On the right side is the quantification showing the specific signal of *ATE1* associated with mitochondria in WT cells. The signal in *ATE1*-KO cells is used as background control for normalization. The error bar represents standard error of mean (SEM) and the statistical significance was calculated by the *t*-test. See also **Supplementary Figure 1B** for the estimate of the percentage of mitochondria-associated *ATE1* in relation to the total cellular *ATE1*. **(D)** The purity of mitochondria isolated from WT and *ATE1*-KO cells were examined by Western blot with antibodies against beta-tubulin, VDAC, and histone 3, which are markers for cytosol, mitochondria, and nucleus, respectively. The whole cell lysate was used as control. On the right side shows the chart of quantification of mitochondrial enrichment, which was calculated from three independent repetitions ( $n = 3$ ) by the ratio of VDAC over tubulin in the mitochondrial fraction vs. the whole lysate. The bar graph represents the mean  $\pm$  SEM. **(E)** Representative Western blot showing the mitochondrial proteinase K protection assay. The signs of “-,” “+,” “++” for proteinase K indicate increasing concentrations (0, 0.32, or 0.64  $\mu$ g/ml) of proteinase K. An arrow indicates the expected size of *ATE1*. On the lower side is the Western blot of the digestions of different mitochondria-associated proteins as controls for localizations. These include COX3, which is located inside the mitochondrial matrix, and TOM20, a transmembrane protein anchored on the outer membrane of mitochondria.

significantly more sensitive to the lack of glucose supply than WT cells (**Figures 5C,D**).

SDH is comprised of four subunits known as SDHA, B, C, and D, all of which are encoded in the nuclear genome and then imported into mitochondria (Van Vranken et al., 2015). When we examined the levels of these subunits in the mitochondrial fraction, we found that the levels of SDHB and SDHC, as well as the palmitoylation level of SDHD, are decreased in mitochondria in *ATE1*-KO MEF, in agreement with the lower levels of CII (**Figure 6A**). However, the total protein levels of these subunits in whole *ATE1*-KO cells were either unchanged or even slightly increased compared to WT cells (**Figure 6B**) while the transcription of SDH subunits is drastically increased in *ATE1*-KO MEF cells (**Figure 6C**), likely as a compensation for the functional SDH deficiency. These data indicate that *ATE1* may affect the mitochondrial import and/or assembly of SDH subunits, ultimately leading to CII deficiency.

## DISCUSSION

This study describes the discovery of uncharacterized physical and functional connections of *ATE1* with the mitochondrion.

The *ATE1* gene is conserved in eukaryotes and bacteria. In eukaryotes, *ATE1* is a nuclear gene whose roles in regulating the functions and/or half-lives of cytosolic or nuclear proteins have been well-documented (Varshavsky, 2011). Here, we found several lines of evidence connecting *ATE1* to mitochondria. First, phylogenetic studies pointed toward an alpha-protobacterial origin for *ATE1*. Second, fluorescence microscopy examinations of recombinant *ATE1* expressed in MEFs and biochemical assays of endogenous *ATE1* determined that a fraction of the protein resides within mitochondria. Third, the absence of *ATE1* in *ATE1*-KO MEFs results in decreased MRC complex II levels and a major reorganization of the MRC into free complexes and supercomplexes. And fourth, decreased respiratory capacity and increased succinate levels in *ATE1*-KO MEFs correlate with elevated dependency on glucose.

The marked decrease in MRC CII and the concomitant rearrangement of the MRC complexes I, III, and IV into CI-containing supercomplexes, as observed in *ATE1*-KO cells, agree with the plasticity model of MRC organization. According to

this model, MRC complexes exist as free entities or in SC associations in a dynamic manner to optimize electron flux from different substrates, adapting the efficiency of the respiratory chain to changes in cellular metabolism (Acin-Perez et al., 2008). Therefore, if electron-transfer from succinate-linked FADH<sub>2</sub> to coenzyme Q-CIII is compromised, NADH-driven respiration would be enhanced by reorganizing the CIII and CIV complexes into I+III<sub>2</sub>+IV<sub>n</sub> supercomplexes. In other words, we interpret the MRC complex re-organization as a consequence of the metabolic remodeling induced by the CII or SDH deficiency. However, at this stage, our studies did not disclose whether the mitochondrial fraction of *ATE1* is directly responsible for the CII assembly/stability defect or whether this is also influenced by the cytoplasmic pool of the *ATE1* protein that, for example, could act to regulate the import of MRC subunits into mitochondria. Nevertheless, the data in our study appear to suggest that the proposed role of *ATE1* in protein degradation in the cytosol (Bachmair et al., 1986; Tasaki et al., 2012) is not very likely to play a significant role in the regulation of mitochondrial respiratory complexes. For example, we found that the transcription of all four SDH subunits is up-regulated by 4–10-folds in the *ATE1*-KO MEF. If the absence of *ATE1* attenuates the degradation of SDH subunits as predicted by the N-end rule theory, one would expect a drastic increase of SDH subunit protein levels accumulating in the cytosol. However, this is not the case since the SDH subunit protein levels measured in whole cells are either unchanged or only slightly elevated. On the other hand, the increased SDH subunits transcription that we have observed in *ATE1*-KO cells is more likely a compensatory cellular response to the functional SDH deficiency.

Given that mitochondria are a major source of ROS and a central regulator of apoptosis, the role of *ATE1* in this organelle may provide an explanation for its observed involvement in the stress response (Bongiovanni et al., 1999; Decca et al., 2007; Carpio et al., 2010, 2013; Lopez Sambrooks et al., 2012; Deka et al., 2016; Kumar et al., 2016; Birnbaum et al., 2019; Kim et al., 2020). Future studies will be devoted to understanding whether the translocation of *ATE1* into mitochondria (or other cellular compartments such as the nucleus) is influenced by stress. Independently, our observations have profound implications in physiological processes such as embryo/tissue development and



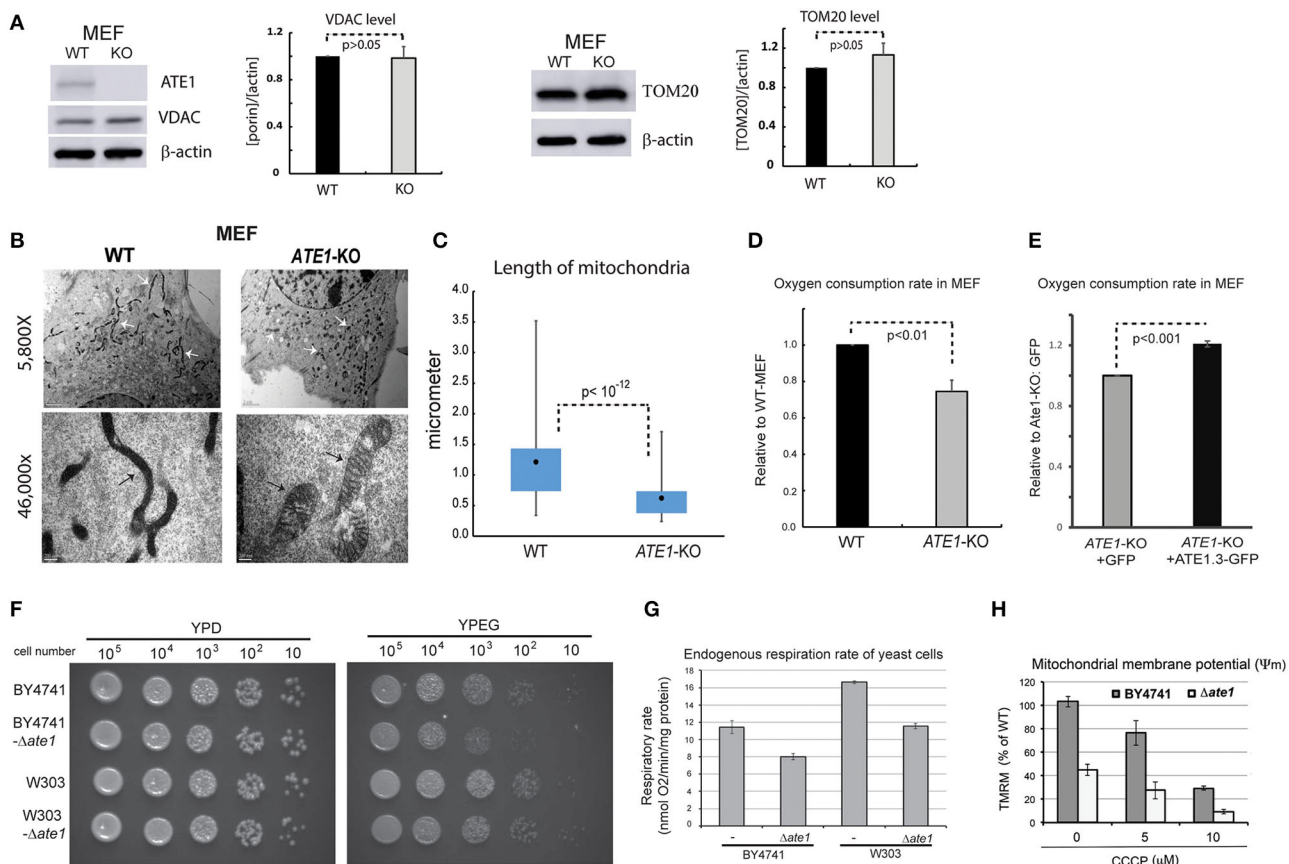


**FIGURE 3 |** ATE1 is essential for the morphology and function of mitochondria. **(A)** The steady state protein levels of mitochondrial mass markers, VDAC and TOM20, in WT and ATE1-KO MEF were examined by Western blot as shown by representative images (left panel) and quantification (right panel) ( $n = 4$  for VDAC;  $n = 3$  for TOM20). Beta-actin was used as a loading control. **(B)** Morphologies and sizes of mitochondria in WT and ATE1-KO MEF shown by negative staining at different magnifications under electron microscopy (5,800X in the upper row and 46,000X in the lower row, as labeled). The scale bars in upper row represent 2 micrometers, while the ones in lower row is 200 nanometers. The white arrows and black arrows indicate a few discrete mitochondria. **(C)** Graph showing box-whisker plots for the lengths of mitochondria in WT and ATE1-KO MEF. The quantification of WT cells were based on 115 discrete mitochondrial filaments ( $n = 115$ ) in 6 electron-microscopy (EM) images containing 6 different cells, while for ATE1-KO was based on 122 discrete mitochondrial filaments in 4 EM images containing 4 different cells. **(D)** Oxygen consumption rates of the whole cell in WT and ATE1-KO MEF. The values in ATE1-KO cells were normalized to those in WT cells in each measurement. The bar graph represents the mean  $\pm$  SEM of four independent measurements ( $n = 4$ ). The  $p$ -value was calculated by  $t$ -test. See also **Supplementary Figure 2** for representative images of the oxygen consumption curve. **(E)** Similar to **(D)**, except that ATE1-KO MEF stably expressing GFP-fused recombinant ATE1, transcript variant 3 was measured. The expression of GFP alone was used as a control. The bar graph represents the mean  $\pm$  SEM of four independent measurements ( $n = 4$ ). The  $p$ -value was calculated by  $t$ -test. **(F)** The growth of yeast of BY4741 or W303 strain, with or without the deletion of the ATE1 gene, was examined by serial dilution on agar plates for either a fermenting condition with the glucose-containing rich media (YPD), or a respiring condition with the glycerol and ethanol-based media (YPEG). **(G)** The cellular oxygen consumption rates of yeast of BY4741 or W303 strain, with or without the deletion of the ATE1 gene. The bar graph represents the mean  $\pm$  SEM of three independent measurements ( $n = 3$ ). The  $p$ -value was calculated by  $t$ -test. **(H)** The level of membrane potential in BY4741 yeast, with or without the deletion of the ATE1 gene, in the increasing level of CCCP, quantified using TMRM staining and flow cytometry. The bar graph represents the mean  $\pm$  SD of three independent measurements ( $n = 3$ ). The  $p$ -value was calculated by  $t$ -test.

aging, and in disease conditions such as cancer and inflammation, in which the involvement of ATE1 is poorly understood.

ATE1 is downregulated in multiple types of cancer, including those observed in the kidney, prostate, and colorectum (Rai et al., 2015; Birnbaum et al., 2019). Therefore, our findings offer a novel explanation for the commonly seen mitochondrial dysregulation in these cancers (Zhong et al., 2005; Rai et al., 2015). Notably, in most normal cells, the balance between glycolysis and mitochondrial respiration is essentially maintained by reciprocal feedback pathways, including the allosteric inhibitory effect of

mitochondrion-generated ATP on AMP-activated protein kinase or citrate on phosphofructose kinase (Gogvadze et al., 2008). However, the downregulation of mitochondria function in cancer is not necessarily a consequence of the increase in glycolysis known as the Warburg effect (Alirol and Martinou, 2006; Viale et al., 2015). It has been proposed that the existence of mutations in genes coding for mitochondrial proteins and/or metabolic enzymes may contribute to tumorigenesis. These include the genes encoding SDH subunits, which are often considered as tumor suppressors (Buffet et al., 2020). SDH mutations result

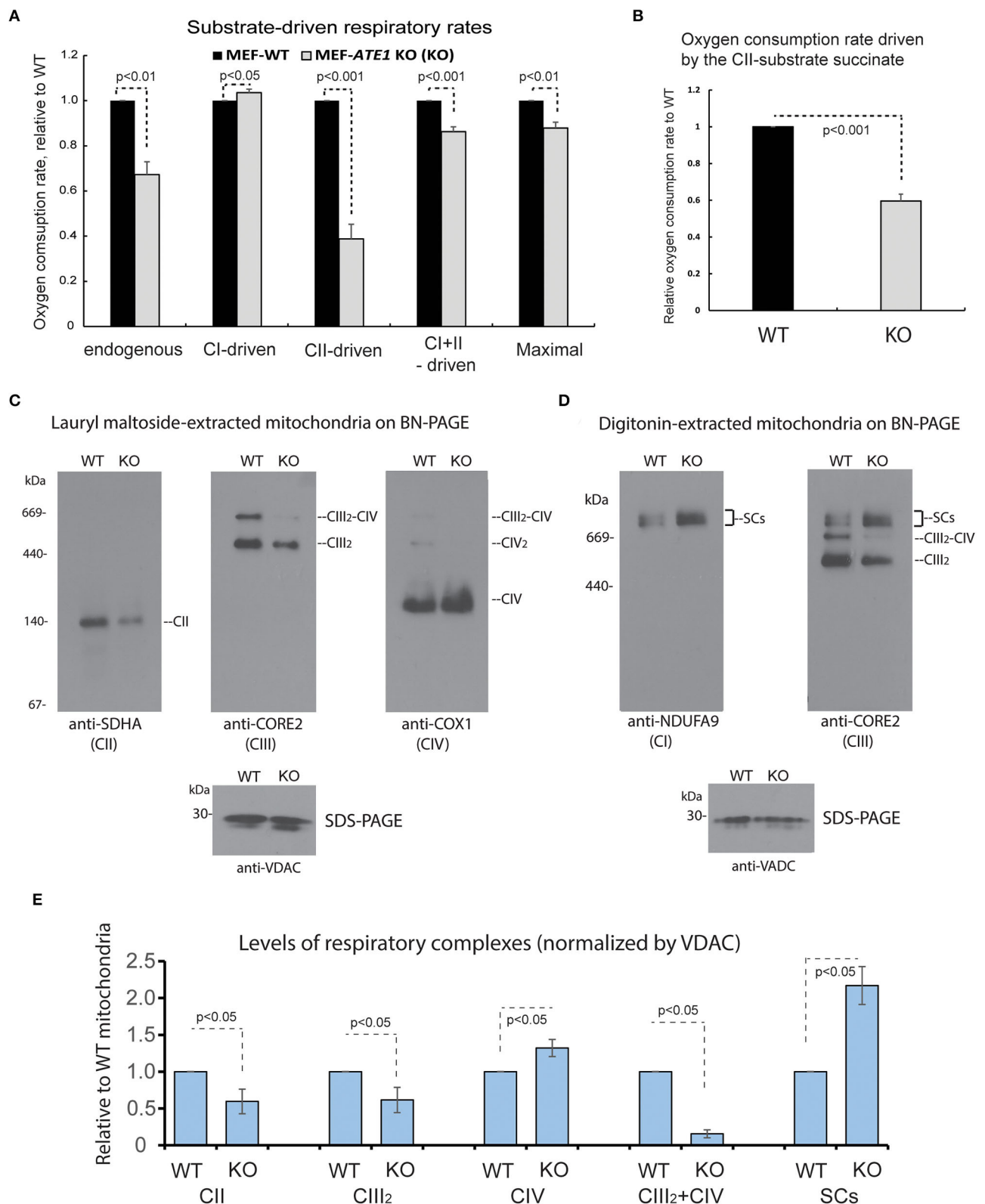


**FIGURE 4 |** ATE1 differentially affects the composition and function of mitochondrial respiration complexes. **(A)** Oxygen consumption rates in intact whole cell (endogenous respiration) before permeabilization and CI and CII substrate-driven coupled respiration in digitonin-permeabilized WT and ATE1-KO (referred as KO) MEF. Glutamate plus malate were used as CI substrates, followed by succinate as a CII substrate. Maximal respiratory rates were measured upon addition of the uncoupler

(Continued)

**FIGURE 4 | FCCP.** The values in *ATE1*-KO cells were normalized to those in WT cells in each measurement. The bar graph represents the mean  $\pm$  SEM of four independent measurements ( $n = 4$ ). The  $p$ -value was calculated by  $t$ -test. See also **Supplementary Figure 2** for representative images of the oxygen consumption curve. **(B)** Oxygen consumption rate in permeabilized cells in presence of only complex II substrate succinate in WT and *ATE1*-KO MEF. The bar graph represents the mean  $\pm$  SD of four independent measurements ( $n = 4$ ). The  $p$ -value was calculated by  $t$ -test. **(C)** Individual respiratory complexes of isolated and lauryl maltoside-extracted mitochondria were separated by blue-native polyacrylamide gel (BN-PAGE) and then examined in Western blot. SDHA, CORE2, and COX1 are established markers for complex II, III, and IV (referred as to CII, CIII, CIV in figure labeling), respectively. The CIII<sub>2</sub>-CIV supercomplex is also indicated. In the bottom panel, VDAC levels assessed by SDS-PAGE and immunoblotting are shown as loading control. **(D)** Similar to **(A)**, except that digitonin was used to extract mitochondrial proteins to preserve supercomplex association. NDUFA9 and CORE2 are established markers for complex I and III (CI and CIII), respectively. SCs indicates CI-containing supercomplexes (CI+CIII<sub>2</sub>+CIVn). **(E)** Quantitative assessment of the assembly and organization of different respiratory complexes and CI-containing supercomplexes (SCs) in mitochondria from WT and *ATE1*-KO MEF, extracted with lauryl maltoside or digitonin and separated by BN-PAGE. The bar graph represents the mean  $\pm$  SEM of three independent repetitions ( $n = 3$ ). The  $p$ -value was calculated by  $t$ -test.

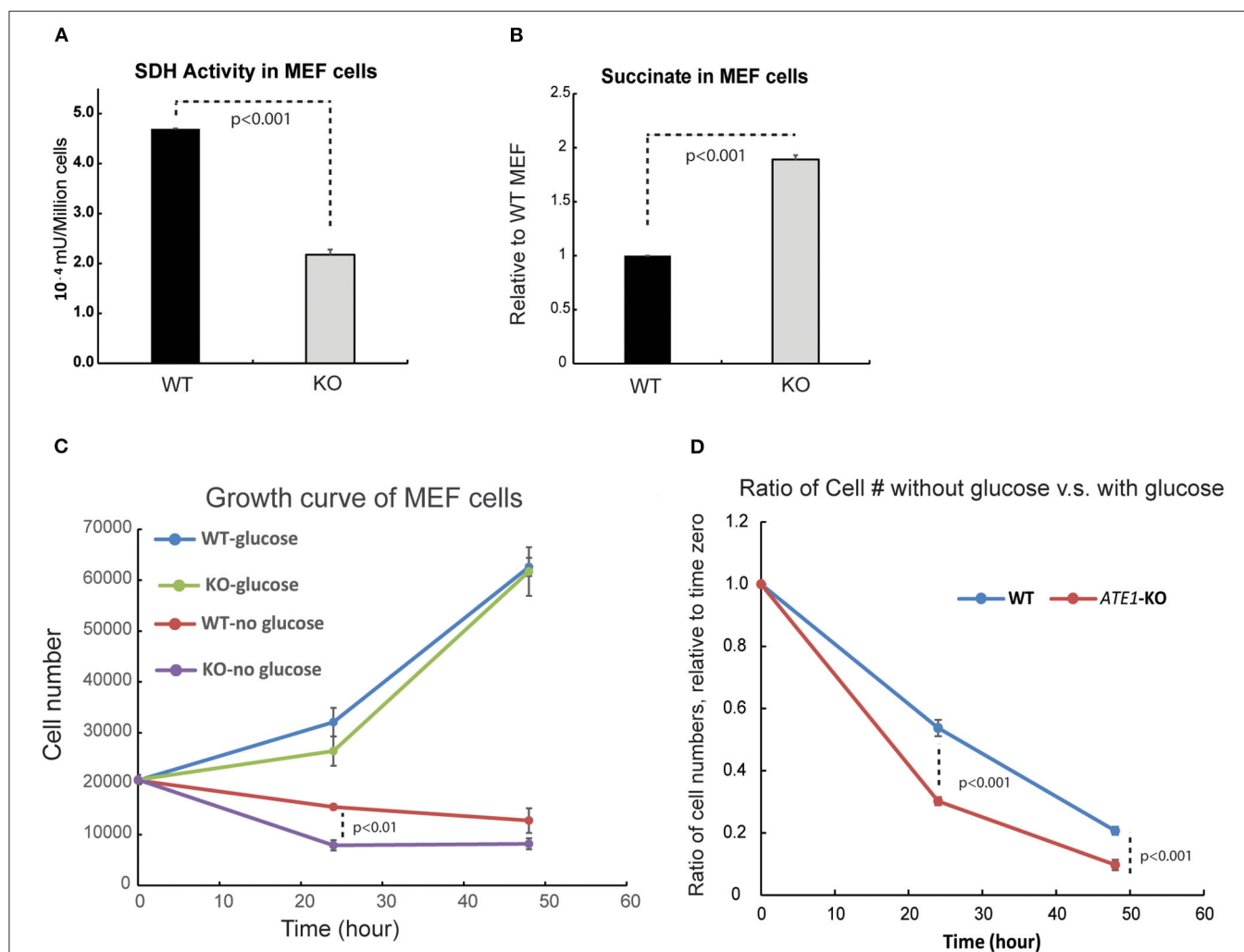


**FIGURE 5 | ATE1 affects the level of succinate and the cellular dependency of glucose.** **(A)** The specific activity of succinate dehydrogenase (SDH) in WT and *ATE1*-KO MEF normalized by cell number. The bar graph represents the mean  $\pm$  SEM of four independent measurements ( $n = 4$ ). The  $p$ -value was calculated by  $t$ -test. **(B)** Comparison of the cellular concentrations of succinate in WT and *ATE1*-KO MEF ( $n = 3$ ), normalized by the concentration in WT cells. The bar graph represents the mean  $\pm$  SEM of three independent measurements ( $n = 3$ ). The  $p$ -value was calculated by  $t$ -test. **(C)** The growth curves of WT and *ATE1*-KO MEF in the presence or absence of glucose. Each point represents the mean  $\pm$  SEM of six independent measurements ( $n = 6$ ). The  $p$ -value was calculated by  $t$ -test. **(D)** The sensitivities of WT and *ATE1*-KO MEF to glucose-starvation, represented by the ratio of cell number in glucose-free condition compared to that in high-glucose condition in the same time point as shown in **(C)**. Each point represents the mean  $\pm$  SEM of six independent measurements ( $n = 6$ ). The  $p$ -value was calculated by  $t$ -test.

in the accumulation of succinate and subsequent stabilization of HIF-1 $\alpha$  (Majmudar et al., 2010), an essential regulator of glycolysis and stress response, and relevant to tumor growth

(Tran et al., 2016). According to our results, the downregulation of ATE1 in multiple cancers may provide another pathway to affect the function of SDH without involving mutations on SDH

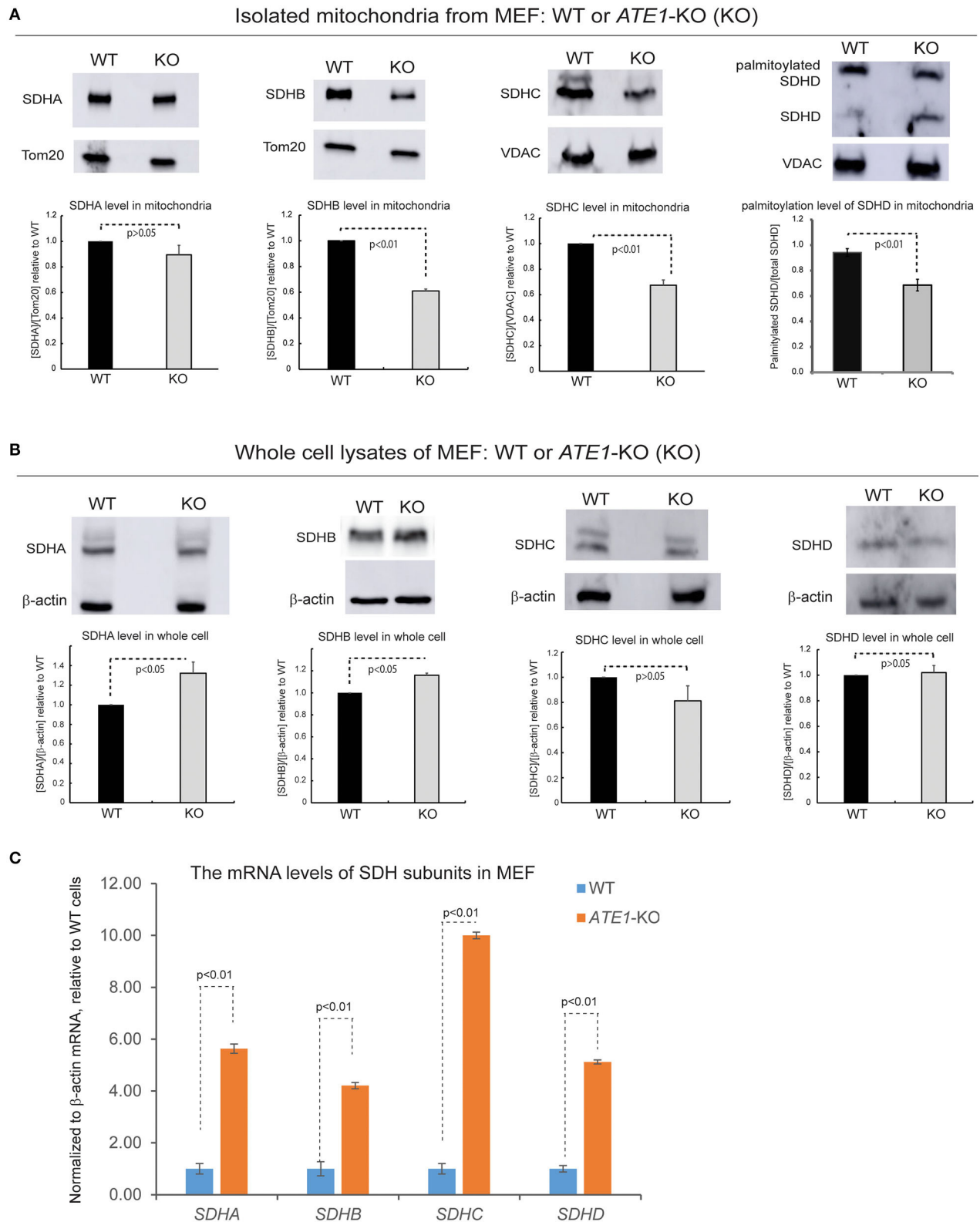


**FIGURE 6 |** ATE1 is required for the biogenesis of succinate dehydrogenase (mitochondrial complex II). **(A)** The protein levels of SDHA, SDHB, SDHC, SDHD in purified mitochondria from WT and *ATE1*-KO MEF. TOM20 or VDAC was used as a loading control. The bar graphs represent the mean  $\pm$  SEM of three independent measurements ( $n = 3$ ) for SDHA, SDHB, and SDHC, or five independent measurements ( $n = 5$ ) for SDHD. The  $p$ -value was calculated by  $t$ -test. **(B)** Similar to **(A)**, (Continued)

**FIGURE 6 |** except that whole cell lysates were used for analysis. Beta-actin was used as a loading control. The quantified results in the charts are shown on the lower panels. The bar graphs represent the mean  $\pm$  SD of three independent measurements ( $n = 3$ ). The  $p$ -value was calculated by  $t$ -test. **(C)** The mRNA level of *SDHA*, *SDHB*, *SDHC*, and *SDHD* in WT and *ATE1*-KO MEF measured by quantitative PCR. The  $\beta$ -*ACTIN* (*ACTB*) mRNA levels were used as loading control. In each testing group containing 4 replicates ( $n = 4$ ), one sample from the WT cells was defined as 1.0 for the normalization of other samples. The bar graphs represent the mean  $\pm$  SD. The  $p$ -value was calculated by  $t$ -test.

genes, which may be an important regulatory mechanism in carcinogenesis. The potential effects of ATE1 on HIF1 $\alpha$  and glycolysis also warrant future investigations.

The role of ATE1 in metabolic regulation may be also relevant in injury response and inflammation since increased arginylation is often observed in these scenarios (Shyne-Athwal et al., 1988; Luo et al., 1990; Jack et al., 1992; Xu et al., 1993; Wang and Ingoglia, 1997). Cells of the innate immune system recognize pathogen-associated molecular patterns via receptors such as Toll-like receptors (TLRs), present on their cell surface and in the cytosol (Janeway and Medzhitov, 2002). In resting conditions, these cells are relatively inactive; however, they respond rapidly upon recognition of foreign material, by adapting to the significant metabolic demands (Pearce and Pearce, 2013). For example, stimulation of dendritic cells and macrophages often result in decreased OXPHOS, which is normally used under resting conditions, and an increase in glycolysis and the pentose-phosphate pathway (Tannahill et al., 2013). There are interesting parallels between tumors and, for example, lipopolysaccharide-activated macrophages concerning succinate metabolism. Succinate levels also increase in macrophages, where a similar process of HIF-1 $\alpha$  stabilization by succinate occurs (Mills and O'Neill, 2014). Whether ATE1 could be involved in these processes deserves further investigations.

In summary, our findings open a new paradigm for studies of metabolism and associated diseases. ATE1 may play an instrumental role in contributing to the metabolic shift from OXPHOS to glycolysis seen in cancer and inflammation, and the adaptation to oxidative, hypoxic, or thermal stresses. Future efforts will be devoted to understanding whether ATE1 translocates to mitochondria upon stress and identify the ATE1 substrates within mitochondria to disclose the precise role/s ATE1 performs in the organelle.

## MATERIALS AND METHODS

### Mammalian Cells and Media

Immortalized mouse embryonic fibroblasts (MEFs) that are either wild-type or genomic knockout for *ATE1* (*ATE1*-KO) were a gift from Dr. Anna Kashina (University of Pennsylvania), prepared as described elsewhere (Zhang et al., 2012). The human embryonic kidney cell line (HEK 293T; clone T7) was obtained from ATCC.

For routine growth and maintenance, unless otherwise indicated, mammalian cells were cultured in media containing high-glucose DMEM supplemented with 1 mM pyruvate and glutamine (Gibco, Cat# 10569) with 10% FBS (HyClone, Cat# SH30910.03). No antibiotics were used for the cell culture to minimize interference with cellular metabolism, and the cultured cells were periodically checked for bacterial or mycoplasma

contamination. The cells were cultured in a 5% CO<sub>2</sub> incubator at 37°C, unless otherwise indicated. To minimize any effects of contact inhibition, only actively growing cells in culture density of <50% confluency were used for any test in this study, unless otherwise indicated.

### Yeast Strains

The *Saccharomyces cerevisiae* strains used in this study include BY4741 (*MATa his3 $\Delta$ 1 leu2 $\Delta$ 0 met15 $\Delta$ 0 ura3 $\Delta$ 0*) and W303-1A (*MATa leu2-3,112 trp1-1 can1-100 ura3-1 ade2-1 his3-11,15 ybp1-1*). They are both obtained from Open Biosystems. A strain carrying a null *ate1 $\Delta$* :KanMX cassette in the BY4741 background was obtained from Open Biosystems. To create *ate1*-deletion in the W303-1A yeast, we applied the knockout cassette amplified from the *ate1 $\Delta$* :KanMX in BY4741-strain yeast with two primers as described before (Kumar et al., 2016):

ATE1300UP: ATGGTGCTGTGCTTGTAATTGCC

ATE1300DOWN: GCTCATCAAAAATAAGAATAAGAG

The strain with a GFP fused to the C-terminal end of endogenous Ate1 in the native chromosome locus in BY4741 genetic background was obtained from Open Biosystems. The identity of each knockout strain listed above was confirmed with PCR genotyping.

### Culture of Yeast

Yeast culture media were prepared as described below:

YPD: 2% glucose, 1% yeast extract, 2% peptone,

SD (Synthetic Defined) Medium (per 1,000 ml): Yeast Nitrogen Base, 1.7g, Ammonium sulfate, 5g, Dextrose/galactose/raffinose, 20g, required amino acids, 50 mg, uracil (if required), 50 mg.

YPEG: 1% yeast extract, 2% peptone, 3% (v/v) glycerol, and 2% ethanol.

For solid media plates, 2% agar was added to the liquid media.

Strains grown in liquid and solid media were incubated at 30°C unless otherwise indicated.

For most serial dilution growth assays, a single colony of yeast was inoculated in liquid medium and allowed to grow to the log phase before spot plating of serial dilutions as described elsewhere (Kumar et al., 2012).

### Antibodies

Primary antibodies used in this study are (unless otherwise indicated): rat anti ATE1 (EMD-Millipore, Billerica, MA, Cat# MABS436, clone 6F11), mouse anti-GFP (Roche Diagnostics, Indianapolis, IN, Cat# 11814460001), mouse anti porin/VDAC1 (Abcam, Cambridge, MA, Cat# ab14734), anti TOM20 (Santa Cruz Biotechnology, Dallas, TX, Cat# SC11415), anti-beta-actin



(Sigma-Aldrich, St. Louis, MO, Cat# A1978), mouse anti-beta-tubulin (Sigma-Aldrich, St. Louis, MO, Cat# T5201), anti-histone H3 (Abcam, Cambridge, MA, Cat# ab1971), rabbit anti-SDHA (One World Lab, San Diego, Ca, Cat# 53800), mouse anti-SDHB (Abcam, Cambridge, MA, Cat# ab14714), rabbit anti-SDHC (Abcam, Cambridge, MA, Cat# ab155999), rabbit anti-SDHD (EMD-Millipore, Billerica, MA, Cat# ABC835), rabbit anti-Hexokinase2 (One World Lab, San Diego, Ca, Cat#55911), mouse anti-PHD2 (Santa Cruz Biotechnology, Dallas, TX, Cat# SC271835).

Secondary antibodies used in this study are (unless otherwise indicated): Anti-mouse-HRP (Pierce, now thermos Scientific, Cat # 31430), Anti-rabbit-HRP (Thermo Fisher Cat # 65-6120), Anti-Rat-HRP (BioLegend, Cat # 405405), Anti-mouse-Alexa 488 (Molecular Probe /Invitrogen, Cat # A21202), Anti-rabbit-Alexa 488 (Molecular Probes/ Invitrogen, Cat # 21206), Anti-Rat-Alexa 594 (Molecular Probe/Invitrogen, Cat # A21209).

## SDS-PAGE and Western Blot

Cell lysate or protein samples were generally prepared in SDS-loading buffer and boiled for 10 min for denaturing. For analysis of membrane-associated proteins, samples were first dissolved in 8M urea/PBS and then added SDS-loading buffer and denatured at 55°C for 10 min. The proteins were separated by electrophoresis in 4–20 or 10% SDS-PAGE (unless otherwise indicated) as needed. The proteins were then transferred to nitrocellulose or PVDF membranes for Western Blot analysis. The protein bands were examined with Chemifluorescence visualization utilizing the HRP conjugated on secondary antibodies and reagents provided in the BM Chemifluorescence Western Blotting Kit Mouse/Rabbit (Roche) or the SuperSignal West Femto Chemiluminescence Kit (Pierce). The chemiluminescent signals were either documented on film (Denville) or by GE Amersham Imager model 600. The films were scanned by an Epson Perfection 2400 photo/film scanner with at least 1,200 dpi resolution to convert into digital forms and then analyzed with Image J (NIH). For images documented by the GE imager, an ImageQuant TL software pack (v8.1) and its 1D gel analysis module were used to examine the intensity of signals by densitometry.

## Analysis of Mitochondrial Complex on Blue Native PAGE (BN-PAGE)

Cells were permeabilized in PBS with 2 mg/ml digitonin (Sigma-Aldrich, Cat# D141) at 4°C for 10 min. Cells were centrifuged at  $10,000 \times g$  for 5 min at 4°C and washed twice with PBS. Cell pellets were resuspended in 1.5 M aminocaproic acid, 50 mM Bis-Tris pH 7.0, and total protein concentration was determined by the Folin method (Lowry et al., 1951). Proteins were extracted either with 1% lauryl maltoside (for monomeric complex analysis) or 1% digitonin (for supercomplex analysis). After centrifugation at  $22,000 \times g$  for 30 min at 4°C, a buffer containing 750 mM aminocaproic acid, 50 mM Bis-Tris pH 7.0, 0.5 mM EDTA, and 5% Serva blue G was added to the clarified extracts. Samples were loaded on a linear 3–12% polyacrylamide blue native gel (Invitrogen), transferred to PVDF membrane, and analyzed by immunoblotting with

the following antibodies: anti-COX1 (Abcam, Cat#Ab14705), anti-COX3 (Abcam, Cat# Ab110259), anti-NDUFA9 (Abcam, Cat# Ab14713), anti-CORE2 (Abcam, Cat# Ab 14745), anti-SDHA (Abcam, Cat# Ab14715), anti-porin/VDAC (Abcam, Cat# Ab14734), anti-TOM20 (Santa Cruz Biotechnology, Cat# sc-11415), second antibodies anti-mouse HRP (Rockland, Cat# 610-4302), anti-rabbit HRP (Rockland, Cat# 611-1302).

## Preparation of Cells Stably Expressing Recombinant ATE1 Proteins

ATE1 KO MEF stably transfected with ATE1-1-GFP, ATE1-2-GFP, ATE1-3-GFP, and ATE1-4-GFP was generated as described previously (Zhang et al., 2015) except cells were enriched with FACS without puromycin selection. Briefly, retroviruses carrying different C-terminal GFP tagged isoform of Ate-1 were constructed by transfecting HEK293T cells with the low-expression pBabe-Puro vectors carrying coding sequence for the desired isoform and the vectors of GAG-Pol and VSV-G vector. The viruses were then allowed to infect ATE1 KO MEF in the presence of 10 mg/mL polybrene. Successfully transfected MEF were enriched by fluorescence sorting.

## Cell Counting and Cell Size Measurement

The numbers of resuspended cells in solution were counted with an automated Biorad TC20 cell counter, and dead cells were excluded with trypan blue unless otherwise indicated. The diameters of the resuspended cells were also measured by the built-in feature of the cell counter. All peaks of size distributions and the associated cell numbers displayed by the counters were used to calculate the average diameter of the cell.

## Measurements of Whole-Cell and Mitochondrial Respiration Activity in Mammalian Cells

For the tests described below, we used actively growing cell cultures at a confluency lower than 50%. The measurements of whole-cell and mitochondrial respiration rates were done according to a protocol published elsewhere (Barrientos et al., 2009). In brief, cells were collected by trypsinization, neutralized in FBS-containing medium, and washed with DPBS. To measure whole-cell respiration, the cells were resuspended in RPMI 1640 medium with L-Glutamine and 25 mM HEPES (Sigma-Aldrich, Cat# SLM-140) at 37°C. The numbers of live cells were counted using Trypan blue on a TC-20 automated cell counter (Bio-Rad). The concentration of all cell lines used in the same test were adjusted to  $4 \times 10^6$  cells/ml and then transferred to the chamber of a polarographic apparatus with a Clark-type O<sub>2</sub> electrode (Hansatech, Oxygraph plus system) for measurement of cell respiration at 37°C. At the end of the measurement, KCN (Sigma-Aldrich, Cat# 60178) was added to the cell suspension to a final concentration of 2 mM to inhibit cell respiration. KCN-sensitive cellular respiratory rates were obtained by subtracting oxygen consumption rates before and after KCN addition.

To measure substrate-driven mitochondrial respiration, the cells were resuspended in warm (37°C) permeabilized-cell respiration buffer (PRB) containing 0.3 M mannitol, 10 mM

KCl, 5 mM MgCl<sub>2</sub>, 0.5 mM EDTA, 0.5 mM EGTA, 1 mg/ml BSA and 10 mM KH<sub>2</sub>PO<sub>4</sub> (pH 7.4). The numbers of live cells were counted using Trypan blue on a TC-20 automated cell counter (Bio-Rad). The concentrations of each cell type in the same test were adjusted to  $4 \times 10^6$  cells/ml. An aliquot of the cell suspension was supplemented with freshly prepared hexokinase (Sigma-Aldrich, Cat# H-5500) to 10 U/mL, and ADP to 2 mM and 1 mL of the cell suspension was transferred to the polarographic chamber/oxygraph containing a Clark-type O<sub>2</sub> electrode (Hansatech, Oxygraph plus system) with a temperature setting of 37°C. The whole-cell respiration was measured before digitonin was added.

To measure substrate-driven respiration, the cell membrane was permeabilized by adding freshly prepared digitonin in optimized ratios of 20 µg per 10<sup>6</sup> cells for WT MEF, or 10 µg per 10<sup>6</sup> cells for *ATE1*-KO MEF. The substrate-driven oxygen consumption rate was then examined by adding specific MRC substrates using a Hamilton microsyringe. To measure complex I-driven respiration, we added 5 mM each of glutamate (Sigma-Aldrich, Cat# G8415) and malate (Sigma-Aldrich, Cat# M1124). To measure complex II, we used 10 mM succinate (ICN Biomedicals, Cat# 102972). To measure uncoupled respiration, we added 3 µM carbonyl cyanide *p*-trifluoromethoxyphenylhydrazone (FCCP) (Sigma-Aldrich, Cat# C2920), and to assess the specificity of the measurements, we inhibited respiration with 2 mM of the CIV inhibitor potassium cyanide (KCN) (Sigma-Aldrich, Cat# 60178).

## Isolation of High-Purity Mitochondria From Cultured Cells for Protein Analysis

Mitochondria were purified from exponentially growing cultured cells based on the Gaines method, updated by Enriquez's group (Fernandez-Vizarra et al., 2010). In brief, cells were harvested by trypsinization and washed twice with cold DPBS before being resuspended in swelling buffer (10 mM Tris-HCl, pH 7.4, 10 mM KCl, 0.5 mM MgCl<sub>2</sub>) and incubation on ice for 5 min. The cells were then homogenized with Teflon-glass douncer until at least 75% of the cells were broken. The homogenized lysate was then mixed with sucrose solution to reach a final concentration of 0.25 M of sucrose and then centrifuged at  $600 \times g$  for 5 min at 4°C twice to remove cell debris. The resulting supernatant was centrifuged at  $7,000 \times g$  for 10 min at 4°C to pellet the mitochondrial fraction. The pellet was washed with the STE buffer (0.32 M sucrose, 1 mM EDTA, and 10 mM Tris-HCl, pH 7.4) and centrifuged again at  $7,000 \times g$  for 10 min at 4°C. The pellet was gently resuspended in freshly prepared, ice-cold mitochondria resuspending buffer (MRB) (250 mM mannitol, 5-mM HEPES (pH 7.4), and 0.5-mM EGTA. The mixture was layered on top of Percoll medium (225-mM mannitol, 25-mM HEPES (pH 7.4), 1-mM EGTA, and 30% Percoll (vol/vol). Additional MRB buffer was added to fill the volume of the centrifuge tube before being centrifuged in a swing-bucket rotor at  $95,000 \times g$  for 30 min at 4°C. A Beckman Coulter Optima L-100 XP ultracentrifuge with an SW40 rotor (Beckman, Fullerton, CA, USA) was used in this study. The purified mitochondria,

which was present in a semi-transparent layer directly above the pellet on the bottom, was then recovered.

## Measurement of Endogenous Cell Respiration in Yeast Cells

The cell respiration of yeasts was assayed polarographically using a Clark-type oxygen electrode (Hansatech Instruments, Norfolk, UK) at 30°C as described elsewhere (Barrientos et al., 2002). The specific activities reported were corrected for KCN-insensitive respiration.

## Measurement of Membrane Potential in Yeast Cells

The measurement of mitochondrial membrane potential ( $\Psi_m$ ) in yeast was performed as described elsewhere (Ocampo et al., 2012). In brief, yeast cells were incubated with 5 µM TMRM of Tetramethyl Rhodamine Methyl Ester (TMRM), a cell-permeant, cationic, fluorescent dye that is readily sequestered by viable mitochondria, at 30°C for 30 min, as reported (Nicholls and Ward, 2000). The cells were then washed twice in PBS and were analyzed with flow cytometry analysis on a Becton Dickinson (BD) FACS Aria™ II Flow Cytometer. Excitation was performed at 532 nm; emission was detected using a 25 nm bandpass filter centered at 575 nm (Becton Dickinson, NJ, USA). Dissipation of  $\Psi_m$  causes TMRM to leak out of mitochondria into the cytosol, where TMRM became unquenched, producing an increase in fluorescence (Nicholls and Ward, 2000). To confirm the mitochondrial specificity of the signal of TMRM, ionophore carbonyl cyanide *m*-chlorophenyl hydrazone (CCCP), which dissipates the membrane potential, was applied to treat the cells as controls.

## Measurement of Cellular Succinate Levels

Actively growing cells below 50% confluency were used. Cells were harvested by trypsin and then immediately washed three times with ice-cold DPBS. The numbers, viability, and diameters of the resuspended cells were measured on the Biorad TC20 automated cell counter. The same number of cells (40 million cells in this test) were used for each cell type. The cells were collected by centrifugation at  $2,500 \times g$  at 4°C for 3 min. The pellets were weighted and 20 volumes of ice-cold H<sub>2</sub>O was added. The cells were then lysed by brief sonication, and the cell debris was removed by centrifugation at  $20,000 \times g$  at 4°C for 10 min. The supernatant was further centrifuged at  $100,000 \times g$  at 4°C for 1 h to remove large cellular complexes. The subsequent supernatant was then filtered through a 10K MWCO membrane (Thermo Scientific, Rockford, IL, Cat#PI88513) by centrifugation at 4°C to remove large proteins. The filtrate protein concentration was quantified by the Bradford assay using reagents from Bio-Rad (Cat# 500 0205). The cell lysate filtrate was then extracted by acetonitrile. The resulting supernatant was dried under N<sub>2</sub> and then derivatized by HCl *n*-butanol. Upon being dried under N<sub>2</sub>, the derivative precipitation was reconstituted with 80% methanol and loaded in LC-MS/MS. The level of succinic acid in the filtrate was quantified by Agilent triple quant LC-MS/MS. The final cellular concentration of succinic

acid was normalized by cell number, cell volumes, dilution factor, and the protein concentration in the filtered lysate.

## Mitochondrial Proteinase K Protection Assay

The experiment was performed according to the previously published method (Clemente et al., 2013). In brief, purified mitochondria were resuspended in a buffer containing 10 mM Tris-HCl, pH 7, 10 mM KCl, 0.15 mM MgSO<sub>4</sub>, and 0.25 M sucrose. As control, one sample was subjected to brief sonication to break the membranes. All samples were then incubated in ice for 45 min in the presence of proteinase K at a final concentration of 0, 0.32, or 0.64 µg/ml. Mitochondria were recovered by centrifugation at 8,000 × g for 15 min at 4°C and analyzed by Western blotting.

## Glucose Starvation Assay

MEF cells (WT or *ATE1*-KO) were cultured in high-glucose DMEM containing 25 mM glucose and 1 mM pyruvate (Gibco Cat#10569) supplemented with 5% FBS (Hyclone, Cat# SH30910.03) for several generations. Immediately before the experiment, the cells were split and cultured for one generation (24 h) in the same high-glucose DMEM except with 5% dialyzed FBS (Life Technologies Cat# 26400-044). At the time of the experiment, the cells were trypsinized, washed with DPBS, and then resuspended in either starving media with glucose-free, pyruvate-free DMEM (Gibco, Cat# 11966) and 5% dialyzed FBS, or non-starving media with high-glucose, 1 mM pyruvate DMEM (Gibco Cat#10569) and 5% dialyzed FBS. The cells were then inoculated into 6-cm culture dishes with 50,000 cells per dish so that the cells would stay at a non-confluent culture density through the duration of tests. Live cells that remained attached to the plate were then counted at given time points, using trypan blue to exclude dead cells.

## Microscopy

Optical and fluorescent images of cells were captured on a Zeiss Observer equipped with a series of objectives and Zen Pro software. Analysis of the images were performed with the Zen Pro software.

## Image Processing

The images were processed in Adobe Photoshop by adjusting the display levels while preserving the linearity of the signals. The figures were assembled in Adobe Illustrator.

## Bioinformatic Analysis

The phylogenetic tree of the ATE1 protein was calculated based on amino acid sequences with Clustal Omega program on the Uniprot website. The detailed alignment of amino acid sequences in ATE-C domain (Pfam ID: PF04377) between two species was performed with NCBI BLASTp. The sunburst graph showing the distribution of ATE-C domain (Pfam ID: PF04377) was generated with corresponding tools from pfam.xfam.org hosted by EMBL-EBI.

## RNA Isolation and Quantitative PCR

RNA was extracted using Quick-RNA MiniPrep Kit (Genesee Scientific, Cat #: 11-328). The corresponding cDNA was prepared by using Superscript First-strand RT-PCR kit (Invitrogen, Cat#: 11904-018). Quantitative real-time PCR was performed by using SsoAdvanced™ Universal SYBR® Green Supermix (Biorad, Cat#: 1725271) on a CFX Connect Real-Time PCR machine (Biorad). The samples were run in multiple replicates on Hard-Shell PCR 96 well plates from Biorad (Cat#: HSP9601). PCR conditions: initial denaturation for 30 s at 95°C, followed by 40 cycles with 95°C for 15 s and 58°C for 1 min. After each run, a melting curve was measured to confirm the specificity of the amplification. The relative expression of the SDH subunits were calculated by delta Ct method. The mRNA of β-actin (ACTB) was used as housekeeping gene/reference gene for loading controls.

The primers targeting different subunits of Succinate dehydrogenase and β-actin are listed below.

```
SDHA_qPCR_F—GCTCCTGCCTCTGTGTTGA
SDHA_qPCR_R—AGCAACACCGATGAGCCTG
SDHB_qPCR_F—TGCGGACCTATGGTGTGGATG
SDHB_qPCR_R—CCAGAGTATTGCCTCCGTTGATG
SDHC_qPCR_F—TGCTCCTTTGGGAACACAGCT
SDHC_qPCR_R—GCAAACGGACAGTGCCATAGGA
SDHD_qPCR_F—GGTTGTCACTGTTCTGCTCTTGG
SDHD_qPCR_R—GTCGGTAACCACTTGTCGAAGG
β-actin_qPCR_F—CAGCTGAGAGGGAAATCGTG
β-actin_qPCR_R—CGTTGCCAATAGTGATGACC
```

## Statistical Analysis

The statistical significance for comparison of quantitative assessments performed in WT and *ATE1*-KO MEF or yeast cells was estimated by the *Student t*-test. The data distribution was considered one-side or two-side based on the presence of the error bars in the displayed data for comparison. Error bars represent standard error of the mean (SEM) or standard deviation (SD), as indicated in the figure legends. A minimum *p*-value of 0.05 was considered significant.

## DATA AVAILABILITY STATEMENT

The original contributions presented in the study are included in the article/**Supplementary Materials**, further inquiries can be directed to the corresponding author/s.

## AUTHOR CONTRIBUTIONS

FZ conceptualized, initiated, and supervised the project. FF designed and supervised most of the mitochondria-related experiments and performed some of them. CJ performed most of the experiments. BM, DP, AK, and WM participated in the performance of some of the experiments under the supervision of FZ and/or FF. BA performed the succinate measurement supervised by JH. DI participated in the bioinformatic analysis. AB and TL participated in the design of metabolism-related experiments. CJ and FZ wrote the manuscript. FF, AB, and DI edited the manuscript. All authors read and approved the manuscript.



## FUNDING

This study was supported by NIGMS R01GM107333, NIGMS R01GM138557, and a Sylvester Comprehensive Cancer Center development grant to FZ. AB was supported by NIGMS-MIRA R35GM118141 and Muscular Dystrophy Association Research Grant MDA-381828. DI was supported by NIGMS-MIRA R35GM119518. Service for flow cytometer and cell

sorting was provided by the core facility of the Sylvester Comprehensive Center.

## SUPPLEMENTARY MATERIAL

The Supplementary Material for this article can be found online at: <https://www.frontiersin.org/articles/10.3389/fcell.2020.603688/full#supplementary-material>

## REFERENCES

- Acin-Perez, R., Fernandez-Silva, P., Peleato, M. L., Perez-Martos, A., and Enriquez, J. A. (2008). Respiratory active mitochondrial supercomplexes. *Mol. Cell* 32, 529–539. doi: 10.1016/j.molcel.2008.10.021
- Alirol, E., and Martinou, J. C. (2006). Mitochondria and cancer: is there a morphological connection? *Oncogene* 25, 4706–4716. doi: 10.1038/sj.onc.1209600
- Bachmair, A., Finley, D., and Varshavsky, A. (1986). *In vivo* half-life of a protein is a function of its amino-terminal residue. *Science* 234, 179–186. doi: 10.1126/science.3018930
- Balzi, E., Choder, M., Chen, W. N., Varshavsky, A., and Goffeau, A. (1990). Cloning and functional analysis of the arginyl-tRNA-protein transferase gene ATE1 of *Saccharomyces cerevisiae*. *J. Biol. Chem.* 265, 7464–7471.
- Barrientos, A., Fontanesi, F., and Diaz, F. (2009). Evaluation of the mitochondrial respiratory chain and oxidative phosphorylation system using polarography and spectrophotometric enzyme assays. *Curr. Protoc. Hum. Genet.* 63, 19.3.1–19.3.14. doi: 10.1002/0471142905.hg1903s63
- Barrientos, A., Korr, D., and Tzagoloff, A. (2002). Shy1p is necessary for full expression of mitochondrial COX1 in the yeast model of Leigh's syndrome. *EMBO J.* 21, 43–52. doi: 10.1093/emboj/21.1.43
- Birnbaum, M. D., Zhao, N., Moorthy, B. T., Patel, D. M., Kryvenko, O. N., Heidman, L., et al. (2019). Reduced arginyltransferase 1 is a driver and a potential prognostic indicator of prostate cancer metastasis. *Oncogene* 38, 838–851. doi: 10.1038/s41388-018-0462-2
- Bock, R. (2017). Witnessing genome evolution: experimental reconstruction of endosymbiotic and horizontal gene transfer. *Annu. Rev. Genet.* 51, 1–22. doi: 10.1146/annurev-genet-120215-035329
- Bongiovanni, G., Fissolo, S., Barra, H. S., and Hallak, M. E. (1999). Posttranslational arginylation of soluble rat brain proteins after whole body hyperthermia. *J. Neurosci. Res.* 56, 85–92.
- Brower, C. S., and Varshavsky, A. (2009). Ablation of arginylation in the mouse N-end rule pathway: loss of fat, higher metabolic rate, damaged spermatogenesis, neurological perturbations. *PLoS ONE* 4:e7757. doi: 10.1371/journal.pone.0007757
- Buffet, A., Burnichon, N., Favier, J., and Gimenez-Roqueplo, A. (2020). An overview of 20 years of genetic studies in pheochromocytoma and paraganglioma. *Best Pract. Res. Clin. Endocrinol. Metab.* 34:101416. doi: 10.1016/j.beem.2020.101416
- Carpio, M. A., Decca, M. B., Lopez Sambrooks, C., Durand, E. S., Montich, G. G., and Hallak, M. E. (2013). Calreticulin-dimerization induced by post-translational arginylation is critical for stress granules scaffolding. *Int. J. Biochem. Cell Biol.* 45, 1223–1235. doi: 10.1016/j.biocel.2013.03.017
- Carpio, M. A., Lopez Sambrooks, C., Durand, E. S., and Hallak, M. E. (2010). The arginylation-dependent association of calreticulin with stress granules is regulated by calcium. *Biochem. J.* 429, 63–72. doi: 10.1042/BJ20091953
- Clemente, P., Peralta, S., Cruz-Bermudez, A., Echevarria, L., Fontanesi, F., Barrientos, A., et al. (2013). hCOA3 stabilizes cytochrome C oxidase 1 (COX1) and promotes cytochrome C oxidase assembly in human mitochondria. *J. Biol. Chem.* 288, 8321–8331. doi: 10.1074/jbc.M112.422220
- Decca, M. B., Carpio, M. A., Bosc, C., Galiano, M. R., Job, D., Andrieux, A., et al. (2007). Post-translational arginylation of calreticulin: a new isospecies of calreticulin component of stress granules. *J. Biol. Chem.* 282, 8237–8245. doi: 10.1074/jbc.M608559200
- Deka, K., Singh, A., Chakraborty, S., Mukhopadhyay, R., and Saha, S. (2016). Protein arginylation regulates cellular stress response by stabilizing HSP70 and HSP40 transcripts. *Cell Death Discov.* 2:16074. doi: 10.1038/cddiscovery.2016.74
- Fernandez-Vizarra, E., Ferrin, G., Perez-Martos, A., Fernandez-Silva, Z. M., and Enriquez, J. A. (2010). Isolation of mitochondria for biogenetical studies: an update. *Mitochondrion* 10, 253–262. doi: 10.1016/j.mito.2009.12.148
- Gogvadze, V., Orrenius, S., and Zhivotovsky, B. (2008). Mitochondria in cancer cells: what is so special about them? *Trends Cell Biol.* 18, 165–173. doi: 10.1016/j.tcb.2008.01.006
- Graciet, E., Hu, R. G., Piatkov, K., Rhee, J. H., Schwarz, E. M., and Varshavsky, A. (2006). Aminoacyl-transferases and the N-end rule pathway of prokaryotic/eukaryotic specificity in a human pathogen. *Proc. Natl. Acad. Sci. U.S.A.* 103, 3078–3083. doi: 10.1073/pnas.0511224103
- Hu, R. G., Brower, C. S., Wang, H., Davydov, I. V., Sheng, J., Zhou, J., et al. (2006). Arginyltransferase, its specificity, putative substrates, bidirectional promoter, splicing-derived isoforms. *J. Biol. Chem.* 281, 32559–32573. doi: 10.1074/jbc.M604355200
- Hu, R. G., Sheng, J., Qi, X., Xu, Z., Takahashi, T. T., and Varshavsky, A. (2005). The N-end rule pathway as a nitric oxide sensor controlling the levels of multiple regulators. *Nature* 437, 981–986. doi: 10.1038/nature04027
- Ingoglia, N. A., Ramanathan, M., Zhang, N., Tzeng, B., Mathur, G., Opuni, K., et al. (2000). What is the signal for the posttranslational arginylation of proteins? *Neurochem. Res.* 25, 51–58. doi: 10.1023/A:1007535331560
- Jack, D. L., Chakraborty, G., and Ingoglia, N. A. (1992). Ubiquitin is associated with aggregates of arginine modified proteins in injured nerves. *Neuroreport* 3, 47–50. doi: 10.1097/00001756-199201000-00012
- Janeway, C. A. Jr. and Medzhitov, R. (2002). Innate immune recognition. *Annu. Rev. Immunol.* 20, 197–216. doi: 10.1146/annurev.immunol.20.083001.084359
- Kim, H. J., Kim, S. Y., Kim, D. H., Park, J. S., Jeong, S. H., Choi, Y. W., et al. (2020). Crosstalk between HSPA5 arginylation and sequential ubiquitination leads to AKT degradation through autophagy flux. *Autophagy* 2020, 1–19. doi: 10.1080/15548627.2020.1740529
- Kumar, A., Birnbaum, M. D., Patel, D. M., Morgan, W. M., Singh, J., Barrientos, A., et al. (2016). Posttranslational arginylation enzyme Ate1 affects DNA mutagenesis by regulating stress response. *Cell Death Dis.* 7:e2378. doi: 10.1038/cddis.2016.284
- Kumar, A., Tikoo, S., Maity, S., Sengupta, S., Kaur, A., and Bachhawat, A. K. (2012). Mammalian proapoptotic factor Chac1 and its homologues function as gamma-glutamyl cyclotransferases acting specifically on glutathione. *EMBO Rep.* 13, 1095–1101. doi: 10.1038/embor.2012.156
- Kurosaka, S., Leu, N. A., Pavlov, I., Han, X., Ribeiro, P. A., Xu, T., et al. (2012). Arginylation regulates myofibrils to maintain heart function and prevent dilated cardiomyopathy. *J. Mol. Cell. Cardiol.* 53, 333–341. doi: 10.1016/j.yjmcc.2012.05.007
- Kurosaka, S., Leu, N. A., Zhang, F., Bunte, R., Saha, S., Wang, J., et al. (2010). Arginylation-dependent neural crest cell migration is essential for mouse development. *PLoS Genet.* 6:e1000878. doi: 10.1371/journal.pgen.1000878
- Kwon, Y. T., Kashina, A. S., Davydov, I. V., Hu, R. G., An, J. Y., Seo, J. W., et al. (2002). An essential role of N-terminal arginylation in cardiovascular development. *Science* 297, 96–99. doi: 10.1126/science.1069531
- Leu, N. A., Kurosaka, S., and Kashina, A. (2009). Conditional Tek promoter-driven deletion of arginyltransferase in the germ line causes defects in gametogenesis and early embryonic lethality in mice. *PLoS ONE* 4:e7734. doi: 10.1371/journal.pone.0007734

- Lopez Sambrooks, C., Carpio, M. A., and Hallak, M. E. (2012). Arginylated calreticulin at plasma membrane increases susceptibility of cells to apoptosis. *J. Biol. Chem.* 287, 22043–22054. doi: 10.1074/jbc.M111.338335
- Lowry, O. H., Rosebrough, N. J., Farr, A. L., and Randall, R. J. (1951). Protein measurement with the Folin phenol reagent. *J. Biol. Chem.* 193, 265–275.
- Luo, D., Chakraborty, G., and Ingoglia, N. A. (1990). Post-translational modification of proteins by arginine and lysine following crush injury and during regeneration of rat sciatic nerves. *Restor. Neurol. Neurosci.* 2, 53–61. doi: 10.3233/RNN-1990-2201
- Majumdar, A. J., Wong, W. J., and Simon, M. C. (2010). Hypoxia-inducible factors and the response to hypoxic stress. *Mol. Cell* 40, 294–309. doi: 10.1016/j.molcel.2010.09.022
- Mills, E., and O'Neill, L. A. (2014). Succinate: a metabolic signal in inflammation. *Trends Cell Biol.* 24, 313–320. doi: 10.1016/j.tcb.2013.11.008
- Nicholls, D. G., and Ward, M. W. (2000). Mitochondrial membrane potential and neuronal glutamate excitotoxicity: mortality and millivolts. *Trends Neurosci.* 23, 166–174. doi: 10.1016/S0166-2236(99)01534-9
- Ocampo, A., Liu, J., Schroeder, E. A., Shadel, G. S., and Barrientos, A. (2012). Mitochondrial respiratory thresholds regulate yeast chronological life span and its extension by caloric restriction. *Cell Metab.* 16, 55–67. doi: 10.1016/j.cmet.2012.05.013
- Pearce, E. L., and Pearce, E. J. (2013). Metabolic pathways in immune cell activation and quiescence. *Immunity* 38, 633–643. doi: 10.1016/j.immuni.2013.04.005
- Rai, R., Colavita, K., Leu, N. A., Kurosaka, S., Kumar, A., Birnbaum, M. D., et al. (2015). Arginyltransferase suppresses cell tumorigenic potential and inversely correlates with metastases in human cancers. *Oncogene* 35, 4058–4068. doi: 10.1038/onc.2015.473
- Rai, R., and Kashina, A. (2005). Identification of mammalian arginyltransferases that modify a specific subset of protein substrates. *Proc. Natl. Acad. Sci. U.S.A.* 102, 10123–10128. doi: 10.1073/pnas.0504500102
- Rai, R., Mushegian, A., Makarova, K., and Kashina, A. (2006). Molecular dissection of arginyltransferases guided by similarity to bacterial peptidoglycan synthases. *EMBO Rep.* 7, 800–805. doi: 10.1038/sj.embor.7400747
- Saha, S., and Kashina, A. (2011). Posttranslational arginylation as a global biological regulator. *Dev. Biol.* 58, 1–8. doi: 10.1016/j.ydbio.2011.06.043
- Shyne-Athwal, S., Chakraborty, G., Gage, E., and Ingoglia, N. A. (1988). Comparison of posttranslational protein modification by amino acid addition after crush injury to sciatic and optic nerves of rats. *Exp. Neurol.* 99, 281–295. doi: 10.1016/0014-4886(88)90148-3
- Tannahill, G. M., Curtis, A. M., Adamik, J., Palsson-McDermott, E. M., McGettrick, A. F., Goel, G., et al. (2013). Succinate is an inflammatory signal that induces IL-1 beta through HIF-1 alpha. *Nature* 496, 238–242. doi: 10.1038/nature11986
- Tasaki, T., Sriram, S. M., Park, K. S., and Kwon, Y. T. (2012). The N-end rule pathway. *Annu. Rev. Biochem.* 81, 261–289. doi: 10.1146/annurev-biochem-051710-093308
- Tran, Q., Lee, H., Park, J., Kim, S. H., and Park, J. (2016). Targeting cancer metabolism - revisiting the warburg effects. *Toxicol Res.* 32, 177–193. doi: 10.5487/TR.2016.32.3.177
- Van Vranken, J. G., Na, U., Winge, D. R., and Rutter, J. (2015). Protein-mediated assembly of succinate dehydrogenase and its cofactors. *Crit. Rev. Biochem. Mol. Biol.* 50, 168–180. doi: 10.3109/10409238.2014.990556
- Varshavsky, A. (2011). The N-end rule pathway and regulation by proteolysis. *Protein Sci.* 20, 1298–1345. doi: 10.1002/pro.666
- Viale, A., Corti, D., and Draetta, G. F. (2015). Tumors and mitochondrial respiration: a neglected connection. *Cancer Res.* 75, 3685–3686. doi: 10.1158/0008-5472.CAN-15-0491
- Wang, J., Han, X., Saha, S., Xu, T., Rai, R., Zhang, F., et al. (2011). Arginyltransferase is an ATP-independent self-regulating enzyme that forms distinct functional complexes *in vivo*. *Chem. Biol.* 18, 121–130. doi: 10.1016/j.chembiol.2010.10.016
- Wang, J., Pavlyk, I., Vedula, S. S., Leu, N. A., Dong, D. W., and Kashina, A. (2017). Arginyltransferase ATE1 is targeted to the neuronal growth cones and regulates neurite outgrowth during brain development. *Dev. Biol.* 430, 41–51. doi: 10.1016/j.ydbio.2017.08.027
- Wang, Y. M., and Ingoglia, N. A. (1997). N-terminal arginylation of sciatic nerve and brain proteins following injury. *Neurochem. Res.* 22, 1453–1459. doi: 10.1023/A:1021998227237
- Wiley, D. J., D'Urso, G., and Zhang, F. L. (2020). Posttranslational arginylation enzyme arginyltransferase1 shows genetic interactions with specific cellular pathways *in vivo*. *Front. Physiol.* 11:427. doi: 10.3389/fphys.2020.00427
- Williams, T. A., Foster, P. G., Cox, C. J., and Embley, T. M. (2013). An archaeal origin of eukaryotes supports only two primary domains of life. *Nature* 504, 231–236. doi: 10.1038/nature12779
- Xu, N. S., Chakraborty, G., Hassankhani, A., and Ingoglia, N. A. (1993). N-terminal arginylation of proteins in explants of injured sciatic nerves and embryonic brains of rats. *Neurochem. Res.* 18, 1117–1123. doi: 10.1007/BF00978361
- Zhang, F., Patel, D. M., Colavita, K., Rodionova, I., Buckley, B., Scott, D. A., et al. (2015). Arginylation regulates purine nucleotide biosynthesis by enhancing the activity of phosphoribosyl pyrophosphate synthase. *Nat. Commun.* 6:7517. doi: 10.1038/ncomms8517
- Zhang, F., Saha, S., and Kashina, A. (2012). Arginylation-dependent regulation of a proteolytic product of talin is essential for cell-cell adhesion. *J. Cell Biol.* 197, 819–836. doi: 10.1083/jcb.201112129
- Zhong, Q., Gao, W. H., Du, F. H., and Wang, X. D. (2005). Mule/ARF-BP1, a BH3-only E3 ubiquitin ligase, catalyzes the polyubiquitination of Mcl-1 and regulates apoptosis. *Cell* 121, 1085–1095. doi: 10.1016/j.cell.2005.06.009

**Conflict of Interest:** The authors declare that the research was conducted in the absence of any commercial or financial relationships that could be construed as a potential conflict of interest.

Copyright © 2020 Jiang, Moorthy, Patel, Kumar, Morgan, Alfonso, Huang, Lampidis, Isom, Barrientos, Fontanesi and Zhang. This is an open-access article distributed under the terms of the Creative Commons Attribution License (CC BY). The use, distribution or reproduction in other forums is permitted, provided the original author(s) and the copyright owner(s) are credited and that the original publication in this journal is cited, in accordance with accepted academic practice. No use, distribution or reproduction is permitted which does not comply with these terms.



# Roles of Lipid Peroxidation-Derived Electrophiles in Pathogenesis of Colonic Inflammation and Colon Cancer

Lei Lei<sup>1,2</sup>, Jianan Zhang<sup>2</sup>, Eric A. Decker<sup>2</sup> and Guodong Zhang<sup>2,3\*</sup>

<sup>1</sup>School of Medicine, Northwest University, Xi'an, China, <sup>2</sup>Department of Food Science, University of Massachusetts, Amherst, MA, United States, <sup>3</sup>Molecular and Cellular Biology Graduate Program, University of Massachusetts, Amherst, MA, United States

## OPEN ACCESS

### Edited by:

Fangliang Zhang,  
University of Miami,  
United States

### Reviewed by:

Oleksii Skorokhod,  
University of Turin, Italy  
Hala Chaaban,  
University of Oklahoma Health  
Sciences Center, United States  
Lidija Milkovic,  
Rudjer Boskovic Institute, Croatia

### \*Correspondence:

Guodong Zhang  
guodongzhang@umass.edu

### Specialty section:

This article was submitted to  
Cellular Biochemistry,  
a section of the journal  
Frontiers in Cell and Developmental  
Biology

**Received:** 08 February 2021

**Accepted:** 22 April 2021

**Published:** 17 May 2021

### Citation:

Lei L, Zhang J, Decker EA and  
Zhang G (2021) Roles of Lipid  
Peroxidation-Derived Electrophiles in  
Pathogenesis of Colonic Inflammation  
and Colon Cancer.  
Front. Cell Dev. Biol. 9:665591.  
doi: 10.3389/fcell.2021.665591

Redox stress is a common feature of gut disorders such as colonic inflammation (inflammatory bowel disease or IBD) and colorectal cancer (CRC). This leads to increased colonic formation of lipid-derived electrophiles (LDEs) such as 4-hydroxynonenal (4-HNE), malondialdehyde (MDA), trans, trans-2,4-decadienal (tt-DDE), and epoxyketo-octadecenoic acid (EKODE). Recent research by us and others support that treatment with LDEs increases the severity of colitis and exacerbates the development of colon tumorigenesis *in vitro* and *in vivo*, supporting a critical role of these compounds in the pathogenesis of IBD and CRC. In this review, we will discuss the effects and mechanisms of LDEs on development of IBD and CRC and lifestyle factors, which could potentially affect tissue levels of LDEs to regulate IBD and CRC development.

**Keywords:** inflammatory bowel disease, colonic inflammation, colorectal cancer, oxidative stress, lipid peroxidation

## INTRODUCTION

Colonic inflammation (inflammatory bowel disease or IBD, including Crohn's disease and ulcerative colitis) and colorectal cancer (CRC) are serious health problems in many countries. The incidence and prevalence of IBD have dramatically increased in the United States and other countries (Molodecky et al., 2012). The symptoms of IBD include abdominal pain, diarrhea, and rectal bleeding; as a result, IBD can severely impact the life quality of the patients. To date, there is no cure of IBD, and the current anti-IBD treatments can lead to serious side effects, such as increased infection risk, bone marrow dysfunction, organ dysfunction, and increased risk of malignancy, making it difficult to manage IBD. In addition, IBD patients have increased risks of developing CRC (Terzić et al., 2010). CRC is the third most common cancer and the second leading cause of cancer-related death worldwide (Bray et al., 2018). There are ~147,950 new cases of CRC in the United States in 2020. Although the majority of these cases occurred in individuals at an age of 50 years and older, ~12% new cases of CRC were diagnosed in individuals aged younger than 50 years (Siegel et al., 2020). It is of critical importance to better understand the pathological components involved in the development of IBD and CRC, in order to develop novel strategies for prevention and/or treatment.

A common feature of IBD and CRC is that the oxidative stress is increased in the colon tissues. Previous studies showed that a variety of reactive oxygen species (ROS), including superoxide ( $O_2^-$ ), hydroxyl (OH), peroxy ( $RO_2$ ), and alkoxy (RO) radicals, are increased in the rodent models and human patients of IBD and CRC (Biasi et al., 2013). These ROS species can attack polyunsaturated fatty acids (PUFAs), notably linoleic acid (LA, the most abundant PUFA in humans diet and tissues), that are incorporated in the membrane phospholipids of colon tissues, leading to formation of endogenous lipid-derived electrophiles (LDEs), such as 4-hydroxynonenal (4-HNE), malondialdehyde (MDA), trans, trans-2,4-decadienal (tt-DDE), and epoxyoctadecenoic acid (EKODE; Van Kuijk et al., 1990; Lin et al., 2007; Blair, 2008; Ayala et al., 2014). Substantial studies have shown that the levels of LDEs are increased in animal models and human patients with IBD or CRC (Skrzydłowska et al., 2005; Rezaie et al., 2007; Lee et al., 2010). In addition, previous studies have shown that the LDEs have potent effects on inflammation and tumorigenesis (Esterbauer et al., 1991). Therefore, some of the LDE compounds are implicated in the pathogenesis of IBD and CRC (Colgan and Taylor, 2010; Iborra et al., 2011; Bhattacharyya et al., 2014). However, most of the previous studies were performed using *in vitro* cell culture models (Esterbauer et al., 1991), which have several limitations: (1) the cell culture models have many limitations to study the complicated pathogenesis of IBD and CRC, (2) the LDEs are chemically reactive toward biomolecules and are metabolically unstable *in vivo*, the extent to, which these compounds can directly interact with intestinal epithelial cells (IECs) or immune cells *in vivo* remain unknown, and (3) some studies treated cultured cells with the LDE at high- $\mu$ M concentrations, which may not be biologically or pathologically relevant.

To address these concerns, recently we performed a series of animal studies to investigate the effects and mechanisms of LDEs, including 4-HNE, tt-DDE, and EKODE, on development of IBD and CRC in mouse models (Wang et al., 2019a, 2020; Lei et al., 2021). Our results showed that systematic, short-time, treatment with low doses of these compounds increased the severity of dextran sodium sulfate (DSS)-induced colitis and exacerbated the development of azoxymethane (AOM)/DSS-induced colon tumorigenesis in mice, supporting a critical role of these compounds in the development of IBD and CRC *in vivo* (Wang et al., 2019a, 2020; Lei et al., 2021). In this review, we will discuss the roles of the LDEs in the pathogenesis of IBD and CRC, and the implications of LDEs in designing strategies to reduce the risks of IBD and CRC (Figure 1).

## LEVELS OF LDEs IN ANIMAL MODELS AND HUMAN PATIENTS OF IBD AND CRC

Previous studies have shown that the concentrations of LDEs are increased in animal models of IBD (Table 1). In both DSS- and 2,4,6-trinitrobenzenesulfonic acid (TNBS)-induced

colitic models, the concentration of 4-HNE is significantly increased in the colon tissues of colitic mice (Lee et al., 2010). Indeed, the colonic concentrations of free-form 4-HNE in normal C3H/HeN mice (not stimulated with DSS) vs. DSS-exposed C3H/HeN mice were  $0.86 \pm 0.85$  ng/ml vs.  $11.92 \pm 7.01$  ng/ml, demonstrating a dramatic increase of colonic 4-HNE in colitis (Lee et al., 2010). The concentration of MDA, another LDE compound, was also increased in the colon tissues of TNBS-induced colitic rats (Liu and Wang, 2011). These effects seemed to be mouse strain-dependent: DSS exposure significantly increased colonic concentration of 4-HNE in both C3H/HeN and C3H/HeJ mice, but the effect was much more dramatic in C3H/HeN mice compared with C3H/HeJ mice (Lee et al., 2010). Overall, these results support that the colonic concentrations of LDEs are increased in animal models of IBD.

Previous studies also showed that the concentrations of LDEs are increased in animal models of CRC (Table 1). Our recent research showed that EKODE, an aldehyde compound derived from oxidative degradation of  $\omega$ -6 PUFAs (Lin et al., 2007), was increased in the colon tissues of AOM/DSS-induced CRC mice (Lei et al., 2021). In our research, we used a liquid chromatography-tandem mass spectrometry (LC-MS/MS)-based metabolomics, which can measure >100 fatty acid metabolites derived from both enzymatic metabolism and non-enzymatic oxidation of PUFAs (Wang et al., 2019b), to systematically profile how fatty acid metabolites are deregulated in the colon of AOM/DSS-induced CRC mice. We found that EKODE was significantly increased in the colon of the AOM/DSS-induced C57BL/6 mice compared with that of the healthy control mice. In addition, EKODE was also among the most dramatically increased fatty acid metabolites in the colon of the mice (Lei et al., 2021). The concentration of EKODE was not significantly increased in the plasma of AOM/DSS-induced CRC mice compared with the healthy control mice (Wang et al., 2019b), and this could be due to the low chemical and/or metabolic stability of EKODE in circulation. Besides the chemically induced CRC models, the levels of LDEs are also increased in the CRC model of the *Il-10*<sup>-/-</sup> mice. Compared with *Il-10*<sup>-/-</sup> mice colonized with a superoxide-deficient strain WY84SS or administered sham, the *Il-10*<sup>-/-</sup> mice colonized with a superoxide-producing *Enterococcus faecalis* strain OG1RFSS developed more severe colon tumorigenesis. Immunohistochemical analyses showed that the levels of 4-HNE-protein adducts are increased in the colonic macrophages and myofibroblasts of *Il-10*<sup>-/-</sup> mice colonized with OG1RFSS (Wang et al., 2012). These results are consistent with other studies, which showed that LDE compounds, such as 4-HNE and MDA, are increased in animal models of CRC (Amerizadeh et al., 2018; Cid-Gallegos et al., 2020).

Human studies also showed that the concentrations of LDEs are increased in IBD and CRC patients (Table 2). Previous studies showed that the circulating concentration of MDA was increased in Crohn's disease patients compared with control subjects (Alzoghbi et al., 2007; Boehm et al., 2012; Achitei et al., 2013). The concentrations of 4-HNE and MDA are increased in human primary CRC tissues (Skrzydłowska et al., 2005).



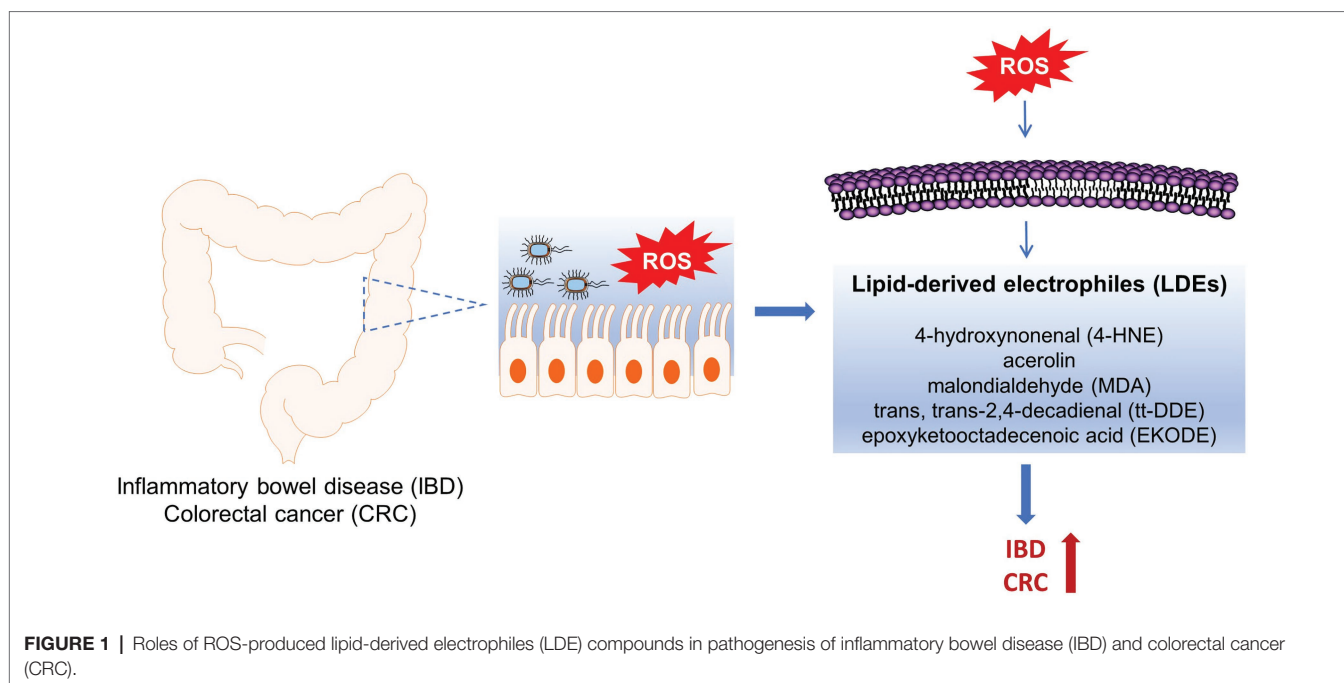


**TABLE 1 |** Concentrations of LDE compounds in animal models of IBD and CRC.

Model	Species	Tissue	Results	References
DSS/TNBS-induced colitis	C3H/HeN or C3H/HeJ mouse	Colon	↑ MDA, ↑ 4-HNE in colon	Lee et al., 2010
TNBS-induced colitis	Sprague-Dawley rat	Colon	↑ MDA in colon	Liu and Wang, 2011
Colitis-CRC model	<i>Il-10<sup>-/-</sup></i> mouse colonized with <i>Enterococcus faecalis</i>	Colon	↑ 4-HNE-protein adducts in colon	Wang et al., 2012
AOM/DSS-induced CRC model	OG1RFSS	Colon	↑ EKODE in colon	Lei et al., 2021
AOM/DSS-induced CRC model	C57BL/6 mouse	Colon	↑ MDA in colon	Amerizadeh et al., 2018
AOM/DSS-induced CRC model	BALB/c mouse	Colon	↑ MDA, ↑ 4-HNE protein in colon	Cid-Gallegos et al., 2020

AOM, azoxymethane; DSS, dextran sodium sulfate; TNBS, 2,4,6-trinitrobenzenesulfonic acid.

In addition, previous studies showed that CRC patients, as well as patients with unresectable colorectal liver metastasis, have higher concentrations of MDA in the urine and/or plasma (Saygili et al., 2003; Leung et al., 2008; Chandramathi et al., 2009). After surgical treatments, the serum concentration of MDA was reduced in CRC patients compared to presurgical status (Surinénaitė et al., 2009). Clinical studies also showed a strong association between LDEs and transforming growth factor  $\beta$ 1 (TGF- $\beta$ 1) levels, related to the tumor malignancy (Tüzün et al., 2012). 4-HNE may make an important contribution toward upregulating TGF- $\beta$ 1 expression (Leonarduzzi et al., 1997). Overall, these results support the clinical importance of LDEs in IBD and CRC.

The increased colonic concentration of LDEs in IBD and CRC could be due to the more severe redox stress in these diseases. Substantial studies have shown that a series of oxidative markers, such as ROS species, nitric oxide, 8-oxo-2'-deoxyguanosine (8-oxodG), and antioxidant or pro-oxidative proteins (e.g., catalase and myeloperoxidase), are altered in IBD and CRC, demonstrating a more severe oxidative microenvironment in IBD and CRC (Perse, 2013; Sies et al., 2017).

In agreement with these studies, we showed that compared with control healthy mice, the AOM/DSS-induced CRC mice had a lower colonic expression of a series of anti-oxidative genes, such as *Sod1* (encoding superoxide dismutase 1), *Cat* (encoding catalase), *Gsr* (encoding glutathione-disulfide reductase), *Gsta1* (encoding glutathione S-transferase A1), *Gstm1* (encoding glutathione S-transferase M1), and *Hmox1* (encoding heme oxygenase-1), and had higher colonic expression of a pro-oxidative gene *Mpo* (encoding myeloperoxidase), demonstrating more severe redox stress in the colon tissues of AOM/DSS-induced CRC mice. Consistent with these findings in animal models, we found that, in the Cancer Genome Atlas (TCGA) database, the expressions of the anti-oxidant genes (*CAT*, *GSR*, *GSTA1*, *GSTM1*, and *HMOX1*) are reduced, while the expression of pro-oxidant gene *MPO* is increased, in the tumor samples of human CRC patients (Lei et al., 2021).

The more severe redox stress in the colon tissues of IBD and CRC could contribute to the high concentrations of LDEs through several mechanisms. First, the colon tissues of IBD and CRC usually have higher levels of ROS species,

**TABLE 2 |** Concentrations of LDE compounds in human patients of IBD and CRC.

Disease	Human subjects	Tissue	Results	References
IBD	IBD patients ( <i>n</i> = 42) and normal adults ( <i>n</i> = 32)	Plasma	↑ MDA in plasma	Alzoghbi et al., 2007
IBD	IBD patients ( <i>n</i> = 41) and normal adults ( <i>n</i> = 18)	Serum	↑ MDA in serum	Achitei et al., 2013
IBD (CD)	CD patients ( <i>n</i> = 52) and healthy adults ( <i>n</i> = 99)	Plasma	↑ MDA in plasma	Boehm et al., 2012
CRC	CRC patients ( <i>n</i> = 81) and most distant location as control ( <i>n</i> = 81)	Colon mucosae	↑ MDA, ↑ 4-HNE in colon mucosae	Skrzydłowska et al., 2005
CRC	CRC patients ( <i>n</i> = 49) and healthy individuals control ( <i>n</i> = 95)	Urine	↑ MDA in urine	Chandramathi et al., 2009
CRC	CRC patients ( <i>n</i> = 20) and healthy individuals control ( <i>n</i> = 20)	Plasma	↑ MDA in plasma	Saygili et al., 2003
CRC	Primary operable patients ( <i>n</i> = 53) and advanced inoperable patients ( <i>n</i> = 53)	Plasma	↑ MDA in plasma	Leung et al., 2008
CRC	CRC patients ( <i>n</i> = 65; comparing the change between presurgical and postsurgical periods)	Serum	↓ MDA in serum compared to presurgical	Surinénaitė et al., 2009

CD, Crohn's disease; TBARS, thiobarbituric acid-reactive substances; UC, ulcerative colitis.

which can directly attack membrane phospholipids and lead to increased production of LDEs such as 4-HNE and EKODE (Lin et al., 2007). Second, the colon tumors or inflamed colons usually have lower expression of glutathione S-transferases (GST), as well as glutathione, and this could lead to decreased metabolism of LDEs and thus contribute to their high abundance in colon tissues. Indeed, previous studies showed that the colonic concentration of glutathione, as well as the colonic activity of GST enzymes, was reduced in DSS-induced colitic model (Oz et al., 2005; Arafa et al., 2009). The GST activity in the distal colon was significantly lower in the carcinoma patients compared with the adenoma patients and healthy controls (Grubben et al., 2006). The GST enzymes are the major enzymes involved in metabolism of lipid peroxidation-derived  $\alpha,\beta$ -unsaturated carbonyl compounds, such as 4-HNE and acrolein, catalyzing the conjugation reaction of these compounds with glutathione to form the corresponding glutathione conjugates (Allocati et al., 2018). Therefore, reduced expression of GST and lower levels of intracellular glutathione in IBD and CRC could lead to attenuated metabolic degradation of the LDEs. Overall, due to the oxidative stress in the colon tissues of IBD and CRC, there could be enhanced production and/or reduced degradation of LDEs in the colon, leading to higher colonic levels of LDEs.

## EFFECTS OF LDEs ON DEVELOPMENT OF IBD AND CRC

### *In vitro* Studies of LDEs on Inflammation and Tumorigenesis

Previous studies by us and others showed that treatment with low-concentration LDE increases inflammatory responses. In our recent study, we treated human CRC (HCT-116) and mouse macrophage (RAW 264.7) cells with EKODE, at a concentration of 300 nM (a dose determined from LC-MS/MS analysis of the concentration of endogenous EKODE in the colon tissues of AOM/DSS-induced CRC mice, see our publication Lei et al., 2021). We found that EKODE treatment induces the expression of pro-inflammatory genes and activates JNK and NF- $\kappa$ B pathways in both CRC and macrophage cells, illustrating a potent pro-inflammatory effect of EKODE *in vitro* (Lei et al., 2021).

Besides EKODE, previous studies by us and others also showed that other LDE compound, such as tt-DDE, induces inflammatory responses *in vitro* (Chang et al., 2005; Wang et al., 2020).

Previous studies also support that LDEs can cause detrimental effects on tumorigenesis *in vitro*. Many LDE compounds, such as 4-HNE, MDA, and acrolein, are chemically reactive and can form covalently-linked conjugates with biomolecules such as DNA, leading to mutagenesis and tumorigenesis. Acrolein, a major component in cigarette smoke, has been shown to be able to directly react guanine residues in DNA to produce DNA adducts (Comes and Eggleton, 2002). It could be a major etiological agent for cigarette smoke-related lung cancer and contributes to lung carcinogenesis through the induction of DNA damage and the inhibition of DNA repair (Feng et al., 2006a). MDA has also been shown to react with nucleosides, such as deoxyguanosine and deoxyadenosine, to form adducts such as pyrimido[1,2-a]purin-10(3H)-one (M1G; Niedernhofer et al., 2003). M1G has been demonstrated to be highly mutagenic in human cells and has been detected in tissues under oxidative stress (Marnett, 1999a,b). MDA treatment inhibits nucleotide excision repair for both UV light- and BPDE-induced DNA damage in CRC cells (Feng et al., 2006b). These results suggest that MDA could play a critical role in oxidative stress-induced mutagenesis and carcinogenesis through two detrimental mechanisms: the induction of DNA damage and the inhibition of DNA repair. Besides MDA, other LDE compound, such as 4-HNE, has been shown to a potential mutagen and could contribute to oxidative stress-induced carcinogenesis (Hu et al., 2002; Nair et al., 2006; Wang et al., 2012, 2015). The effects of LDEs on inflammation and tumorigenesis have been summarized and discussed in several reviews (Poli et al., 2008; Ayala et al., 2014; Zhong and Yin, 2015) and will not be discussed in detail here.

Previous studies showed that LDEs can cause different, or even opposite, effects at different concentrations *in vitro*. For example, EKODE at a concentration of 10  $\mu$ M can activate nuclear factor erythroid 2-related factor 2 (Nrf2) signaling (Wang et al., 2009), which is an important pathway involved in cellular defense against oxidative stress (Guina et al., 2015). While at lower concentrations, EKODE did not have such an effect and instead induced inflammatory responses (Wang et al., 2009; Lei et al., 2021). This could be, at least in part, due to the

mode of actions of these compounds. LDEs are chemically reactive and can covalently modify cellular proteins, it is feasible that at different concentrations, the LDE compound can interact with different cellular proteins: at low concentrations, the LDE compound could selectively interact with the cellular proteins, which have the most reactive amino acid residues; while at high concentrations, the LDE compound could interact with more proteins in a less selective manner, resulting in varied or even opposite biological responses. This notion is supported by previous studies of click chemistry-based imaging of LDE compounds such as 4-HNE and tt-DDE (Vila et al., 2008; Wang et al., 2020). To better understand the biological effect of LDE compound, it is important to perform cell culture studies using a dose that is biologically or pathologically relevant. As we discussed in “Levels of LDEs in Animal Models and Human Patients of IBD and CRC” section above, substantial studies have reported the concentrations of endogenous LDEs in animal models and human patients of IBD and CRC: for example, previous studies showed that the colonic concentrations of 4-HNE are ~11.9 ng/ml (~76 nM) in DSS-exposed C3H/HeN mice and ~15.9 ng/ml (~102 nM) in TNBS-exposed C3H/HeN mice (Lee et al., 2010). These reported concentrations can help us to perform *in vitro* studies to study the actions of these compounds under biologically relevant conditions.

### **In vivo Studies of LDEs on IBD and CRC**

Our recent research showed that systematic, short-time, treatment with low doses of the LDEs, such as 4-HNE, tt-DDE, or EKODE, increased the severity of DSS-induced colitis and exacerbated the development of AOM/DSS-induced CRC in mouse models, supporting critical roles of these compounds in the development of IBD and CRC (Wang et al., 2019a, 2020; Lei et al., 2021). In our experiment, we treated C57BL/6 mice with 2% DSS in drinking water, with or without administration of 4-HNE, tt-DDE, or EKODE (*via* intraperitoneal injection, dose = 1–5 mg/kg/day), for 6–7 days, then sacrificed the mice for analysis. We found that LDE treatment increased the severity of DSS-induced colitis in mice, with increased infiltration of immune cells, expression of pro-inflammatory genes, and enhanced crypt damage, in the colon tissues. Furthermore, we showed that LDE treatment exacerbated intestinal barrier dysfunction, leading to enhanced translocation of bacteria or toxic bacterial products from the gut into the systemic circulation and distant organs. Overall, these results support that LDEs have a pro-colitic activity *in vivo* (Wang et al., 2019a, 2020; Lei et al., 2021). In addition, we also found that LDE treatment exacerbated the development of AOM/DSS-induced colon tumorigenesis in mice. In this experiment, we stimulated AOM and DSS to initiate colon tumorigenesis, then treated the mice with an intraperitoneal injection of EKODE (dose = 1 mg/kg/day). EKODE treatment increased tumor number and tumor size, and increased expression of pro-inflammatory and pro-tumorigenic markers in the colon, demonstrating its CRC-enhancing effects *in vivo* (Lei et al., 2021).

TLR4 plays a critical role in gut bacteria-host interactions by recognizing LPS, which is expressed by Gram-negative

bacteria and certain Gram-positive bacteria (Abreu, 2010). Activation of TLR4 contributes to the development and maintenance of inflammatory responses (O’Shea and Murray, 2008), and the expression of TLR4 is significantly upregulated in the colon of DSS-induced colitic mice (Hou et al., 2013). TLR4 is generally expressed at the basolateral surface of intestinal epithelial cells; as a result, TLR4 signaling will only be activated when the gut bacteria penetrate the intestinal epithelium layer (Kubinak and Round, 2012). We found that in the DSS-induced colitic model, treatment with 4-HNE suppressed expression of tight-junction proteins in colon tissues, leading to increased translocation of bacteria or bacterial product (e.g., LPS) from the gut into the systemic circulation, resulting in increased activation of TLR4 signaling *in vivo* (Wang et al., 2019a). Furthermore, we showed that 4-HNE failed to promote DSS-induced colitis in *Tlr4*<sup>-/-</sup> mice, supporting that TLR4 signaling is required for the pro-colitic activity of 4-HNE (Wang et al., 2019a). Our finding is consistent with previous studies, which showed that 4-HNE induces the production of pro-inflammatory cytokines (IL-8, IL-1 $\beta$ , and TNF $\alpha$ ) and upregulates matrix metalloproteinase-9 by TLR4/NF- $\kappa$ B-dependent mechanisms *in vitro* (Gargiulo et al., 2015). Besides 4-HNE, we also found that EKODE treatment impaired intestinal barrier function and enhanced bacterial translocation *in vivo*, which could lead to activation of TLR4 signaling and contribute to its pro-colitic activity (Lei et al., 2021).

The potential roles of TLR4 in mediating the pro-colitic actions of LDEs suggest that gut microbiota could be involved in the actions of LDEs. The LDE compounds, which are increased in the colon tissues under IBD or CRC status, could directly interact with bacterial cells that reside in the colon, leading to alteration of gut microbiota and contributing to increased development of IBD or CRC (Sekirot et al., 2010). A healthy gut is a mostly oxygen-free environment and is mainly inhabited by obligate anaerobes (Sekirot et al., 2010). Previous studies have supported the notion that many beneficial gut bacteria are sensitive to oxygen or redox stress, while the pathologic bacteria are more resistant to redox stress (Sekirot et al., 2010). Therefore, increased formation of LDEs, which are chemically and redox-active, could perturb gut microbiota through suppressing the growth of beneficial anaerobic bacteria and enhancing the growth of redox-resistant pathological bacteria, resulting in microbiota dysbiosis. To date, few studies have characterized the roles of LDEs on gut microbiota, and the functional roles of the altered microbiota in promoting IBD or CRC. Further studies are needed to better understand how IBD or CRC-associated redox microenvironment interacts with the gut microbiota to affect the development of gut diseases.

Overall, our results support a model that during the development of colitis and CRC, there is enhanced production of ROS species in the colon, leading to increased production of LDEs such as 4-HNE and EKODE in the colon tissues. These compounds could interact with the cells that reside in the gut, such as IECs, inflammatory cells, or even gut bacteria cells, leading to increased inflammatory responses and tumorigenesis, and resulting in increased development of IBD and CRC. In support of this notion, the results by us and

others showed that treatment with LDEs, at pathologically relevant concentrations, induced inflammatory responses in IECs and macrophages (Wang et al., 2019a, 2020; Lei et al., 2021). Therefore, these compounds could be important pathological components in the development of IBD and CRC. Future studies are needed to determine whether we could develop strategies to selectively target LDEs to reduce the risks of IBD and CRC.

We want to point out that our animal studies have limitations. The purpose of our research is to study the extent to, which LDE compounds modulate the development of colitis and CRC in mouse models. Since, the LDEs are produced by non-enzymatic oxidation of tissue PUFAs, it is difficult for us to use genetically engineered mouse models to alter colonic concentrations of LDEs and study their biological actions. In our experiments, we treated mice with these compounds, such as 4-HNE and EKODE (dose = 1–5 mg/kg/day), *via* intraperitoneal injection (Wang et al., 2019a, 2020; Lei et al., 2021). We used this dose range, since a previous study has shown to intraperitoneal injection of 5 mg/kg/day 4-HNE caused no toxic effects in mice (Nishikawa et al., 2000). However, intraperitoneal injection of LDEs leads to systematic delivery of LDEs and could also increase the concentrations of LDEs in other tissues. In addition, it remains to determine whether the colonic concentrations of LDEs in the LDEs-treated mice are relevant with those in IBD and CRC patients.

## FACTORS THAT AFFECT THE FORMATION OF LDEs IN TISSUES

Since, LDEs are produced from tissue PUFAs (notably LA) by the actions of ROS, factors that can affect the formation of LDEs in tissues, such as dietary intake of LA, heme irons, and antioxidants, could modulate the risks of IBD and CRC. The details are discussed below.

### Dietary Intake of LA

LA is abundant in vegetable oils, such as corn, soybean, and canola oils, as well as fried food, salad dressing, and mayonnaise (Blasbalg et al., 2011). Since the last century, there has been a dramatic increase of dietary consumption of LA in the United States and other countries: the consumption of soybean oil, which is a major vegetable oil on the market, has risen more than 47% since 1980 and more than 1,000-fold since 1909 (Blasbalg et al., 2011). It is feasible that a high intake of dietary LA would increase the abundance of LA in membrane phospholipids and leads to increased formation of LDEs under redox stress, which could result in increased development of IBD and CRC. In consistent with this notion, animal experiments showed that a high intake of LA increased both AOM- and *Apc* mutation-induced CRC, suggesting its potential adverse effect on CRC (Reddy et al., 1985; Wu et al., 2004; Fujise et al., 2007; Enos et al., 2016; Liu et al., 2020). Human studies also support that a high intake of LA increases the risks of CRC (Pot et al., 2008; Daniel et al., 2009) and colitis (Shoda et al., 1996; Tjonneland et al., 2009; Strassburg et al., 2014; Rashvand et al., 2015). Notably, the European

Prospective Investigation into Cancer and Nutrition (EPIC) study showed that high intake of LA more than doubled the risks of IBD and could be responsible for ~30% of ulcerative colitis cases (Tjonneland et al., 2009), though we need to point out there are also inconsistent studies, which showed that a high dietary intake of LA did not increase risks of CRC in human populations (Zock and Katan, 1998; Bartsch et al., 1999; Azrad et al., 2013). Further studies are needed to better characterize the molecular mechanisms for the potential CRC-enhancing effects of dietary LA, in order to clarify its health effects and make dietary recommendations or guidelines for the optimal intake of LA.

### Dietary Intake of Heme Iron

Overall meat consumption has continued to rise in the United States and the rest of the developed world. Red meat represents the largest proportion of meat consumed in the United States (58%; Daniel et al., 2011). Heme has been proposed as the key molecule contributing to tumorigenesis upon red and processed meat intake (Fiorito et al., 2020). Heme iron plays important role in lipid peroxidation. Previous studies support that a high dietary intake of heme iron increases tissue levels of LDEs, leading to increased risks of CRC. Heme iron can increase lipid peroxidation in food products: Gasc et al. (2007) showed that heme iron can interact with dietary LA, leading to increased levels of 4-HNE in food products. In addition, Pierre et al. showed that administration of a diet rich in heme iron increased the urinal concentration of 1,4-dihydroxynonane mercapturic acid (DHN-MA), which is a major urinary metabolite of 4-HNE, in both animal models and human subjects, suggesting that dietary intake of heme iron increases lipid peroxidation *in vivo* (Pierre et al., 2006). Animal and human studies also support that heme iron increases risks of CRC. Feeding of a diet rich in heme iron increased the number of preneoplastic lesions in an AOM-induced CRC model in rats and increased tumor load in a spontaneous CRC model in *Apc*<sup>Min</sup> mice (Bastide et al., 2015). A meta-analysis of cohort studies showed that high heme iron intake was associated with increased risks of CRC, supporting that heme iron increases risks of CRC in humans (Bastide et al., 2011).

### Dietary Intake of Antioxidants

Radical scavenging antioxidants, which counteract the detrimental actions of ROS species and are used to inhibit lipid peroxidation in food products, are widely regarded to be beneficial. Previous studies support that some naturally occurring antioxidants, such as lycopene, flavonoids, phenolic, and polyphenolic compounds, have anti-tumor effects (Khurana et al., 2018) and could attenuate the risks of IBD and CRC (Murtaugh et al., 2004; Moura et al., 2015). Administration of antioxidant has been shown to reduce tissue levels of LDE compounds, such as MDA or its DHA adduct M1G, supporting a link of antioxidant intake with LDE compounds (Sharma et al., 2001; Vezza et al., 2016). However, there are recent studies that suggest that antioxidants can increase the risks



of cancers in animal models and human subjects. Gallic acid, which is a phenolic acid widely found in plants, has been shown to increase the risks of CRC in *Apc<sup>Min/+</sup>p53<sup>R172H</sup>* mice (*Apc<sup>Min/+</sup>* mice with *p53* mutation), while it had no effects on *Apc<sup>Min/+</sup>* mice that express wild-type *p53* (Kadosh et al., 2020). In other types of cancers, Sayin et al. showed that dietary administration with the antioxidants, N-acetylcysteine (NAC) and vitamin E, markedly increased tumor progression and reduced survival in mouse models of B-RAF- and K-RAS-induced lung cancer (Sayin et al., 2014). Tumor metastasis, which is a process of the cancer cells to migrate from primary tumors to other distant organs, is the cause for ~90% of human cancer death (Chaffer and Weinberg, 2011). Piskounova et al. showed that metastasizing melanoma cells experience severe oxidative stress in the blood and visceral organs, resulting in poor metastases, while supplementations with antioxidants increase tumor metastasis (Piskounova et al., 2015). Le Gal et al. (2015) also showed that the dietary administration of antioxidant NAC increases lymph node metastases in an endogenous mouse model of malignant melanoma. Some human studies also support that intake of antioxidants may cause detrimental effects on cancer development in human subjects (Albanes et al., 1996). Overall, these results support a potential detrimental effect of the antioxidant supplement on tumorigenesis.

There could be many reasons for the inconsistent results: e.g., different antioxidants could have different biological actions and varied effects on IBD and CRC. In addition, some antioxidants can reduce transition metals to a more active state, which can then decompose hydroperoxides into high-energy free radicals. Since, phenolics can act as both antioxidants and prooxidants, it can be difficult to predict their net effects in biological systems (Decker, 1997). Further studies are urgently needed in this area, since many dietary antioxidants are widely

consumed by the general public, a better understanding of their effects could lead to a major impact on public health.

## CONCLUSION

Research by us and others support that the LDEs are increased in the colon tissues of IBD and CRC and play critical roles in promoting the disease development of these two types of diseases. A better understanding of the mode of actions of these compounds could help us to identify novel therapeutic targets of IBD and CRC, helping us to design mechanism-based strategies to reduce the risks of these diseases. In addition, dietary factors, such as LA, heme iron, and antioxidants, could have important implications in regulating the development of IBD and CRC, at least in part, through modulating colonic levels of LDEs. Since these dietary compounds are commonly consumed by the general public, a better understanding of their effects on IBD and CRC could lead to a significant impact on public health.

## AUTHOR CONTRIBUTIONS

LL and JZ wrote the review. ED and GZ edited the review. All authors contributed to the article and approved the submitted version.

## FUNDING

This research is supported by USDA NIFA 2016-67017-24423, 2019-67017-29248, 2020-67017-30844, and USDA/Hatch MAS00556 (to GZ).

## REFERENCES

- Abreu, M. T. (2010). Toll-like receptor signaling in the intestinal epithelium: how bacterial recognition shapes intestinal function. *Nat. Rev. Immunol.* 10, 131–144. doi: 10.1038/nri2707
- Achitei, D., Ciobica, A., Balan, G., Gologan, E., Stanciu, C., and Stefanescu, G. (2013). Different profile of peripheral antioxidant enzymes and lipid peroxidation in active and non-active inflammatory bowel disease patients. *Dig. Dis. Sci.* 58, 1244–1249. doi: 10.1007/s10620-012-2510-z
- Albanes, D., Heinonen, O. P., Taylor, P. R., Virtamo, J., Edwards, B. K., Rautalahti, M., et al. (1996).  $\alpha$ -Tocopherol and  $\beta$ -carotene supplements and lung cancer incidence in the  $\alpha$ -Tocopherol, Beta-carotene cancer prevention study: effects of base-line characteristics and study compliance. *J. Natl. Cancer Inst.* 88, 1560–1570. doi: 10.1093/jnci/88.21.1560
- Allocati, N., Masulli, M., Di Ilio, C., and Federici, L. (2018). Glutathione transferases: substrates, inhibitors and pro-drugs in cancer and neurodegenerative diseases. *Oncogenesis* 7:8. doi: 10.1038/s41389-017-0025-3
- Alzoghaibi, M. A., Al Mofleh, I. A., and Al-Jebreen, A. M. (2007). Lipid peroxides in patients with inflammatory bowel disease. *Saudi J. Gastroenterol.* 13:187. doi: 10.4103/1319-3767.36750
- Amerizadeh, F., Rezaei, N., Rahmani, F., Hassanian, S. M., Moradi-Marjaneh, R., Fiuji, H., et al. (2018). Crocin synergistically enhances the antiproliferative activity of 5-fluorouracil through Wnt/PI3K pathway in a mouse model of colitis-associated colorectal cancer. *J. Cell. Biochem.* 119, 10250–10261. doi: 10.1002/jcb.27367
- Arafa, H. M., Hemeida, R. A., El-Bahrawy, A. I., and Hamada, F. M. (2009). Prophylactic role of curcumin in dextran sulfate sodium (DSS)-induced ulcerative colitis murine model. *Food Chem. Toxicol.* 47, 1311–1317. doi: 10.1016/j.fct.2009.03.003
- Ayala, A., Muñoz, M. F., and Argüelles, S. (2014). Lipid peroxidation: production, metabolism, and signaling mechanisms of malondialdehyde and 4-hydroxy-2-nonenal. *Oxidative Med. Cell. Longev.* 2014:360438. doi: 10.1155/2014/360438
- Azrad, M., Turgeon, C. E., and Demark-Wahnefried, W. (2013). Current evidence linking polyunsaturated fatty acids with cancer risk and progression. *Front. Oncol.* 3:224. doi: 10.3389/fonc.2013.00224
- Bartsch, H., Nair, J., and Owen, R. W. (1999). Dietary polyunsaturated fatty acids and cancers of the breast and colorectum: emerging evidence for their role as risk modifiers. *Carcinogenesis* 20, 2209–2218. doi: 10.1093/carcin/20.12.2209
- Bastide, N. M., Chenni, F., Audebert, M., Santarelli, R. L., Taché, S., Naud, N., et al. (2015). A central role for heme iron in colon carcinogenesis associated with red meat intake. *Cancer Res.* 75, 870–879. doi: 10.1158/0008-5472.CAN-14-2554
- Bastide, N. M., Pierre, F. H., and Corpet, D. E. (2011). Heme iron from meat and risk of colorectal cancer: a meta-analysis and a review of the mechanisms involved. *Cancer Prev. Res.* 4, 177–184. doi: 10.1158/1940-6207.CAPR-10-0113
- Bhattacharyya, A., Chattopadhyay, R., Mitra, S., and Crowe, S. E. (2014). Oxidative stress: an essential factor in the pathogenesis of gastrointestinal mucosal diseases. *Physiol. Rev.* 94, 329–354. doi: 10.1152/physrev.00040.2012

- Biasi, F., Leonarduzzi, G., Oteiza, P. I., and Poli, G. (2013). Inflammatory bowel disease: mechanisms, redox considerations, and therapeutic targets. *Antioxid. Redox Signal.* 19, 1711–1747. doi: 10.1089/ars.2012.4530
- Blair, I. A. (2008). DNA adducts with lipid peroxidation products. *J. Biol. Chem.* 283, 15545–15549. doi: 10.1074/jbc.R700051200
- Blasbalg, T., Hibbeln, J., Ramsden, C., Majchrzak, S., and Rawlings, R. (2011). Changes in consumption of omega-3 and omega-6 fatty acids in the United States during the 20th century. *Am. J. Clin. Nutr.* 93, 950–962. doi: 10.3945/ajcn.110.006643
- Boehm, D., Krzystek-Korpacka, M., Neubauer, K., Matusiewicz, M., Paradowski, L., and Gamian, A. (2012). Lipid peroxidation markers in Crohn's disease: the associations and diagnostic value. *Clin. Chem. Lab. Med.* 50, 1359–1366. doi: 10.1515/cclm-2011-0817
- Bray, F., Ferlay, J., Soerjomataram, I., Siegel, R. L., Torre, L. A., and Jemal, A. (2018). Global cancer statistics 2018: GLOBOCAN estimates of incidence and mortality worldwide for 36 cancers in 185 countries. *CA Cancer J. Clin.* 68, 394–424. doi: 10.3322/caac.21492
- Chaffer, C. L., and Weinberg, R. A. (2011). A perspective on cancer cell metastasis. *Science* 331, 1559–1564. doi: 10.1126/science.1203543
- Chandramathi, S., Suresh, K., Anita, Z., and Kuppusamy, U. (2009). Comparative assessment of urinary oxidative indices in breast and colorectal cancer patients. *J. Cancer Res. Clin. Oncol.* 135, 319–323. doi: 10.1007/s00432-008-0462-7
- Chang, L. W., Lo, W.-S., and Lin, P. (2005). Trans, trans-2, 4-decadienal, a product found in cooking oil fumes, induces cell proliferation and cytokine production due to reactive oxygen species in human bronchial epithelial cells. *Toxicol. Sci.* 87, 337–343. doi: 10.1093/toxsci/kfi258
- Cid-Gallegos, M. S., Sánchez-Chino, X. M., Álvarez-González, I., Madrigal-Bujaidar, E., Vásquez-Garzón, V. R., Baltiérrez-Hoyos, R., et al. (2020). Modification of in vitro and in vivo antioxidant activity by consumption of cooked chickpea in a colon cancer model. *Nutrients* 12:2572. doi: 10.3390/nu12092572
- Colgan, S. P., and Taylor, C. T. (2010). Hypoxia: an alarm signal during intestinal inflammation. *Nat. Rev. Gastroenterol. Hepatol.* 7, 281–287. doi: 10.1038/nrgastro.2010.39
- Comes, R., and Eggleton, M. (2002). *Concise International Chemical Assessment Document No 43*. Geneva: World Health Organization.
- Daniel, C. R., Cross, A. J., Koebnick, C., and Sinha, R. (2011). Trends in meat consumption in the USA. *Public Health Nutr.* 14, 575–583. doi: 10.1017/S1368980010002077
- Daniel, C. R., McCullough, M. L., Patel, R. C., Jacobs, E. J., Flanders, W. D., Thun, M. J., et al. (2009). Dietary intake of ω-6 and ω-3 fatty acids and risk of colorectal cancer in a prospective cohort of US men and women. *Cancer Epidemiol. Prev. Biomarkers* 18, 516–525. doi: 10.1158/1055-9965.EPI-08-0750
- Decker, E. A. (1997). Phenolics: prooxidants or antioxidants? *Nutr. Rev.* 55, 396–398. doi: 10.1111/j.1753-4887.1997.tb01580.x
- Enos, R. T., Velazquez, K. T., McClellan, J. L., Cranford, T. L., Nagarkatti, M., Nagarkatti, P. S., et al. (2016). High-fat diets rich in saturated fat protect against azoxymethane/dextran sulfate sodium-induced colon cancer. *Am. J. Physiol. Gastrointest. Liver Physiol.* 310, G906–G919. doi: 10.1152/ajpgi.00345.2015
- Esterbauer, H., Schaur, R. J., and Zollner, H. (1991). Chemistry and biochemistry of 4-hydroxynonenal, malonaldehyde and related aldehydes. *Free Radic. Biol. Med.* 11, 81–128. doi: 10.1016/0891-5849(91)90192-6
- Feng, Z., Hu, W., Hu, Y., and Tang, M.-S. (2006a). Acrolein is a major cigarette-related lung cancer agent: preferential binding at p53 mutational hotspots and inhibition of DNA repair. *Proc. Natl. Acad. Sci.* 103, 15404–15409. doi: 10.1073/pnas.0607031103
- Feng, Z., Hu, W., Marnett, L. J., and Tang, M.-S. (2006b). Malondialdehyde, a major endogenous lipid peroxidation product, sensitizes human cells to UV- and BPDE-induced killing and mutagenesis through inhibition of nucleotide excision repair. *Mutat. Res.* 601, 125–136. doi: 10.1016/j.mrfmmm.2006.06.003
- Fiorito, V., Chiabrand, D., Petrillo, S., Bertino, F., and Tolosano, E. (2020). The multifaceted role of heme in cancer. *Front. Oncol.* 9:1540. doi: 10.3389/fonc.2019.01540
- Fujise, T., Iwakiri, R., Kakimoto, T., Shiraishi, R., Sakata, Y., Wu, B., et al. (2007). Long-term feeding of various fat diets modulates azoxymethane-induced colon carcinogenesis through Wnt/beta-catenin signaling in rats. *Am. J. Physiol. Gastrointest. Liver Physiol.* 292, G1150–G1156. doi: 10.1152/ajpgi.00269.2006
- Gargiulo, S., Gamba, P., Testa, G., Rossin, D., Biasi, F., Poli, G., et al. (2015). Relation between TLR4/NF-κB signaling pathway activation by 27-hydroxycholesterol and 4-hydroxynonenal, and atherosclerotic plaque instability. *Aging Cell* 14, 569–581. doi: 10.1111/ace.12322
- Gasc, N., Taché, S., Rathahao, E., Bertrand-Michel, J., Roques, V., and Guéraud, F. (2007). 4-hydroxynonenal in foodstuffs: heme concentration, fatty acid composition and freeze-drying are determining factors. *Redox Rep.* 12, 40–44. doi: 10.1179/135100007X162257
- Grubben, M., van Den Braak, C., Nagengast, F., and Peters, W. (2006). Low colonic glutathione detoxification capacity in patients at risk for colon cancer. *Eur. J. Clin. Invest.* 36, 188–192. doi: 10.1111/j.1365-2362.2006.01618.x
- Guina, T., Biasi, F., Calfapietra, S., Nano, M., and Poli, G. (2015). Inflammatory and redox reactions in colorectal carcinogenesis. *Ann. N. Y. Acad. Sci.* 1340, 95–103. doi: 10.1111/nyas.12734
- Hou, Y.-C., Chu, C.-C., Ko, T.-L., Yeh, C.-L., and Yeh, S.-L. (2013). Effects of alanyl-glutamine dipeptide on the expression of colon-inflammatory mediators during the recovery phase of colitis induced by dextran sulfate sodium. *Eur. J. Nutr.* 52, 1089–1098. doi: 10.1007/s00394-012-0416-3
- Hu, W., Feng, Z., Eveleigh, J., Iyer, G., Pan, J., Amin, S., et al. (2002). The major lipid peroxidation product, trans-4-hydroxy-2-nonenal, preferentially forms DNA adducts at codon 249 of human p53 gene, a unique mutational hotspot in hepatocellular carcinoma. *Carcinogenesis* 23, 1781–1789. doi: 10.1093/carcin/23.11.1781
- Iborra, M., Moret, I., Rausell, F., Bastida, G., Aguas, M., Cerrillo, E., et al. (2011). Role of oxidative stress and antioxidant enzymes in Crohn's disease. *Biochem. Soc. Trans.* 39, 1102–1106. doi: 10.1042/BST0391102
- Kadosh, E., Snir-Alkalay, I., Venkatachalam, A., May, S., Lasry, A., Elyada, E., et al. (2020). The gut microbiome switches mutant p53 from tumour-suppressive to oncogenic. *Nature* 586, 133–138. doi: 10.1038/s41586-020-2541-0
- Khurana, R. K., Jain, A., Jain, A., Sharma, T., Singh, B., and Kesharwani, P. (2018). Administration of antioxidants in cancer: debate of the decade. *Drug Discov. Today* 23, 763–770. doi: 10.1016/j.drudis.2018.01.021
- Kubinak, J. L., and Round, J. L. (2012). Toll-like receptors promote mutually beneficial commensal-host interactions. *PLoS Pathog.* 8:e1002785. doi: 10.1371/journal.ppat.1002785
- Le Gal, K., Ibrahim, M. X., Wiel, C., Sayin, V. I., Akula, M. K., Karlsson, C., et al. (2015). Antioxidants can increase melanoma metastasis in mice. *Sci. Transl. Med.* 7:308re8. doi: 10.1126/scitranslmed.aad3740
- Lee, I.-A., Bae, E.-A., Hyun, Y.-J., and Kim, D.-H. (2010). Dextran sulfate sodium and 2, 4, 6-trinitrobenzene sulfonic acid induce lipid peroxidation by the proliferation of intestinal gram-negative bacteria in mice. *J. Inflamm.* 7:7. doi: 10.1186/1476-9255-7-7
- Lei, L., Yang, J., Zhang, J., and Zhang, G. (2021). The lipid peroxidation product EKODE exacerbates colonic inflammation and colon tumorigenesis. *Redox Biol.* 101880. doi: 10.1016/j.redox.2021.101880 [Epub ahead of print]
- Leonarduzzi, G., Scavazza, A., Biasi, F., Chiarpotto, E., Camandola, S., Vogl, S., et al. (1997). The lipid peroxidation end product 4-hydroxy-2, 3-nonenal up-regulates transforming growth factor β1 expression in the macrophage lineage: a link between oxidative injury and fibrosclerosis 1. *FASEB J.* 11, 851–857. doi: 10.1096/fasebj.11.11.9285483
- Leung, E. Y., Crozier, J. E., Talwar, D., O'Reilly, D. S. J., McKee, R. F., Horgan, P. G., et al. (2008). Vitamin antioxidants, lipid peroxidation, tumour stage, the systemic inflammatory response and survival in patients with colorectal cancer. *Int. J. Cancer* 123, 2460–2464. doi: 10.1002/ijc.23811
- Lin, D., Zhang, J., and Sayre, L. M. (2007). Synthesis of six epoxyketooctadecenoic acid (EKODE) isomers, their generation from nonenzymatic oxidation of linoleic acid, and their reactivity with imidazole nucleophiles. *J. Org. Chem.* 72, 9471–9480. doi: 10.1021/jo701373f
- Liu, X., and Wang, J. (2011). Anti-inflammatory effects of iridoid glycosides fraction of *Folium syringae* leaves on TNBS-induced colitis in rats. *J. Ethnopharmacol.* 133, 780–787. doi: 10.1016/j.jep.2010.11.010
- Liu, F., Zuo, X., Liu, Y., Deguchi, Y., Moussalli, M. J., Chen, W., et al. (2020). Suppression of membranous LRP5 recycling, Wnt/β-catenin signaling, and colon carcinogenesis by 15-LOX-1 peroxidation of linoleic acid in PI3P. *Cell Rep.* 32:108049. doi: 10.1016/j.celrep.2020.108049
- Marnett, L. (1999a). Chemistry and biology of DNA damage by malondialdehyde. *IARC Sci. Publ.* 150, 17–27.

- Marnett, L. J. (1999b). Lipid peroxidation—DNA damage by malondialdehyde. *Mutat. Res.* 424, 83–95. doi: 10.1016/s0027-5107(99)00010-x
- Molodecky, N. A., Soon, I. S., Rabi, D. M., Ghali, W. A., Ferris, M., Chernoff, G., et al. (2012). Increasing incidence and prevalence of the inflammatory bowel diseases with time, based on systematic review. *Gastroenterology* 142, 46–54. doi: 10.1053/j.gastro.2011.10.001
- Moura, F. A., de Andrade, K. Q., Dos Santos, J. C. F., Araújo, O. R. P., and Goulart, M. O. F. (2015). Antioxidant therapy for treatment of inflammatory bowel disease: does it work? *Redox Biol.* 6, 617–639. doi: 10.1016/j.redox.2015.10.006
- Murtaugh, M. A., Ma, K.-N., Benson, J., Curtin, K., Caan, B., and Slattery, M. L. (2004). Antioxidants, carotenoids, and risk of rectal cancer. *Am. J. Epidemiol.* 159, 32–41. doi: 10.1093/aje/kwh013
- Nair, J., Gansauge, F., Beger, H., Dolara, P., Winde, G., and Bartsch, H. (2006). Increased etheno-DNA adducts in affected tissues of patients suffering from Crohn's disease, ulcerative colitis, and chronic pancreatitis. *Antioxid. Redox Signal.* 8, 1003–1010. doi: 10.1089/ars.2006.8.1003
- Niedernhofer, L. J., Daniels, J. S., Rouzer, C. A., Greene, R. E., and Marnett, L. J. (2003). Malondialdehyde, a product of lipid peroxidation, is mutagenic in human cells. *J. Biol. Chem.* 278, 31426–31433. doi: 10.1074/jbc.M212549200
- Nishikawa, A., Furukawa, F., Kasahara, K.-I., Ikezaki, S., Itoh, T., Suzuki, T., et al. (2000). Trans-4-hydroxy-2-nonenal, an aldehydic lipid peroxidation product, lacks genotoxicity in lacI transgenic mice. *Cancer Lett.* 148, 81–86. doi: 10.1016/S0304-3835(99)00318-3
- O'Shea, J. J., and Murray, P. J. (2008). Cytokine signaling modules in inflammatory responses. *Immunity* 28, 477–487. doi: 10.1016/j.immuni.2008.03.002
- Oz, H. S., Chen, T. S., McClain, C. J., and de Villiers, W. J. (2005). Antioxidants as novel therapy in a murine model of colitis. *J. Nutr. Biochem.* 16, 297–304. doi: 10.1016/j.jnutbio.2004.09.007
- Perse, M. (2013). Oxidative stress in the pathogenesis of colorectal cancer: cause or consequence? *Biomed. Res. Int.* 2013:725710. doi: 10.1155/2013/725710
- Pierre, F., Peiro, G., Taché, S., Cross, A. J., Bingham, S. A., Gasc, N., et al. (2006). New marker of colon cancer risk associated with heme intake: 1, 4-dihydroxynonane mercapturic acid. *Cancer Epidemiol. Prev. Biomarkers* 15, 2274–2279. doi: 10.1158/1055-9965.EPI-06-0085
- Piskounova, E., Agathocleous, M., Murphy, M. M., Hu, Z., Huddleston, S. E., Zhao, Z., et al. (2015). Oxidative stress inhibits distant metastasis by human melanoma cells. *Nature* 527, 186–191. doi: 10.1038/nature15726
- Poli, G., Schaur, R. J., Siems, W. a., and Leonarduzzi, G. (2008). 4-Hydroxynonenal: a membrane lipid oxidation product of medicinal interest. *Med. Res. Rev.* 28, 569–631. doi: 10.1002/med.20117
- Pot, G. K., Geelen, A., van Heijningen, E. M. B., Siezen, C. L., van Kranen, H. J., and Kampman, E. (2008). Opposing associations of serum n-3 and n-6 polyunsaturated fatty acids with colorectal adenoma risk: an endoscopy-based case-control study. *Int. J. Cancer* 123, 1974–1977. doi: 10.1002/ijc.23729
- Rashvand, S., Somi, M. H., Rashidkhani, B., and Hekmatdoost, A. (2015). Dietary fatty acid intakes are related to the risk of ulcerative colitis: a case-control study. *Int. J. Color. Dis.* 30, 1255–1260. doi: 10.1007/s00384-015-2232-8
- Reddy, B. S., Tanaka, T., and Simi, B. (1985). Effect of different levels of dietary trans fat or corn oil on azoxymethane-induced colon carcinogenesis in F344 rats. *J. Natl. Cancer Inst.* 75, 791–798.
- Rezaie, A., Parker, R. D., and Abdollahi, M. (2007). Oxidative stress and pathogenesis of inflammatory bowel disease: an epiphenomenon or the cause? *Dig. Dis. Sci.* 52, 2015–2021. doi: 10.1007/s10620-006-9622-2
- Saygili, E., Konukoglu, D., Papila, C., and Akcay, T. (2003). Levels of plasma vitamin E, vitamin C, TBARS, and cholesterol in male patients with colorectal tumors. *Biochem. Mosc.* 68, 325–328. doi: 10.1023/A:1023010418230
- Sayin, V. I., Ibrahim, M. X., Larsson, E., Nilsson, J. A., Lindahl, P., and Bergo, M. O. (2014). Antioxidants accelerate lung cancer progression in mice. *Sci. Transl. Med.* 6:221ra15. doi: 10.1126/scitranslmed.3007653
- Sekirov, I., Russell, S. L., Antunes, L. C. M., and Finlay, B. B. (2010). Gut microbiota in health and disease. *Physiol. Rev.* 90, 859–904. doi: 10.1152/physrev.00045.2009
- Sharma, R. A., Ireson, C. R., Verschöyle, R. D., Hill, K. A., Williams, M. L., Leuratti, C., et al. (2001). Effects of dietary curcumin on glutathione S-transferase and malondialdehyde-DNA adducts in rat liver and colon mucosa: relationship with drug levels. *Clin. Cancer Res.* 7, 1452–1458.
- Shoda, R., Matsueda, K., Yamato, S., and Umeda, N. (1996). Epidemiologic analysis of Crohn disease in Japan: increased dietary intake of n-6 polyunsaturated fatty acids and animal protein relates to the increased incidence of Crohn disease in Japan. *Am. J. Clin. Nutr.* 63, 741–745. doi: 10.1093/ajcn/63.5.741
- Siegel, R. L., Miller, K. D., Goding Sauer, A., Fedewa, S. A., Butterly, L. F., Anderson, J. C., et al. (2020). Colorectal cancer statistics, 2020. *CA Cancer J. Clin.* 70, 145–164. doi: 10.3322/caac.21601
- Sies, H., Berndt, C., and Jones, D. P. (2017). Oxidative stress. *Annu. Rev. Biochem.* 86, 715–748. doi: 10.1146/annurev-biochem-061516-045037
- Skrzydłowska, E., Sulkowski, S., Koda, M., Zalewski, B., Kanczuga-Koda, L., and Sulkowska, M. (2005). Lipid peroxidation and antioxidant status in colorectal cancer. *World J. Gastroenterol.* 11:403. doi: 10.3748/wjg.v11.i3.403
- Strassburg, K., Esser, D., Vreeken, R. J., Hankemeier, T., Müller, M., van Duynhoven, J., et al. (2014). Postprandial fatty acid specific changes in circulating oxylipins in lean and obese men after high-fat challenge tests. *Mol. Nutr. Food Res.* 58, 591–600. doi: 10.1002/mnfr.201300321
- Surinēnaitė, B., Prasmickienė, G., Milašienė, V., Stratilovas, E., and Didžiapetrienė, J. (2009). The influence of surgical treatment and red blood cell transfusion on changes in antioxidative and immune system parameters in colorectal cancer patients. *Medicina* 45:785. doi: 10.3390/medicina45100102
- Terzić, J., Grivennikov, S., Karin, E., and Karin, M. (2010). Inflammation and colon cancer. *Gastroenterology* 138, 2101.e2105–2114.e2105. doi: 10.1053/j.gastro.2010.01.058
- Tjonneland, A., Overvad, K., Bergmann, M., Nagel, G., Linseisen, J., Hallmans, G., et al. (2009). Linoleic acid, a dietary n-6 polyunsaturated fatty acid, and the aetiology of ulcerative colitis: a nested case-control study within a European prospective cohort study. *Gut* 58, 1606–1611. doi: 10.1136/gut.2008.169078
- Tüzün, S., Yücel, A. F., Pergel, A., Kemik, A. S., and Kemik, Ö. (2012). Lipid peroxidation and transforming growth factor-β1 levels in gastric cancer at pathologic stages. *Balkan Med. J.* 29:273. doi: 10.5152/balkanmedj.2012.026
- Van Kuijk, F. J., Holte, L. L., and Dratz, E. A. (1990). 4-Hydroxyhexenal: a lipid peroxidation product derived from oxidized docosahexaenoic acid. *Biochim. Biophys. Acta* 1043, 116–118. doi: 10.1016/0005-2760(90)90118-h
- Veza, T., Rodríguez-Nogales, A., Algieri, F., Utrilla, M. P., Rodríguez-Cabezas, M. E., and Galvez, J. (2016). Flavonoids in inflammatory bowel disease: a review. *Nutrients* 8:211. doi: 10.3390/nu8040211
- Vila, A., Tallman, K. A., Jacobs, A. T., Liebler, D. C., Porter, N. A., and Marnett, L. J. (2008). Identification of protein targets of 4-hydroxynonenal using click chemistry for ex vivo biotinylation of azido and alkynyl derivatives. *Chem. Res. Toxicol.* 21, 432–444. doi: 10.1021/tx700347w
- Wang, Y., Dattmore, D. A., Wang, W., Pohnert, G., Wolfram, S., Zhang, J., et al. (2020). Trans, trans-2, 4-Decadienal, a lipid peroxidation product, induces inflammatory responses via Hsp90- or 14-3-3ζ-dependent mechanisms. *J. Nutr. Biochem.* 76:108286. doi: 10.1016/j.jnutbio.2019.108286
- Wang, R., Kern, J. T., Goodfriend, T. L., Ball, D. L., and Luesch, H. (2009). Activation of the antioxidant response element by specific oxidized metabolites of linoleic acid. *Prostaglandins Leukot. Essent. Fat. Acids* 81, 53–59. doi: 10.1016/j.plefa.2009.04.008
- Wang, Y., Wang, W., Yang, H., Shao, D., Zhao, X., and Zhang, G. (2019a). Intraperitoneal injection of 4-hydroxynonenal (4-HNE), a lipid peroxidation product, exacerbates colonic inflammation through activation of toll-like receptor 4 signaling. *Free Radic. Biol. Med.* 131, 237–242. doi: 10.1016/j.freeradbiomed.2018.11.037
- Wang, W., Yang, J., Edin, M. L., Wang, Y., Luo, Y., Wan, D., et al. (2019b). Targeted metabolomics identifies the cytochrome P450 monooxygenase eicosanoid pathway as a novel therapeutic target of colon tumorigenesis. *Cancer Res.* 79, 1822–1830. doi: 10.1158/0008-5472.CAN-18-3221
- Wang, X., Yang, Y., and Huycke, M. M. (2015). Commensal bacteria drive endogenous transformation and tumour stem cell marker expression through a bystander effect. *Gut* 64, 459–468. doi: 10.1136/gutjnl-2014-307213
- Wang, X., Yang, Y., Moore, D. R., Nimmo, S. L., Lightfoot, S. A., and Huycke, M. M. (2012). 4-Hydroxy-2-nonenal mediates genotoxicity and bystander effects caused by *Enterococcus faecalis*-infected macrophages. *Gastroenterology* 142, 543.e547–551.e547. doi: 10.1053/j.gastro.2011.11.020

- Wu, B., Iwakiri, R., Ootani, A., Tsunada, S., Fujise, T., Sakata, Y., et al. (2004). Dietary corn oil promotes colon cancer by inhibiting mitochondria-dependent apoptosis in azoxymethane-treated rats. *Exp. Biol. Med.* 229, 1017–1025. doi: 10.1177/153537020422901005
- Zhong, H., and Yin, H. (2015). Role of lipid peroxidation derived 4-hydroxynonenal (4-HNE) in cancer: focusing on mitochondria. *Redox Biol.* 4, 193–199. doi: 10.1016/j.redox.2014.12.011
- Zock, P. L., and Katan, M. B. (1998). Linoleic acid intake and cancer risk: a review and meta-analysis. *Am. J. Clin. Nutr.* 68, 142–153. doi: 10.1093/ajcn/68.1.142

**Conflict of Interest:** The authors declare that the research was conducted in the absence of any commercial or financial relationships that could be construed as a potential conflict of interest.

Copyright © 2021 Lei, Zhang, Decker and Zhang. This is an open-access article distributed under the terms of the Creative Commons Attribution License (CC BY). The use, distribution or reproduction in other forums is permitted, provided the original author(s) and the copyright owner(s) are credited and that the original publication in this journal is cited, in accordance with accepted academic practice. No use, distribution or reproduction is permitted which does not comply with these terms.



# Protein Lipidation by Palmitoylation and Myristoylation in Cancer

Chee Wai Fhu\* and Azhar Ali\*

Cancer Science Institute of Singapore, National University of Singapore, Singapore

## OPEN ACCESS

### Edited by:

Yong Liu,  
Xuzhou Medical University, China

### Reviewed by:

Ji Cao,  
Zhejiang University, China  
Yang Sun,  
Massachusetts General Hospital and  
Harvard Medical School,  
United States

### \*Correspondence:

Chee Wai Fhu  
csifcw@nus.edu.sg  
Azhar Ali  
csiazhar@nus.edu.sg

### Specialty section:

This article was submitted to  
Cellular Biochemistry,  
a section of the journal  
Frontiers in Cell and Developmental  
Biology

**Received:** 28 February 2021

**Accepted:** 06 April 2021

**Published:** 20 May 2021

### Citation:

Fhu CW and Ali A (2021) Protein  
Lipidation by Palmitoylation  
and Myristoylation in Cancer.  
Front. Cell Dev. Biol. 9:673647.  
doi: 10.3389/fcell.2021.673647

Posttranslational modification of proteins with lipid moieties is known as protein lipidation. The attachment of a lipid molecule to proteins endows distinct properties, which affect their hydrophobicity, structural stability, localization, trafficking between membrane compartments, and influences its interaction with effectors. Lipids or lipid metabolites can serve as substrates for lipidation, and the availability of these lipid substrates are tightly regulated by cellular metabolism. Palmitoylation and myristoylation represent the two most common protein lipid modifications, and dysregulation of protein lipidation is strongly linked to various diseases such as metabolic syndromes and cancers. In this review, we present recent developments in our understanding on the roles of palmitoylation and myristoylation, and their significance in modulating cancer metabolism toward cancer initiation and progression.

**Keywords:** protein lipidation, palmitoylation, myristoylation, depalmitoylation, metabolism, cancer

## INTRODUCTION

The hallmarks of cancer are characterized by biological properties, which include continuous proliferation, resistance to apoptosis, metastasis and epithelial mesenchymal transition, sustained angiogenesis, and metabolic reprogramming (Hanahan and Weinberg, 2011). Cancer phenotypes are attributed by the function of oncoproteins affected by posttranslational modifications (PTMs) in tumor cells (Lothrop et al., 2013). PTMs alter subcellular localization, stability, and activity of protein molecules. Multiple classes of PTMs have been identified in mammalian cells including phosphorylation, acetylation, sumoylation, and lipidation (Lothrop et al., 2013; Blanc et al., 2015). Protein lipidation, one of the most important and diverse classes of PTMs, can reversibly or irreversibly attach up to six different lipid types including fatty acids, isoprenoids, sterols, phospholipids, glycosylphosphatidylinositol (GPI) anchors, and lipid-derived electrophiles (LDEs) to proteins. Protein lipidation is hypothesized to be tightly regulated and may partially contribute to the pathogenesis of cancer with dysregulated lipid metabolism. Palmitoylation, myristoylation, and farnesylation are the three major lipidation processes. It is, therefore, important to understand the mechanisms, functions and pathological relevance of protein lipidation, which can ultimately lead to identification of novel therapeutic targets. In this review, we will cover the two most common protein lipidation, palmitoylation and myristoylation, and discuss their roles on cancer initiation and pathogenesis.

## PALMITOYLATION

Palmitoylation is a dynamic process where it influences protein distribution, localization, accumulation, secretion, stability, and function by altering the protein's membrane affinity.



Through specific methods such as radioactive isotope-labeled lipids or acyl-biotin exchange, early studies have identified hundreds of cancer-related protein palmitoylation (Kang et al., 2008; Yang et al., 2010; Ivaldi et al., 2012; Chen et al., 2018). These proteins can either be mono-palmitoylated or poly-palmitoylated, and the presence of palmitoylated proteins in tumor cells indicate a functional role in cancer. Palmitoylation is categorized into S-palmitoylation or the less frequently occurring O-palmitoylation and N-palmitoylation. O-palmitoylation is the addition of fatty acyl group to serine residues, while N-palmitoylation is the addition of fatty acyl group to the N-terminus. To date, a few oncoproteins are identified to be O- or N-palmitoylated where two well-known examples of O-palmitoylated proteins are Wnt and Histone H4 (Zou et al., 2011; Miranda et al., 2014), while Hedgehog proteins are N-palmitoylated (Pepinsky et al., 1998).

## S-Palmitoylation

S-palmitoylation is the major form of palmitoylation and involves the addition of fatty acyl group, usually palmitic acid, to cysteine residues of protein. In certain circumstances, other fatty acids with varied carbon lengths are utilized (Senyilmaz et al., 2015). Due to the labile nature of thioester bonds, S-palmitoylation is reversible and dynamic, and S-palmitoylated proteins can undergo cycles of palmitoylation and de-palmitoylation within seconds to hours in response to upstream signals. Some proteins are exclusively S-palmitoylated, while others undergo a combination of S-palmitoylation and an additional modification of protein lipidation such as myristoylation or farnesylation. Examples of such proteins include the Src family of kinase, p59fyn, and H-Ras (Cadwallader et al., 1994). Although S-palmitoylation was discovered several decades ago, little is known on the mechanisms and participating players involved in both palmitoylation and de-palmitoylation processes and, more importantly, the recognition of protein sequences on substrate proteins for palmitoylation. S-palmitoylation is catalyzed by a specific class of enzymes called palmitoyl S-acyltransferases (PATs). PATs family comprises 23 distinct members in mammals. Active sites of PATs contain zinc finger Asp-His-His-Cys (DHHC) domain required for palmitic acid transferring activity to substrate protein (Putilina et al., 1999). Most DHHC proteins are localized primarily to the endoplasmic reticulum (ER) and Golgi apparatus. **Figure 1** provides a simplified mechanism of action of PAT. Briefly, the Asp-His-His-Cys (DHHC) domain is critical for PAT enzymatic activity where palmitoyl-CoA reacts with the cysteine residue within the DHHC motif, forming an acyl intermediate and subsequent release of coenzyme A (CoA-SH). The fatty acid chain is then transferred directly to a substrate protein. Cysteine residues, which are located close to the DHHC domain, is essential as it anchors two zinc atoms for proper enzyme folding and function; however, it does not play any catalytic role in palmitate transfer (González Montoro et al., 2013).

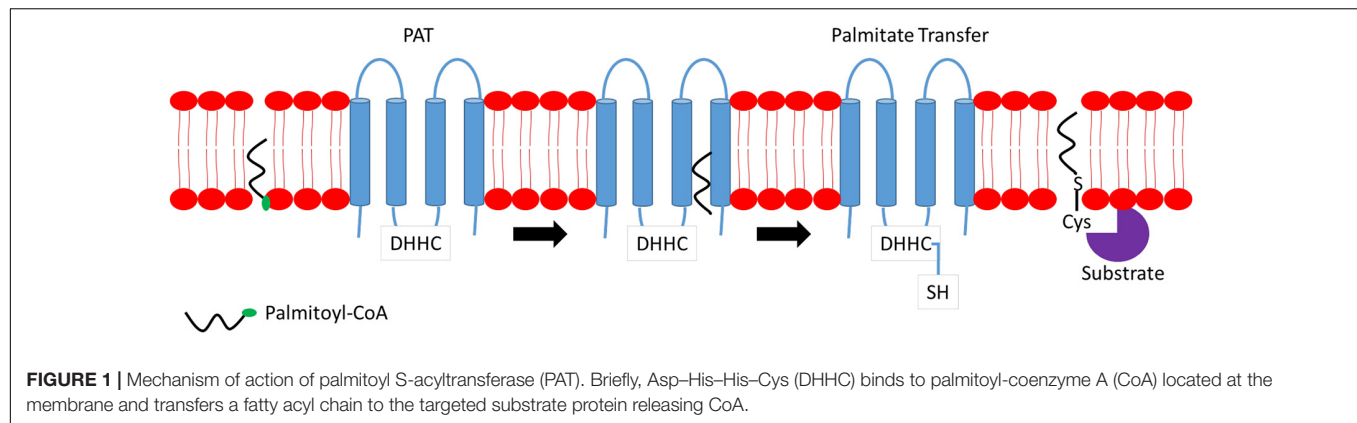
Despite the high similarity in amino acid sequences between all DHHC enzymes, each individual DHHC member exhibits distinctive differences in catalytic efficiency and fatty acyl preferences. Structural and functional studies have shown

a region in each DHHC enzyme that promotes substrate interaction and palmitoylation, thus, suggesting unique substrate-binding preferences guiding palmitoylation of certain proteins. However, the exact consensus palmitoylation sequence remains unknown, and the mechanism(s) as to how each individual DHHC enzyme selects a specific substrate for palmitoylation remains entirely unclear. S-palmitoylation is a highly specific modification process on a given protein, and it occurs on a particular internal cysteine residue. The success of palmitoylation on peripheral proteins though is dependent on DHHC-substrate binding conformation. One such example is the DHHC7-mediated scribble planar cell polarity protein (SCRIB) palmitoylation. DHHC7 palmitoylates SCRIB to promote tumorigenesis where DHHC7 is shown to interact with N-terminal leucine-rich repeat (LRR) domain of SCRIB. Site-directed mutagenesis at amino acid residue 305 from proline to leucine (P305L) at the LRR domain affects its local structure where increased binding is observed between DHHC7 and SCRIB P305L mutant. Furthermore, DHHC7 is unable to transfer palmitate acid to SCRIB P305L mutant due to its altered binding conformation (Chen et al., 2016). These observations highlight the importance of correct DHHC-substrate binding conformation for palmitoylation to occur.

Asp-His-His-Cys enzymes exhibit redundancy in substrate binding. However, each DHHC also exhibits stronger binding affinity and palmitoylation efficiency toward specific protein substrates. DHHC enzymes' substrate selection and binding are affected by three main factors. Subcellular localization is the first factor for palmitoylation to occur, a substrate protein has to be bound to the membrane and interacts with a DHHC enzyme. For certain proteins, this can be accomplished by undergoing an initial lipidation event such as prenylation and myristoylation prior to the palmitoylation process. The initial lipidation event must occur at the amino acid residue positioned in close proximity to the Cys residue(s) to be palmitoylated, thus, rendering help to the protein, which is bound weakly to the membrane and facilitating their anchoring to the DHHC enzyme. Two protein examples on the requirement of pre-lipidation event are RAS C-terminal farnesylation and Src-family N-terminal myristoylation (Willumsen et al., 1984; Hancock et al., 1991; Patwardhan and Resh, 2010). Another factor that regulates DHHC activity and expression is the presence of specific accessory or cofactor proteins. DHHC9 is shown to form a stable complex with GCP16, which helps stabilize DHHC9 in HEK293 cells. In the absence of GCP16, DHHC9 partially undergoes proteolysis. Furthermore, DHHC9 fails to S-acylate H-Ras in the absence of GCP16 suggesting that GCP16 does not only stabilizes DHHC9 but also contributes to DHHC9 S-acylation reaction (Swarthout et al., 2005).

## Depalmitoylation

S-palmitoylation is a dynamic and reversible modification process, and depalmitoylation is carried out by the enzyme cysteine deacylase. This “eraser” enzyme belongs to the family of serine hydrolases. Acyl-protein thioesterase (APT) is the first depalmitoylation enzyme identified. There are two APT paralogs – APT1 and APT2. Both isoforms are ~64% identical



and share a similar structure (Toyoda et al., 1999). However, they exhibit a different localization pattern within the cell. APT2 is a cytosolic protein, whereas APT1 is found in both cytosol and mitochondria (Kathayat et al., 2018). Different cellular distributions may contribute to the functional differences between APT1 and APT2 functions. As cytosolic proteins, APT1 and APT2 do share some common targeted proteins such as H-Ras, growth-associated protein-43 (GAP-43) (Kong et al., 2013), and NMNAT2 (Milde and Coleman, 2014). Until now, the consensus sequences flanking the thioacyl group, which is recognized by APT1/2, has not been reported. APTs do not depalmitoylate substrate proteins indiscriminately, and this is shown by failure to remove the acyl group from acylated caveolin by recombinant APT1, whereas endothelial nitric oxide synthase (eNOS) diacylation is readily noticed (Dietzen et al., 1995; Yeh et al., 1999).

Palmitoyl protein thioesterase 1 (PPT1) exhibits capability to depalmitoylate [ $^3\text{H}$ ]-palmitate-labeled H-Ras,  $\text{G}\alpha$  subunits, and acyl-CoA *in vitro*, with preference to 14–18 carbon lengths (Camp and Hofmann, 1993; Camp et al., 1994). PPT1 is a lysosomal protein and unlikely to play any role in deacylating cytoplasmic proteins (Verkruyse and Hofmann, 1996). PPT2, a lysosomal protein as well, possesses a substrate specificity for palmitoyl-CoA and not palmitoylated proteins. In recent years, a family of mammals  $\alpha/\beta$  hydrolase domain containing proteins (ABHD), comprising at least 19 members, has been proposed to be depalmitoylation enzymes. Within the ABHD family, ABHD17 hydrolase is the most well-studied protein, and it is divided into three subspecies: ABHD17A, ABHD17B, and ABHD17C, which are broadly expressed in all vertebrates and harbor multiple conserved cysteine residues near their N-termini. ABHD17 has been reported to regulate palmitate turnover on postsynaptic density protein 95 (PSD95) and N-Ras (Lin and Conibear, 2015).

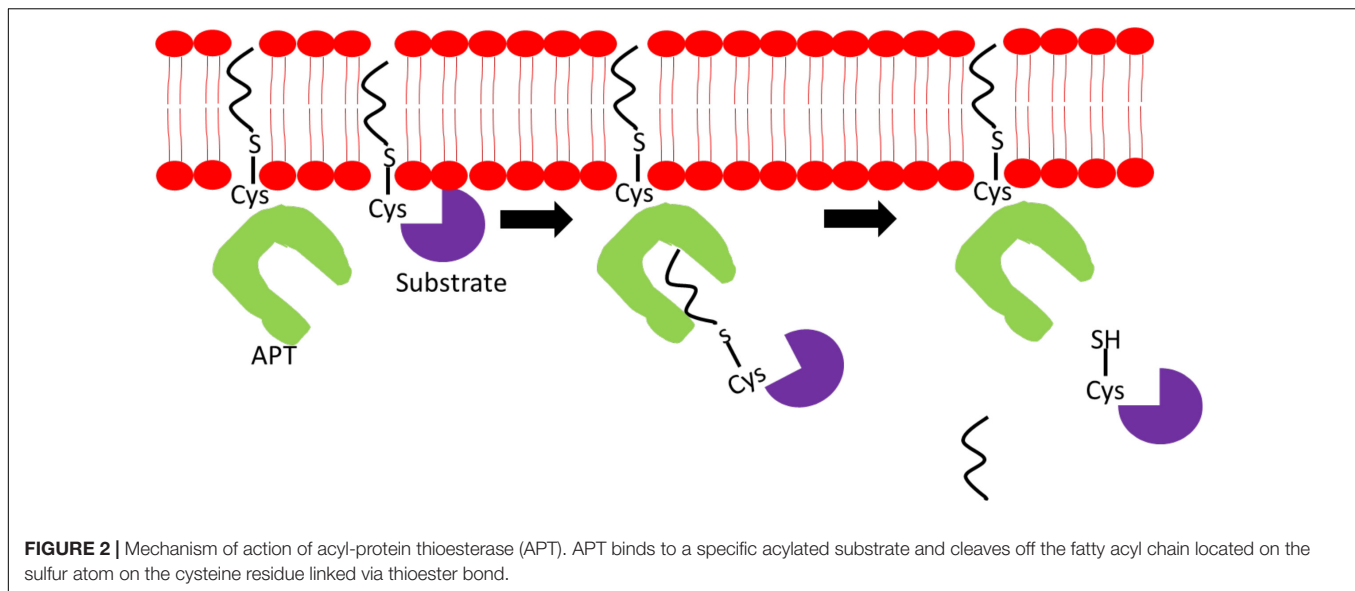
## Functional Interactions Between Palmitoylation and Depalmitoylation Enzymes

Due to the continuous cycles of protein palmitoylation and depalmitoylation to maintain optimal cellular functions, PPTs, APTs, and DHHCs have to work cooperatively and coexist in

highly complex networks. Palmitoylation of APT1/2 and ABHD-family of thioesterases is critical for their proper localization and function. Palmitoylation of APT1 and APT2, at cysteine-2 residues, facilitates their cytosol-membrane shuttling and cellular membrane anchoring to execute depalmitoylation of Ras and GAP-43 proteins. Adding further complexity to the network, APT1 also regulates APT2 palmitoylation levels but not vice versa (Kong et al., 2013). **Figure 2** illustrates a simplified mechanism of APTs' ability to deacylate substrate proteins. ABHD17A-C harbors multiple conserved cysteine residues at the N-termini, which are essential for S-palmitoylation and membrane anchoring (Martin and Cravatt, 2009). Deletion of N-terminal cysteine-rich domain has no effect on ABHD17 activity suggesting that palmitoylation is essential for its membrane localization but not enzymatic activity. Palmitoylation is shown to affect PPT1 activity, but not its localization, as demonstrated by its palmitoylation by DHHC3 and DHHC7 enzymes. Palmitoylation of mutated PPT1 at C6S did not alter its intracellular location; however, the non-palmitoylated form of PPT1 exhibited a higher depalmitoylation activity (Segal-Salto et al., 2016). Under certain conditions, a single palmitoylation process involves multiple DHHC enzymes and APTs as observed in the complex network surrounding DHHC6. To exert its function, DHHC6 requires palmitoylation by DHHC16 at three cysteine residues in its SH3\_2 domain. This acylation is required for the subsequent acylation of its substrates, calnexin and transferrin receptor, at the ER. Although palmitoylated DHHC6 possesses high acylation activity, it also contributes DHHC6 to undergo ER-regulated degradation thus providing a reason as to why DHHC6 needs to be depalmitoylated rapidly by APT2 to maintain its cellular level (Abrami et al., 2017).

## N-MYRISTOYLATION

N-myristoylation is a process involving the covalent attachment of myristate, a 14-carbon saturated fatty acid, to the N-terminal glycine residue of protein (Farazi et al., 2001). The N-myristoylation process is catalyzed by N-myristoyltransferase (NMT), which is a member of the Gcn5-related N-acetyltransferase (GNAT) superfamily. In contrast to palmitoylation, myristoylation is irreversible and can



occur co- and posttranslationally. Cotranslational myristoylation occurs when an initiator methionine residue is removed by methionine aminopeptidase, followed by the attachment of NMT-regulated myristate. The entire process occurs more efficiently when a glycine residue is located right after the initiator methionine as shown in **Figure 3A** (Frottin et al., 2006). Posttranslational myristoylation takes place when the internal glycine residue, within a cryptic myristoylation consensus sequence, is exposed by the action of caspase in apoptotic cells as shown by **Figure 3B** (Zha et al., 2000). Similar to S-palmitoylation, N-myristoylation is critical for subcellular targeting, protein–protein and protein–membrane interactions, and is required for the activities of certain oncoproteins including Src and ADP-ribosylation factor 1 (ARF1) (Liu et al., 2009; Patwardhan and Resh, 2010). Although protein myristoylation is necessary for membrane binding, it must be augmented with additional downstream modification for enhanced membrane anchoring (Peitzsch and McLaughlin, 1993; Shahinian and Silviu, 1995). A well-known example would be the Src family of kinases, in which Src protein requires both myristoylation and palmitoylation to accurately position itself at the cellular membrane, and myristoylation is shown to be a prerequisite for palmitoylation to occur (Alland et al., 1994; Koegl et al., 1994). While myristoylation modification is irreversible, acylated proteins can bind reversibly to membrane owing to its weak hydrophobic nature. The half-life of a myristoylated protein bound to membrane is in the order of minutes, in contrast to hours for palmitoylated or double (myristoylated and palmitoylated) modified protein (Martin et al., 2011). It is postulated that the orientation of myristoyl moiety within the protein is highly dynamic. N-myristoylated protein can exist in two conformations where the myristoyl moiety is either sequestered in a hydrophobic pocket within the protein or flipped out and exposed to participate in membrane binding. The transition between these two conformations is regulated by a “myristoyl switch.” “Myristoyl switch” is categorized into three

classes: ligand binding, electrostatic, and proteolysis. Recoverin is a calcium-binding protein in retina that regulates the phosphorylation of photoexcited rhodopsin through rhodopsin kinase inhibition. In a calcium-free environment, the myristoyl group is sequestered in a hydrophobic pocket where calcium-binding induces a conformational change within recoverin and releases myristate for membrane binding (Tanaka et al., 1995).

Another factor that influences myristoyl group–membrane binding is electrostatic charge. Myristoylated alanine-rich c-kinase substrate (MARCKS) protein is a substrate of protein kinase C (PKC) where myristoylated MARCKS is displaced from the membrane upon phosphorylation by PKC. MARCKS phosphorylation, occurring within the basic domain, introduces negative charge to the positively charged region. This reduces interaction between the positively charged myristoylated region of protein and negatively charged acidic phospholipids thus leading to its removal from the membrane (Thelen et al., 1991). The significance of electrostatic charge on membrane-binding Src is demonstrated where myristoylation of Src contributes to its strong affinity binding to plasma membrane. The strength of this interaction is ~2,500-fold higher when binding occurs on vesicles with membranes containing a physiological ratio of 2:1 phosphatidylcholine (PC)/phosphatidylserine (PS) than the neutral PC bilayer. Src mutants, with basic residues at the amino terminus replaced by neutral asparagine, exhibit a significant reduction in interaction strength (Sigal et al., 1994). The final factor affecting myristoylated protein–membrane interaction is the myristoyl–proteolytic switch. An example to illustrate this modification is the human immunodeficiency virus type I gene (HIV-1) Pr55<sup>gag</sup>. Pr55<sup>gag</sup> is directed to the plasma membrane by a myristate with basic motif (Zhou et al., 1994). Myristoylation at the N-terminal, together with the highly basic region, is critical to acid phospholipid membrane binding. Pr55<sup>gag</sup> is cleaved by HIV-1 protease to yield N-terminal cleavage product, P17MA. This cleavage process triggers myristoyl switch where the myristate group is found sequestered in P17MA, thus,



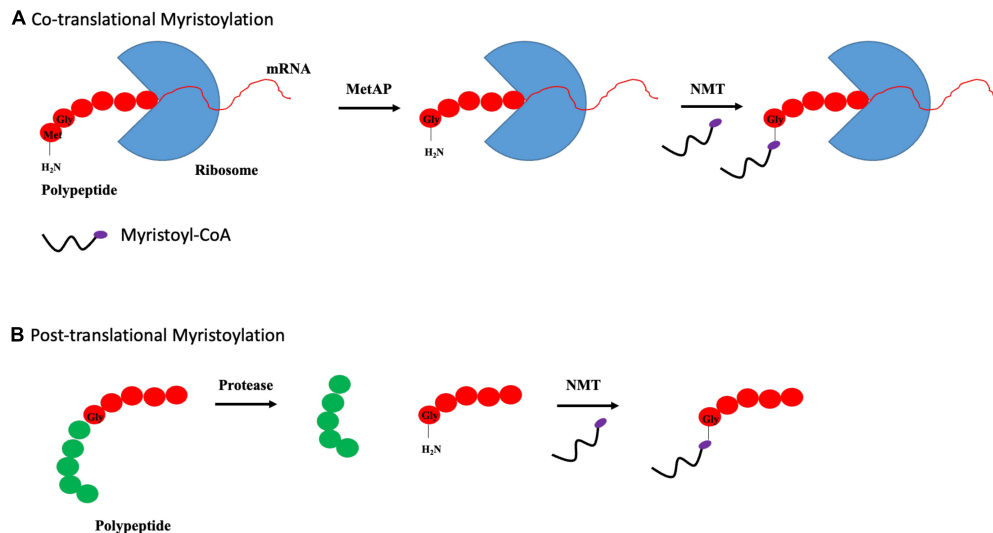


**FIGURE 3 |** Types of myristoylation. **(A)** Schematic illustration of steps involved in cotranslational myristoylation. During cotranslational myristoylation, the myristoyl group is added to the N-terminal glycine residue following cleavage of the N-terminal methionine residue on the growing polypeptide chain. **(B)** Posttranslational myristoylation normally occurs following caspase cleavage event, resulting in the exposure of internal glycine residue, which allows myristic acid addition.

rendering low binding affinity to the membrane (Hermida-Matsumoto and Resh, 1999). This feature is highly critical for the infectivity of HIV virus.

## N-Myristoyltransferase

N-myristoylation is catalyzed by the enzyme N-myristoyltransferase (NMT). The mechanism of action by NMT, in *Saccharomyces cerevisiae*, shows that this enzyme performs its catalyst activity via an ordered Bi-bi reaction. Myristoyl-CoA first binds to NMT followed by a peptide substrate and subsequent transfer of myristyl-CoA to N-terminal glycine residue of substrate. CoA molecule and myristoylated protein are then released from NMT at the end of the process (Rudnick et al., 1991). Two human NMT isoforms have been identified, namely, NMT1 and NMT2, and they share ~77% amino acid sequence similarity (Giang and Cravatt, 1998). Similar to DHHC, both NMTs exhibit distinctive differences in function and demonstrate a certain degree of functional redundancy. This is clearly shown by NMT1 knock-out ( $NMT^{-/-}$ ) mice suggesting that NMT1 is critical for early embryonic development. Intercross of NMT heterozygous mice did not produce any  $NMT^{-/-}$  offspring as  $NMT^{-/-}$  embryos died between embryonic days 3.5 and 7.5, and heterozygotes offspring were born at a lesser frequency. Furthermore,  $NMT^{-/-}$  embryonic stem (ES) cells revealed that, although NMT2 isoform was detected in ES cells, total NMT activity was greatly reduced by ~95%. These data suggest that NMT2 expression does not compensate for loss of NMT1 during embryogenesis (Yang et al., 2005). NMT1 and NMT2 share redundant and specific effects on protein processing, apoptosis, and cellular proliferation. Specific small interfering RNAs (siRNAs) against each individual NMT isoform can reduce the expressions of both NMT isoforms by at least 90%, respectively. Ablation of NMT1, but not

NMT2 expression, can suppress cellular proliferation through reduced Src activation and signaling *in vitro* and *in vivo* models. However, suppression of both NMT1 and NMT2 can induce apoptotic effect on ovarian cancer cell line, SK-OV-3, with NMT2 inhibition showing greater apoptotic effect compared with NMT1 (Ducker et al., 2005).

N-myristoyltransferases possess preferential fatty acyl substrate specificities where 14-carbon chain myristoyl-CoA is the preferred substrate. It is noteworthy to mention that palmitoyl-CoA can also bind to NMT with approximately the same Michaelis constant ( $K_m$ ) value as myristoyl-CoA; however, palmitoyl-CoA is not transferred to proteins by NMT. It is intriguing how NMT selects myristoyl-CoA over palmitoyl-CoA, which exhibits similar binding affinity and higher intracellular concentrations (palmitoyl-CoA is ~5- to 20-fold higher). Structural analyses of various fatty acyl-CoA analogs show that the geometry of enzyme's acyl-CoA binding site requires the acyl chain of active substrate to acquire a bend confirmation within the C5 vicinity. Furthermore, the distance between C1 and bend is critical for optimal positioning of acyl-CoA for peptide substrate binding through ordered Bi-bi reaction mechanism (Rudnick et al., 1992). Additionally, carbon chain length of fatty acyl-CoA rather than hydrophobicity plays a determinant role in NMT substrate selection (Heuckeroth et al., 1988). Together, these data demonstrate that myristoyl-CoA is the preferred substrate for NMT instead of palmitoyl-CoA.

## Lysine Acylation and Deacylation

Lysine residue was first discovered to be myristoylated on the membrane-bound precursors of cytokine interleukin 1- $\alpha$  (IL-1) and tumor necrosis factor- $\alpha$  (TNF- $\alpha$ ) about 30 years ago (Stevenson et al., 1992, 1993). Apart from myristoylation, recent findings revealed that lysine residues can be palmitoylated, and

lysine fatty acylation has garnered much attention over the years due to the diverse functions of lysine fatty acylation (Wilson et al., 2011). Until now, protein candidates, which are responsible for lysine fatty acylation or de-acylation are still unknown. There are numerous ongoing studies to identify the players involved in the lysine acylation process. Recently, an unexpected function of NMT1 and NMT2 was reported where they were found to efficiently myristoylate lysine 3 residue on ARF6. This step is essential for ARF6 attachment to the membrane during GTPase cycle. More importantly, this study shows that Sirtuin (Sirt) 2 can remove the myristoyl group from lysine residue on ARF6 suggesting a complex network of NMT/Sirt2-ARF6 regulatory network in GTPase cycle (Kosciuk et al., 2020). Sirtuin belongs to the family of seven NAD-dependent deacetylases that remove the acetyl group from acetylated histone. However, it was reported in *in vitro* assays that deacetylase activity in certain members of the Sirt family is weak, and they are more catalytically efficient toward long-chain peptide substrate (myristoylated) compared with acetylated peptide substrate (Jiang et al., 2013; Feldman et al., 2015).

The physiology significance of Sirt deacetylase activity started after the discovery of its involvement in demyristoylating a lysine residue in TNF- $\alpha$  maturation and extracellular secretion. Sirt 6 is shown to hydrolyze the myristoyl group of both lysine 19 (K19) and 20 (K20), which helps in matured TNF- $\alpha$  secretion (Jiang et al., 2013). Replacement of K19 and K20 with arginine affects TNF- $\alpha$  secretion, which is promoted by Sirt 6 deacylation activity. Progressively, the candidates for Sirt deacetylase activity are shown to include K-Ras 4a (Jing et al., 2017) and RalB (Spiegelman et al., 2019); the diacylation of these proteins play essential roles in cancer progression.

Interestingly, findings *in vitro* demonstrates reciprocal regulation of deacetylation, and diacylation showed that the addition of long-chain fatty acid such as palmitic and myristoylic acid can stimulate Sirt 6 deacetylated activity on H3K9Ac. A detailed steady-state inhibition analysis revealed that myristoylic acid competes with the myristoylated peptide for the same binding pocket on Sirt 6, which eventually led to a lower demyristoylation activity. Binding of myristoylic acid to

Sirt 6 also contributes to conformational changes, thus, allowing efficient deacetylation (Feldman et al., 2013).

## PALMITOYLATION AND N-MYRISTOYLATION IN CANCER

Palmitoylation and myristoylation are shown to play crucial roles in cancer progression as demonstrated by past studies investigating the roles of DHHCs, APTs, and NMTs in aberrant activation of oncogenic signaling networks such as Src and Ras, among others. The aberrant oncogene signaling confers a more aggressive, and imparts a higher proliferative, capacity of cancer cells. However, the impact of palmitoylation or myristoylation on cancer metabolism such as mitochondrial respiration, glycolysis, and fatty acid oxidation (FAO) are not well documented. Cancer metabolism has now garnered attention since its inclusion as a hallmark of cancer (Hanahan and Weinberg, 2011). Cancer metabolism is highly dynamic and complex, and disruption of an arm of a metabolic process can shift the entire cellular metabolism in an attempt to maintain a new equilibrium for survival. Cancer lipid metabolism is also found to play an essential link between lipid synthesis and lipid consumption by providing the building blocks required for membrane synthesis as well as lipid moieties for protein lipidation. Hence, we will discuss the impact of protein lipidation on cancer metabolism in this review.

### Palmitoylation/Depalmitoylation and Cancer Metabolism

Due to technological advances in research, the list of identified palmitoylated proteins is growing (Table 1). Proteins that can be palmitoylated are shown to span across various categories including proteins involved in cellular metabolic regulation particularly mitochondrial proteins. Hence, factors that can influence metabolic protein palmitoylation are postulated to affect cancer cell respiration as well. Cellular metabolism is tightly dependent on various variables such as nutrient uptake, morphology of mitochondria, and metabolic enzyme

**TABLE 1 |** Summary of palmitoylation and depalmitoylation involvement in cancer metabolism.

Target protein	Modification	Enzymes	Consequences	References
CD36	Palmitoylation	DHHC4 and DHHC5	Increased fatty acid uptake and fatty acid oxidation	Zhao et al., 2018; Wang et al., 2019
Erx	Palmitoylation	DHHC7 and DHHC21	Increased glucose uptake	Pedram et al., 2012; Garrido et al., 2013
GLUT4	Palmitoylation	DHHC7	Increased glucose uptake	Ren et al., 2015
KRAS4A	Depalmitoylation	Unknown	Increased glycolytic flux	Amendola et al., 2019
TMX-1	Palmitoylation	Unknown	Increased mitochondrial respiration and ATP production	Raturi et al., 2016
CKAP4	Palmitoylation	DHHC2	Increased basal mitochondrial respiration and maximal respiratory activity	Zhang et al., 2008; Harada et al., 2020
DRP-1	Palmitoylation	DHHC13	Increased oxidative phosphorylation	Napoli et al., 2017
Mitochondrial EGFR	Palmitoylation	Unknown	Increased mitochondrial fusion	Bollu et al., 2014
PRDX5	Depalmitoylation	ABHD10	Increased mitochondrial redox buffering capacity	Cao et al., 2019
Malonyl CoA-acyl carrier protein transacylase and Catenin delta-a	Palmitoylation	DHHC13	Decreased mitochondrial function and increased oxidative stress	Shen et al., 2017

activities. Hepatic cell plays an important role in metabolizing lipids in the body. Palmitoyltransferases DHHC4 and DHHC5 regulate fatty acid uptake by palmitoylating and targeting CD36 to the plasma membrane. DHHC4 is shown localized at the Golgi apparatus, while DHHC5 can be found at the plasma membrane. Depletion of either DHHC4 or 5 disrupts fatty acid uptake capability of adipose tissues. Furthermore, both DHHC4 knock-out or adipose-specific DHHC5 knock-out mice exhibit reduced fatty acid uptake. DHHC4 and DHHC5 isoforms are not functionally redundant and do not share a similar localization pattern within the cell (Wang et al., 2019). Prior progressing into liver cancer, non-alcoholic steatohepatitis (NASH) features abnormal lipid metabolism with palmitoylated CD36 upregulation. CD36 functions as a fatty acid transporter, and its expression is significantly enhanced at cellular plasma membrane in NASH samples. In the NASH mouse model, enhanced expression of membranous CD36 is linked to increased palmitoylation on CD36, which, in turn, helps CD36 trafficking and anchoring to the cellular membrane. Further validation utilizing a liver cancer cell line, HepG2, cultured under conditions with exogenous palmitic acid, shows upregulation of both CD36 mRNA expression and protein palmitoylation. CD36 palmitoylation inhibition protects mice from developing NASH. Palmitoylated CD36 enhances long-chain fatty acid binding and uptake but lowers FAO through AMPK pathway resulting in lipid accumulation in liver cancer cells. The data clearly shows that palmitoylated CD36 plays an important role in the development of NASH (Zhao et al., 2018).

Apart from fatty acid uptake and oxidation, palmitoylation influences glucose uptake as demonstrated in estrogen receptor (ER)-positive breast cancer. Both DHHC7 and 21 can palmitoylate ER $\alpha$  at cysteine 451 (Pedram et al., 2012). Using an ER-positive breast cancer cell line, MCF-7, the activation of ER $\alpha$  receptors enhance glucose uptake through GLUT4 membrane translocation to fulfill the energy demand of highly proliferative tumor cells. Stimulation of ER $\alpha$  by 17 $\beta$ -estradiol promotes ER $\alpha$  membrane translocation and its concomitant depalmitoylation, and allows its dissociation from the plasma membrane to interact with proximal kinases, PI3K/Akt. Activated ER $\alpha$  interacts with p85 $\alpha$ , a key member of the insulin-signaling cascade, and forms a complex capable of inducing Akt activation through Ser473 phosphorylation. This eventually leads to GLUT4 membrane translocation and enhances cellular glucose uptake that can be inhibited using PI3K/Akt-specific inhibitor, LY294002 (Garrido et al., 2013). Interestingly, direct GLUT4 palmitoylation, at Cys223, induces GLUT4 membrane translocation and improves glucose uptake in 3T3 cell line (Ren et al., 2015). DHHC7 has been subsequently identified to be the PAT responsible for GLUT4 palmitoylation (Du et al., 2017). Palmitoylation also regulates hexokinase 1 (HK1) activity in glycolysis. Depalmitoylation of KRAS4A, at cysteine 180 residue, is crucial for HK1 association at the outer mitochondria membrane (OMM). Palmitoylation-deficient KRAS4A mutant and 2-BP treatment reduce KRAS4A-HK1 association at the OMM. KRAS4A-HK1 association ameliorates the inhibitory effect of 2-deoxyglucose (2-DG) on HK-1

suggesting a functional role of KRAS4A-HK1 association. Binding of KRAS4A to HK1 is shown to boost HK1 activity, induces higher glycolytic flux with both glucose consumption, and basal extracellular acidification rates are elevated significantly (Amendola et al., 2019).

Cancer metabolism is highly dependent on the physiological state of the mitochondria. The mitochondrion and endoplasmic reticulum (ER) are connected through sites called mitochondrial-associated membrane (MAM). MAM is important for the regulation of Ca<sup>2+</sup> flux between ER and mitochondrion to achieve optimal cellular function and mitochondrial ATP production. ER-localized thioredoxin-related transmembrane protein (TMX) is shown to localize at MAM sites in a palmitoylation-dependent manner. Comparisons between wild type and mutated TMX, with altered putative palmitoylated sites, revealed that altered dual palmitoylation sequence reduces mutant TMX level in the MAM from >50% to <20%. Furthermore, inhibition of TMX palmitoylation using 2-bromopalmitate (2-BP) diminishes TMX levels at MAM sites (Lynes et al., 2012). These observations are supported in a separate study where palmitoylated TMX-1 is observed to interact with SERCA2b in a calnexin-dependent manner to regulate Ca<sup>2+</sup> flux between the ER and the mitochondria. Modification of palmitoylated sites from cysteine to alanine on TMX-1 impairs its MAM localization and ability to interact with SERCA2b. Furthermore, suppression of TMX-1 expression induces high retention of Ca<sup>2+</sup> in the ER and low Ca<sup>2+</sup> flux to the mitochondria, which indirectly affects its metabolism through ER. Respiratory capacity of TMX-1-knocked down Hela cells is lowered by 50% when compared with scrambled. Furthermore, mitochondria capacity of the melanoma cell line, A375, is shown to be elevated by 20% when TMX-1 levels are overexpressed in these cells. TMX-1 knockdown in Hela and A375 cells is shown to significantly reduce ATP production when compared with the respective controls (Raturi et al., 2016).

Cytoskeleton-associated protein 4 (CKAP4), which is localized at MAM sites, is reported to exert its role in cellular respiration and requires palmitoylation to achieve optimal function. CKAP4 is a known substrate of DHHC2 (Zhang et al., 2008). Structural analyses of mitochondria in CKAP4 KO cells revealed significant fragmentation and attenuated mitochondrial network when compared with tubular mitochondrial reticulum in control cells. CKAP4 KO cells also exhibit increased mitochondrial number but smaller in mitochondrial sizes compared with the control. Furthermore, CKAP4 KO cells possess lower basal oxygen consumption and maximal respiration capacity, and the levels of oxidative phosphorylation-related proteins remained unchanged. CKAP4 has been proposed to regulate mitochondrial function by forming a functional complex with voltage-dependent anion-selective channel protein 2 (VDAC2). Formation of this complex, however, requires palmitoylation of CKAP4. A palmitoylation-deficient variant of CKAP4 and CKAP4<sup>C100S</sup> is shown to be incapable of binding to VDAC2 and disrupts mitochondrial function. Expression of CKAP4<sup>WT</sup> or CKAP4<sup>C100S</sup> in CKAP4 KO cells, which show abnormal mitochondrial structure and oxidative phosphorylation, can be rescued by CKAP4<sup>WT</sup> but

not CKAP<sup>C100S</sup>. These evidence highlight the importance of palmitoylation for proper CKAP4 function. Furthermore, SCID mice carrying a tumor with CKAP KO and CKAP<sup>C100S</sup> showed a significantly smaller tumor volume and mass due to reduced mitochondria size and function (Harada et al., 2020).

Palmitoylation can directly affect mitochondria protein function. 2-BP treatment is shown to shift the balance of mitochondrial fusion and fission by influencing dynamin-related protein 1 (Drp-1) and optic atrophy 1 (OPA1) levels. 2-BP relieves bone cancer pain through disruption of mitochondrial dynamics together with reduced production of proapoptotic factors and proinflammatory cytokines. In a bone cancer pain rat model (BCP) inoculated with MRMT-1 rat mammary gland carcinoma cells, proteins from spinal cord extracts showed significant upregulation of Drp-1 expression in BCP rats compared with sham, and 2-BP treatment attenuated Drp-1 levels. Conversely, OPA-1 expression is downregulated extensively in the BCP group compared with sham, and 2-BP treatment restores OPA-1 expression (Meng et al., 2019). The impact of 2-BP on Drp-1 is further shown where DHHC13 palmitoylates Drp-1 and affects its mitochondrial localization and activity (Napoli et al., 2017). *De novo* synthesis of palmitate by fatty acid synthase (FASN) is reported to contribute to mitochondrial epidermal growth factor receptor (mtEGFR) palmitoylation in mtEGFR-positive prostate and breast cancer cell lines. EGF induces *de novo* palmitate synthesis, and excessive palmitate is shown to assist mtEGFR palmitoylation, which improves its activity by enhancing phosphorylation. Activated mtEGFR promotes mitochondrial fusion by upregulating OPA-1 and prohibitin-2 (PHB-2) expressions where PHB-2 is required to protect OPA-1 from proteolysis. Palmitoylated sites on the mtEGFR have been identified to be cysteines 781, 797, 1,058, and 1,146, and through site-directed mutagenesis, C797 is found critical for both palmitoylation and phosphorylation of mtEGFR (Bollu et al., 2014).

Additionally, a new role of alpha/beta hydrolase domain-containing 10 (ABHD10) in the mitochondria has been proposed. Mitochondrial-specific pan-APT inhibitor is shown to specifically inhibit ABHD10 and affects mitochondrial redox buffering capacity. Subsequent interrogation showed that ABHD10 is a novel mitochondrial APT candidate and possesses mitochondrial S-deacylase activity *in vitro*. Perturbation of ABHD10 expression, in the form of ABHD10 overexpression, upregulates mitochondrial buffering capacity, or hydrogen peroxide lowers this capacity. Peroxiredoxin-5 (PRDX5) is shown to be the downstream target of ABDH10 where cysteine residues at position 100 of PRDX5 are identified to be sites of depalmitoylation and plays a crucial part for its activity (Cao et al., 2019).

## Myristoylation and Cancer Metabolism

Compared with palmitoylation, the available information on myristoylation and cancer respiration is scarce (Table 2). A direct relationship between myristoylation and mitochondrial respiration has yet to be established. However, a possible

**TABLE 2 |** Summary of myristoylation involvement in cancer metabolism.

Protein	Modification agent	Consequences	References
AMPK	NMT1	Increased mitophagy	Liang et al., 2015
AMPK	Unknown	Increased fatty acid oxidation	Zhang et al., 2021
SAMM50, MIC19, TOMM40, and MIC25	Unknown	Maintain mitochondrial structure	Utsumi et al., 2018
Akt	Unknown	Increased aerobic glycolysis and reduced fatty acid oxidation	Elstrom et al., 2004; Buzzai et al., 2005; Deberardinis et al., 2006
LAMTOR1	NMT1	Reduced lysosomal degradation	Chen et al., 2020

functional link between myristoylation and mitochondria has been reported where myristoylation is shown to affect AMP-activated protein kinase (AMPK) signaling and participates in mitochondrial surveillance in lung and breast cancer cell lines. When mitochondria are damaged under stress or induced by mitochondrial depolarizing agent, carbonyl cyanide 3-chlorophenylhydrazone (CCCP), an autophagy-related event termed mitophagy is initiated to recycle damaged mitochondria. AMPK is required in both autophagy and mitophagy processes. AMPK is physically shown to associate with damaged mitochondria where upon CCCP treatment, the total and T172-phosphorylated AMPK are upregulated in mitochondrial fractions. Concomitantly, recruited AMPK initiates mitophagy process through interaction with ATG16 complexes. AMPK kinase activity is required to accelerate the recruitment of ATG complex following CCCP-induced mitochondria damage. Localization of AMPK is found to be entirely dependent on myristoylation of the  $\beta$ -subunit of AMPK by NMT1. Following CCCP treatment, AMPK is completely abrogated from the mitochondria after the introduction of N-myristoylated-deficient mutant, AMPK $\beta$ 1G2A-GFP, into cells. The importance of N-myristoylation on AMPK mitochondria localization is confirmed when treatment of cells with myristoylation inhibitor, 2-hydroxymyristic acid (2-HA), suppresses AMPK $\beta$  myristoylation and affects its localization at the mitochondria membrane. These observations highlight an important role of myristoylated AMPK $\beta$  subunit for proper mitochondria localization and mitophagy process but not for non-selective autophagy (Liang et al., 2015).

A link between metabolic reprogramming and metastasis through myristoylated AMPK has been recently reported where two isogenic cell lines, one highly metastatic (HM) and the other non-metastatic (NM), were characterized for proteomic and metabolic profiles. Lipid reprogramming were observed in HM cells, and expression of ACSL-1 was significantly elevated compared with NM cells. *In vitro* and *in vivo* data suggest that enhanced expression of ACSL-1 contributes to a higher rate of proliferation and confers more tumorigenic properties. Furthermore, higher levels of ACSL-1 seen in HM cells induce a shift in lipidomic profiles through upregulating myristoylic acid production, which strongly associates with cancer progression



and metastasis. Excessive amounts of myristoylic acid boost myristoylation process on AMPK leading to AMPK pathway activation and concomitantly upregulates expression of FAO-related ACADM, ACADVL, and HAHA. To confirm that AMPK myristoylation by ACSL-1 is critical in FAO process regulation, an AMPK inhibitor, dorsomorphin, was utilized, and suppression of AMPK pathway activation failed to promote FAO protein expression even in ACSL-1-overexpressing cells (Zhang et al., 2021).

Myristoylation is critical for proper membrane localization. The same observation also applies to mitochondrial proteins. Myristoylation is detected on four mitochondrial proteins, SAMM50, TOMM40, MIC19, and MIC25, through *in vitro* and *in vivo* metabolic labeling experiments. Myristoylation of these mitochondrial proteins is important for mitochondrial membrane localization and functions as components within the mitochondrial intermembrane space-bridging complex playing a critical role in the maintenance of the mitochondria structure and function. N-myristoylation is shown to play a crucial role in mitochondrial membrane targeting for SAMM50 and MIC19 but not TOMM40 and MIC25. Data from immunoprecipitation assays suggest that MIC19 is a major N-myristoylated binding partner of SAMM50 and that the N-myristoylation of MIC19 is essential for interaction with SAMM50 (Utsumi et al., 2018).

Myristoylation of Akt is critical for its plasma membrane anchoring and confers a higher basal kinase activity. Constitutively active Akt is important to stimulate aerobic glycolysis in cancer cells. Myristoylated Akt is often found overexpressed in leukemia cell lines, and this overexpression is driven by doxycycline. Akt myristoylation can also enhance aerobic glycolysis without affecting oxidative phosphorylation. Excessive amounts of glycolytic end-products are converted to lactate and secreted. These observations suggest that Akt activity contributes to the differences in glucose metabolism rates and glucose dependency for survival. Furthermore, PI3K inhibition, which is upstream of Akt, with LY294002, reduces Akt phosphorylation, glucose consumption rate, and lactate production (Elstrom et al., 2004). Other than glycolysis, Akt myristoylation affects fatty acid metabolism in glioblastoma cells. Glioblastoma cell line, LN18, contains constitutively active Akt and is highly dependent on glucose for survival, while LN229, another glioblastoma cell line, lacks active Akt and exhibits low glucose dependence. Under glucose withdrawal condition, LN18 cell viability is greatly reduced, while LN229 cell survival remains unaffected. Forced myristoylated Akt expression in LN229 (LN229 + myr Akt) induces a metabolic shift, in which cellular viability becomes highly dependent on glucose, and glucose withdrawal greatly reduces LN229 + myr Akt cell viability. Akt activation can suppress the expression of phosphorylated AMPK at T172. Expression of phosphorylated AMPK is crucial to shift the metabolic substrate preference from glucose to fatty acid, and this allows cells to survive under glucose-deprived conditions. Furthermore, LN229 control cells exhibit higher FAO and lower rate of fatty acid synthesis when glucose is removed. However, LN229 + myr Akt cells demonstrate a reverse phenotype where treatment with an AMPK activator, 5-aminoimidazole-4-carboxamide-1- $\beta$ -D-ribofuranoside

(AICAR), improves FAO rate and cell survival rate under a glucose-depleted condition (Buzzai et al., 2005). The suppression of FAO by Akt activation has also been suggested to be a result of carnitine palmitoyltransferase 1A (CPT1A) downregulation (Deberardinis et al., 2006).

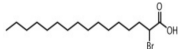
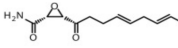
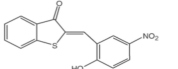
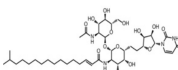
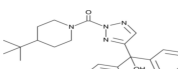
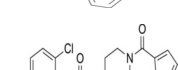
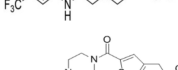
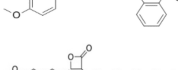
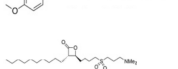
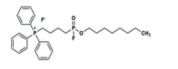
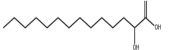
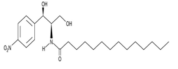
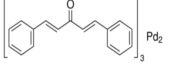
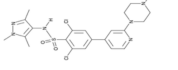
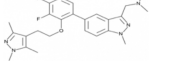
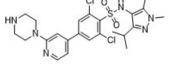
Lysosomes are complex cellular organelles involved in modulating cancer cell metabolic homeostasis. NMT1 is necessary for lysosomal degradation and mTORC1 activation in cancer cells. Knock-down of NMT1 in H460 (non-small cell lung carcinoma) and H1792 (lung adenocarcinoma) cells, without affecting the NMT2 expression, is shown to significantly reduce the autophagy flux. Furthermore, decreased NMT1 expression led to reduction in global myristoylation in tumor cells, and this contributed to weakened lysosomal degradation, accumulation of late endosomes/lysosomes, and simultaneous mTORC1 dissociation from lysosome surface leading to attenuated mTORC1 activation. Regulation of lysosomal functions by NMT1 is shown to be mediated through lysosomal adaptor, LAMTOR1. Upon NMT1 knock-down, LAMTOR1 myristoylation is downregulated significantly and failed to position itself at the lysosomal membrane, thus, disrupting mTORC1 activation. All these eventually led to slower cancer cell proliferation (Chen et al., 2020).

## TARGETING PROTEIN LIPIDATION IN CANCER

Protein lipidation plays an essential role in cancer progression and initiation, which renders it an attractive cancer therapeutic target. However, the development of anti-lipidation drugs (Table 3) face huge hurdles as illustrated by farnesylation inhibitors, which have shown strong *in vitro* antitumor activity but limited clinical success (Berndt et al., 2011). Nevertheless, several lines of evidence provide strong rationale for targeting PATs as a potential therapeutic avenue. Presently, there are no potent and specific inhibitors against DHHC proteins. 2-Bromopalmitate (2-BP), a broad-spectrum palmitoylation inhibitor, is widely used to validate the anticancer effects of DHHC preclinically. Although it is also referred to as “specific” PAT inhibitor, extensive studies have suggested otherwise. 2-BP treatment has been observed to non-selectively inactivate several types of membrane-bound enzymes including several lipid metabolism-related enzymes including triacylglycerol biosynthesis, fatty acid Co-A ligase, and glycerol-3-phosphate acyltransferase (Coleman et al., 1992) as well as deacylating enzymes, APT1 and APT2 (Pedro et al., 2013). These attributes render 2-BP to be an unreliable lead compound for further development.

The delay in the development of specific DHHC inhibitors lies on the mechanism of action and high similarity protein sequences as well as structures shared among members of the DHHC family. A large number of proteins can be palmitoylated by more than one member of DHHC enzymes. This functional redundancy suggests that specific inhibitors of individual DHHC enzymes may not be clinically useful as they may target multiple DHHC family members. This is similar to the pharmacology

**TABLE 3 |** Summary of PAT, APT, and NMT inhibitors.

Inhibitors	Blocking target	Structure	Developmental stage	References
2-BP	General depalmitoylation agent		<i>In vitro</i> study	Davda et al., 2013
Cerulenin	General depalmitoylation agent		<i>In vitro</i> and <i>in vivo</i> study	Jochen et al., 1995; Lawrence et al., 1999
Compound V	Reversible inhibitor of palmitoylation and myristoylation		<i>In vitro</i> study	Jennings et al., 2009
Tunicamycin	General depalmitoylation agent		<i>In vitro</i> study	Patterson and Skene, 1995; Hurley et al., 2000
ML211	ABHD11		<i>In vitro</i> study	Adibekian et al., 2010
ML348	APT1, IC <sub>50</sub> = 0.21 μM		<i>In vitro</i> and <i>in vivo</i> study	Adibekian et al., 2012; Vujic et al., 2016; Hernandez et al., 2017
ML349	APT2, IC <sub>50</sub> = 0.144 μM		<i>In vitro</i> and <i>in vivo</i> study	Vujic et al., 2016; Hernandez et al., 2017
Palmostatin B	APT1 and APT2, IC <sub>50</sub> = 0.67 μM (Ras depalmitoylation)		<i>In vitro</i> study	Coleman et al., 1992; Hedberg et al., 2011; Pedro et al., 2013; Vujic et al., 2016
Palmostatin M	APT1 and APT2, IC <sub>50</sub> = 2.5 nM for APT1 and IC <sub>50</sub> = 19.6 nM for APT2		<i>In vitro</i> study	Hedberg et al., 2011; Rusch et al., 2011
Mitochondrial pan-APT inhibitor, MitoFP	ABHD10		<i>In vitro</i> study	Cao et al., 2019
2-Hydroxymyristic acid	NMT, inhibitory activity observed from 100 μM to 1 mM		<i>In vitro</i> study	Paige et al., 1989, 1990
D-NMAPDD	NMT1, IC <sub>50</sub> = 77.6 μM		<i>In vitro</i> and <i>in vivo</i> study	Kim et al., 2017
Tris-DBA palladium	NMT1		<i>In vitro</i> and <i>in vivo</i> study	Bhandarkar et al., 2008
IMP-366	NMT1 and NMT2		<i>In vitro</i> and <i>in vivo</i> study	Frearson et al., 2010
IMP-1088	NMT1 and NMT2		<i>In vitro</i> study	Mousnier et al., 2018
PCLX-001	NMT1 and NMT2		<i>In vitro</i> , <i>in vivo</i> , and phase I clinical trial	Davda et al., 2013; Randeep et al., 2020; Mackey et al., 2021

of the pan-kinase inhibitor, lapatinib, which inhibits epidermal growth factor receptor and Her2/neu receptor simultaneously. A possible solution to this problem would be to develop pan-DHHC inhibitors that can block the function of several palmitoylation enzymes of a single target. Another way to overcome the limitation is to design specific small molecules targeting specific binding domains of DHHC enzymes. Such an example is the essential ankyrin repeat domains of DHHC13 and DHHC17 for substrate protein to interact and palmitoylate. An alternative method of targeting DHHC enzymes is to promote an irreversible covalent modification of individual cysteine

residue with palmitate by targeting protein structure essential for DHHC binding. An example would be the development of covalent inhibitors targeting the transcriptional enhanced associate domain (TEAD) transcription factor. Kojic acid analogs are shown to covalently target the cysteine residues at the central pocket of TEAD. This covalent binding prevents interaction between TEAD with coactivator yes-associated protein (YAP) and reduces TEAD target gene expression (Karatas et al., 2020).

In certain cases, targeting protein depalmitoylation would be more efficient than palmitoylation inhibition. APTs are generally more druggable, and inhibition of APT enzymes can suppress

tumor formation. An effort to identify novel APT inhibitors has been based on use of weight loss drug Orlistat, a prototypical serine hydrolase inhibitor, after the discovery that APTs share structural homology with gastric lipase. Structural analysis of Orlistat reveals the presence of an electrophilic  $\beta$ -lactone moiety that covalently inactivates certain serine hydrolases (Hadvary et al., 1991). Modification of  $\beta$ -lactone scaffold has led to the discovery of palmostatins, the first compound capable of preventing Ras depalmitoylation (Dekker et al., 2010). Further optimization and modification to the chemical structure of palmostatin B led to the development of a better APT inhibitor, palmostatin M. Both inhibitors bind covalently to the serine residue at the active site, thus, blocking the recognition by APTs. Pharmacological analyses of palmostatin B and palmostatin M show that these inhibitors are effective against both APT1 and APT2 without any selective preferences. Palmostatin B and palmostatin M were used to inhibit depalmitoylation of H-Ras (Hedberg et al., 2011). A new class of APT1 and APT2 inhibitors were identified recently, and these potent and non-toxic APT1/2 inhibitors were derived from boronic acid. These compounds were discovered through extensive library screening using chemical arrays, and their effectiveness were later confirmed on Ras protein depalmitoylation *in vitro*. These inhibitors act by competing with APT1/2 at binding sites on the substrate protein. The advantages of these inhibitors are that they exhibit APT isoform specificity and possess slower binding-off rates compared with palmostatin inhibitors (Zimmermann et al., 2013). Depalmitoylation inhibitors could be beneficial for anticancer treatment as most of the oncogene activity or function requires palmitoylation modification for proper localization at the cellular membrane. Furthermore, depalmitoylation inhibitors may be useful to target palmitoylation-induced cancer metabolism reprogramming shown by examples presented utilizing 2-BP. Future studies are required to fully investigate the beneficial effects of depalmitoylation inhibitors in targeting cancer progression or more specifically in targeting cancer metabolism.

N-myristoyltransferase expression and activity are found upregulated in cancers including colorectal (Magnuson et al., 1995), gallbladder (Rajala et al., 2000), and brain (Lu et al., 2005). These observations suggest that NMT expression can be used as biomarkers and a possible cancer therapeutic target. Until now, NMT inhibitors have been used extensively as antifungal agents; however, NMT as a target in cancer is still in the infancy stage. Over the years, several compounds such as 2-hydroxymyristic acid, D-NMAPDD, and Tris-DBA-palladium (Tris-DBA) complex have been utilized as NMT inhibitors in numerous studies. However, these inhibitors are deemed not to be good NMT inhibitors due to several pitfalls. 2-Hydroxymyristic acid, an NMT inhibitor, does not show inhibitory activity at concentrations below 100  $\mu$ M. Reduced N-myristoylation is only observed when 2-hydroxymyristic acid is applied at concentrations between 100  $\mu$ M and 1 mM. However, usage at such high concentrations is not favorable due to its precipitation in the culture medium and inducing cell death. Moreover, millimolar concentration is also likely to cause off-target toxicity effects as demonstrated on porcine

alveolar macrophages (Du et al., 2010). The application of D-NMAPDD is controversial as it was initially developed as an inhibitor for lysosomal acid ceramidase (Bielawska et al., 1996). D-NMAPDD exhibits NMT1 activity inhibition and reduces Src kinase myristoylation at an  $IC_{50}$  of 77.6  $\mu$ M (Kim et al., 2017). However, this observation was not reproducible in a later study by Kallemijn et al. (2019). Moreover, D-NMAPDD at 30  $\mu$ M induces a significant cytotoxic effect within 24 h of exposure by a mechanism unrelated to NMT inhibition as shown by losses of caspase 3 activation and metabolic activity (Kallemijn et al., 2019). The Tris-DBA palladium complex has been proposed to be an NMT1 inhibitor and inhibits growth of melanoma *in vitro* and *in vivo*. Furthermore, the same complex also shows promising anticancer activity against multiple myeloma (de la Puente et al., 2016), leukemia B cells (Kay et al., 2016), and prostate cancer (Dıaz et al., 2016). However, the  $IC_{50}$  of the Tris-DBA palladium complex is reported to be 4.2  $\mu$ M similar to the precipitation concentration in previous findings. It is suggested that the inhibitory effect imparted by the Tris-DBA palladium complex is due to precipitation effect rather than specific interactions. Using similar experimental settings, Kallemijn et al. (2019) failed to reproduce the NMT1 inhibitory effect of the Tris-DBA palladium complex on A375, a melanoma cell line, as shown by Bhandarkar et al. (2008) in an earlier study. Downregulation of myristoylated protein can be partly explained by the overall reduction in protein production identified through chemical proteomics.

Two small molecule inhibitors, IMP-366 and IMP-1088, were recently developed NMT inhibitors and shown to possess superior specificity. The binding mode of these inhibitors is supported by X-ray co-crystal structural analyses of human NMT1 and NMT2, which demonstrate high specificity of these inhibitors on NMTs. Later on, an improved version of IMP-366 was developed, named PCLX-001, which possessed anticancer activity preclinically. PCLX-001 is reported to possess a greater inhibitory effect in hematological malignancies but less so in solid tumor cell lines. The proposed mechanism of PCLX-001 on tumors is apoptotic cell death through the attenuation of Src myristoylation, basal Src levels, and downstream survival signaling of B-cell receptor (Beauchamp et al., 2020). Other than B-cell lymphoma, PCLX-001 has been reported to effectively kill several breast cancer cell line subtypes ranging from breast carcinoma, ductal carcinoma, and breast adenocarcinoma in both *in vitro* and *in vivo* models (Mackey et al., 2021). The encouraging preclinical data has prompted an open label phase I clinical trial in several Canadian Cancer Centres to establish the antitumor effect maximum tolerable dose of PCLX-001 in B-cell lymphoma and advanced solid tumors. Data obtained from these phase I trials will then be utilized to establish the recommended dose for phase II trial and to evaluate the safety pharmacokinetics of PCLX-001 later on (Randeep et al., 2020).

## CONCLUSION

In recent years, technological advances have provided better understanding of protein palmitoylation and myristoylation

processes. Scientists and researchers are currently exploring the possibility of targeting protein lipidation as a paradigm for cancer therapy; however, there are still some unanswered questions that requires attention. First, apart from DHHC enzymes, it is unclear if there are other enzymes capable of palmitoylating proteins. DHHC enzymes are membrane bound and localized in the ER, Golgi, and plasma membrane. However, there are other non-membrane-bound palmitoylated proteins roaming freely in cells. The recent discovery of LPCAT1, as a palmitoylating agent for histone K4, unveils the possibility of proteins functioning as non-conventional palmitoylation enzymes. Second, the degree of protein palmitoylation of a protein substrate is shown to be highly dependent on the expression and stability of DHHC enzymes as well as APTs, thus, adding further complexity of DHHC enzymes and APT network on palmitoylation. An example would be the DHHC16–DHHC6–APT2 network observed in ER protein palmitoylation. This highlights that DHHC and APT are connected to maintain optimal cellular functions. Understanding the role of each player in this network can help explore and identify possible APTs as a target when a specific inhibitor against the corresponding DHHC is unavailable. Myristoylation process, in general, is less complicated compared with palmitoylation.

## REFERENCES

- Abrami, L., Dallavilla, T., Sandoz, P. A., Demir, M., Kunz, B., Savoglidis, G., et al. (2017). Identification and dynamics of the human ZDHHC16–ZDHHC6 palmitoylation cascade. *Elife* 6:e27826. doi: 10.7554/eLife.27826
- Adibekian, A., Martin, B. R., Chang, J. W., Hsu, K. L., Tsuboi, K., Bachovchin, D. A., et al. (2012). Confirming target engagement for reversible inhibitors in vivo by kinetically tuned activity-based probes. *J. Am. Chem. Soc.* 134, 10345–10348. doi: 10.1021/ja303400u
- Adibekian, A., Martin, B. R., Speers, A. E., Brown, S. J., Spicer, T., Fernandez-Vega, V., et al. (2010). “Optimization and characterization of a triazole urea dual inhibitor for lysophospholipase 1 (LYPLA1) and lysophospholipase 2 (LYPLA2),” in *Probes Report in the NIH Molecular Libraries Program*. Bethesda, MD: National Center for Biotechnology Information (US). Available online at: <https://www.ncbi.nlm.nih.gov/books/NBK133440/>
- Alland, L., Peseckis, S. M., Atherton, R. E., Berthiaume, L., and Resh, M. D. (1994). Dual myristylation and palmitoylation of Src family member p59fyn affects subcellular localization. *J. Biol. Chem.* 269, 16701–16705.
- Amendola, C. R., Mahaffey, J. P., Parker, S. J. I., Ahearn, M., Chen, W. C., Zhou, M., et al. (2019). KRAS4A directly regulates hexokinase 1. *Nature* 576, 482–486. doi: 10.1038/s41586-019-1832-9
- Beauchamp, E., Yap, M. C., Iyer, A., Perinpanayagam, M. A., Gamma, J. M., Vincent, K. M., et al. (2020). Targeting N-myristoylation for therapy of B-cell lymphomas. *Nat. Commun.* 11:5348. doi: 10.1038/s41467-020-18998-1
- Berndt, N., Hamilton, A. D., and Sebt, S. M. (2011). Targeting protein prenylation for cancer therapy. *Nat. Rev. Cancer* 11, 775–791. doi: 10.1038/nrc3151
- Bhandarkar, S. S., Bromberg, J., Carrillo, C., Selvakumar, P., Sharma, R. K., Perry, B. N., et al. (2008). Tris (dibenzylideneacetone) dipalladium, a N-myristoyltransferase-1 inhibitor, is effective against melanoma growth in vitro and in vivo. *Clin. Cancer Res.* 14, 5743–5748. doi: 10.1158/1078-0432.CCR-08-0405
- Bielawska, A., Greenberg, M. S., Perry, D., Jayadev, S., Shayman, J. A., McKay, C., et al. (1996). (1S,2R)-D-erythro-2-(N-myristoylamino)-1-phenyl-1-propanol as an inhibitor of ceramidase. *J. Biol. Chem.* 271, 12646–12654. doi: 10.1074/jbc.271.21.12646
- Blanc, M., David, F., Abrami, L., Migliozi, D., Armand, F., Bürgi, J., et al. (2015). SwissPalm: protein Palmitoylation database. *F1000Res* 4:261. doi: 10.12688/f1000research.6464.1
- The greatest concern in targeting myristoylation will be technical challenges that prevents identification of myristoylated proteins in tumor cells. Improved structural analyses and computational approaches are, thus, paramount to accurately identify the three-dimensional structure of myristoylated proteins or NMT for inhibitor development. Furthermore, thorough studies on its efficacy and cytotoxic effect are greatly warranted when exploring the possibility of using NMT inhibitor either as a single or combination therapies against cancers.
- ## AUTHOR CONTRIBUTIONS
- CF and AA conceptualized the study and wrote and edited the manuscript. AA acquired the funding. Both authors contributed to the article and approved the submitted version.
- ## FUNDING
- This research was funded by the R713-000-216-720.
- Bollu, L. R., Ren, J., Blessing, A. M., Katreddy, R. R., Gao, G., Xu, L., et al. (2014). Involvement of de novo synthesized palmitate and mitochondrial EGFR in EGF induced mitochondrial fusion of cancer cells. *Cell Cycle* 13, 2415–2430. doi: 10.4161/cc.29338
- Buzzai, M., Bauer, D. E., Jones, R. G., Deberardinis, R. J., Hatzivassiliou, G., Elstrom, R. L., et al. (2005). The glucose dependence of Akt-transformed cells can be reversed by pharmacologic activation of fatty acid beta-oxidation. *Oncogene* 24, 4165–4173. doi: 10.1038/sj.onc.1208622
- Cadwallader, K. A., Paterson, H., Macdonald, S. G., and Hancock, J. F. (1994). N-terminally myristoylated Ras proteins require palmitoylation or a polybasic domain for plasma membrane localization. *Mol. Cell. Biol.* 14, 4722–4730. doi: 10.1128/mcb.14.7.4722
- Camp, L. A., and Hofmann, S. L. (1993). Purification and properties of a palmitoyl-protein thioesterase that cleaves palmitate from H-Ras. *J. Biol. Chem.* 268, 22566–22574.
- Camp, L. A., Verkruyse, L. A., Afendis, S. J., Slaughter, C. A., and Hofmann, S. L. (1994). Molecular cloning and expression of palmitoyl-protein thioesterase. *J. Biol. Chem.* 269, 23212–23219.
- Cao, Y., Qiu, T., Kathayat, R. S., Azizi, S. A., Thorne, A. K., Ahn, D., et al. (2019). ABHD10 is an S-depalmitoylase affecting redox homeostasis through peroxiredoxin-5. *Nat. Chem. Biol.* 15, 1232–1240. doi: 10.1038/s41589-019-0399-y
- Chen, B., Sun, Y., Niu, J., Jarugumilli, G. K., and Wu, X. (2018). Protein lipidation in cell signaling and diseases: function, regulation, and therapeutic opportunities. *Cell Chem. Biol.* 25, 817–831. doi: 10.1016/j.chembiol.2018.05.003
- Chen, B., Zheng, B., DeRan, M., Jarugumilli, G. K., Fu, J., Brooks, Y. S., et al. (2016). ZDHHC7-mediated S-palmitoylation of Scribble regulates cell polarity. *Nat. Chem. Biol.* 12, 686–693. doi: 10.1038/nchembio.2119
- Chen, Y. C., Navarrete, M. S., Wang, Y., McClintock, N. C., Sakurai, R., Wang, F., et al. (2020). N-myristoyltransferase-1 is necessary for lysosomal degradation and mTORC1 activation in cancer cells. *Sci. Rep.* 10:11952. doi: 10.1038/s41598-020-68615-w
- Coleman, R. A., Rao, P., Fogelson, R. J., and Bardes, E. S. (1992). 2-Bromopalmitoyl-CoA and 2-bromopalmitate: promiscuous inhibitors of membrane-bound enzymes. *Biochim. Biophys. Acta* 1125, 203–209. doi: 10.1016/0005-2760(92)90046-x
- Davda, D., El Azzouny, M. A., Tom, C. T., Hernandez, J. L., Majmudar, J. D., Kennedy, R. T., et al. (2013). Profiling targets of the irreversible palmitoylation



- inhibitor 2-bromopalmitate. *ACS Chem. Biol.* 8, 1912–1917. doi: 10.1021/cb400380s
- de la Puente, P., Azab, F., Muz, B., Luderer, M., Arbiser, J., and Azab, A. K. (2016). Tris DBA palladium overcomes hypoxia-mediated drug resistance in multiple myeloma. *Leuk. Lymphoma* 57, 1677–1686. doi: 10.3109/10428194.2015
- Deberardinis, R. J., Lum, J. J., and Thompson, C. B. (2006). Phosphatidylinositol 3-kinase-dependent modulation of carnitine palmitoyltransferase 1A expression regulates lipid metabolism during hematopoietic cell growth. *J. Biol. Chem.* 281, 37372–37380. doi: 10.1074/jbc.M608372200
- Dekker, F. J., Rocks, O., Vartak, N., Menninger, S., Hedberg, C., Balamurugan, R., et al. (2010). Small-molecule inhibition of APT1 affects Ras localization and signaling. *Nat. Chem. Biol.* 6, 449–456. doi: 10.1038/nchembio.362
- Díaz, B., Ostapoff, K. T., Toombs, J. E., Lo, J., Bonner, M. Y., Curatolo, A., et al. (2016). Tris DBA palladium is highly effective against growth and metastasis of pancreatic cancer in an orthotopic model. *Oncotarget* 7, 51569–51580. doi: 10.18632/oncotarget.10514
- Dietzen, D. J., Hastings, W. R., and Lublin, D. M. (1995). Caveolin is palmitoylated on multiple cysteine residues. Palmitoylation is not necessary for localization of caveolin to caveolae. *J. Biol. Chem.* 270, 6838–6842. doi: 10.1074/jbc.270.12.6838
- Du, K., Murakami, S., Sun, Y., Kilpatrick, C. L., and Luscher, B. (2017). DHHC7 palmitoylates glucose transporter 4 (Glut4) and regulates Glut4 membrane translocation. *J. Biol. Chem.* 292, 2979–2991. doi: 10.1074/jbc.M116.747139
- Du, Y., Zuckermann, F. A., and Yoo, D. (2010). Myristoylation of the small envelope protein of porcine reproductive and respiratory syndrome virus is non-essential for virus infectivity but promotes its growth. *Virus Res.* 147, 294–299. doi: 10.1016/j.virusres.2009.11.016
- Ducker, C. E., Upson, J. J., French, K. J., and Smith, C. D. (2005). Two N-myristoyltransferase isozymes play unique roles in protein myristoylation, proliferation, and apoptosis. *Mol. Cancer Res.* 3, 463–476. doi: 10.1158/1541-7786.MCR-05-0037
- Elstrom, R. L., Bauer, D. E., Buzzai, M., Karnauskas, R., Harris, M. H., Plas, D. R., et al. (2004). Akt stimulates aerobic glycolysis in cancer cells. *Cancer Res.* 64, 3892–3899. doi: 10.1158/0008-5472.CAN-03-2904
- Farazi, T. A., Waksman, G., and Gordon, J. I. (2001). The biology and enzymology of protein N-myristoylation. *J. Biol. Chem.* 276, 39501–39504. doi: 10.1074/jbc.R100042200
- Feldman, J. L., Baeza, J., and Denu, J. M. (2013). Activation of the protein deacetylase SIRT6 by long-chain fatty acids and widespread deacylation by mammalian sirtuins. *J. Biol. Chem.* 288, 31350–31356. doi: 10.1074/jbc.C113.511261
- Feldman, J. L., Dittenhafer-Reed, K. E., Kudo, N., Thelen, J. N., Ito, A., Yoshida, M., et al. (2015). Kinetic and structural basis for Acyl-Group selectivity and NAD(+) dependence in sirtuin-catalyzed deacylation. *Biochemistry* 54, 3037–3050. doi: 10.1021/acs.biochem.5b00150
- Frearson, J. A., Brand, S., McElroy, S. P., Cleghorn, L. A., Smid, O., Stojanovski, L., et al. (2010). N-myristoyltransferase inhibitors as new leads to treat sleeping sickness. *Nature* 464, 728–732. doi: 10.1038/nature08893
- Frottin, F., Martinez, A., Peynot, P., Mitra, S., Holz, R. C., Giglione, C., et al. (2006). The proteomics of N-terminal methionine cleavage. *Mol. Cell. Proteomics* 5, 2336–2349. doi: 10.1074/mcp.M600225-MCP200
- Garrido, P., Morán, J., Alonso, A., González, S., and González, C. (2013). 17 $\beta$ -estradiol activates glucose uptake via GLUT4 translocation and PI3K/Akt signaling pathway in MCF-7 cells. *Endocrinology* 154, 1979–1989. doi: 10.1210/en.2012-1558
- Giang, D. K., and Cravatt, B. F. (1998). A second mammalian N-myristoyltransferase. *J. Biol. Chem.* 273, 6595–6598. doi: 10.1074/jbc.273.12.6595
- González Montoro, A., Quiroga, R., and Valdez Taubas, J. (2013). Zinc co-ordination by the DHHC cysteine-rich domain of the palmitoyltransferase Swf1. *Biochem. J.* 454, 427–435. doi: 10.1042/BJ20121693
- Hadváry, P., Sidler, W., Meister, W., Vetter, W., and Wolfer, H. (1991). The lipase inhibitor tetrahydrolipstatin binds covalently to the putative active site serine of pancreatic lipase. *J. Biol. Chem.* 266, 2021–2027.
- Hanahan, D., and Weinberg, R. A. (2011). Hallmarks of cancer: the next generation. *Cell* 144, 646–674. doi: 10.1016/j.cell.2011.02.013
- Hancock, J. F., Cadwallader, K., Paterson, H., and Marshall, C. J. (1991). A CAAX or a CAAL motif and a second signal are sufficient for plasma membrane targeting of ras proteins. *EMBO J.* 10, 4033–4039.
- Harada, T., Sada, R., Osugi, Y., Matsumoto, S., Matsuda, T., Hayashi-Nishino, M., et al. (2020). Palmitoylated CKAP4 regulates mitochondrial functions through an interaction with VDAC2 at ER-mitochondria contact sites. *J. Cell Sci.* 133:jcs249045. doi: 10.1242/jcs.249045
- Hedberg, C., Dekker, F. J., Rusch, M., Renner, S., Wetzel, S., Vartak, N., et al. (2011). Development of highly potent inhibitors of the Ras-targeting human acyl protein thioesterases based on substrate similarity design. *Angew Chem. Int. Ed. Engl.* 50, 9832–9837. doi: 10.1002/anie.201102965
- Hermida-Matsumoto, L., and Resh, M. D. (1999). Human immunodeficiency virus type 1 protease triggers a myristoyl switch that modulates membrane binding of Pr55(gag) and p17MA. *J. Virol.* 73, 1902–1908. doi: 10.1128/JVI.73.3.1902-1908.1999
- Hernandez, J. L., Davda, D., Cheung See Kit, M., Majmudar, J. D., Won, S. J., Gang, M., et al. (2017). APT2 inhibition restores scribble localization and S-Palmitoylation in snail-transformed cells. *Cell Chem. Biol.* 24, 87–97. doi: 10.1016/j.chembiol.2016.12.007
- Heuckeroth, R. O., Glaser, L., and Gordon, J. I. (1988). Heteroatom-substituted fatty acid analogs as substrates for N-myristoyltransferase: an approach for studying both the enzymology and function of protein acylation. *Proc. Natl. Acad. Sci. U.S.A.* 85, 8795–8799. doi: 10.1073/pnas.85.23.8795
- Hurley, J. H., Cahill, A. L., Currie, K. P., and Fox, A. P. (2000). The role of dynamic palmitoylation in Ca<sup>2+</sup> channel inactivation. *Proc. Natl. Acad. Sci. U.S.A.* 97, 9293–9298. doi: 10.1073/pnas.160589697
- Ivaldi, C., Martin, B. R., Kieffer-Jaquinod, S., Chapel, A., Levade, T., Garin, J., et al. (2012). Proteomic analysis of S-acylated proteins in human B cells reveals palmitoylation of the immune regulators CD20 and CD23. *PLoS One* 7:e37187. doi: 10.1371/journal.pone.0037187
- Jennings, B. C., Nadolski, M. J., Ling, Y., Baker, M. B., Harrison, M. L., Deschenes, R. J., et al. (2009). 2-Bromopalmitate and 2-(2-hydroxy-5-nitro-benzylidene)-benzo[b]thiophen-3-one inhibit DHHC-mediated palmitoylation in vitro. *J. Lipid Res.* 50, 233–242. doi: 10.1194/jlr.M800270-JLR200
- Jiang, H., Khan, S., Wang, Y., Charron, G., He, B., Sebastian, C., et al. (2013). SIRT6 regulates TNF- $\alpha$  secretion through hydrolysis of long-chain fatty acyl lysine. *Nature* 496, 110–113. doi: 10.1038/nature12038
- Jing, H., Zhang, X., Wisner, S. A., Chen, X., Spiegelman, N. A., Linder, M. E., et al. (2017). SIRT2 and lysine fatty acylation regulate the transforming activity of K-Ras4a. *Elife* 6:e32436. doi: 10.7554/eLife.32436
- Jochen, A. L., Hays, J., and Mick, G. (1995). Inhibitory effects of cerulenin on protein palmitoylation and insulin internalization in rat adipocytes. *Biochim. Biophys. Acta* 1259, 65–72. doi: 10.1016/0005-2760(95)00147-5
- Kallemeijn, W. W., Lueg, G. A., Faronato, M., Hadavizadeh, K., Goya Grocin, A., Song, O. R., et al. (2019). Validation and invalidation of chemical probes for the human N-myristoyltransferases. *Cell Chem. Biol.* 26, 892–900.e894. doi: 10.1016/j.chembiol.2019.03.006
- Kang, R., Wan, J., Arstikaitis, P., Takahashi, H., Huang, K., Bailey, A. O., et al. (2008). Neural palmitoyl-proteomics reveals dynamic synaptic palmitoylation. *Nature* 456, 904–909. doi: 10.1038/nature07605
- Karatas, H., Akbarzadeh, M., Adihou, H., Hahne, G., Pobbati, A. V., Yihui Ng, E., et al. (2020). Discovery of covalent inhibitors targeting the transcriptional enhanced associate domain central pocket. *J. Med. Chem.* 63, 11972–11989. doi: 10.1021/acs.jmedchem.0c01275
- Kathayat, R. S., Cao, Y., Elvira, P. D., Sandoz, P. A., Zaballa, M. E., Springer, M. Z., et al. (2018). Active and dynamic mitochondrial S-depalmitoylation revealed by targeted fluorescent probes. *Nat. Commun.* 9:334. doi: 10.1038/s41467-017-02655-1
- Kay, N. E., Sassoon, T., Secreto, C., Sinha, S., Shanafelt, T. D., Ghosh, A. K., et al. (2016). Tris (dibenzylideneacetone) dipalladium: a small-molecule palladium complex is effective in inducing apoptosis in chronic lymphocytic leukemia B-cells. *Leuk. Lymphoma* 57, 2409–2416. doi: 10.3109/10428194.2016.1161186
- Kim, S., Alsaïdan, O. A., Goodwin, O., Li, Q., Sulejmani, E., Han, Z., et al. (2017). Blocking myristoylation of Src inhibits its kinase activity and suppresses prostate cancer progression. *Cancer Res.* 77, 6950–6962. doi: 10.1158/0008-5472.CAN-17-0981

- Koegl, M., Zlatkine, P., Ley, S. C., Courtneidge, S. A., and Magee, A. I. (1994). Palmitoylation of multiple Src-family kinases at a homologous N-terminal motif. *Biochem. J.* 303(Pt 3), 749–753. doi: 10.1042/bj3030749
- Kong, E., Peng, S., Chandra, G., Sarkar, C., Zhang, Z., Bagh, M. B., et al. (2013). Dynamic palmitoylation links cytosol-membrane shuttling of acyl-protein thioesterase-1 and acyl-protein thioesterase-2 with that of proto-oncogene H-ras product and growth-associated protein-43. *J. Biol. Chem.* 288, 9112–9125. doi: 10.1074/jbc.M112.421073
- Kosciuk, T. I., Price, R., Zhang, X., Zhu, C., Johnson, K. N., Zhang, S., et al. (2020). NMT1 and NMT2 are lysine myristoyltransferases regulating the ARF6 GTPase cycle. *Nat. Commun.* 11:1067. doi: 10.1038/s41467-020-14893-x
- Lawrence, D. S., Zilfou, J. T., and Smith, C. D. (1999). Structure-activity studies of cerulenin analogues as protein palmitoylation inhibitors. *J. Med. Chem.* 42, 4932–4941. doi: 10.1021/jm980591s
- Liang, J., Xu, Z. X., Ding, Z., Lu, Y., Yu, Q., Werle, K. D., et al. (2015). Myristoylation confers noncanonical AMPK functions in autophagy selectivity and mitochondrial surveillance. *Nat. Commun.* 6:7926. doi: 10.1038/ncomms8926
- Lin, D. T., and Conibear, E. (2015). ABHD17 proteins are novel protein depalmitoylases that regulate N-Ras palmitate turnover and subcellular localization. *Elife* 4:e11306. doi: 10.7554/eLife.11306
- Liu, Y., Kahn, R. A., and Prestegard, J. H. (2009). Structure and membrane interaction of myristoylated ARF1. *Structure* 17, 79–87. doi: 10.1016/j.str.2008.10.020
- Lothrop, A. P., Torres, M. P., and Fuchs, S. M. (2013). Deciphering post-translational modification codes. *FEBS Lett.* 587, 1247–1257. doi: 10.1016/j.febslet.2013.01.047
- Lu, Y., Selvakumar, P., Ali, K., Shrivastav, A., Bajaj, G., Resch, L., et al. (2005). Expression of N-myristoyltransferase in human brain tumors. *Neurochem. Res.* 30, 9–13. doi: 10.1007/s11064-004-9680-9
- Lynes, E. M., Bui, M., Yap, M. C., Benson, M. D., Schneider, B., Ellgaard, L., et al. (2012). Palmitoylated TMX and calnexin target to the mitochondria-associated membrane. *EMBO J.* 31, 457–470. doi: 10.1038/emboj.2011.384
- Mackey, J. R., Lai, J., Chauhan, U., Beauchamp, E., Dong, W. F., Glubrecht, D., et al. (2021). N-myristoyltransferase proteins in breast cancer: prognostic relevance and validation as a new drug target. *Breast Cancer Res. Treat.* 186, 79–87. doi: 10.1007/s10549-020-06037-y
- Magnuson, B. A., Raju, R. V., Moyana, T. N., and Sharma, R. K. (1995). Increased N-myristoyltransferase activity observed in rat and human colonic tumors. *J. Natl. Cancer Inst.* 87, 1630–1635. doi: 10.1093/jnci/87.21.1630
- Martin, B. R., and Cravatt, B. F. (2009). Large-scale profiling of protein palmitoylation in mammalian cells. *Nat. Methods* 6, 135–138. doi: 10.1038/nmeth.1293
- Martin, D. D., Beauchamp, E., and Berthiaume, L. G. (2011). Post-translational myristoylation: fat matters in cellular life and death. *Biochimie* 93, 18–31. doi: 10.1016/j.biochi.2010.10.018
- Meng, W., Hao, M. M., Yu, N., Li, M. Y., Ding, J. Q., Wang, B. H., et al. (2019). 2-Bromopalmitate attenuates bone cancer pain via reversing mitochondrial fusion and fission imbalance in spinal astrocytes. *Mol. Pain* 15:1744806919871813. doi: 10.1177/1744806919871813
- Milde, S., and Coleman, M. P. (2014). Identification of palmitoyltransferase and thioesterase enzymes that control the subcellular localization of axon survival factor nicotinamide mononucleotide adenyltransferase 2 (NMNAT2). *J. Biol. Chem.* 289, 32858–32870. doi: 10.1074/jbc.M114.582338
- Miranda, M., Galli, L. M., Enriquez, M., Szabo, L. A., Gao, X., Hannoush, R. N., et al. (2014). Identification of the WNT1 residues required for palmitoylation by Porcupine. *FEBS Lett.* 588, 4815–4824. doi: 10.1016/j.febslet.2014.11.016
- Mousnier, A., Bell, A. S., Swieboda, D. P., Morales-Sanfrutos, J., Pérez-Dorado, I., Brannigan, J. A., et al. (2018). Fragment-derived inhibitors of human N-myristoyltransferase block capsid assembly and replication of the common cold virus. *Nat. Chem.* 10, 599–606. doi: 10.1038/s41557-018-0039-2
- Napoli, E., Song, G., Liu, S., Espejo, A., Perez, C. J., Benavides, F., et al. (2017). Zdhc13-dependent Drp1 S-palmitoylation impacts brain bioenergetics, anxiety, coordination and motor skills. *Sci. Rep.* 7:12796. doi: 10.1038/s41598-017-12889-0
- Paige, L. A., Zheng, G. Q., DeFrees, S. A., Cassady, J. M., and Geahlen, R. L. (1989). S-(2-oxopentadecyl)-CoA, a nonhydrolyzable analogue of myristoyl-CoA, is a potent inhibitor of myristoyl-CoA:protein N-myristoyltransferase. *J. Med. Chem.* 32, 1665–1667. doi: 10.1021/jm00128a001
- Paige, L. A., Zheng, G. Q., DeFrees, S. A., Cassady, J. M., and Geahlen, R. L. (1990). Metabolic activation of 2-substituted derivatives of myristic acid to form potent inhibitors of myristoyl CoA:protein N-myristoyltransferase. *Biochemistry* 29, 10566–10573. doi: 10.1021/bi00498a021
- Patterson, S. I., and Skene, J. H. (1995). Inhibition of dynamic protein palmitoylation in intact cells with tunicamycin. *Methods Enzymol.* 250, 284–300. doi: 10.1016/0076-6879(95)50079-0
- Patwardhan, P., and Resh, M. D. (2010). Myristoylation and membrane binding regulate c-Src stability and kinase activity. *Mol. Cell. Biol.* 30, 4094–4107. doi: 10.1128/MCB.00246-10
- Pedram, A., Razandi, M., Deschenes, R. J., and Levin, E. R. (2012). DHHC-7 and -21 are palmitoylacyltransferases for sex steroid receptors. *Mol. Biol. Cell* 23, 188–199. doi: 10.1091/mbc.E11-07-0638
- Pedro, M. P., Vilcaes, A. A., Tomatis, V. M., Oliveira, R. G., Gomez, G. A., and Daniotti, J. L. (2013). 2-Bromopalmitate reduces protein deacylation by inhibition of acyl-protein thioesterase enzymatic activities. *PLoS One* 8:e75232. doi: 10.1371/journal.pone.0075232
- Peitzsch, R. M., and McLaughlin, S. (1993). Binding of acylated peptides and fatty acids to phospholipid vesicles: pertinence to myristoylated proteins. *Biochemistry* 32, 10436–10443. doi: 10.1021/bi00090a020
- Pepinsky, R. B., Zeng, C., Wen, D., Rayhorn, P., Baker, D. P., Williams, K. P., et al. (1998). Identification of a palmitic acid-modified form of human Sonic hedgehog. *J. Biol. Chem.* 273, 14037–14045. doi: 10.1074/jbc.273.22.14037
- Putilina, T., Wong, P., and Gentleman, S. (1999). The DHHC domain: a new highly conserved cysteine-rich motif. *Mol. Cell. Biochem.* 195, 219–226. doi: 10.1023/a:1006932522197
- Rajala, R. V., Radhi, J. M., Kakkar, R., Datla, R. S., and Sharma, R. K. (2000). Increased expression of N-myristoyltransferase in gallbladder carcinomas. *Cancer* 88, 1992–1999.
- Randeep, S., Sangha, L. H. S., Kuruvilla, J., Weickert, M., Mackey, J. R., and Berthiaume, L. G. (2020). An open-label, first-in-human, phase I trial of the safety and efficacy of daily PCLX-001. *J. Clin. Oncol.* 38 (Suppl. 15):TPS3656. doi: 10.1200/JCO.2020.38.15\_suppl.TPS3656
- Raturi, A., Gutiérrez, T., Ortiz-Sandoval, C., Ruangkittisakul, A., Herrera-Cruz, M. S., Rockley, J. P., et al. (2016). TMX1 determines cancer cell metabolism as a thiol-based modulator of ER-mitochondria Ca<sup>2+</sup> flux. *J. Cell. Biol.* 214, 433–444. doi: 10.1083/jcb.201512077
- Ren, W., Sun, Y., and Du, K. (2015). Glut4 palmitoylation at Cys223 plays a critical role in Glut4 membrane trafficking. *Biochem. Biophys. Res. Commun.* 460, 709–714. doi: 10.1016/j.bbrc.2015.03.094
- Rudnick, D. A., Lu, T., Jackson-Machelski, E., Hernandez, J. C., Li, Q., Gokel, G. W., et al. (1992). Analogs of palmitoyl-CoA that are substrates for myristoyl-CoA:protein N-myristoyltransferase. *Proc. Natl. Acad. Sci. U.S.A.* 89, 10507–10511. doi: 10.1073/pnas.89.21.10507
- Rudnick, D. A., McWherter, C. A., Rocque, W. J., Lennon, P. J., Getman, D. P., and Gordon, J. I. (1991). Kinetic and structural evidence for a sequential ordered Bi Bi mechanism of catalysis by *Saccharomyces cerevisiae* myristoyl-CoA:protein N-myristoyltransferase. *J. Biol. Chem.* 266, 9732–9739.
- Rusch, M., Zimmermann, T. J., Bürger, M., Dekker, F. J., Görmer, K., Triola, G., et al. (2011). Identification of acyl protein thioesterases 1 and 2 as the cellular targets of the Ras-signaling modulators palmostatin B and M. *Angew Chem. Int. Ed. Engl.* 50, 9838–9842. doi: 10.1002/anie.201102967
- Segal-Salto, M., Sapir, T., and Reiner, O. (2016). Reversible cysteine acylation regulates the activity of human palmitoyl-protein thioesterase 1 (PPT1). *PLoS One* 11:e0146466. doi: 10.1371/journal.pone.0146466
- Senyilmaz, D., Virtue, S., Xu, X., Tan, C. Y., Griffin, J. L., Miller, A. K., et al. (2015). Regulation of mitochondrial morphology and function by stearoylation of TFR1. *Nature* 525, 124–128. doi: 10.1038/nature14601
- Shahinian, S., and Silvius, J. R. (1995). Doubly-lipid-modified protein sequence motifs exhibit long-lived anchorage to lipid bilayer membranes. *Biochemistry* 34, 3813–3822. doi: 10.1021/bi00011a039
- Shen, L. F., Chen, Y. J., Liu, K. M., Haddad, A. N. S., Song, I. W., Roan, H. Y., et al. (2017). Role of S-Palmitoylation by ZDHHC13 in Mitochondrial function and Metabolism in Liver. *Sci. Rep.* 7:2182. doi: 10.1038/s41598-017-02159-4
- Sigal, C. T., Zhou, W., Buser, C. A., McLaughlin, S., and Resh, M. D. (1994). Amino-terminal basic residues of Src mediate membrane binding through

- electrostatic interaction with acidic phospholipids. *Proc. Natl. Acad. Sci. U.S.A.* 91, 12253–12257. doi: 10.1073/pnas.91.25.12253
- Spiegelman, N. A., Zhang, X., Jing, H., Cao, J. I., Kotliar, B., Aramsangtienchai, P., et al. (2019). SIRT2 and lysine fatty acylation regulate the activity of RalB and cell migration. *ACS Chem. Biol.* 14, 2014–2023. doi: 10.1021/acscchembio.9b00492
- Stevenson, F. T., Bursten, S. L., Fanton, C., Locksley, R. M., and Lovett, D. H. (1993). The 31-kDa precursor of interleukin 1 alpha is myristoylated on specific lysines within the 16-kDa N-terminal propeptide. *Proc. Natl. Acad. Sci. U.S.A.* 90, 7245–7249. doi: 10.1073/pnas.90.15.7245
- Stevenson, F. T., Bursten, S. L., Locksley, R. M., and Lovett, D. H. (1992). Myristyl acylation of the tumor necrosis factor alpha precursor on specific lysine residues. *J. Exp. Med.* 176, 1053–1062. doi: 10.1084/jem.176.4.1053
- Swarthout, J. T., Lobo, S., Farh, L., Croke, M. R., Greentree, W. K., Deschenes, R. J., et al. (2005). DHHC9 and GCP16 constitute a human protein fatty acyltransferase with specificity for H- and N-Ras. *J. Biol. Chem.* 280, 31141–31148. doi: 10.1074/jbc.M504113200
- Tanaka, T., Ames, J. B., Harvey, T. S., Stryer, L., and Ikura, M. (1995). Sequestration of the membrane-targeting myristoyl group of recoverin in the calcium-free state. *Nature* 376, 444–447. doi: 10.1038/376444a0
- Thelen, M., Rosen, A., Nairn, A. C., and Aderem, A. (1991). Regulation by phosphorylation of reversible association of a myristoylated protein kinase C substrate with the plasma membrane. *Nature* 351, 320–322. doi: 10.1038/351320a0
- Toyoda, T., Sugimoto, H., and Yamashita, S. (1999). Sequence, expression in *Escherichia coli*, and characterization of lysophospholipase II. *Biochim. Biophys. Acta* 1437, 182–193. doi: 10.1016/s1388-1981(99)00007-4
- Utsumi, T., Matsuzaki, K., Kiwado, A., Tanikawa, A., Kikkawa, Y., Hosokawa, T., et al. (2018). Identification and characterization of protein N-myristoylation occurring on four human mitochondrial proteins, SAMM50, TOMM40, MIC19, and MIC25. *PLoS One* 13:e0206355. doi: 10.1371/journal.pone.0206355
- Verkruyse, L. A., and Hofmann, S. L. (1996). Lysosomal targeting of palmitoyl-protein thioesterase. *J. Biol. Chem.* 271, 15831–15836. doi: 10.1074/jbc.271.26.15831
- Vujic, I., Sanlorenzo, M., Esteve-Puig, R., Vujic, M., Kwong, A., Tsumura, A., et al. (2016). Acyl protein thioesterase 1 and 2 (APT-1, APT-2) inhibitors palmostatin B, ML348 and ML349 have different effects on NRAS mutant melanoma cells. *Oncotarget* 7, 7297–7306. doi: 10.18632/oncotarget.6907
- Wang, J., Hao, J. W., Wang, X., Guo, H., Sun, H. H., Lai, X. Y., et al. (2019). DHHC4 and DHHC5 facilitate fatty acid uptake by palmitoylating and targeting CD36 to the plasma membrane. *Cell Rep.* 26, 209–221.e205. doi: 10.1016/j.celrep.2018.12.022
- Willumsen, B. M., Christensen, A., Hubbert, N. L., Papageorge, A. G., and Lowy, D. R. (1984). The p21 ras C-terminus is required for transformation and membrane association. *Nature* 310, 583–586. doi: 10.1038/310583a0
- Wilson, J. P., Raghavan, A. S., Yang, Y. Y., Charron, G., and Hang, H. C. (2011). Proteomic analysis of fatty-acylated proteins in mammalian cells with chemical reporters reveals S-acylation of histone H3 variants. *Mol. Cell. Proteomics* 10:M110.001198. doi: 10.1074/mcp.M110.001198
- Yang, S. H., Shrivastav, A., Kosinski, C., Sharma, R. K., Chen, M. H., Berthiaume, L. G., et al. (2005). N-myristoyltransferase 1 is essential in early mouse development. *J. Biol. Chem.* 280, 18990–18995. doi: 10.1074/jbc.M412917200
- Yang, W., Di Vizio, D., Kirchner, M., Steen, H., and Freeman, M. R. (2010). Proteome scale characterization of human S-acylated proteins in lipid raft-enriched and non-raft membranes. *Mol. Cell. Proteomics* 9, 54–70. doi: 10.1074/mcp.M800448-MCP200
- Yeh, D. C., Duncan, J. A., Yamashita, S., and Michel, T. (1999). Depalmitoylation of endothelial nitric-oxide synthase by acyl-protein thioesterase 1 is potentiated by Ca(2+)-calmodulin. *J. Biol. Chem.* 274, 33148–33154. doi: 10.1074/jbc.274.46.33148
- Zha, J., Weiler, S., Oh, K. J., Wei, M. C., and Korsmeyer, S. J. (2000). Posttranslational N-myristoylation of BID as a molecular switch for targeting mitochondria and apoptosis. *Science* 290, 1761–1765. doi: 10.1126/science.290.5497.1761
- Zhang, J., Planey, S. L., Ceballos, C., Stevens, S. M., Keay, S. K., and Zacharias, D. A. (2008). Identification of CKAP4/p63 as a major substrate of the palmitoyl acyltransferase DHHC2, a putative tumor suppressor, using a novel proteomics method. *Mol. Cell. Proteomics* 7, 1378–1388. doi: 10.1074/mcp.M800069-MCP200
- Zhang, Q., Zhou, W., Yu, S., Ju, Y., To, S. K. Y., Wong, A. S. T., et al. (2021). Metabolic reprogramming of ovarian cancer involves ACSL1-mediated metastasis stimulation through upregulated protein myristoylation. *Oncogene* 40, 97–111. doi: 10.1038/s41388-020-01516-4
- Zhao, L., Zhang, C., Luo, X., Wang, P., Zhou, W., Zhong, S., et al. (2018). CD36 palmitoylation disrupts free fatty acid metabolism and promotes tissue inflammation in non-alcoholic steatohepatitis. *J. Hepatol.* 69, 705–717. doi: 10.1016/j.jhep.2018.04.006
- Zhou, W., Parent, L. J., Wills, J. W., and Resh, M. D. (1994). Identification of a membrane-binding domain within the amino-terminal region of human immunodeficiency virus type 1 Gag protein which interacts with acidic phospholipids. *J. Virol.* 68, 2556–2569. doi: 10.1128/JVI.68.4.2556-2569.1994
- Zimmermann, T. J., Bürger, M., Tashiro, E., Kondoh, Y., Martinez, N. E., Görmer, K., et al. (2013). Boron-based inhibitors of acyl protein thioesterases 1 and 2. *Chembiochem* 14, 115–122. doi: 10.1002/cbic.201200571
- Zou, C., Ellis, B. M., Smith, R. M., Chen, B. B., Zhao, Y., and Mallampalli, R. K. (2011). Acyl-CoA:lysophosphatidylcholine acyltransferase I (Lpcat1) catalyzes histone protein O-palmitoylation to regulate mRNA synthesis. *J. Biol. Chem.* 286, 28019–28025. doi: 10.1074/jbc.M111.253385

**Conflict of Interest:** The authors declare that the research was conducted in the absence of any commercial or financial relationships that could be construed as a potential conflict of interest.

Copyright © 2021 Fhu and Ali. This is an open-access article distributed under the terms of the Creative Commons Attribution License (CC BY). The use, distribution or reproduction in other forums is permitted, provided the original author(s) and the copyright owner(s) are credited and that the original publication in this journal is cited, in accordance with accepted academic practice. No use, distribution or reproduction is permitted which does not comply with these terms.



# Functions and Mechanisms of Lysine Glutarylation in Eukaryotes

Longxiang Xie<sup>††</sup>, Yafei Xiao<sup>††</sup>, Fucheng Meng<sup>††</sup>, Yongqiang Li<sup>1</sup>, Zhenyu Shi<sup>1\*</sup> and Keli Qian<sup>2\*</sup>

<sup>1</sup> Institute of Biomedical Informatics, Cell Signal Transduction Laboratory, Bioinformatics Center, Henan Provincial Engineering Center for Tumor Molecular Medicine, School of Basic Medical Sciences, Huaihe Hospital, Henan University, Kaifeng, China,

<sup>2</sup> Infection Control Department, The First Affiliated Hospital of Chongqing Medical University, Chongqing, China

## OPEN ACCESS

### Edited by:

Fangliang Zhang,  
University of Miami, United States

### Reviewed by:

Tzong-Yi Lee,  
The Chinese University of Hong Kong,  
Shenzhen, China  
Yong Liu,  
Xuzhou Medical University, China

### \*Correspondence:

Zhenyu Shi  
shizhenyu@henu.edu.cn  
Keli Qian  
qiankeli86@163.com

<sup>††</sup> These authors have contributed  
equally to this work and share first  
authorship

### Specialty section:

This article was submitted to  
Cellular Biochemistry,  
a section of the journal  
Frontiers in Cell and Developmental  
Biology

**Received:** 14 February 2021

**Accepted:** 01 June 2021

**Published:** 24 June 2021

### Citation:

Xie L, Xiao Y, Meng F, Li Y, Shi Z  
and Qian K (2021) Functions  
and Mechanisms of Lysine  
Glutarylation in Eukaryotes.  
Front. Cell Dev. Biol. 9:667684.  
doi: 10.3389/fcell.2021.667684

Lysine glutarylation (Kglu) is a newly discovered post-translational modification (PTM), which is considered to be reversible, dynamic, and conserved in prokaryotes and eukaryotes. Recent developments in the identification of Kglu by mass spectrometry have shown that Kglu is mainly involved in the regulation of metabolism, oxidative damage, chromatin dynamics and is associated with various diseases. In this review, we firstly summarize the development history of glutarylation, the biochemical processes of glutarylation and deglutarylation. Then we focus on the pathophysiological functions such as glutaric acidemia 1, asthenospermia, etc. Finally, the current computational tools for predicting glutarylation sites are discussed. These emerging findings point to new functions for lysine glutarylation and related enzymes, and also highlight the mechanisms by which glutarylation regulates diverse cellular processes.

**Keywords:** glutarylation, SIRT5, glutaryl-CoA, PTM, proteomic

## INTRODUCTION

Protein post-translational modifications (PTMs), covalent chemical modifications of amino acid residues (Macek et al., 2019), are a conserved mechanism adopted by organisms to effectively modulate biological activities, enabling them to make rapid adaptive responses to environmental changes (Bernal et al., 2014). PTMs have been reported to be involved in various biological processes (Walsh et al., 2005; Xu et al., 2016). They play crucial roles in the diversification of protein functions in different biological and physiological interactions (Walsh et al., 2005; Xu et al., 2016). To date, 676 different PTMs have been identified in the UniProt database<sup>1</sup>, including lysine (Lys) acylation, phosphorylation, ubiquitination, SUMOylation, and so forth (Venne et al., 2014; Harmel and Fiedler, 2018). Lysine acylation is a widely occurring PTM of proteins (Diallo et al., 2019). Besides the well-known acetylation (Kac) (Kim et al., 2006; Choudhary et al., 2009; Zhao et al., 2010; Lundby et al., 2012), eight types of short-chain Lys acylations have recently been identified on histones, including Lys propionylation (Kpr) (Chen et al., 2007), butyrylation (Kbu) (Chen et al., 2007), 2-hydroxyisobutyrylation (Khib) (Dai et al., 2014), succinylation (Ksucc) (Xie et al., 2012), malonylation (Kma) (Xie et al., 2012), glutarylation (Kglu) (Tan et al., 2014), crotonylation (Kcr) (Tan et al., 2011), and  $\beta$ -hydroxybutyrylation (Kbhb) (Xie Z. et al., 2016). These modifications are

<sup>1</sup> <http://www.uniprot.org/docs/ptmlist>



similar to the well-studied Kac in their  $\epsilon$ -amine linkage, but different in hydrocarbon chain length, hydrophobicity or charge (Sabari et al., 2017). Such as, compared to the Kac changing the charge of lysine from +1 to 0 and adding a 2-carbon acyl group to lysine (Hirsche and Zhao, 2015), Kglu means adding glutaryl groups to specific lysine residues (Dou et al., 2021). Kglu changes the charge of lysine from +1 to -1 and adds a 5-carbon acyl group to lysine (Hirsche and Zhao, 2015). These changes may lead to structural alterations on proteins, affecting their physiological functions and disrupting any interactions between the lysine side chains of glutarylated proteins and negative charged molecules (Hirsche and Zhao, 2015).

The Kglu was first identified by Tan et al. (2014). They performed immunoblot analysis with whole-cell lysates from *Escherichia coli*, *Saccharomyces cerevisiae*, *Drosophila melanogaster* (S2), mouse (MEFs), and human cells (HeLa). The results showed that Kglu is a conserved PTM and exists in both eukaryotic and prokaryotic cells. Afterward, more proteins including histone and non-histone proteins were identified as glutarylated proteins, and they were found to play important roles in mitochondrial functions (Schmiesing et al., 2018), oxidative damage (Zhou et al., 2016), sperm motility (Cheng et al., 2019), and glutaric aciduria 1 (GA1) (Dimitrov et al., 2020).

To systematically review the roles of Kglu in prokaryotes and eukaryotes, we searched PubMed for studies that mentioned glutarylation. Our specific advanced search terms included: "Glutaric acylation" OR "glutarylation" OR "Kglu" OR "glutarylated." The results provided 186 papers as of January 10, 2021. Two investigators reviewed each initial study to determine whether it was related with glutarylation. Finally, 23 papers were preserved by exclusion criteria described in **Figure 1**. In this review, we mainly summarized recent studies about Kglu and discussed its implications. The scope mainly includes mechanism, function, identification and prediction of glutarylated proteins.

## PROTEOMIC PROFILING OF LYSINE GLUTARYLATION

With the development of proteomic technology, the landscape of glutarylation is expanding (**Figure 2**). The proteomic method combining the sensitive immune-affinity purification and high-resolution liquid chromatography-tandem mass spectrometry (LC-MS/MS) has been used to find new glutarylated proteins and modification sites. Recently, four studies have identified new glutarylated proteins and glutarylated lysine residues in *Mycobacterium tuberculosis*, mouse and human serum. Xie L. et al. (2016), our group identified a total of 24 glutarylated proteins and 41 Kglu sites in *M. tuberculosis*. Schmiesing et al. (2018) found 37 glutarylated proteins with 73 Kglu sites in the brain of mice. Bao et al. (2019) revealed that Kglu occurs at 27 lysine residues on human core histones. Zhou et al. (2020) reported 4 kinds of glutarylated proteins with 10 sites in human serum. It shows that Kglu occurred in different species, and most of glutarylated proteins contain at least two Kglu sites in **Table 1**.

Since the discovery of immonium ion on acetylated lysine, most of the modifications based on acylation have their corresponding immonium ion characteristics. Parameter 86 m/z was set for detecting this PTM after MS/MS searches.

Antibodies are crucial for experimental studies, especially for the identification of protein PTMs. Therefore, we have reviewed the experimental studies on antibody for lysine glutarylation, and found eight related articles (Tan et al., 2014; Xie L. et al., 2016; Zhou et al., 2016, 2020; Schmiesing et al., 2018; Bao et al., 2019; Cheng et al., 2019; Wang et al., 2020). The specific Methods and reagents used in previous studies were summarized in **Supplementary Table 1**. Among eight studies, the glutarylation antibodies used in five studies are from the same company BioLabs (Tan et al., 2014; Xie L. et al., 2016; Zhou et al., 2016; Schmiesing et al., 2018; Cheng et al., 2019). Tan et al. (2014) found that the number of glutarylated peptides is 157, and the number of unmodified peptides is 297. Meanwhile, they performed Dot-blot assay using anti-Kglu antibody by incubation of the peptide libraries bearing a fixed unmodified lysine (K), acetyl-lysine (Kac), malonyl-lysine (Kmal), succinyl-lysine (Ksucc), glutaryl-lysine (Kglu), respectively. Each peptide library includes 10 residues CXXXXKXXXX, where X is a mixture of 19 amino acids (excluding cysteine), C is cysteine, and the 6th residue is a fixed lysine residue. The results showed that only peptide bearing a fixed Kglu can be detected, whereas other types of peptides cannot be detected. This shows the specificity of this glutarylation antibody (Tan et al., 2014). For the remaining three studies, Bao et al. (2019) raised a rabbit polyclonal antibody which is site specific against histones glutarylation and conducted dot-blot and western blot analysis to verify whether the antibody has high specificity. Although the origin of the antibodies was not specified in the remaining two papers, western blot analysis or mass spectrometer were also performed to verify the specificity of antibodies (Wang et al., 2020; Zhou et al., 2020).

Anyway, proteomic profiling of Kglu provides a key resource for finding novel properties and regulatory functions of Kglu.

## THE DISCOVERY OF LYSINE GLUTARYLATION

Tan et al. (2014) first identified and validated Kglu as a PTM by four independent approaches, which is present in both prokaryotes and eukaryotes. They not only first discovered the presence of Kglu in *E. coli*, but also detected 23 Kglu sites in 13 glutarylated proteins. In addition, they isolated 10 glutarylated proteins in HeLa cells and detected 10 Kglu sites, and they also detected 683 sites in 191 glutarylated proteins in mouse liver cells. They also demonstrated that Kglu could be regulated by sirtuin 5 (SIRT5) and nutrient and showed that glutaryl-CoA could directly lead to non-enzymatic Kglu. They further showed that carbamoyl phosphate synthase (1), as a glutarylated protein, is associated with glutaric acidemia type 1 (GA1). Furthermore, they identified three Kglu sites on core histone H2B (H2BK5, H2BK116, and H2BK120), which are critical for regulation of gene expression (Tan et al., 2014). This research is significant, and it opens the door for further biological studies of Kglu (**Figure 2**).

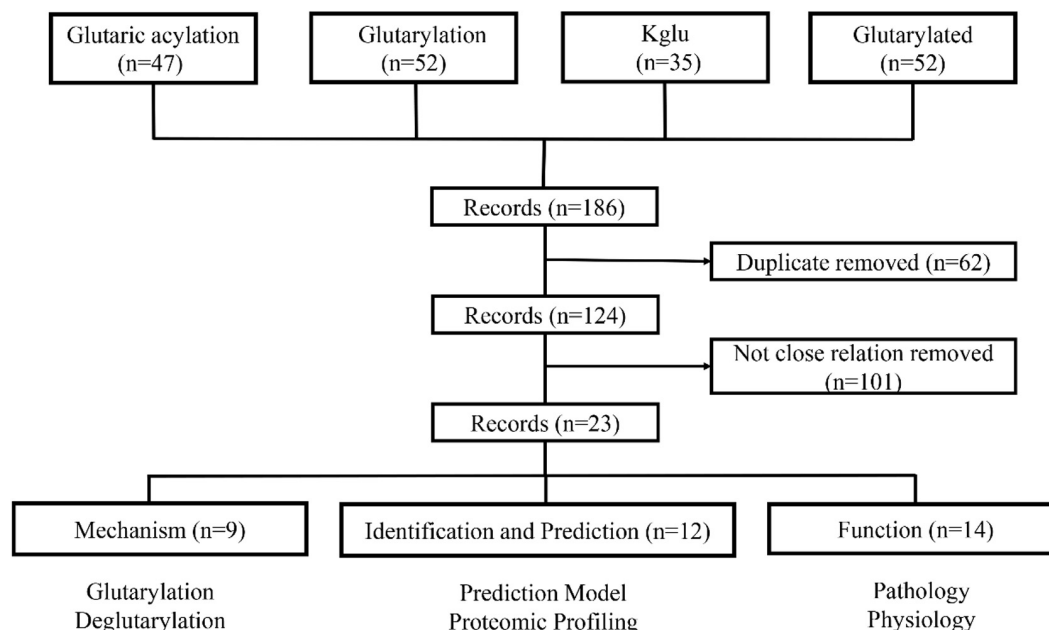


**FIGURE 1 |** The process of literature screening. The articles were sorted into three categories: mechanism, function, identification and prediction of glutarylated proteins. *N* = number of literature records.

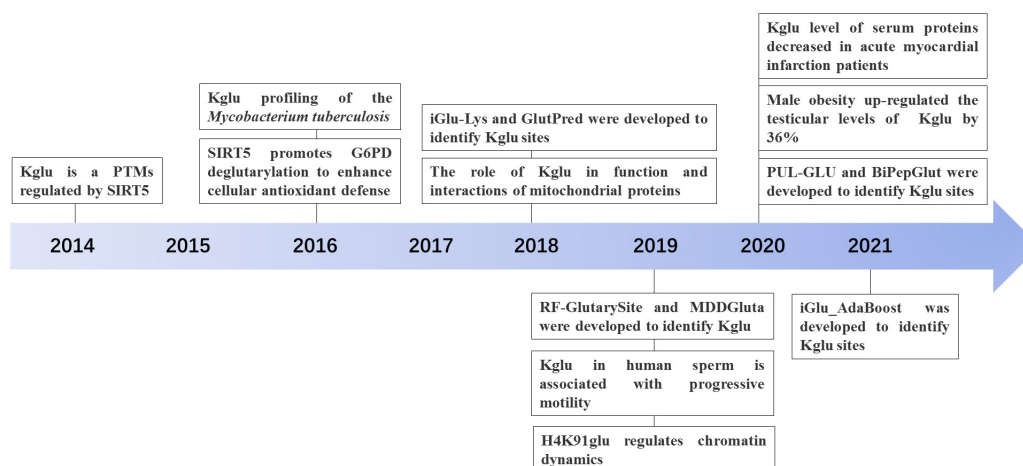


**FIGURE 2 |** The discovery and development history of Lysine glutarylation (Kglu).

## LYSINE GLUTARYLATION AND DEGLUTARYLATION

Glutaryl coenzyme A (CoA) serves as the main acyl donor molecule for Kglu reaction (Schmiesing et al., 2018). SIRT5, which relies on nicotinamide adenine dinucleotide (NAD<sup>+</sup>), can catalyze lysine deglutarylation *in vivo* and *in vitro* (Schmiesing et al., 2018). Glutarylation was considered a non-enzymatic process in the past (Tan et al., 2014), but in recent years, it has been found that glutarylation can be achieved enzymatically in histones (Bao et al., 2019; **Figure 3**).

## Lysine Glutarylation

**Non-enzymatic reactions:** Similar to acetyl coenzyme A and succinyl coenzyme A, glutaryl-CoA can directly induce the non-enzymatic Kglu (Tan et al., 2014). Cellular glutaryl-CoA forms a reactive cyclic anhydride that readily glutarylates lysine residues (Harmel and Fiedler, 2018). The level of Kglu is affected by multiple factors: (1) decreasing the concentration of other CoAs, thus reducing the competition with glutaryl-CoA; (2) increasing the concentration of glutaryl-CoA, both means could enhance the level of Kglu *in vivo* (Sabari et al., 2017).

**TABLE 1** | Information on glutarylated proteins and sites that have been found.

Time (year)	Experimental subject	Position		Protein (n)	Sites (n)	References
		Organ	Ultra structure			
2014	<i>E. coli</i>	-	-	13	23	Tan et al., 2014
2014	HeLa cell	-	-	10	10	Tan et al., 2014
2014	Mouse	liver	-	191	683	Tan et al., 2014
2014	Mouse	liver	nucleus	1 (H2B)	3	Tan et al., 2014
2016	<i>Mycobacterium tuberculosis</i>	-	-	24	41	Xie L. et al., 2016
2018	Mouse	brain	-	37	73	Schmiesing et al., 2018
2018	Mouse	liver	-	154	425	Schmiesing et al., 2018
2019	HeLa cell	-	nucleus	4	27	Bao et al., 2019
2020	Human serum	-	-	4	13	Zhou et al., 2020
2020	Rat serum	-	-	2	4	Zhou et al., 2020

Enzymatic reaction: P300, a member of histone acetyltransferases (HATs), is a well-studied transcription co-activator (Sabari et al., 2017). Apart from its initially described acetyltransferase activity (Bannister and Kouzarides, 1996; Ogryzko et al., 1996), P300 was also found to catalyze the Ksucc (Sabari et al., 2017) and Kglu (Tan et al., 2014) of histone. Although P300 has enzymatic activity for the modification of Kglu *in vitro*, no acyltransferase could catalyze the transfer of malonyl, succinyl, or glutaryl to proteins *in vivo* (Tan et al., 2014). Bao et al. (2019) found that KAT2A (lysine acetyltransferase 2A) and  $\alpha$ -ketoadipate dehydrogenase ( $\alpha$ -KADH) complex were conjugated, which could play the role of histone glutamyltransferase in cells. This implies that both P300 and KAT2A may be the glutaryl transferase responsible for the histone glutarylation. It will be very interesting to study whether these two glutaryl transferases also can catalyze the glutarylation of non-histone proteins in the cytoplasm and mitochondria.

## Lysine Deglutarylation

Sirtuins are a class of protein deacylases and/or ADP ribosyltransferases that depend on NAD<sup>+</sup> (Kumar and Lombard, 2018). In mammals, the sirtuin family consists of seven members (sirt1–7) that have conserved NAD<sup>+</sup> binding and catalytic domains (Kumar and Lombard, 2017). Zhao et al. (2010) proved that the previously annotated deacetylase SIRT5 is a lysine depentadiene Chemase (Tan et al., 2014). One recent research showed that SIRT5 is mainly present in mitochondria, cytoplasm, and nuclear loci (Park et al., 2013). SIRT5 is involved in glycolysis, tricarboxylic acid (TCA) cycle, fatty acid oxidation, and reactive oxygen species (ROS) detoxification (Kumar and Lombard, 2018).

Kglu is a PTM regulated by SIRT5, which possesses potent desuccinylase, demalonylase, and deglutarylase activities (Tan

et al., 2014). At physiological pH, succinyl, malonyl and glutaryl will negatively charge the modified lysine residue (Hirschey and Zhao, 2015). There are two positively charged amino acid groups in the active center of SIRT5 (Du et al., 2011; Peng et al., 2011; Zhou et al., 2012). Therefore, it is not difficult to understand that SIRT5 displays a unique affinity for negatively charged acetyllysine modification and catalyzes protein desuccinylation, demalonylation, and deglutarylation. The SIRT5-catalyzed deglutarylation reaction requires NAD<sup>+</sup> as a cofactor, which is inhibited by nicotinamide, a class III HDAC inhibitor (Tan et al., 2014). Expression of SIRT5 can be regulated by peroxisome proliferator-activated receptor coactivator-1 $\alpha$  (PGC-1 $\alpha$ ) and AMP-activated protein kinase (AMPK) (Buler et al., 2014). Overexpression of PGC-1 $\alpha$  increased SIRT5 mRNA and protein levels, whereas AMPK overexpression inhibited SIRT5 expression in primary mouse hepatocytes (Buler et al., 2014). Under normal basal conditions, the depletion of SIRT5 does not result in an indispensable effect on cell metabolism (Osborne et al., 2016).

Another study showed that SIRT7 catalyzed the hydrolysis of glutaryl peptides in the presence of nicotinamide adenine dinucleotide (NAD) and DNA *in vitro* and in cells (Bao et al., 2019). This implies that SIRT7 may be a compensatory mechanistic pathway. However, whether the SIRT7 possesses potent deglutarylase activities remains to be verified *in vivo*.

## FUNCTIONAL ROLES OF LYSINE GLUTARYLATION

### Regulation of Metabolism

Glutaryl-CoA, one of the precursors of glutarylation, is a thiol ester compound of glutaric acid and coenzyme A (Menon and Stern, 1960; Nishizuka et al., 1960). Glutaric acid, derived from lysine and tryptophan, is mainly metabolized in mitochondria, and the metabolism of glutaryl-CoA is also mainly located in the mitochondria (Besrat et al., 1969; Vamecq et al., 1985). Glutaryl-CoA dehydrogenase (GCDH) is a key enzyme in the metabolic process of glutaryl-CoA (Cheng et al., 2019). GCDH catalyzes the oxidative decarboxylation of glutaryl-CoA to crotonyl-CoA in the lysine and tryptophan degradation pathways, and the increase of glutaryl-CoA content in GCDH KO mice elevated the level of Kglu (Goodman and Frerman, 1995; Koeller et al., 2002; Tan et al., 2014).

It has been discovered that protein glutaryl metabolism mainly occurs in mitochondria (Schmiesing et al., 2018). For example, proteomic analysis of mouse liver revealed that there are 191 glutarylated proteins, of which 148 are mainly or partly located in mitochondria, accounting for more than three-quarters of all identified glutarylated proteins (Tan et al., 2014). There are two reasons why glutaryl metabolism mainly exists in mitochondria: It may be because glutaryl-CoA is mainly located in mitochondria (Besrat et al., 1969; Vamecq et al., 1985); in addition, this may be related to the higher pH (7.9) of mitochondrial matrix which is associated with the deprotonation of the  $\epsilon$ -amino group of lysine, making them more susceptible to acylation (Carrico et al., 2018). Mitochondria

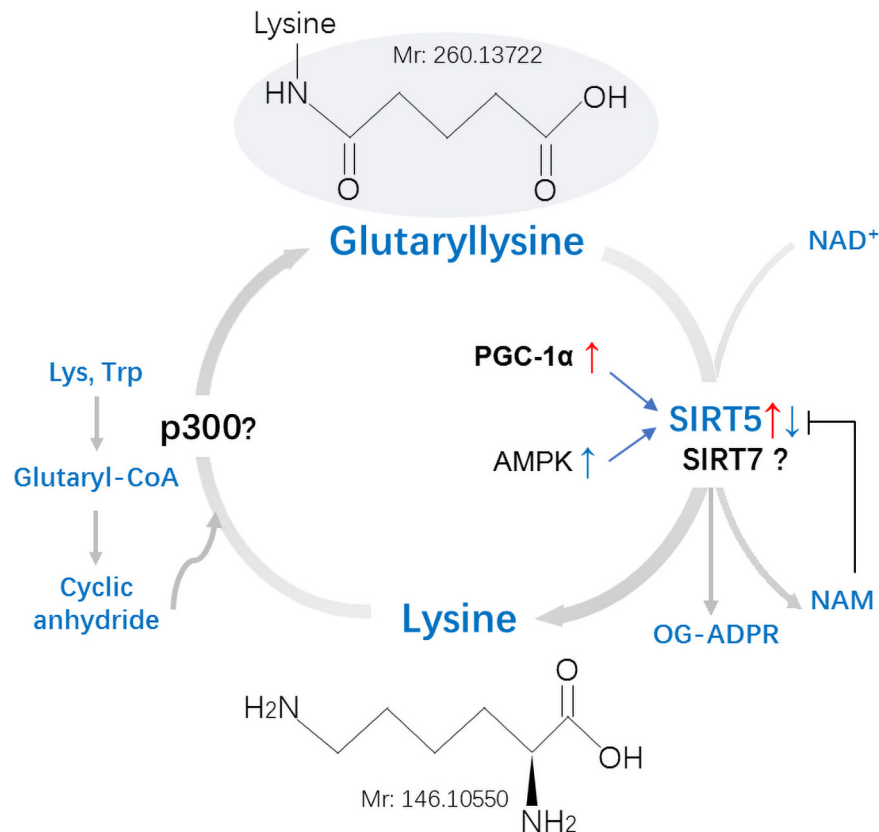


**FIGURE 3 |** Mechanisms and regulation of non-histones lysine glutarylation (Kglu). Glutaryl-CoA forms a reactive cyclic anhydride that readily glutarylates lysine residues on target proteins. No enzymes were found in this process *in vivo*. Whether the p300 is involved in the process of Kglu remains to be identified. Kglu is targeted for removal by the NAD<sup>+</sup>-dependent SIRT5. Expression of SIRT5 can be inhibited by NAM and be regulated by PGC-1α and AMPK. Whether the SIRT7 possesses potent deglutarylase activities remains to be verified *in vivo*. Lys, Lysine; Trp, Tryptophan; NAM, Nicotinamide; OG-ADPR, O-Glutaryl ADP-Ribose; PGC-1α, peroxisome proliferator-activated receptor coactivator-1α; AMPK, AMP-activated protein kinase; Mr, molecular mass.

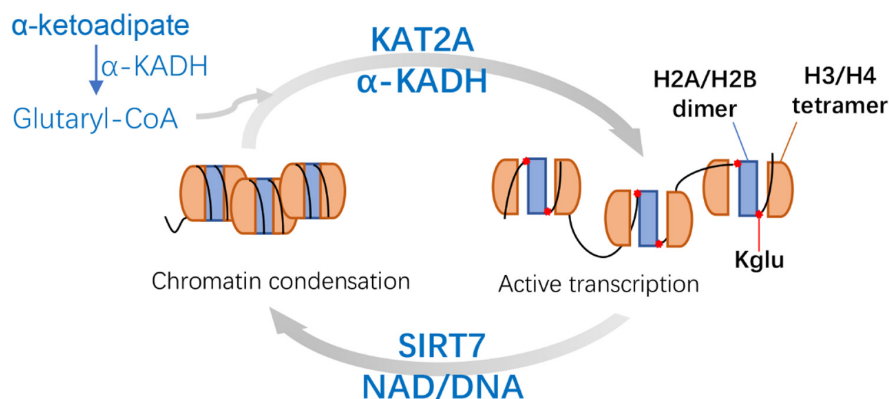


**FIGURE 4 |** Mechanisms and features of Histone H4 Lysine 91 glutarylation (H4K91glu). KAT2A is coupled with α-KADH to catalyze the H4K91glu as the histone glutaryl transferase. H4K91glu could regulate chromatin structure and enhance active gene expression. SIRT7-catalyzed removal of H4K91glu is related to chromatin condensation. KAT2A, lysine acetyltransferase 2A; α-KADH, α-ketoadipate dehydrogenase; NAD, nicotinamide adenine dinucleotide.

play a key role in energy production, cell signaling and cell survival, and mitochondrial dysfunction can lead to the aging and aging-related diseases, such as metabolic diseases, cancer,

and neurodegeneration (Osborne et al., 2016). Since acyl-CoA cannot penetrate the inner mitochondrial membrane, its accumulation in the mitochondrial compartment is easy.



Accumulation of toxic acyl-CoA will affect mitochondrial energy metabolism (Dimitrov et al., 2020). Glutaryl-CoA inhibits the E2 subunit of  $\alpha$ -ketoglutarate dehydrogenase complex (KGDHC), similar to the feedback inhibition of its physiological product, succinyl-CoA, leading to mitochondrial TCA cycle dysfunction (Sauer et al., 2005). Notably, the reduction of  $\alpha$ -ketoglutarate dehydrogenase (KGDH) activity has recently been demonstrated in other neurodegenerative diseases, such as Alzheimer (Gibson et al., 1988), Parkinson (Mizuno et al., 1994, 1995), and Huntington diseases (Klivenyi et al., 2004), sharing neuropathological similarities with GCDH deficiency (Strauss and Morton, 2003).

In addition, lysine glutarylation can also affect mitochondrial metabolism and other mitochondrial functions (Ju and He, 2018). CPS1, mainly found in mitochondria (Summar et al., 1995), is the first rate-limiting enzyme in the urea cycle (UC), which is responsible for directly incorporating ammonia into the intermediate of UC (Nitzahn and Lipshutz, 2020). It is verified that CPS1 is a substrate of Kglu, and that Kglu of CPS1 inhibits its enzymatic activity (Tan et al., 2014). Excessive glutarylation will reduce the activity of CPS1 enzyme, resulting in increased blood ammonia levels and damage to nerve cells (Nakagawa et al., 2009; Tan et al., 2014; Nitzahn and Lipshutz, 2020).

## Regulation of Asthenospermia

Unlike somatic cells, mature sperm has a highly concentrated chromatin structure. Except for a few genes that are expressed in sperm mitochondria, there is almost no transcription and translation activities (Gur and Breitbart, 2008). Therefore, compared with somatic cells, the function regulation of mature sperm cells is more dependent on PTMs (Cheng et al., 2019).

The most widespread PTM in human sperm studies is phosphorylation, followed by acetylation, and these modifications are essential for sperm differentiation, maturation, and function (Porambo et al., 2012; Yu et al., 2015). Cheng et al. (2019), for the first time, reported the cofactor and regulatory protein of human sperm Kglu, and also discussed the correlation between sperm Kglu and sperm motility, as well as the role of Kglu in asthenospermia. As the energy metabolism center, mitochondria are vital to sperm motility (Yu et al., 2015). They found that Kglu is clearly present in the mitochondria of normal male sperm, while the content of Kglu is reduced in weak sperm (Bakos et al., 2011). Therefore, they speculated that Kglu is involved in the regulation of human sperm mitochondrial function. The decrease of Kglu in mitochondria may damage mitochondrial function and ultimately affect sperm motility (Cheng et al., 2019).

In addition, many studies have proven that obesity can reduce sperm quality and functions, which cause sperm DNA damage, and lead to hypogonadism (Jensen et al., 2004; Ghanayem et al., 2010; MacDonald et al., 2010; Bakos et al., 2011; Dupont et al., 2013; Samavat et al., 2014; Ramaraju et al., 2018). Wang et al. (2020) found that obesity in men can increase testicular histone Kglu levels by 36%. Although they proved that Kglu is related to male reproductive dysfunction caused by obesity, whether there is a causal relationship between increased histone Kglu and decreased sperm motility still needs to be verified.

## Regulation of Oxidative Stress

It has been reported that Kglu is closely related to oxidative metabolism (Tan et al., 2014; Zhou et al., 2016; Chen et al., 2020). Tan et al. (2014) through GO enrichment analysis, found that Kglu was significantly enriched in many cellular metabolic processes, including redox and aerobic respiration. They also found the potential impact of Kglu on metabolic pathways of oxidative metabolism through KEGG and Pfam enrichment analysis (Tan et al., 2014). Study has showed that reactive oxygen regulatory proteins such as superoxidase dismutase could be a substrate of the enzymes involved in the addition of glutarylation (Xie L. et al., 2016).

The central nervous system has a high metal content, which can catalyze the formation of oxygen free radicals, and its antioxidant defense ability is relatively low, so it is vulnerable to free radical damage (Facheris et al., 2004). It is known that excessive mitochondrial ROS are the main cause of cellular oxidative stress (Tojyo et al., 1989; Turrens, 2003; Orrenius et al., 2007; Park et al., 2011). GSH can remove ROS and protect cells from oxidative damage (Zhou et al., 2016). Nicotinamide Adenine Dinucleotide Phosphate (NADPH) is the main intracellular reducing agent and plays a key role in keeping glutathione in its reduced form of GSH. Zhou et al. found that deglutarylation can activate one NADPH-producing enzyme: glucose-6-phosphate dehydrogenase (G6PD) (Zhou et al., 2016). In conclusion, Kglu may reduce or inactivate the activity of the enzyme, and the amount of NADPH will decrease, thus reducing the antioxidant defense ability of the nervous system and leading to nervous system damage. However, this still needs to be further verified.

Chen et al. (2020) found that mitochondrial ROS can cause endothelial dysfunction and hypertension. Therefore, oxidative stress is not only related to the nervous system but may also be an important mechanism of stress-induced cardiovascular disease (CVD). CVD is the main cause of morbidity and mortality worldwide, and metabolic dysfunction is the basic core mechanism of CVDs. Protein acylation plays an important role in the physiological and pathological processes of the heart and blood vessels (Chen et al., 2020). For example, malonylation can damage the activity of mTORC1 kinase and ultimately lead to angiogenesis defects, which is an important part of myocardial infarction (Bruning et al., 2018). Although the current studies on the relationship between Kglu and myocardial damage are less than that of malonylation, some important results have been discovered in recent years. For example, it's found that the serum protein Kglu level decreased after acute myocardial infarction (Zhou et al., 2020). In addition, Zhou et al. (2016) found that SIRT5 KO mice showed higher sensitivity to cardiac ischemia-reperfusion injury, which was related to the increased production of ROS. Relevant experiments have confirmed that by reducing ROS production and alleviating mitochondrial swelling, the damage caused by mitochondrial membrane potential in mice's cardiovascular system can be partially saved (Nagao et al., 2016; Yu et al., 2018). The association between Kglu and CVD is a new research field. In the future, it may be possible to reduce the oxidative stress after myocardial

**TABLE 2 |** Statistics of information on developed site prediction models.

Time (year)	Tool	10-fold cross-validation				References	URL
		SN	SP	ACC	MCC		
2018	GlutPred	65%	77%	75%	0.32	Ju and He, 2018	<a href="http://dx.doi.org/10.1016/j.ab">http://dx.doi.org/10.1016/j.ab</a>
2018	iGlu-Lys	50%	95%	88%	0.51	Xu et al., 2018	<a href="http://app.aporc.org/iGlu-Lys/">http://app.aporc.org/iGlu-Lys/</a>
2019	MDDGlutar	68%*	62%*	64%*	0.28*	Huang et al., 2019	<a href="http://csb.cse.yzu.edu.tw/MDDGlutar/">http://csb.cse.yzu.edu.tw/MDDGlutar/</a>
2019	RF-GlutarySite	81%	68%	75%	0.50	Al-Barakati et al., 2019	-
2020	PUL-GLU	72%	75%	75%	0.35	Ju and Wang, 2020	-
2020	BiPepGlut	70%	93%	82%	0.64	Arafat et al., 2020	<a href="http://www.brl.uiu.ac.bd/bioglutarylation">www.brl.uiu.ac.bd/bioglutarylation</a>
2021	iGlu_AdaBoost	87%	74%	80%	0.61	Dou et al., 2021	-

SN: sensitivity; SP: specificity; ACC: accuracy; MCC: matthew correlation coefficient.

\*5-fold cross-validation.

infarction by regulating the enzymes of Kglu, thereby reducing the damage to the heart.

## Regulation of Glutaric Aciduria Type 1

Glutariduria type 1 (GA1), a type of organic aciduria (Mahoney, 1976), was first reported by Goodman and Kohlhoff (1975). It is an autosomal recessive genetic disease that causes lysine and tryptophan metabolism disorders due to insufficient GCDH activity (Goodman et al., 1977). It is characterized by intermittent metabolic acidemia, dystonia, asthenia, and mental retardation (Stokke et al., 1976). The GCDH gene is located on human chromosome 19p13.2, spans about 7 kb, contains 11 exons and 10 introns (Goodman et al., 1977; Shadmehri et al., 2019), and it is involved in the degradation of L-lysine and L-tryptophan (Tan et al., 2014). It is known that GCDH degrades glutaryl-CoA, thereby reducing the Kglu level of the protein, and the GCDH deficiency will lead to the increase of glutaryl-CoA and Kglu (Tan et al., 2014).

Glutaric aciduria 1 is a multi-organ disease, and the organ most affected during metabolic abnormalities in patients is the brain (Zhou et al., 2016). GA1 is caused by a mutation in the gene of the mitochondrial stromal enzyme GCDH, which elevates the level of glutaric acid (GA) in the brain and blood (Koeller et al., 2002). GCDH deficiency could impair the degradation of lysine/tryptophan (Zhou et al., 2016), which may be an important reason for the increase of glutaric acid, because lysine/tryptophan is the source of glutaric acid. It is known that glutaric acid is one of the precursors of glutaryl-CoA, and the augment of glutaric acid will indirectly lead to the increase of glutarylation (Tan et al., 2014; Chen et al., 2020). Schmiesing et al. (2018) also believed that GCDH deficiency is related to the mitochondrial protein lysine Kglu in the pathogenesis of GA1 disease, which leads to the heterogeneity and fragility of glial cell mitochondria (Zhou et al., 2016). Is it possible to treat or alleviate the neurological symptoms of GA1 by regulating the protein Kglu? This is a challenging subject for researchers.

## Regulation of Chromatin Dynamics

Nucleosome is the basic repetitive unit of chromatin. Both structures are highly dynamic, and one main mechanism for controlling their dynamics is through PTMs of histone. H4K91 is a residue located at the interface between H3-H4 tetramer and H2A-H2B dimer (Bao et al., 2019). There are salt bridges between

H4K91 and glutamate residues from histone H2B in nucleosome (Cosgrove et al., 2004).

It has been reported that a known histone acetyltransferase KAT2A (Grant et al., 1997; Wang and Dent, 2014) is coupled with  $\alpha$ -ketoacid dehydrogenase to catalyze the oxidative decarboxylation of  $\alpha$ -ketoacid to glutaryl-CoA as the histone glutaryl transferase (Bao et al., 2019). Then SIRT7 can catalyze the removal of H4K91glu. H4K91glu disturbs the

**TABLE 3 |** The number of positive and negative samples in the training and testing data sets.

Time (year)	Tool	Testing data set		Training data set	
		Positive	Negative	Positive	Negative
2018	GlutPred	56	428	590	3498
2018	iGlu-Lys	-	-	-	-
2019	MDDGlutar	46	92	430	860
2019	RF-GlutarySite	44	203	400	400
2020	PUL-GLU	56	428	590	3498
2020	BiPepGlut	217	192	1952	1731
2021	iGlu_AdaBoost	44	203	400	1703

-, Data are not available.

**TABLE 4 |** Scientific questions for future studies about Kglu.

No.	Classification	Questions
1	Mechanism	Is there any relationship between the regulation of Kglu, acetylation and succinylation overlap sites?
2		Does glutaryl transferase also exist in other parts such as the glutarylation of proteins in the cytoplasm and mitochondria?
3		Why are there so few sites found in eukaryotes?
4		Is Kglu present in prokaryotes other than <i>E. coli</i> and <i>M. tuberculosis</i> ?
5	Function	Is there Kglu of prokaryotic biofilm proteins?
6		Is it possible to treat asthenospermia and GA1 by regulating Kglu of proteins?
7		Is there any connection between Kglu and the development of cancer?
8		Except for H4K91, what is the function of other histone glutaric acid sites?

efficient assembly of H2A/H2B dimer and H3/H4 tetramer to form octamer (Bao et al., 2019; **Figure 4**). Therefore, glutaryl groups of histones affect the stability of nucleosomes and chromatin. In mammalian cells, H4K91glu is mainly enriched in the promoter region of highly expressed genes. The downregulation of H4K91glu is closely associated with chromatin aggregation during mitosis and the response to DNA damage (Bao et al., 2019), suggesting that H4K91glu plays a vital role in modulating gene expression and chromatin damage. In addition, histone H4K91 was mutated into glutamate (K91E) in *S. cerevisiae* to simulate Kglu. The results consistently showed significant delays during S and G2/M phase in H4K91E mutant cells, suggesting that the K91E mutations (mimicking K91glu) may also destroy the assembly of nucleosome and chromatin during S phase and mitosis (Bao et al., 2019).

## PREDICTION OF GLUTARYLATION BY COMPUTATIONAL TOOLS

To better understand the molecular mechanism of Kglu, it is important to accurately identify the substrate of Kglu and its corresponding Kglu sites. The traditional method of identifying Kglu is based on affinity enrichment proteomics method (Chen et al., 2012): pan anti-Kglu antibody was used to enrich the glutarylated peptide, and then the HPLC-mass spectrometry (MS)/MS was used to analyze it (Chen et al., 2005). This experimental method is expensive, cumbersome and time-consuming (Xu et al., 2018). Therefore, some computational tools for predicting Kglu sites have been developed (**Table 2**). Based on known protein interaction data, using feature extraction and feature selection techniques (Chen et al., 2019), combined with probability theory and mathematical statistics, using recognized machine learning algorithms, such as support vector machines (SVMs) (Huang et al., 2019), random forest (RF) (Al-Barakati et al., 2019), to discover possible proteins Interaction site.

Ju and He (2018) discovered that kspaced amino acid pair features play an important role in the prediction of glutarylation sites. Then they established a predictive model GlutPred based on comprehensive features composed of amino acid factor (AAF), binary code (BE), and composition of k-spaced Amino Acid Pairs (CKSAAP). In the same year, Xu et al. (2018) used the characteristics of the position-specific propensity matrices (PSPM) to build a model iGlu-Lys, which improved the prediction performance. Huang et al. (2019) later developed a model MDDGlutar based on SVM, which combines six motifs identified by maximal dependence decomposition (MDD). This model significantly improves the predictive performance of Kglu sites recognition and takes into account sensitivity and specificity. Then Al-Barakati et al. (2019) used Random Forest (RF) to predict the Kglu sites from the primary amino acid sequence and established the model RF-GlutarySite. In terms of performance indicators that are most affected by TP rate (such as SN, PR, and F1 scores), RF-GlutarySite is superior to the existing glutaric acid site predictors. On the contrary, for indicators that are more sensitive to the TN rate (such as SP and ACC), it does not work well. Ju and Wang (2020)

regarded the experimentally verified glutaric acid sites as positive samples, and the remaining unverified lysine sites as unlabeled samples. A new type of glutaric acid site predictor PUL-GLU was developed by using positive unlabeled (PU) learning technology. Based on the evolutionary characteristics of double peptides, Arafat et al. (2020) used Extra-Trees (ET) classifier to build the model BiPepGlut. Recently, Dou et al. (2021) believed that the physical and chemical properties of charge, polarity, and van der Waals volume play a key role in the recognition of protein glutarylation, especially the positively charged R and K residues around the Kglu sites. They used the ensemble classifier AdaBoost to identify Kglu sites and built a new computational predictor called iGlu\_AdaBoost. Here is a comparison of these predictors. iGlu-Lys did not utilize the secondary structure and tertiary structure characteristics of protein, and not balance positive and negative data. The SN of iGlu-Lys is the lowest (Xu et al., 2018). GlutPred used a biased SVM algorithm to handle the unbalanced problem in the prediction of glutarylation sites and showed good performance in specificity (SP) and accuracy (ACC). However, there was a large gap between the positive and negative prediction abilities (Ju and He, 2018). The prediction results of iGlu-Lys and GlutPred were significantly biased toward the majority of samples (i.e., non-glutarylation sites), and the prediction efficiency of positive samples was lower (Dou et al., 2021). RF-GlutarySite helps discover the relationship between glutarylation and well-known lysine modifications, such as acetylation, methylation, and some recently identified lysine modifications. PUL-GLU could predict more non-glutaryl lysine sites (Al-Barakati et al., 2019). iGlu\_AdaBoost has good prediction generalization ability, and the prediction results have high consistency between positive samples and negative samples (Dou et al., 2021).

From GlutPred to iGlu\_AdaBoost, which was recently developed (not yet online), there are currently seven computational prediction models (**Table 2**). Besides, the number of positive and negative samples in the training and testing data sets were shown in **Table 3**. These tools provide researchers an easy way to discover new Kglu sites and proteins.

## CONCLUSION

Although the study of Kglu of biological proteins started late, the research on Kglu is increasing quickly and has achieved great results. The development of high-resolution LC-MS/MS methods has made it possible for the identification of massive Kglu proteins. Kglu is involved in various pathways that control diverse cellular functions ranging from mitochondria to chromosomal histones. Current studies mainly focus on mitochondrial metabolism and related content (Tan et al., 2014; Schmiesing et al., 2018). The emergence of Kglu site prediction tools also accelerates the discovery of new Kglu sites.

However, some limitations in the previous reported studies still need to be addressed. One important question is the reasons for the small number of sites found in eukaryotes. We consider the following four aspects: (1) The antibody specificity. Although eight studies stated that their antibodies were highly specific



and verified, the relevant data about the number of glutarylated peptides vs. unmodified peptides were not easily accessed from three studies. Hence, it is better to firstly collect these antibodies to evaluate their specificity in the same species/tissues, and then use the antibody with highest specificity to identify the glutarylated protein and sites in the new species/tissues. (2) The low stoichiometry of this modification (Schmiesing et al., 2018). It is well known that discovering a new, unknown PTM with low stoichiometry is a great challenge for analytical techniques. (3) The sample preparation. Different preparation methods will influence the purity of the sample, which in turn affects the specific binding of antibodies. During the sample preparation, if deglutarylase inhibitors are used in advance to inhibit deglutarylation, the number of identified glutarylated protein and sites will be increased. For example, Tan et al. (2014) identified more glutarylated proteins and sites from *Sirt5*<sup>-/-</sup> mice, which can block deglutarylation with the deletion of *SIRT5*, and maximize the number of sites in tissues. But in other studies, these did not use inhibitors to block deglutarylation during sample preparation, which may reduce the number of sites (Schmiesing et al., 2018; Bao et al., 2019; Zhou et al., 2020). (4) The lability of this PTM. Kglu sites are characterized by instability and low abundance *in vivo* (Huang et al., 2019). If this PTM is decomposed before detection, it will result in a small number of sites found in eukaryotes. Hence, it is very important to add the stabilizer of PTM during sample preparation.

Another important question is the relationship between Kglu and cancer. As early as Tanaka et al. (1993) glutarylated the serum proteins of mice with glutaric anhydride, and found that glutarylation reduced the distribution of carrier protein in normal tissues, resulting in higher accumulation of tumor tissues. Therefore, they believed that glutaryl serum proteins have relative tumor selectivity and can be used as a macromolecular carrier for anti-tumor drugs, but this requires further research and verification. It is known that *SIRT5* is responsible for de-glutarylation of Kglu (Tan et al., 2014). Recently, Osborne et al. (2016); Bringman-Rodenbarger et al. (2018), and Kumar and Lombard (2018) showed that *SIRT5* plays an important role in cancer models, including tumor suppression and tumor metabolism (Osborne et al., 2016; Bringman-Rodenbarger et al., 2018; Kumar and Lombard, 2018). In addition, Carrico et al. (2018) believed that a potential key role of mitochondrial acylation in tumorigenesis is to initiate the

Warburg effect. Hence, future studies are needed to uncover the role of Kglu in cancer.

For other questions about glutarylation, we have made a table (Table 4). For example, there are some Kglu sites that partially overlap with other PTMs such as Kac or Ksucc (Du et al., 2011; Chen et al., 2012; Park et al., 2013). Is there any crosstalk in the regulation of overlapping sites? Currently, most of the Kglu studies focus on the non-histone proteins, while the research on histone Kglu is relatively rare. Therefore, more research on histone Kglu is needed. As there are many problems, it is not necessary to list them all here, but these issues are basic and critical. We hope these questions can provide some enlightenment for future researchers.

## AUTHOR CONTRIBUTIONS

YX, FM, and LX conceived the study protocol, participated in the literature search and the data collection, analyzed the data, drafted the manuscript, and revised the manuscript. All authors read and approved the final manuscript.

## FUNDING

This study was funded by the National Natural Science Foundation of China (No. 82002172), Program for Science and Technology Development in Henan Province (Nos. 202102310205, 192102310350, and 192102310379), Key Scientific Research Project Plan of Henan Province (No. 20A180001), China Postdoctoral Science Foundation (No. 2020M682279), and Henan University Medical National Natural Science Foundation Cultivation Program.

## SUPPLEMENTARY MATERIAL

The Supplementary Material for this article can be found online at: <https://www.frontiersin.org/articles/10.3389/fcell.2021.667684/full#supplementary-material>

**Supplementary Table 1** | The main methods and reagents used in previous researches.

## REFERENCES

- Al-Barakati, H. J., Saigo, H., Newman, R. H., and Kc, D. B. (2019). RF-GlutarySite: A random forest based predictor for glutarylation sites. *Mol. Omics* 15, 189–204. doi: 10.1039/c9mo00028c
- Arafat, M. E., Ahmad, M. W., Shovan, S. M., Dehzangi, A., Dipta, S. R., Hasan, M. A. M., et al. (2020). Accurately predicting glutarylation sites using sequential bi-peptide-based evolutionary features. *Genes (Basel)* 11:1023. doi: 10.3390/genes11091023
- Bakos, H. W., Mitchell, M., Setchell, B. P., and Lane, M. (2011). The effect of paternal diet-induced obesity on sperm function and fertilization in a mouse model. *Int. J. Androl.* 34, 402–410. doi: 10.1111/j.1365-2605.2010.01092.x
- Bannister, A. J., and Kouzarides, T. (1996). The CBP co-activator is a histone acetyltransferase. *Nature* 384, 641–643. doi: 10.1038/384641a0
- Bao, X., Liu, Z., Zhang, W., Gladysz, K., Fung, Y. M. E., Tian, G., et al. (2019). Glutarylation of histone H4 lysine 91 regulates chromatin dynamics. *Mol. Cell* 76, 660–675.e9.
- Bernal, V., Castano-Cerezo, S., Gallego-Jara, J., Ecija-Conesa, A., de Diego, T., Iborra, J. L., et al. (2014). Regulation of bacterial physiology by lysine acetylation of proteins. *N. Biotechnol.* 31, 586–595. doi: 10.1016/j.nbt.2014.03.002
- Besrat, A., Polan, C. E., and Henderson, L. M. (1969). Mammalian metabolism of glutaric acid. *J. Biol. Chem.* 244, 1461–1467. doi: 10.1016/s0021-9258(18)01782-5



- Bringman-Rodenbarger, L. R., Guo, A. H., Lyssiotis, C. A., and Lombard, D. B. (2018). Emerging roles for SIRT5 in metabolism and cancer. *Antioxid. Redox Signal.* 28, 677–690. doi: 10.1089/ars.2017.7264
- Bruning, U., Morales-Rodriguez, F., Kalucka, J., Goveia, J., Taverna, F., Queiroz, K. C. S., et al. (2018). Impairment of angiogenesis by fatty acid synthase inhibition involves mTOR malonylation. *Cell Metab.* 28, 866–880.e15.
- Buler, M., Aatsinki, S. M., Izzi, V., Uusimaa, J., and Hakkola, J. (2014). SIRT5 is under the control of PGC-1 $\alpha$  and AMPK and is involved in regulation of mitochondrial energy metabolism. *FASEB J.* 28, 3225–3237. doi: 10.1096/fj.13-245241
- Carrico, C., Meyer, J. G., He, W., Gibson, B. W., and Verdin, E. (2018). The mitochondrial acylome emerges: proteomics, regulation by sirtuins, and metabolic and disease implications. *Cell Metab.* 27, 497–512. doi: 10.1016/j.cmet.2018.01.016
- Chen, X. F., Chen, X., and Tang, X. (2020). Short-chain fatty acid, acylation and cardiovascular diseases. *Clin. Sci. (Lond.)* 134, 657–676. doi: 10.1042/cs20200128
- Chen, Y., Kwon, S. W., Kim, S. C., and Zhao, Y. (2005). Integrated approach for manual evaluation of peptides identified by searching protein sequence databases with tandem mass spectra. *J. Proteome Res.* 4, 998–1005. doi: 10.1021/pr049754t
- Chen, Y., Sprung, R., Tang, Y., Ball, H., Sangras, B., Kim, S. C., et al. (2007). Lysine propionylation and butyrylation are novel post-translational modifications in histones. *Mol. Cell. Proteomics* 6, 812–819. doi: 10.1074/mcp.m700021-mcp200
- Chen, Y., Zhao, W., Yang, J. S., Cheng, Z., Luo, H., Lu, Z., et al. (2012). Quantitative acetylome analysis reveals the roles of SIRT1 in regulating diverse substrates and cellular pathways. *Mol. Cell. Proteomics* 11, 1048–1062. doi: 10.1074/mcp.m112.019547
- Chen, Z., Liu, X., Li, F., Li, C., Marquez-Lago, T., Leier, A., et al. (2019). Large-scale comparative assessment of computational predictors for lysine post-translational modification sites. *Brief. Bioinform.* 20, 2267–2290. doi: 10.1093/bib/bby089
- Cheng, Y. M., Hu, X. N., Peng, Z., Pan, T. T., Wang, F., Chen, H. Y., et al. (2019). Lysine glutarylation in human sperm is associated with progressive motility. *Hum. Reprod.* 34, 1186–1194. doi: 10.1093/humrep/dez068
- Choudhary, C., Kumar, C., Gnäd, F., Nielsen, M. L., Rehman, M., Walther, T. C., et al. (2009). Lysine acetylation targets protein complexes and co-regulates major cellular functions. *Science* 325, 834–840. doi: 10.1126/science.1175371
- Cosgrove, M. S., Boeke, J. D., and Wolberger, C. (2004). Regulated nucleosome mobility and the histone code. *Nat. Struct. Mol. Biol.* 11, 1037–1043. doi: 10.1038/nsmb851
- Dai, L., Peng, C., Montellier, E., Lu, Z., Chen, Y., Ishii, H., et al. (2014). Lysine 2-hydroxyisobutyrylation is a widely distributed active histone mark. *Nat. Chem. Biol.* 10, 365–370. doi: 10.1038/nchembio.1497
- Diallo, I., Seve, M., Cunin, V., Minassian, F., Poisson, J. F., Michelland, S., et al. (2019). Current trends in protein acetylation analysis. *Expert Rev. Proteomics* 16, 139–159. doi: 10.1080/14789450.2019.1559061
- Dimitrov, B., Molema, F., Williams, M., Schmiesing, J., Muhlhausen, C., Baumgartner, M. R., et al. (2020). Organic acidurias: Major gaps, new challenges, and a yet unfulfilled promise. *J. Inherit. Metab. Dis.* 44, 9–21. doi: 10.1002/jimd.12254
- Dou, L., Li, X., Zhang, L., Xiang, H., and Xu, L. (2021). iGlu\_AdaBoost: identification of lysine glutarylation using the AdaBoost classifier. *J. Proteome Res.* 20, 191–201. doi: 10.1021/acs.jproteome.0c00314
- Du, J., Zhou, Y., Su, X., Yu, J. J., Khan, S., Jiang, H., et al. (2011). Sirt5 is a NAD-dependent protein lysine demethylase and desuccinylase. *Science* 334, 806–809. doi: 10.1126/science.1207861
- Dupont, C., Faure, C., Sermondade, N., Boubaya, M., Eustache, F., Clement, P., et al. (2013). Obesity leads to higher risk of sperm DNA damage in infertile patients. *Asian J. Androl.* 15, 622–625. doi: 10.1038/aja.2013.65
- Facheris, M., Beretta, S., and Ferrarese, C. (2004). Peripheral markers of oxidative stress and excitotoxicity in neurodegenerative disorders: tools for diagnosis and therapy? *J. Alzheimers Dis.* 6, 177–184. doi: 10.3233/jad-2004-6210
- Ghanayem, B. I., Bai, R., Kissling, G. E., Travlos, G., and Hoffer, U. (2010). Diet-induced obesity in male mice is associated with reduced fertility and potentiation of acrylamide-induced reproductive toxicity. *Biol. Reprod.* 82, 96–104. doi: 10.1095/biolreprod.109.078915
- Gibson, G. E., Sheu, K. F., Blass, J. P., Baker, A., Carlson, K. C., Harding, B., et al. (1988). Reduced activities of thiamine-dependent enzymes in the brains and peripheral tissues of patients with Alzheimer's disease. *Arch. Neurol.* 45, 836–840. doi: 10.1001/archneur.1988.00520320022009
- Goodman, S. I., and Frerman, F. E. (1995). "Organic Acidemias due to defects in lysine oxidation: 2-ketoadipic academia and glutaric academia," in *The Metabolic and Molecular Bases of Inherited Disease*, 8th Edn, eds C. R. Scriver, A. L. Beaudet, W. S. Sly, and D. Valle (New York, NY: McGraw-Hill), 2195–2204.
- Goodman, S. I., and Kohlhoff, J. G. (1975). Glutaric aciduria: inherited deficiency of glutaryl-CoA dehydrogenase activity. *Biochem. Med.* 13, 138–140. doi: 10.1016/0006-2944(75)90149-0
- Goodman, S. I., Norenberg, M. D., Shikes, R. H., Breslich, D. J., and Moe, P. G. (1977). Glutaric aciduria: biochemical and morphologic considerations. *J. Pediatr.* 90, 746–750. doi: 10.1016/s0022-3476(77)81240-7
- Grant, P. A., Duggan, L., Cote, J., Roberts, S. M., Brownell, J. E., Candau, R., et al. (1997). Yeast Gcn5 functions in two multisubunit complexes to acetylate nucleosomal histones: characterization of an Ada complex and the SAGA (Spt/Ada) complex. *Genes Dev.* 11, 1640–1650. doi: 10.1101/gad.11.13.1640
- Gur, Y., and Breitbart, H. (2008). Protein synthesis in sperm: dialog between mitochondria and cytoplasm. *Mol. Cell. Endocrinol.* 282, 45–55. doi: 10.1016/j.mce.2007.11.015
- Harmel, R., and Fiedler, D. (2018). Features and regulation of non-enzymatic post-translational modifications. *Nat. Chem. Biol.* 14, 244–252. doi: 10.1038/nchembio.2575
- Hirschey, M. D., and Zhao, Y. (2015). Metabolic regulation by lysine malonylation, succinylation, and glutarylation. *Mol. Cell. Proteomics* 14, 2308–2315. doi: 10.1074/mcp.r114.046664
- Huang, K. Y., Kao, H. J., Hsu, J. B., Weng, S. L., and Lee, T. Y. (2019). Characterization and identification of lysine glutarylation based on intrinsic interdependence between positions in the substrate sites. *BMC Bioinformatics* 19:384. doi: 10.1186/s12859-018-2394-9
- Jensen, T. K., Andersson, A. M., Jorgensen, N., Andersen, A. G., Carlsen, E., Petersen, J. H., et al. (2004). Body mass index in relation to semen quality and reproductive hormones among 1,558 Danish men. *Fertil. Steril.* 82, 863–870. doi: 10.1016/j.fertnstert.2004.03.056
- Ju, Z., and He, J. J. (2018). Prediction of lysine glutarylation sites by maximum relevance minimum redundancy feature selection. *Anal. Biochem.* 550, 1–7. doi: 10.1016/j.ab.2018.04.005
- Ju, Z., and Wang, S. Y. (2020). Computational identification of lysine glutarylation sites using positive-unlabeled learning. *Curr. Genomics* 21, 204–211. doi: 10.2174/1389202921666200511072327
- Kim, S. C., Sprung, R., Chen, Y., Xu, Y., Ball, H., Pei, J., et al. (2006). Substrate and functional diversity of lysine acetylation revealed by a proteomics survey. *Mol. Cell* 23, 607–618. doi: 10.1016/j.molcel.2006.06.026
- Klivenyi, P., Starkov, A. A., Calingasan, N. Y., Gardian, G., Browne, S. E., Yang, L., et al. (2004). Mice deficient in dihydrolipoamide dehydrogenase show increased vulnerability to MPTP, malonate and 3-nitropropionic acid neurotoxicity. *J. Neurochem.* 88, 1352–1360. doi: 10.1046/j.1471-4159.2003.02263.x
- Koeller, D. M., Woontner, M., Crnic, L. S., Kleinschmidt-DeMasters, B., Stephens, J., Hunt, E. L., et al. (2002). Biochemical, pathologic and behavioral analysis of a mouse model of glutaric acidemia type I. *Hum. Mol. Genet.* 11, 347–357. doi: 10.1093/hmg/11.4.347
- Kumar, S., and Lombard, D. B. (2017). For Certain, SIRT4 Activities! *Trends Biochem. Sci.* 42, 499–501. doi: 10.1016/j.tibs.2017.05.008
- Kumar, S., and Lombard, D. B. (2018). Functions of the sirtuin deacylase SIRT5 in normal physiology and pathobiology. *Crit. Rev. Biochem. Mol. Biol.* 53, 311–334. doi: 10.1080/10409238.2018.1458071
- Lundby, A., Lage, K., Weinert, B. T., Bekker-Jensen, D. B., Secher, A., Skovgaard, T., et al. (2012). Proteomic analysis of lysine acetylation sites in rat tissues reveals organ specificity and subcellular patterns. *Cell Rep.* 2, 419–431. doi: 10.1016/j.celrep.2012.07.006
- MacDonald, A. A., Herbison, G. P., Showell, M., and Farquhar, C. M. (2010). The impact of body mass index on semen parameters and reproductive hormones in human males: a systematic review with meta-analysis. *Hum. Reprod. Update* 16, 293–311. doi: 10.1093/humupd/dmp047

- Macek, B., Forchhammer, K., Hardouin, J., Weber-Ban, E., Grangeasse, C., and Mijakovic, I. (2019). Protein post-translational modifications in bacteria. *Nat. Rev. Microbiol.* 17, 651–664.
- Mahoney, M. J. (1976). Organic acidemias. *Clin. Perinatol.* 3, 61–78. doi: 10.1017/9781107323704.020
- Menon, G. K., and Stern, J. R. (1960). Enzymic synthesis and metabolism of malonyl coenzyme A and glutaryl coenzyme A. *J. Biol. Chem.* 235, 3393–3398. doi: 10.1016/s0021-9258(18)64478-3
- Mizuno, Y., Ikebe, S., Hattori, N., Nakagawa-Hattori, Y., Mochizuki, H., Tanaka, M., et al. (1995). Role of mitochondria in the etiology and pathogenesis of Parkinson's disease. *Biochim. Biophys. Acta* 1271, 265–274.
- Mizuno, Y., Matuda, S., Yoshino, H., Mori, H., Hattori, N., and Ikebe, S. (1994). An immunohistochemical study on alpha-ketoglutarate dehydrogenase complex in Parkinson's disease. *Ann. Neurol.* 35, 204–210. doi: 10.1002/ana.410350212
- Nagao, M., Toh, R., Irino, Y., Mori, T., Nakajima, H., Hara, T., et al. (2016). beta-Hydroxybutyrate elevation as a compensatory response against oxidative stress in cardiomyocytes. *Biochem. Biophys. Res. Commun.* 475, 322–328. doi: 10.1016/j.bbrc.2016.05.097
- Nakagawa, T., Lomb, D. J., Haigis, M. C., and Guarente, L. (2009). SIRT5 Deacetylates carbamoyl phosphate synthetase 1 and regulates the urea cycle. *Cell* 137, 560–570. doi: 10.1016/j.cell.2009.02.026
- Nishizuka, Y., Kuno, S., and Hayaishi, O. (1960). Enzymic formation of acetyl-CoA and carbon dioxide from glutaryl-CoA. *Biochim. Biophys. Acta* 43, 357–360. doi: 10.1016/0006-3002(60)90456-x
- Nitzahn, M., and Lipshutz, G. S. (2020). CPS1: Looking at an ancient enzyme in a modern light. *Mol. Genet. Metab.* 131, 289–298. doi: 10.1016/j.ymgme.2020.10.003
- Ogryzko, V. V., Schiltz, R. L., Russanova, V., Howard, B. H., and Nakatani, Y. (1996). The transcriptional coactivators p300 and CBP are histone acetyltransferases. *Cell* 87, 953–959. doi: 10.1016/s0092-8674(00)82001-2
- Orrenius, S., Gogvadze, V., and Zhivotovsky, B. (2007). Mitochondrial oxidative stress: implications for cell death. *Annu. Rev. Pharmacol. Toxicol.* 47, 143–183. doi: 10.1146/annurev.pharmtox.47.120505.105122
- Osborne, B., Bentley, N. L., Montgomery, M. K., and Turner, N. (2016). The role of mitochondrial sirtuins in health and disease. *Free Radic. Biol. Med.* 100, 164–174. doi: 10.1016/j.freeradbiomed.2016.04.197
- Park, J., Chen, Y., Tishkoff, D. X., Peng, C., Tan, M., Dai, L., et al. (2013). SIRT5-mediated lysine desuccinylation impacts diverse metabolic pathways. *Mol. Cell* 50, 919–930. doi: 10.1016/j.molcel.2013.06.001
- Park, J., Lee, J., and Choi, C. (2011). Mitochondrial network determines intracellular ROS dynamics and sensitivity to oxidative stress through switching inter-mitochondrial messengers. *PLoS One* 6:e23211. doi: 10.1371/journal.pone.0023211
- Peng, C., Lu, Z., Xie, Z., Cheng, Z., Chen, Y., Tan, M., et al. (2011). The first identification of lysine malonylation substrates and its regulatory enzyme. *Mol. Cell. Proteomics* 10:M111012658.
- Porambo, J. R., Salicioni, A. M., Visconti, P. E., and Platt, M. D. (2012). Sperm phosphoproteomics: historical perspectives and current methodologies. *Expert Rev. Proteomics* 9, 533–548. doi: 10.1586/epr.12.41
- Ramaraju, G. A., Teppala, S., Prathigudupu, K., Kalagara, M., Thota, S., Kota, M., et al. (2018). Association between obesity and sperm quality. *Andrologia* 50:e12888. doi: 10.1111/and.12888
- Sabari, B. R., Zhang, D., Allis, C. D., and Zhao, Y. (2017). Metabolic regulation of gene expression through histone acylations. *Nat. Rev. Mol. Cell Biol.* 18, 90–101. doi: 10.1038/nrm.2016.140
- Samavat, J., Natali, I., Degl'Innocenti, S., Filimberti, E., Cantini, G., Di Franco, A., et al. (2014). Acrosome reaction is impaired in spermatozoa of obese men: a preliminary study. *Fertil. Steril.* 102, 1274–1281.e2.
- Sauer, S. W., Okun, J. G., Schwab, M. A., Crnic, L. R., Hoffmann, G. F., Goodman, S. I., et al. (2005). Bioenergetics in glutaryl-coenzyme A dehydrogenase deficiency: a role for glutaryl-coenzyme A. *J. Biol. Chem.* 280, 21830–21836. doi: 10.1074/jbc.m502845200
- Schmiesing, J., Storch, S., Dorfler, A. C., Schweizer, M., Makrypidi-Fraune, G., Thelen, M., et al. (2018). Disease-Linked glutarylation impairs function and interactions of mitochondrial proteins and contributes to mitochondrial heterogeneity. *Cell Rep.* 24, 2946–2956. doi: 10.1016/j.celrep.2018.08.014
- Shadmehri, A. A., Fattahi, N., Pourreza, M. R., Koochian, M., Zariifi, S., Darbouy, M., et al. (2019). Molecular genetic study of glutaric aciduria, type I: Identification of a novel mutation. *J. Cell. Biochem.* 120, 3367–3372. doi: 10.1002/jcb.27607
- Stokke, O., Goodman, S. I., and Moe, P. G. (1976). Inhibition of brain glutamate decarboxylase by glutarate, glutaconate, and beta-hydroxyglutarate: explanation of the symptoms in glutaric aciduria? *Clin. Chim. Acta* 66, 411–415. doi: 10.1016/0009-8981(76)90241-2
- Strauss, K. A., and Morton, D. H. (2003). Type I glutaric aciduria, part 2: a model of acute striatal necrosis. *Am. J. Med. Genet. Part C Semin. Med. Genet.* 121c, 53–70. doi: 10.1002/ajmg.c.20008
- Summar, M. L., Dasouki, M. J., Schofield, P. J., Krishnamani, M. R., Vnencak-Jones, C., Tuchman, M., et al. (1995). Physical and linkage mapping of human carbamyl phosphate synthetase I (CPS1) and reassignment from 2p to 2q35. *Cytogenet. Cell Genet.* 71, 266–267. doi: 10.1159/000134124
- Tan, M., Luo, H., Lee, S., Jin, F., Yang, J. S., Montellier, E., et al. (2011). Identification of 67 histone marks and histone lysine crotonylation as a new type of histone modification. *Cell* 146, 1016–1028. doi: 10.1016/j.cell.2011.08.008
- Tan, M., Peng, C., Anderson, K. A., Chhoy, P., Xie, Z., Dai, L., et al. (2014). Lysine glutarylation is a protein posttranslational modification regulated by SIRT5. *Cell Metab.* 19, 605–617. doi: 10.1016/j.cmet.2014.03.014
- Tanaka, T., Kaneo, Y., Shiramoto, S., and Iguchi, S. (1993). The disposition of serum proteins as drug-carriers in mice bearing Sarcoma 180. *Biol. Pharm. Bull.* 16, 1270–1275. doi: 10.1248/bpb.16.1270
- Tojyo, Y., Okumura, K., Kanazawa, M., and Matsumoto, Y. (1989). Effect of cytochalasin D on acinar cell structure and secretion in rat parotid salivary glands in vitro. *Arch. Oral Biol.* 34, 847–855. doi: 10.1016/0003-9969(89)90140-4
- Turrens, J. F. (2003). Mitochondrial formation of reactive oxygen species. *J. Physiol.* 552, 335–344. doi: 10.1113/jphysiol.2003.049478
- Vamecq, J., de Hoffmann, E., and Van Hoof, F. (1985). Mitochondrial and peroxisomal metabolism of glutaryl-CoA. *Eur. J. Biochem.* 146, 663–669. doi: 10.1111/j.1432-1033.1985.tb08702.x
- Venne, A. S., Kollipara, L., and Zahedi, R. P. (2014). The next level of complexity: crosstalk of posttranslational modifications. *Proteomics* 14, 513–524. doi: 10.1002/pmic.201300344
- Walsh, C. T., Garneau-Tsodikova, S., and Gatto, G. J. Jr. (2005). Protein posttranslational modifications: the chemistry of proteome diversifications. *Angew. Chem. Int. Ed Engl.* 44, 7342–7372. doi: 10.1002/anie.200501023
- Wang, F., Chen, H., Chen, Y., Cheng, Y., Li, J., Zheng, L., et al. (2020). Diet-induced obesity is associated with altered expression of sperm motility-related genes and testicular post-translational modifications in a mouse model. *Theriogenology* 158, 233–238. doi: 10.1016/j.theriogenology.2020.09.023
- Wang, L., and Dent, S. Y. (2014). Functions of SAGA in development and disease. *Epigenomics* 6, 329–339. doi: 10.2217/epi.14.22
- Xie, L., Wang, G., Yu, Z., Zhou, M., Li, Q., Huang, H., et al. (2016). Proteome-wide lysine glutarylation profiling of the *Mycobacterium tuberculosis* H37Rv. *J. Proteome Res.* 15, 13179–13185. doi: 10.1021/acs.jproteome.5b00917
- Xie, Z., Dai, J., Dai, L., Tan, M., Cheng, Z., Wu, Y., et al. (2012). Lysine succinylation and lysine malonylation in histones. *Mol. Cell. Proteomics* 11, 100–107. doi: 10.1074/mcp.m111.015875
- Xie, Z., Zhang, D., Chung, D., Tang, Z., Huang, H., Dai, L., et al. (2016). Metabolic regulation of gene expression by histone lysine beta-hydroxybutyrylation. *Mol. Cell* 62, 194–206. doi: 10.1016/j.molcel.2016.03.036
- Xu, Y., Ding, J., and Wu, L. Y. (2016). iSulf-Cys: prediction of S-sulfonylation sites in proteins with physicochemical properties of amino acids. *PLoS One* 11:e0154237. doi: 10.1371/journal.pone.0154237
- Xu, Y., Yang, Y., Ding, J., and Li, C. (2018). iGlu-Lys: a predictor for lysine glutarylation through amino acid pair order features. *IEEE Trans. Nanobioscience* 17, 394–401. doi: 10.1109/tnb.2018.2848673
- Yu, H., Diao, H., Wang, C., Lin, Y., Yu, F., Lu, H., et al. (2015). Acetylproteomic analysis reveals functional implications of lysine acetylation in human spermatozoa (sperm). *Mol. Cell. Proteomics* 14, 1009–1023. doi: 10.1074/mcp.m114.041384

- Yu, Y., Yu, Y., Zhang, Y., Zhang, Z., An, W., and Zhao, X. (2018). Treatment with D- $\beta$ -hydroxybutyrate protects heart from ischemia/reperfusion injury in mice. *Eur. J. Pharmacol.* 829, 121–128. doi: 10.1016/j.ejphar.2018.04.019
- Zhao, S., Xu, W., Jiang, W., Yu, W., Lin, Y., Zhang, T., et al. (2010). Regulation of cellular metabolism by protein lysine acetylation. *Science* 327, 1000–1004.
- Zhou, B., Du, Y., Xue, Y., Miao, G., Wei, T., and Zhang, P. (2020). Identification of malonylation, succinylation, and glutarylation in serum proteins of acute myocardial infarction patients. *Proteomics Clin. Appl.* 14:e1900103.
- Zhou, L., Wang, F., Sun, R., Chen, X., Zhang, M., Xu, Q., et al. (2016). SIRT5 promotes IDH2 desuccinylation and G6PD deglutarylation to enhance cellular antioxidant defense. *EMBO Rep.* 17, 811–822. doi: 10.15252/embr.201541643
- Zhou, Y., Zhang, H., He, B., Du, J., Lin, H., Cerione, R. A., et al. (2012). The bicyclic intermediate structure provides insights into the desuccinylation mechanism of human sirtuin 5 (SIRT5). *J. Biol. Chem.* 287, 28307–28314. doi: 10.1074/jbc.m112.384511

**Conflict of Interest:** The authors declare that the research was conducted in the absence of any commercial or financial relationships that could be construed as a potential conflict of interest.

Copyright © 2021 Xie, Xiao, Meng, Li, Shi and Qian. This is an open-access article distributed under the terms of the Creative Commons Attribution License (CC BY). The use, distribution or reproduction in other forums is permitted, provided the original author(s) and the copyright owner(s) are credited and that the original publication in this journal is cited, in accordance with accepted academic practice. No use, distribution or reproduction is permitted which does not comply with these terms.



# Lysine Fatty Acylation: Regulatory Enzymes, Research Tools, and Biological Function

Garrison Komaniecki<sup>1,2</sup> and Hening Lin<sup>1,2,3\*</sup>

<sup>1</sup> Graduate Field of Biochemistry, Molecular, and Cell Biology, Cornell University, Ithaca, NY, United States, <sup>2</sup> Department of Chemistry and Chemical Biology, Cornell University, Ithaca, NY, United States, <sup>3</sup> Howard Hughes Medical Institute, Cornell University, Ithaca, NY, United States

## OPEN ACCESS

### Edited by:

Lianjun Zhang,  
Center of Systems Medicine, Chinese  
Academy of Medical Sciences,  
Suzhou Institute of Systems Medicine  
(ISM), China

### Reviewed by:

James Galligan,  
University of Arizona, United States  
Valeria De Pasquale,  
University of Naples Federico II, Italy

### \*Correspondence:

Hening Lin  
hl379@cornell.edu

### Specialty section:

This article was submitted to  
Cellular Biochemistry,  
a section of the journal  
Frontiers in Cell and Developmental  
Biology

**Received:** 31 May 2021

**Accepted:** 30 June 2021

**Published:** 22 July 2021

### Citation:

Komaniecki G and Lin H (2021)  
Lysine Fatty Acylation: Regulatory  
Enzymes, Research Tools,  
and Biological Function.  
Front. Cell Dev. Biol. 9:717503.  
doi: 10.3389/fcell.2021.717503

Post-translational acylation of lysine side chains is a common mechanism of protein regulation. Modification by long-chain fatty acyl groups is an understudied form of lysine acylation that has gained increasing attention recently due to the characterization of enzymes that catalyze the addition and removal this modification. In this review we summarize what has been learned about lysine fatty acylation in the approximately 30 years since its initial discovery. We report on what is known about the enzymes that regulate lysine fatty acylation and their physiological functions, including tumorigenesis and bacterial pathogenesis. We also cover the effect of lysine fatty acylation on reported substrates. Generally, lysine fatty acylation increases the affinity of proteins for specific cellular membranes, but the physiological outcome depends greatly on the molecular context. Finally, we will go over the experimental tools that have been used to study lysine fatty acylation. While much has been learned about lysine fatty acylation since its initial discovery, the full scope of its biological function has yet to be realized.

**Keywords:** lysine fatty acylation, protein lipidation, sirtuin, HDAC, RTX toxin, NMT, myristoylation, palmitoylation

## INTRODUCTION

Post-translational modification of proteins is a key biological regulatory mechanism that impacts every aspect of life. One class of post-translational modifications is protein lipidation which involves the attachment of hydrophobic moieties such as fatty acyl groups, isoprenoid lipids, or cholesterol (Jiang et al., 2018). These hydrophobic species partition into the lipophilic environment of cellular membranes, bringing the modified protein to the membranes (Resh, 1999). N-terminal glycine myristoylation and cysteine palmitoylation and prenylation are well studied forms of protein lipidation known to regulate biological processes from development and cancer to inflammation and microbial pathogenesis (Resh, 2006; Schlott et al., 2018; Wang et al., 2021). In comparison, fatty acylation of lysine residues is under-examined. However, recent progress in the understanding of the enzymes that regulate lysine fatty acylation and the effect of the modification on substrates has opened the door to exciting new research directions.

Lysine fatty acylation (KFA) is the addition of long-chain fatty acyl groups to lysine side chains via amide bonds. Myristoylation (C<sub>14</sub>) and palmitoylation (C<sub>16</sub>) are the most common forms of KFA, but the identity of the endogenous acyl group is often unknown making fatty acylation a more inclusive and general description (**Figure 1**). KFA of mammalian proteins was first discovered by Bursten et al., 1988 when studying the membrane affinity of IL-1 $\alpha$ . Since this initial discovery,



seven other human proteins and an entire class of bacterial proteins were identified to be modified by KFA. In addition, several proteins of both human and bacterial origin were found to be able to add or remove this modification. These discoveries, along with the tools that make them possible, will be covered in this review.

## FATTY ACYL LYSINE HYDROLASES

To date, all enzymes known to have KFA hydrolase activity fall into the lysine deacetylase (KDAC) family of proteins. This includes both  $\text{Zn}^{2+}$ -dependent histone deacetylases (HDACs) and the  $\text{NAD}^+$ -dependent sirtuins (SIRT). Archaeobacterial sirtuins Sir2A1 and Sir2A2 from the archaea *Archaeoglobus fulgidus*, were also reported to be able to remove KFA, but there are no known substrates for this activity (Ringel et al., 2014). The KFA hydrolases discussed below were originally assumed to only remove acetyl groups so it is possible that some of the bacterial deacetylases could also have KFA hydrolase activity (Gregoret et al., 2004). Sir2A from the malaria parasite *Plasmodium falciparum* has also been found to have KFA hydrolase activity, but again no substrates for this activity have been identified (Zhu et al., 2012). Human enzymes HDAC8 and HDAC11 along with SIRT1, 2, 3, 6, and 7 can all remove KFA *in vitro* (Table 1). We will highlight the enzymes with known endogenous substrates for this activity in order of their discovery.

### SIRT6

The first mammalian protein identified to hydrolyze KFA is SIRT6 (Jiang et al., 2013). SIRT6 is involved in several physiological processes such as regulating immune signaling and suppressing tumorigenesis (Chang et al., 2020). SIRT6 is recruited to chromatin by DNA double strand breaks and by transcription factors such as HIF-1 $\alpha$  to remodel chromatin and regulate gene expression (Zhong et al., 2010; Toiber et al., 2013). SIRT6 is best characterized as a lysine deacetylase. Targets of SIRT6 deacetylase activity include histone H3 and GCN5, which represses NF- $\kappa$ B levels and regulates glucose production, respectively (Michishita et al., 2008, 2009; Kawahara et al., 2009; Zhong et al., 2010; Dominy et al., 2012). However, *in vitro* SIRT6 deacetylase activity is relatively weak compared to other sirtuin family members, raising the possibility of additional enzymatic activities (Pan et al., 2011).

Jiang et al. (2013) explored alternative SIRT6 deacylation activities using various acyl-lysine peptides. Like previous studies, SIRT6 had very little deacetylation activity on peptide substrates *in vitro*. However, SIRT6 was able to efficiently hydrolyze octanoyl, myristoyl, and palmitoyl lysine peptides. A SIRT6 structure was obtained by co-crystallization with a myristoyl-lysine peptide revealing a hydrophobic groove in which bound the myristoyl group (Figure 2). Interestingly, free fatty acids were found to activate SIRT6 deacetylase activity but to inhibit deKFA activity (Feldman et al., 2013). Together, these observations suggest that binding of fatty acyl groups, whether free or on a lysine, to the acyl pocket of SIRT6 may activate SIRT6.

Given the reported tumor suppressor activity of SIRT6, it is attractive to imagine compounds that could selectively activate

SIRT6 through interactions with the hydrophobic groove. Indeed, multiple studies have identified compounds able to activate SIRT6 deacetylation activity (You et al., 2017, 2019; Tenhunen et al., 2021). Crystal structures consistently reveal SIRT6 activating compounds bound in the hydrophobic groove. It is therefore unsurprising that when tested in demyristoylation assays these compounds act as inhibitors (You et al., 2017, 2019). SIRT6 deacetylation inhibitors have also been developed and have been shown to have potential efficacy in type II diabetes and multiple sclerosis models (Parenti et al., 2014; Sociali et al., 2017; Ferrara et al., 2020). These inhibitors were not tested against SIRT6 deKFA activity so what role SIRT6 deKFA activity has in these contexts is unclear. Thiomyristoyl peptides can inhibit SIRT6 deKFA by taking advantage of SIRT6 activity to generate a covalent stalled intermediate (He et al., 2014). Future SIRT6 inhibitors could use this as a starting point for more potent compounds. Such an approach has proven successful for SIRT2 inhibitors as will be discussed below.

### SIRT2

SIRT2 was the next enzyme found to have endogenous substrates for its deKFA activity (Jing et al., 2017; Spiegelman et al., 2019; Kosciuk et al., 2020). SIRT2 has been extensively studied due to its diverse physiological roles and its potential as a therapeutic target for certain cancers and neurological disorders (Liu et al., 2019; Wang et al., 2019; Chen et al., 2020). In cancer, SIRT2 can play both a tumor promoting and tumor suppressing role (Chen et al., 2020). For instance, SIRT2 can promote breast cancer development by deacetylating Slug and aldehyde dehydrogenase 1A1 (ALDH1A1) (Zhao et al., 2014; Zhou et al., 2016). On the other hand, SIRT2 can reduce the activity of peroxiredoxin-1 (Prdx-1) through deacetylation which leads to breast cancer cells accumulating reactive oxygen species (ROS) and becoming less viable (Fiskus et al., 2016). Regardless, inhibition of SIRT2 leads to degradation of c-Myc and reduced growth in a broad variety of cancer cells, demonstrating its efficacy as a drug target (Jing et al., 2016).

Unlike SIRT6, SIRT2 has strong *in vitro* deacetylase activity and has a plethora of reported deacetylase targets (Feldman et al., 2013; Wang et al., 2019). While SIRT2 is a well-established deacetylase, it was also found to be able to hydrolyze lysine myristoylation with comparable efficiency to acetylation (Feldman et al., 2013; Teng et al., 2015). Similar to SIRT6, structural analysis of SIRT2 crystalized with a myristoyl-lysine peptide revealed a hydrophobic pocket that can readily accommodate a fatty acyl group (Figure 2; Teng et al., 2015).

SIRT2 inhibitors are numerous and diverse. Inhibitors of SIRT2 can be broadly categorized into two classes: activity-based and non-activity-based. Activity-based SIRT2 inhibitors usually have a peptide backbone and contain a thioacyl moiety that reacts with  $\text{NAD}^+$  in the SIRT2 active site to form a covalent stalled intermediate. Non-activity-based SIRT2 inhibitors function through a more typical manner by binding tightly at or near the active site. Direct comparison of SIRT2 inhibitors revealed that non-activity-based inhibitors AGK2, SirReal2, and Tenovin-6 can inhibit *in vitro* SIRT2 deacetylase activity, but not deKFA activity. Activity-based inhibitor TM was able to inhibit both activities *in vitro* (Spiegelman et al., 2018),

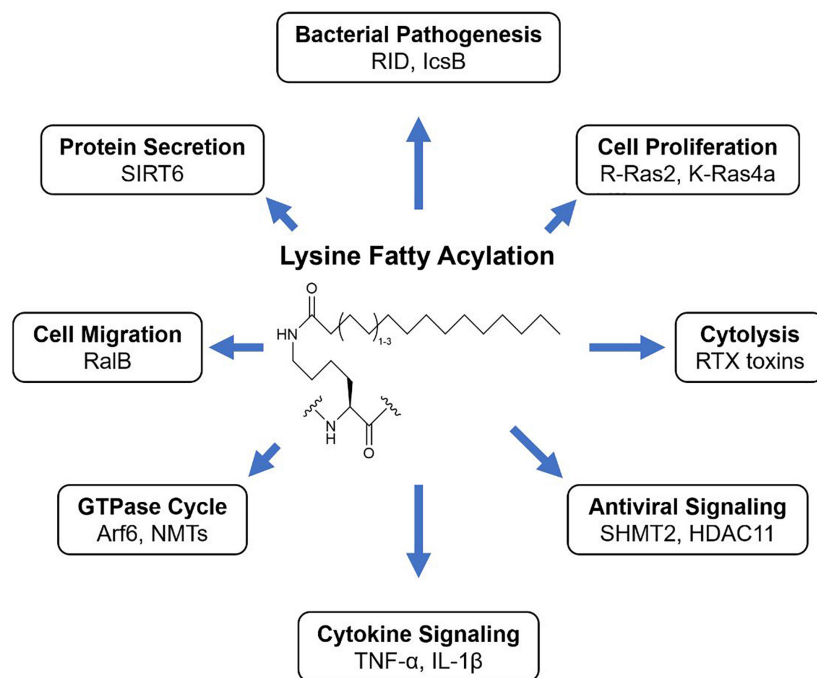


**FIGURE 1** | KFA is the modification of lysine side chains with long fatty acyl groups. How KFA affects a modified substrate is not always understood but known outcomes of KFA are diverse.

**TABLE 1** | Enzymes that regulate lysine fatty acylation.

	Name	Species	$k_{cat}/K_M$ ( $s^{-1}/M^{-1}$ )	Known Substrates	References
Lysine fatty-acyl transferases	RtxC Family	Many gram negative bacteria	NA	RtxA toxins	Benz, 2020
	RID	<i>V. cholerae</i>	NA	RhoA-family GTPases	Zhou et al., 2017
	IcsB	<i>S. flexneri</i>	NA	Several—see citation.	Liu et al., 2018
	NMT1, NMT2	Human	NMT1: 144 <sup>a</sup> NMT2: 133 <sup>a</sup>	Arf6	Dian et al., 2020; Kosciuk et al., 2020
Lysine fatty-acyl hydrolases	HDAC8	Human	120 <sup>b</sup>	NA	Aramsangtienchai et al., 2016
	HDAC11	Human	$1.54 \times 10^4$ <sup>b</sup>	SHMT2	Cao et al., 2019
	SIRT1	Human	$1.44 \times 10^5$ <sup>b</sup>	NA	Gai et al., 2016
	SIRT2	Human	$7.4 \times 10^4$ <sup>b</sup>	K-Ras4a, RalB, Arf6	Jing et al., 2017; Spiegelman et al., 2019
	SIRT3	Human	$2.51 \times 10^5$ <sup>b</sup>	NA	Gai et al., 2016
	SIRT6	Human	$1.4 \times 10^3$ <sup>b</sup>	TNF- $\alpha$ , R-Ras2	Jiang et al., 2013; Zhang et al., 2017
	SIRT7	Human	> 167 <sup>c</sup>	NA	Tong et al., 2017

<sup>a</sup>Myristoylation of Arf6 G2A peptide. Analysis using HPLC.

<sup>b</sup>Demyristoylation Myr-H3K9 peptide. Analysis using HPLC.

<sup>c</sup>Demyristoylation Myr-H3K9 peptide in the presence of rRNA. Analysis using HPLC.

but not much deKFA activity in cells. However, simultaneous inhibition of SIRT2 deacetylase and deKFA activity can be achieved with a proteolytic targeting chimera (PROTAC) strategy to selectively degrade SIRT2 (Schiedel et al., 2018; Hong et al., 2020). Crystal structures of inhibitors bound SIRT2 have been solved for several inhibitors (Rumpf et al., 2015; Mellini et al., 2017; Moniot et al., 2017; Hong et al., 2019). A recurring theme in these structures is the contribution of residues in the SIRT2 hydrophobic pocket for interaction with the inhibitors. While SIRT2 inhibitors have yet to be used in a clinical setting, cellular and mouse studies have yielded encouraging results for the use of SIRT2 inhibitors in treating disease. As mentioned above SIRT2i

reduced growth of numerous different cancer cell lines (Jing et al., 2016). SIRT2i has also been shown to decrease  $\alpha$ -synuclein toxicity in Parkinson's disease models (Outeiro et al., 2007). The exact mechanism of action for this effect is still unclear and there is some debate about the causative or protective role for SIRT2 in Parkinson's disease (Liu et al., 2019).

## HDAC11

The most recent enzyme found to hydrolyze KFA is HDAC11 (Kutil et al., 2018; Moreno-Yruea et al., 2018; Cao et al., 2019). HDAC11 is the newest member of the HDAC family and is the only class IV HDAC in humans. Since its discovery, HDAC11

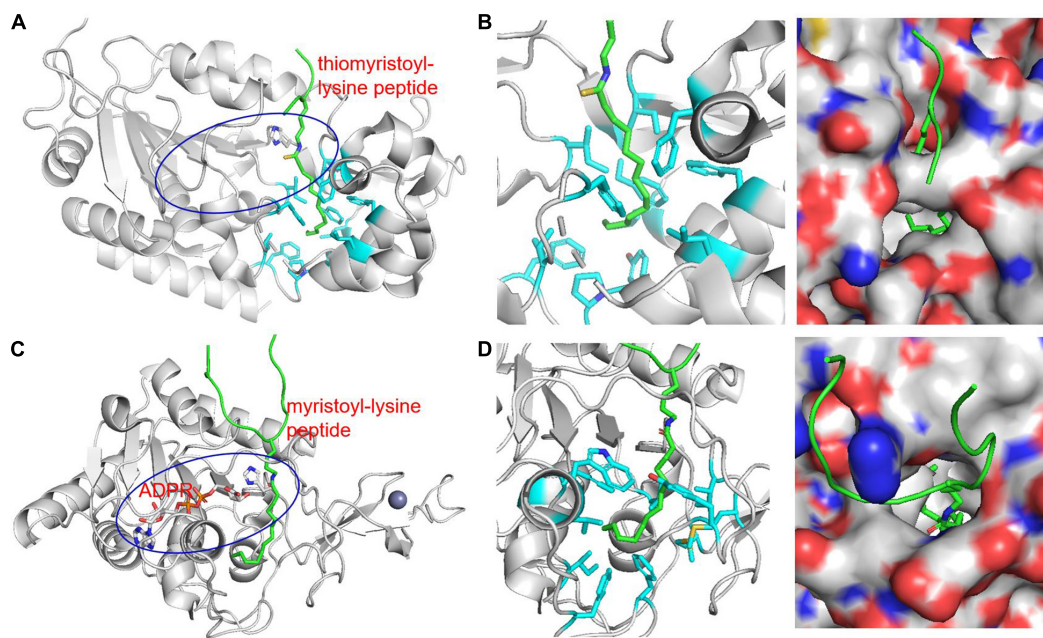


**FIGURE 2 |** Structure of KFA hydrolases SIRT2 (**A,B**, PDB 4R8M) and SIRT6 (**C,D**, PDB 3ZG6) highlighting hydrophobic pockets that accommodate long-chain fatty acyl groups (**B,D**). (**A**) Overall structure of SIRT2 in complex with a thiomristoyl-lysine peptide. The peptide is shown in green. The blue oval highlights the overall active site of SIRT2 and the catalytic histidine residue is shown in stick representation. (**B**) Zoom-in view of the SIRT2 hydrophobic pocket that accommodates the myristoyl group. The hydrophobic side chains are shown in cyan stick representations. A surface representation showing the hydrophobic pocket in a slightly different orientation is also shown. (**C**) Overall structure of SIRT6 in complex with a myristoyl-lysine peptide. The peptide is shown in green. The blue oval highlights the overall active site of SIRT6 and the catalytic histidine residue is shown in stick representation. (**D**) Zoom-in view of the SIRT6 hydrophobic pocket that accommodates the myristoyl group. The hydrophobic side chains are shown in cyan stick representations. A surface representation showing the hydrophobic pocket in a different orientation is also shown.

has been found to play a role in neuronal function, immune regulation, and metabolic homeostasis (Bagchi et al., 2018; Sun et al., 2018a,b; Yanginlar and Logie, 2018; Nunez-Alvarez and Suelves, 2021; Yang et al., 2021). In addition, HDAC11 is overexpressed in several cancers and silencing HDAC11 can cause cell death in some cancer cell lines (Deubzer et al., 2013; Thole et al., 2017).

In *in vitro* studies, HDAC11 lacks detectable deacetylation activity. Instead, HDAC11 is highly active toward KFA modified substrates (Kutil et al., 2018; Moreno-Yruela et al., 2018; Cao et al., 2019). HDAC11 kinetics are similar to SIRT2 in hydrolyzing KFA, but HDAC11 is far more selective toward this unique modification. Unfortunately, no crystal structure has been obtained for HDAC11. HDAC11 modulation has been shown to affect acetylation of several proteins, but catalytic dead HDAC11 mutants were not utilized in any of these studies so whether or not HDAC11 has any bona-fide deacetylation substrates remains unclear (Glozak and Seto, 2009; Wang et al., 2017; Gong et al., 2019; Yuan et al., 2019). HDAC11 is reported to interact with HDAC6 so it is possible that changes in acetylation following HDAC11 modulation occur indirectly through HDAC6 or with the help of some unidentified cofactor or interacting partner that is lost in purification of HDAC11 for *in vitro* assays (Gao et al., 2002). Further work is necessary to determine whether and how HDAC11 regulates protein acetylation.

Compared to SIRT6 and SIRT2, HDAC11 is understudied. The number of published inhibitors reflects this. A common strategy for creating inhibitors for  $\text{Zn}^{2+}$ -dependent HDACs is to design a molecule that can chelate  $\text{Zn}^{2+}$  and has isoform specific interactions with residues surrounding the active site. This strategy was successfully employed in the design of SIS17, with a fatty acyl moiety which likely interacts with HDAC11 in a similar manner to a KFA substrate (Son et al., 2019). Another HDAC11 inhibitor, FT895, has shown promising anti-cancer activity in lung adenocarcinoma cells by suppressing Sox2 expression (Martin et al., 2018; Bora-Singhal et al., 2020). Additionally, a natural product garcinol was shown to inhibit HDAC11 selectively (Son et al., 2020). Garcinol has several reported biological activities. Although the relevance of HDAC11 inhibition in garcinol's various biological activities is unclear, it is interesting to note that biological effects of garcinol in mouse models share some commonality with HDAC11 knockout (Son et al., 2020). Given HDAC11's substrate specificity for KFA hydrolysis, use of HDAC11-specific inhibitors could help illuminate the role of KFA in a biological context.

## LYSINE FATTY ACYL TRANSFERASES

One of the major impediments to studying KFA is the identification of human KFA transferase enzymes. Knowledge of



how proteins acquire KFA would be invaluable in understanding the purpose of this modification. For instance, some bacterial toxins with known physiological importance take advantage of this activity during pathogenesis to promote infection (Figure 3). Although human lysine fatty acyl transferases are known, the acyl transferases for many of the reported KFA-modified proteins are still unknown. It is possible that such enzymes do exist but require more future effort to identify. However, an alternative explanation for the presence of endogenous KFA is that this modification simply arises from an S-to-N transfer. In this model a free lysine acts as a nucleophile to steal a fatty acyl group from a palmitoylated cysteine or palmitoyl-CoA. An amide bond is more stable than a thioester bond, making this reaction thermodynamically favorable. Several KFA transferases have been characterized and are reviewed below in order of discovery.

## RtxC Proteins

Several species of bacterial pathogens employ a class of secreted toxin proteins known as Repeats in ToXin (RTX) toxins. RTX toxins function in various ways, but typically act as cytotoxins by forming pores in the plasma membrane of mammalian cells (Benz, 2016). Structures in the RTX toxin operon vary, but typically consist of four genes: *rtxA-D*. *rtxA* encodes the actual toxin which is secreted through a type one secretion system encoded by *rtxB*, *rtxD*, and a third gene, *tolC*, located elsewhere on the bacterial chromosome. RtxA is synthesized as a protoxin that is activated by fatty acylation on one or two highly conserved lysine residues catalyzed by RtxC (Figure 3A; Benz, 2020).

The best characterized RtxC member is HlyC, which catalyzes KFA on the *Escherichia coli* hemolysin toxin HlyA. Initial characterization of the HlyA toxin revealed that HlyC activates proHlyA in a manner dependent on the acylated acyl carrier protein (acyl-ACP) (Issartel et al., 1991). Follow-up studies determined through mass spectrometry that HlyC activates HlyA by directing fatty acylation of two internal lysines (Stanley et al., 1994). While the majority of HlyA lysine acylation is myristoylation (C14), HlyC apparently has some flexibility in substrate preference as saturated C15 and C17 acylation was also detected at appreciable amounts (Lim et al., 2000). Similar findings were made for the *Bordetella pertussis* CyaA toxin which is palmitoylated on a single lysine (Hackett et al., 1994). Interestingly, when recombinantly expressed with its cognate acyl transferase CyaC in *E. coli*, CyaA is palmitoylated on a second lysine (Hackett et al., 1995). This reveals that the number of lysines and the nature of the transferred acyl chain vary by each unique enzyme as well as the species background.

More detailed information of RtxC enzymology was revealed using HlyC (Trent et al., 1999; Worsham et al., 2001). HlyC acylation of proHlyA occurs through a ping-pong mechanism involving two steps. In the proposed model, the acyl group from acyl-ACP is first transferred to His23 to form a covalent acyl-HlyC intermediate. This His is conserved throughout RtxC proteins. Then, the acyl group is transferred to the lysine residues on proHlyA. Ser20 is also important for optimal activity. While detailed enzymology has not been carried out for many RtxC proteins, the enzymatic mechanism is likely to be similar due to the conservation of relevant catalytic residues. Indeed, the

analogous active site His and Ser in CyaC are necessary for its activity (Basar et al., 2001).

Structural information for RtxC proteins is sparse but revealing. Despite unidentifiable sequence homology, ApxIC, the RtxC from *Actinobacillus pleuropneumoniae*, has conspicuous structural homology to the Gcn5-like N-acetyl transferase (GNAT) superfamily (Greene et al., 2015). GNAT proteins are well established acyl-transferases that use acyl-CoA as an acyl donor (Salah Ud-Din et al., 2016). The ApxIC structure is differentiated from other GNAT proteins by the lack of elements that typically interact with CoA, explaining why characterized RtxC proteins do not utilize acyl-CoA as the acyl donor. The conserved active site residues reside within a deep surface groove. While further structural information is needed, this study, along with the fact that RtxC proteins are well conserved, opens the door for further understanding of these unique enzymes and raises the possibility of designing inhibitors to block toxin function.

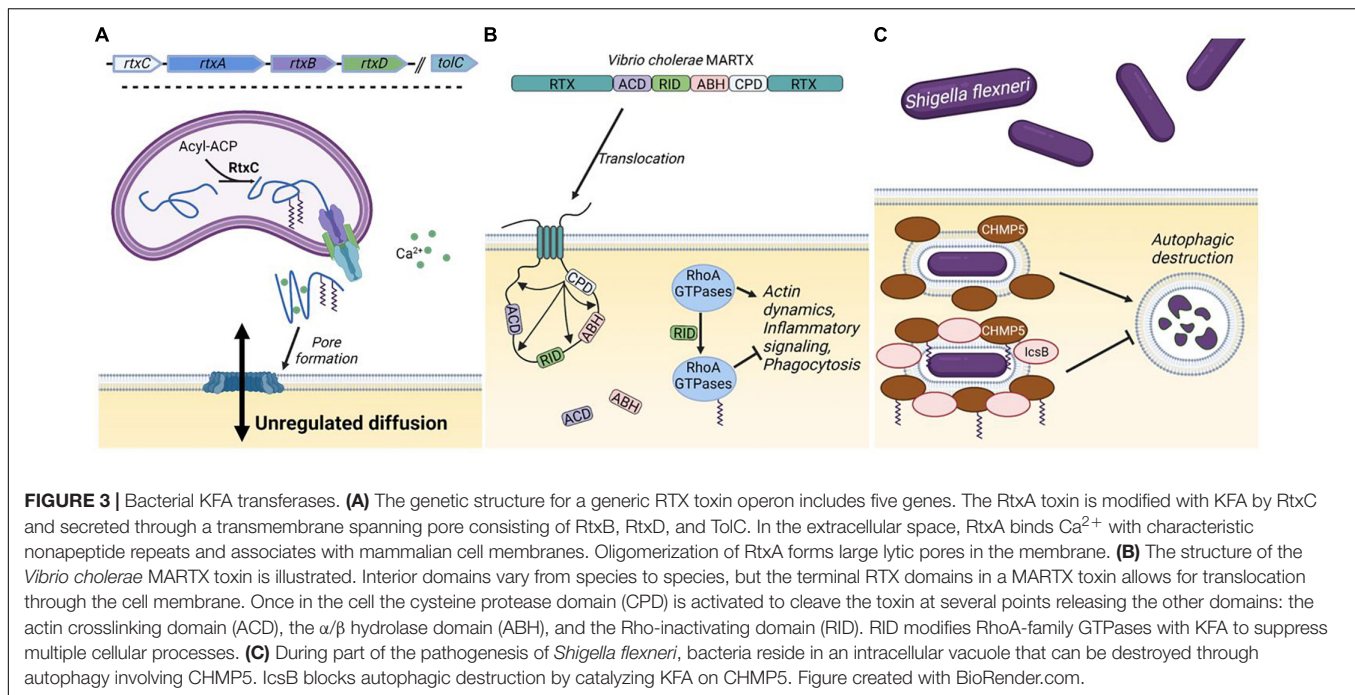
## RID

There is a subset of multifunctional RtxA toxins that are much larger called Multifunctional Autoprocessing Repeats in ToXin (MARTX) toxins. MARTX toxins contain the trademark non-peptide repeats in both the N- and C-terminus, which forms a pore in the cell membrane that translocates the interior portion of the toxin encoding a modular array of effector domains into the cytoplasm (Satchell, 2007). While the number and type of interior domains varies, a cysteine protease domain (CPD) is universally conserved in MARTX toxins. Once internalized, the CPD is activated and proteolytically cleaves the toxin at several points, releasing additional effector domains into the cell (Satchell, 2011). One of these effectors present in multiple species was dubbed the Rho inactivation domain (RID).

RID is present in several known MARTX toxins (Satchell, 2007). The best characterized RID domain is the one in the *Vibrio cholerae* toxin, MARTX<sub>Vc</sub> (Figure 3B). MARTX<sub>Vc</sub> is known to induce cell rounding through an actin crosslinking domain (ACD) that covalently links actin monomers, preventing actin polymerization (Cordero et al., 2006). However, cell rounding was still observed when this domain was knocked out. Follow up studies determined that this occurred through RID, which substantially decreases the amount of GTP-bound Rho GTPases Rho, Rac, and Cdc42 (Sheahan and Satchell, 2007). The mechanism by which RID functions was not known until a structure of the *Vibrio vulnificus* RID domain was solved (Zhou et al., 2017). Clues from this structure allowed the authors to determine that RID catalyzes palmitoylation on lysines in the polybasic region of RhoA-family GTPases. This activity was dependent on C-terminal prenylation of the GTPases and could utilize palmitoyl-CoA as a acyl donor. Small GTPases are activated by guanine nucleotide exchange factors (GEFs) by stimulating the release of GDP, to allow the binding of GTP. RID-catalyzed KFA on Rac1 inhibits its interaction with GEFs, but how KFA prevents GEF interaction is unclear.

Both the ACD and RID from MARTX<sub>Vc</sub> lead to an obvious cell rounding phenotype by preventing actin dynamics. It is reasonable to wonder why *V. cholerae* would evolve to have





two domains to carry out the same role. Woida and Satchell (2020) recently discovered that RID and a third domain in the MARTX<sub>VC</sub>, a  $\alpha/\beta$  hydrolase (ABH) domain, function to suppress proinflammatory signaling. Cytoskeletal collapse caused by ACD activates mitogen-activated protein kinase (MAPK) signaling, leading to upregulation and enhanced secretion of proinflammatory cytokines. RID inactivation of Rac1 blocks MAPK signaling and subsequent cytokine secretion (Figure 3B). RhoA-family GTPases also have other functions in immune processes, so RID could be playing a broad immunosuppressive function to prevent *V. cholerae* clearance by leukocytes (Biro et al., 2014; Bros et al., 2019; Guo, 2021).

## IcsB

The *Shigella flexneri* toxin IcsB is another enzyme identified to catalyze KFA (Liu et al., 2018). *Shigella* are gram negative bacteria that can colonize the intestinal epithelium through a complicated mechanism with the aid of toxin effectors secreted by a type three secretion system (Parsot, 2009). Following ingestion, *Shigella* induce endocytosis by M cells in the epithelium of the colon (Wassef et al., 1989). Endocytosed *Shigella* are transferred to resident macrophages where they employ a barrage of secreted effectors to escape the vacuole and replicate in the cytosol of the macrophage (Zychlinsky et al., 1992). This leads to lysis of the macrophage and dissemination of bacterial progeny. One of the critical effectors that enables this mode of infection is IcsB.

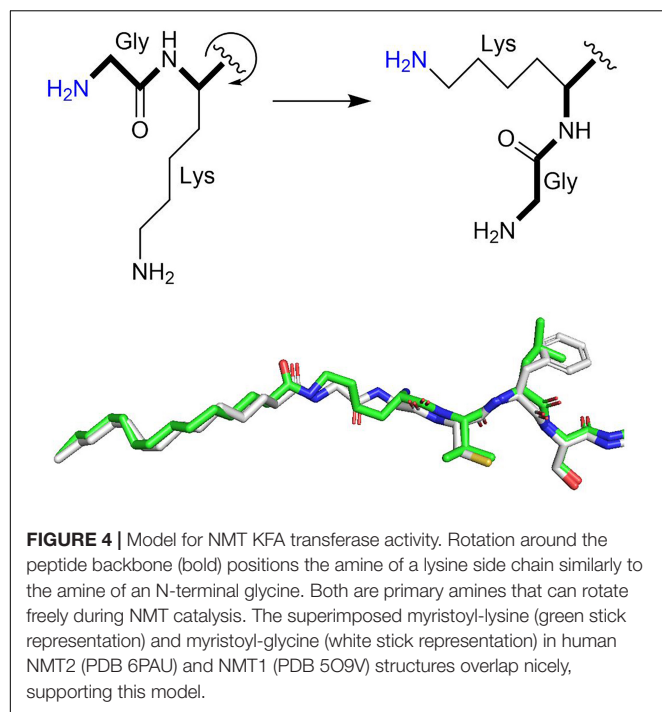
IcsB promotes infection in several ways including preventing autophagic destruction and promoting cell lysis (Allaoui et al., 1992; Ogawa et al., 2005). How IcsB functions to modulate multiple cellular processes had been unclear, but it was predicted to be an enzyme through bioinformatic analysis (Pei and Grishin, 2009). IcsB was found to be a potential homolog of RID

and ectopic expression of IcsB was found to disrupt the actin cytoskeleton. In line with these observations, IcsB was also found to catalyze KFA on lysines in the polybasic region of Rho GTPases (Liu et al., 2018). The eighteen-carbon stearyl-CoA seems to be the preferred acyl donor and prenylation of Rho GTPases is also necessary for IcsB activity. Proteomic analysis identified numerous IcsB substrates in addition to Rho GTPases. KFA on one of these substrates, CHMP5, was identified to inhibit the autophagic destruction of *S. flexneri* thus providing a mechanism for sustained intercellular survival (Figure 3C).

While RID and IcsB are both bacterial toxins that catalyze KFA of host substrates, they differ in a few key aspects. IcsB transfected cells exhibit cell rounding whereas *S. flexneri* infected cells do not. Cells introduced to RID or infected with *V. cholerae* both exhibit cell rounding. This discrepancy is in part due to the presence of the *V. cholerae* ACD as well as to the observation that *S. flexneri* activate actin polymerization for part of their pathogenesis. Additionally, while no proteomic search for substrates has been done, RID is only known to modify Rho GTPases while IcsB can modify many other substrates in addition to Rho GTPases. What role KFA plays on these other substrates is an area for future study.

## NMT1 and NMT2

N-myristoyltransferases (NMTs) have long been known to transfer a myristoyl group from myristoyl-CoA to the  $\alpha$ -amine of an N-terminal glycine following cleavage of the initiator methionine (Towler et al., 1987). This modification happens co-translationally or after proteolytic events that result in a free N-terminal glycine such as caspase cleavage (Farazi et al., 2001; Yuan et al., 2020). There are no known enzymes that can hydrolyze N-terminal myristoylation and as such it is



thought to be irreversible. Like KFA, N-terminal myristoylation increases a protein's affinity for membranes. Knocking out NMT is embryonically lethal in mice and fruit flies (Ntwasa et al., 2001; Yang et al., 2005). NMT levels are elevated in several cancers and NMT inhibition has advanced to clinical trials for the treatment of NMT-deficient blood cancers (Selvakumar et al., 2007; Berthiaume and Beauchamp, 2018). Additionally, several viruses utilize host NMTs for their replication and infectivity raising the possibility of using NMT inhibitors as an antiviral agent (Mousnier et al., 2018).

Because NMTs catalyze the fatty acylation of a primary amine, they can do the same chemistry as a potential KFA transferase. Indeed, two groups found that the human NMT1 and NMT2 can catalyze KFA on lysines toward the N-terminus of a peptide (Dian et al., 2020; Kosciuk et al., 2020). The proposed mechanism for this reaction requires rotation around the peptide bond to present the lysine  $\epsilon$ -amine into the active site typically occupied by the  $\alpha$ -amine of glycine (Figure 4). Both amines can freely rotate during NMT catalysis and myristoyl-glycine and myristoyl-lysine are similarly positioned in the active site of NMT structures, supporting the proposed activity (Figure 4). The precise sequence requirements for this activity are still being clarified, but it is clear that this activity is strongest when lysine is closer to the N-terminus. While glycine is the preferred substrate, KFA is efficiently catalyzed on a lysine that is right after the glycine, especially when the N-terminal amine is blocked. KFA transferase activity is decreased when an extra glycine is added before the modified lysine and is absent when two additional glycines are inserted. This narrows the scope of potential substrates for NMT KFA transferase activity. Peptide experiments indicate that a good KFA transferase substrate for NMTs has a small amino acid at position two, a lysine at position three, a serine at position six,

and lysine at position seven. This was confirmed when Arf6 was identified to be a substrate of NMT KFA transferase activity (Kosciuk et al., 2020). The Arf6 N-terminal sequence following initiator methionine cleavage is GKVLSKIF. Arf6 can be doubly myristoylated at both G2 and K3. It was proposed that NMTs can accommodate both myristoyl groups when one is inserted into a solvent channel in the protein structure. While Arf6 is currently the only known substrate for NMT KFA transferase activity, it is feasible that additional proteins with N-termini similar to Arf6 could also be modified (Kosciuk and Lin, 2020).

## FUNCTIONS OF LYSINE FATTY ACYLATION

A diverse set of proteins has been identified to have KFA (Table 2). How exactly KFA affects the modified protein is often unclear, but a common theme is a change in membrane affinity (Figure 5). If a protein is otherwise soluble, KFA can lead to membrane localization as is the case for IL-1 $\alpha$  or SHMT2. For proteins that already have membrane targeting elements, KFA can change which cellular membranes they are localized to. This is the case for several small GTPases which are targeted to membranes through electrostatic interactions and other lipid modifications. In this section we review proteins known to have KFA, how KFA on the protein was found, and what is known about how KFA affects protein function. Not discussed in this section are the substrates for RID and IcsB toxins which are examined above or in other publications (Zhou et al., 2017; Liu et al., 2018).

### IL-1 $\alpha$

Interleukins (ILs) are a family of secreted proteins used in cell-to-cell communication that regulate inflammatory signaling. The IL-1 family of proteins contains 11 different members that are synthesized as precursor proteins, requiring proteolytic processing for optimal biologic activity (Afonina et al., 2015). IL-1 $\alpha$  and IL-1 $\beta$  are closely related pro-inflammatory members of the IL-1 family. Despite obvious structural similarity between the two proteins, they differ in some key respects (Priestle et al., 1989; Ren et al., 2017). While IL-1 $\beta$  functions exclusively as a secreted protein, IL-1 $\alpha$  has activity both secreted and bound to the cell membrane (Kim et al., 2013). In examining its affinity for membranes, it was determined that IL-1 $\alpha$  was doubly myristoylated on the N-terminal portion of the protein (Bursten et al., 1988; Stevenson et al., 1993). This was determined through the incorporation of radiolabeled myristic acid. Incubation of synthetic peptides with monocyte lysates identified lysines 82 and 83 as sites of myristoylation (Stevenson et al., 1993). Myristoylation was also observed for IL-1 $\beta$ , but to a much less extent. While the precise role KFA plays on IL-1 $\alpha$  function is unclear, only the uncleaved IL-1 $\alpha$ , with modified lysines present, associates with the cell membrane (Beuscher and Colten, 1988). It is not known what enzymes could regulate IL-1 $\alpha$  KFA, but acylation in the presence of lysates raises the possibility of an unidentified KFA transferase. Membrane associated IL-1 $\alpha$

**TABLE 2 |** Proteins with lysine fatty acylation.

Name	Species	KFA transferase	KFA hydrolase	Effect of KFA	References
IL-1 $\alpha$	Human	NA	NA	NA	Bursten et al., 1988; Stevenson et al., 1993
Aquaporin-0	Human, Bovine	NA	NA	NA	Schey et al., 2010
TNF- $\alpha$	Human	NA	SIRT6	Decreased TNF- $\alpha$ secretion	Stevenson et al., 1992; Jiang et al., 2016
R-Ras2	Human	NA	SIRT6	Increased R-Ras2 activity and cell proliferation	Zhang et al., 2017
K-Ras4	Human	NA	SIRT2	Decreased interaction with A-Raf and cell proliferation	Jing et al., 2017
H-Ras	Human	NA	NA	NA	Jing et al., 2017
RalB	Human	NA	SIRT2	Increased RalB activity and cell migration	Spiegelman et al., 2019
Arf6	Human	NMT1/NMT2	SIRT2	Promotes Arf6 GTPase cycle	Kosciuk et al., 2020
SHMT2	Human	NA	HDAC11	Reduced ubiquitination and enhanced signaling of INF $\alpha$ R1	Cao et al., 2019
RhoA GTPases	Human	RID	NA	GTPase inactivation; defect in actin polymerization; reduced inflammatory signaling	Zhou et al., 2017; Woida and Satchell, 2020
CHMP5*	Human	IcsB	NA	Defect in <i>S. flexneri</i> autophagic destruction	Liu et al., 2018
RTX toxins	Many gram negative bacteria	RtxC	NA	Increased binding to $\beta_2$ -integrins; promotion of oligomerization	Benz, 2020

\*CHMP5 is one of many identified IcsB substrates. For a complete list see Liu et al., 2018.

contributes to arthritis in a mouse model, so modulating IL-1 $\alpha$  KFA could have therapeutic applications (Niki et al., 2004).

## Aquaporin-0

Aquaporins are a family of transmembrane channel proteins that facilitate the transport of water across the plasma membrane. Aquaporin-0 (AQP0) is highly abundant in the ocular lens where it plays an important role, not only in circulating water, but as a cell to cell adhesion protein for maintenance of proper tissue structure (Mathias et al., 1997; Sindhu Kumari et al., 2015). There is very little protein turnover in lens proteins due to the loss of fiber cell organelles during differentiation, making proteins in this tissue an interesting model for aging. AQP0 is known to accumulate post-translational modifications with age (Ball et al., 2004). To determine what fatty acylations may be accumulating on AQP0, Schey et al. (2010) carried out mass spectrometric analysis of hydrophobic peptides from bovine and human lens tissue. They identified AQP0 as containing two fatty acylations: one on the N-terminal methionine and one on a highly conserved lysine. The identity of AQP0 KFA modification varies from C16 to C20 with up to 4 desaturations at ratios closely resembling the abundance of phosphoethanolamine lipids in lens membranes (Ismail et al., 2016). This suggests that either the modification is accumulating non-enzymatically or that a potential KFA transferase has limited preference in acyl group. The effect KFA has on AQP0 function is unknown, but the modified protein partitions to detergent-resistant membrane fractions. This suggests a role in membrane domain targeting.

## TNF- $\alpha$

Tumor necrosis factor  $\alpha$  (TNF- $\alpha$ ) is a proinflammatory cytokine secreted by several immune cells. TNF- $\alpha$  is translated with a single transmembrane domain that is cleaved at the plasma membrane to release a soluble form that binds TNF receptors

(TNFRs). TNFR1 is universally expressed on almost every cell type meaning that TNF- $\alpha$  signaling is both ubiquitous and tightly regulated (Locksley et al., 2001). In a follow up study to the IL-1 $\alpha$  findings highlighted above, TNF- $\alpha$  was also identified to have KFA (Stevenson et al., 1992). Modification is present on two lysines, K19 and K20, at the intracellular end of the transmembrane helix. SIRT6 was found to hydrolyze KFA on TNF- $\alpha$  which in turn promotes its secretion (Jiang et al., 2013). KFA causes TNF- $\alpha$  to accumulate in the lysosome where it is degraded (Jiang et al., 2016). In this context, KFA thus serves an anti-inflammatory role by decreasing the amount of secreted TNF- $\alpha$  (Figure 5A). In addition to TNF- $\alpha$ , a proteomic study revealed that SIRT6 deKFA activity regulates the secretion of numerous other proteins (Zhang et al., 2016). Interestingly, SIRT6 deKFA activity decreases the secretion of ribosomal proteins via exosomes, but the detailed mechanism for how this happens is unknown.

## R-Ras2

The only other known endogenous substrate for SIRT6 deKFA activity is R-Ras2, a member of the Ras family of GTPases (Zhang et al., 2017). Ras GTPases are known to be targeted to cellular membranes by their C-terminal hypervariable regions through cysteine lipidation and polybasic regions. R-Ras2 was identified to have KFA in its polybasic region using mass spectrometry. Mutating a patch of four lysine residues to arginine in the polybasic region of R-Ras2 abolished KFA. Immunofluorescence analysis demonstrated that KFA enhances R-Ras2 plasma membrane localization. There, R-Ras2 exist more in the GTP-bound state, interacts with PI3K, activates Akt signaling, and upregulates cell proliferation. SIRT6 KO MEFs are more proliferative than WT, an effect which is rescued by suppressing R-Ras2 level. Together this provides a model where

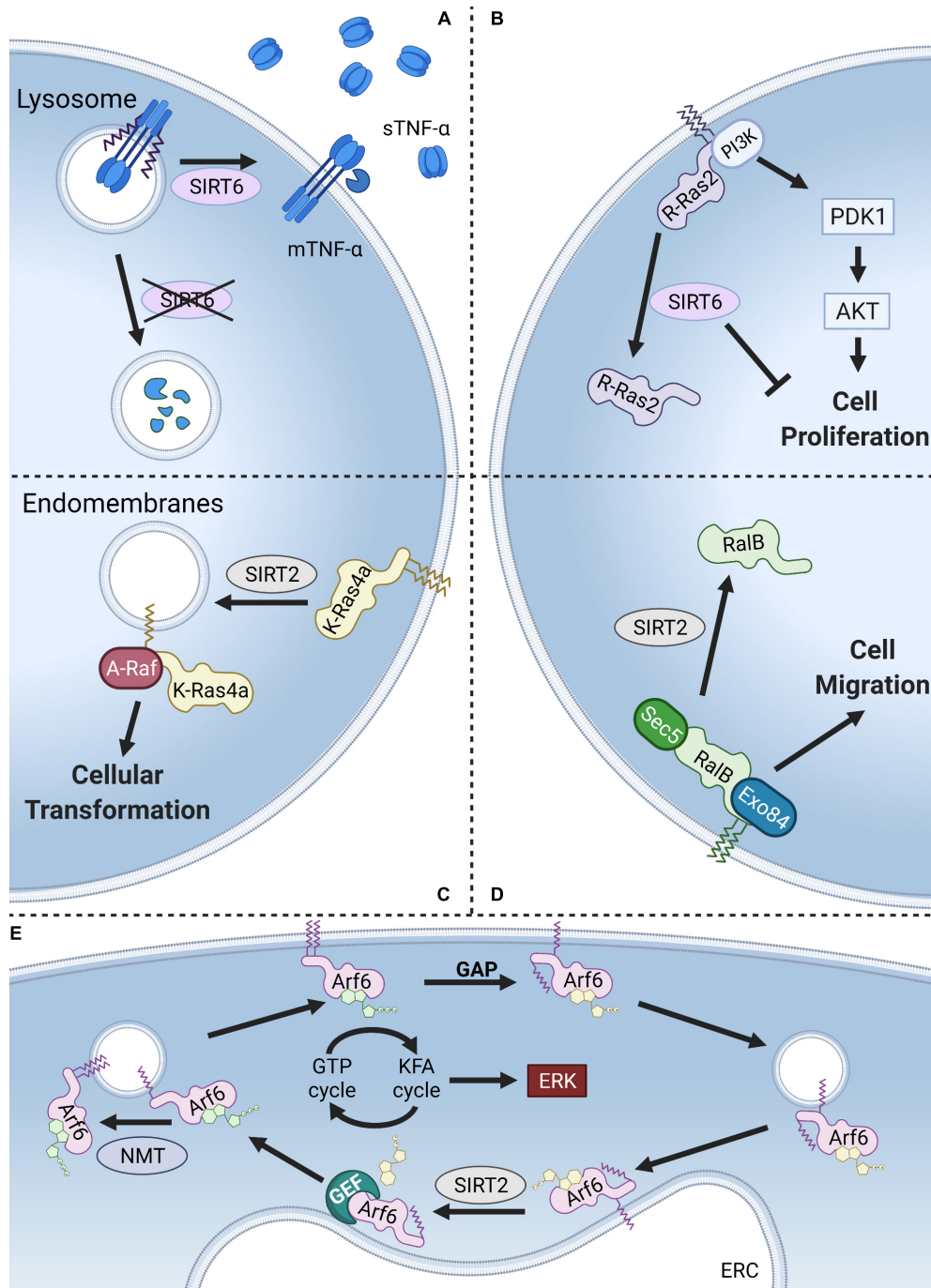


**FIGURE 5 |** Models of KFA regulation. **(A)** KFA on TNF- $\alpha$  directs it to the lysosome for degradation. SIRT6 hydrolyzes TNF- $\alpha$  KFA leading to higher levels on the plasma membrane and increased secretion of cleaved, soluble TNF- $\alpha$ . **(B)** KFA on the polybasic region of R-Ras2 results in increased plasma membrane localization, PI3K interaction, AKT signaling, and cell proliferation. SIRT6 hydrolyzes R-Ras2 KFA, releasing it from the membrane and decreasing cell proliferation. **(C)** K-Ras4a with KFA preferentially localizes at the plasma membrane. SIRT2 hydrolyzes K-Ras4a KFA and promotes its localization to endomembranes where K-Ras4a interacts with the signaling kinase A-Raf leading to downstream cellular transformation. **(D)** KFA on RalB also directs it to the plasma membrane to interact with Sec5 and Exo84 and promote cell migration. SIRT2 hydrolyzes RalB KFA, decreasing plasma membrane localization. **(E)** NMT-catalyzed KFA on K3 of Arf6 increases plasma membrane localization. GTP hydrolysis at the plasma membrane aided by a GTPase activating protein (GAP) causes Arf6 N-terminal glycine myristoylation to be sequestered. Arf6 is then trafficked to the endocytic recycling compartment (ERC) where SIRT2 hydrolyzes KFA and Arf6 is reloaded with GTP. NMT then starts the cycle again. Thus, a KFA and deKFA cycle promotes Arf6 activation, which in turn promotes ERK signaling. Figure created with BioRender.com.



SIRT6 acts as a tumor suppressor by inhibiting R-Ras2 and downregulating proliferative PI3K/Akt signaling (**Figure 5B**).

## K-Ras4a

The first identified SIRT2 deKFA substrate was K-Ras4a (Jing et al., 2017). After the identification of R-Ras2 as a KFA substrate, Jing et al. (2017) examined other small GTPases with polybasic regions similar to R-Ras2 for potential KFA modification. These included the well-known oncoproteins H-Ras, N-Ras, K-Ras4a, and K-Ras4b. Using mass spectrometry, they identified both H-Ras, and K-Ras4a as having KFA in their polybasic region. Sirtuins with known deKFA activity were screened against both H-Ras and K-Ras4a and SIRT2 was found to remove K-Ras4a KFA. Removal of H-Ras KFA was not observed for any of the screened enzymes. The oncogene *KRAS* (which is alternatively spliced into K-Ras4a and K-Ras4b) is the most frequently mutated gene in cancer, so identifying how modifications regulate its activity is of great interest (Simanshu et al., 2017). KFA on K-Ras4a was found to inhibit intracellular puncta localization, interaction with the signaling kinase A-Raf, and downstream cellular proliferation (**Figure 5C**). By removing K-Ras4a KFA, SIRT2 serves a tumor promoting role.

## RalB

The identification of R-Ras2 and K-Ras4a as proteins with KFA motivated Spiegelman et al. (2019) to further expand the search further into the of Ras subfamily small GTPases. In so doing they identified RalB having KFA. Like R-Ras2 and K-Ras4a, RalB is modified with KFA in its C-terminal polybasic region. Mutating all eight lysines in this region to arginines abolished KFA signal. Screening enzymes with deKFA activity identified SIRT2 as being able to remove KFA from RalB. RalB has been identified to promote multiple cancer phenotypes (Martin et al., 2011; Guin et al., 2013; Tecleab et al., 2014). Studying the effect of RalB KFA on these phenotypes revealed that RalB KFA enhanced migration of A549 lung cancer cells but did not affect cell proliferation. KFA of RalB was also found to increase GTP loading, plasma membrane localization, and co-localization with its effector proteins Sec5 and Exo84 (**Figure 5D**). Contrary to the K-Ras4a mechanism, SIRT2 by removing RalB KFA, decreases RalB activation and cell migration. This juxtaposition underscores the diverse, context-dependent role of KFA and the enzymes that modulate it.

## Arf6

Arf6 is a small GTPase in the ADP-ribosylation factor (Arf) subfamily that has been found to be modified with KFA (Kosciuk et al., 2020). While members of the Ras subfamily of GTPases discussed above are anchored to membranes through lipidation and electrostatic interactions in their C-terminus, the Arf family is targeted to membranes via N-terminal glycine myristoylation catalyzed by NMTs (Gillingham and Munro, 2007). Unlike KFA, there are no enzymes that are known to hydrolyze glycine myristoylation. For Arf proteins, regulating membrane association occurs through a nucleotide-dependent conformational shift that flips the myristoyl group back into the protein to sequester it in a hydrophobic pocket (Goldberg,

1998). Unlike Arf1–5, Arf6 has a lysine in the third position of its sequence. Interestingly, K3 was found to be modified with KFA by NMT enzymes and the modification is hydrolyzed by SIRT2. NMT activity is greatest toward the active, GTP-bound, form of Arf6 where SIRT2 prefers the inactive, GDP-bound, form. This enzyme preference links a dynamic KFA cycle to the GTPase cycle. Indeed, inhibiting either SIRT2 or NMTs decreased phosphorylation of ERK, a downstream target of Arf6 activation. A cycle of dynamic KFA modification thus drives the Arf6 GTPase cycle (**Figure 5E**).

## SHMT2

Serine hydroxymethyltransferase 2 (SHMT2) is a key member of one-carbon metabolism. SHMT2 catalyzes the reversible conversion of serine and THF to glycine and methylene-THF in the mitochondria. High levels of SHMT2 are associated with poor patient prognosis in several cancers and inhibitors that target both SHMT2 and SHMT1 (which catalyzes the same reaction in the cytoplasm) have shown promising results in initial cellular and mouse studies (Cuthbertson et al., 2021). Additionally, SHMT2 was found to regulate immune signaling as a component of the BRISC deubiquitylase complex. The BRISC complex is known to hydrolyze K63-linked polyubiquitin chains on type I IFN receptor chain 1 (IFN $\alpha$ R1), a key receptor in the antiviral response. BRISC prevents degradation of the receptor and promotes recycling to the plasma membrane (Zheng et al., 2013; Rabl et al., 2019; Walden et al., 2019; Rabl, 2020). SHMT2 was identified to have KFA during a search for substrates of HDAC11 (Cao et al., 2019). KFA on SHMT2 did not affect its *in vitro* activity in converting serine and THF to glycine and methylene-THF. Instead, KFA was found to be relevant in SHMT2's role in the BRISC complex. Increasing SHMT2 KFA, through HDAC11 knock out or knock down, increased SHMT2 localization to the endosomes/lysosomes where the BRISC complex can hydrolyze IFN $\alpha$ R1 ubiquitination. Correspondingly, HDAC11 KO cells had more IFN $\alpha$ R1 on the cell surface following IFN $\alpha$  treatment. Further, HDAC11 KO cells had stronger downstream signaling following IFN $\alpha$  stimulation and HDAC11 KO mice also had a stronger antiviral response when challenged with vesicular stomatitis virus. In this context, KFA again controls intracellular localization of the substrate protein, here leading to enhanced cellular activity of a deubiquitylase complex. Inhibiting HDAC11 may therefore enhance antiviral responses.

## RTX Toxins

The RtxA family of proteins are toxins that are secreted by many pathogenic gram-negative bacteria (Linhartova et al., 2010). As discussed above, RtxA proteins, hereby referred to as RTX toxins, are activated via lysine fatty acylation catalyzed by RtxC proteins. Once secreted, RTX toxins function in a variety of different ways. The best-known mode of action for RTX toxins is cytolysis and hemolysis through formation of pores in the cell membrane (Ostolaza et al., 2019). RTX toxins primarily target leukocytes and form pores in the cell membrane in a calcium dependent manner (Knapp et al., 2003). Hydrophobic regions toward the N-terminus are believed to interact with the target cell membrane to form cation-selective pores, leading to cell

lysis (Iwaki et al., 1995; Welch, 2001). KFA is necessary for the cytotoxicity of all known pore forming RTX toxins, but the mechanism by which KFA affects RTX toxin function is still unclear. Unacylated RTX toxins from *E. coli* and *B. pertussis*, HlyA and CyaA, respectively, are both able to form pores in liposomes and planar lipid bilayers (Ludwig et al., 1996; Masin et al., 2005). At concentrations insufficient to cause cell lysis, RTX toxins bind to  $\beta_2$ -integrins and activate downstream signaling pathways that lead to apoptosis (Atapattu and Czuprynski, 2007; Frey, 2019). KFA was found to increase the affinity to  $\beta_2$ -integrin receptors for CyaC and the *A. actinomycetemcomitans* toxin LtxA (El-Azami-El-Idrissi et al., 2003; Balashova et al., 2009). It was reported that KFA on HlyA is important for the formation of oligomers in erythrocyte membranes, but the physiological importance of RTX toxin oligomerization is unclear (Herlax et al., 2009). It is conceivable that KFA on RTX toxins may promote localization to appropriate membrane subdomains such as lipid rafts, somehow increasing toxin function. For instance, the *K. kingae* RtxA binds cholesterol, a membrane component enriched in lipid rafts, for optimal activity and palmitoylation on cysteines is thought to target transmembrane proteins to lipid rafts (Levental et al., 2010; Osickova et al., 2018). KFA on RTX toxins could also potentially play a role in maintaining an appropriate structural confirmation. Additional studies are necessary to identify the precise mechanism by which KFA regulates RTX toxins.

## TOOLS FOR STUDYING LYSINE FATTY ACYLATION

### Methods to Detect Endogenous KFA

Research involving KFA is well suited to a chemical biology approach. The most commonly used approach when assaying KFA is the use of fatty acyl alkyne probes as discussed below. However, this approach has inherent limitations. First, one must add alkyne probes exogenously which is difficult for applications in mice or other tissue samples. Second, when used in cell cultures, a working concentration is  $\sim 50 \mu\text{M}$  which may be sufficient to unintentionally stimulate signaling pathways involving fatty acids or to increase protein lipidation due to artificially high amounts of fatty acids. One way to assay levels of endogenous KFA is to purify a protein of interest and to attempt to identify KFA with mass spectrometry (Kosciuk et al., 2020). Mass spectrometry can directly identify the modified residue but is technically challenging due to the relatively low abundance of KFA and the hydrophobicity of the modification which makes processing samples for MS difficult. Endogenous KFA can be indirectly detected using a  $[^{32}\text{P}]\text{NAD}^+$  TLC assay if the modification is able to be hydrolyzed by a sirtuin (Jing et al., 2017; Zhang et al., 2017; Kosciuk et al., 2020). In this assay, a protein of interest is incubated with a sirtuin that has KFA hydrolase activity and radiolabeled  $[^{32}\text{P}]\text{NAD}^+$ . Sirtuin-catalyzed lysine deacylation results in the formation of  $[^{32}\text{P}]\text{O-acylADPR}$ . Fatty acyl-ADPR is drastically more hydrophobic than  $\text{NAD}^+$  and can be easily separated on a TLC plate. Phosphorescence detection can then be used to analyze the presence of fatty acyl-ADPR

and, by extension, KFA on the protein of interest (**Figure 6A**). Additional tools to study endogenous KFA could be inspired by research of similar post translational modifications. Studies concerning lysine acetylation commonly employ antibodies specific to acetyl-lysine. Antibodies that could specifically bind KFA would allow for purification and analysis of endogenously modified proteins without any exogenous treatment. Additional tools for studying KFA are necessary to fully realize the full scope of biological importance.

### Enzyme Activity Assays

Assays measuring *in vitro* enzyme activity are necessary for establishing enzyme kinetics, substrate preferences, and for testing inhibitors. Once the proper cofactors and buffer conditions are determined for an enzyme of interest, measuring its activity in regulating KFA can be straightforward. Assays for RtxC enzymes indirectly measure activity by taking advantage of the hemolytic action of their cognate RtxA proteins (Bellalou et al., 1990; Linhartova et al., 2010; Osickova et al., 2020). This is not a broadly applicable technique for KFA enzymes and as such will not be further elaborated on. Here we briefly introduce several proven strategies for measuring the activity of KFA hydrolases or transferases (**Figure 6**).

A commonly used approach to assaying KFA hydrolase activity is to incubate the enzyme of interest with a short peptide containing a KFA-modified lysine. After quenching the reaction, the products can be analyzed using HPLC or LC/MS (**Figure 6B**). For standard HPLC detection, the peptide ideally should have a strong chromophore which can be something as simple as a tryptophan residue. While this approach has been successfully implemented to study sirtuins, HDACs, and NMTs, it could theoretically be applied for studying RtxC enzymes (Feldman et al., 2013; Teng et al., 2015; Aramsangtienchai et al., 2016; Cao et al., 2019; Kosciuk et al., 2020). One of the benefits of this assay is that a peptide closely resembling the physiological protein substrate can be used. It allows for determination of an enzyme's substrate specificity by assaying peptides of various amino acid sequences. Additionally, tandem MS can be used to confirm the site of modification. Drawbacks for this approach include the need for HPLC or LC/MS instruments and relatively low throughput.

Acyl-peptide based assays for KFA hydrolases can also be analyzed with a fluorescence readout (**Figure 6C**). In this approach, peptides containing amino acids of choice with the acyl lysine at the C-terminal end followed by a fluorescent moiety such as 7-amino-4-methylcoumarin moiety (AMC) which will only fluoresce if released from the peptide (Young Hong et al., 2019). After incubation with enzyme the reaction is quenched by adding trypsin which cleaves amide bonds after lysines. Increased KFA hydrolase activity can thus be measured by increased fluorescence. This assay can be done quickly in a 96-well plate which allows researchers to test many different conditions at once and in replicates. This assay is well suited to screening libraries of compounds for enzyme inhibitors or activators.  $\text{IC}_{50}$  and  $\text{EC}_{50}$  values can be easily calculated by relating fluorescence values to the concentration of inhibitor or activator in the well. The drawback of this assay is the potential

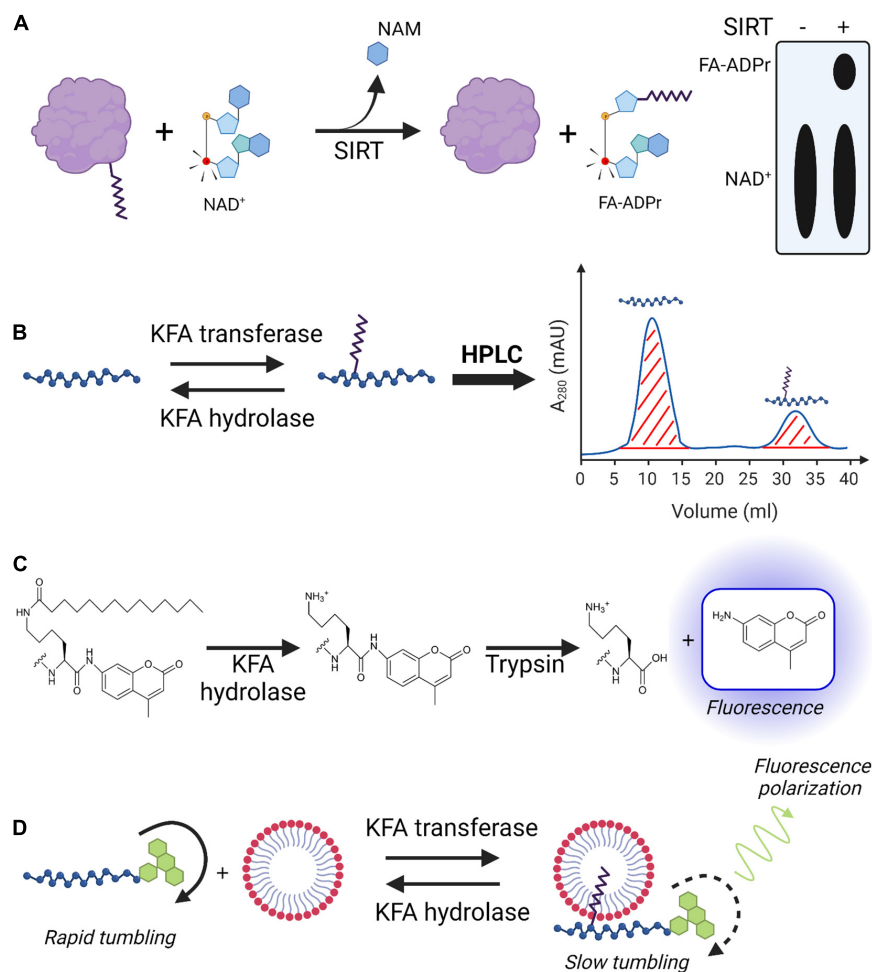


**FIGURE 6 |** Techniques for studying KFA enzyme activity. **(A)** [ $^{32}\text{P}$ ]NAD $^{+}$  sirtuin assay.  $^{32}\text{P}$  (red atom) is incorporated into NAD $^{+}$  to be used by a sirtuin with KFA hydrolase activity. During the hydrolysis mechanism, the sirtuin transfers the fatty acyl group from a modified protein to the cofactor releasing nicotinamide (NAM) and resulting in the formation of [ $^{32}\text{P}$ ]fatty acyl-ADPr. TLC plates are used to separate, visualize, and quantify radiolabeled species. **(B)** HPLC analysis of KFA enzyme activity on peptides. Unmodified and KFA-modified peptides are separated with HPLC and the area of the corresponding peaks are determined for quantification. **(C)** Fluorescence-based peptide KFA hydrolase assay. KFA is hydrolyzed from a lysine immediately preceding and AMC group. Trypsin hydrolyzes the amide bond following only the unmodified lysine releasing the AMC, which then exhibits fluorescence. **(D)** Acyl-cLIP assay for KFA enzymes. KFA on a peptide modified with fluorescein increases its affinity for micellar membranes. Fluorescein has slower tumbling when bound to the bulky micelles, resulting in increased fluorescence polarization. Figure created with BioRender.com.

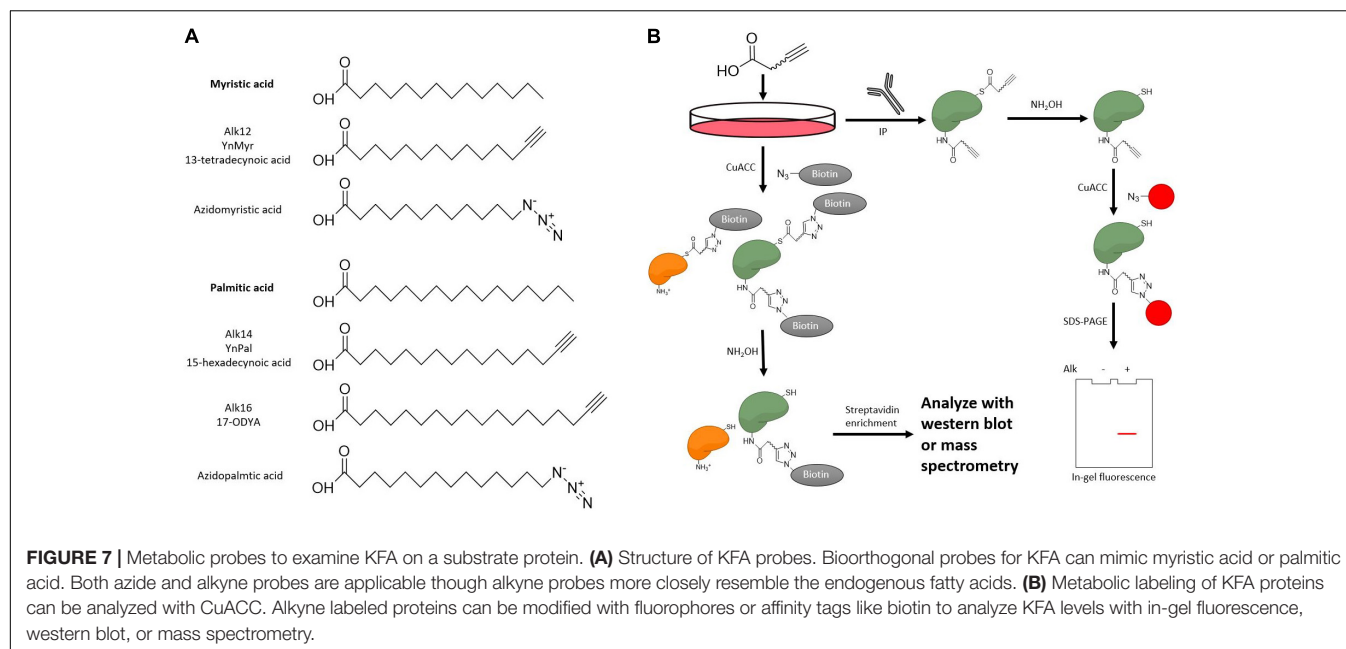
difficulty in synthesizing the appropriate peptide substrates. Furthermore, there are no amino acids on the C-terminal of the acyl-lysine, limiting the degree to which sequence specificity of a given enzyme can be ascertained. A similar technique is to modify a lysine with a fluorescent acyl group and to incorporate a fluorescence quenching moiety into the peptide. Hydrolysis separates the fluorophore from the quenching moiety and results in increased fluorescence. While this assay is also fast, the acyl group is necessarily bulky and may not have broad applicability (Kutil et al., 2019).

A promising novel technique for studying protein lipidation is acylation-coupled lipophilic induction of polarization (Acyl-cLIP) (Lanyon-Hogg et al., 2019). In this assay, an enzymatic protein lipidation reaction is carried out on a fluorescein tagged peptide in the presence of detergent micelles. Changes

in lipidation affect the peptides affinity for the micelles. When bound to the micelles, the fluorescein has decreased molecular tumbling and a corresponding increase in polarized fluorescence emission. The change in polarized fluorescence can be detected with fluorescence anisotropy measurements and this change can be attributed to the lipidation status of the peptide (Figure 6D). Drawbacks of this assay are the same as other peptide-based assays mentioned above. Benefits of this assay include a high throughput for kinetics and inhibitor studies, the ability to assay both lipid transferase and hydrolase enzymes, and a universal applicability to any type of lipid modification.

## Measuring KFA With Fatty Acyl Probes

If a target protein can be readily purified in large quantities, endogenous KFA levels can be analyzed with mass spectrometry,



such as for APQ0 (Schey et al., 2010). However, this approach is not broadly applicable for reasons outlined above. More commonly used tools for studying levels of KFA on a target protein involve the addition of exogenous fatty acid analogs (Figure 7A). An important caveat for all approaches that involve the incorporation of fatty acids is that more than just lysines can be fatty acylated. Cysteine palmitoylation and glycine myristoylation are both abundant modifications that involve fatty acyl groups and must be ruled out as the source of fatty acylation signal. Cysteine palmitoylation can be hydrolyzed by hydroxylamine while lysine acylations cannot. Treating a fatty-acylated sample with hydroxylamine can thus eliminate an experimental signal from cysteine fatty-acylation. Glycine myristoylation cannot be removed with hydroxylamine but does require a glycine at the most N-terminal position so a cursory examination of the protein's sequence can reveal if the modification is possible.

One class of exogenous fatty acyl probes is radioactive-isotope-labeled fatty acids. Cells treated with radioactive fatty acids can then form radioactive fatty acyl-CoA for use by KFA transferases. A protein of interest can then be purified and monitored for radioactivity to assay for fatty acylation (Bursten et al., 1988).  $^3\text{H}$ - and  $^{14}\text{C}$ -labeled fatty acids are the best choice for this application as the isotopes can be incorporated into the fatty acid without modifying the structure. However, these isotopes have relatively low signal and must be monitored for a long time.

Clickable fatty acid analogs have proven to be a more powerful tool for studying KFA. After treating cells with these probes, proteins are modified with fluorophores or biotin via click chemistry to track levels of fatty acylation using fluorescence scanning, western blot, or various mass spectrometry approaches (Figure 7B). While azido fatty acids have been implemented for the study of cysteine palmitoylation, alkyne fatty acids have lower background and more closely resemble the structure of

the endogenous fatty acids (Speers and Cravatt, 2004). There is a suite of fatty acyl alkyne probes that analogize natural fatty acids (Figure 7A). In addition to analyzing a protein of interest, clickable fatty acid probes can help identify substrates of KFA transferases or hydrolases as has been done for IcsB and HDAC11 (Liu et al., 2018; Cao et al., 2019). In this SILAC (stable isotope labeling with amino acids in cell culture) experiment, cells are cultured in media containing normal or isotopically heavy amino acids. KFA modulating enzymes are then overexpressed or suppressed and cells are treated with fatty acid alkyne probes. After probe incubation, cells are lysed and lysates from heavy and light media are mixed. Alkyne-labeled proteins are modified with biotin via click chemistry then treated with hydroxylamine to remove cysteine palmitoylation signal. The remaining biotinylated proteins are enriched with streptavidin and analyzed via MS. Further proteomic analysis in this way is necessary to fully appreciate the scope of KFA during various biological processes.

## SUMMARY AND FUTURE QUESTIONS

Since the initial discovery of KFA on IL-1 $\alpha$ , significant progress has been made in studying KFA. This is especially true of the last 10 or so years as several enzymes were identified to add or remove KFA. Additionally, implementation of clickable probes has allowed for the identification of many new proteins with KFA and has hastened the pace of discovery. We now know that KFA can regulate a variety of biological processes such as protein secretion, tumorigenesis, and immune signaling. The knowledge gained surrounding KFA can now serve as a basis for further exploration.

Multiple species of pathogenic bacteria utilize KFA to enhance their pathogenesis. While mammalian cells are not yet



known to have KFA transferases that act on a broad range of substrates, the presence of multiple enzymes with strong KFA hydrolase activity suggests an evolutionarily beneficial role for this activity. Is it possible that during certain bacterial infections KFA hydrolase activity serves a protective role against toxins like RID and IcsB? Is it possible that KFA hydrolase enzymes could remove RTX toxin KFA to inactivate the pore-forming toxin?

Additional lines of future study are myriad. In addition to bacteria, could other pathogens modulate KFA during infection? In addition to infection, KFA has already been shown to modulate tumor phenotypes. What other diseases could be regulated by KFA? Can KFA guide the creation of therapeutics to counteract these diseases? Addressing these questions, will require identifying more proteins modified by KFA and additional enzymes that regulate this modification,

as well as the development of small molecules targeting the regulatory enzymes. Future work needs to address these issues to fully understand the biological impact of KFA.

## AUTHOR CONTRIBUTIONS

GK and HL surveyed the literature and wrote the manuscript. Both authors contributed to the article and approved the submitted version.

## FUNDING

This work was supported by a grant from NIH/NCI CA240529.

## REFERENCES

- Afonina, I. S., Muller, C., Martin, S. J., and Beyaert, R. (2015). Proteolytic processing of Interleukin-1 family cytokines: variations on a common theme. *Immunity* 42, 991–1004. doi: 10.1016/j.immuni.2015.06.003
- Allaoui, A., Mounier, J., Prevost, M. C., Sansonetti, P. J., and Parsot, C. (1992). icsB: a *Shigella flexneri* virulence gene necessary for the lysis of protrusions during intercellular spread. *Mol. Microbiol.* 6, 1605–1616. doi: 10.1111/j.1365-2958.1992.tb00885.x
- Aramsangtienchai, P., Spiegelman, N. A., He, B., Miller, S. P., Dai, L., Zhao, Y., et al. (2016). HDAC8 catalyzes the hydrolysis of long chain fatty acyl lysine. *ACS Chem. Biol.* 11, 2685–2692. doi: 10.1021/acscchembio.6b00396
- Atapattu, D. N., and Czuprynski, C. J. (2007). Mannheimia haemolytica leukotoxin binds to lipid rafts in bovine lymphoblastoid cells and is internalized in a dynamin-2- and clathrin-dependent manner. *Infect. Immun.* 75, 4719–4727. doi: 10.1128/IAI.00534-07
- Bagchi, R. A., Ferguson, B. S., Stratton, M. S., Hu, T., Cavaasin, M. A., Sun, L., et al. (2018). HDAC11 suppresses the thermogenic program of adipose tissue via BRD2. *JCI Insight* 3:e120159. doi: 10.1172/jci.insight.120159
- Balashova, N. V., Shah, C., Patel, J. K., Megalla, S., and Kachlany, S. C. (2009). Aggregatibacter actinomycetemcomitans LtxC is required for leukotoxin activity and initial interaction between toxin and host cells. *Gene* 443, 42–47. doi: 10.1016/j.gene.2009.05.002
- Ball, L. E., Garland, D. L., Crouch, R. K., and Schey, K. L. (2004). Post-translational modifications of aquaporin 0 (AQPO) in the normal human lens: spatial and temporal occurrence. *Biochemistry* 43, 9856–9865. doi: 10.1021/bi0496034
- Basar, T., Havlicek, V., Bezouskova, S., Hackett, M., and Sebo, P. (2001). Acylation of lysine 983 is sufficient for toxin activity of *Bordetella pertussis* adenylate cyclase. Substitutions of alanine 140 modulate acylation site selectivity of the toxin acyltransferase CyaC. *J. Biol. Chem.* 276, 348–354. doi: 10.1074/jbc.M006463200
- Bellalou, J., Sakamoto, H., Ladant, D., Geoffroy, C., and Ullmann, A. (1990). Deletions affecting hemolytic and toxin activities of *Bordetella pertussis* adenylate cyclase. *Infect. Immun.* 58, 3242–3247. doi: 10.1128/IAI.58.10.3242-3247.1990
- Benz, R. (2016). Channel formation by RTX-toxins of pathogenic bacteria: basis of their biological activity. *Biochim. Biophys. Acta* 1858, 526–537. doi: 10.1016/j.bbmem.2015.10.025
- Benz, R. (2020). RTX-toxins. *Toxins (Basel)* 12, 359. doi: 10.3390/toxins12060359
- Berthiaume, L. G., and Beauchamp, E. (2018). *Epigenetic Silencing of NMT2*, Patent US 20180208990A1. Edmonton CMA: Pacylex Pharmaceuticals.
- Beuscher, H. U., and Colten, H. R. (1988). Structure and function of membrane IL-1. *Mol. Immunol.* 25, 1189–1199. doi: 10.1016/0161-5890(88)90155-1
- Biro, M., Munoz, M. A., and Weninger, W. (2014). Targeting Rho-GTPases in immune cell migration and inflammation. *Br. J. Pharmacol.* 171, 5491–5506. doi: 10.1111/bph.12658
- Bora-Singhal, N., Mohankumar, D., Saha, B., Colin, C. M., Lee, J. Y., Martin, M. W., et al. (2020). Novel HDAC11 inhibitors suppress lung adenocarcinoma stem cell self-renewal and overcome drug resistance by suppressing Sox2. *Sci. Rep.* 10:4722. doi: 10.1038/s41598-020-61295-6
- Bros, M., Haas, K., Moll, L., and Grabbe, S. (2019). RhoA as a key regulator of innate and adaptive immunity. *Cells* 8:733. doi: 10.3390/cells8070733
- Bursten, S. L., Locksley, R. M., Ryan, J. L., and Lovett, D. H. (1988). Acylation of monocyte and glomerular mesangial cell proteins. Myristyl acylation of the interleukin 1 precursors. *J. Clin. Invest.* 82, 1479–1488. doi: 10.1172/JCI113755
- Cao, J., Sun, L., Aramsangtienchai, P., Spiegelman, N. A., Zhang, X., Huang, W., et al. (2019). HDAC11 regulates type I interferon signaling through deacetylation of SHMT2. *Proc. Natl. Acad. Sci. U.S.A.* 116, 5487–5492. doi: 10.1073/pnas.1815365116
- Chang, A. R., Ferrer, C. M., and Mostoslavsky, R. (2020). SIRT6, a mammalian deacetylase with multitasking abilities. *Physiol. Rev.* 100, 145–169. doi: 10.1152/physrev.00030.2018
- Chen, G., Huang, P., and Hu, C. (2020). The role of SIRT2 in cancer: a novel therapeutic target. *Int. J. Cancer* 147, 3297–3304. doi: 10.1002/ijc.33118
- Cordero, C. L., Kudryashov, D. S., Reisler, E., and Satchell, K. J. (2006). The actin cross-linking domain of the *Vibrio cholerae* RTX toxin directly catalyzes the covalent cross-linking of actin. *J. Biol. Chem.* 281, 32366–32374. doi: 10.1074/jbc.M605275200
- Cuthbertson, C. R., Arabzade, Z., Bankhead, A. III, Kyani, A., and Neamati, N. (2021). A review of small-molecule inhibitors of one-carbon enzymes: SHMT2 and MTHFD2 in the spotlight. *ACS Pharmacol. Transl. Sci.* 4, 624–646. doi: 10.1021/acspstsci.0c00223
- Deubzer, H. E., Schier, M. C., Oehme, I., Lodrini, M., Haendler, B., Sommer, A., et al. (2013). HDAC11 is a novel drug target in carcinomas. *Int. J. Cancer* 132, 2200–2208. doi: 10.1002/ijc.27876
- Dian, C., Perez-Dorado, I., Riviere, F., Asensio, T., Legrand, P., Ritzfeld, M., et al. (2020). High-resolution snapshots of human N-myristoyltransferase in action illuminate a mechanism promoting N-terminal Lys and Gly myristoylation. *Nat. Commun.* 11:1132. doi: 10.1038/s41467-020-14847-3
- Dominy, J. E. Jr., Lee, Y., Jedrychowski, M. P., Chim, H., Jurczak, M. J., Camporez, J. P., et al. (2012). The deacetylase Sirt6 activates the acetyltransferase GCN5 and suppresses hepatic gluconeogenesis. *Mol. Cell* 48, 900–913. doi: 10.1016/j.molcel.2012.09.030
- El-Azami-El-Idrissi, M., Bauche, C., Loucka, J., Osicka, R., Sebo, P., Ladant, D., et al. (2003). Interaction of *Bordetella pertussis* adenylate cyclase with CD11b/CD18: role of toxin acylation and identification of the main integrin interaction domain. *J. Biol. Chem.* 278, 38514–38521. doi: 10.1074/jbc.M304387200
- Farazi, T. A., Waksman, G., and Gordon, J. I. (2001). The biology and enzymology of protein N-myristoylation. *J. Biol. Chem.* 276, 39501–39504. doi: 10.1074/jbc.R100042200
- Feldman, J. L., Baeza, J., and Denu, J. M. (2013). Activation of the protein deacetylase SIRT6 by long-chain fatty acids and widespread deacylation by mammalian sirtuins. *J. Biol. Chem.* 288, 31350–31356. doi: 10.1074/jbc.C113.511261

- Ferrara, G., Benzi, A., Sturla, L., Marubbi, D., Frumento, D., Spinelli, S., et al. (2020). Sirt6 inhibition delays the onset of experimental autoimmune encephalomyelitis by reducing dendritic cell migration. *J. Neuroinflammation* 17:228. doi: 10.1186/s12974-020-01906-1
- Fiskus, W., Coothankandaswamy, V., Chen, J., Ma, H., Ha, K., Saenz, D. T., et al. (2016). SIRT2 deacetylates and inhibits the peroxidase activity of Peroxiredoxin-1 to sensitize breast cancer cells to oxidant stress-inducing agents. *Cancer Res.* 76, 5467–5478. doi: 10.1158/0008-5472.CAN-16-0126
- Frey, J. (2019). RTX toxins of animal pathogens and their role as antigens in vaccines and diagnostics. *Toxins (Basel)* 11:719. doi: 10.3390/toxins11120719
- Gai, W., Li, H., Jiang, H., Long, Y., and Liu, D. (2016). Crystal structures of SIRT3 reveal that the alpha2-alpha3 loop and alpha3-helix affect the interaction with long-chain acyl lysine. *FEBS Lett.* 590, 3019–3028. doi: 10.1002/1873-3468.12345
- Gao, L., Cueto, M. A., Asselbergs, F., and Atadja, P. (2002). Cloning and functional characterization of HDAC11, a novel member of the human histone deacetylase family. *J. Biol. Chem.* 277, 25748–25755. doi: 10.1074/jbc.M111871200
- Gillingham, A. K., and Munro, S. (2007). The small G proteins of the Arf family and their regulators. *Annu. Rev. Cell Dev. Biol.* 23, 579–611. doi: 10.1146/annurev.cellbio.23.090506.123209
- Glozak, M. A., and Seto, E. (2009). Acetylation/deacetylation modulates the stability of DNA replication licensing factor Cdt1. *J. Biol. Chem.* 284, 11446–11453. doi: 10.1074/jbc.M809394200
- Goldberg, J. (1998). Structural basis for activation of ARF GTPase: mechanisms of guanine nucleotide exchange and GTP-myristoyl switching. *Cell* 95, 237–248. doi: 10.1016/s0092-8674(00)81754-7
- Gong, D., Zeng, Z., Yi, F., and Wu, J. (2019). Inhibition of histone deacetylase 11 promotes human liver cancer cell apoptosis. *Am. J. Transl. Res.* 11, 983–990.
- Greene, N. P., Crow, A., Hughes, C., and Koronakis, V. (2015). Structure of a bacterial toxin-activating acyltransferase. *Proc. Natl. Acad. Sci. U.S.A.* 112, E3058–E3066. doi: 10.1073/pnas.1503832112
- Gregoret, I. V., Lee, Y. M., and Goodson, H. V. (2004). Molecular evolution of the histone deacetylase family: functional implications of phylogenetic analysis. *J. Mol. Biol.* 338, 17–31. doi: 10.1016/j.jmb.2004.02.006
- Guin, S., Ru, Y., Wynes, M. W., Mishra, R., Lu, X., Owens, C., et al. (2013). Contributions of KRAS and RAL in non-small-cell lung cancer growth and progression. *J. Thorac. Oncol.* 8, 1492–1501. doi: 10.1097/JTO.0000000000000007
- Guo, F. (2021). RhoA and Cdc42 in T cells: are they targetable for T cell-mediated inflammatory diseases? *Precis. Clin. Med.* 4, 56–61. doi: 10.1093/pccmedi/pbaa039
- Hackett, M., Guo, L., Shabanowitz, J., Hunt, D. F., and Hewlett, E. L. (1994). Internal lysine palmitoylation in adenylate cyclase toxin from *Bordetella pertussis*. *Science* 266, 433–435. doi: 10.1126/science.7939682
- Hackett, M., Walker, C. B., Guo, L., Gray, M. C., Van Cuyk, S., Ullmann, A., et al. (1995). Hemolytic, but not cell-invasive activity, of adenylate cyclase toxin is selectively affected by differential fatty-acylation in *Escherichia coli*. *J. Biol. Chem.* 270, 20250–20253. doi: 10.1074/jbc.270.35.20250
- He, B., Hu, J., Zhang, X., and Lin, H. (2014). Thiomyristoyl peptides as cell-permeable Sirt6 inhibitors. *Org. Biomol. Chem.* 12, 7498–7502. doi: 10.1039/c4ob00860j
- Herlax, V., Mate, S., Rimoldi, O., and Bakas, L. (2009). Relevance of fatty acid covalently bound to *Escherichia coli* alpha-hemolysin and membrane microdomains in the oligomerization process. *J. Biol. Chem.* 284, 25199–25210. doi: 10.1074/jbc.M109.009365
- Hong, J. Y., Jing, H., Price, I. R., Cao, J., Bai, J. J., and Lin, H. (2020). Simultaneous Inhibition of SIRT2 deacetylase and defatty-acylase activities via a PROTAC strategy. *ACS Med. Chem. Lett.* 11, 2305–2311. doi: 10.1021/acsmedchemlett.0c00423
- Hong, J. Y., Price, I. R., Bai, J. J., and Lin, H. (2019). A glycoconjugated SIRT2 inhibitor with aqueous solubility allows structure-based design of SIRT2 inhibitors. *ACS Chem. Biol.* 14, 1802–1810. doi: 10.1021/acscchembio.9b00384
- Ismail, V. S., Mosely, J. A., Tapodi, A., Quinlan, R. A., and Sanderson, J. M. (2016). The lipidation profile of aquaporin-0 correlates with the acyl composition of phosphoethanolamine lipids in lens membranes. *Biochim. Biophys. Acta* 1858, 2763–2768. doi: 10.1016/j.bbame.2016.06.026
- Issartel, J. P., Koronakis, V., and Hughes, C. (1991). Activation of *Escherichia coli* prohaemolysin to the mature toxin by acyl carrier protein-dependent fatty acylation. *Nature* 351, 759–761. doi: 10.1038/351759a0
- Iwaki, M., Ullmann, A., and Sebo, P. (1995). Identification by in vitro complementation of regions required for cell-invasive activity of *Bordetella pertussis* adenylate cyclase toxin. *Mol. Microbiol.* 17, 1015–1024. doi: 10.1111/j.1365-2958.1995.mmi.17061015.x
- Jiang, H., Khan, S., Wang, Y., Charron, G., He, B., Sebastian, C., et al. (2013). SIRT6 regulates TNF-alpha secretion through hydrolysis of long-chain fatty acyl lysine. *Nature* 496, 110–113. doi: 10.1038/nature12038
- Jiang, H., Zhang, X., Chen, X., Aramsangtienchai, P., Tong, Z., and Lin, H. (2018). Protein lipidation: occurrence, mechanisms, biological functions, and enabling technologies. *Chem. Rev.* 118, 919–988. doi: 10.1021/acs.chemrev.6b00750
- Jiang, H., Zhang, X., and Lin, H. (2016). Lysine fatty acylation promotes lysosomal targeting of TNF-alpha. *Sci. Rep.* 6:24371. doi: 10.1038/srep24371
- Jing, H., Hu, J., He, B., Negron Abril, Y. L., Stupinski, J., Weiser, K., et al. (2016). A SIRT2-selective inhibitor promotes c-Myc oncoprotein degradation and exhibits broad anticancer activity. *Cancer Cell* 29, 767–768. doi: 10.1016/j.ccell.2016.04.005
- Jing, H., Zhang, X., Wisner, S. A., Chen, X., Spiegelman, N. A., Linder, M. E., et al. (2017). SIRT2 and lysine fatty acylation regulate the transforming activity of K-Ras4a. *Elife* 6:e32436. doi: 10.7554/eLife.32436
- Kawahara, T. L., Michishita, E., Adler, A. S., Damian, M., Berber, E., Lin, M., et al. (2009). SIRT6 links histone H3 lysine 9 deacetylation to NF-kappaB-dependent gene expression and organismal life span. *Cell* 136, 62–74. doi: 10.1016/j.cell.2008.10.052
- Kim, B., Lee, Y., Kim, E., Kwak, A., Ryoo, S., Bae, S. H., et al. (2013). The Interleukin-1alpha precursor is biologically active and is likely a key alarmin in the IL-1 family of cytokines. *Front. Immunol.* 4:391. doi: 10.3389/fimmu.2013.00391
- Knapp, O., Maier, E., Polleichtner, G., Masin, J., Sebo, P., and Benz, R. (2003). Channel formation in model membranes by the adenylate cyclase toxin of *Bordetella pertussis*: effect of calcium. *Biochemistry* 42, 8077–8084. doi: 10.1021/bi034295f
- Kosciuk, T., and Lin, H. (2020). N-Myristoyltransferase as a glycine and lysine myristoyltransferase in cancer, immunity, and infections. *ACS Chem. Biol.* 15, 1747–1758. doi: 10.1021/acscchembio.0c00314
- Kosciuk, T., Price, I. R., Zhang, X., Zhu, C., Johnson, K. N., Zhang, S., et al. (2020). NMT1 and NMT2 are lysine myristoyltransferases regulating the ARF6 GTPase cycle. *Nat. Commun.* 11:1067. doi: 10.1038/s41467-020-14893-x
- Kutil, Z., Mikesova, J., Zessin, M., Meleshin, M., Novakova, Z., Alquicer, G., et al. (2019). Continuous activity assay for HDAC11 enabling reevaluation of HDAC inhibitors. *ACS Omega* 4, 19895–19904. doi: 10.1021/acsomega.9b02808
- Kutil, Z., Novakova, Z., Meleshin, M., Mikesova, J., Schutkowski, M., and Barinka, C. (2018). Histone deacetylase 11 is a fatty-acid deacylase. *ACS Chem. Biol.* 13, 685–693. doi: 10.1021/acscchembio.7b00942
- Lanyon-Hogg, T., Ritzfeld, M., Sefer, L., Bickel, J. K., Rudolf, A. F., Panyain, N., et al. (2019). Acylation-coupled lipophilic induction of polarisation (Acyl-cLIP): a universal assay for lipid transferase and hydrolase enzymes. *Chem. Sci.* 10, 8995–9000. doi: 10.1039/c9sc01785b
- Levental, I., Lingwood, D., Grzybek, M., Coskun, U., and Simons, K. (2010). Palmitoylation regulates raft affinity for the majority of integral raft proteins. *Proc. Natl. Acad. Sci. U.S.A.* 107, 22050–22054. doi: 10.1073/pnas.1016184107
- Lim, K. B., Walker, C. R., Guo, L., Pellett, S., Shabanowitz, J., Hunt, D. F., et al. (2000). *Escherichia coli* alpha-hemolysin (HlyA) is heterogeneously acylated in vivo with 14-, 15-, and 17-carbon fatty acids. *J. Biol. Chem.* 275, 36698–36702. doi: 10.1074/jbc.C000544200
- Linhardtova, I., Bumba, L., Masin, J., Basler, M., Osicka, R., Kamanova, J., et al. (2010). RTX proteins: a highly diverse family secreted by a common mechanism. *FEMS Microbiol. Rev.* 34, 1076–1112. doi: 10.1111/j.1574-6976.2010.00231.x
- Liu, W., Zhou, Y., Peng, T., Zhou, P., Ding, X., Li, Z., et al. (2018). N(epsilon)-fatty acylation of multiple membrane-associated proteins by *Shigella* IcsB effector to modulate host function. *Nat. Microbiol.* 3, 996–1009. doi: 10.1038/s41564-018-0215-6
- Liu, Y., Zhang, Y., Zhu, K., Chi, S., Wang, C., and Xie, A. (2019). Emerging role of Sirtuin 2 in Parkinson's disease. *Front. Aging Neurosci.* 11:372. doi: 10.3389/fnagi.2019.00372

- Locksley, R. M., Killeen, N., and Lenardo, M. J. (2001). The TNF and TNF receptor superfamilies: integrating mammalian biology. *Cell* 104, 487–501. doi: 10.1016/S0092-8674(01)00237-9
- Ludwig, A., Garcia, F., Bauer, S., Jarchau, T., Benz, R., Hoppe, J., et al. (1996). Analysis of the in vivo activation of hemolysin (HlyA) from *Escherichia coli*. *J. Bacteriol.* 178, 5422–5430. doi: 10.1128/jb.178.18.5422-5430.1996
- Martin, M. W., Lee, J. Y., Lancia, D. R. Jr., Ng, P. Y., Han, B., Thomason, J. R., et al. (2018). Discovery of novel N-hydroxy-2-arylisoindoline-4-carboxamides as potent and selective inhibitors of HDAC11. *Bioorg. Med. Chem. Lett.* 28, 2143–2147. doi: 10.1016/j.bmcl.2018.05.021
- Martin, T. D., Samuel, J. C., Routh, E. D., Der, C. J., and Yeh, J. J. (2011). Activation and involvement of Ral GTPases in colorectal cancer. *Cancer Res.* 71, 206–215. doi: 10.1158/0008-5472.CAN-10-1517
- Masin, J., Basler, M., Knapp, O., El-Azami-El-Idrissi, M., Maier, E., Konopasek, I., et al. (2005). Acylation of lysine 860 allows tight binding and cytotoxicity of Bordetella adenylate cyclase on CD11b-expressing cells. *Biochemistry* 44, 12759–12766. doi: 10.1021/bi050459b
- Mathias, R. T., Rae, J. L., and Baldo, G. J. (1997). Physiological properties of the normal lens. *Physiol. Rev.* 77, 21–50. doi: 10.1152/physrev.1997.77.1.21
- Mellini, P., Itoh, Y., Tsumoto, H., Li, Y., Suzuki, M., Tokuda, N., et al. (2017). Potent mechanism-based sirtuin-2-selective inhibition by an in situ-generated occupant of the substrate-binding site, “selectivity pocket” and NAD(+)-binding site. *Chem. Sci.* 8, 6400–6408. doi: 10.1039/c7sc02738a
- Michishita, E., Mccord, R. A., Berber, E., Kioi, M., Padilla-Nash, H., Damian, M., et al. (2008). SIRT6 is a histone H3 lysine 9 deacetylase that modulates telomeric chromatin. *Nature* 452, 492–496. doi: 10.1038/nature06736
- Michishita, E., Mccord, R. A., Boxer, L. D., Barber, M. F., Hong, T., Gozani, O., et al. (2009). Cell cycle-dependent deacetylation of telomeric histone H3 lysine K56 by human SIRT6. *Cell Cycle* 8, 2664–2666. doi: 10.4161/cc.8.16.9367
- Moniot, S., Forgione, M., Lucidi, A., Hailu, G. S., Nebbioso, A., Carafa, V., et al. (2017). Development of 1,2,4-oxadiazoles as potent and selective inhibitors of the human deacetylase Sirtuin 2: structure-activity relationship, X-Ray crystal structure, and anticancer activity. *J. Med. Chem.* 60, 2344–2360. doi: 10.1021/acs.jmedchem.6b01609
- Moreno-Yruea, C., Galleano, I., Madsen, A. S., and Olsen, C. A. (2018). Histone deacetylase 11 is an epsilon-N-Myristoyllysine hydrolase. *Cell Chem. Biol.* 25, 849–856.e8. doi: 10.1016/j.chembiol.2018.04.007
- Mousnier, A., Bell, A. S., Swiebeda, D. P., Morales-Sanfrutos, J., Perez-Dorado, I., Brannigan, J. A., et al. (2018). Fragment-derived inhibitors of human N-myristoyltransferase block capsid assembly and replication of the common cold virus. *Nat. Chem.* 10, 599–606. doi: 10.1038/s41557-018-0039-2
- Niki, Y., Yamada, H., Kikuchi, T., Toyama, Y., Matsumoto, H., Fujikawa, K., et al. (2004). Membrane-associated IL-1 contributes to chronic synovitis and cartilage destruction in human IL-1 alpha transgenic mice. *J. Immunol.* 172, 577–584. doi: 10.4049/jimmunol.172.1.577
- Ntwasa, M., Aapies, S., Schiffmann, D. A., and Gay, N. J. (2001). Drosophila embryos lacking N-myristoyltransferase have multiple developmental defects. *Exp. Cell Res.* 262, 134–144. doi: 10.1006/excr.2000.5086
- Nunez-Alvarez, Y., and Suelves, M. (2021). HDAC11: a multifaceted histone deacetylase with proficient fatty deacylase activity and its roles in physiological processes. *FEBS J.* doi: 10.1111/febs.15895 [Epub ahead of print].
- Ogawa, M., Yoshimori, T., Suzuki, T., Sagara, H., Mizushima, N., and Sasakawa, C. (2005). Escape of intracellular *Shigella* from autophagy. *Science* 307, 727–731. doi: 10.1126/science.1106036
- Osickova, A., Balashova, N., Masin, J., Sulc, M., Roderova, J., Wald, T., et al. (2018). Cytotoxic activity of Kingella kingae RtxA toxin depends on post-translational acylation of lysine residues and cholesterol binding. *Emerg. Microbes Infect.* 7:178. doi: 10.1038/s41426-018-0179-x
- Osickova, A., Khaliq, H., Masin, J., Jurnecka, D., Sukova, A., Fiser, R., et al. (2020). Acyltransferase-mediated selection of the length of the fatty acyl chain and of the acylation site governs activation of bacterial RTX toxins. *J. Biol. Chem.* 295, 9268–9280. doi: 10.1074/jbc.RA120.014122
- Ostolaza, H., Gonzalez-Bullon, D., Uribe, K. B., Martin, C., Amuategi, J., and Fernandez-Martinez, X. (2019). Membrane permeabilization by pore-forming RTX Toxins: what kind of lesions do these toxins form? *Toxins (Basel)* 11:354. doi: 10.3390/toxins11060354
- Outeiro, T. F., Kontopoulos, E., Altmann, S. M., Kufareva, I., Strathearn, K. E., Amore, A. M., et al. (2007). Sirtuin 2 inhibitors rescue alpha-synuclein-mediated toxicity in models of Parkinson's disease. *Science* 317, 516–519. doi: 10.1126/science.1143780
- Pan, P. W., Feldman, J. L., Devries, M. K., Dong, A., Edwards, A. M., and Denu, J. M. (2011). Structure and biochemical functions of SIRT6. *J. Biol. Chem.* 286, 14575–14587. doi: 10.1074/jbc.M111.218990
- Parenti, M. D., Grozio, A., Bauer, I., Galeno, L., Damonte, P., Millo, E., et al. (2014). Discovery of novel and selective SIRT6 inhibitors. *J. Med. Chem.* 57, 4796–4804. doi: 10.1021/jm500487d
- Parsot, C. (2009). *Shigella* type III secretion effectors: how, where, when, for what purposes? *Curr. Opin. Microbiol.* 12, 110–116. doi: 10.1016/j.mib.2008.12.002
- Pei, J., and Grishin, N. V. (2009). The Rho GTPase inactivation domain in *Vibrio cholerae* MARTX toxin has a circularly permuted papain-like thiol protease fold. *Proteins* 77, 413–419. doi: 10.1002/prot.22447
- Priestle, J. P., Schar, H. P., and Grutter, M. G. (1989). Crystallographic refinement of interleukin 1 beta at 2.0 Å resolution. *Proc. Natl. Acad. Sci. U.S.A.* 86, 9667–9671. doi: 10.1073/pnas.86.24.9667
- Rabl, J. (2020). BRCA1-A and BRISC: multifunctional molecular machines for ubiquitin signaling. *Biomolecules* 10:1503. doi: 10.3390/biom10111503
- Rabl, J., Bunker, R. D., Schenk, A. D., Cavadini, S., Gill, M. E., Abdulrahman, W., et al. (2019). Structural basis of BRCC36 function in DNA repair and immune regulation. *Mol. Cell* 75, 483–497.e9. doi: 10.1016/j.molcel.2019.06.002
- Ren, X., Gelin, A. D., Von Carlowitz, I., Janjic, N., and Pyle, A. M. (2017). Structural basis for IL-1alpha recognition by a modified DNA aptamer that specifically inhibits IL-1alpha signaling. *Nat. Commun.* 8:810. doi: 10.1038/s41467-017-00864-2
- Resh, M. D. (1999). Fatty acylation of proteins: new insights into membrane targeting of myristoylated and palmitoylated proteins. *Biochim. Biophys. Acta* 1451, 1–16. doi: 10.1016/S0167-4889(99)00075-0
- Resh, M. D. (2006). Trafficking and signaling by fatty-acylated and prenylated proteins. *Nat. Chem. Biol.* 2, 584–590. doi: 10.1038/nchembio834
- Ringel, A. E., Roman, C., and Wolberger, C. (2014). Alternate deacylating specificities of the archaeal sirtuins Sir2Afl and Sir2Afl2. *Protein Sci.* 23, 1686–1697. doi: 10.1002/pro.2546
- Rumpf, T., Schiedel, M., Karaman, B., Roessler, C., North, B. J., Lehotzky, A., et al. (2015). Selective Sirt2 inhibition by ligand-induced rearrangement of the active site. *Nat. Commun.* 6:6263. doi: 10.1038/ncomms7263
- Salah Ud-Din, A. I., Tikhomirova, A., and Roujeinikova, A. (2016). Structure and functional diversity of GCN5-Related N-Acetyltransferases (GNAT). *Int. J. Mol. Sci.* 17:1018. doi: 10.3390/ijms17071018
- Satchell, K. J. (2007). MARTX, multifunctional autoprocessing repeats-in-toxin toxins. *Infect. Immun.* 75, 5079–5084. doi: 10.1128/IAI.00525-07
- Satchell, K. J. (2011). Structure and function of MARTX toxins and other large repetitive RTX proteins. *Annu. Rev. Microbiol.* 65, 71–90. doi: 10.1146/annurev-micro-090110-102943
- Schey, K. L., Gutierrez, D. B., Wang, Z., Wei, J., and Grey, A. C. (2010). Novel fatty acid acylation of lens integral membrane protein aquaporin-0. *Biochemistry* 49, 9858–9865. doi: 10.1021/bi101415w
- Schiedel, M., Herp, D., Hammelmann, S., Swyter, S., Lehotzky, A., Robaa, D., et al. (2018). Chemically induced degradation of Sirtuin 2 (Sirt2) by a proteolysis targeting chimera (PROTAC) based on sirtuin rearranging ligands (SirReals). *J. Med. Chem.* 61, 482–491. doi: 10.1021/acs.jmedchem.6b01872
- Schlott, A. C., Holder, A. A., and Tate, E. W. (2018). N-Myristoylation as a drug target in malaria: exploring the role of N-Myristoyltransferase substrates in the inhibitor mode of action. *ACS Infect. Dis.* 4, 449–457. doi: 10.1021/acsinfecdis.7b00203
- Selvakumar, P., Lakshmikuttyamma, A., Shrivastav, A., Das, S. B., Dimmock, J. R., and Sharma, R. K. (2007). Potential role of N-myristoyltransferase in cancer. *Prog. Lipid Res.* 46, 1–36. doi: 10.1016/j.plipres.2006.05.002
- Sheahan, K. L., and Satchell, K. J. (2007). Inactivation of small Rho GTPases by the multifunctional RTX toxin from *Vibrio cholerae*. *Cell Microbiol.* 9, 1324–1335. doi: 10.1111/j.1462-5822.2006.00876.x
- Simanshu, D. K., Nissley, D. V., and McCormick, F. (2017). RAS proteins and their regulators in human disease. *Cell* 170, 17–33. doi: 10.1016/j.cell.2017.06.009



- Sindhu Kumari, S., Gupta, N., Shiels, A., Fitzgerald, P. G., Menon, A. G., Mathias, R. T., et al. (2015). Role of Aquaporin 0 in lens biomechanics. *Biochem. Biophys. Res. Commun.* 462, 339–345. doi: 10.1016/j.bbrc.2015.04.138
- Sociali, G., Magnone, M., Ravera, S., Damonte, P., Vigliarolo, T., Von Holtey, M., et al. (2017). Pharmacological Sirt6 inhibition improves glucose tolerance in a type 2 diabetes mouse model. *FASEB J.* 31, 3138–3149. doi: 10.1096/fj.201601294R
- Son, S. I., Cao, J., Zhu, C. L., Miller, S. P., and Lin, H. (2019). Activity-guided design of HDAC11-specific inhibitors. *ACS Chem. Biol.* 14, 1393–1397. doi: 10.1021/acschembio.9b00292
- Son, S. I., Su, D., Ho, T. T., and Lin, H. (2020). Garcinol is an HDAC11 inhibitor. *ACS Chem. Biol.* 15, 2866–2871. doi: 10.1021/acschembio.0c00719
- Speers, A. E., and Cravatt, B. F. (2004). Profiling enzyme activities in vivo using click chemistry methods. *Chem. Biol.* 11, 535–546. doi: 10.1016/j.chembiol.2004.03.012
- Spiegelman, N. A., Price, I. R., Jing, H., Wang, M., Yang, M., Cao, J., et al. (2018). Direct comparison of SIRT2 inhibitors: potency, specificity, activity-dependent inhibition, and on-target anticancer activities. *ChemMedChem* 13, 1890–1894. doi: 10.1002/cmdc.201800391
- Spiegelman, N. A., Zhang, X., Jing, H., Cao, J., Kotliar, I. B., Aramsangtienchai, P., et al. (2019). SIRT2 and lysine fatty acylation regulate the activity of RalB and cell migration. *ACS Chem. Biol.* 14, 2014–2023. doi: 10.1021/acschembio.9b00492
- Stanley, P., Packman, L. C., Koronakis, V., and Hughes, C. (1994). Fatty acylation of two internal lysine residues required for the toxic activity of *Escherichia coli* hemolysin. *Science* 266, 1992–1996. doi: 10.1126/science.7801126
- Stevenson, F. T., Bursten, S. L., Fanton, C., Locksley, R. M., and Lovett, D. H. (1993). The 31-kDa precursor of interleukin 1 alpha is myristoylated on specific lysines within the 16-kDa N-terminal propeptide. *Proc. Natl. Acad. Sci. U.S.A.* 90, 7245–7249. doi: 10.1073/pnas.90.15.7245
- Stevenson, F. T., Bursten, S. L., Locksley, R. M., and Lovett, D. H. (1992). Myristyl acylation of the tumor necrosis factor alpha precursor on specific lysine residues. *J. Exp. Med.* 176, 1053–1062. doi: 10.1084/jem.176.4.1053
- Sun, L., Marin De Esvikova, C., Bian, K., Achille, A., Telles, E., Pei, H., et al. (2018a). Programming and regulation of metabolic homeostasis by HDAC11. *EBioMedicine* 33, 157–168. doi: 10.1016/j.ebiom.2018.06.025
- Sun, L., Telles, E., Karl, M., Cheng, F., Luetetke, N., Sotomayor, E. M., et al. (2018b). Loss of HDAC11 ameliorates clinical symptoms in a multiple sclerosis mouse model. *Life Sci. Alliance* 1:e201800039. doi: 10.26508/lsa.201800039
- Tecleab, A., Zhang, X., and Sebt, S. M. (2014). Ral GTPase down-regulation stabilizes and reactivates p53 to inhibit malignant transformation. *J. Biol. Chem.* 289, 31296–31309. doi: 10.1074/jbc.M114.565796
- Teng, Y. B., Jing, H., Aramsangtienchai, P., He, B., Khan, S., Hu, J., et al. (2015). Efficient demyristoylase activity of SIRT2 revealed by kinetic and structural studies. *Sci. Rep.* 5:8529. doi: 10.1038/srep08529
- Tenhunen, J., Kucera, T., Huovinen, M., Kublbeck, J., Bisenieks, E., Vigante, B., et al. (2021). Screening of SIRT6 inhibitors and activators: a novel activator has an impact on breast cancer cells. *Biomed. Pharmacother.* 138:111452. doi: 10.1016/j.biopha.2021.111452
- Thole, T. M., Lodrini, M., Fabian, J., Wuenschel, J., Pfeil, S., Hielscher, T., et al. (2017). Neuroblastoma cells depend on HDAC11 for mitotic cell cycle progression and survival. *Cell Death Dis.* 8:e2635. doi: 10.1038/cddis.2017.49
- Toiber, D., Erdel, F., Bouazoune, K., Silberman, D. M., Zhong, L., Mulligan, P., et al. (2013). SIRT6 recruits SNF2H to DNA break sites, preventing genomic instability through chromatin remodeling. *Mol. Cell* 51, 454–468. doi: 10.1016/j.molcel.2013.06.018
- Tong, Z., Wang, M., Wang, Y., Kim, D. D., Grenier, J. K., Cao, J., et al. (2017). SIRT7 is an RNA-activated protein lysine deacylase. *ACS Chem. Biol.* 12, 300–310. doi: 10.1021/acschembio.6b00954
- Towler, D. A., Adams, S. P., Eubanks, S. R., Towery, D. S., Jackson-Machelski, E., Glaser, L., et al. (1987). Purification and characterization of yeast myristoyl CoA:protein N-myristoyltransferase. *Proc. Natl. Acad. Sci. U.S.A.* 84, 2708–2712. doi: 10.1073/pnas.84.9.2708
- Trent, M. S., Worsham, L. M., and Ernst-Fonberg, M. L. (1999). HlyC, the internal protein acyltransferase that activates hemolysin toxin: role of conserved histidine, serine, and cysteine residues in enzymatic activity as probed by chemical modification and site-directed mutagenesis. *Biochemistry* 38, 3433–3439. doi: 10.1021/bi982491u
- Walden, M., Tian, L., Ross, R. L., Sykora, U. M., Byrne, D. P., Hesketh, E. L., et al. (2019). Metabolic control of BRISC-SHMT2 assembly regulates immune signalling. *Nature* 570, 194–199. doi: 10.1038/s41586-019-1232-1
- Wang, B., Dai, T., Sun, W., Wei, Y., Ren, J., Zhang, L., et al. (2021). Protein N-myristoylation: functions and mechanisms in control of innate immunity. *Cell. Mol. Immunol.* 18, 878–888. doi: 10.1038/s41423-021-00663-2
- Wang, W., Fu, L., Li, S., Xu, Z., and Li, X. (2017). Histone deacetylase 11 suppresses p53 expression in pituitary tumor cells. *Cell Biol. Int.* 41, 1290–1295. doi: 10.1002/cbin.10834
- Wang, Y., Yang, J., Hong, T., Chen, X., and Cui, L. (2019). SIRT2: controversy and multiple roles in disease and physiology. *Ageing Res. Rev.* 55:100961. doi: 10.1016/j.arr.2019.100961
- Wassef, J. S., Keren, D. F., and Mailloux, J. L. (1989). Role of M cells in initial antigen uptake and in ulcer formation in the rabbit intestinal loop model of shigellosis. *Infect. Immun.* 57, 858–863. doi: 10.1128/IAI.57.3.858-863.1989
- Welch, R. A. (2001). RTX toxin structure and function: a story of numerous anomalies and few analogies in toxin biology. *Curr. Top. Microbiol. Immunol.* 257, 85–111. doi: 10.1007/978-3-642-56508-3\_5
- Woida, P. J., and Satchell, K. J. F. (2020). The *Vibrio cholerae* MARTX toxin silences the inflammatory response to cytoskeletal damage before inducing actin cytoskeleton collapse. *Sci. Signal.* 13:eaw9447. doi: 10.1126/scisignal.aaw9447
- Worsham, L. M., Trent, M. S., Earls, L., Jolly, C., and Ernst-Fonberg, M. L. (2001). Insights into the catalytic mechanism of HlyC, the internal protein acyltransferase that activates *Escherichia coli* hemolysin toxin. *Biochemistry* 40, 13607–13616. doi: 10.1021/bi011032h
- Yang, H., Chen, L., Sun, Q., Yao, F., Muhammad, S., and Sun, C. (2021). The role of HDAC11 in obesity-related metabolic disorders: a critical review. *J. Cell. Physiol.* 236, 5582–5591. doi: 10.1002/jcp.30286
- Yang, S. H., Shrivastav, A., Kosinski, C., Sharma, R. K., Chen, M. H., Berthiaume, L. G., et al. (2005). N-myristoyltransferase 1 is essential in early mouse development. *J. Biol. Chem.* 280, 18990–18995. doi: 10.1074/jbc.M412917200
- Yanginlar, C., and Logie, C. (2018). HDAC11 is a regulator of diverse immune functions. *Biochim. Biophys. Acta* 1861, 54–59. doi: 10.1016/j.bbagr.2017.12.002
- You, W., Rotili, D., Li, T. M., Kambach, C., Meleshin, M., Schutkowski, M., et al. (2017). Structural basis of Sirtuin 6 activation by synthetic small molecules. *Angew. Chem. Int. Ed. Engl.* 56, 1007–1011. doi: 10.1002/anie.201610082
- You, W., Zheng, W., Weiss, S., Chua, K. F., and Steegborn, C. (2019). Structural basis for the activation and inhibition of Sirtuin 6 by quercetin and its derivatives. *Sci. Rep.* 9:19176. doi: 10.1038/s41598-019-55654-1
- Young Hong, J., Cao, J., and Lin, H. (2019). Fluorogenic assays for the defatty-acylase activity of Sirtuins. *Methods Mol. Biol.* 2009, 129–136. doi: 10.1007/978-1-4939-9532-5\_10
- Yuan, M., Song, Z. H., Ying, M. D., Zhu, H., He, Q. J., Yang, B., et al. (2020). N-myristoylation: from cell biology to translational medicine. *Acta Pharmacol. Sin.* 41, 1005–1015. doi: 10.1038/s41401-020-0388-4
- Yuan, Y., Zhao, K., Yao, Y., Liu, C., Chen, Y., Li, J., et al. (2019). HDAC11 restricts HBV replication through epigenetic repression of cccDNA transcription. *Antiviral Res.* 172:104619. doi: 10.1016/j.antiviral.2019.104619
- Zhang, X., Khan, S., Jiang, H., Antonyak, M. A., Chen, X., Spiegelman, N. A., et al. (2016). Identifying the functional contribution of the defatty-acylase activity of SIRT6. *Nat. Chem. Biol.* 12, 614–620. doi: 10.1038/nchembio.2106
- Zhang, X., Spiegelman, N. A., Nelson, O. D., Jing, H., and Lin, H. (2017). SIRT6 regulates Ras-related protein R-Ras2 by lysine defatty-acylation. *Elife* 6:e25158. doi: 10.7554/eLife.25158
- Zhao, D., Mo, Y., Li, M. T., Zou, S. W., Cheng, Z. L., Sun, Y. P., et al. (2014). NOTCH-induced aldehyde dehydrogenase 1A1 deacetylation promotes breast cancer stem cells. *J. Clin. Invest.* 124, 5453–5465. doi: 10.1172/JCI76611
- Zheng, H., Gupta, V., Patterson-Fortin, J., Bhattacharya, S., Katlinski, K., Wu, J., et al. (2013). A BRISC-SHMT complex deubiquitinates IFNAR1 and regulates interferon responses. *Cell Rep.* 5, 180–193. doi: 10.1016/j.celrep.2013.08.025
- Zhong, L., D'urso, A., Toiber, D., Sebastian, C., Henry, R. E., Vadysirisack, D. D., et al. (2010). The histone deacetylase Sirt6 regulates glucose homeostasis via Hif1alpha. *Cell* 140, 280–293. doi: 10.1016/j.cell.2009.12.041



- Zhou, W., Ni, T. K., Wronski, A., Glass, B., Skibinski, A., Beck, A., et al. (2016). The SIRT2 deacetylase stabilizes slug to control malignancy of basal-like breast cancer. *Cell Rep.* 17, 1302–1317. doi: 10.1016/j.celrep.2016.10.006
- Zhou, Y., Huang, C., Yin, L., Wan, M., Wang, X., Li, L., et al. (2017). N(epsilon)-Fatty acylation of Rho GTPases by a MARTX toxin effector. *Science* 358, 528–531. doi: 10.1126/science.aam8659
- Zhu, A. Y., Zhou, Y., Khan, S., Deitsch, K. W., Hao, Q., and Lin, H. (2012). Plasmodium falciparum Sir2A preferentially hydrolyzes medium and long chain fatty acyl lysine. *ACS Chem. Biol.* 7, 155–159. doi: 10.1021/cb200230x
- Zychlinsky, A., Prevost, M. C., and Sansonetti, P. J. (1992). *Shigella flexneri* induces apoptosis in infected macrophages. *Nature* 358, 167–169. doi: 10.1038/358167a0

**Conflict of Interest:** HL was a founder and consultant for Sedec Therapeutics.

The remaining author declares that the research was conducted in the absence of any commercial or financial relationships that could be construed as a potential conflict of interest.

Copyright © 2021 Komaniecki and Lin. This is an open-access article distributed under the terms of the Creative Commons Attribution License (CC BY). The use, distribution or reproduction in other forums is permitted, provided the original author(s) and the copyright owner(s) are credited and that the original publication in this journal is cited, in accordance with accepted academic practice. No use, distribution or reproduction is permitted which does not comply with these terms.



# Cardioprotective Role of SIRT5 in Response to Acute Ischemia Through a Novel Liver-Cardiac Crosstalk Mechanism

Boda Zhou<sup>1†</sup>, Min Xiao<sup>2,3†</sup>, Hao Hu<sup>2†</sup>, Xiaoxia Pei<sup>2</sup>, Yajun Xue<sup>1</sup>, Guobin Miao<sup>1</sup>, Jifeng Wang<sup>2</sup>, Wanqi Li<sup>4</sup>, Yipeng Du<sup>2</sup>, Ping Zhang<sup>1\*</sup> and Taotao Wei<sup>2,3\*</sup>

<sup>1</sup> Department of Cardiology, Beijing Tsinghua Changgung Hospital, School of Clinical Medicine, Tsinghua University, Beijing, China, <sup>2</sup> National Laboratory of Biomacromolecules, Institute of Biophysics, Chinese Academy of Sciences, Beijing, China, <sup>3</sup> College of Life Sciences, University of Chinese Academy of Sciences, Beijing, China, <sup>4</sup> Yuanpei College, Peking University, Beijing, China

## OPEN ACCESS

### Edited by:

Lianjun Zhang,  
Center of Systems Medicine, Chinese  
Academy of Medical Sciences,  
Suzhou Institute of Systems Medicine  
(ISM), China

### Reviewed by:

Hui Gong,  
Fudan University, China  
Chun Li,  
Beijing University of Chinese  
Medicine, China

### \*Correspondence:

Ping Zhang  
zhpdoc@126.com  
Taotao Wei  
weitt@ibp.ac.cn

<sup>†</sup>These authors have contributed  
equally to this work

### Specialty section:

This article was submitted to  
Cellular Biochemistry,  
a section of the journal  
Frontiers in Cell and Developmental  
Biology

**Received:** 29 March 2021

**Accepted:** 30 June 2021

**Published:** 22 July 2021

### Citation:

Zhou B, Xiao M, Hu H, Pei X,  
Xue Y, Miao G, Wang J, Li W, Du Y,  
Zhang P and Wei T (2021)  
Cardioprotective Role of SIRT5  
in Response to Acute Ischemia  
Through a Novel Liver-Cardiac  
Crosstalk Mechanism.  
*Front. Cell Dev. Biol.* 9:687559.  
doi: 10.3389/fcell.2021.687559

Protein posttranslational modifications play important roles in cardiovascular diseases. The authors' previous report showed that the abundance of succinylated and glutarylated proteins was significantly lower in the serum of patients with acute myocardial infarction (AMI) than in that of healthy volunteers, suggesting a potential relationship between protein acylation and AMI. Sirtuin 5 (SIRT5) facilitates the removal of malonyl, succinyl, and glutaryl modification; however, its effects on AMI remain unknown. In this study, the levels of SIRT5 in AMI mouse model was compared. Results showed elevated hepatic SIRT5 after myocardial infarction. Hepatocyte-specific SIRT5 overexpressing mice (liver SIRT5 OE) were generated to address the possible involvement of hepatic SIRT5 in AMI. The areas of myocardial infarction, myocardial fibrosis, and cardiac function in a model of experimental myocardial infarction were compared between liver SIRT5 OE mice and wild-type (WT) mice. The liver SIRT5 OE mice showed a significantly smaller area of myocardial infarction and myocardial fibrosis than the WT mice. The fibroblast growth factor 21 (FGF21) in the blood and myocardium of liver SIRT5 OE mice after AMI was markedly elevated compared with that in WT mice. The results of mass spectrometry showed increased levels of proteins regulating tricarboxylic acid cycle, oxidative phosphorylation, and fatty acid  $\beta$ -oxidation pathways in the liver mitochondria of liver SIRT5 OE mice. These findings showed that SIRT5 may exhibit a cardioprotective effect in response to acute ischemia through a liver-cardiac crosstalk mechanism, probably by increasing the secretion of FGF21 and the improvement of energy metabolism.

**Keywords:** Sirt5, acute myocardial infarction, acylation, liver-cardiac crosstalk, FGF-21

## INTRODUCTION

Lysine acylation is a large family of protein posttranslational modifications that use metabolic intermediates as group donors (Zhao et al., 2010; Lin et al., 2012). Acetylation occurring on histones facilitates the epigenetic regulation of gene expression, while acetylation on metabolic enzymes regulates the flux of metabolism (Zhao et al., 2010; Zhou et al., 2011). However, the physiological and pathophysiological functions of non-acetyl acylation have been

under-investigated. Malonylation, succinylation, and glutarylation, which were found in histones (Xie et al., 2012) and metabolic enzymes (Du et al., 2015; Sadhukhan et al., 2016), use malonyl-CoA, succinyl-CoA, and glutaryl-CoA as substrates in their reaction, respectively (Hirschey and Zhao, 2015). Several groups have demonstrated the important roles of non-acetyl acylation in metabolism regulation in hepatic steatosis, diabetes, and heart failure (Rardin et al., 2013; Du et al., 2015, 2018; Sadhukhan et al., 2016), suggesting their potential importance in homeostasis and pathogenesis of metabolic disease. Recently we reported that the abundance of serum protein succinylation and glutarylation was significantly lower in the peripheral serum of patients with ST-elevation myocardial infarction and experimental acute myocardial infarction (AMI) rats than in healthy volunteers or sham surgery rats (Zhou et al., 2020). As the protein levels of cardiac SIRT5 were comparable before and after myocardial infarction, other mechanisms may be responsible for the removal of serum protein acylation during AMI. By profiling the expression of SIRT5 before and after myocardial infarction in mice, we found AMI resulted in elevated hepatic SIRT5 protein levels. Then we established a hepatocyte-specific SIRT5-overexpressing (liver SIRT5 OE) mouse model to investigate the pathophysiological functions of hepatic SIRT5 in AMI. Interestingly, the liver SIRT5 OE mice showed significantly smaller areas of myocardial infarction and myocardial fibrosis than the wild-type (WT) mice. Overexpression of SIRT5 increased the levels of blood and cardiac fibroblast growth factor 21 (FGF21) and elevated the expression of enzymes responsible for fatty acid  $\beta$ -oxidation in AMI mice, suggesting that SIRT5 may exhibit a cardioprotective role through a novel liver-cardiac crosstalk mechanism.

## MATERIALS AND METHODS

### Antibodies and Reagents

Antibodies against SIRT5 (15122-1-AP), VDAC (10866-1-AP), Oxoglutarate Dehydrogenase L (OGDHL) (17110-1-AP), Hydroxyacyl-CoA Dehydrogenase Trifunctional Multienzyme Complex Subunit Alpha (HADHA) (1-758-1-AP),  $\beta$ -tubulin (10068-1-AP),  $\alpha$ -tubulin (11224-1-AP),  $\beta$ -actin (66009-1-Ig), and HRP-conjugated  $\alpha$ -tubulin (HRP-66031) were purchased from ProteinTech (Beijing, China). An antibody against FGF21 (ab171941) was from Abcam. An antibody against ATP synthase, H<sup>+</sup> transporting, mitochondrial Fo complex, subunit d (ATP5H) (A4425) was from ABclonal. An anti-pan-succinyl-lysine (PTM-419) antibody was purchased from PTM Biolabs (Hangzhou, China). FGF21 ELISA kits were from R&D System (MF2100) and Abcam (ab212160). A list of chemicals used for mass spectroscopy could be found in the previously published paper (Du et al., 2015).

### Animals

Male C57BL/6J mice (12–16 weeks old, WT) were purchased from Vital River Co., Ltd. (Beijing, China). Hepatic SIRT5-overexpressing mice in C57BL/6 background (liver SIRT5 OE) was established by using the CRISPR/Cas9 gene editing tool

described previously (Du et al., 2018). The males of this strain at the age of 12–28 weeks were used for the experiments. The mouse studies were approved by the Ethics Committee of Beijing Tsinghua Changgung Hospital (19032-0-01) and the National Health and Medical Research Council of China Guidelines on Animal Experimentation. All efforts were made to minimize animal suffering.

### Myocardial Infarction Experiments

Ligation of LCA in mice was performed as described previously (Lindsey et al., 2018). The mice were intubated and anesthetized with an animal anesthesia machine (Soft Lander; Sin-ei Industry Co., Ltd., Saitama, Japan). Left thoracotomy was performed to visualize the left auricle. LCA was ligated using a 7-0 suture (Ethicon, Inc., Somerville, NJ, United States). The muscle layers and skin were closed using a 3-0 suture. In sham-surgery mice, the same surgical procedures were performed without ligation of LCA. The body temperature of mice was maintained at 37°C with a heat lamp during the procedures. In total, 12 WT mice received myocardial infarction surgery (AMI-WT), 12 WT mice received sham surgery (Sham-WT), 12 liver SIRT5 OE mice received LCA ligation surgery at the same site as WT mice (AMI-SIRT5 OE), and 12 liver SIRT5 OE mice received sham surgery (Sham-SIRT5 OE). The peripheral blood was collected in all mice before and 24 h after surgery. Plasma or serum was isolated from whole blood and kept in  $-80^{\circ}\text{C}$  until use. All mice were anesthetized and sacrificed 5 days after the surgery. Heart, liver, and other organs were sectioned.

### Histopathology

The heart was excised and sliced horizontally into 6–7 slices from base to apex. The morphological characteristics were analyzed via hematoxylin/eosin staining. Frozen heart sections (5  $\mu\text{m}$  thickness) were fixed with acetone for 15 min, followed by Masson's trichrome staining. The samples were incubated for 30 min in 1% 2,3,5-triphenyltetrazolium chloride (TTC) diluted in PBS (pH 7.4) at 37°C. The stained myocardial samples were visualized under a bright field microscope (Leica DM2500, Tokyo, Japan), and pictures of the entire slice were taken with identical exposure settings for all sections. The infarct/fibrotic area was compared with the total left ventricular (LV) area by using Image J software (NIH, Bethesda, MD, United States). The percentage of infarct area = infarct area/(infarct area + non-infarct area)  $\times$  100%, while the percentage of fibrotic area = fibrotic area/(fibrotic area + non-fibrotic area)  $\times$  100%.

### Echocardiography

Cardiac function was evaluated in the anesthesia. Ultrasound examinations were carried out using a high-resolution imaging system (Vevo 770, VisualSonics, Canada) with high-frequency ultrasound probe (RMV-707B, VisualSonics). M-mode images were obtained for measurements of LV wall thickness, LV end diastolic diameter (LVEDD), and LV end systolic diameter (LVESD). Ejection fraction (EF)% =  $\frac{\text{LVEDV} - \text{LVESV}}{\text{LVEDV}} \times 100\%$ , while fractional shortening (FS)% =  $\frac{\text{LVEDD} - \text{LVESD}}{\text{LVEDD}} \times 100\%$ .

## Western Blotting

Tissues were homogenized in 1 mL lysis buffer (50 mM Tris-Cl pH 7.4, 150 mM NaCl, 0.5 mM EDTA, 1 mM dithiothreitol, 1% Triton X-100, 0.5% sodium deoxycholate, and 0.1% sodium dodecyl sulfate). The homogenized tissues were centrifuged at 12,000 rpm, and the supernatant containing the tissue lysates were collected. The protein concentration was quantified with Pierce BCA Kit (Thermo Fisher Scientific). Western blot analysis was performed as described previously (Du et al., 2018).

## Measurements of FGF21

The FGF21 levels in mouse plasma were analyzed via ELISA with the use of Quantikine mouse FGF21 Immunoassay kit (R&D Systems) following the protocols provided by the manufacturer. The FGF21 levels in the culture medium of primary hepatocytes isolated from WT or SIRT5 OE mice were analyzed using an ELISA kit (Abcam) in accordance with the protocols provided by the manufacturer.

## Mass Spectrometry

Mitochondria were isolated from the liver of WT or liver SIRT5 OE mice, and proteins were extracted from the mitochondria following standard protocols (Du et al., 2018). The purified mitochondrial samples were disrupted by an ultrasonic processor on ice in lysis buffer (8 M urea/0.1 M Tris-HCl, pH 8.0) containing 1× Protease Inhibitor Cocktail (Roche). The protein solution was diluted 1:5 with 50 mM triethylammonium bicarbonate (TEAB) and digested with trypsin (1:50) at 37°C overnight. The digestion was desalted on OASIS HLB column, and peptides eluted with 60% acetonitrile were lyophilized via vacuum centrifugation. The dried peptides were dissolved with 100 mM TEAB buffer prior to labeling with tandem mass tags (TMTs). One hundred microgram of protein from each biological replicate of different experimental conditions was labeled with TMT 10plex (Thermo Fisher Scientific) in accordance with the manufacturer's instructions.

All nano LC-MS/MS experiments were performed on Q Exactive (Thermo Fisher Scientific) equipped with an Easy n-LC 1000 HPLC system. The labeled peptides were loaded onto a 100  $\mu$ m id  $\times$  2 cm fused silica trap column packed in-house with reversed phase silica (Reprosil-Pur C18 AQ, 5  $\mu$ m, Dr. Maisch GmbH) and then separated on an a 75  $\mu$ m id  $\times$  20 cm C18 column packed with reversed phase silica (Reprosil-Pur C18 AQ, 3  $\mu$ m, Dr. Maisch GmbH). MS analysis was performed with Q Exactive mass spectrometer (Thermo Fisher Scientific). Under data-dependent acquisition mode, the MS data were acquired at a high resolution of 70,000 ( $m/z$  200) across the mass range of 300–1600  $m/z$ . The target value was 3.00E + 06, with a maximum injection time of 60 ms. The top 20 precursor ions were selected from each MS full scan with isolation width of 2  $m/z$  for fragmentation in the HCD collision cell with normalized collision energy of 32%. Subsequently, MS/MS spectra were acquired at a resolution of 17,500 ( $m/z$  200). The target value was 5.00E + 04, with a maximum injection time of 80 ms. The dynamic exclusion time was 40 s. The nano electrospray ion-source setting was as

follows: spray voltage of 2.0 kV, no sheath gas flow, and heated capillary temperature of 320°C.

The raw data from Q Exactive were analyzed with Proteome Discovery version 2.2.0.388 using Sequest HT search engine for protein identification and Percolator for false discovery rate (FDR) analysis. FDR < 1% was set for protein identification. The peptide confidence was set as high for peptide filter. Protein quantification was also performed on Proteome Discovery 2.2.0.388 using the ratio of the intensity of reporter ions from the MS/MS spectra. Only the unique and razor peptides of proteins were selected for protein relative quantification. The co-isolation threshold was specified as 50%, and the average reporter S/N value should be above 10. Normalization mode was selected for the total peptide amount to correct experimental bias. The abundance values were normalized using Z-score to visualize the profiles of metabolic proteins in the hepatic mitochondria between the WT and liver SIRT5 OE mice. The normalized values were used to generate heat maps by using the pheatmap R-package in R (version 3.61).

## Statistical Analysis

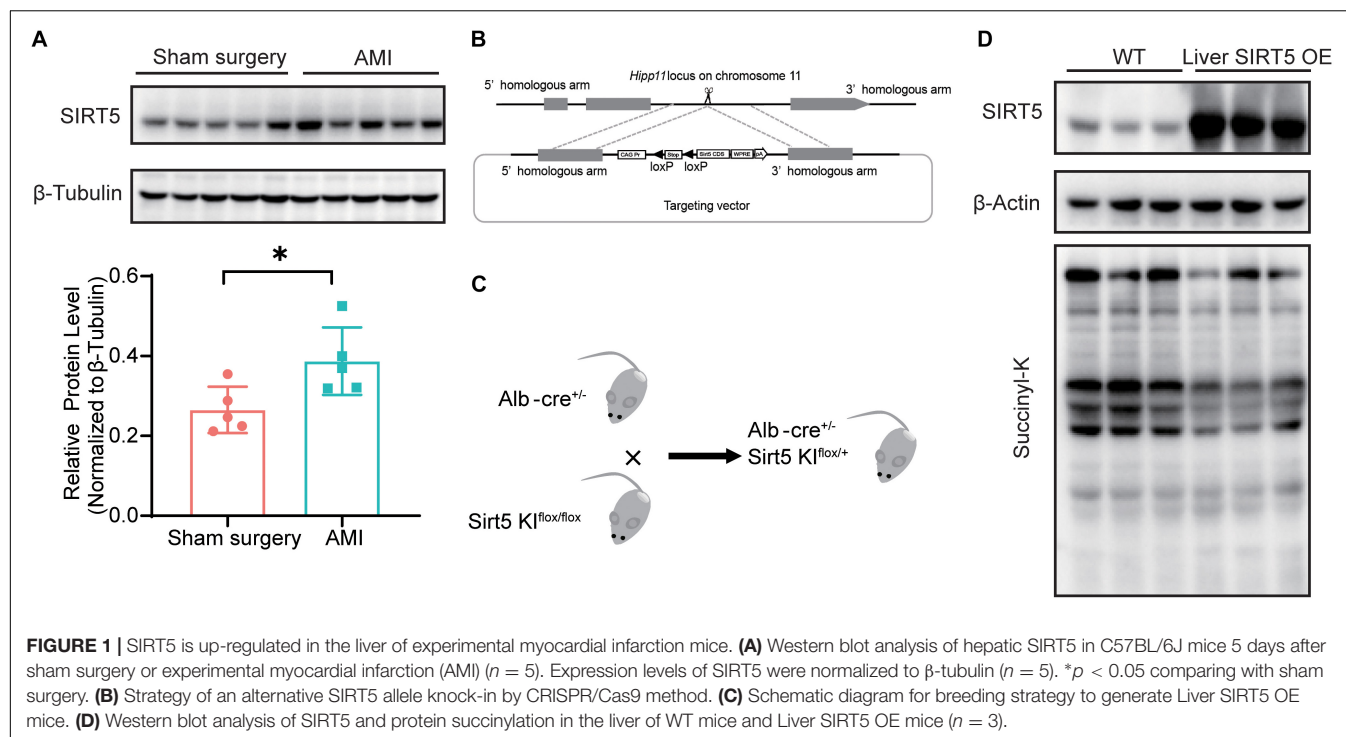
Descriptive data were presented as the mean  $\pm$  standard deviation (SD) for continuous variables. Data were analyzed using independent *t* test or one-way analysis of variance for continuous variables. Significance was assumed at a two-sided *p* value < 0.05. Statistical analysis was performed using GraphPad Prism (version 8.3.1).

## RESULTS

### Generation of Liver SIRT5 OE Mice

We recently reported decreased serum protein succinylation and glutarylation in patients and rats with AMI, but the levels of cardiac SIRT5 were comparable before and after myocardial infarction. Thus, the protein levels of SIRT5 in WT mice 5 days after AMI or sham surgery were compared. The results showed significantly elevated hepatic SIRT5 levels after AMI compared with sham surgery (Figure 1A). A hepatic specific SIRT5-overexpressing mouse model (liver SIRT5 OE) was established to further investigate the possible pathophysiological effects of hepatic SIRT5 in AMI. An alternative SIRT5 coding sequence was inserted into the Hipp 11 locus on the chromosome 11 of WT C57BL/6 mice via CRISPR/Cas9 method (Figure 1B). Hepatic SIRT5-overexpressing mice (liver SIRT5 OE) were generated by crossing between the SIRT5 allele knock-in mice (SIRT5  $K^{lox/flox}$ ) and Alb-cre mice (Alb-cre<sup>±</sup>), as shown in Figure 1C. Overexpression of SIRT5 in the liver but not in the kidney, brain, or heart was confirmed by Western blot (Figure 1D and Supplementary Figure 1). A marked decrease in total protein succinylation was found in the liver tissues of liver SIRT5 OE mice compared with that of WT mice (Figure 1D). Altogether, SIRT5 was specifically overexpressed in the liver of mice, and this overexpression significantly reduced levels of succinylation on multiple hepatic proteins.





## Hepatic Overexpression of SIRT5 Reduced Myocardial Infarction and Cardiac Fibrosis

To understand the effect of hepatic overexpression of SIRT5 on myocardial infarction, we first compared the cardiac function by using echocardiography between liver SIRT5 OE and WT mice 4 days after experimental myocardial infarction. Although no significant difference was noticed before surgery (**Supplementary Figure 2**), we observed a trend toward higher ( $p = 0.081$ ) LVEF in liver SIRT5 OE mice ( $27.55 \pm 12.73\%$ ) compared with WT mice ( $18.97 \pm 8.78\%$ ) after AMI, and a trend toward higher ( $p = 0.099$ ) LVFS in liver SIRT5 OE mice ( $12.72 \pm 4.36\%$ ) compared with WT mice ( $8.78 \pm 6.29\%$ ) after AMI (**Figures 2E,F**). Second, the percentage of infarction area between the liver SIRT5 OE and WT mice 5 days after experimental myocardial infarction was compared using TTC staining. The results showed a significantly lower ( $p = 0.027$ ) percentage of myocardial infarction in liver SIRT5 OE mice ( $22.84 \pm 7.80\%$ ) than in WT mice ( $30.33 \pm 7.20\%$ , **Figures 2A,B**). Third, the percentage of fibrosis area between liver SIRT5 OE and WT mice 5 days after experimental myocardial infarction was compared using Masson staining. The results revealed a significantly lower ( $p = 0.019$ ) percentage of fibrosis in liver SIRT5 OE mice ( $16.44 \pm 7.71\%$ ) than in WT mice ( $25.17 \pm 9.51\%$ , **Figures 2C,D**).

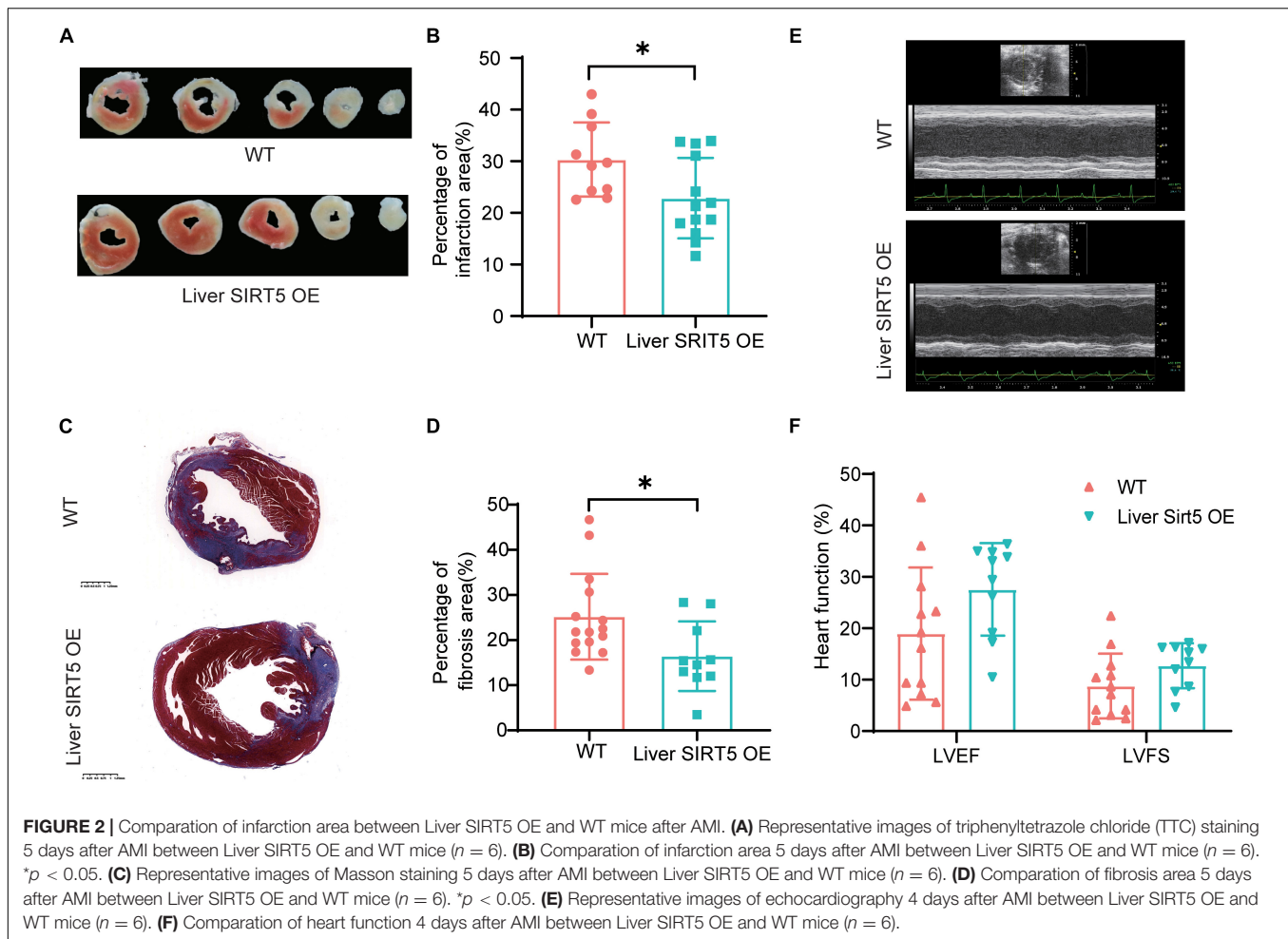
## Hepatic Overexpression of SIRT5 Promoted Endocrine FGF21 From Liver

Fibroblast growth factor 21 played an important role in liver-cardiac crosstalk during myocardial ischemia by regulating energy expenditure. Therefore, we hypothesized that hepatic

overexpression of SIRT5 may interfere with FGF21. The hepatic FGF21 protein level between sham surgery and AMI WT mice 5 days after surgery was detected, and the results showed a significantly elevated hepatic FGF21 protein level in AMI WT mice (**Figure 3A**). Surprisingly, a comparable hepatic FGF21 protein level was found in liver SIRT5 OE mice after sham surgery or AMI surgery, different from the results of WT mice (**Figure 3A**). Then, the blood FGF21 protein level between WT and liver SIRT5 OE mice before and after AMI surgery was compared. A significantly elevated blood FGF21 protein level was observed in liver SIRT5 OE mice after AMI surgery, whereas comparable blood FGF21 protein level was found in WT mice (**Figure 3B**). Interestingly, the cardiac but not muscular FGF21 protein level was significantly elevated in liver SIRT5 OE mice 5 days after AMI surgery compared with that in WT mice 5 days after AMI surgery (**Figure 3C** and **Supplementary Figure 3A**). Moreover, comparison of FGF21 secretion in the culture medium of primary hepatocytes isolated from liver SIRT5 OE or WT mice revealed significantly higher FGF21 level in hepatocytes from liver SIRT5 OE mice (**Supplementary Figure 3B**). These results suggested that the hepatic overexpression of SIRT5 promoted the secretion of FGF21 from the liver. There is also a possibility that hepatic overexpression of SIRT5 increased the expression or secretion of FGF21 from heart by potential mechanisms.

## Hepatic Overexpression of SIRT5 Improved Cell Metabolism

LC-MS/MS analysis of the hepatic mitochondria was performed to investigate the potential pathways regulated by the hepatic overexpression of SIRT5 ( $n = 8$ , **Supplementary Figure 4**).



Western blot revealed significantly upregulated SIRT5 in the hepatic mitochondria isolated from liver SIRT5 OE mice (Figure 4A). Bioinformatic analysis reported 269 upregulated peptides and 104 downregulated peptides with at least 1.3-fold change in the hepatic mitochondria of liver SIRT5 OE mice (Figure 4B). Pathway enrichment analysis showed enrichment in the pathways regulating fatty acid metabolism, tricarboxylic acid cycle, and oxidative phosphorylation (Figure 4C). The heat map of the total hepatic mitochondrial proteins confirmed the significant upregulation of multiple proteins in fatty acid  $\beta$ -oxidation, tricarboxylic acid cycle, and oxidative phosphorylation pathways in liver SIRT5 OE mice compared with that in WT mice (Figure 4D), indicating the enhancement of mitochondrial metabolism. These results were verified by western blot and showed upregulation of OGDHL and ATP5H in the hepatic mitochondria isolated from liver SIRT5 OE mice (Figure 4E).

## DISCUSSION

Cardiovascular diseases, especially myocardial infarction, have been the leading cause of death worldwide, even after modern therapeutic methods became prevalent, with ischemic injury

secondary to energy shortage as the potential pathological basis (Pedersen et al., 2014). Activated upon caloric restriction, sirtuins control critical cellular processes in the nucleus, cytoplasm, and mitochondria to maintain metabolic homeostasis and reduce cellular damage to protect against ischemic injury (Winnik et al., 2015). SIRT5 has been reported to exhibit a protective role in the pathological process of AMI, as global knockout of SIRT5 increased the infarct size in a model of cardiac ischemia-reperfusion injury (Boylston et al., 2015) and developed heart failure (Sadhukhan et al., 2016). Surprisingly, the global knockout of SIRT5 (Hershberger et al., 2017) but not the cardiac-specific knockout of SIRT5 (Hershberger et al., 2018) resulted in increased mortality in response to pressure overload, thus suggesting that the cardioprotective role of SIRT5 is not dependent on the heart. The SIRT5 in other tissues and organs may also be responsible for the cardioprotection. In the present study, SIRT5 expression was profiled in an AMI mouse model, and significantly elevated SIRT5 levels were found in the liver of AMI mice, indicating a possible role of hepatic SIRT5 in AMI. To confirm the relationship between SIRT5 and AMI, a hepatic-specific SIRT5-overexpressing mouse model was established by using the CRISPR/Cas9-based transgenic strategy. The results showed a significantly smaller area of myocardial infarction and myocardial fibrosis in liver SIRT5 OE mice than

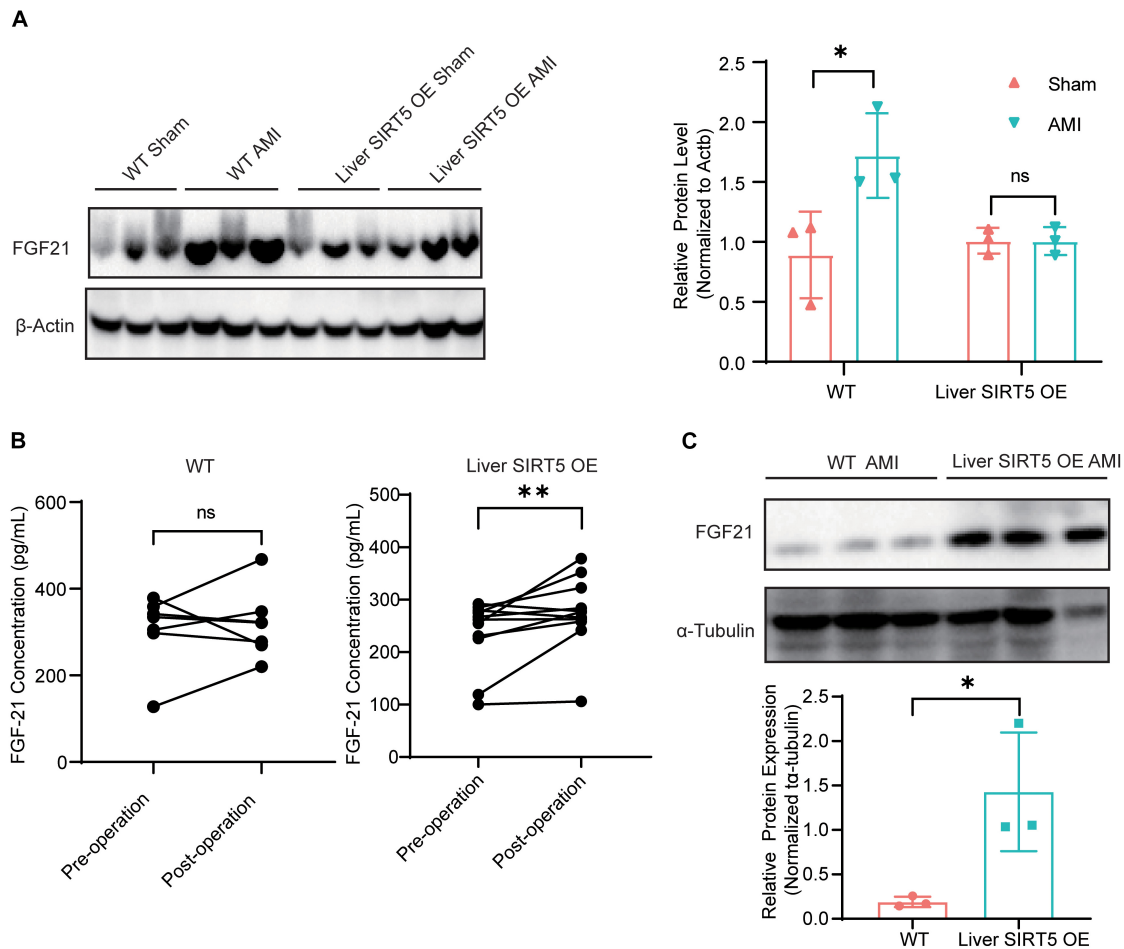


**FIGURE 3 |** Expression and secretion of FGF21 in mice after AMI. **(A)** Western blot analysis of hepatic FGF21 in WT or Liver SIRT5 OE 5 days after sham surgery or AMI. Expression levels of FGF21 were normalized to  $\beta$ -tubulin ( $n = 3$ ). \* $p < 0.05$  comparing with sham surgery ( $n = 3$ ). **(B)** Comparison of serum FGF21 level in mice before and after AMI ( $n = 5$ ). \*\* $p < 0.01$ . **(C)** Western blot analysis of cardiac FGF21 in WT or Liver SIRT5 OE 5 days after sham surgery or AMI. Expression levels of FGF21 were normalized to  $\beta$ -tubulin ( $n = 3$ ). \* $p < 0.05$ .

in WT mice, suggesting a novel cardioprotective mechanism of SIRT5 through a liver-cardiac crosstalk mechanism.

Fibroblast growth factor 21 has been reported to play key roles via liver-cardiac crosstalk in response to AMI. Of note, Liu et al. (2013) demonstrated that FGF21 was upregulated and released from the liver and adipose tissues in myocardial infarction. In the present study, a significant elevation in the hepatic FGF21 levels of WT mice in response to AMI operation was also observed. FGF21 protected the myocardium via attenuation of apoptosis, prevention of oxidative stress, and inhibition of inflammation (Tanajak et al., 2015). The signaling pathway involved in the regulation of FGF21 expression was well-documented. In the liver, the SIRT1-mediated activation of FGF21 prevented liver steatosis caused by fasting (Jegere et al., 2014), indicating the possible relationship between sirtuins and FGF21. By using hepatocyte-specific SIRT5 overexpressed mice, the effects of SIRT5 in hepatic FGF21 were explored in AMI mouse models. Different from the case of WT mice, in which the hepatic FGF21 was elevated as a result of AMI operation, no apparent upregulation of FGF21 was observed in the liver SIRT5 OE mice

after AMI operation. However, the blood and cardiac FGF21 levels in liver SIRT5 OE mice in response to AMI operation were significantly higher than those in WT mice. These data suggested that hepatic SIRT5 promoted the secretion of FGF21 from the liver into the circulation system, where it showed cardioprotective effects in AMI models.

Fibroblast growth factor 21 improved the energy supply to the heart by modulating the  $\beta$ -oxidation of fatty acid (Tanajak et al., 2015). Fatty acid oxidation is the major (50–70%) source of energy in the heart (Opie and Stubbs, 1976). During AMI, carbohydrate metabolism is temporarily disturbed. Instead, circulating free fatty acids are generally increased (Opie and Stubbs, 1976). LC-MS/MS analysis revealed an elevated expression of proteins regulating tricarboxylic acid cycle, oxidative phosphorylation, and fatty acid  $\beta$ -oxidation, the three essential pathways in the process of fatty acid oxidation, in liver SIRT5 OE mice. Western blot indicated that three proteins, OGDHL involved in the TCA cycle, ATP5H involved in the synthesis of ATP, and HADHA involved in the oxidation of fatty acids, were up-regulated in SIRT5 OE mice. This

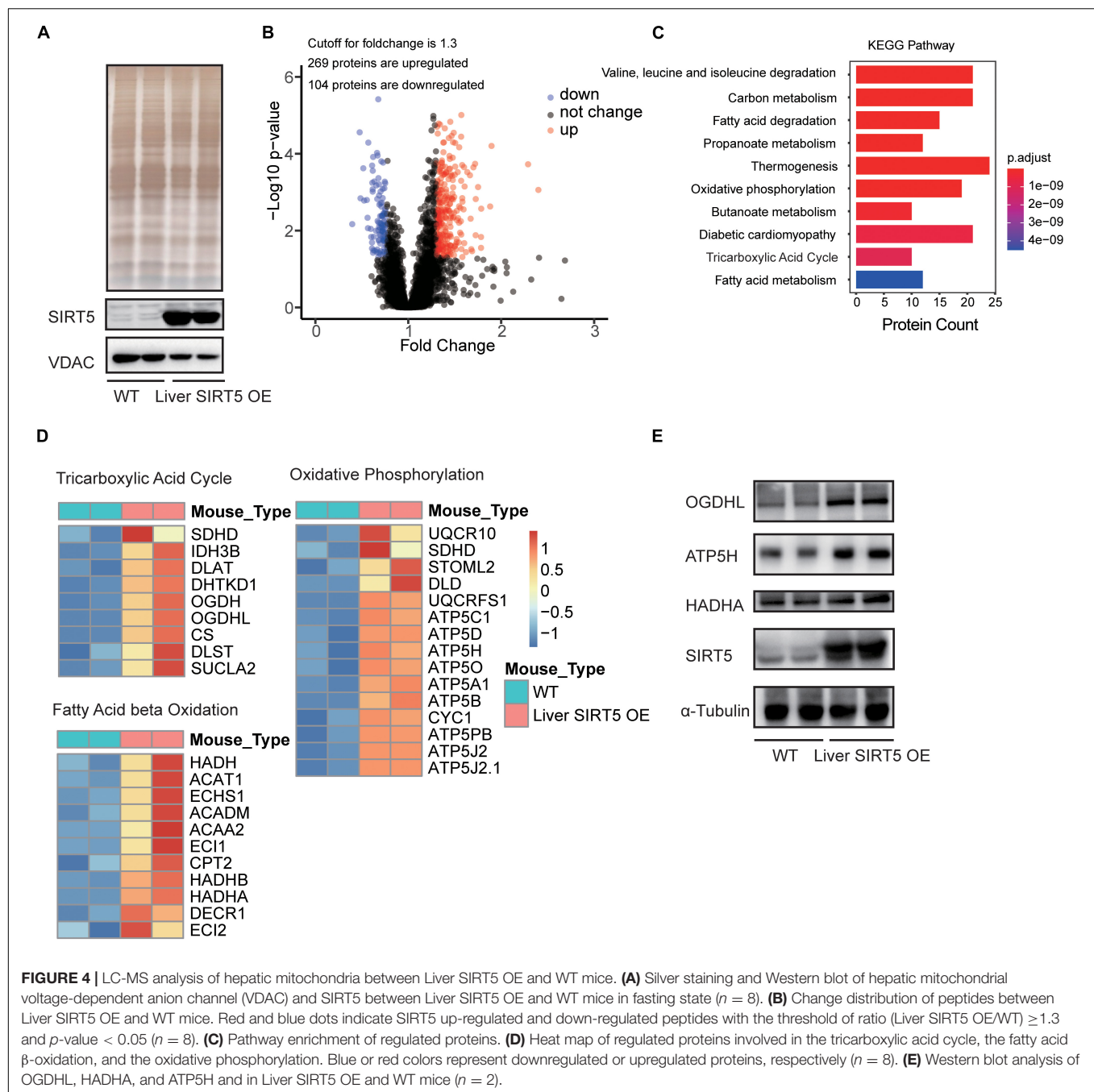


**FIGURE 4 |** LC-MS analysis of hepatic mitochondria between Liver SIRT5 OE and WT mice. **(A)** Silver staining and Western blot of hepatic mitochondrial voltage-dependent anion channel (VDAC) and SIRT5 between Liver SIRT5 OE and WT mice in fasting state ( $n = 8$ ). **(B)** Change distribution of peptides between Liver SIRT5 OE and WT mice. Red and blue dots indicate SIRT5 up-regulated and down-regulated peptides with the threshold of ratio (Liver SIRT5 OE/WT)  $\geq 1.3$  and  $p$ -value  $< 0.05$  ( $n = 8$ ). **(C)** Pathway enrichment of regulated proteins. **(D)** Heat map of regulated proteins involved in the tricarboxylic acid cycle, the fatty acid  $\beta$ -oxidation, and the oxidative phosphorylation. Blue or red colors represent downregulated or upregulated proteins, respectively ( $n = 8$ ). **(E)** Western blot analysis of OGDHL, HADHA, and ATP5H and in Liver SIRT5 OE and WT mice ( $n = 2$ ).

finding suggested that hepatic SIRT5 may accelerate fatty acid metabolism, which may promote energy supply to the heart during AMI. All these results were consistent with the findings observed in ob/ob mice (Du et al., 2018).

In conclusion, the results provided direct experimental evidence supporting a possible cardio-protective role of SIRT5 in response to acute ischemia. The increase in FGF21 secretion and the improvement of fatty acid metabolism may be crucial for the novel liver-cardiac crosstalk mechanism, which may shed light on the prevention and treatment of AMI and related heart diseases.

## DATA AVAILABILITY STATEMENT

The original contributions presented in the study are included in the article/Supplementary Material, further inquiries can be directed to the corresponding authors.

## ETHICS STATEMENT

The animal study was reviewed and approved by the Ethics Committee of Beijing Tsinghua Changgung Hospital.



## AUTHOR CONTRIBUTIONS

BZ, PZ, and TW initiated the study and developed the concept of the manuscript. BZ, MX, HH, YD, PZ, and TW designed the experiments. BZ, MX, HH, XP, YX, GM, JW, and WL performed the experiments. BZ, MX, PZ, and TW analyzed and interpreted the data and wrote the manuscript. All authors contributed to the article and approved the submitted version.

## FUNDING

This project was supported by grants 81970299, 92054108, and 31771257 from the National Natural Science Foundation of China, grants 2019YFA0508602 and 2017YFA0205501 from the National Key R&D Program of China, grant DFL20190902 from Beijing Hospitals Authority Ascent Plan, special funding support ZYLX201831 from Beijing Municipal Administration of Hospitals Clinical Medicine Development, and special funding support 2020-4-2243 from the Capital Health Research and Development.

## REFERENCES

- Boylston, J. A., Sun, J., Chen, Y., Gucek, M., Sack, M. N., and Murphy, E. (2015). Characterization of the cardiac succinylome and its role in ischemia-reperfusion injury. *J. Mol. Cell. Cardiol.* 88, 73–81. doi: 10.1016/j.jmcc.2015.09.005
- Du, Y., Cai, T., Li, T., Xue, P., Zhou, B., He, X., et al. (2015). Lysine malonylation is elevated in type 2 diabetic mouse models and enriched in metabolic associated proteins. *Mol. Cell. Proteomics* 14, 227–236. doi: 10.1074/mcp.M114.041947
- Du, Y., Hu, H., Qu, S., Wang, J., Hua, C., Zhang, J., et al. (2018). SIRT5 deacylates metabolism-related proteins and attenuates hepatic steatosis in ob/ob mice. *EBioMedicine* 36, 347–357. doi: 10.1016/j.ebiom.2018.09.037
- Hershberger, K. A., Abraham, D. M., Liu, J., Locasale, J. W., Grimsrud, P. A., and Hirschey, M. D. (2018). Ablation of Sirtuin5 in the postnatal mouse heart results in protein succinylation and normal survival in response to chronic pressure overload. *J. Biol. Chem.* 293, 10630–10645. doi: 10.1074/jbc.RA118.002187
- Hershberger, K. A., Abraham, D. M., Martin, A. S., Mao, L., Liu, J., Gu, H., et al. (2017). Sirtuin 5 is required for mouse survival in response to cardiac pressure overload. *J. Biol. Chem.* 292, 19767–19781. doi: 10.1074/jbc.M117.809897
- Hirschey, M. D., and Zhao, Y. (2015). Metabolic Regulation by Lysine Malonylation, Succinylation, and Glutarylation. *Mol. Cell. Proteomics* 14, 2308–2315. doi: 10.1074/mcp.R114.046664
- Jegere, S., Narbute, I., and Erglis, A. (2014). Use of intravascular imaging in managing coronary artery disease. *World J. Cardiol.* 6, 393–404. doi: 10.4330/wjc.v6.i6.393
- Lin, H., Su, X., and He, B. (2012). Protein lysine acylation and cysteine succinylation by intermediates of energy metabolism. *ACS Chem. Biol.* 7, 947–960. doi: 10.1021/cb3001793
- Lindsey, M. L., Bolli, R., Canty, J. M. Jr., Du, X. J., Frangogiannis, N. G., Frantz, S., et al. (2018). Guidelines for experimental models of myocardial ischemia and infarction. *Am. J. Physiol. Heart Circ. Physiol.* 314, H812–H838. doi: 10.1152/ajpheart.00335.2017
- Liu, S. Q., Roberts, D., Kharitonov, A., Zhang, B., Hanson, S. M., Li, Y. C., et al. (2013). Endocrine protection of ischemic myocardium by FGF21 from the liver and adipose tissue. *Sci. Rep.* 3:2767. doi: 10.1038/srep02767
- Opie, L. H., and Stubbs, W. A. (1976). Carbohydrate metabolism in cardiovascular disease. *Clin. Endocrinol. Metab.* 5, 703–729. doi: 10.1016/s0300-595x(76)80047-3
- Pedersen, F., Butrymovich, V., Kelbaek, H., Wachtell, K., Helqvist, S., Kastrup, J., et al. (2014). Short- and long-term cause of death in patients treated with

## SUPPLEMENTARY MATERIAL

The Supplementary Material for this article can be found online at: <https://www.frontiersin.org/articles/10.3389/fcell.2021.687559/full#supplementary-material>

**Supplementary Figure 1** | Western blot analysis of SIRT5 in the kidney, brain, and heart of WT mice and Liver SIRT5 OE mice ( $n = 3$ ).

**Supplementary Figure 2** | Comparison of heart function before AMI. **(A)** Representative images of echocardiography before AMI between Liver SIRT5 OE and WT mice ( $n = 8$ ). **(B)** Comparison of heart function before AMI between Liver SIRT5 OE and WT mice ( $n = 8$ ).

**Supplementary Figure 3** | Detection of FGF21 in WT mice and Liver SIRT5 OE mice. **(A)** Western blot analysis of FGF21 in the muscle of WT mice and Liver SIRT5 OE mice ( $n = 3$ ). **(B)** Primary hepatocytes were isolated from Liver SIRT5 OE or WT mice, and cultured *in vitro*. FGF21 protein was detected in the culture medium by ELISA and compared.

**Supplementary Figure 4** | Sample preparation for LC-MS analysis of hepatic mitochondria ( $n = 8$ ): A total of eight WT c57 mice and eight Liver SIRT5 OE mice were subject to starvation for 12 h before experiment, then hepatic mitochondria were isolated from every four mice and processed as one sample in TMT-MS.

- primary PCI for STEMI. *J. Am. Coll. Cardiol.* 64, 2101–2108. doi: 10.1016/j.jacc.2014.08.037
- Rardin, M. J., He, W., Nishida, Y., Newman, J. C., Carrico, C., Danielson, S. R., et al. (2013). SIRT5 regulates the mitochondrial lysine succinylome and metabolic networks. *Cell Metab.* 18, 920–933. doi: 10.1016/j.cmet.2013.11.013
- Sadhukhan, S., Liu, X., Ryu, D., Nelson, O. D., Stupinski, J. A., Li, Z., et al. (2016). Metabolomics-assisted proteomics identifies succinylation and SIRT5 as important regulators of cardiac function. *Proc. Natl. Acad. Sci. U. S. A.* 113, 4320–4325. doi: 10.1073/pnas.1519858113
- Tanajak, P., Chattipakorn, S. C., and Chattipakorn, N. (2015). Effects of fibroblast growth factor 21 on the heart. *J. Endocrinol.* 227, R13–R30. doi: 10.1530/JOE-15-0289
- Winnik, S., Auwerx, J., Sinclair, D. A., and Mather, C. M. (2015). Protective effects of sirtuins in cardiovascular diseases: from bench to bedside. *Eur. Heart J.* 36, 3404–3412. doi: 10.1093/eurheartj/ehv290
- Xie, Z., Dai, J., Dai, L., Tan, M., Cheng, Z., Wu, Y., et al. (2012). Lysine succinylation and lysine malonylation in histones. *Mol. Cell. Proteomics* 11, 100–107. doi: 10.1074/mcp.M111.015875
- Zhao, S., Xu, W., Jiang, W., Yu, W., Lin, Y., Zhang, T., et al. (2010). Regulation of cellular metabolism by protein lysine acetylation. *Science* 327, 1000–1004. doi: 10.1126/science.1179689
- Zhou, B., Du, Y., Xue, Y., Miao, G., Wei, T., and Zhang, P. (2020). Identification of Malonylation, Succinylation, and Glutarylation in Serum Proteins of Acute Myocardial Infarction Patients. *Proteomics Clin. Appl.* 14:e1900103. doi: 10.1002/prca.201900103
- Zhou, B., Margariti, A., Zeng, L., and Xu, Q. (2011). Role of histone deacetylases in vascular cell homeostasis and arteriosclerosis. *Cardiovasc. Res.* 90, 413–420. doi: 10.1093/cvr/cvr003

**Conflict of Interest:** The authors declare that the research was conducted in the absence of any commercial or financial relationships that could be construed as a potential conflict of interest.

Copyright © 2021 Zhou, Xiao, Hu, Pei, Xue, Miao, Wang, Li, Du, Zhang and Wei. This is an open-access article distributed under the terms of the Creative Commons Attribution License (CC BY). The use, distribution or reproduction in other forums is permitted, provided the original author(s) and the copyright owner(s) are credited and that the original publication in this journal is cited, in accordance with accepted academic practice. No use, distribution or reproduction is permitted which does not comply with these terms.



# Post-translational Modifications of the Protein Termini

Li Chen and Anna Kashina\*

Department of Biomedical Sciences, School of Veterinary Medicine, University of Pennsylvania, Philadelphia, PA, United States

## OPEN ACCESS

### Edited by:

Fangliang Zhang,  
University of Miami, United States

### Reviewed by:

Akhilesh Kumar,  
Banaras Hindu University, India  
Marta E. Hallak,  
National University of Córdoba,  
Argentina  
Aaron Smith,  
University of Maryland, Baltimore  
County, United States

### \*Correspondence:

Anna Kashina  
akashina@upenn.edu

### Specialty section:

This article was submitted to  
Cellular Biochemistry,  
a section of the journal  
Frontiers in Cell and Developmental  
Biology

**Received:** 02 June 2021

**Accepted:** 30 June 2021

**Published:** 29 July 2021

### Citation:

Chen L and Kashina A (2021)  
Post-translational Modifications of the  
Protein Termini.  
Front. Cell Dev. Biol. 9:719590.  
doi: 10.3389/fcell.2021.719590

Post-translational modifications (PTM) involve enzyme-mediated covalent addition of functional groups to proteins during or after synthesis. These modifications greatly increase biological complexity and are responsible for orders of magnitude change between the variety of proteins encoded in the genome and the variety of their biological functions. Many of these modifications occur at the protein termini, which contain reactive amino- and carboxy-groups of the polypeptide chain and often are pre-primed through the actions of cellular machinery to expose highly reactive residues. Such modifications have been known for decades, but only a few of them have been functionally characterized. The vast majority of eukaryotic proteins are N- and C-terminally modified by acetylation, arginylation, tyrosination, lipidation, and many others. Post-translational modifications of the protein termini have been linked to different normal and disease-related processes and constitute a rapidly emerging area of biological regulation. Here we highlight recent progress in our understanding of post-translational modifications of the protein termini and outline the role that these modifications play *in vivo*.

**Keywords:** N-terminome, C-terminome, acetylation, lipidation, Met-AP, arginylation, ubiquitination

## INTRODUCTION

Post-translational modifications (PTMs) involve enzyme-mediated covalent addition of functional groups to proteins during or after synthesis. These modifications greatly increase biological complexity and are responsible for orders of magnitude of change between the variety of proteins encoded in the genome and the variety of their biological functions. Thus, PTMs dramatically expand the encoded flexibility of a living system (Marino et al., 2015). As an example, the human genome encodes 20,379 proteins, which serve as targets for 191,837 PTMs<sup>1</sup>. Many of these modifications occur at the protein termini, which contain reactive amino- and carboxy-groups of the polypeptide chain and often are pre-primed through the actions of cellular machinery to expose highly reactive residues. Such modifications have been known for decades, but only a few of them have been functionally characterized.

Proteins with distinct N- and C-termini possess specific biochemical properties and functions, and are collectively referred to as the protein terminome (Figures 1, 2). Since every translated protein originally contains an N-terminal Met, specialized machinery in the cell removes this residue co- or post-translationally (Figure 1). This is the critical step that makes the N-terminus accessible to many modifications that target the primary amino group of residues other than

<sup>1</sup><https://www.nextprot.org/about/human-proteome>

Met. Similar pre-processing can occur at the C-termini—e.g., in the case of tubulin tyrosination-detyrosination cycle, where the C-terminal Tyr originally encoded in the tubulin gene can be removed and re-ligated through the action of specialized enzymes (Murofushi, 1980; Schroder et al., 1985; Aillaud et al., 2017; Nieuwenhuis et al., 2017; reviewed in Nieuwenhuis and Brummelkamp, 2019; **Figure 2**). Some PTMs at the protein termini can be more abundant than PTMs targeting the internal sites; for example, N-terminal acetylation can modify 80–90% of soluble human proteins and 50–70% of yeast proteins (Arnesen et al., 2009; Van Damme et al., 2011b). Terminal modifications target over 90% of the mammalian proteome and are essential for a variety of biological functions and processes such as protein sorting, membrane integration, cellular signaling, protein transport, enzyme activity, and formation of protein complexes. Thus, terminal modifications represent an important contribution to proteomic diversity and complexity.

In this review we discuss the major types of N- and C-terminal modifications that have been characterized to date, focusing on eukaryotic and mammalian systems.

## N-TERMINAL POST-TRANSLATIONAL MODIFICATIONS

### N-Terminal Removal of Amino Acid Residues and Signal Peptides

Since the ribosome recognizes the AUG codon as the translation initiation site, all naturally synthesized proteins contain an initiator Met at their N-terminus. This Met in itself is a reactive residue that can be modified by acetylation (Van Damme et al., 2012), as well as potentially serve as a target for other PTMs, e.g., as oxidation target for reactive oxygen species, though biological examples of such modifications have yet to be described. In many eukaryotic proteins the initiator Met is co- or post-translationally removed by Met-aminopeptidases (Met-APs), to expose the second residue in the sequence, which can in turn be removed or targeted by other PTMs.

Eukaryotic cells contain two of major Met-APs, Met-AP1 and Met-AP2 (Arfin et al., 1995; Li and Chang, 1995). These enzymes remove the Met preceding small and uncharged amino acid residues (e.g., Gly, Ala, Ser, Cys, Pro, Thr, and Val) (Boissel et al., 1985; Tsunasawa et al., 1985; Flinta et al., 1986; Ben-Bassat et al., 1987; Xiao et al., 2010; Wingfield, 2017). While the exact biological functions of these enzymes have not been characterized in detail, the overall activity of these enzymes is required for cell viability: their deletion leads to lethality in yeast (Li and Chang, 1995), and inhibition of their activity causes cell death in mammalian cell cultures (Towbin et al., 2003).

While no other Met-APs have been described, the repertoire of proteins found *in vivo* with removed N-terminal Met increasingly suggests that other classes of Met-APs must exist in cells, with specificity for residues in the second position that goes beyond the limited list of those recognized by Met-AP1 and Met-AP2. For example, cytoplasmic actins are processed by removal of N-terminal Met preceding negatively charged

residues (Asp or Glu), which occurs after Met acetylation (Redman and Rubenstein, 1981; Rubenstein and Martin, 1983; Martin and Rubenstein, 1987; Van Damme et al., 2012). The enzyme mediating this removal has been biochemically enriched but never definitively identified (Sheff and Rubenstein, 1992). Emerging mass spectrometry data suggest that initiator Met removal may occur even outside this residue specificity, suggesting that other Met-APs with different target sites might also exist in cells. Identification of these enzymes constitutes an exciting potential direction of research.

Removal of N-terminal Met exposes the next residue in the sequence to other, non-Met aminopeptidases, which can catalyze sequential removal of amino acid residues from the N-terminus unless it becomes structurally or chemically protected. According to MEROPS database (Rawlings, 2009), there are currently 269 aminopeptidases of different specificity found across the kingdoms of life<sup>2</sup>. While some of these aminopeptidases have been characterized in different systems, the global contribution of this processing to the functional N-terminome has not been systematically addressed.

Another type of N-terminal protein processing involves removal of signal peptides, e.g., from proteins secreted through the ER or targeted to other intracellular compartments. This cleavage exposes reactive residues on the N-termini that are further targeted by various modifications, both in the intracellular compartments and in the extracellular space.

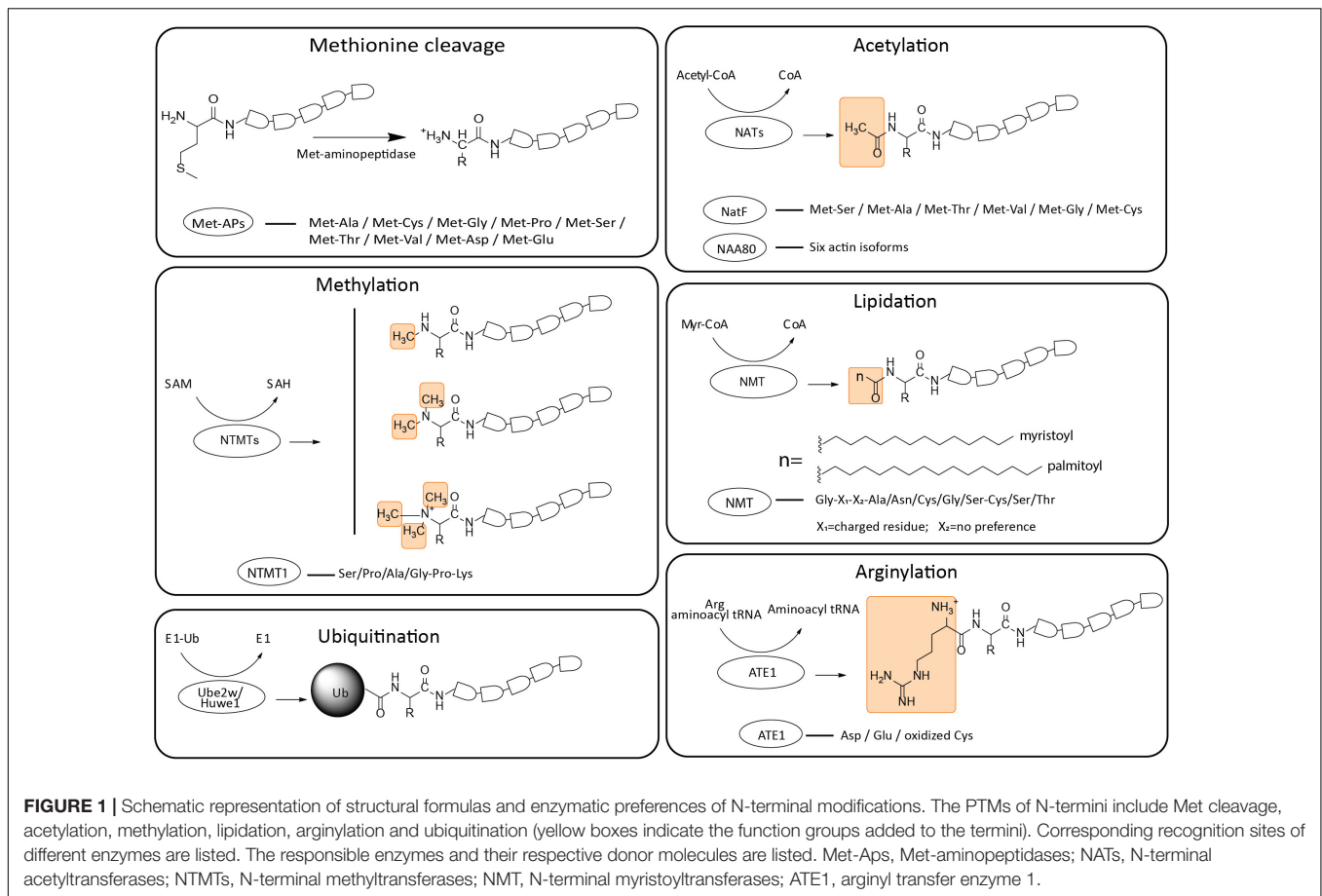
Both signal peptide cleavage and the action of endopeptidases generate neo N-termini that can be subjected to a multitude of different N-terminal modifications (Gevaert et al., 2003; Auf dem Keller et al., 2013). For example, an estimated 64 to 77% of identified termini in human erythrocytes and platelets differ from the genetically encoded termini and originate largely through proteolytic cleavage (Lange et al., 2014; Prudova et al., 2014). Collectively, these events increase the complexity of the N-terminome *in vivo* and the variety of N-terminal modifications on the same protein during different physiological processes *in vivo*.

### Acetylation

N-terminal acetylation is one of the most abundant protein modifications in eukaryotes. This modification involves the transfer of an acetyl moiety from acetyl-CoA to the  $\alpha$ -amino group of a nascent polypeptide or the fully synthesized protein. Even though some acetylation occurs directly on the initiator Met, most of these events in eukaryotes require Met removal and target the second or third residue in the protein sequence (Polevoda and Sherman, 2000). 80–90% of all proteins in human and 50–70% in yeast are N-terminally acetylated (Arnesen et al., 2009).

N-terminal acetylation is catalyzed by one of seven N-terminal acetyltransferases (NATs) (NatA to NatF and NatH). All NATs are oligomeric complexes composed of at least one catalytic subunit and one or more auxiliary subunit(s), including a unique ribosomal anchor, which contribute to substrate specificity and interactions with nascent polypeptides (Ree et al., 2018). Five

<sup>2</sup><https://www.ebi.ac.uk/merops/index.shtml>



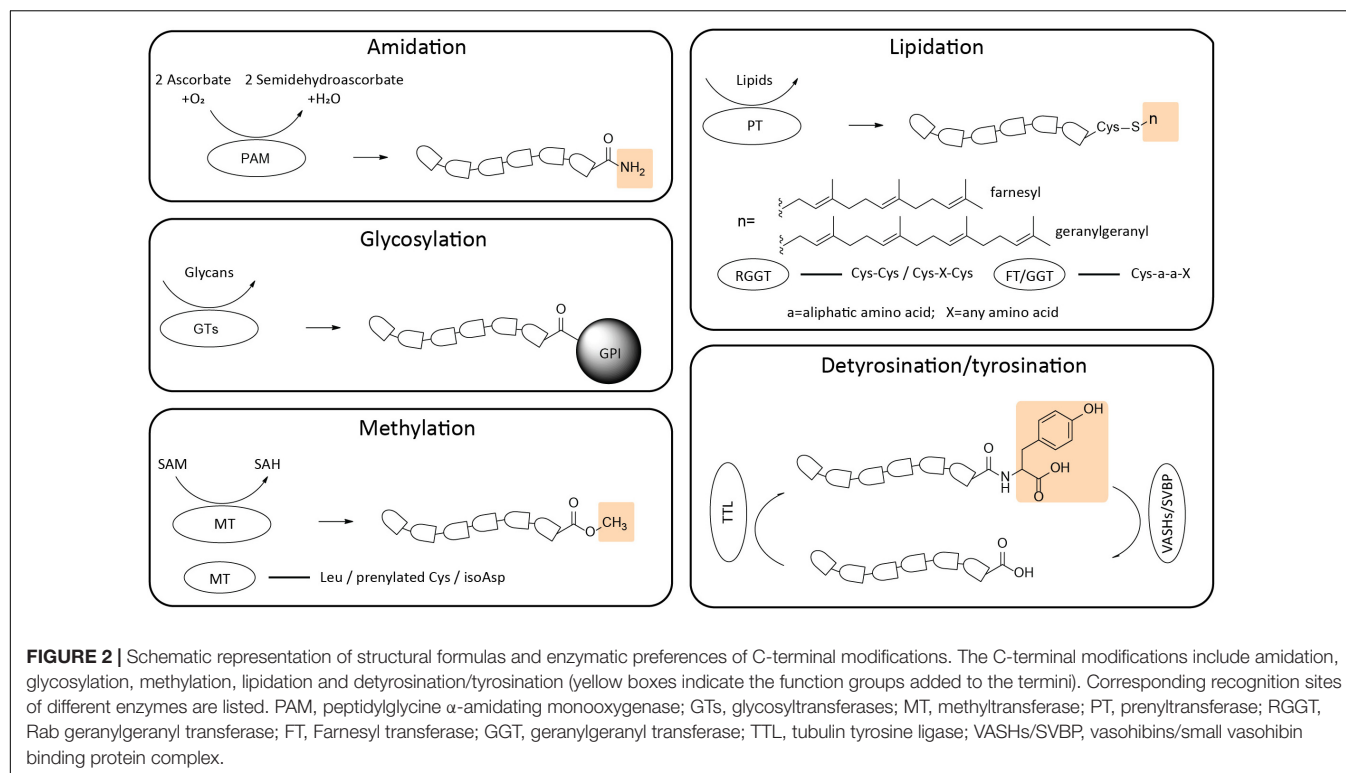
of the NATs (NatA to NatE) act co-translationally on nascent peptides emerging from the ribosome. NatF binds to the Golgi membrane and acetylates transmembrane proteins (Chen et al., 2016), most likely in a post-translational manner (Aksnes et al., 2015). Different NATs exhibit different target site specificity. Out of the three major NATs responsible for the majority of acetylations in eukaryotes, the NatA complex, acetylates N-termini starting with Ala, Cys, Gly, Ser, Thr or Val following the removal of the preceding initiator Met. Of note, removal of the auxiliary subunit from this enzyme complex changes its specificity to target the acidic N-termini (Polevoda et al., 1999; Arnesen et al., 2009; Van Damme et al., 2011a), though it is unclear whether this mechanism regulates N-terminal acetylation *in vivo*. The NatB complex acetylates the initiator Met preceding Asn, Asp, Gln, or Glu (Polevoda and Sherman, 2003). NatC targets the initiator Met that precedes Ile, Leu, Phe, or Trp. Other NATs also exhibit specific acetylation signatures, and sometimes show preference toward specific classes of proteins (e.g., histones in the case of NatD). These specificities are not absolute, and some overlapping protein targets have been observed between different NATs.

In addition to these broader specificity NATs, some additional N-terminal acetyltransferases exist that are uniquely specialized to target specific proteins *in vivo*. The recently identified NAA80 uniquely recognizes actin (Drazic et al., 2018). NAA80 acts

post-translationally, recognizing fully synthesized and folded actin and targeting all six mammalian actin isoforms in unique processing steps that occur differently in muscle and non-muscle actins.

Actin N-terminal processing constitutes a striking example of the complexity of the machinery mediating N-terminal acetylation and removal of specific residues in a protein. Non-muscle actins, containing a string of negatively charged residues following the initiator Met (DDD in beta actin and EEE in gamma actin), are co-translationally acetylated on the initiator Met *via* NatB, followed by removal of the acetylated Met by an unidentified actin N-acetyl-aminopeptidase (ANAP) (Sheff and Rubenstein, 1992). Muscle actins, typically containing a Cys in the second position, are processed by Met-AP1/2 to remove the N-terminal Met, followed by Cys acetylation, likely by NatA, and acetylated Cys removal by ANAP, to expose the acidic residue in the third position. In all cases, this acidic residue is then recognized by NAA80 in a posttranslational manner after actin's emergence from the ribosome and folding. Notably, NAA80 appears to have uniquely coevolved with actin to enable this preferential recognition, facilitated by the negatively charged actin's N-terminus, as well as the actin-profilin complex (Rebowski et al., 2020). It appears likely that other proteins may also have dedicated acetyltransferases that are yet to be discovered.





While the exact biological role of N-terminal acetylation is still being investigated, studies of individual proteins, as well as knockouts of individual N-acetyltransferases, enable some insights into their functions. Acetylation of fetal hemoglobin promotes subunit interactions in the hemoglobin tertiary complex (Manning and Manning, 2001), while tropomyosin requires acetylation for binding to actin (Urbancikova and Hitchcock-DeGregori, 1994). NAT knockouts in yeast lead to systemic growth and mating defects (Polevoda et al., 1999). In the case of actin, NAA80 knockout results in disrupted cytoskeleton structure and dynamics, including increased ratio of filamentous to globular actin, increased filopodia and lamellipodia formation, and accelerated cell motility (Drazic et al., 2018).

To date, no N-terminal deacetylases that globally remove N-terminally added acetyl groups have been identified, and thus N-terminal acetylation of proteins is believed to be irreversible.

## Lipidation

N-terminal lipidation refers to the transfer of fatty acids from acyl-CoA to the N-terminal amino acid residue. The most extensively studied type of lipidation is called myristoylation, which involves the addition of myristic acid to the N-terminal glycine (Gly) of the target protein. This chemical reaction is catalyzed by N-terminal myristoyltransferases (NMTs), which modify proteins in a co-translational manner in most of the cases (Glover et al., 1997; Varland et al., 2015) by targeting the amino acid residue N-terminally exposed after the removal of the initiator Met.

Two NMTs exist in mammalian systems, NMT1 and NMT2 (Gordon et al., 1991). These enzymes recognize an N-terminal

5-residue consensus sequence, which always starts with a Gly, followed by a charged residue in the second position, Ala/Asn/Cys/Gly, or Ser in the fourth position, and a preferred Cys/Ser, or Thr in the fifth position. There is no preference for the third position. Aromatic residues and Pro in the second position and/or Pro in the fifth position are incompatible with myristoylation (Towler et al., 1987; Martin et al., 2011).

N-terminal myristoylation targets an estimated 0.5% of cellular proteins (Thinon et al., 2014). Global profiling of N-terminal post-translational myristoylation found 40 substrates of NMTs in human cells. These proteins distribute in most of the organelles and are responsible for a variety of cell functions including apoptosis, DNA damage and repair, cell cycle regulation, and others. While our understanding of the biological role of myristoylation is still far from complete, studies demonstrate its key involvement in immune response (Udenwobe et al., 2017), protein turnover (Timms et al., 2019), G-protein signaling (Linder et al., 1993), and targeting of proteins to the membranes in different intracellular compartments (Resh, 2006; Baekkeskov and Kanaani, 2009). Huntingtin protein (HTT) is post-translationally myristoylated following the cleavage by caspases, and disruption of this myristoylation process on HTT fragment might be involved in the pathophysiology of Huntington disease (Martin et al., 2014).

Pro-apoptotic protein fragments with exposed N-terminal Gly undergo extensive myristoylation events in apoptotic cells (Zha et al., 2000; Utsumi et al., 2003). Strictly speaking, such myristoylation is not exactly N-terminal, since it occurs on pre-proteolyzed peptides, however, it is mediated by the same enzymes and thus belongs in this overview of NMT-mediated

protein regulation. By definition, such myristoylation in apoptotic cells is always post-translational, targeting fully synthesized and proteolyzed proteins. A prominent example is BID, a pro-apoptotic Bcl-2 protein containing only the BH3 domain, which is cleaved by caspase 8, generating a truncated 15-kd fragment (tBID) that translocates to the mitochondria within 1 hour. Myristoylation of tBID fragment acts as an activating switch, enhancing BID-induced release of cytochrome c and cell death (Zha et al., 2000). N-myristoylation of p21-activated kinase 2 (PAK2) targets its C-terminal fragment (ctPAK2), facilitating its relocation from the cytosol to the plasma membrane and membrane ruffles to maintain the normal apoptosis (Vilas et al., 2006).

Another type of N-terminal lipidation is palmitoylation, the addition of a palmitoyl group that can occur both N-terminally and internally in the protein. In the latter case, palmitoylation targets the side chains of Cys residues. N-terminal palmitoylation is far less abundant, and only a few examples of protein regulation by this modification have been identified. A palmitic acid-modified form of Sonic Hedgehog plays a role in regulating its intracellular functions (Pepinsky et al., 1998). Palmitoylation of the alpha subunit of the heterotrimeric G protein on the N-terminal Gly facilitates G-protein-dependent activation of adenylyl cyclase (Kleuss and Krause, 2003). Further studies are needed to uncover additional biological roles of this modification.

## Methylation

N-terminal methylation catalyzes the transfer of a methyl group from S-adenosylmethionine (SAM) to the exposed N-terminal  $\alpha$ -amino group after the initiator Met cleavage. The properties of methylated proteins differ by the degree of residue methylation. Monomethylation slightly increases basicity of the  $\alpha$ -amino group, and also introduces minor steric hindrance that may reduce its reactivity. However, dimethylation and trimethylation generate a permanent positive charge on the N-terminal amino group. The reversed electric charge properties cause the loss of nucleophilicity generated by  $\alpha$ -amino nitrogen. Up until now, no N-terminal demethylase has been found and this process is believed to be irreversible.

Although this modification was found more than 40 years ago, its physiological function was not clear until the discovery of its importance in protein-DNA interactions (Chen et al., 2007). In 2010, two different groups identified N-terminal methyltransferases (NTMTs) in yeast and human, respectively (Tooley et al., 2010; Webb et al., 2010). Two NTMTs are identified to date: NTMT1 is a tri-methyltransferase responsible for mono-, di-, and trimethylation of its substrates whereas NTMT2 is primarily responsible for monomethylation (Varland et al., 2015).

NTMT1, highly conserved from yeast to humans, recognizes the substrates with consensus sequence X-Pro-Lys (X = Ser/Pro/Ala/Gly). However, a recent study found that NTMT1 has broader recognition of peptides *in vitro*, where X can also include Phe, Tyr, Cys, Met, Lys, Arg, Asn, Gln, or His, suggesting that this enzyme, under different conditions, can also have broader substrate specificity *in vivo* (Petkowski et al., 2012). A crystal structure revealed that NTMT1 contains a

typical methyltransferase Rossmann fold which is composed of a seven-strand  $\beta$ -sheet and five  $\alpha$ -helices. Two  $\alpha$ -helices ( $\alpha 6$  and  $\alpha 7$ ) pack on one side of the  $\beta$ -sheet, and the other three  $\alpha$ -helices ( $\alpha 3, \alpha 4$ , and  $\alpha 5$ ) pack on the other side of the  $\beta$ -sheet. Besides its highly conserved Rossmann fold, NTMT1 has two unique structural elements distinct from other methyltransferases: a  $\beta$  hairpin inserted between strand  $\beta 5$  and helix  $\alpha 7$  and an N-terminal extension consisting of two  $\alpha$ -helices ( $\alpha 1$  and  $\alpha 2$ ). These two unique structures, which are involved in substrate binding, contribute to substrate specificity (Dong et al., 2015).

Many N-methylated proteins are components of large multisubunit complexes, suggesting a role of N-methylation in the regulation of protein-protein interactions (Stock et al., 1987). N-terminal  $\alpha$ -methylation on Ser2 of RCC1, the only known guanine nucleotide-exchange factor for the Ran GTPase, is indispensable for stable chromatin association and normal mitosis (Chen et al., 2007). During mitosis, CENP-A recruits the constitutive centromere associated network (CCAN) complex to govern the centromere function. N-terminal trimethylation on Gly2, followed by removal of the initiator Met, keeps the appropriate function of CENP-A, and loss of trimethylation can lead to lagging chromosomes and spindle pole defects (Sathyan et al., 2017). Mass spectrometric analysis revealed that the N-terminal Ala of PARP3 [poly(ADP-ribose) polymerase 3] is heavily methylated; however, the function of this methylation is not yet known (Dai et al., 2015).

N-terminal methyltransferases play important roles in maintaining proper cell function. Loss of the N-terminal methyltransferase NRMT1 disrupts the DNA damage repair and promotes mammary oncogenesis (Bonsignore et al., 2015a). The NRMT1 knockout (Nrmt1<sup>-/-</sup>) mice show high mortality after birth, and the surviving minority of these mice exhibit a variety of defects including decreased body size, female-specific infertility, kyphosis, decreased mitochondrial function, and early-onset liver degeneration (Bonsignore et al., 2015b).

## Arginylation

Protein arginylation was originally discovered in 1963, when it was found that ribosome-free extracts from cells and tissues exhibit prominent incorporation of specific radioactive amino acids (Kaji et al., 1963a,b). In eukaryotes, this catalytic reaction transfers Arg from aminoacyl tRNA to the target protein independently of the ribosome (Kashina, 2015). The enzyme mediating this reaction was first cloned and characterized in yeast, and termed arginyl transfer enzyme 1 (ATE1), or arginyltransferase (Balzi et al., 1990). To date, no stable binding partners or cofactors modulating ATE1 activity have been characterized, with the exception of Liat1 that was shown to bind to ATE1 and stimulate its ability to N-terminally arginylate a model substrate *in vitro* (Brower et al., 2014). The *Ate1* gene exists in nearly all eukaryotes [with the exception of two protozoan species (Jiang et al., 2020)], and plants have an additional gene, *Ate2*, which is believed to have arisen through gene duplication and carries a redundant biological function (Graciet and Wellmer, 2010; Domitrovic et al., 2017). The *Ate1* gene in human and mouse encodes four isoforms, generated by alternative splicing (Rai and Kashina, 2005). Additional two

isoforms, containing a tandem assembly of normally alternatively spliced exons, have been reported in one study (Hu et al., 2006), but the existence of these two isoforms has not been corroborated in studies by other groups.

ATE1 preferentially targets the unacetylated acidic N-terminal residues, including Asp and Glu (Wang et al., 2018), and has also been found to target oxidized Cys (Hu et al., 2008; Sriram et al., 2011). Targeting of unmodified Cys and other N-terminal amino acid residues has also been reported (Wong et al., 2007), likely at far lesser frequency than that of the “canonical” sites, and this targeting was found to differ between different ATE1 isoforms (Rai et al., 2006; Wang et al., 2019). While early studies did not observe any apparent consensus sequence for arginylation, recent high throughput analysis of arginylation using peptide arrays and advanced prediction tools suggested the existence of a consensus motif that may potentially be used to predict arginylation sites *in vivo* (Wang et al., 2019). Furthermore, recent studies uncovered the ability of ATE1 to arginylate the acidic side chains of Asp and Glu located internally in the protein sequence, expanding the role of this enzyme beyond the N-terminome (Wang et al., 2018).

ATE1-mediated arginylation has been initially characterized as part of the N-degron (N-end rule) pathway that relates the protein's half-life to the identity of the N-terminal amino acid residue (Bachmair et al., 1986; Varshavsky, 2019). In this pathway, the N-terminally arginylated proteins are recognized by specific E3 ligases of the ubiquitin–proteasome system (UPS), which then ubiquitinate a nearby Lys for the follow-up degradation. However, many arginylated proteins do not contain an accessible Lys for this targeting and thus remain metabolically stable after arginylation. Moreover, global analysis of protein arginylation targets suggest that regulation of protein stability constitutes only a small subset of ATE1's *in vivo* functions (Wong et al., 2007). To date, only a few proteins regulated by ATE1-dependent degradation have been uncovered, including members of the RGS family (Lee et al., 2005), and Apetala2/Ethylene Response Factors in plants (Gibbs et al., 2011; Licausi et al., 2011; Phukan et al., 2017). At the same time, non-degradatory targets of ATE1 have also been reported, including calreticulin (Carpio et al., 2010), phosphoribosyl pyrophosphate synthase (Zhang et al., 2015), and non-muscle  $\beta$ -actin (Karakozova et al., 2006).  $\beta$ -actin is N-arginylated at the third residue from the N-terminus, Asp3, after removal of the initiator Met and Asp2, and this arginylation is believed to regulate its functions in cytoskeleton maintenance and cell motility (Saha et al., 2010; Pavlyk et al., 2018), however, these mechanisms have not yet been fully characterized. Arginylated calreticulin is less susceptible to proteasomal degradation compared to the non-arginylated one (Goitea and Hallak, 2015), and its arginylation, following retrotranslocation of calreticulin from the ER into the cytosol, has been shown to increase apoptotic response (Comba et al., 2019). Further studies are underway and will eventually unravel the full complexity of the N-terminal arginylome.

## Ubiquitination

N-terminal ubiquitination involves the addition of a ubiquitin moiety to the free  $\alpha$ -amino group of the first

residue of a protein. The N-terminal ubiquitin may serve as a target for polyubiquitination, which is a well-known degradation signal recognized by the 26S proteasome complex. The addition of ubiquitin to the N-terminus of a target protein requires the same enzymatic machinery as ubiquitination of internal residues in the protein sequence, including ubiquitin activating, conjugating, and ligating enzymes.

N-terminal ubiquitination was first discovered by Ciechanover's lab (Breitschopf et al., 1998), which observed that ubiquitin-dependent degradation of myogenic transcriptional switch protein MyoD was not significantly affected by substitution of all nine internal Lys residues, but was abolished by chemical modification of the  $\alpha$ -amino group (Breitschopf et al., 1998). Direct evidence of N-terminal protein ubiquitination was obtained later by mass spectrometry, using tumor suppressor protein p16INK4a and the human papillomavirus oncoprotein-58 E7 (Ben-Saadon et al., 2004). Recently, it was found that  $\alpha$ -synuclein and a tau tetra-repeat domain can be N-terminally ubiquitinated *in vitro*. This ubiquitination affects aggregation properties, and was proposed to enable targeting of the modified  $\alpha$ -synuclein and a tau tetra-repeat domain by the proteasome, suggesting a role of N-terminal ubiquitination in the removal of amyloidogenic proteins (Ye et al., 2020).

Until now, two enzymes in the ubiquitin pathway, Ube2w and Huwe1, are reported to have the ability for N-terminal ubiquitination. Ube2w is an E2 ligase that conjugates ubiquitin to the N-terminal residue of Ataxin-3 and tau protein. Comparison of the active sites of Ube2w and classical E2s shows distinctive features, which make the Ube2w better suited for a neutral  $\alpha$ -amino group rather than a positively charged Lys side chain (Scaglione et al., 2013; Tatham et al., 2013). Huwe1 is the ubiquitin E3 ligase responsible for MyoD N-terminal ubiquitination. It was reported to play an important role in the nervous system, including neural progenitor proliferation, differentiation, cell migration, axon development, and inhibitory neurotransmission (Giles and Grill, 2020). Loss of function of Ube2w increases the susceptibility to early postnatal lethality and defects in skin, immune, and Male reproductive systems (Wang et al., 2016).

## N-Degron

Earlier studies of protein degradation revealed that protein's N-terminus often determines the protein's half-life, leading to the discovery of the “N-end rule pathway” (Bachmair et al., 1986) (later termed N-degron pathway) that related ubiquitin-dependent protein degradation to the identity of the N-terminal residue [see, e.g., (Varshavsky, 2011; Eldeeb and Fahlman, 2016; Winter et al., 2021) for an overview]. Since all proteins initially contain a Met at the N-termini, generation of the N-degrons requires additional processing that can include the action of the Met-APs, discussed earlier in this review, or regulated proteolysis that can expose a destabilizing N-terminal residue (Rao et al., 2001; Piatkov et al., 2012, 2014). Additional pathways can include N-terminal deamidation of Asn or Gln, followed by their Ate1-mediated arginylation (termed secondary and

tertiary steps of the N-end rule pathway, see Varshavsky (2019) for a recent review). In eukaryotes, N-terminal acetylation can serve as a degradation signal (Shemorry et al., 2013; Varshavsky, 2019), even though other studies propose that the hydrophobicity of the N-terminus, rather than acetylation, might serve a defining role in this mechanism (Eldeeb et al., 2019). More recently, the scope of the N-degron pathway was expanded from solely ubiquitin-proteasome degradation to autophagy and lysosomal pathways (Cha-Molstad et al., 2015, 2017; Yoo et al., 2017, 2018; Shim et al., 2018; Ji et al., 2019; Winter et al., 2021). Through all these processes, N-degrons are believed to regulate protein quality control as an integral part of key intracellular processes (Tasaki and Kwon, 2007; Gibbs et al., 2016; Ji and Kwon, 2017; Kwon and Ciechanover, 2017; Timms and Koren, 2020).

## C-TERMINAL POST-TRANSLATIONAL MODIFICATIONS

### Amidation

Carboxy-terminal  $\alpha$ -amidation—the addition of an amide group to the end of the polypeptide chain—is an important post-translational modification found widely in cells. The  $\alpha$ -amide group neutralizes the negatively charged C-termini, preventing ionization of the C-terminus and improves receptor binding ability of proteins and peptides (Cui et al., 2013; Marino et al., 2015). The most representative  $\alpha$ -amidated peptides are found in the nervous and endocrine systems, including neurokinin A, calcitonin, and amylin (Kim and Seong, 2001).

The  $\alpha$ -amidation reaction is catalyzed by peptidylglycine  $\alpha$ -amidating monooxygenase (PAM), a bifunctional enzyme composed of peptidylglycine- $\alpha$ -hydroxylating monooxygenase (PHM: E.C. 1.14.17.3) and peptidyl- $\alpha$ -hydroxyglycine- $\alpha$ -amidating lyase (PAL: E.C. 4.3.2.5) domains. The first step of amidation is catalyzed by PHM, a dicopper and ascorbate-dependent monooxygenase, which hydroxylates peptidylglycine generated from precursor proteins by sequential endo- and exoproteolysis. The hydroxylated product of this reaction, peptidyl- $\alpha$ -hydroxyglycine, is N-oxidatively cleaved by PAL, a zinc-bounded lyase (Chufán et al., 2009). X-ray structure analysis of PHM catalytic core (Prigge et al., 1997) revealed that this core is organized into N- and C-terminal domains of about 150 residues connected by a linker peptide. Each domain contains nine  $\beta$  strands and binds one copper ion ( $\text{Cu}_M$  and  $\text{Cu}_H$ ). Crystal structure shows that PAL folds as a six-bladed  $\beta$ -propeller. The active site is composed of a Zn(II) ion, coordinated by three histidine residues; the substrate binds to the active site through its  $\alpha$ -hydroxyl group linked to the Zn(II) ion (Chufán et al., 2009).

Over half of all biologically active peptides and peptide hormones are C-terminally  $\alpha$ -amidated, which is essential for their full biological activities (Kim and Seong, 2001). In most cases, this structural feature is essential for receptor recognition, signal transduction, and ligand binding. Mutation of the PAM gene leads to larval lethality in *Drosophila* and embryonic lethality in mice (Kolhekar et al., 1997; Czyzyk et al., 2005).

### Glycosylation

Glycosylation involves addition of carbohydrate moieties to proteins *in vivo*. Protein glycosylation plays an important overall role in protein maturation and sorting, affecting a wide variety of normal and pathological functions [e.g., (Varki, 2017; Reily et al., 2019) for recent reviews]. Protein glycosylation is a complicated multistep process that can target different chemical groups in proteins by addition of different sugar moieties (glycans) and utilizes around 200 glycosyltransferases (GTs) with different specificities. Common types of glycosylation include N-linked glycosylation, O-linked glycosylation, addition of phosphorylated glycans and glycosaminoglycans to different amino acid residues in protein midchain sites, as well as C-terminal addition of glycosylphosphatidylinositol (GPI).

One well-described example of C-terminal glycosylation involves addition of GPI to serve as a lipid anchor for protein binding to the cell surface. GPI is conjugated to the protein C-terminus *via* an amide bond between the carboxyl group and an amino group of the terminal ethanolamine phosphate. This is a multi-step process, in which the core GPI is assembled on the endoplasmic reticulum (ER) membrane and then transferred to the precursor proteins immediately after their ER translocation. Following this, the nascent GPI-linked protein undergoes several modification steps, including addition of side glycans in the ER and the Golgi apparatus (Homans et al., 1988; Kinoshita, 2020). The final products are transported to the plasma membrane.

In humans, at least 150 GPI-anchored proteins have been identified, and these proteins play a variety of different roles in cells, serving as receptors, adhesion molecules, enzymes, transporters, and protease inhibitors (Kinoshita, 2016). Complete loss or severe reduction in GPI biosynthesis lead to early embryonic lethality in mice (Alfieri et al., 2003; Reily et al., 2019). Inherited GPI deficiency causes neurological problems, including seizures, developmental delay/intellectual disability, cerebral atrophy and hypotonia (Knaus et al., 2018; Bellai-Dussault et al., 2019).

Another type of C-terminal glycosylation involves perforin, a pore-forming cytolytic protein found in the granules of cytotoxic T lymphocytes and natural killer cells. Perforin forms transmembrane pores on the target cell membrane, which allow for the passive diffusion of granzymes into the target cell and lead to cell apoptosis (Podack et al., 1985; Stinchcombe et al., 2006). N-linked glycosylation of the perforin's C-terminal Asn549 plays a vital role in protecting cytotoxic lymphocytes from perforin cytotoxicity by preventing perforin pores formation prior to granule exocytosis (House et al., 2017).

### Lipidation

Protein C-terminal lipidation, also called prenylation, refers to the addition of multiple isoprene units to cysteine residues close to the C-termini of proteins. For an estimation, about 2% of the total proteins in mammalian cells are prenylated (Epstein et al., 1991; Jiang et al., 2018). Two types of lipid groups, farnesyl and geranylgeranyl, target the cysteine at the C-termini of protein with conserved motifs CaaX CC and CXC (C = cysteine, a = an aliphatic amino acid, X = any amino acid). The majority of prenylated



proteins undergo geranylgeranylation (Epstein et al., 1991). This modification is thought to be irreversible, as no enzymes have been found to be responsible for de-prenylation of intact proteins. However, studies revealed that a prenylcysteine lyase exists in lysosomes and is responsible for thioether bond of prenylcysteines cleavage during degradation of prenylated proteins (Tschantz et al., 1999, 2001).

There are three members of prenyltransferase (PT) family in eukaryotes, including farnesyl transferase, geranylgeranyl transferase, and Rab geranylgeranyl transferase. Farnesyl transferase (FT) catalyzes 15-carbon farnesyl group transfer to target protein; geranylgeranyl transferase (GGT) is responsible for transfer of 20-carbon geranylgeranyl group. After these two transferases target Cys within the C-terminal CaaX motif, the C-terminal aaX is further processed through endoplasmic reticulum (ER) protease cleavage, followed by carboxylmethylation on prenylated cysteine residue in the ER (Boyartchuk et al., 1997; Dai et al., 1998). The Rab geranylgeranyl transferase (RGGT) recognizes Rab protein CC or CXC motifs and transfers geranylgeranyl groups on the C-terminal double cysteine (Jiang et al., 2018). Crystal structures analyses of GGT and FT revealed that the active sites of these two enzymes are composed of conserved aromatic residues that bind hydrophobic isoprene units, located in the  $\beta$  subunits. Zn(II) ions are required for their enzymatic activity (Park et al., 1997; Taylor et al., 2003).

Prenylation modulates protein membrane localization and protein-protein interaction. Defects in isoprene units biosynthesis or regulation can lead to cancer, cardiovascular and metabolic diseases, and neurodegenerative disorders (Xu et al., 2015). For example, lamin B requires farnesylation to assemble into the lamina for its association with the nuclear membrane during mitosis (Sinensky, 2011). Defects in lamin B1 prenylation can lead to abnormal brain development, and non-farnesylated form of lamin B1 causes mouse death soon after birth (Mical and Monteiro, 1998; Jung et al., 2013).

## Methylation

C-terminal methylation is an important branch of protein methylation, involving the enzymatic transfer of methyl groups from S-adenosylmethionine (SAM) to proteins. C-terminal methylation targets several amino acid residues, including Leu, prenylated Cys, and abnormal aspartyl and isoaspartyl residues on age-damaged proteins [see (Grillo and Colombatto, 2005) for a comprehensive overview].

One well-studied case is leucine methylation of mammalian protein phosphatase 2A (PP2A), which is involved in carbohydrate, amino acid, and lipid metabolism, and cell cycle control. PP2A is a dimeric core enzyme, composed of a structural A and catalytic C subunits, and a regulatory B subunit. The catalytic C subunit is methylated by leucine carboxylmethyltransferase-1 (LCMT-1). This is a reversible process, and the removal of the C-terminal methyl group is catalyzed by protein phosphatase methylesterase 1 (PME1) (Lee and Stock, 1993; Xie and Clarke, 1994; Ogris et al., 1999; Wandzioch et al., 2014). A crystal structure of human LCMT-1 shows that it contains a canonical SAM-dependent methyltransferase (MT) domain and a unique lid domain

composed of  $\alpha$  helices. The lid domain forms a deep active-site pocket that presumably binds to the carboxyl terminus of the PP2A tail (Stanevich et al., 2011). Interestingly, the extensive contacts between PP2A active site and LCMT-1 are essential for methylation of the PP2A tail. This mechanism suggests that efficient conversion of activated PP2A into substrate-specific holoenzyme minimizes unregulated phosphatase activity or formation of inactive holoenzymes (Stanevich et al., 2011). The active form of PP2A is critical for dephosphorylation of tau protein, which plays a crucial role in maintaining microtubule stability (Barbier et al., 2019). Deficiency of methylation on the catalytic subunit of PP2A has been associated with tau hyperphosphorylation, which leads to its aggregation into neurofibrillary tangles that correlate with the severity of phospho-tau pathology in Alzheimer's disease (Sontag et al., 2004).

The prenylated Cys of CaaX motif undergoes methylation after the cleavage of the aaX tripeptide (Grillo and Colombatto, 2005). Methylation of prenylated Cys increases the hydrophobicity of the prenyl membrane anchor, mediating its membrane association. Evidence showed that methylation plays a very important role in localizing prenylated proteins to the membrane (Michaelson et al., 2005). Prenylcysteine methylation also enhances protein-protein interactions such as interactions between lamin B and the nuclear envelope associated proteins, as well as K-Ras association with microtubules, and Rho GTPases binding to RhoGDI (Chen et al., 2000; Maske et al., 2003; Cushman and Casey, 2009). Cys methylation is catalyzed by isoprenylcysteine carboxyl methyltransferase (ICMT), an ER membrane-associated methyltransferase. The first crystal structure of a eukaryotic ICMT was solved in 2018, using ICMT from beetle *Tribolium castaneum* (Diver et al., 2018). X-ray structure shows that ICMT contains eight transmembrane  $\alpha$ -helices (M1-M8), and that almost the entire structure resides within the ER membrane. The active site is located mostly within the cytosolic leaflet of the membrane, and is contained between the M4 region and the C terminus (Diver et al., 2018). Two arginine residues Arg173 (on M6) and Arg246 (on M8) coordinate and position the carboxylate of the prenylcysteine substrate for catalysis, and also provide specificity for the carboxylate. Defects of methylation on prenylated cysteines affect a variety of biological processes; ICMT catalyzes methylation on terminal isoprenylcysteine of lamin A to ensure its incorporation into the nuclear envelope (Casasola et al., 2016). Inhibition of the ICMT activity results in unmethylated Ras and B-Raf, a signaling component downstream of Ras, which disrupts the transformation of cells (Bergo et al., 2004). Disruption of the methylation of Rho proteins severely impairs both random and directed cell migration (Cushman and Casey, 2011). A recent study showed that deficiency of isoprenylcysteine ICMT leads to progressive loss of photoreceptor function in mice (Christiansen et al., 2016).

## Tyrosination

Tyrosination, addition of Tyr to a protein, has been identified exclusively on tubulin, the main structural constituent of the microtubules. The microtubule lattice is formed by evolutionarily

conserved  $\alpha$ - and  $\beta$ -tubulin dimers, which can be modified by a broad range of functional groups. Enzymatic detyrosination and subsequent tyrosination of tubulin is a cyclic process that plays very important roles in modulating microtubule functions in mitosis, neuronal differentiation, and cardiomyocyte contraction (Aillaud et al., 2017; Nieuwenhuis and Brummelkamp, 2019) and likely affects other microtubule functions. This cyclic event happens solely on  $\alpha$ -tubulin. Most of the  $\alpha$ -tubulin isoforms encode a C-terminal tyrosine, except for TUBA8 that ends with phenylalanine, and TUBA4A that contains a terminus resembling deetyrosinated  $\alpha$ -tubulin (Gadadhar et al., 2017).

The deetyrosination/tyrosination cycle of tubulin was discovered more than 40 years ago, following an observation that rat brain homogenate has the capacity to incorporate tyrosine into  $\alpha$ -tubulin in a translation-independent manner (Arce et al., 1975). The enzyme responsible for this  $\alpha$ -tubulin-specific incorporation was shortly thereafter purified and designated tubulin tyrosine ligase (TTL). While the first TTL was discovered in 1970s (Arce et al., 1975), the enzyme responsible for deetyrosination was not identified until 2017, when two groups independently found that vasohibins/small vasohibin binding protein complex (VASHs/SVBP) possess the ability to remove tyrosine at the C-terminus (Arce et al., 1975; Aillaud et al., 2017; Nieuwenhuis and Brummelkamp, 2019). Biochemical studies revealed that TTL exclusively modifies unpolymerized tubulin, however, VASHs/SVBP preferentially catalyze the deetyrosination step on microtubules.

TTL includes three structurally distinct domains: N-terminal (residues 1–71), central (residues 72–188) and C-terminal (residues 189–377); the enzyme's active site is located in the C-terminal domain (Szyk et al., 2011). TTL binds to the heterodimer interface of tubulin and interacts with the major part of  $\alpha$ -tubulin, recognizing the conformation specific to non-polymerized tubulin and absent from the microtubules (Szyk et al., 2011; Protá et al., 2013). VASHs recognize  $\alpha$ -tubulin tail through its transglutaminase-like cysteine protease domain, which contains helical N- and C-lobes with the active site located at the interface between these two lobes. VASHs form complexes with SVBP, which stabilizes the active site of VASH (Li et al., 2019). Its specificity toward C-terminal tyrosine is determined by a serine residue (S221 in VASH1 and S210 in VASH2) and an adjacent arginine (R222 in VASH1 and R211 in VASH2), however, the preference of VASH1 and VASH2 toward microtubules is yet to be determined (Li et al., 2019). It is possible that this enzyme also acts on other Tyr-containing protein substrates.

The deetyrosination/tyrosination cycle affects the binding of microtubule-associated proteins (MAPs) and the microtubule motors, kinesins, modulating their processivity (Nieuwenhuis and Brummelkamp, 2019). Through these effects, enzymes involved in deetyrosination/tyrosination mediate microtubule-dependent biological processes *in vivo*. Mice lacking TTL die perinatally, with poorly developed neuronal networks, even though microtubule distribution is not grossly affected in TTL-deficient cells (Erck et al., 2005). In mice hemizygous for TTL (TTL<sup>±</sup>), reduced TTL expression, leads to a significant change in the deetyrosinated/tyrosinated tubulin ratio, resulting

in deficiencies in synaptic plasticity and memory; moreover, a reduced TTL level is characteristic for Alzheimer's Disease (Peris et al., 2021). Defects in tubulin deetyrosination cause structural brain abnormalities and cognitive impairments in mice, and these effects are recapitulated in human patients with familial mutations in deetyrosination enzymes (Pagnamenta et al., 2019). Tubulin tyrosination-deetyrosination cycle is required for stabilizing of kinesin-mediated microtubule-kinetochore attachment to promote mitotic error corrections (Ferreira et al., 2020). Inhibition of tubulin deetyrosination by using parthenolide disrupts microtubule anchoring at the Z disks of the sarcomeres, leading to reduced stiffness of the cardiomyocytes (Robison et al., 2016). It has been found that Phe can incorporate into the tubulin C-terminus in place of Tyr that can also serve as a site for dopamine binding (Ditamo et al., 2016; Dentesano et al., 2018). Blocking the tubulin C-terminus to prevent these modifications interferes with the microtubule-dependent transport in neurons (Zorgniotti et al., 2021).

## C-Degrans

Protein termini can determine metabolic stability of proteins and mediate protein degradation (Varshavsky, 2019). The terminal degradation signals are called degrons. N-degrons, created by proteolytic cleavage or enzymatic modifications of the N-termini to facilitate these proteins' turnover, have been known for a long time [e.g., (Hwang et al., 2010; Piatkov et al., 2014) for an overview]. Recently, it was discovered that stereo-chemically unique C-terminal polypeptides can serve as degradation signals, prompting the term "C-degron" (Lin et al., 2015, 2018). Such C-degrons are grouped into three different groups, including full length proteins, C-termini generated by cleavage, and prematurely terminated products (Lin et al., 2018; Varshavsky, 2019). A detailed characterization of C-degrons and related functional pathways are yet to be determined (Yeh et al., 2021). It appears likely that other intracellular mechanisms could contribute to this pathway. For example, as the N-terminal arginylation can occasionally act as an N-degron; similarly, C-terminal modifications could be potential contributors to the C-degron pathway.

## CONCLUSION

With the development and application of mass spectrometry technology, more and more new post-translational protein modifications are being identified and emerge as previously unknown regulatory mechanisms. Modifications at both N- and C-termini of proteins make an important contribution to proteomic diversity and complexity in post-translational modifications. N- and C-terminomes play a vital role in global biological pathways including protein regulation, cytoskeleton function, cellular signaling, embryogenesis, and cell viability.

Often, modifications of the protein termini have different effects on their *in vivo* targets. For example, N-terminal arginylation affects not only the half-life of proteins through the ubiquitin mediated degradation but also the  $\beta$ -actin cytoskeleton which influences the cell motility (Karakozova et al., 2006;

Sriram et al., 2011). C-terminal lipidation influences protein membrane localization and protein-protein interactions, and its dysfunction can lead to various diseases, such as cancer, cardiovascular diseases, neurodegeneration, and metabolic disorders (Xu et al., 2015). Collectively, investigation of the terminal post-translational modifications broadens our knowledge on protein terminome. Dysfunction and dysregulation of terminal modification enzymes lead to human diseases including cancer and neurodegenerative disorders, attracting great attention and efforts to this field.

Since terminal modifications often target the same reactive groups on different proteins, they likely exist *in vivo* in a complex interplay, in which choices between different modification can drive the metabolic fate and functions of specific proteins. Such interplay further adds to the post-translationally generated complexity of the proteome, and is virtually unexplored. We are aware of only a few examples of such interplay—e.g., actin, which is normally ~98% N-terminally acetylated, has been discovered to also undergo arginylation at nearly the same site (Karakozova et al., 2006). Structural predictions suggest that arginylation and acetylation at the actin's N-terminus are mutually exclusive (Rebowski et al., 2020). Indeed, direct and indirect evidence suggest that these two modifications exist in a potentially

functional interplay. While abolishment of arginylation reduces cell motility and actin polymerization (Saha et al., 2010), knockout of actin acetyltransferase NAA80 facilitates these events (Drazic et al., 2018), as well as dramatically increasing the arginylated actin level (Chen and Kashina, 2019), indicating a potentially antagonistic relationship between N-arginylation and N-acetylation. Beyond a doubt, other terminal modifications of proteins also exhibit structural and functional interplay. Uncovering these mechanisms constitutes an exciting direction of future studies.

## AUTHOR CONTRIBUTIONS

LC and AK wrote the manuscript and prepared the figures. Both authors contributed to the article and approved the submitted version.

## FUNDING

This work was supported by NIH R35GM122505 and R01NS102435 to AK.

## REFERENCES

- Aillaud, C., Bosc, C., Peris, L., Bosson, A., Heemeryck, P., Van Dijk, J., et al. (2017). Vasohibins/SVBP are tubulin carboxypeptidases (T) that regulate neuron differentiation. *Science* 358, 1448–1453. doi: 10.1126/science.aao4165
- Aksnes, H., Van Damme, P., Goris, M., Starheim, K. K., Marie, M., Støve, S. I., et al. (2015). An organellar  $\alpha$ -acetyltransferase, naa60, acetylates cytosolic N termini of transmembrane proteins and maintains Golgi integrity. *Cell Rep.* 10, 1362–1374. doi: 10.1016/j.celrep.2015.01.053
- Alfieri, J. A., Martin, A. D., Takeda, J., Kondoh, G., Myles, D. G., and Primakoff, P. (2003). Infertility in female mice with an oocyte-specific knockout of GPI-anchored proteins. *J. Cell Sci.* 116, 2149–2155. doi: 10.1242/jcs.00430
- Arce, C. A., Rodriguez, J. A., Barra, H. S., and Caputo, R. (1975). Incorporation of L-tyrosine, L-phenylalanine and L-3,4-dihydroxyphenylalanine as single units into rat brain tubulin. *Eur. J. Biochem.* 59, 145–149. doi: 10.1111/j.1432-1033.1975.tb02435.x
- Arfin, S. M., Kendall, R. L., Hall, L., Weaver, L. H., Stewart, A. E., Matthews, B. W., et al. (1995). Eukaryotic methionyl aminopeptidases: two classes of cobalt-dependent enzymes. *Proc. Natl. Acad. Sci. U.S.A.* 92, 7714–7718. doi: 10.1073/pnas.92.17.7714
- Arnesen, T., Van Damme, P., Plevoda, B., Helsens, K., Evjenth, R., Colaert, N., et al. (2009). Proteomics analyses reveal the evolutionary conservation and divergence of N-terminal acetyltransferases from yeast and humans. *Proc. Natl. Acad. Sci. U.S.A.* 106, 8157–8162. doi: 10.1073/pnas.0901931106
- Auf dem Keller, U., Prudova, A., Eckhard, U., Fingleton, B., and Overall, C. M. (2013). Systems-level analysis of proteolytic events in increased vascular permeability and complement activation in skin inflammation. *Sci. Signal.* 6:rs2. doi: 10.1126/scisignal.2003512
- Bachmair, A., Finley, D., and Varshavsky, A. (1986). *In vivo* half-life of a protein is a function of its amino-terminal residue. *Science* 234, 179–186. doi: 10.1126/science.3018930
- Baekkeskov, S., and Kanaani, J. (2009). Palmitoylation cycles and regulation of protein function (Review). *Mol. Membr. Biol.* 26, 42–54. doi: 10.1080/09687680802680108
- Balzi, E., Choder, M., Chen, W., Varshavsky, A., and Goffeau, A. (1990). Cloning and functional analysis of the arginyl-tRNA-protein transferase gene ATE1 of *Saccharomyces cerevisiae*. *J. Biol. Chem.* 265, 7464–7471. doi: 10.1016/s0021-9258(19)39136-7
- Barbier, P., Zejneli, O., Martinho, M., Lasorsa, A., Belle, V., Smet-Nocca, C., et al. (2019). Role of tau as a microtubule-associated protein: structural and functional aspects. *Front. Aging Neurosci.* 11:204. doi: 10.3389/fnagi.2019.00204
- Bellai-Dussault, K., Nguyen, T. T. M., Baratang, N. V., Jimenez-Cruz, D. A., and Campeau, P. M. (2019). Clinical variability in inherited glycosylphosphatidylinositol deficiency disorders. *Clin. Genet.* 95, 112–121. doi: 10.1111/cge.13425
- Ben-Bassat, A., Bauer, K., Chang, S. Y., Myambo, K., Boosman, A., and Chang, S. (1987). Processing of the initiation methionine from proteins: properties of the *Escherichia coli* methionine aminopeptidase and its gene structure. *J. Bacteriol.* 169, 751–757. doi: 10.1128/jb.169.2.751-757.1987
- Ben-Saadon, R., Fajerman, I., Ziv, T., Hellman, U., Schwartz, A. L., and Ciechanover, A. (2004). The tumor suppressor protein p16INK4a and the human papillomavirus oncoprotein-58 E7 are naturally occurring lysine-less proteins that are degraded by the ubiquitin system: direct evidence for ubiquitination at the N-terminal residue. *J. Biol. Chem.* 279, 41414–41421. doi: 10.1074/jbc.m407201200
- Bergo, M. O., Gavino, B. J., Hong, C., Beigneux, A. P., McMahon, M., Casey, P. J., et al. (2004). Inactivation of Icm1 inhibits transformation by oncogenic K-Ras and B-Raf. *J. Clin. Invest.* 113, 539–550. doi: 10.1172/jci200418829
- Boissel, J. P., Kasper, T. J., Shah, S. C., Malone, J. I., and Bunn, H. F. (1985). Amino-terminal processing of proteins: hemoglobin South Florida, a variant with retention of initiator methionine and N alpha-acetylation. *Proc. Natl. Acad. Sci. U.S.A.* 82, 8448–8452. doi: 10.1073/pnas.82.24.8448
- Bonsignore, L. A., Butler, J. S., Klinge, C. M., and Tooley, C. E. S. (2015a). Loss of the N-terminal methyltransferase NRMT1 increases sensitivity to DNA damage and promotes mammary oncogenesis. *Oncotarget* 6, 12248–12263. doi: 10.18632/oncotarget.3653
- Bonsignore, L. A., Tooley, J. G., Van, P., Hoose, M., Wang, E., Cheng, A., et al. (2015b). NRMT1 knockout mice exhibit phenotypes associated with impaired DNA repair and premature aging. *Mech. Ageing Dev.* 146, 42–52. doi: 10.1016/j.mad.2015.03.012
- Boyartchuk, V. L., Ashby, M. N., and Rine, J. (1997). Modulation of Ras and a-factor function by carboxyl-terminal proteolysis. *Science* 275, 1796–1800. doi: 10.1126/science.275.5307.1796
- Breitschopf, K., Bengal, E., Ziv, T., Admon, A., and Ciechanover, A. (1998). A novel site for ubiquitination: the N-terminal residue, and not internal lysines



- of MyoD, is essential for conjugation and degradation of the protein. *EMBO J.* 17, 5964–5973. doi: 10.1093/emboj/17.20.5964
- Brower, C. S., Rosen, C. E., Jones, R. H., Wadas, B. C., Piatkov, K. I., and Varshavsky, A. (2014). Liat1, an arginyltransferase-binding protein whose evolution among primates involved changes in the numbers of its 10-residue repeats. *Proc. Natl. Acad. Sci. U.S.A.* 111, E4936–E4945.
- Carpio, M. A., Lopez Sambrooks, C., Durand, E. S., and Hallak, M. E. (2010). The arginylation-dependent association of calreticulin with stress granules is regulated by calcium. *Biochem. J.* 429, 63–72. doi: 10.1042/bj20091953
- Casasola, A., Scalzo, D., Nandakumar, V., Halow, J., Recillas-Targa, F., Groudine, M., et al. (2016). Prelamin A processing, accumulation and distribution in normal cells and laminopathy disorders. *Nucleus* 7, 84–102. doi: 10.1080/19491034.2016.1150397
- Cha-Molstad, H., Sung, K. S., Hwang, J., Kim, K. A., Yu, J. E., Yoo, Y. D., et al. (2015). Amino-terminal arginylation targets endoplasmic reticulum chaperone BiP for autophagy through p62 binding. *Nat. Cell Biol.* 17, 917–929. doi: 10.1038/ncb3177
- Cha-Molstad, H., Yu, J. E., Feng, Z., Lee, S. H., Kim, J. G., Yang, P., et al. (2017). p62/SQSTM1/Sequestosome-1 is an N-recognin of the N-end rule pathway which modulates autophagosome biogenesis. *Nat. Commun.* 8:102.
- Chen, J.-Y., Liu, L., Cao, C.-L., Li, M.-J., Tan, K., Yang, X., et al. (2016). Structure and function of human Naa60 (NatF), a Golgi-localized bi-functional acetyltransferase. *Sci. Rep.* 6:31425.
- Chen, L., and Kashina, A. (2019). Quantification of intracellular N-terminal  $\beta$ -actin arginylation. *Sci. Rep.* 9:16669.
- Chen, T., Muratore, T. L., Schaner-Tooley, C. E., Shabanowitz, J., Hunt, D. F., and Macara, I. G. (2007). N-terminal  $\alpha$ -methylation of RCC1 is necessary for stable chromatin association and normal mitosis. *Nat. Cell Biol.* 9, 596–603. doi: 10.1038/ncb1572
- Chen, Z., Otto, J. C., Bergo, M. O., Young, S. G., and Casey, P. J. (2000). The C-terminal polylysine region and methylation of K-Ras are critical for the interaction between K-Ras and microtubules. *J. Biol. Chem.* 275, 41251–41257. doi: 10.1074/jbc.m006687200
- Christiansen, J. R., Pendse, N. D., Kolandaivelu, S., Bergo, M. O., Young, S. G., and Ramamurthy, V. (2016). Deficiency of isoprenylcysteine carboxyl methyltransferase (ICMT) leads to progressive loss of photoreceptor function. *J. Neurosci.* 36, 5107–5114. doi: 10.1523/jneurosci.0176-16.2016
- Chufán, E. E., De, M., Eipper, B. A., Mains, R. E., and Amzel, L. M. (2009). Amidation of bioactive peptides: the structure of the lyase domain of the amidating enzyme. *Structure* 17, 965–973. doi: 10.1016/j.str.2009.05.008
- Comba, A., Bonnet, L. V., Goitea, V. E., Hallak, M. E., and Galiano, M. R. (2019). Arginylated calreticulin increases apoptotic response induced by Bortezomib in Glioma Cells. *Mol. Neurobiol.* 56, 1653–1664. doi: 10.1007/s12035-018-1182-x
- Cui, W., Niu, S., Zheng, L., Hu, L., Huang, T., Gu, L., et al. (2013). Prediction of protein amidation sites by feature selection and analysis. *Mol. Genet. Genomics* 288, 391–400. doi: 10.1007/s00438-013-0760-x
- Cushman, I., and Casey, P. J. (2009). Role of isoprenylcysteine carboxylmethyltransferase-catalyzed methylation in Rho function and migration. *J. Biol. Chem.* 284, 27964–27973. doi: 10.1074/jbc.m109.025296
- Cushman, I., and Casey, P. J. (2011). RHO methylation matters: a role for isoprenylcysteine carboxylmethyltransferase in cell migration and adhesion. *Cell Adh. Migr.* 5, 11–15. doi: 10.4161/cam.5.1.13196
- Czyzyk, T. A., Ning, Y., Hsu, M.-S., Peng, B., Mains, R. E., Eipper, B. A., et al. (2005). Deletion of peptide amidation enzymatic activity leads to edema and embryonic lethality in the mouse. *Dev. Biol.* 287, 301–313. doi: 10.1016/j.ydbio.2005.09.001
- Dai, Q., Choy, E., Chiu, V., Romano, J., Slivka, S. R., Steitz, S. A., et al. (1998). Mammalian prenylcysteine carboxyl methyltransferase is in the endoplasmic reticulum. *J. Biol. Chem.* 273, 15030–15034. doi: 10.1074/jbc.273.24.15030
- Dai, X., Rulten, S. L., You, C., Caldecott, K. W., and Wang, Y. (2015). Identification and functional characterizations of N-terminal  $\alpha$ -N-methylation and phosphorylation of serine 461 in human poly (ADP-ribose) polymerase 3. *J. Proteome Res.* 14, 2575–2582. doi: 10.1021/acs.jproteome.5b00126
- Dentesano, Y. M., Ditamo, Y., Hansen, C., Arce, C. A., and Bisig, C. G. (2018). Post-translational incorporation of 3,4-dihydroxyphenylalanine into the C terminus of alpha-tubulin in living cells. *FEBS J.* 285, 1064–1078. doi: 10.1111/febs.14386
- Ditamo, Y., Dentesano, Y. M., Purro, S. A., Arce, C. A., and Bisig, C. G. (2016). Post-translational incorporation of L-phenylalanine into the C-terminus of alpha-tubulin as a possible cause of neuronal dysfunction. *Sci. Rep.* 6:38140.
- Diver, M. M., Pedi, L., Koide, A., Koide, S., and Long, S. B. (2018). Atomic structure of the eukaryotic intramembrane RAS methyltransferase ICMT. *Nature* 553, 526–529. doi: 10.1038/nature25439
- Domitrovic, T., Fausto, A. K., Silva, T. F., Romanel, E., and Vaslin, M. F. S. (2017). Plant arginyltransferases (ATEs). *Genet. Mol. Biol.* 40, 253–260. doi: 10.1590/1678-4685-gmb-2016-0084
- Dong, C., Mao, Y., Tempel, W., Qin, S., Li, L., Loppnau, P., et al. (2015). Structural basis for substrate recognition by the human N-terminal methyltransferase 1. *Genes Dev.* 29, 2343–2348. doi: 10.1101/gad.270611.115
- Drazic, A., Aksnes, H., Marie, M., Boczkowska, M., Varland, S., Timmerman, E., et al. (2018). NAA80 is actin's N-terminal acetyltransferase and regulates cytoskeleton assembly and cell motility. *Proc. Natl. Acad. Sci. U.S.A.* 115, 4399–4404. doi: 10.1073/pnas.1718336115
- Eldeeb, M., and Fahlman, R. (2016). The N-end rule: the beginning determines the end. *Protein Pept. Lett.* 23, 343–348. doi: 10.2174/0929866523666160108115809
- Eldeeb, M. A., Fahlman, R. P., Ragheb, M. A., and Esmaili, M. (2019). Does N-terminal protein acetylation lead to protein degradation? *Bioessays* 41:e1800167.
- Epstein, W., Lever, D., Leining, L., Bruenger, E., and Rilling, H. (1991). Quantitation of prenylcysteines by a selective cleavage reaction. *Proc. Natl. Acad. Sci. U.S.A.* 88, 9668–9670. doi: 10.1073/pnas.88.21.9668
- Erck, C., Peris, L., Andrieux, A., Meissirel, C., Gruber, A. D., Vernet, M., et al. (2005). A vital role of tubulin-tyrosine-ligase for neuronal organization. *Proc. Natl. Acad. Sci. U.S.A.* 102, 7853–7858. doi: 10.1073/pnas.0409626102
- Ferreira, L. T., Orr, B., Rajendraprasad, G., Pereira, A. J., Lemos, C., Lima, J. T., et al. (2020). alpha-Tubulin dephosphorylation impairs mitotic error correction by suppressing MCAK centromeric activity. *J. Cell Biol.* 219:e201910064.
- Flinta, C., Persson, B., Jornvall, H., and von Heijne, G. (1986). Sequence determinants of cytosolic N-terminal protein processing. *Eur. J. Biochem.* 154, 193–196. doi: 10.1111/j.1432-1033.1986.tb09378.x
- Gadadhar, S., Bodakuntla, S., Natarajan, K., and Janke, C. (2017). The tubulin code at a glance. *J. Cell Sci.* 130, 1347–1353.
- Gevaert, K., Goethals, M., Martens, L., Van Damme, J., Staes, A., Thomas, G. R., et al. (2003). Exploring proteomes and analyzing protein processing by mass spectrometric identification of sorted N-terminal peptides. *Nat. Biotechnol.* 21, 566–569. doi: 10.1038/nbt810
- Gibbs, D. J., Bailey, M., Tedds, H. M., and Holdsworth, M. J. (2016). From start to finish: amino-terminal protein modifications as degradation signals in plants. *New Phytol.* 211, 1188–1194. doi: 10.1111/nph.14105
- Gibbs, D. J., Lee, S. C., Isa, N. M., Gramuglia, S., Fukao, T., Bassel, G. W., et al. (2011). Homeostatic response to hypoxia is regulated by the N-end rule pathway in plants. *Nature* 479, 415–418. doi: 10.1038/nature10534
- Giles, A. C., and Grill, B. (2020). Roles of the HUWE1 ubiquitin ligase in nervous system development, function and disease. *Neural Dev.* 15, 1–18.
- Glover, C. J., Hartman, K. D., and Felsted, R. L. (1997). Human N-myristoyltransferase amino-terminal domain involved in targeting the enzyme to the ribosomal subcellular fraction. *J. Biol. Chem.* 272, 28680–28689. doi: 10.1074/jbc.272.45.28680
- Goitea, V. E., and Hallak, M. E. (2015). Calreticulin and arginylated calreticulin have different susceptibilities to proteasomal degradation. *J. Biol. Chem.* 290, 16403–16414. doi: 10.1074/jbc.m114.626127
- Gordon, J. I., Duronio, R., Rudnick, D., Adams, S., and Gokel, G. (1991). Protein N-myristoylation. *J. Biol. Chem.* 266, 8647–8650.
- Graciet, E., and Wellmer, F. (2010). The plant N-end rule pathway: structure and functions. *Trends Plant Sci.* 15, 447–453. doi: 10.1016/j.tplants.2010.04.011
- Grillo, M., and Colombatto, S. (2005). S-adenosylmethionine and protein methylation. *Amino Acids* 28, 357–362. doi: 10.1007/s00726-005-0197-6
- Homans, S. W., Ferguson, M. A., Dwek, R. A., Rademacher, T. W., Anand, R., and Williams, A. F. (1988). Complete structure of the glycosyl phosphatidylinositol membrane anchor of rat brain Thy-1 glycoprotein. *Nature* 333, 269–272. doi: 10.1038/333269a0
- House, I. G., House, C. M., Brennan, A. J., Gilan, O., Dawson, M. A., Whisstock, J. C., et al. (2017). Regulation of perforin activation and pre-synaptic toxicity through C-terminal glycosylation. *EMBO Rep.* 18, 1775–1785. doi: 10.15252/embr.201744351
- Hu, R. G., Brower, C. S., Wang, H., Davydov, I. V., Sheng, J., Zhou, J., et al. (2006). Arginyltransferase, its specificity, putative substrates, bidirectional promoter,



- and splicing-derived isoforms. *J. Biol. Chem.* 281, 32559–32573. doi: 10.1074/jbc.m604355200
- Hu, R. G., Wang, H., Xia, Z., and Varshavsky, A. (2008). The N-end rule pathway is a sensor of heme. *Proc. Natl. Acad. Sci. U.S.A.* 105, 76–81. doi: 10.1073/pnas.0710568105
- Hwang, C.-S., Shemorry, A., and Varshavsky, A. (2010). N-terminal acetylation of cellular proteins creates specific degradation signals. *Science* 327, 973–977. doi: 10.1126/science.1183147
- Ji, C. H., Kim, H. Y., Heo, A. J., Lee, S. H., Lee, M. J., Kim, S. B., et al. (2019). The N-degron pathway mediates ER-phagy. *Mol. Cell* 75, 1058–1072.e9.
- Ji, C. H., and Kwon, Y. T. (2017). Crosstalk and interplay between the ubiquitin-proteasome system and autophagy. *Mol. Cells* 40, 441–449.
- Jiang, C., Moorthy, B. T., Patel, D. M., Kumar, A., Morgan, W. M., Alfonso, B., et al. (2020). Regulation of mitochondrial respiratory chain complex levels, organization, and function by arginyltransferase 1. *Front. Cell Dev. Biol.* 8:603688. doi: 10.3389/fcell.2020.603688
- Jiang, H., Zhang, X., Chen, X., Aramsangtienchai, P., Tong, Z., and Lin, H. (2018). Protein lipidation: occurrence, mechanisms, biological functions, and enabling technologies. *Chem. Rev.* 118, 919–988. doi: 10.1021/acs.chemrev.6b00750
- Jung, H.-J., Nobumori, C., Goulbourne, C. N., Tu, Y., Lee, J. M., Tatar, A., et al. (2013). Farnesylation of lamin B1 is important for retention of nuclear chromatin during neuronal migration. *Proc. Natl. Acad. Sci. U.S.A.* 110, E1923–E1932.
- Kaji, A., Kaji, H., and Novelli, G. D. (1963a). A soluble amino acid incorporating system. *Biochem. Biophys. Res. Commun.* 10, 406–409. doi: 10.1016/0006-291x(63)90546-1
- Kaji, H., Novelli, G. D., and Kaji, A. (1963b). A soluble amino acid-incorporating system from rat liver. *Biochim. Biophys. Acta* 76, 474–477. doi: 10.1016/0926-6550(63)90070-7
- Karakozova, M., Kozak, M., Wong, C. C., Bailey, A. O., Yates, J. R. III, Mogilner, A., et al. (2006). Arginylation of beta-actin regulates actin cytoskeleton and cell motility. *Science* 313, 192–196. doi: 10.1126/science.1129344
- Kashina, A. S. (2015). Protein arginylation: over 50 years of discovery. *Methods Mol Biol.* 1337, 1–11. doi: 10.1007/978-1-4939-2935-1\_1
- Kim, K.-H., and Seong, B. L. (2001). Peptide amidation: production of peptide hormones *in vivo* and *in vitro*. *Biotechnol. Bioprocess Eng.* 6, 244–251. doi: 10.1007/bf02931985
- Kinoshita, T. (2016). Glycosylphosphatidylinositol (GPI) anchors: biochemistry and cell biology: introduction to a thematic review series. *J. Lipid Res.* 57, 4–5. doi: 10.1194/jlr.e065417
- Kinoshita, T. (2020). Biosynthesis and biology of mammalian GPI-anchored proteins. *Open Biol.* 10:190290. doi: 10.1098/rsob.190290
- Kleuss, C., and Krause, E. (2003). Galpha(s) is palmitoylated at the N-terminal glycine. *EMBO J.* 22, 826–832. doi: 10.1093/emboj/cdg095
- Knaus, A., Pantel, J. T., Pendziwiat, M., Hajjir, N., Zhao, M., Hsieh, T.-C., et al. (2018). Characterization of glycosylphosphatidylinositol biosynthesis defects by clinical features, flow cytometry, and automated image analysis. *Genome Med.* 10, 1–13.
- Kolhekar, A. S., Roberts, M. S., Jiang, N., Johnson, R. C., Mains, R. E., Eipper, B. A., et al. (1997). Neuropeptide amidation in *Drosophila*: separate genes encode the two enzymes catalyzing amidation. *J. Neurosci.* 17, 1363–1376. doi: 10.1523/jneurosci.17-04-01363.1997
- Kwon, Y. T., and Ciechanover, A. (2017). The ubiquitin code in the ubiquitin-proteasome system and autophagy. *Trends Biochem. Sci.* 42, 873–886. doi: 10.1016/j.tibs.2017.09.002
- Lange, P. F., Huesgen, P. F., Nguyen, K., and Overall, C. M. (2014). Annotating N termini for the human proteome project: N termini and N $\alpha$ -acetylation status differentiate stable cleaved protein species from degradation remnants in the human erythrocyte proteome. *J. Proteome Res.* 13, 2028–2044. doi: 10.1021/pr401191w
- Lee, J., and Stock, J. (1993). Protein phosphatase 2A catalytic subunit is methyl-esterified at its carboxyl terminus by a novel methyltransferase. *J. Biol. Chem.* 268, 19192–19195. doi: 10.1016/s0021-9258(19)36497-x
- Lee, M. J., Tasaki, T., Moroi, K., An, J. Y., Kimura, S., Davydov, I. V., et al. (2005). RGS4 and RGS5 are *in vivo* substrates of the N-end rule pathway. *Proc. Natl. Acad. Sci. U.S.A.* 102, 15030–15035. doi: 10.1073/pnas.0507533102
- Li, F., Hu, Y., Qi, S., Luo, X., and Yu, H. (2019). Structural basis of tubulin deetyrosination by vasohibins. *Nat. Struct. Mol. Biol.* 26, 583–591. doi: 10.1038/s41594-019-0242-x
- Li, X., and Chang, Y. H. (1995). Amino-terminal protein processing in *Saccharomyces cerevisiae* is an essential function that requires two distinct methionine aminopeptidases. *Proc. Natl. Acad. Sci. U.S.A.* 92, 12357–12361. doi: 10.1073/pnas.92.26.12357
- Licausi, F., Kosmacz, M., Weits, D. A., Giuntoli, B., Giorgi, F. M., Voesenek, L. A., et al. (2011). Oxygen sensing in plants is mediated by an N-end rule pathway for protein destabilization. *Nature* 479, 419–422. doi: 10.1038/nature10536
- Lin, H.-C., Ho, S.-C., Chen, Y.-Y., Khoo, K.-H., Hsu, P.-H., and Yen, H.-C. S. (2015). CRL2 aids elimination of truncated selenoproteins produced by failed UGA/Sec decoding. *Science* 349, 91–95. doi: 10.1126/science.aa.b0515
- Lin, H.-C., Yeh, C.-W., Chen, Y.-F., Lee, T.-T., Hsieh, P.-Y., Rusnac, D. V., et al. (2018). C-terminal end-directed protein elimination by CRL2 ubiquitin ligases. *Mol. Cell* 70, 602–613.e3.
- Linder, M. E., Middleton, P., Hepler, J. R., Taussig, R., Gilman, A. G., and Mumby, S. M. (1993). Lipid modifications of G proteins: alpha subunits are palmitoylated. *Proc. Natl. Acad. Sci. U.S.A.* 90, 3675–3679. doi: 10.1073/pnas.90.8.3675
- Manning, L. R., and Manning, J. M. (2001). The acetylation state of human fetal hemoglobin modulates the strength of its subunit interactions: long-range effects and implications for histone interactions in the nucleosome. *Biochemistry* 40, 1635–1639. doi: 10.1021/bi002157%2B
- Marino, G., Eckhard, U., and Overall, C. M. (2015). Protein termini and their modifications revealed by positional proteomics. *ACS Chem. Biol.* 10, 1754–1764. doi: 10.1021/acschembio.5b00189
- Martin, D. D., Beauchamp, E., and Berthiaume, L. G. (2011). Post-translational myristoylation: fat matters in cellular life and death. *Biochimie* 93, 18–31. doi: 10.1016/j.biochi.2010.10.018
- Martin, D. D., Heit, R. J., Yap, M. C., Davidson, M. W., Hayden, M. R., and Berthiaume, L. G. (2014). Identification of a post-translationally myristoylated autophagy-inducing domain released by caspase cleavage of huntingtin. *Hum. Mol. Genet.* 23, 3166–3179. doi: 10.1093/hmg/ddu027
- Martin, D. J., and Rubenstein, P. A. (1987). Alternate pathways for removal of the class II actin initiator methionine. *J. Biol. Chem.* 262, 6350–6356. doi: 10.1016/s0021-9258(18)45577-9
- Maske, C. P., Hollinshead, M. S., Higbee, N. C., Bergo, M. O., Young, S. G., and Vaux, D. J. (2003). A carboxyl-terminal interaction of lamin B1 is dependent on the CAAX endoprotease Rce1 and carboxymethylation. *J. Cell Biol.* 162, 1223–1232. doi: 10.1083/jcb.200303113
- Mical, T. I., and Monteiro, M. J. (1998). The role of sequences unique to nuclear intermediate filaments in the targeting and assembly of human lamin B: evidence for lack of interaction of lamin B with its putative receptor. *J. Cell Sci.* 111, 3471–3485. doi: 10.1242/jcs.111.23.3471
- Michaelson, D., Ali, W., Chiu, V. K., Bergo, M., Silletti, J., Wright, L., et al. (2005). Postprenylation CAAX processing is required for proper localization of Ras but not Rho GTPases. *Mol. Biol. Cell* 16, 1606–1616. doi: 10.1091/mbc.e04-11-0960
- Murofushi, H. (1980). Purification and characterization of tubulin-tyrosine ligase from porcine brain. *J. Biochem.* 87, 979–984. doi: 10.1093/oxfordjournals.jbchem.a132828
- Nieuwenhuis, J., Adamopoulos, A., Bleijerveld, O. B., Mazouzi, A., Stickel, E., Celie, P., et al. (2017). Vasohibins encode tubulin deetyrosinating activity. *Science* 358, 1453–1456. doi: 10.1126/science.aao5676
- Nieuwenhuis, J., and Brummelkamp, T. R. (2019). The tubulin deetyrosination cycle: function and enzymes. *Trends Cell Biol.* 29, 80–92. doi: 10.1016/j.tcb.2018.08.003
- Ogris, E., Du, X., Nelson, K. C., Mak, E. K., Yu, X. X., Lane, W. S., et al. (1999). A protein phosphatase methyltransferase (PME-1) is one of several novel proteins stably associating with two inactive mutants of protein phosphatase 2A. *J. Biol. Chem.* 274, 14382–14391. doi: 10.1074/jbc.274.20.14382
- Pagnamenta, A. T., Heemeryck, P., Martin, H. C., Bosc, C., Peris, L., Uszynski, I., et al. (2019). Defective tubulin deetyrosination causes structural brain abnormalities with cognitive deficiency in humans and mice. *Hum. Mol. Genet.* 28, 3391–3405. doi: 10.1093/hmg/ddz186
- Park, H.-W., Boduluri, S. R., Moomaw, J. F., Casey, P. J., and Beese, L. S. (1997). Crystal structure of protein farnesyltransferase at 2.25 angstrom resolution. *Science* 275, 1800–1805. doi: 10.1126/science.275.5307.1800

- Pavlyk, I., Leu, N. A., Vedula, P., Kurosaka, S., and Kashina, A. (2018). Rapid and dynamic arginylation of the leading edge  $\beta$ -actin is required for cell migration. *Traffic* 19, 263–272. doi: 10.1111/tra.12551
- Pepinsky, R. B., Zeng, C., Wen, D., Rayhorn, P., Baker, D. P., Williams, K. P., et al. (1998). Identification of a palmitic acid-modified form of human Sonic hedgehog. *J. Biol. Chem.* 273, 14037–14045. doi: 10.1074/jbc.273.22.14037
- Peris, L., Qu, X., Soleilhac, J.-M., Parato, J., Lante, F., Kumar, A., et al. (2021). Impaired  $\alpha$ -tubulin re-tyrosination leads to synaptic dysfunction and is a feature of Alzheimer's disease. *bioRxiv* [Preprint]. doi: 10.1101/2021.05.17.443847
- Petkowski, J. J., Schaner Tooley, C. E., Anderson, L. C., Shumilin, I. A., Balsbaugh, J. L., Shabanowitz, J., et al. (2012). Substrate specificity of mammalian N-terminal  $\alpha$ -amino methyltransferase NRMT. *Biochemistry* 51, 5942–5950. doi: 10.1021/bi300278f
- Phukan, U. J., Jeena, G. S., Tripathi, V., and Shukla, R. K. (2017). Regulation of Apetala2/Ethylene response factors in plants. *Front. Plant Sci.* 8:150. doi: 10.3389/fpls.2017.00150
- Piatkov, K. I., Brower, C. S., and Varshavsky, A. (2012). The N-end rule pathway counteracts cell death by destroying proapoptotic protein fragments. *Proc. Natl. Acad. Sci. U.S.A.* 109, E1839–E1847.
- Piatkov, K. I., Oh, J.-H., Liu, Y., and Varshavsky, A. (2014). Calpain-generated natural protein fragments as short-lived substrates of the N-end rule pathway. *Proc. Natl. Acad. Sci. U.S.A.* 111, E817–E826.
- Podack, E. R., Young, J., and Cohn, Z. A. (1985). Isolation and biochemical and functional characterization of perforin 1 from cytolytic T-cell granules. *Proc. Natl. Acad. Sci. U.S.A.* 82, 8629–8633. doi: 10.1073/pnas.82.24.8629
- Polevoda, B., Norbeck, J., Takakura, H., Blomberg, A., and Sherman, F. (1999). Identification and specificities of N-terminal acetyltransferases from *Saccharomyces cerevisiae*. *EMBO J.* 18, 6155–6168. doi: 10.1093/emboj/18.21.6155
- Polevoda, B., and Sherman, F. (2000). Nalpha-terminal acetylation of eukaryotic proteins. *J. Biol. Chem.* 275, 36479–36482. doi: 10.1074/jbc.R000023200
- Polevoda, B., and Sherman, F. (2003). N-terminal acetyltransferases and sequence requirements for N-terminal acetylation of eukaryotic proteins. *J. Mol. Biol.* 325, 595–622. doi: 10.1016/S0022-2836(02)01269-X
- Prigge, S. T., Kolhekar, A. S., Eipper, B. A., Mains, R. E., and Amzel, L. M. (1997). Amidation of bioactive peptides: the structure of peptidylglycine  $\alpha$ -hydroxylating monooxygenase. *Science* 278, 1300–1305. doi: 10.1126/science.278.5341.1300
- Prota, A. E., Magiera, M. M., Kuijpers, M., Bargsten, K., Frey, D., Wieser, M., et al. (2013). Structural basis of tubulin tyrosination by tubulin tyrosine ligase. *J. Cell Biol.* 200, 259–270. doi: 10.1083/jcb.201211017
- Prudova, A., Serrano, K., Eckhard, U., Fortelny, N., Devine, D. V., and Overall, C. M. (2014). TAILS N-terminomics of human platelets reveals pervasive metalloproteinase-dependent proteolytic processing in storage. *Blood* 124, e49–e60.
- Rai, R., and Kashina, A. (2005). Identification of mammalian arginyltransferases that modify a specific subset of protein substrates. *Proc. Natl. Acad. Sci. U.S.A.* 102, 10123–10128. doi: 10.1073/pnas.0504500102
- Rai, R., Mushegian, A., Makarova, K., and Kashina, A. (2006). Molecular dissection of arginyltransferases guided by similarity to bacterial peptidoglycan synthases. *EMBO Rep.* 7, 800–805. doi: 10.1038/sj.embor.7400747
- Rao, H., Uhlmann, F., Nasmyth, K., and Varshavsky, A. (2001). Degradation of a cohesin subunit by the N-end rule pathway is essential for chromosome stability. *Nature* 410, 955–959. doi: 10.1038/35073627
- Rawlings, N. D. (2009). A large and accurate collection of peptidase cleavages in the MEROPS database. *Database* 2009:ba015.
- Rebowski, G., Boczkowska, M., Drazic, A., Ree, R., Goris, M., Arnesen, T., et al. (2020). Mechanism of actin N-terminal acetylation. *Sci. Adv.* 6:eay8793. doi: 10.1126/sciadv.aay8793
- Redman, K., and Rubenstein, P. A. (1981). NH<sub>2</sub>-terminal processing of *Dictyostelium discoideum* actin in vitro. *J. Biol. Chem.* 256, 13226–13229. doi: 10.1016/S0021-9258(18)43032-3
- Ree, R., Varland, S., and Arnesen, T. (2018). Spotlight on protein N-terminal acetylation. *Exp. Mol. Med.* 50, 1–13. doi: 10.1038/s12276-018-0116-z
- Reily, C., Stewart, T. J., Renfrow, M. B., and Novak, J. (2019). Glycosylation in health and disease. *Nat. Rev. Nephrol.* 15, 346–366.
- Resh, M. D. (2006). Palmitoylation of ligands, receptors, and intracellular signaling molecules. *Sci. STKE* 2006:re14. doi: 10.1126/stke.3592006re14
- Robison, P., Caporizzo, M. A., Ahmadzadeh, H., Bogush, A. I., Chen, C. Y., Margulies, K. B., et al. (2016). Detyrosinated microtubules buckle and bear load in contracting cardiomyocytes. *Science* 352:aaf0659. doi: 10.1126/science.aaf0659
- Rubenstein, P. A., and Martin, D. J. (1983). NH<sub>2</sub>-terminal processing of actin in mouse L-cells in vivo. *J. Biol. Chem.* 258, 3961–3966. doi: 10.1016/S0021-9258(18)32761-3
- Saha, S., Mundia, M. M., Zhang, F., Demers, R. W., Korobova, F., Svitkina, T., et al. (2010). Arginylation regulates intracellular actin polymer level by modulating actin properties and binding of capping and severing proteins. *Mol. Biol. Cell* 21, 1350–1361. doi: 10.1091/mbc.e09-09-0829
- Sathyan, K. M., Fachinetti, D., and Foltz, D. R. (2017).  $\alpha$ -amino trimethylation of CENP-A by NRMT is required for full recruitment of the centromere. *Nat. Commun.* 8:14678.
- Scaglione, K. M., Basrur, V., Ashraf, N. S., Konen, J. R., Elenitoba-Johnson, K. S., Todi, S. V., et al. (2013). The ubiquitin-conjugating enzyme (E2) Ube2w ubiquitinates the N terminus of substrates. *J. Biol. Chem.* 288, 18784–18788. doi: 10.1074/jbc.M113.477596
- Schroder, H. C., Wehland, J., and Weber, K. (1985). Purification of brain tubulin-tyrosine ligase by biochemical and immunological methods. *J. Cell Biol.* 100, 276–281. doi: 10.1083/jcb.100.1.276
- Sheff, D. R., and Rubenstein, P. (1992). Isolation and characterization of the rat liver actin N-acetylaminopeptidase. *J. Biol. Chem.* 267, 20217–20224. doi: 10.1016/S0021-9258(19)88689-1
- Shemorry, A., Hwang, C. S., and Varshavsky, A. (2013). Control of protein quality and stoichiometries by N-terminal acetylation and the N-end rule pathway. *Mol. Cell* 50, 540–551. doi: 10.1016/j.molcel.2013.03.018
- Shim, S. M., Choi, H. R., Sung, K. W., Lee, Y. J., Kim, S. T., Kim, D., et al. (2018). The endoplasmic reticulum-residing chaperone BiP is short-lived and metabolized through N-terminal arginylation. *Sci. Signal.* 11:eaan0630. doi: 10.1126/scisignal.aan0630
- Sinensky, M. (2011). “Insights into the Function of Prenylation from Nuclear Lamin Farnesylation,” in *The Enzymes*, Vol. 29, eds F. Tamanoi, C. A. Hrycyna, and M. O. Bergo (Amsterdam: Elsevier), 5–20. doi: 10.1016/B978-0-12-381339-8.00002-0
- Sontag, E., Hladik, C., Montgomery, L., Luangpirom, A., Mudrak, I., Ogris, E., et al. (2004). Downregulation of protein phosphatase 2A carboxyl methylation and methyltransferase may contribute to Alzheimer disease pathogenesis. *J. Neuropathol. Exp. Neurol.* 63, 1080–1091. doi: 10.1093/jnen/63.10.1080
- Sriram, S. M., Kim, B. Y., and Kwon, Y. T. (2011). The N-end rule pathway: emerging functions and molecular principles of substrate recognition. *Nat. Rev. Mol. Cell Biol.* 12, 735–747. doi: 10.1038/nrm3217
- Stanevich, V., Jiang, L., Satyshur, K. A., Li, Y., Jeffrey, P. D., Li, Z., et al. (2011). The structural basis for tight control of PP2A methylation and function by LCMT-1. *Mol. Cell* 41, 331–342. doi: 10.1016/j.molcel.2010.12.030
- Stinchcombe, J. C., Majorovits, E., Bossi, G., Fuller, S., and Griffiths, G. M. (2006). Centrosome polarization delivers secretory granules to the immunological synapse. *Nature* 443, 462–465. doi: 10.1038/nature05071
- Stock, A., Clarke, S., Clarke, C., and Stock, J. (1987). N-terminal methylation of proteins: structure, function and specificity. *FEBS Lett.* 220, 8–14. doi: 10.1016/0014-5793(87)80866-9
- Szyk, A., Deaconescu, A. M., Piszczek, G., and Roll-Mecak, A. (2011). Tubulin tyrosine ligase structure reveals adaptation of an ancient fold to bind and modify tubulin. *Nat. Struct. Mol. Biol.* 18, 1250–1258. doi: 10.1038/nsmb.2148
- Tasaki, T., and Kwon, Y. T. (2007). The mammalian N-end rule pathway: new insights into its components and physiological roles. *Trends Biochem. Sci.* 32, 520–528. doi: 10.1016/j.tibs.2007.08.010
- Tatham, M. H., Plechanovová, A., Jaffray, E. G., Salmen, H., and Hay, R. T. (2013). Ube2W conjugates ubiquitin to  $\alpha$ -amino groups of protein N-termini. *Biochem. J.* 453, 137–145. doi: 10.1042/bj20130244
- Taylor, J. S., Reid, T. S., Terry, K. L., Casey, P. J., and Beese, L. S. (2003). Structure of mammalian protein geranylgeranyltransferase type-I. *EMBO J.* 22, 5963–5974. doi: 10.1093/emboj/cdg571
- Thinon, E., Serwa, R. A., Broncel, M., Brannigan, J. A., Brassat, U., Wright, M. H., et al. (2014). Global profiling of co- and post-translationally N-myristoylated proteomes in human cells. *Nat. Commun.* 5:4919.

- Timms, R. T., and Koren, I. (2020). Tying up loose ends: the N-degron and C-degron pathways of protein degradation. *Biochem. Soc. Trans.* 48, 1557–1567. doi: 10.1042/bst20191094
- Timms, R. T., Zhang, Z., Rhee, D. Y., Harper, J. W., Koren, I., and Elledge, S. J. (2019). A glycine-specific N-degron pathway mediates the quality control of protein N-myristoylation. *Science* 365:eaaw4912. doi: 10.1126/science.aaw4912
- Tooley, C. E. S., Petkowski, J. J., Muratore-Schroeder, T. L., Balsbaugh, J. L., Shabanowitz, J., Sabat, M., et al. (2010). NRMT is an  $\alpha$ -N-methyltransferase that methylates RCC1 and retinoblastoma protein. *Nature* 466, 1125–1128. doi: 10.1038/nature09343
- Towbin, H., Bair, K. W., DeCaprio, J. A., Eck, M. J., Kim, S., Kinder, F. R., et al. (2003). Proteomics-based target identification: bengamides as a new class of methionine aminopeptidase inhibitors. *J. Biol. Chem.* 278, 52964–52971.
- Towler, D. A., Eubanks, S. R., Towery, D. S., Adams, S. P., and Glaser, L. (1987). Amino-terminal processing of proteins by N-myristoylation. Substrate specificity of N-myristoyl transferase. *J. Biol. Chem.* 262, 1030–1036.
- Tschantz, W. R., Digits, J. A., Pyun, H.-J., Coates, R. M., and Casey, P. J. (2001). Lysosomal prenylcysteine lyase is a FAD-dependent thioether oxidase. *J. Biol. Chem.* 276, 2321–2324. doi: 10.1074/jbc.c000616200
- Tschantz, W. R., Zhang, L., and Casey, P. J. (1999). Cloning, expression, and cellular localization of a human prenylcysteine lyase. *J. Biol. Chem.* 274, 35802–35808. doi: 10.1074/jbc.274.50.35802
- Tsunasawa, S., Stewart, J. W., and Sherman, F. (1985). Amino-terminal processing of mutant forms of yeast iso-1-cytochrome c. The specificities of methionine aminopeptidase and acetyltransferase. *J. Biol. Chem.* 260, 5382–5391. doi: 10.1016/s0021-9258(18)90333-0
- Udenwobele, D. I., Su, R.-C., Good, S. V., Ball, T. B., Varma Shrivastav, S., and Shrivastav, A. (2017). Myristoylation: an important protein modification in the immune response. *Front. Immunol.* 8:751. doi: 10.3389/fimmu.2017.00751
- Urbancikova, M., and Hitchcock-DeGregori, S. E. (1994). Requirement of amino-terminal modification for striated muscle alpha-tropomyosin function. *J. Biol. Chem.* 269, 24310–24315. doi: 10.1016/s0021-9258(19)51083-3
- Utsumi, T., Sakurai, N., Nakano, K., and Ishisaka, R. (2003). C-terminal 15 kDa fragment of cytoskeletal actin is posttranslationally N-myristoylated upon caspase-mediated cleavage and targeted to mitochondria. *FEBS Lett.* 539, 37–44. doi: 10.1016/s0014-5793(03)00180-7
- Van Damme, P., Evjenth, R., Foyn, H., Demeyer, K., De, P., Bock, J., et al. (2011a). Proteome-derived peptide libraries allow detailed analysis of the substrate specificities of N(alpha)-acetyltransferases and point to hNaa10p as the post-translational actin N(alpha)-acetyltransferase. *Mol. Cell. Proteomics* 10:M110004580.
- Van Damme, P., Hole, K., Pimenta-Marques, A., Helsens, K., Vandekerckhove, J., Martinho, R. G., et al. (2011b). NatF contributes to an evolutionary shift in protein N-terminal acetylation and is important for normal chromosome segregation. *PLoS Genet.* 7:e1002169. doi: 10.1371/journal.pgen.1002169
- Van Damme, P., Lasa, M., Polevoda, B., Gazquez, C., Elosegui-Artola, A., Kim, D. S., et al. (2012). N-terminal acetylome analyses and functional insights of the N-terminal acetyltransferase NatB. *Proc. Natl. Acad. Sci. U.S.A.* 109, 12449–12454. doi: 10.1073/pnas.1210303109
- Varki, A. (2017). Biological roles of glycans. *Glycobiology* 27, 3–49. doi: 10.1093/glycob/cww086
- Varland, S., Osberg, C., and Arnesen, T. (2015). N-terminal modifications of cellular proteins: the enzymes involved, their substrate specificities and biological effects. *Proteomics* 15, 2385–2401. doi: 10.1002/pmic.201400619
- Varshavsky, A. (2011). The N-end rule pathway and regulation by proteolysis. *Protein Sci.* 20, 1298–1345. doi: 10.1002/pro.666
- Varshavsky, A. (2019). N-degron and C-degron pathways of protein degradation. *Proc. Natl. Acad. Sci. U.S.A.* 116, 358–366. doi: 10.1073/pnas.1816596116
- Vilas, G. L., Corvi, M. M., Plummer, G. J., Seime, A. M., Lambkin, G. R., and Berthiaume, L. G. (2006). Posttranslational myristoylation of caspase-activated p21-activated protein kinase 2 (PAK2) potentiates late apoptotic events. *Proc. Natl. Acad. Sci. U.S.A.* 103, 6542–6547. doi: 10.1073/pnas.0600824103
- Wandzioch, E., Pusey, M., Werda, A., Bail, S., Bhaskar, A., Nestor, M., et al. (2014). PME-1 modulates protein phosphatase 2A activity to promote the malignant phenotype of endometrial cancer cells. *Cancer Res.* 74, 4295–4305. doi: 10.1158/0008-5473.can-13-3130
- Wang, B., Merillat, S. A., Vincent, M., Huber, A. K., Basrur, V., Mangelberger, D., et al. (2016). Loss of the ubiquitin-conjugating enzyme UBE2W results in susceptibility to early postnatal lethality and defects in skin, immune, and Male reproductive systems. *J. Biol. Chem.* 291, 3030–3042. doi: 10.1074/jbc.m115.676601
- Wang, J., Pejaver, V. R., Dann, G. P., Wolf, M. Y., Kellis, M., Huang, Y., et al. (2018). Target site specificity and *in vivo* complexity of the mammalian arginylome. *Sci. Rep.* 8:16177.
- Wang, J., Yates, J. R. III, and Kashina, A. (2019). Biochemical analysis of protein arginylation. *Methods Enzymol.* 626, 89–113. doi: 10.1016/bs.mie.2019.07.028
- Webb, K. J., Lipson, R. S., Al-Hadid, Q., Whitelegge, J. P., and Clarke, S. G. (2010). Identification of protein N-terminal methyltransferases in yeast and humans. *Biochemistry* 49, 5225–5235. doi: 10.1021/bi100428x
- Wingfield, P. T. (2017). N-terminal methionine processing. *Curr. Protoc. Protein Sci.* 88, 6.14.1–6.14.3.
- Winter, N., Novatchkova, M., and Bachmair, A. (2021). Cellular control of protein turnover via the modification of the amino terminus. *Int. J. Mol. Sci.* 22:3545. doi: 10.3390/ijms22073545
- Wong, C. C., Xu, T., Rai, R., Bailey, A. O., Yates, J. R. III, Wolf, Y. I., et al. (2007). Global analysis of posttranslational protein arginylation. *PLoS Biol.* 5:e258. doi: 10.1371/journal.pbio.0050258
- Xiao, Q., Zhang, F., Nacev, B. A., Liu, J. O., and Pei, D. (2010). Protein N-terminal processing: substrate specificity of *Escherichia coli* and human methionine aminopeptidases. *Biochemistry* 49, 5588–5599. doi: 10.1021/bi1005464
- Xie, H., and Clarke, S. (1994). Protein phosphatase 2A is reversibly modified by methyl esterification at its C-terminal leucine residue in bovine brain. *J. Biol. Chem.* 269, 1981–1984. doi: 10.1016/s0021-9258(17)42124-7
- Xu, N., Shen, N., Wang, X., Jiang, S., Xue, B., and Li, C. (2015). Protein prenylation and human diseases: a balance of protein farnesylation and geranylgeranylation. *Sci China Life Sci.* 58, 328–335. doi: 10.1007/s11427-015-4836-1
- Ye, Y., Klennerman, D., and Finley, D. (2020). N-terminal ubiquitination of amyloidogenic proteins triggers removal of their oligomers by the proteasome holoenzyme. *J. Mol. Biol.* 432, 585–596. doi: 10.1016/j.jmb.2019.08.021
- Yeh, C. W., Huang, W. C., Hsu, P. H., Yeh, K. H., Wang, L. C., Hsu, P. W. C., et al. (2021). The C-degron pathway eliminates mislocalized proteins and products of deubiquitinating enzymes. *EMBO J.* 40:e105846.
- Yoo, Y. D., Lee, D. H., Cha-Molstad, H., Kim, H., Mun, S. R., Ji, C., et al. (2017). Glioma-derived cancer stem cells are hypersensitive to proteasomal inhibition. *EMBO Rep.* 18, 150–168. doi: 10.15252/embr.201642360
- Yoo, Y. D., Mun, S. R., Ji, C. H., Sung, K. W., Kang, K. Y., Heo, A. J., et al. (2018). N-terminal arginylation generates a bimodal degron that modulates autophagic proteolysis. *Proc. Natl. Acad. Sci. U.S.A.* 115, E2716–E2724.
- Zha, J., Weiler, S., Oh, K. J., Wei, M. C., and Korsmeyer, S. J. (2000). Posttranslational N-myristoylation of BID as a molecular switch for targeting mitochondria and apoptosis. *Science* 290, 1761–1765. doi: 10.1126/science.290.5497.1761
- Zhang, F., Patel, D. M., Colavita, K., Rodionova, I., Buckley, B., Scott, D. A., et al. (2015). Arginylation regulates purine nucleotide biosynthesis by enhancing the activity of phosphoribosyl pyrophosphate synthase. *Nat. Commun.* 6:7517.
- Zorgnotti, A., Ditamo, Y., Arce, C. A., and Bisig, C. G. (2021). Irreversible incorporation of L-dopa into the C-terminus of alpha-tubulin inhibits binding of molecular motor KIF5B to microtubules and alters mitochondrial traffic along the axon. *Neurobiol. Dis.* 147:105164. doi: 10.1016/j.nbd.2020.105164

**Conflict of Interest:** The authors declare that the research was conducted in the absence of any commercial or financial relationships that could be construed as a potential conflict of interest.

**Publisher's Note:** All claims expressed in this article are solely those of the authors and do not necessarily represent those of their affiliated organizations, or those of the publisher, the editors and the reviewers. Any product that may be evaluated in this article, or claim that may be made by its manufacturer, is not guaranteed or endorsed by the publisher.

Copyright © 2021 Chen and Kashina. This is an open-access article distributed under the terms of the Creative Commons Attribution License (CC BY). The use, distribution or reproduction in other forums is permitted, provided the original author(s) and the copyright owner(s) are credited and that the original publication in this journal is cited, in accordance with accepted academic practice. No use, distribution or reproduction is permitted which does not comply with these terms.





# Sirtuin 5 is Dispensable for CD8<sup>+</sup> T Cell Effector and Memory Differentiation

Qianqian Duan<sup>1,2†</sup>, Jiying Ding<sup>1,2,3†</sup>, Fangfang Li<sup>1,2,4</sup>, Xiaowei Liu<sup>1,2</sup>, Yunan Zhao<sup>4</sup>, Hongxiu Yu<sup>5</sup>, Yong Liu<sup>6,7,8</sup> and Lianjun Zhang<sup>1,2,8\*</sup>

<sup>1</sup>Institute of Systems Medicine, Chinese Academy of Medical Sciences and Peking Union Medical College, Beijing, China, <sup>2</sup>Suzhou Institute of Systems Medicine, Suzhou, China, <sup>3</sup>School of Life Science and Technology, China Pharmaceutical University, Nanjing, China, <sup>4</sup>Institute of Biomedical Electromagnetic Engineering, Shenyang University of Technology, Shenyang, China, <sup>5</sup>Department of Systems Biology for Medicine, School of Basic Medical Sciences, Fudan University, Shanghai, China, <sup>6</sup>Cancer Institute, Xuzhou Medical University, Xuzhou, China, <sup>7</sup>Center of Clinical Oncology, The Affiliated Hospital of Xuzhou Medical University, Xuzhou, China, <sup>8</sup>Jiangsu Center for the Collaboration and Innovation of Cancer Biotherapy, Cancer Institute, Xuzhou Medical University, Xuzhou, China

## OPEN ACCESS

### Edited by:

Alejandro Vaquero,  
Josep Carreras Leukaemia Research  
Institute (LRC), Spain

### Reviewed by:

Berta N. Vazquez,  
Josep Carreras Leukaemia Research  
Institute (LRC), Spain  
Dan Ye,  
Fudan University, China

### \*Correspondence:

Lianjun Zhang  
zlj@ism.cams.cn

<sup>†</sup>These authors have contributed  
equally to this work

### Specialty section:

This article was submitted to  
Cellular Biochemistry,  
a section of the journal  
Frontiers in Cell and Developmental  
Biology

**Received:** 19 August 2021

**Accepted:** 15 November 2021

**Published:** 13 December 2021

### Citation:

Duan Q, Ding J, Li F, Liu X, Zhao Y,  
Yu H, Liu Y and Zhang L (2021) Sirtuin  
5 is Dispensable for CD8<sup>+</sup> T Cell  
Effector and Memory Differentiation.  
Front. Cell Dev. Biol. 9:761193.  
doi: 10.3389/fcell.2021.761193

CD8<sup>+</sup> T cell effector and memory differentiation is tightly controlled at multiple levels including transcriptional, metabolic, and epigenetic regulation. Sirtuin 5 (SIRT5) is a protein deacetylase mainly located at mitochondria, but it remains unclear whether SIRT5 plays key roles in regulating CD8<sup>+</sup> T cell effector or memory formation. Herein, with adoptive transfer of Sirt5<sup>+/+</sup> or Sirt5<sup>-/-</sup> OT-1 cells and acute *Listeria monocytogenes* infection model, we demonstrate that SIRT5 deficiency does not affect CD8<sup>+</sup> T cell effector function and that SIRT5 is not required for CD8<sup>+</sup> T cell memory formation. Moreover, the recall response of SIRT5 deficient memory CD8<sup>+</sup> T cells is comparable with Sirt5<sup>+/+</sup> memory CD8<sup>+</sup> T cells. Together, these observations suggest that SIRT5 is dispensable for the effector function and memory differentiation of CD8<sup>+</sup> T cells.

**Keywords:** sirtuin 5 (SIRT5), CD8 T cell, memory T cell, infection, effector T cell

## INTRODUCTION

CD8<sup>+</sup> T cells are the main immune effector cells, protecting host against viral/bacterial infection and tumor development. Upon antigen stimulation, naïve CD8<sup>+</sup> T cells undergo extensive proliferation and acquisition of effector functions, which is followed by memory T cell formation. In response to acute infection, the memory formation of CD8<sup>+</sup> T cells consists of the expansion phase, contraction phase, and memory formation and maintenance phase (Williams and Bevan, 2007). The activation of naïve CD8<sup>+</sup> T cells is marked with the upregulation of multiple surface markers including CD25, CD44, CD69, and CD98 and downregulation of CD62L. Meanwhile, T cell activation process is accompanied by striking metabolic switch from oxidative phosphorylation to aerobic glycolysis, and glycolytic metabolism is the key required for acquisition of CD8<sup>+</sup> T cell effector functions (Chang et al., 2013). Central memory CD8<sup>+</sup> T cells (T<sub>cm</sub>) display high level expression of CD62L, allowing their homing to lymph node (LN). Importantly, T<sub>cm</sub> cells exhibit substantial mitochondrial spare respiratory capacity (SRC) and fatty acid oxidation (FAO), which allows to sustain their long-term survival and metabolically prepared for secondary expansion (Zhang and Romero, 2018). Indeed, accumulating evidence suggests that T cell activation and differentiation are coupled to metabolic reprogramming, and alterations of metabolic activity can determine the CD8<sup>+</sup> T cell fate (Zhang and Romero, 2018).

The sirtuins possess NAD<sup>+</sup>-dependent protein deacetylase activity and contain seven members in mammalian cells with different subcellular localization and functions, the SIRT1~SIRT7 (Houtkooper et al., 2012; Song et al., 2018). SIRT1, SIRT6, and SIRT7 are mainly located in the



nucleus and SIRT3-5 in the mitochondria, whereas SIRT2 is predominantly located in the cytoplasm. Sirtuins have been shown to play important roles in regulating diverse key biological processes, including gluconeogenesis, glycolysis, the tricarboxylic acid (TCA) cycle, and lipid metabolism (Houtkooper et al., 2012). Yet, emerging studies demonstrated that sirtuin members were involved in diverse stages of immune response, and more detailed roles of sirtuins are currently under investigation. For instance, SIRT2 inhibits T cell metabolism by targeting multiple key enzymes, such as hexokinase, ATP-dependent 6-phosphofructokinase, aldolase, glyceraldehyde-3-phosphate dehydrogenase (GAPDH), enolase, 2-oxoglutarate dehydrogenase, and succinate dehydrogenase, through its deacetylase activity (Hamaidi et al., 2020). Of note, SIRT2 deficiency in T cells increases both glycolysis and oxidative phosphorylation to enhance their proliferation and anti-tumor effector functions. Moreover, SIRT1 regulates glycolytic activity in innate immune cells by cooperating with hypoxia-inducible factor-1 $\alpha$  (HIF1 $\alpha$ ) to impact their functional differentiation (Yu et al., 2018). In addition, SIRT1 programs the differentiation of CD4 $^{+}$  T cells by driving the production of cytokine interleukin-12 (IL-12) and transforming growth factor- $\beta$ 1 in dendritic cell through a HIF1 $\alpha$ -dependent signaling pathway (Liu et al., 2015). Therefore, sirtuins are likely novel therapeutic targets against tumor or other diseases *via* modulating metabolism or epigenetic activity.

Sirtuin 5 (SIRT5) is a unique member amongst the seven sirtuins, because it not only has deacetylase activity but also possesses stronger demalonylase, desuccinylase, and deglutarylase functions (Du et al., 2011; Tan et al., 2014; Wang et al., 2017; Kumar and Lombard, 2018). So far, thousands of potential substrates of SIRT5 have been identified *via* proteomic analysis including various critical metabolic enzymes involved in ketogenesis (Rardin et al., 2013), amino acid degradation, TCA cycle, fatty acid metabolism (Park et al., 2013), and glycolysis (Nishida et al., 2015). SIRT5 has been well recognized as a regulator of various metabolic processes, which was involved in multiple diseases such as DSS-induced colitis and hypertrophic cardiomyopathy (Rardin et al., 2013; Nishida et al., 2015; Sadhukhan et al., 2016; Kumar and Lombard, 2018). Previous studies indicated that the modulation of cellular metabolism plays a key role in dictating immune cell development and function (Norata et al., 2015). For instance, Wang et al. (2017) have revealed that SIRT5 reprograms the metabolism process of macrophage to repress the pro-inflammatory response by activating the PKM2 kinase activity and block macrophage IL-1 $\beta$  production. In addition, Jeng et al. (2018) reported that the metabolic reprogramming of resting memory CD8 $^{+}$  T cell is closely correlated with the loss of SIRT1. Given that SIRT5 is an important metabolic or epigenetic regulator, a better understanding of its roles in regulating CD8 $^{+}$  T cell immune response is needed.

Herein, our present study aimed to explore the effects of SIRT5 on the effector function and memory differentiation of CD8 $^{+}$  T cells with OT-1 TCR transgenic mice and acute *Listeria monocytogenes* infection model. To our surprise, we did not observe significant phenotypic changes regarding the activation, differentiation, and effector function of CD8 $^{+}$  T cells in the absence of SIRT5. Furthermore, SIRT5 deficiency did not affect the recall of memory CD8 $^{+}$  T cells.

Together, although SIRT5 affected the mitochondrial function to some extent, it is dispensable for differentiation and function of CD8 $^{+}$  T cells.

## METHODS

### Animal

Female C57BL/6N mice (6–8 weeks old, WT) were purchased from Vital River Co., Ltd. (Beijing, China). B6;129-Sirt5<sup>tm1Fwa/J</sup> (Sirt5<sup>-/-</sup>) mice were kindly provided by Prof. Hongxiu Yu and were described by Wang et al. (2017). CD45.1 $^{+}$  OT-1 TCR transgenic mice on a C57BL/6 background were housed under specific pathogen-free conditions in the animal facility of Suzhou Institute of Systems Medicine (Suzhou, China). CD45.2 $^{+}$  Sirt5<sup>-/-</sup> mouse was crossed with CD45.1 $^{+}$  OT-1 mouse to obtain CD45.1/2 $^{+}$  Sirt5<sup>+/-</sup> OT-1 and CD45.1/2 $^{+}$  Sirt5<sup>+/-</sup> offspring mice, and then, the CD45.1/2 $^{+}$  Sirt5<sup>+/-</sup> OT-1 mouse was crossed with CD45.1/2 $^{+}$  Sirt5<sup>+/-</sup> mouse to produce CD45.1 $^{+}$  Sirt5<sup>+/-</sup> OT-1, CD45.1/2 $^{+}$  Sirt5<sup>+/-</sup> OT-1, CD45.1 $^{+}$  Sirt5<sup>-/-</sup> OT-1, CD45.1/2 $^{+}$  Sirt5<sup>-/-</sup> OT-1, and other genotype offspring mice. *Listeria* infection experiments were performed in Animal Biosafety Level-2 laboratories.

### CD8 $^{+}$ T Cell Activation and *in vitro* Culture

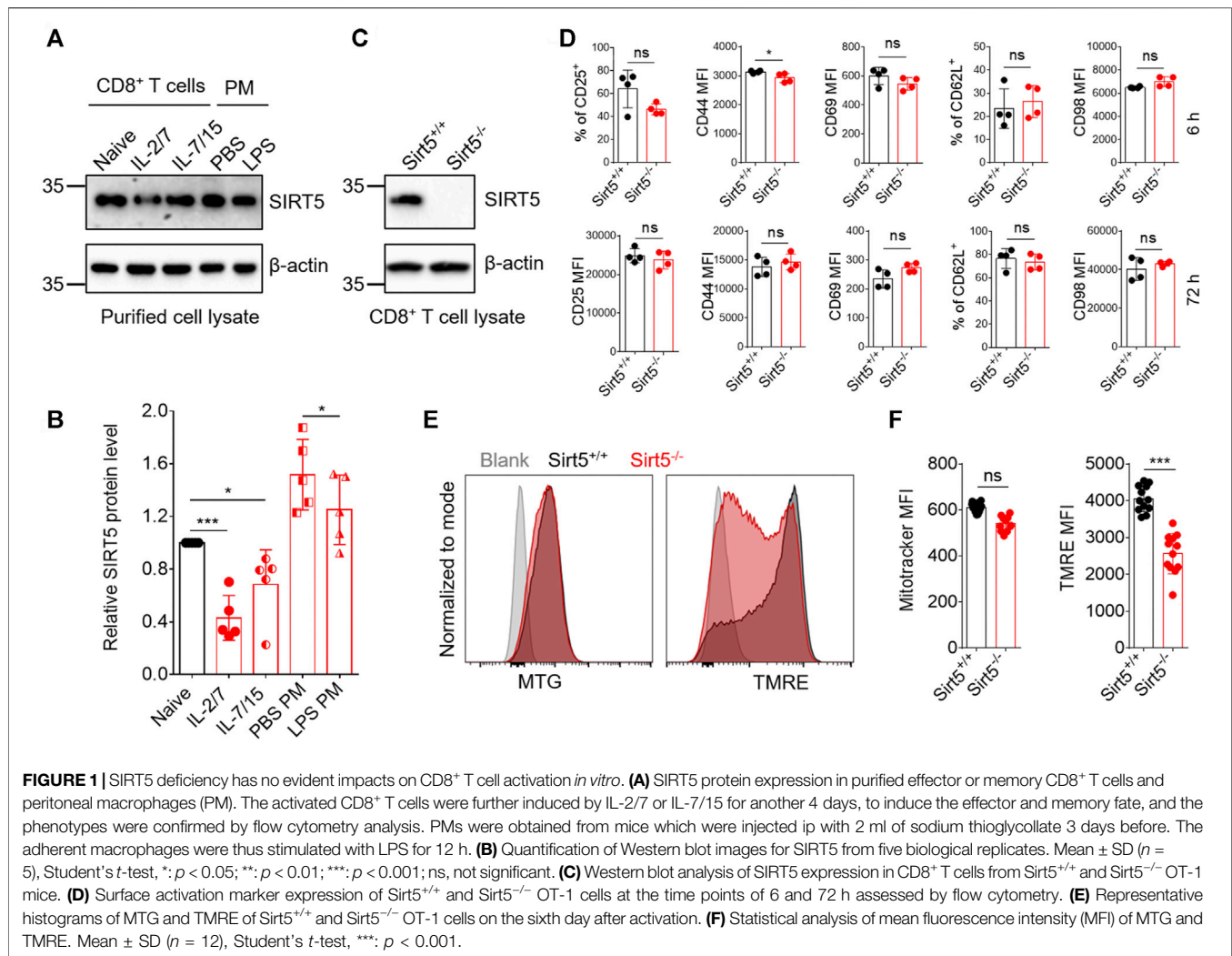
CD8 $^{+}$  T cells were sorted from the spleens of Sirt5<sup>+/-</sup> OT-1 mice and Sirt5<sup>-/-</sup> OT-1 mice by the Mouse CD8 $^{+}$  Naïve T Cell Isolation Kit (BioLegend, no. 480044). CD8 $^{+}$  T cells ( $2 \times 10^6$ ) were plated into each well of 24-well plate in 2-ml medium, which was precoated with  $\alpha$ CD3 (Invitrogen, no. 16-0031-86) and  $\alpha$ CD28 (Invitrogen, no. 16-0281-86) antibody. IL-2 (PeproTech, no. 200-02) was added into the culture medium, and the final concentration was 10 ng/ml. The activation phenotype of CD8 $^{+}$  T cells was assessed at the time points of 6 h, 24 h, 72 h, and 6 days after activation. On third day, dead cells were removed by Ficoll-Paque (GE Healthcare, no. 17-1440-03), and the rest live CD8 $^{+}$  T cells were continually cultured in the medium containing IL-2 (10 ng/ml) and IL-7 (10 ng/ml) (PeproTech, no. 200-07). On the sixth day, CD8 $^{+}$  T cells were collected to measure the cytokine secretion ability by restimulation with N4 peptide.

### Quantitative Polymerase Chain Reaction

Quantitative PCR analysis was performed according to a previously described method (Duan et al., 2019).  $\beta$ -actin was used as the internal reference. Four technical replicates were performed. The following primers were used: SIRT5 forward primer: 5'-GTCATCACCCAGAACATCGA-3', SIRT5 reversed primer: 5'-ACGTGAGGTCGCAGCAAGCC-3' (Ogura et al., 2010), and  $\beta$ -actin forward primer: 5'-GGGCTATGCTCTCCC TCAC-3',  $\beta$ -actin reversed primer: 5'-GATGTCACGCACGAT TTCC-3' (Cheeran et al., 2007).

### Adoptive Naïve T Cell Transfer and Bacterial Infection

Sirt5<sup>+/-</sup> and Sirt5<sup>-/-</sup> naïve OT-1 cells were sorted using the Mouse CD8 $^{+}$  Naïve T Cell Isolation Kit (BioLegend, no. 480044). CD45.1 and CD45.2 are allelic variants of CD45 expressed in all leukocytes

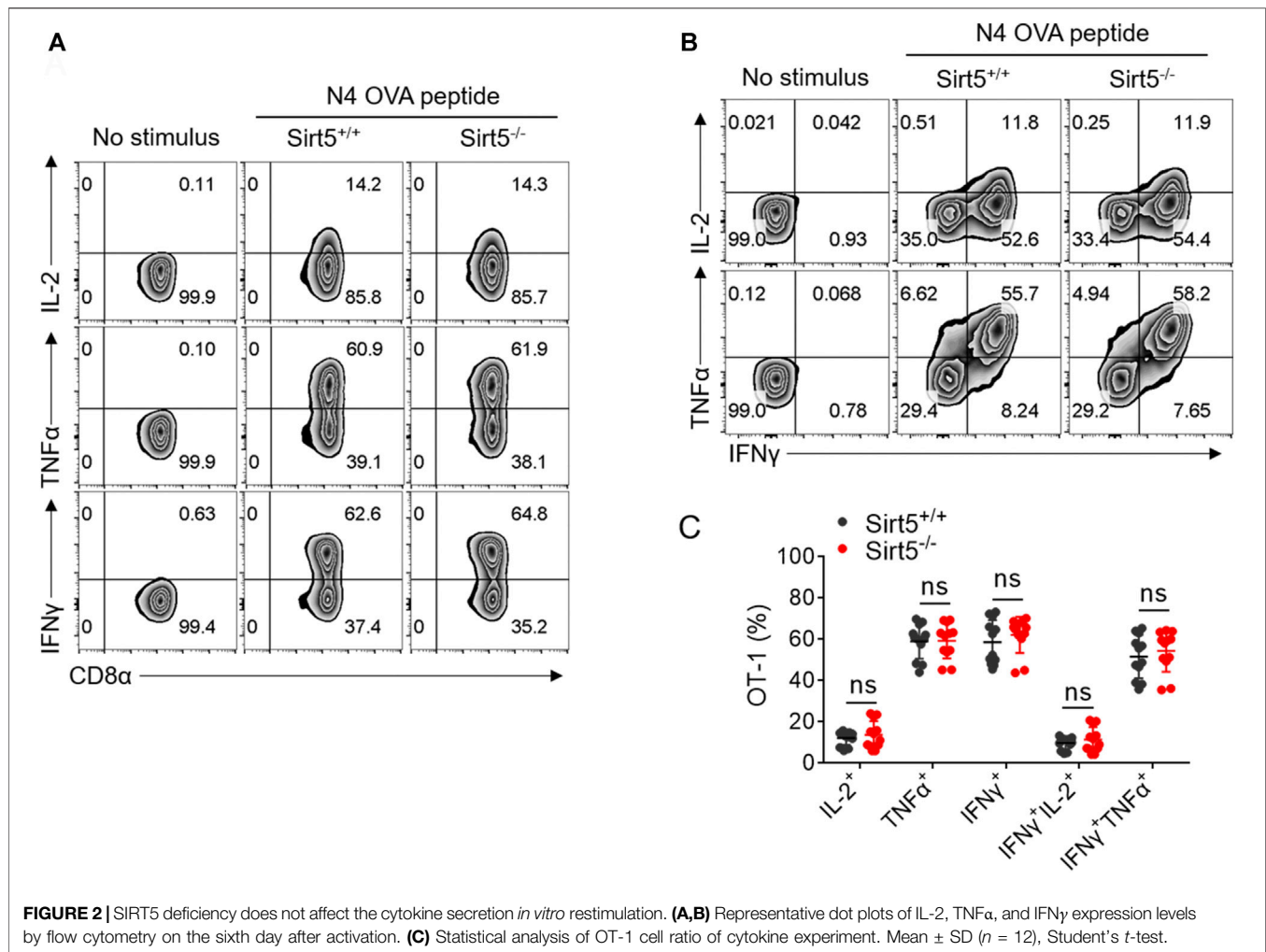


including CD8<sup>+</sup> T cell and can be efficiently distinguished by flow cytometry. In the adoptive naïve T cell transfer experiments, CD45.1 and CD45.2 were used to be as congenic marker to distinguish donor CD8<sup>+</sup> T cells and host CD8<sup>+</sup> T cells. The recipients were all CD45.2<sup>+</sup> mice, and the transferred naïve CD8<sup>+</sup> T cells were CD45.1<sup>+</sup> or CD45.1/2<sup>+</sup> OT-1 cells. For separate transfer of Sirt5<sup>+/+</sup> and Sirt5<sup>-/-</sup> naïve OT-1 cells,  $5 \times 10^4$  cells were transferred into naïve host intravenously (i.v.), separately. For co-transfer of Sirt5<sup>+/+</sup> and Sirt5<sup>-/-</sup> naïve OT-1 cells, a total of  $1 \times 10^5$  cells was transferred i.v., as the amount of Sirt5<sup>+/+</sup> and Sirt5<sup>-/-</sup> naïve OT-1 cells were both  $5 \times 10^4$ . Each mouse was injected i.v. 2,000 CFU *Listeria monocytogenes* stably expressing ovalbumin (LM-OVA) at primary infection. Co-transferred mice were used for recall experiments and were injected i.v.  $1 \times 10^4$  CFU LM-OVA on the 40th day at secondary infection.

## Flow Cytometry (Surface and Intracellular Staining)

Single-cell suspensions obtained from the blood, spleen, and lymphocyte node were used for flow cytometry analysis. For cell

surface staining, cells were first performed by viability staining with Fixable Viability Dye eFluor 506 (eBioscience, no. 65-0866-18) for 20 min on ice. Then, the cells were surface stained for 25 min on ice: anti-CD8 (Brilliant Violet 711, BioLegend, no. 100748), anti-CD25 (PB, 102022, no. 100748), anti-CD44 (APC-Cy7, BioLegend, no. 103028), anti-CD69 (FITC, BioLegend, no. 104506), anti-CD98 (Alexa Fluor 647, BioLegend, no. 128210), anti-CD62L (PE or APC, BioLegend, no. 104408 or 104412), anti-CD45.1 (FITC or Percp/Cy5.5, BioLegend, no. 110706 or 110728), anti-CD45.2 (Pacific Blue, BioLegend, no. 109820), anti-KLRG1 (PE-Cy7, Invitrogen, no. 25-5893-82), and anti-CD127 (PE, BioLegend, no. 135010). For intracellular cytokine staining, cells were first fixed with Fixation Buffer (BioLegend, no.420801) for 20 min on ice and permeabilized with Permeabilization Buffer (BioLegend, no.421002). Then, cells were stained with anti-IL-2 (PE, BioLegend, no. 503808), anti-tumor necrosis factor- $\alpha$  (TNF $\alpha$ ) (FITC, BioLegend, no. 506306), and anti-interferon- $\gamma$  (IFN $\gamma$ ) (APC, BioLegend, no. 505810) for 25 min on ice. For intracellular transcription factor staining, cells were first fixed with eBioscience Foxp3/Transcription Factor Staining Buffer (Invitrogen, no.00-5223-56 and 00-5123-43), permeabilized with Permeabilization Buffer (Invitrogen, no.00-8333-56), and then



were stained with anti-Tcf1 (Alexa Fluor 647, BioLegend, no. 655204) and anti-T-bet (PE-Cy7, BioLegend, no. 644824). The stained cell samples were resuspended in FACS buffer (phosphate-buffered saline containing 2% fetal bovine serum) and loaded in an LSR Fortessa flow cytometer (Becton Dickinson, San Jose, CA). The FCA data were analyzed by FlowJo software.

## Mitochondrial Potential Measurement by Flow Cytometry

Mitochondrial mass and activity were assessed by MitoTracker green (MTG) (Invitrogen, no. M7514) and tetramethylrhodamine ethyl ester (TMRE) (Invitrogen, no. T669) staining, respectively. In brief, cells were stained with MTG and TMRE at 37°C in dark for 30 min, which was followed by incubation with Fixable Viability Dye eFluor 506 for 20 min and subsequent cell surface staining. Finally, cells were resuspended in FACS buffer for further analysis.

## *In vitro* Restimulation

Single-cell suspensions obtained from the blood, spleen, and lymphocyte node were used for restimulation *in vitro* to measure cytokine secretion ability. At indicated time points, single-cell

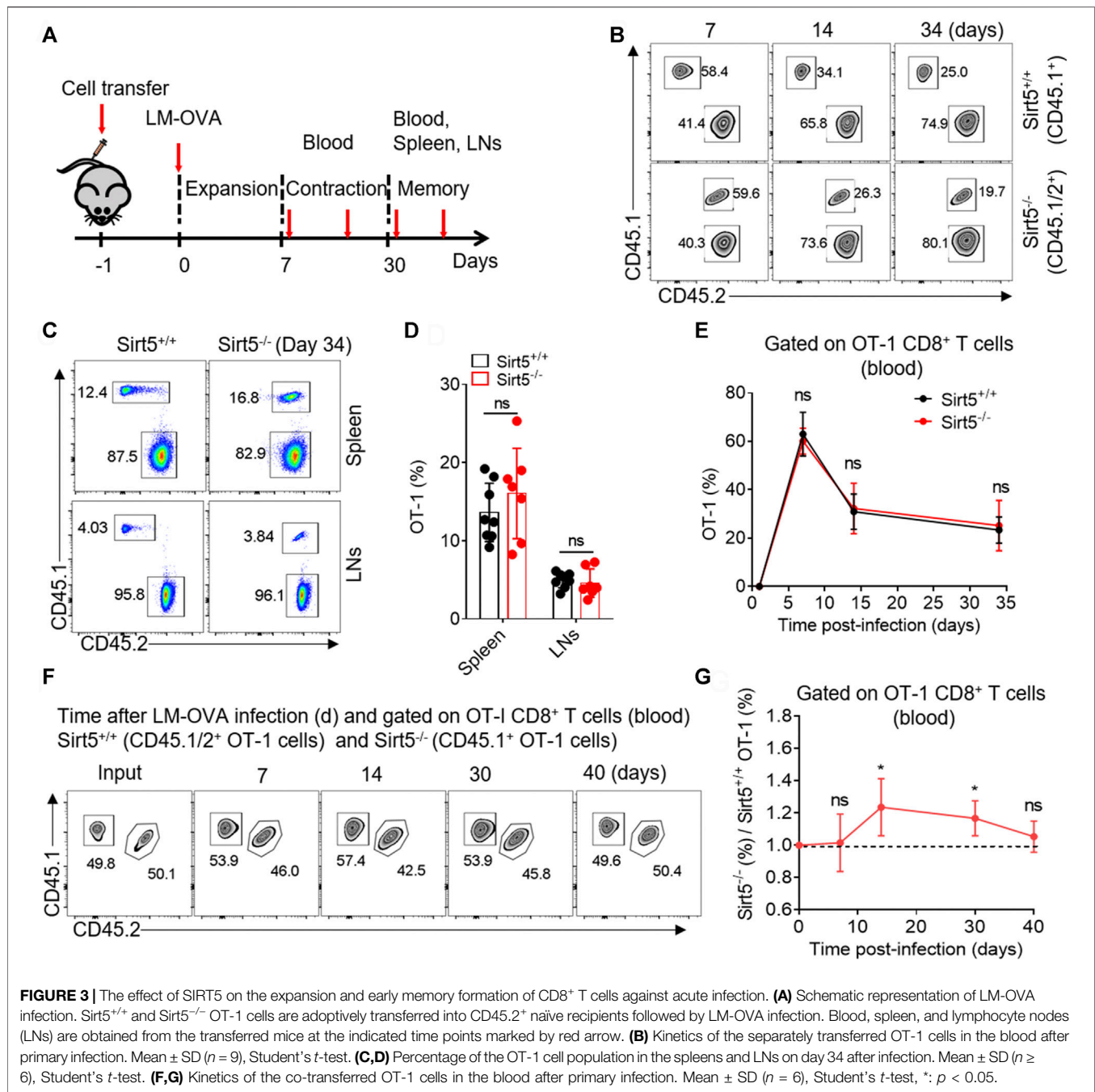
suspensions were seeded into 96-well plate. The cells were pre-stimulated with 1  $\mu$ M SIINFEKL (N4) peptide (synthesized by China Abcepta Biotech Ltd., Co.) for 30 min. Then, cells were restimulated for another 4 h, and meanwhile, the medium was added eBioscience Brefeldin A (Invitrogen, no. 00-4506-51) and eBioscience Monensin Solution (Invitrogen, no. 00-4505-51).

## Western Blot Analysis

Western blot analysis was performed according to a previously described method (Duan et al., 2019). Total protein lysates were generated by lysing the purified CD8<sup>+</sup> T cells from Sirt5<sup>+/+</sup> and Sirt5<sup>-/-</sup> OT-1 mice in RIPA buffer containing 50 mM Tris-HCl, 150 mM NaCl, 1% Triton X-100, 0.1% SDS, 1 mM EDTA, protease inhibitor cocktail tablet (Roche, no. 11697498001). The SIRT5 antibody was purchased from Cell Signaling Technology (no. 8782S), and  $\beta$ -actin was from ABclonal Technology (no. AC026).

## Statistical Analysis

Statistical analysis was performed with GraphPad Prism software. The comparison of two groups was done by two-tailed Student's *t*-test. Data are presented as the mean  $\pm$  SD. Difference was



considered statistically significant when  $p < 0.05$  (\* $p < 0.05$ ; \*\* $p < 0.01$ ; \*\*\* $p < 0.001$ ).

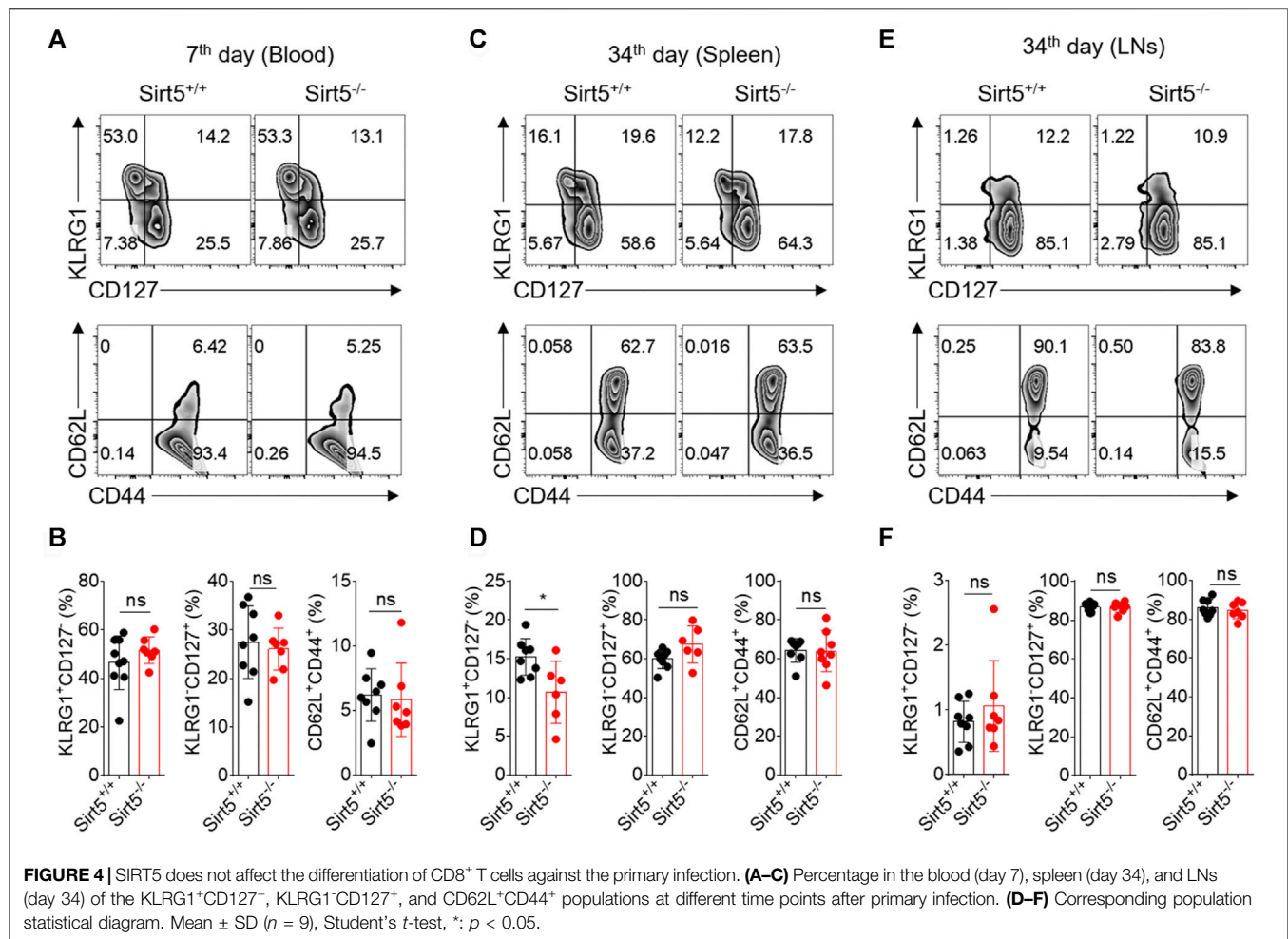
## RESULTS

### SIRT5 Deficiency Does Not Impact the Activation and Functionality of CD8<sup>+</sup> T Cells

First, we compared the expression pattern of SIRT5 at both mRNA and protein levels in different CD8<sup>+</sup> T cell subtypes including naïve, effector, and memory CD8<sup>+</sup> T cells and other cell types such as

macrophages, where SIRT5 has been reported to play important roles (Wang et al., 2017) (Figures 1A,B; Supplementary Figure S1A). Results showed that SIRT5 protein levels were downregulated in the effector CD8<sup>+</sup> T cells (cultured with IL-2/7) and CD8<sup>+</sup> T cells with memory phenotype (cultured with IL-7/15) (Zoon, et al., 2017). In particular, we demonstrated that the mRNA expression of SIRT5 was also decreased in purified antigen-specific memory CD8<sup>+</sup> T cells after bacterial infection (Supplementary Figure S1A), indicating the potential roles of SIRT5 in regulating CD8<sup>+</sup> T cell effector and memory differentiation. Of note, the mRNA expression of SIRT5 was relatively lower in CD8<sup>+</sup> T cells as compared to peritoneal





macrophages. To characterize the precise role of SIRT5 in CD8<sup>+</sup> T cells, Sirt5<sup>-/-</sup> mice were crossed with OT-1 TCR transgenic mice on a C57BL/6 background to generate Sirt5<sup>-/-</sup> OT-1 mice. With western blot analysis, we confirmed that SIRT5 was successfully knocked out in OT-1 mice (Figure 1C). The effects of SIRT5 on the activation phenotype of CD8<sup>+</sup> T cells was assessed by measuring the surface marker expression at different time points. Flow cytometry analysis demonstrated that SIRT5 deficiency did not affect the expression pattern of CD25, CD44, CD69, CD98, and CD62L significantly (Figure 1D; Supplementary Figure S1B). In addition, we assessed the cytokine secretion ability of Sirt5<sup>+/+</sup> and Sirt5<sup>-/-</sup> OT-1 cells by *in vitro* restimulation but did not observe significant difference between Sirt5<sup>+/+</sup> and Sirt5<sup>-/-</sup> OT-1 cells (Figures 2A–C), which indicates that SIRT5 deficiency may not affect the CD8<sup>+</sup> T effector function. As SIRT5 is mainly located in the mitochondria, it is unclear whether SIRT5 affects the mitochondrial mass and function of CD8<sup>+</sup> T cells. Thus, we measured the mitochondrial mass with MTG staining and mitochondrial membrane potential with TMRE staining. SIRT5-deficient CD8<sup>+</sup> T cells showed similar MTG MFI with that of Sirt5<sup>+/+</sup> CD8<sup>+</sup> T cells (Figures 1E,F), which is consistent with previously report that SIRT5 did not affect the mitochondrial mass (Buler et al., 2014). Mitochondrial membrane potential ( $\Delta\psi_m$ ) is a critical factor in the energy transformation and production and

performs many non-energetic functions for mitochondria. Normal  $\Delta\psi_m$  is a requisite for maintenance of mitochondrial function. Interestingly, SIRT5 deficiency in CD8<sup>+</sup> T cells led to decreased TMRE MFI (Figures 1E,F), indicating of potential alteration of mitochondrial function in the absence of SIRT5.

## SIRT5 is Not Required for the Proliferation and Survival of CD8<sup>+</sup> T Cells Upon Acute Infection

SIRT5 is an important regulator of various energy metabolisms. Next, we want to know whether SIRT5 affects the expansion and the effector and memory differentiation of CD8<sup>+</sup> T cells *in vivo*. We thus transferred Sirt5<sup>+/+</sup> and Sirt5<sup>-/-</sup> naïve OT-1 cells into wild-type mice *i.v.* and infected them with LM-OVA and then analyzed the proliferative response of OT-1 cells by flow cytometry at different time points during expansion, contraction, and memory maintenance phase of memory CD8<sup>+</sup> T cell formation process (Figure 3A). We performed the kinetic analysis of Sirt5<sup>+/+</sup> and Sirt5<sup>-/-</sup> OT-1 cells in the blood of LM-OVA infected mice (Figures 3B,E). At the peak of expansion phase (seventh day after infection), we did not observe significant differences in the expansion of Sirt5<sup>+/+</sup> and Sirt5<sup>-/-</sup> OT-1 cells. The *in vivo* kinetic curves of Sirt5<sup>+/+</sup> and Sirt5<sup>-/-</sup> OT-1 cells were

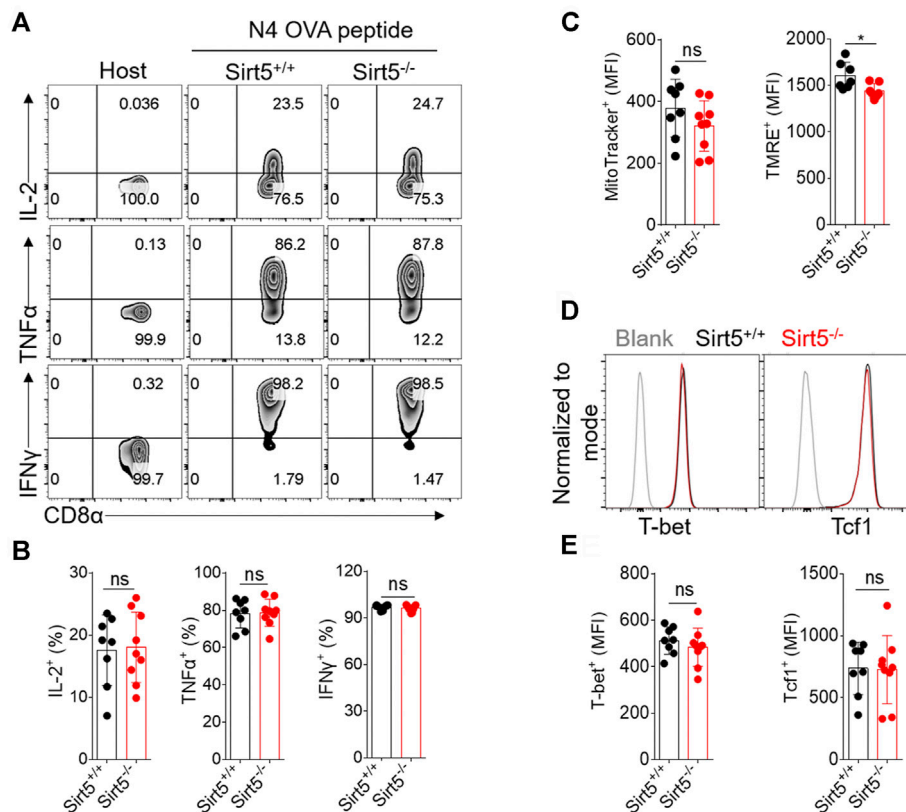


**FIGURE 5 |** The effect of SIRT5 on the effector function, mitochondrial function, and transcription factor expression of CD8<sup>+</sup> T cells from the spleens of transferred mice. **(A)** Representative dot plots of IL-2, TNFα, and IFNγ expression levels of OT-1 cells from the spleen tissues by flow cytometry *in vitro* restimulation. The transferred mice are sacrificed on day 34 after primary LM-OVA infection. **(B)** Statistical analysis of OT-1 cell ratio of cytokine experiment. Mean ± SD (*n* = 9), Student's *t*-test. **(C)** Statistical analysis of MTG and TMRE MFI. Mean ± SD (*n* = 9), Student's *t*-test, \*: *p* < 0.05. **(D)** Representative histograms of Tcf1 and Tbet protein expression level of Sirt5<sup>+/+</sup> and Sirt5<sup>-/-</sup> OT-1 cells from the spleens. **(E)** Statistical analysis of Tcf1 and Tbet MFI. Mean ± SD (*n* = 9), Student's *t*-test.

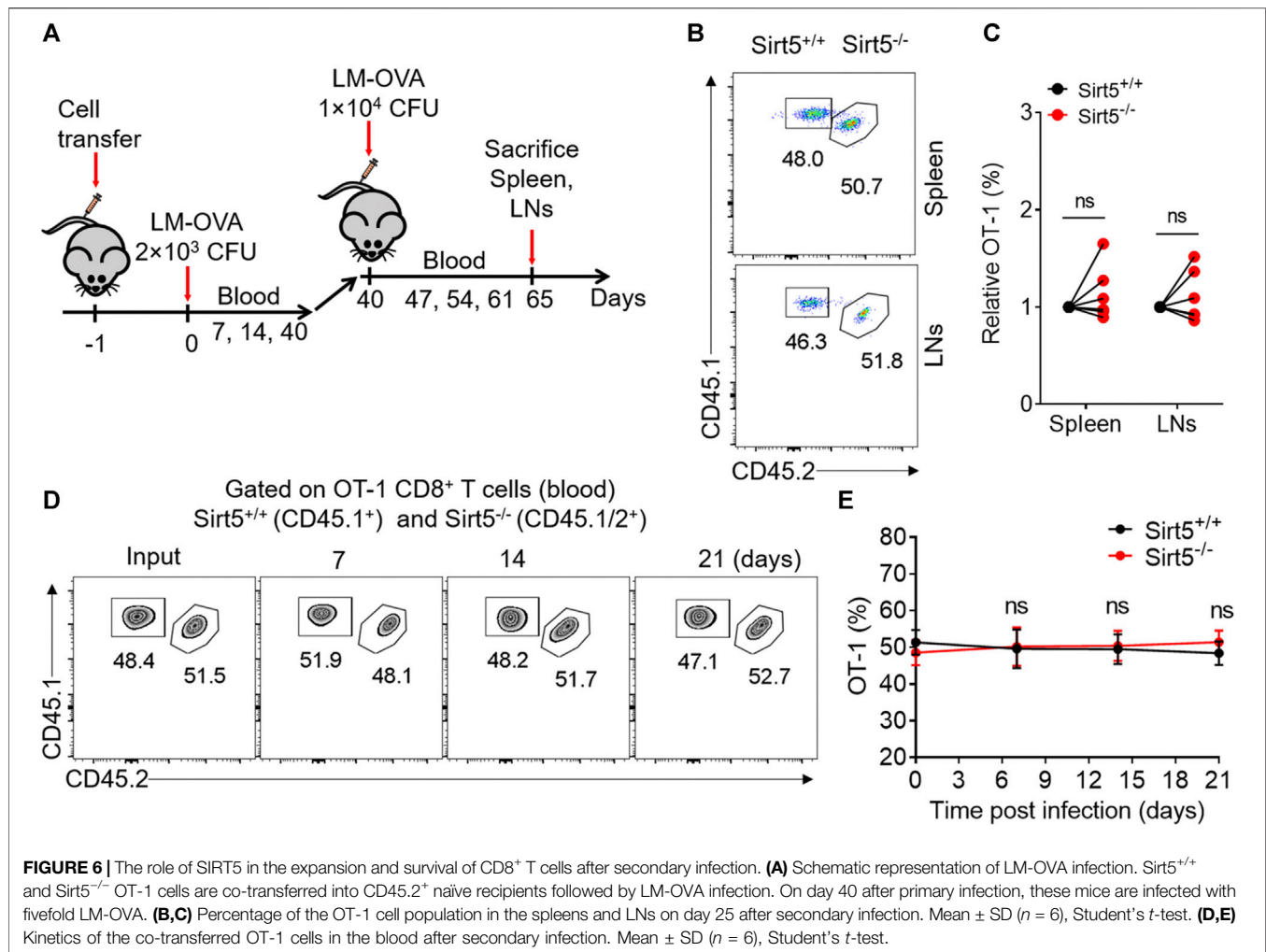
similar, suggesting that SIRT5 is unrelated to the proliferation and survival of CD8<sup>+</sup> T cells. Next, we separated the spleens and lymphocyte nodes from infected mice and quantified their early memory CD8<sup>+</sup> T cell of Sirt5<sup>+/+</sup> and Sirt5<sup>-/-</sup> OT-1 cells on the 34th day (Figures 3C,D). However, the ratio of early memory cell of Sirt5<sup>-/-</sup> OT-1 cells in total CD8<sup>+</sup> T subset was similar with that of Sirt5<sup>+/+</sup> OT-1 cells. To avoid any effects of different host microenvironment, we carried out co-transfer mouse model experiment. Although Sirt5<sup>-/-</sup> OT-1 cells had slight survival advantage during contraction phase (14 days after infection) in the co-transfer model, consistent with separate transfer model, they formed the comparable ratio of early memory cell with Sirt5<sup>+/+</sup> OT-1 cells in memory maintenance phase (Figures 3F,G).

## SIRT5 Deficiency Does Not Impact Differentiation and Function of CD8<sup>+</sup> T Cells *In vivo*

KLRG1, CD127, CD62L, and CD44 have been reported to define functionally distinct CD8<sup>+</sup> T cell populations [short-lived effector cells (SLEC): KLRG1<sup>+</sup>CD127<sup>-</sup>, and memory-precursor effector cells (MPEC): KLRG1<sup>-</sup>CD127<sup>+</sup>; and central memory T cells (Tcm):

CD62L<sup>+</sup>CD44<sup>+</sup>] (Bengsch et al., 2007; Sukumar et al., 2016; Renkema et al., 2020). Next, we measured the expression pattern of these surface markers by flow cytometry to characterize the OT-1 cell differentiation *in vivo*. The percentages of Tcm, SLEC, and MPEC population were all comparable between Sirt5<sup>+/+</sup> OT-1 cells and Sirt5<sup>-/-</sup> OT-1 cells on seventh day in blood of the separately transferred mice (Figures 4A,B). Consistently, there were no significant differences in these three subsets between the two genotypes in co-transfer model at different time points: 7th, 14th, 30th, and 40th day (data not shown). Similarly, in the spleens and lymphocyte nodes, there was no statistical significance in Tcm and MPEC populations (Figures 4C–F). On the basis of these results, we concluded that SIRT5 deficiency may not affect the transition of OT-1 cells from effector to memory CD8<sup>+</sup> T cells.

Next, we investigated whether SIRT5 affects the CD8<sup>+</sup> T cell effector function *in vivo*. Yet, we observed comparable IFNγ, TNFα, and IL-2 production between Sirt5<sup>+/+</sup> OT-1 cells and Sirt5<sup>-/-</sup> OT-1 cells in the spleens and lymphocyte nodes (Figures 5A,B; Supplementary Figure S2). Consistently, the cytokine production capacity was comparable between the two genotypes in the blood of both separate transferred and co-transferred mice on the 7th, 14th, 30th, and 40th days (data not shown). In addition, we



detected the mitochondria mass and function of OT-1 cells with MTG and TMRE staining in the spleens and lymphocyte nodes, and consistent with *in vitro* results, we found that SIRT5 did not affect the MFI of MTG, but decreased the TMRE MFI (Figure 5C). Tcf1 is a critical transcription factor required for CD8<sup>+</sup> T cell memory formation and T-bet is highly expressed in the effector T cells; we thus detected the protein expression of transcription factors Tcf1 and T-bet (Figures 5D,E). However, SIRT5 did not significantly affect the protein expression of Tcf1 and T-bet.

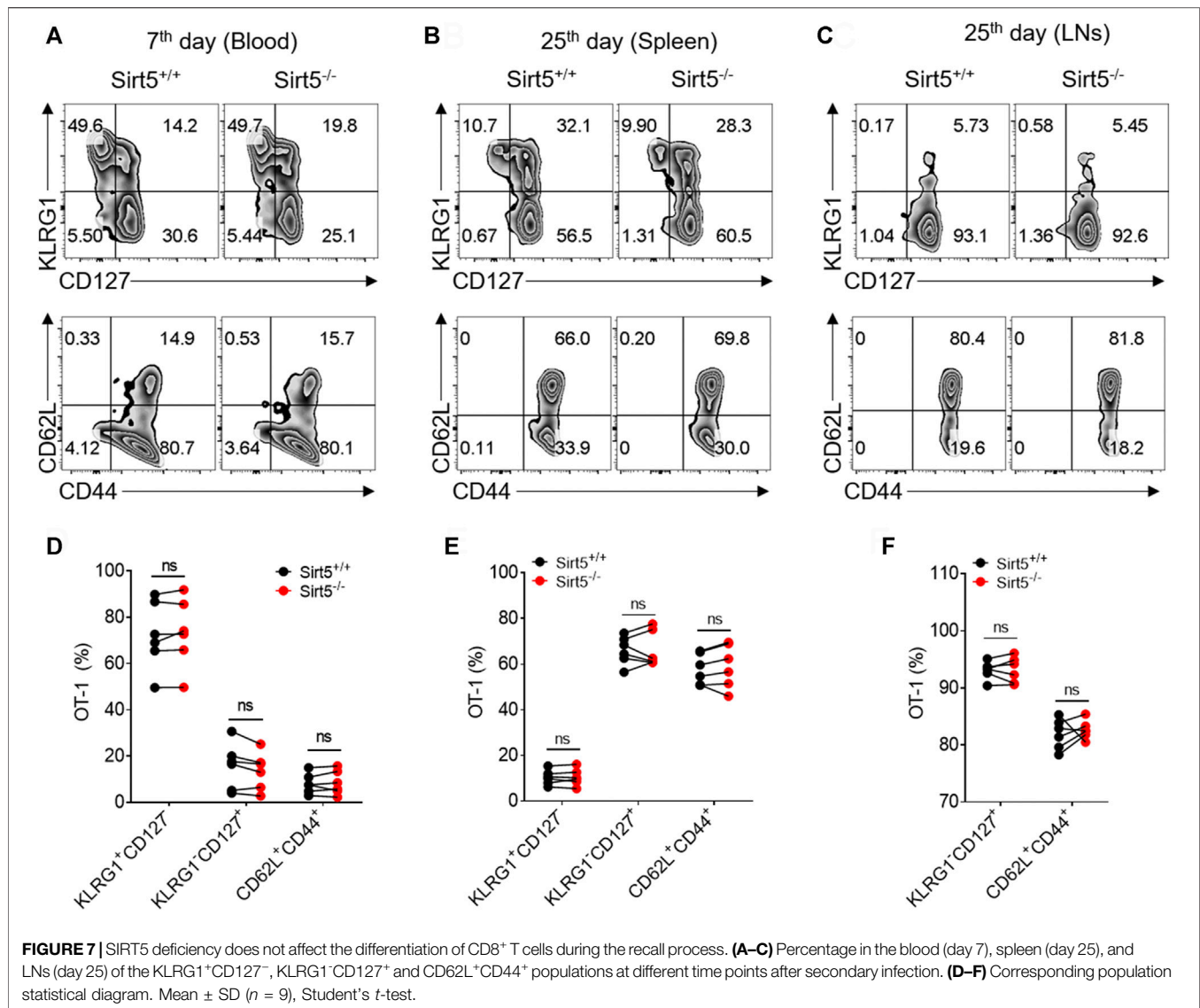
### SIRT5 Deficient Memory CD8<sup>+</sup> T Cells Mounted Comparable Recall Responses

Memory CD8<sup>+</sup> T cells exhibit quick expansion ability and strong effector function when encountering same antigen again, which is different from naïve CD8<sup>+</sup> T cells. We thus measured the recall response of memory Sirt5<sup>+/+</sup> and Sirt5<sup>-/-</sup> OT-1 cells with the co-transfer model followed by secondary infection with relatively higher dose of bacteria (Figure 6A). The detection of blood samples demonstrated that SIRT5-deficient OT-1 cells did not show significant expansion advantage (Figures 6D,E). Consistently, Sirt5<sup>-/-</sup> OT-1 cells did not show significant

differences with that of Sirt5<sup>+/+</sup> OT-1 cells in the survival in the spleens and lymphocyte nodes (Figures 6B,C). In addition, SIRT5 deficiency did not affect the differentiation of memory CD8<sup>+</sup> T cells in the blood (seventh day), spleen, and lymphocyte nodes (25th day) (Figures 7A–F). Similar results were obtained in the blood on the 14th day and 21st day (data not shown). Moreover, regarding the cytokine production of IL-2, TNF $\alpha$ , and IFN $\gamma$  and the protein expression of transcription factor Tcf1 and T-bet in the spleens and lymphocyte nodes, SIRT5 deficiency did not cause marked changes in the recall experiment (Figures 8A,B,D,E; Supplementary Figure S3). Of note, SIRT5 deficiency decreased the TMRE MFI of OT-1 cells (Figure 8C). Therefore, SIRT5 may be not required for the function, differentiation, and survival of memory CD8<sup>+</sup> T cells upon secondary infection.

## DISCUSSION

The roles of sirtuins in regulating CD8<sup>+</sup> T cell differentiation and function are largely unknown, and it remains unclear whether SIRT5 regulates CD8<sup>+</sup> T cell effector function and memory



differentiation. Given that SIRT5 impacts on many mitochondrial enzyme activities and is involved in multiple cellular metabolism pathways, it is necessary to investigate the role of SIRT5 in CD8<sup>+</sup> T cell effector or memory differentiation and functionality. Surprisingly, our results demonstrate that SIRT5 is dispensable for CD8<sup>+</sup> T cell activation, proliferation, and transition to memory, and the survival and recall response of memory CD8<sup>+</sup> T cells are also not dependent on SIRT5.

SIRT5 is currently the only enzyme known to possess demalonylase, desuccinylase, and deglutarylase activity and has been shown to exert multiple effects of desuccinylation, demalonylation, and deglutarylation on intracellular biological pathways *via* modulating a large range of substrates, such as PKM2, isocitrate dehydrogenase 2 (IDH2), glucose-6-phosphate 1-dehydrogenase (G6PD), GAPDH, and carbamoyl-phosphate synthase (Tan et al., 2014; Nishida et al., 2015; Zhou et al., 2016; Wang et al., 2017). SIRT5 may play a role in regulating the development and function of immune cells by modulating their

cellular metabolism pathways. Both Zhang et al. and Heinonen et al. have explored the innate immune responses of Sirt5<sup>-/-</sup> mice to bacterial infections, respectively, but they obtained contradictory results due to utilization of the different mouse lines and bacterial strains (Heinonen et al., 2018; Zhang et al., 2020).

In this present study, although SIRT5 did not affect the activation process and cytokine secretion of CD8<sup>+</sup> T cells *in vitro*, SIRT5 deficiency decreased the TMRE MFI (Figures 1E, 5C). The mitochondrial membrane potential is a crucial parameter affecting the T cell differentiation, as low- $\Delta\psi_m$  T cells exhibited memory phenotype with increased FAO and enhanced *in vivo* self-renewal and anti-tumor function (Sukumar et al., 2016). Thus, we transferred Sirt5<sup>+/+</sup> and Sirt5<sup>-/-</sup> OT-1 cells into the mice to monitor the *in vivo* dynamic changes. In the primary infection experiment, Sirt5<sup>+/+</sup> and Sirt5<sup>-/-</sup> OT-1 cells have comparable expansion, early memory differentiation capacity, and effector function in the blood, spleens, and



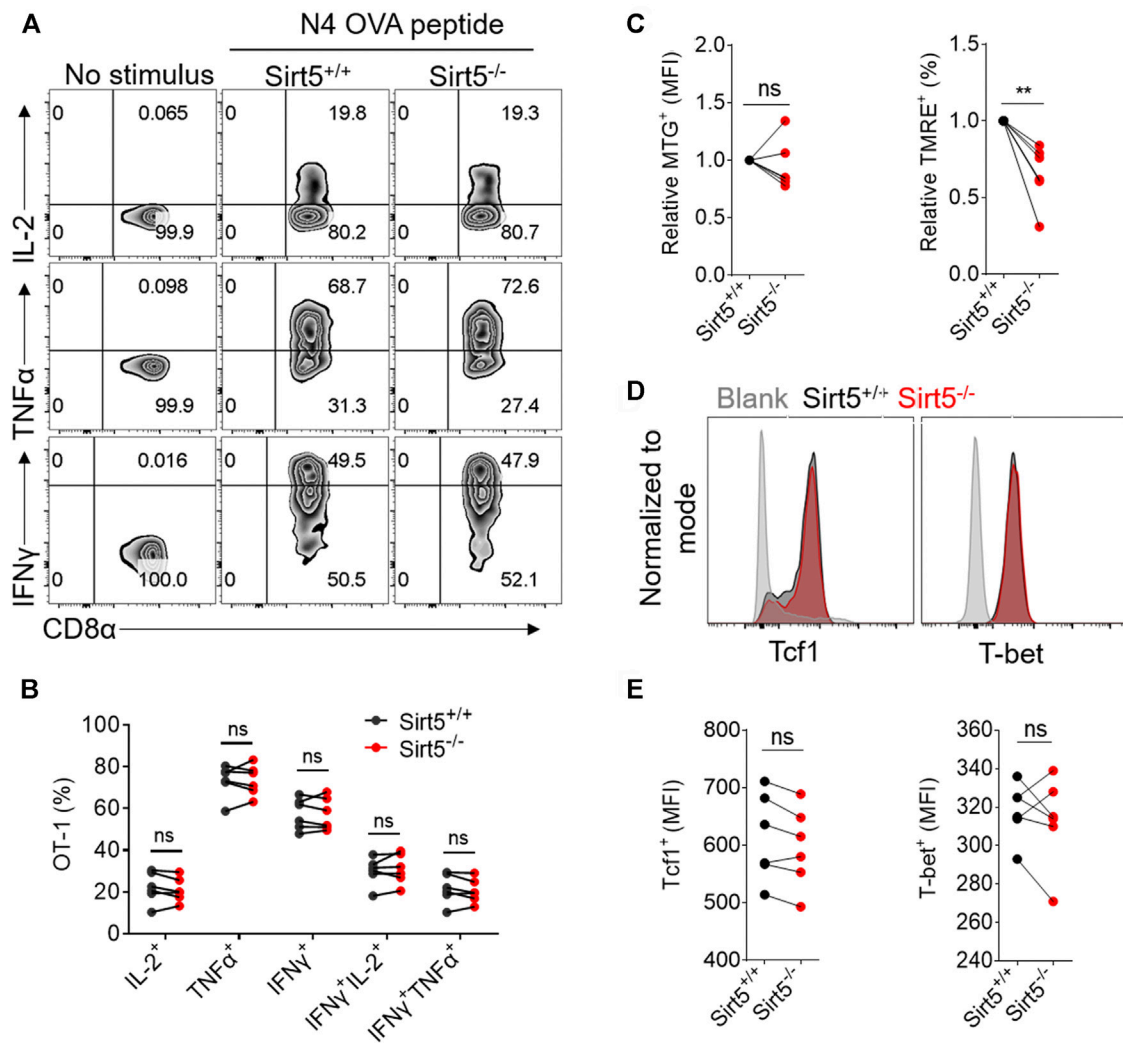


**FIGURE 8 |** The effect of SIRT5 on the effector function, mitochondrial function and transcription factor expression of CD8<sup>+</sup> T cells from the spleens of co-transferred mice. **(A)** Representative dot plots of IL-2, TNFα, and IFNγ expression levels of OT-1 cells from the spleen tissues by flow cytometry *in vitro* restimulation. The transferred mice are sacrificed on day 25 after secondary LM-OVA infection. **(B)** Statistical analysis of OT-1 cell ratio of cytokine experiment. Mean ± SD (*n* = 6), Student's *t*-test. **(C)** Statistical analysis of relative MTG and TMRE MFI. Mean ± SD (*n* = 6), Student's *t*-test, \*\*: *p* < 0.01. **(D)** Representative histograms of Tcf1 and T-bet protein expression level of Sirt5<sup>+/+</sup> and Sirt5<sup>-/-</sup> OT-1 cells from the spleens. **(E)** Statistical analysis of Tcf1 and T-bet MFI. Mean ± SD (*n* = 6), Student's *t*-test.

lymphocyte nodes, regardless of separate-transfer or co-transfer. Next, we investigated the possibility that SIRT5 might affect the recall response, because memory T cells harbor specific metabolic or epigenetic programs to mount the recall response when encountered with same antigen. Yet, upon secondary infection, we observed similar expansion, survival capacity, differentiation, and effector function between Sirt5<sup>+/+</sup> and Sirt5<sup>-/-</sup> memory CD8<sup>+</sup> T cells. Although Sirt5<sup>-/-</sup> CD8<sup>+</sup> T cells tended to have a slightly decreased mitochondrial membrane potential (Figure 8C), this SIRT5-induced TMRE decrement may be not sufficient for altering the immune response of CD8<sup>+</sup> T cells. Tcf1 and T-bet are the two important transcription factors coordinately regulating the function and differentiation of CD8<sup>+</sup> T cells; when Tcf1 is highly expressed in MPEC and Tcm cells, T-bet is highly upregulated in the SLEC cells (Pritchard et al., 2019;

Zhao et al., 2021). However, comparable expression of Tcf1 and T-bet were observed between Sirt5<sup>+/+</sup> and Sirt5<sup>-/-</sup> OT-1 cells in our assay.

To this end, our observations that SIRT5 is not necessary for CD8<sup>+</sup> T cell effector and memory differentiation are likely to be explained as follows. First, there exists a certain degree of functional overlap between SIRT5 and other sirtuin members. For example, SIRT3 protected calorie restriction on oxidative stress by deacetylating superoxide dismutase 2 (SOD2) and promoting its antioxidative activity (Qiu et al., 2010). SIRT3 altered the lipid metabolism of macrophages by targeting its deacetylated substrate IDH2 (Sheng et al., 2015). Similar to SIRT3, SIRT5 can deacetylated SOD1, IDH1, and IDH2 and affected the oxidative stress and mitochondrial functions (Lin et al., 2013; Li et al., 2015; Zhou et al., 2016). As SIRT3 and SIRT5

share the similar subcellular location and targets, maybe due to their compensated functions, neither Sirt3 nor Sirt5 knockout altered host defenses against bacterial infection (Ciarlo et al., 2017; Heinonen et al., 2018), but dual deficiency of SIRT3 and SIRT5 exhibited a modest protection against listeriosis host defense (Heinonen et al., 2019). In addition, individual SIRT5 or SIRT3 deficiency did not lead to significant global metabolic abnormalities of mice (Fernandez-Marcos et al., 2012; Yu et al., 2013). Second, the functions of SIRT5 may be induced under specific conditions. Twenty-four of forty-eight hours of food withdraw significantly promoted the expression of SIRT5 in mouse hepatocytes (Ogura et al., 2010; Buler et al., 2014). Meanwhile, Yu et al. (2013) confirmed that, under steady state, SIRT5 was not necessary for the metabolic homeostasis. However, when exposed to extreme stress such as feeding with high-fat diet (HFD) for 12 months (not 1 week or 3 months), Sirt3<sup>-/-</sup> mice displayed multiple metabolic syndromes including obesity, insulin resistance, hepatic steatosis, nonalcoholic steatohepatitis, or hyperlipidemias (Hirschey et al., 2011). During caloric restriction, SIRT3 modulated amino acid catabolism and  $\beta$ -oxidation by regulating ornithine transcarbamoylase activity and urea cycle (Hallows et al., 2011). Glucose limitation activated AMPK and its subsequent SENP1-SIRT3 signaling, promoting OXPHOS and mitochondrial fusion, which was beneficial to the anti-tumor immunity of T cells (He et al., 2021). Therefore, it remains unclear whether SIRT5 may play an important role under other physiological or pathological conditions, such as long time HFD, fasting, hypoxia, low glucose, low glutamine, or the tumor microenvironment. Third, CD8<sup>+</sup> cells used in our experiments were derived from the whole-body Sirt5<sup>-/-</sup> mice, in which the CD8<sup>+</sup> cells may have adapted to SIRT5 deficiency throughout development. Immune cells including CD8<sup>+</sup> T cells can reprogram their metabolism and adapt to the changes in the living environment to fulfill their biological functions (O'Neill and Pearce, 2016; Zhang and Romero, 2018). We cannot exclude this possibility that SIRT5 deletion triggers striking adaptation of CD8<sup>+</sup> T cells. Therefore, the acute SIRT5 deletion with a conditional Cre recombinase or other SIRT5 deficiency/inhibition models such as retrovirus or lentivirus-mediated knockdown may provide valuable insights into CD8<sup>+</sup> T cell functionality and differentiation due to the lack of systemic adaptations.

In summary, we reported here that CD8<sup>+</sup> T cell memory differentiation and effector function were not impacted in the absence of SIRT5. Strikingly, the deletion of SIRT5 in CD8<sup>+</sup> T cells did not lead to significant phenotypic changes through our *in vitro* and *in vivo* analysis, indicating that SIRT5 may be dispensable for differentiation and function of CD8<sup>+</sup> T cells. Considering the redundant functions of other sirtuin family members that could compensate the deficiency of SIRT5 and the requirement of extreme induction condition in CD8<sup>+</sup> T cells, we will focus our studies on the roles of SIRT5 in the CD8<sup>+</sup> T cell immune response under specific conditions, such as the tumor microenvironment.

## DATA AVAILABILITY STATEMENT

The original contributions presented in the study are included in the article/**Supplementary Material**, further inquiries can be directed to the corresponding author.

## ETHICS STATEMENT

The animal study was reviewed and approved by Animal experiments were approved by the Institutional Animal Care and Use Committee (IACUC) of Suzhou Institution of System Medicine.

## AUTHOR CONTRIBUTIONS

QD and JD performed most experiments. QD wrote the manuscript. FL provided help to maintain the mouse line. XL helped for the genotyping. HY kindly provided the Sirt5<sup>-/-</sup> mice and valuable discussions. YZ, YL, and LZ revised the manuscript. LZ designed and supervised the project. All authors read the manuscript and approved the submitted version.

## FUNDING

QD was supported by the Natural Science Foundation of Jiangsu Province (BK20200240), the China Postdoctoral Science Foundation (2020M670219), and Natural Science Foundation of China (NSFC 82101829). LZ was supported, in part, by Natural Science Foundation of China (NSFC 81971466), the Special Research Fund for Central Universities, Peking Union Medical College (2021-PT180-001) and CAMS Innovation Fund for Medical Sciences (CIFMS 2021-1-I2M-061).

## ACKNOWLEDGMENTS

We thank HY at Department of Systems Biology for Medicine, School of Basic Medical Sciences, Fudan University, for kindly providing C57BL/6 Sirt5<sup>-/-</sup> mice.

## SUPPLEMENTARY MATERIAL

The Supplementary Material for this article can be found online at: <https://www.frontiersin.org/articles/10.3389/fcell.2021.761193/full#supplementary-material>

**Supplementary Figure S1 | (A)** The mRNA expression of SIRT5 in purified CD8<sup>+</sup> T cell populations including naïve, effector, and memory CD8<sup>+</sup> T cells, and PMs stimulated with LPS or not. The activated CD8<sup>+</sup> T cells were further induced by IL-2/7 or IL-7/15 for 4 days, as indicated in **Figure 1**. *In vivo* memory CD8<sup>+</sup> T cells were sorted from the spleens of OT-1 transferred mice on day 45 after LM-OVA infection. PMs were obtained as indicated in **Figure 1** and were stimulated with LPS for 12 hours. **(B)** Surface activation marker expression of Sirt5<sup>+/+</sup> and Sirt5<sup>-/-</sup> OT-1 cells at the time points of 24 h and 6 days assessed by flow cytometry.

**Supplementary Figure S2** | The effect of SIRT5 on the cytokine secretion ability of CD8<sup>+</sup> T cells from lymphocyte nodes of separate transferred mice. **(A)** Representative dot plots of IL-2, TNF $\alpha$ , and IFN $\gamma$  expression levels of OT-1 cells from lymphocyte nodes by flow cytometry in vitro restimulation. The transferred mice are sacrificed on day 34 after primary LM-OVA infection. **(B)** Statistical analysis of OT-1 cell ratio of cytokine experiment. Mean  $\pm$  SD ( $n = 9$ ), Student's t-test; ns, not significant.

**Supplementary Figure S3** | The effect of SIRT5 on the cytokine secretion ability of CD8<sup>+</sup> T cells from lymphocyte nodes of co-transferred mice. **(A)** Representative dot plots of IL-2, TNF $\alpha$ , and IFN $\gamma$  expression levels of OT-1 cells from lymphocyte nodes by flow cytometry in vitro restimulation. The transferred mice are sacrificed on day 25 after secondary LM-OVA infection. **(B)** Statistical analysis of OT-1 cell ratio of cytokine experiment. Mean  $\pm$  SD ( $n = 6$ ), Student's t-test; ns, not significant.

## REFERENCES

- Bengsch, B., Spangenberg, H. C., Kersting, N., Neumann-Haefelin, C., Panther, E., von Weizsäcker, F., et al. (2007). Analysis of CD127 and KLRG1 Expression on Hepatitis C Virus-specific CD8<sup>+</sup> T Cells Reveals the Existence of Different Memory T-Cell Subsets in the Peripheral Blood and Liver. *J. Virol.* 81, 945–953. doi:10.1128/JVI.01354-06
- Buler, M., Aatsinki, S. M., Izzi, V., Uusimaa, J., and Hakkola, A. J. (2014). SIRT5 Is under the Control of PGC-1 $\alpha$  and AMPK and Is Involved in Regulation of Mitochondrial Energy Metabolism. *FASEB J.* 28, 3225–3237. doi:10.1096/fj.13-245241
- Chang, C.-H., Curtis, J. D., Maggi, L. B., Jr., Faubert, B., Villarino, A. V., O'Sullivan, A., et al. (2013). Posttranscriptional Control of T Cell Effector Function by Aerobic Glycolysis. *Cell* 153, 1239–1251. doi:10.1016/j.cell.2013.05.016
- Cheeran, M. C., Hu, S., Palmquist, J. M., Bakken, T., Gekker, G., and Lokensgard, J. R. (2007). Dysregulated Interferon-Gamma Responses during Lethal Cytomegalovirus Brain Infection of IL-12-deficient Mice. *Virus Res.* 130, 96–102. doi:10.1016/j.virusres.2007.05.022
- Ciarlo, E., Heinonen, T., Lugrin, J., Acha-Orbea, H., Le Roy, D., Auwerx, J., et al. (2017). Sirtuin 3 Deficiency Does Not Alter Host Defenses against Bacterial and Fungal Infections. *Sci. Rep.* 7, 3853. doi:10.1038/s41598-017-04263-x
- Du, J., Zhou, Y., Su, X., Yu, J. J., Khan, S., Jiang, H., et al. (2011). Sirt5 Is a NAD-dependent Protein Lysine Demalonylase and Desuccinylase. *Science* 334, 806–809. doi:10.1126/science.1207861
- Duan, Q., Li, D., Xiong, L., Chang, Z., and Xu, G. (2019). SILAC Quantitative Proteomics and Biochemical Analyses Reveal a Novel Molecular Mechanism by Which ADAM12S Promotes the Proliferation, Migration, and Invasion of Small Cell Lung Cancer Cells through Upregulating Hexokinase 1. *J. Proteome Res.* 18, 2903–2914. doi:10.1021/acs.jproteome.9b00208
- Fernandez-Marcos, P. J., Jenning, E. H., Canto, C., Harach, T., De Boer, V. C. J., Andreux, P., et al. (2012). Muscle or Liver-specific Sirt3 Deficiency Induces Hyperacetylation of Mitochondrial Proteins without Affecting Global Metabolic Homeostasis. *Sci. Rep.* 2, 425. doi:10.1038/srep00425
- Hallows, W. C., Yu, W., Smith, B. C., Devires, M. K., Ellinger, J. J., Someya, S., et al. (2011). Sirt3 Promotes the Urea Cycle and Fatty Acid Oxidation during Dietary Restriction. *Mol. Cell* 41, 139–149. doi:10.1016/j.molcel.2011.01.002
- Hamaidi, L., Zhang, L., Kim, N., Wang, M.-H., Iclozan, C., Fang, B., et al. (2020). Sirt2 Inhibition Enhances Metabolic Fitness and Effector Functions of Tumor-Reactive T Cells. *Cel Metab.* 32, 420–436. doi:10.1016/j.cmet.2020.07.008
- He, J., Shanguan, X., Zhou, W., Cao, Y., Zheng, Q., Tu, J., et al. (2021). Glucose Limitation Activates AMPK Coupled SENP1-Sirt3 Signalling in Mitochondria for T Cell Memory Development. *Nat. Commun.* 12, 4371. doi:10.1038/s41467-021-24619-2
- Heinonen, T., Ciarlo, E., Le Roy, D., and Roger, T. (2019). Impact of the Dual Deletion of the Mitochondrial Sirtuins SIRT3 and SIRT5 on Anti-microbial Host Defenses. *Front. Immunol.* 10, 2341. doi:10.3389/fimmu.2019.02341
- Heinonen, T., Ciarlo, E., Théroude, C., Pelekanou, A., Herderschee, J., Le Roy, D., et al. (2018). Sirtuin 5 Deficiency Does Not Compromise Innate Immune Responses to Bacterial Infections. *Front. Immunol.* 9, 2675. doi:10.3389/fimmu.2018.02675
- Hirschey, M. D., Shimazu, T., Jing, E., Grueter, C. A., Collins, A. M., Auouizerat, B., et al. (2011). SIRT3 Deficiency and Mitochondrial Protein Hyperacetylation Accelerate the Development of the Metabolic Syndrome. *Mol. Cell* 44, 177–190. doi:10.1016/j.molcel.2011.07.019
- Houtkooper, R. H., Pirinen, E., and Auwerx, J. (2012). Sirtuins as Regulators of Metabolism and Healthspan. *Nat. Rev. Mol. Cell Biol.* 13, 225–238. doi:10.1038/nrm3293
- Jeng, M. Y., Hull, P. A., Fei, M., Kwon, H.-S., Tsou, C.-L., Kasler, H., et al. (2018). Metabolic Reprogramming of Human CD8<sup>+</sup> Memory T Cells through Loss of SIRT1. *J. Exp. Med.* 215, 51–62. doi:10.1084/jem.20161066
- Kumar, S., and Lombard, D. B. (2018). Functions of the Sirtuin Deacetylase SIRT5 in normal Physiology and Pathobiology. *Crit. Rev. Biochem. Mol. Biol.* 53, 311–334. doi:10.1080/10409238.2018.1458071
- Li, F., He, X., Ye, D., Lin, Y., Yu, H., Yao, C., et al. (2015). NADP<sup>+</sup>-IDH Mutations Promote Hypersuccinylation that Impairs Mitochondria Respiration and Induces Apoptosis Resistance. *Mol. Cell* 60, 661–675. doi:10.1016/j.molcel.2015.10.017
- Lin, Z.-F., Xu, H.-B., Wang, J.-Y., Lin, Q., Ruan, Z., Liu, F.-B., et al. (2013). SIRT5 Desuccinylates and Activates SOD1 to Eliminate ROS. *Biochem. Biophysical Res. Commun.* 441, 191–195. doi:10.1016/j.bbrc.2013.10.033
- Liu, G., Bi, Y., Xue, L., Zhang, Y., Yang, H., Chen, X., et al. (2015). Dendritic Cell SIRT1-Hif1 $\alpha$  axis Programs the Differentiation of CD4<sup>+</sup> T Cells through IL-12 and TGF- $\beta$ 1. *Proc. Natl. Acad. Sci. USA* 112, E957–E965. doi:10.1073/pnas.1420419112
- Nishida, Y., Rardin, M. J., Carrico, C., He, W., Sahu, A. K., Gut, P., et al. (2015). SIRT5 Regulates Both Cytosolic and Mitochondrial Protein Malonylation with Glycolysis as a Major Target. *Mol. Cell* 59, 321–332. doi:10.1016/j.molcel.2015.05.022
- Norata, G. D., Caligiuri, G., Chavakis, T., Matarese, G., Netea, M. G., Nicoletti, A., et al. (2015). The Cellular and Molecular Basis of Translational Immunometabolism. *Immunity* 43, 421–434. doi:10.1016/j.immuni.2015.08.023
- Ogura, M., Nakamura, Y., Tanaka, D., Zhuang, X., Fujita, Y., Obara, A., et al. (2010). Overexpression of SIRT5 Confirms its Involvement in Deacetylation and Activation of Carbamoyl Phosphate Synthetase 1. *Biochem. Biophysical Res. Commun.* 393, 73–78. doi:10.1016/j.bbrc.2010.01.081
- O'Neill, L. A. J., and Pearce, E. J. (2016). Immunometabolism Governs Dendritic Cell and Macrophage Function. *J. Exp. Med.* 213, 15–23. doi:10.1084/jem.20151570
- Park, J., Chen, Y., Tishkoff, D. X., Peng, C., Tan, M., Dai, L., et al. (2013). SIRT5-mediated Lysine Desuccinylation Impacts Diverse Metabolic Pathways. *Mol. Cell* 50, 919–930. doi:10.1016/j.molcel.2013.06.001
- Pritchard, G. H., Kedl, R. M., and Hunter, C. A. (2019). The Evolving Role of T-Bet in Resistance to Infection. *Nat. Rev. Immunol.* 19, 398–410. doi:10.1038/s41577-019-0145-4
- Qiu, X., Brown, K., Hirschey, M. D., Verdin, E., and Chen, D. (2010). Calorie Restriction Reduces Oxidative Stress by SIRT3-Mediated SOD2 Activation. *Cel Metab.* 12, 662–667. doi:10.1016/j.cmet.2010.11.015
- Rardin, M. J., He, W., Nishida, Y., Newman, J. C., Carrico, C., Danielson, S. R., et al. (2013). SIRT5 Regulates the Mitochondrial Lysine Succinylome and Metabolic Networks. *Cel Metab.* 18, 920–933. doi:10.1016/j.cmet.2013.11.013
- Renkema, K. R., Huggins, M. A., Borges Da Silva, H., Knutson, T. P., Henzler, C. M., and Hamilton, S. E. (2020). KLRG1<sup>+</sup> Memory CD8<sup>+</sup> T Cells Combine Properties of Short-Lived Effectors and Long-Lived Memory. *J. I.* 205, 1059–1069. doi:10.4049/jimmunol.1901512
- Sadhukhan, S., Liu, X., Ryu, D., Nelson, O. D., Stupinski, J. A., Li, Z., et al. (2016). Metabolomics-assisted Proteomics Identifies Succinylation and SIRT5 as Important Regulators of Cardiac Function. *Proc. Natl. Acad. Sci. USA* 113, 4320–4325. doi:10.1073/pnas.1519858113
- Sheng, S., Kang, Y., Guo, Y., Pu, Q., Cai, M., and Tu, Z. (2015). Overexpression of Sirt3 Inhibits Lipid Accumulation in Macrophages through Mitochondrial IDH2 Deacetylation. *Int. J. Clin. Exp. Pathol.* 8, 9196–9201.
- Song, J., Yang, B., Jia, X., Li, M., Tan, W., Ma, S., et al. (2018). Distinctive Roles of Sirtuins on Diabetes, Protective or Detrimental? *Front. Endocrinol.* 9, 724. doi:10.3389/fendo.2018.00724
- Sukumar, M., Liu, J., Mehta, G. U., Patel, S. J., Roychoudhuri, R., Crompton, J. G., et al. (2016). Mitochondrial Membrane Potential Identifies Cells with Enhanced Stemness for Cellular Therapy. *Cel Metab.* 23, 63–76. doi:10.1016/j.cmet.2015.11.002
- Tan, M., Peng, C., Anderson, K. A., Chhoy, P., Xie, Z., Dai, L., et al. (2014). Lysine Glutarylation Is a Protein Posttranslational Modification Regulated by SIRT5. *Cel Metab.* 19, 605–617. doi:10.1016/j.cmet.2014.03.014

- Wang, F., Wang, K., Xu, W., Zhao, S., Ye, D., Wang, Y., et al. (2017). SIRT5 Desuccinylates and Activates Pyruvate Kinase M2 to Block Macrophage IL-1 $\beta$  Production and to Prevent DSS-Induced Colitis in Mice. *Cel Rep.* 19, 2331–2344. doi:10.1016/j.celrep.2017.05.065
- Williams, M. A., and Bevan, M. J. (2007). Effector and Memory CTL Differentiation. *Annu. Rev. Immunol.* 25, 171–192. doi:10.1146/annurev.immunol.25.022106.141548
- Yu, J., Sadhukhan, S., Noriega, L. G., Moullan, N., He, B., Weiss, R. S., et al. (2013). Metabolic Characterization of a Sirt5 Deficient Mouse Model. *Sci. Rep.* 3, 2806. doi:10.1038/srep02806
- Yu, Q., Dong, L., Li, Y., and Liu, G. (2018). SIRT1 and HIF1 $\alpha$  Signaling in Metabolism and Immune Responses. *Cancer Lett.* 418, 20–26. doi:10.1016/j.canlet.2017.12.035
- Zhang, C., Wang, K., Hu, Z., Yang, L., Wei, B., Li, S., et al. (2020). SIRT5 Is Important for Bacterial Infection by Regulating Insulin Secretion and Glucose Homeostasis. *Protein Cell* 11, 846–851. doi:10.1007/s13238-020-00709-7
- Zhang, L., and Romero, P. (2018). Metabolic Control of CD8(+) T Cell Fate Decisions and Antitumor Immunity. *Trends Mol. Med.* 24, 30–48. doi:10.1016/j.molmed.2017.11.005
- Zhao, X., Shan, Q., and Xue, H. H. (2021). TCF1 in T Cell Immunity: a Broadened Frontier. *Nat. Rev. Immunol.* doi:10.1038/s41577-021-00563-6
- Zhou, L., Wang, F., Sun, R., Chen, X., Zhang, M., Xu, Q., et al. (2016). SIRT5 Promotes IDH2 Desuccinylation and G6PD Deglutarylation to Enhance Cellular Antioxidant Defense. *EMBO Rep.* 17, 811–822. doi:10.15252/embr.201541643
- Zoon, C. K., Wan, W., Graham, L., and Bear, H. D. (2017). Expansion of T Cells with Interleukin-21 for Adoptive Immunotherapy of Murine Mammary Carcinoma. *Int. J. Mol. Sci.* 18, 270. doi:10.3390/ijms18020270

**Conflict of Interest:** The authors declare that the research was conducted in the absence of any commercial or financial relationships that could be construed as a potential conflict of interest.

The reviewer DY declared a shared affiliation with one of the authors HY to the handling Editor.

**Publisher's Note:** All claims expressed in this article are solely those of the authors and do not necessarily represent those of their affiliated organizations or those of the publisher, the editors, and the reviewers. Any product that may be evaluated in this article, or claim that may be made by its manufacturer, is not guaranteed or endorsed by the publisher.

Copyright © 2021 Duan, Ding, Li, Liu, Zhao, Yu, Liu and Zhang. This is an open-access article distributed under the terms of the Creative Commons Attribution License (CC BY). The use, distribution or reproduction in other forums is permitted, provided the original author(s) and the copyright owner(s) are credited and that the original publication in this journal is cited, in accordance with accepted academic practice. No use, distribution or reproduction is permitted which does not comply with these terms.





# Arginylation Regulates G-protein Signaling in the Retina

Marie E. Fina<sup>1</sup>, Junling Wang<sup>1</sup>, Pavan Vedula<sup>1</sup>, Hsin-Yao Tang<sup>2</sup>, Anna Kashina<sup>1\*</sup> and Dawei W. Dong<sup>1,3\*</sup>

<sup>1</sup>Department of Biomedical Sciences, School of Veterinary Medicines, University of Pennsylvania, Philadelphia, PA, United States,

<sup>2</sup>Proteomics and Metabolomics Facility, The Wistar Institute, Philadelphia, PA, United States, <sup>3</sup>Institute for Biomedical Informatics, Perelman School of Medicine, University of Pennsylvania, Philadelphia, PA, United States

## OPEN ACCESS

### Edited by:

Fangliang Zhang,  
University of Miami, United States

### Reviewed by:

Marta E. Hallak,  
National University of Cordoba,  
Argentina  
Tomomi Ichinose,  
Wayne State University, United States

### \*Correspondence:

Anna Kashina  
akashina@upenn.edu  
Dawei W. Dong  
ddong@upenn.edu

### Specialty section:

This article was submitted to  
Cellular Biochemistry,  
a section of the journal  
Frontiers in Cell and Developmental  
Biology

**Received:** 02 November 2021

**Accepted:** 17 December 2021

**Published:** 21 January 2022

### Citation:

Fina ME, Wang J, Vedula P, Tang H-Y,  
Kashina A and Dong DW (2022)  
Arginylation Regulates G-protein  
Signaling in the Retina.  
Front. Cell Dev. Biol. 9:807345.  
doi: 10.3389/fcell.2021.807345

Arginylation is a post-translational modification mediated by the arginyltransferase (Ate1). We recently showed that conditional deletion of Ate1 in the nervous system leads to increased light-evoked response sensitivities of ON-bipolar cells in the retina, indicating that arginylation regulates the G-protein signaling complexes of those neurons and/or photoreceptors. However, none of the key players in the signaling pathway were previously shown to be arginylated. Here we show that Gαt1, Gβ1, RGS6, and RGS7 are arginylated in the retina and RGS6 and RGS7 protein levels are elevated in Ate1 knockout, suggesting that arginylation plays a direct role in regulating their protein level and the G-protein-mediated responses in the retina.

**Keywords:** arginylation, G-protein signaling, RGS, retina, mass spectrometry

## 1 INTRODUCTION

Arginylation is a post-translational modification that has been implicated in a large number of key physiological processes (see, e.g., Zanakakis et al., 1984; Bongiovanni et al., 1999; Kwon et al., 2002; Hu et al., 2005; Karakozova et al., 2006; Decca et al., 2007; Rai et al., 2008; Saha and Kashina, 2011; Lee et al., 2012; Jiang et al., 2016; Wang et al., 2017a; Wang et al., 2017b). It was initially characterized as a post-translational modification of the protein N-termini for ubiquitin-proteasomal degradation (Ciechanover et al., 1988; Balzi et al., 1990). N-terminal arginylation can target proteins for degradation both *in vitro* (Davydov and Varshavsky, 2000) and *in vivo* (Lee et al., 2005) via ubiquitin-proteasome dependent N-end rule pathway (Varshavsky, 2011). While initially arginylation was believed to be exclusively targeting the N-terminal Asp, Glu, or Cys, as well as Asn and Gln upon deamidation, it has been later shown that arginylation can also target internal Asp and Glu residues by conjugating Arg to their acidic side chains (Wang et al., 2014). This discovery expands the scope of potentially arginylated proteins.

G-protein signaling is involved in virtually every known physiological process and plays a major role in neural signal transduction (Stewart and Fisher, 2015; Squires et al., 2018). It involves three crucial components: G-protein coupled receptors (GPCRs), G-protein heterotrimers, and Regulator of G-protein signaling (RGS) proteins. Upon stimulation, GPCRs facilitate the formation of Gα-GTP and promote the dissociation of Gα and Gβγ from each other and from GPCRs. Opposite to GPCRs, RGS proteins accelerate the termination of G-protein signaling by facilitating hydrolysis of the GTP bound to the Gα subunit of the G-protein, and thus promoting its re-association with Gβγ subunits and GPCRs (De Vries et al., 1995; Dohlman et al., 1995; Druey et al., 1996; Hunt et al., 1996; Koelle and Horvitz, 1996; Watson et al., 1996).

We recently discovered that conditional deletion of arginyltransferase (Ate1) in the nervous system affects G-protein signaling in the retina. In particular, lack of Ate1 leads to increased light-

**TABLE 1 |** Components of the G-protein signaling complexes in the retina screened for arginylation. The coverage is calculated with the MS/MS peptides identified during tryptic/P search against the whole mouse proteome without including arginylation into the search. The depth is the average number of MS/MS scans of the identified peptides over each covered amino acid (AA) base. Rgs9 (short) isoform and Gnb5 (long) isoform are listed. The latter encodes two protein isoforms: G $\beta$ 5 and G $\beta$ 5L. The three well-known G-protein signaling complexes in the retina are: RHO-G $\alpha$ t1-G $\beta$ 1-G $\gamma$ t1-RGS9-G $\beta$ 5L, OPN1MW/OPN1SW-G $\alpha$ t2-G $\beta$ 3-G $\gamma$ 2-RGS9-G $\beta$ 5L, mGluR6-G $\alpha$ o-G $\beta$ 3-G $\gamma$ 13-RGS7/RGS11-G $\beta$ 5.

Gene name	AA length	Coverage(%)	depth	protein symbol	protein name
Gnao1	354	63	131	G $\alpha$ o	G-proteins
Gnat1	350	75	373	G $\alpha$ t1	G-protein Go subunit alpha
Gnat2	354	64	132	G $\alpha$ t2	G-protein Gt subunit alpha-1
Gnb1	340	74	285	G $\beta$ 1	G-protein Gi,s,t subunit beta-1
Gnb3	340	67	53	G $\beta$ 3	G-protein Gi,s,t subunit beta-3
Gng2	71	72	11	G $\gamma$ 2	G-protein Gi,s,o subunit gamma-2
Gng13	67	84	7	G $\gamma$ 13	G-protein Gi,s,o subunit gamma-13
Gngt1	74	84	225	G $\gamma$ t1	G-protein Gt subunit gamma-T1
Grm6	871	19	2	mGluR6	G-protein coupled receptors
Opn1mw	359	19	6	OPN1MW	Metabotropic glutamate receptor 6
Opn1sw	346	29	16	OPN1SW	Medium-wave-sensitive opsin 1
Rho	348	32	202	RHO	Short-wave-sensitive opsin 1
					Rhodopsin
Gnb5	395	56	31	G $\beta$ 5(L)	GTPase accelerating proteins
Rgs6	472	47	11	RGS6	G-protein subunit beta-5
Rgs7	469	28	13	RGS7	Regulator of G-protein signaling 6
Rgs9	484	75	23	RGS9	Regulator of G-protein signaling 7
Rgs11	443	2.9	2	RGS11	Regulator of G-protein signaling 9
					Regulator of G-protein signaling 11

evoked response sensitivities of ON-bipolar cells, as well as their downstream neurons (Fina et al., 2021), indicating that arginylation might be involved in the three G-protein signaling complexes of the first two stages of visual signal transduction. Among the GPCRs, G-proteins, and RGSs in the mouse retina (see Table 1), RHO, G $\beta$ 5L, G $\gamma$ 13, and RGS11 have the N-end rule residues, while others have the potential to be arginylated on the side chains. However, none of them are known to be arginylated.

Here we performed mass spectrometry analysis of mouse retina, using both our own data and data from the public domain, to investigate if any of the proteins involved in G-protein signaling in the retina are arginylated. We found that G $\alpha$ t1, G $\beta$ 1, RGS6 and RGS7 were arginylated. Immunostaining revealed a prominent increase in the levels of RGS6 and its obligatory binding partner G $\beta$ 5 in synaptic processes of starburst amacrine cells of Ate1 knockout retina, corroborating our previous finding that RGS7 and G $\beta$ 5 increase in synaptic processes of ON-bipolar cells. We propose that arginylation regulates RGS6 and RGS7 levels and thus regulates G-protein signaling in the retina.

## 2 METHODS

### 2.1 Generation of Ate1 Conditional Knockout Mice

To obtain brain-specific Ate1 knockout mice, Ate1-floxed mice (Leu et al., 2009; Kurosaka et al., 2010) were crossed with the Jackson Laboratory strain B6.Cg-Tg(Nes-cre)1Kln/J, expressing Cre recombinase under Nesting promoter. Mice were maintained

in C57BL6/129SVJ background in accordance with the University of Pennsylvania IACUC.

### 2.2 Immunohistochemistry and Data Processing

Retina collection and immunostaining was performed as previously described (Fina et al., 2021). Briefly, mice were dark adapted overnight and euthanized with a mixture containing ketamine/xylazine (300  $\mu$ g each per g body-weight). Immediately after the euthanasia, eyes were enucleated and the cornea removed under dim red-light. Eyeballs were fixed in the dark in 4% paraformaldehyde for 60 min, rinsed in phosphate buffer (PB) 3 times, cryoprotected overnight at 4°C in 0.1M PB containing 30% sucrose and then, with the lens removed, embedded in a mixture of two parts 20% sucrose in PB and one part optimal cutting temperature compound (Tissue Tek, Electron Microscopy Sciences, Hateld, PA, United States). Radial sections were stained with antibodies and imaged using a confocal laser scanning microscope (Olympus Fluoview 1,000, Center Valley, PA, United States) under an oil-immersion objective (Tummala et al., 2016). Littermate retinas from WT and KO mice were immunostained and imaged in parallel under the same conditions and settings. To compensate the exposure difference between imaging of retinal slides, each set of images from the same retinal slide was normalized by the non-specific signal in the outer nuclear layer (ONL).

For image quantification, a region of interest (ROI, of the same 6  $\times$  6  $\mu$ m area size for WT and KO mice) was positioned on the lines drawn manually along the bands of stained starburst amacrine cell (SAC) processes in the inner plexiform layer

(IPL), and the intensity measurement for each pixel was taken from the average z-stacks (of the same 0.3  $\mu\text{m}$ /slice thickness for WT and KO mice) using MATLAB software (MathWorks, Natick, MA, United States). The pixel intensity was thresholded by the background—the non-specific signal in ONL. The average intensity of the pixels in the ROI was calculated for each section to represent the immunostaining level in IPL, averaged along the SAC bands for each section, and then averaged over 1 to 4 sections per retina.

## 2.3 mRNA Sequencing and Analysis

Tissue collection and processing was performed as previously described (Fina et al., 2021). Briefly, freshly excised mouse brains were flash-frozen in liquid nitrogen and ground in liquid nitrogen using mortar and pestle to obtain whole brain lysates. Total RNA was extracted using Trizol, and RNA sequencing (stranded TruSeq with Ribo-Zero, Illumina, San Diego, CA, United States) was used to quantify mRNA levels in the whole brain lysates of 3 littermate pairs of 3 month old mice and analyzed using STAR software package (Dobin et al., 2013).

## 2.4 Mass Spectrometry

Freshly excised mouse retinas, with the cornea and the lens removed, were flash-frozen in liquid nitrogen and ground up in liquid nitrogen to obtain retinal lysates. The retinal proteins were pulled down with phalloidin (manuscript in preparation).

For mass spectrometry, the resulting protein samples of 4 retinas of 6 month old mice were reduced with tris(2-carboxyethyl)phosphine (TCEP), alkylated with iodoacetamide, and digested with trypsin. Tryptic digests were analyzed using a 1.5 h LC gradient on the Thermo Q Exactive Plus mass spectrometer.

## 2.5 Mass Spectrometry Data Analysis

Data analysis was performed on the samples described above (processed as .raw files), as well as the original raw data files from public data sets (ProteomeXchange Consortium accession number PXD003441 (Zhao et al., 2016), PXD009909 (Harman et al., 2018), PXD014459 (Sze et al., 2021), and PXD023439 (Chen et al., 2021)), all of which are wild-type mice of C57BL6 backgrounds. The raw data files were processed using MaxQuant software (Version 1.6.7.0 for PXD014459 and 1.6.17.0 for the rest) from Max-Planck Institute for Biochemistry, Martinsried, Germany (Tyanova et al., 2016). To avoid mis-assignment of arginylation to a peptide, for each raw data file, we did two complete search runs, one without arginylation and one with arginylation modifications.

In the first run (without arginylation modifications), all searches were against the mouse protein reference UP000000589 and a locally compiled list of contaminants. In the second run, the “MS/MS first search” (used for mass recalibration in MaxQuant) was the same as the first run but the “MS/MS main search” and the “Second peptide search” were against the proteins of interest (Table 1). In addition, “Match between runs” and “Dependent peptides” were enabled in the second run. Consensus identification lists were generated with false discovery rates of 1% at protein, peptide and site levels. The

two parameter .xml files and the two locally compiled. fasta files are included in the **Supplementary Material**. We excluded the “arginylated” peptides identified in the second run if they were from the scans which have at least one peptide identified in the first run. In addition, we also inspected MS/MS spectra to exclude “arginylated” peptides which could be mistaken for N-terminal or C-terminal arginine due to missed cleavage.

## 2.6 Antibodies and Constructs

Rabbit anti-G $\beta$ 5 (dilution 1:500) was a gift from Dr. C.K. Chen, Baylor College of Medicine, Houston, TX, United States; rabbit anti-RGS6/RGS7 (dilution 1:100) was a gift from Dr. T.G. Wensel, Baylor College of Medicine, Houston, TX, United States.

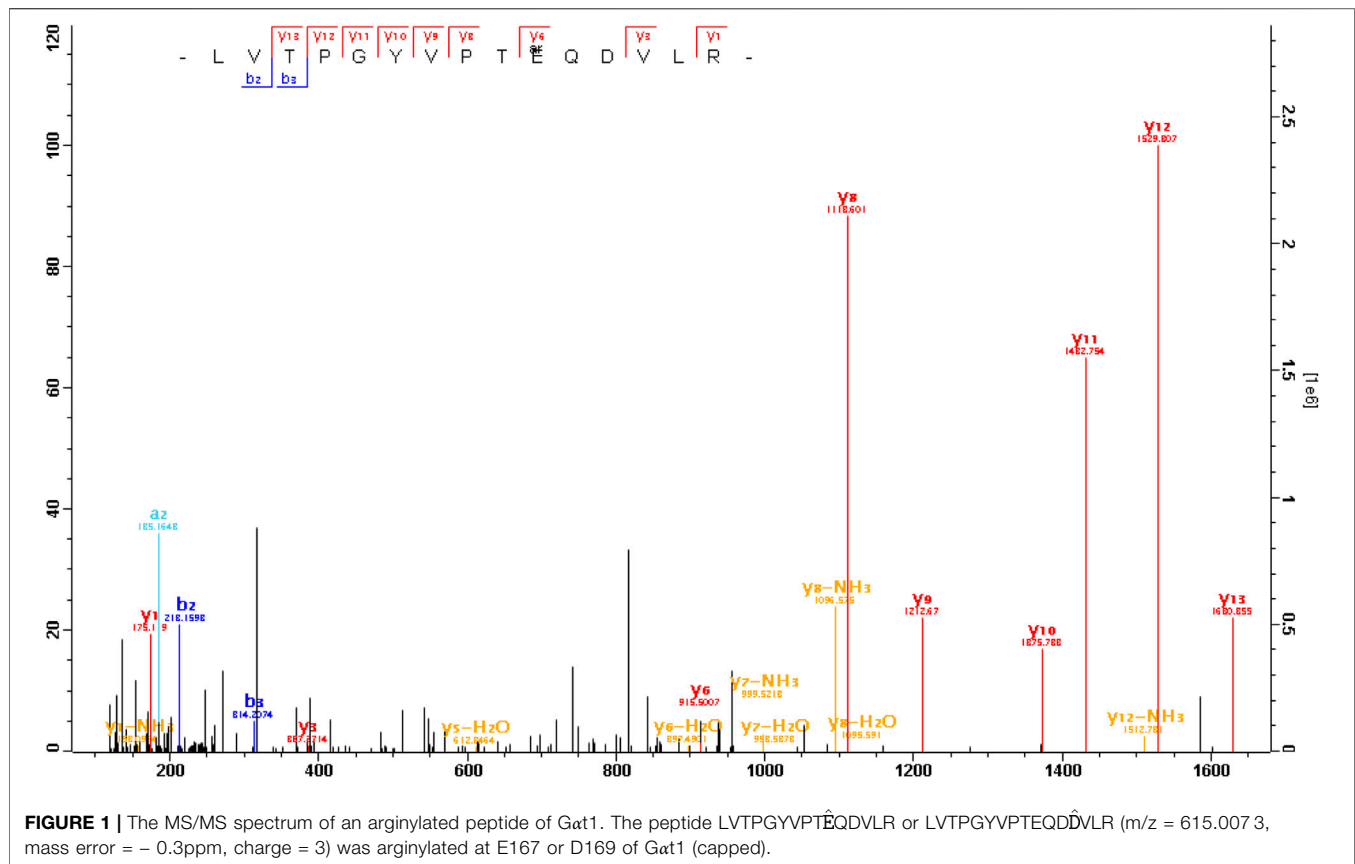
## 2.7 Experimental Design and Statistical Analysis

In the RNA sequencing and the immunostaining experiments, KO and WT littermate pairs were compared pairwise, and the p-values for these comparisons were calculated using paired Student's t-test and paired Wilcoxon t-test (signed-rank test for median) on the 3 and 7 KO/WT pairs, respectively. For the immunostaining experiments, the average staining intensity of all samples on each slide was normalized to 1 and then the average staining intensity of all samples of each WT and KO pair was normalized to 1 in order to reduce the potential experimental variation.

# 3 RESULTS AND DISCUSSIONS

## 3.1 Proteomic Screening for Arginylation of the Components of the G-protein Signaling Complex

We previously reported that the ON-bipolar responses and RGS7 protein levels are regulated by Ate1, however arginylation of RGS7 or in the components of the G-protein signaling complexes which give rise to ON-bipolar responses has never been directly demonstrated. To test whether any of these proteins are arginylated, we analyzed retina samples by mass spectrometry, and searched the results from LC-MS/MS runs for potential arginylation against a limited database including G-proteins, GPCRs, and RGS proteins (Table 1). These candidate proteins were chosen based on the existence of three well characterized G-protein signaling complexes in the retina. In rod and cone photoreceptors, rhodopsins and opsins are the GPCRs responding to photon stimulation in dim and bright light, respectively, and they activate G-proteins Gat1-G $\beta$ 1-G $\gamma$ 1 and Gat2-G $\beta$ 3-G $\gamma$ 2 which are deactivated by RGS9 in the obligatory heterodimer with G $\beta$ 5L (Cowan et al., 1998; He et al., 1998). In ON-bipolar cells, glutamate released by photoreceptors activates the ON-bipolar cells' GPCR, the metabotropic glutamate receptor 6 (mGluR6) receptor, which in turn activates the G $\alpha$ -G $\beta$ 3-G $\gamma$ 13 proteins that can be deactivated by RGS7-G $\beta$ 5 and RGS11-G $\beta$ 5 (Mojumder et al., 2009; Chen et al., 2010; Zhang et al., 2010; Cao et al., 2012). We also included RGS6 in this screen, since it is the



closest family member to RGS7 and is widely distributed in the retina, including prominent representation in the dendrites of cholinergic starburst amacrine cells (Voigt, 1986; Haverkamp and Wässle, 2000; Song et al., 2007).

To search for arginylation of these proteins, we used MaxQuant (Tyanova et al., 2016). To avoid mis-assignment, we first searched all MS/MS scans without arginylation modifications and then searched the unidentified scans with arginylation modifications, including potential addition of unmodified as well as mono- and di-methylated Arg. The search covered the G-proteins (Table 1, top) really well with the coverage ranging between 63 and 84 percent. However, the coverage for GPCRs was low, between 19 and 32 percent (Table 1, middle). This low coverage is likely related to the fact that GPCRs are tightly membrane-bound, and thus a majority of these proteins would be excluded from the soluble retina homogenate. The coverage of RGS and Gβ5, the GTPase accelerating proteins in the retina, varied a lot (Table 1, bottom). Most surprisingly, we found only one peptide for RGS11 in two MS/MS scans, despite the fact that RGS11 has similar molar amounts to RGS7 in the retina (Sarria et al., 2015).

This search revealed several putative arginylated sites, on Gαt1, Gβ1, RGS6, and RGS7. These were the only G-protein and RGS family members identified. We found no instance of arginylation of the GPCRs. In the next sections, we detail the evidence for these arginylation sites.

### 3.2 Putative Arginylated Sites of Gαt1

In outer segments of rod photoreceptors, the transducin Gαt1 binds with Gβ1Gγt1 heterodimer in the dark. Light stimulation activates rhodopsin, which facilitates the formation of Gαt1-GTP and hence promotes the dissociation of Gαt1 from Gβ1γt1 and rhodopsin. This activated Gαt1 then interacts with the downstream phosphodiesterase (PDE6) and starts the phototransduction cascade.

We found that Gαt1 was arginylated at the site of E167 or D169 (Figure 1). This site is located in the middle of the protein and on the opposite side of the interface with PDE6 (Figure 2A). It is within the α-helical domain, near a linker with the β-sheets of the GTPase domain (Figure 2B). This site is also on the solvent-exposed surface of Gαt1Gβ1Gγt1 heterotrimer in the GDP-bound state (Lambright et al., 1996), in a region of Gαt1 α-helical domain, which interacts with Gβ1 when Gαt1 is activated by rhodopsin, thus helping to provide an open route between the α-helical and GTPase domains and facilitating GDP and GTP exchange (Gao et al., 2019). This site is shared between Gαt1, Gαt2, and Gao (Figure 2B). Arginylation of this site can affect the rate of GDP-GTP exchange of these Gα proteins and the G-protein signaling in rods, cones, and ON-bipolar cells.

### 3.3 Putative Arginylated Sites of Gβ1

In the outer segments of the rods, Gβ1 is the important link between Gαt1 and Gγt1. Each of Gαt1 and Gγt1 has a membrane domain, which is not strong enough to anchor Gαt1 or Gβ1Gγt1



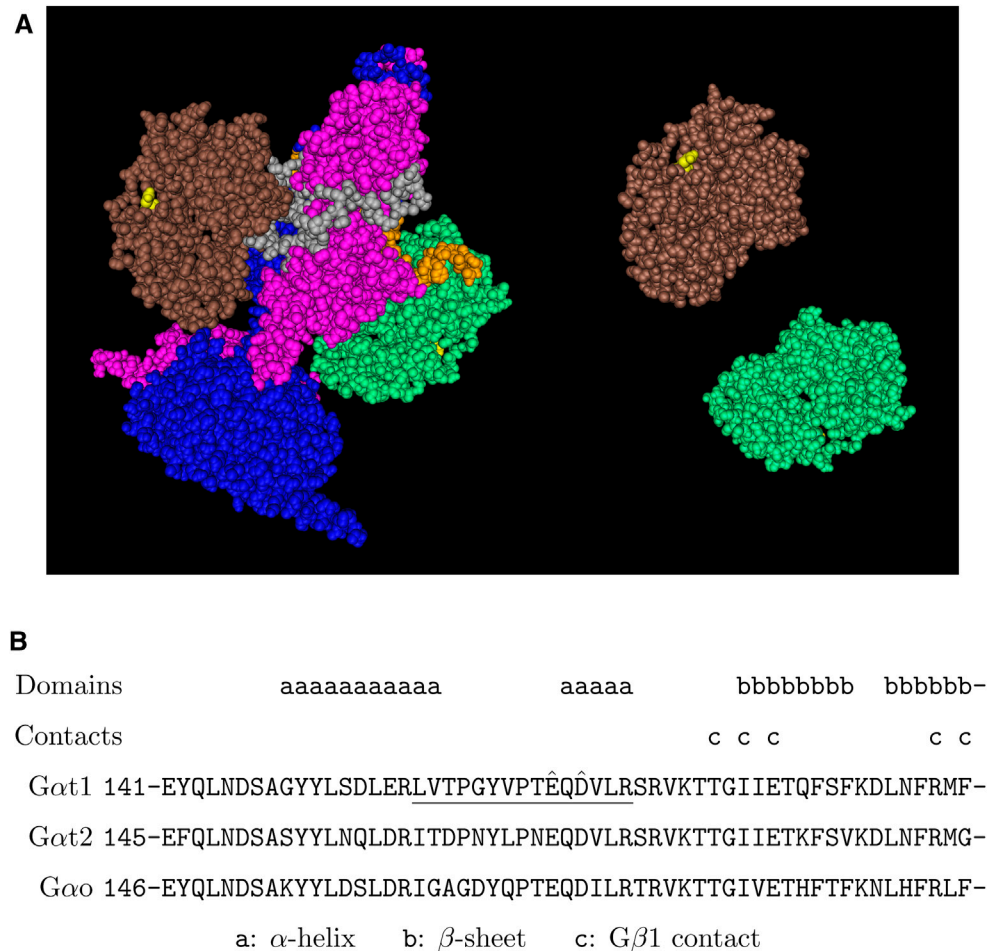


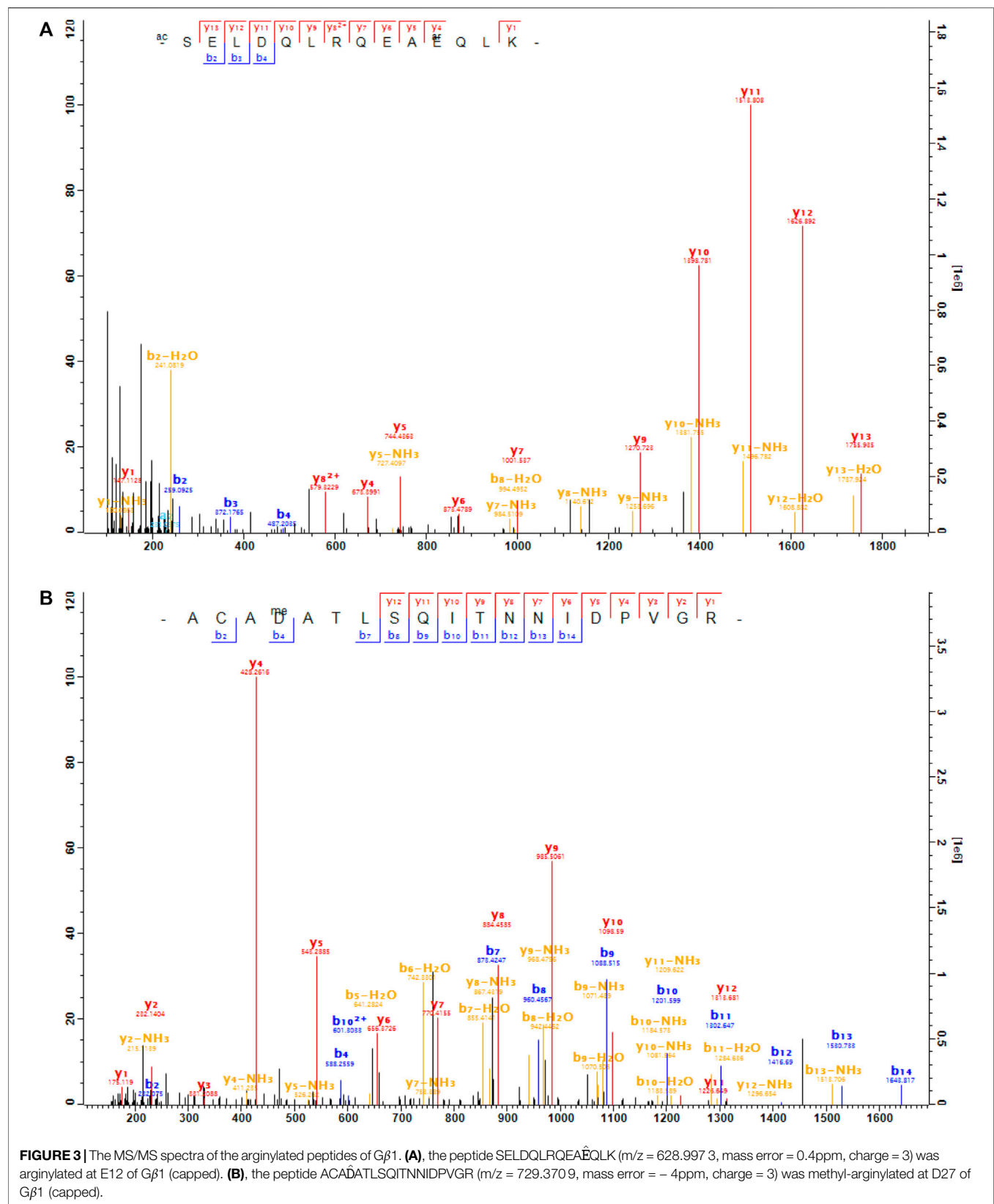
**FIGURE 2 |** Putative arginylation sites of Gat1. **(A)** The 3D structure of 2 Gat1 in the complex with PDE6 based on the structure data 7JSN (Gao et al., 2020). Brown/green: Gat1, blue: PDEα, pink: PDEβ, gray/orange: PDEγ, yellow: Gat1 E167. **(B)** The putative arginylation sites (capped), the peptide (underlined), and the surrounding regions are shown. The putative arginylation sites E167 and D169 are within the α-helical domain of six helices, near the beginning of the 6th α-helix which is connected by a linker region to the 2nd of the six-stranded β-sheets of the Ras-like GTPase domain (Lambright et al., 1996). These sites are shared between Gat1, Gat2, and Gαo.

separately to the disk membrane, but both of them together anchor the heterotrimer in the GDP-bound inactive state. Recently, it has been proposed to play an important role in facilitating GDP-GTP exchange during Gat1 activation (Gao et al., 2019). Gβ1 is also found in the synaptic terminals of the rods (Peng et al., 1992). Interestingly, Gβ1, when translocated to the synaptic terminals of the rods during light adaptation (Whelan and McGinnis, 1988; Sokolov et al., 2002) facilitates the synaptic transmission to ON-bipolar cells (Majumder et al., 2013).

We found that Gβ1 was arginylated at two sites: E12 and D27 (Figure 3). These sites are located near the N-terminus of the protein before the seven-bladed β-propellers (WD40 domains) and in particular D27 is at the junction of the Gβ1 N-terminus, seven-blades, and Gy (Figure 4A). These sites are located within a region of high homology and is conserved between Gβ1, Gβ3, and Gβ5 (Figure 4B). Based on this homology, we propose that these sites can also be arginylated in Gβ3 and possibly in Gβ5. Gβ3

bound with Gy2 plays a similar role in the cones as Gβ1 in the rods. Gβ3 is also found in the synaptic terminals of the cones (Peng et al., 1992). Arginylation of Gβ1 and Gβ3 can potentially affect the phototransduction in the outer segments and the signal transmission to ON-bipolar cells (OBCs) at the synaptic terminals of rods and cones, respectively. In addition, Gβ3 in complex with Gy13 in OBCs facilitates the post-synaptic light-on responses of both rod-OBCs and cone-OBCs (Dhingra et al., 2012; Ramakrishnan et al., 2015) and thus arginylation of Gβ3, if it happens, can potentially affect post-synaptic responses to both rod and cone signals.

Gβ5 is a special Gβ existing as an obligatory heterodimer with all R7 family (RGS6, RGS7, RGS9, RGS11) proteins (Cabrera et al., 1998; Liang et al., 2000; Witherow et al., 2000; Zhang and Simonds, 2000). It has 2 splice variants, Gβ5 (short) and Gβ5L, which includes additional 42 N-terminal amino acid residues added to the Gβ5 (short) sequence. In the retina, the Gβ5L isoform forms an obligatory heterodimer with RGS9 (short),



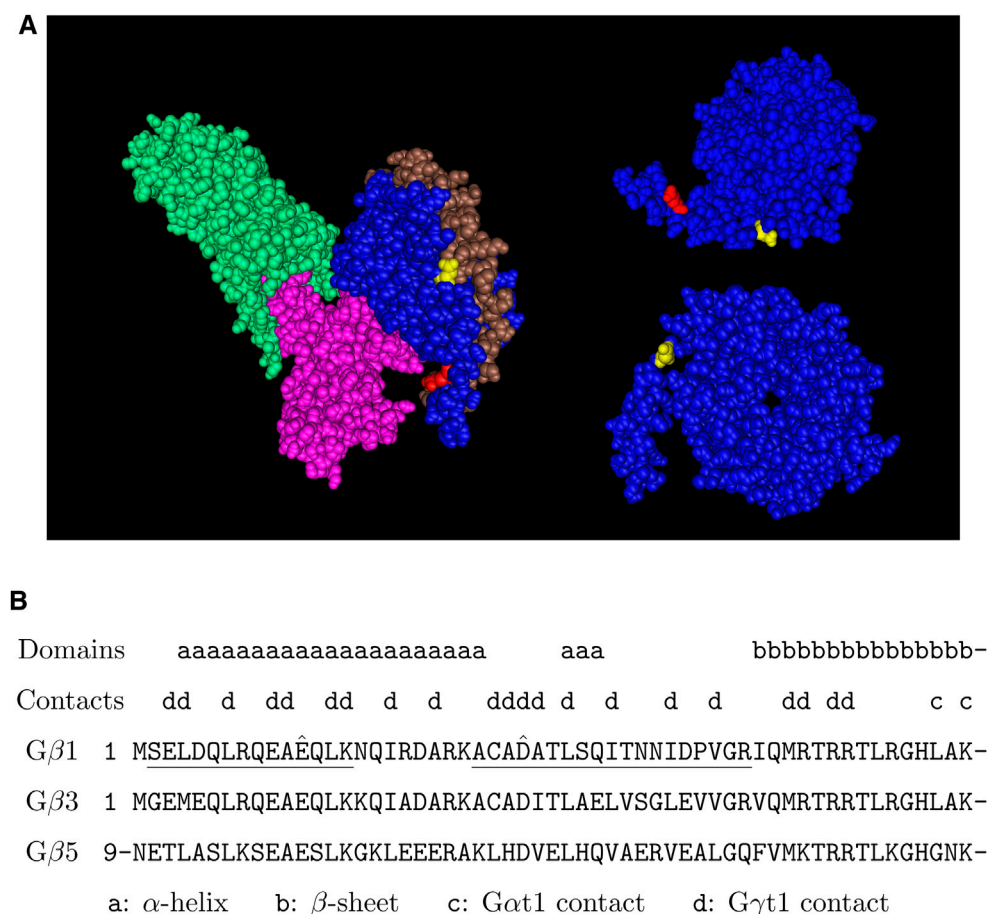


**FIGURE 4 |** Putative arginylation sites of Gβ1. **(A)** The 3D structure of Gβ1 in the Gαt1-Gβ1-Gγt1 heterotrimer in complex with rhodopsin based on the structure data 6OYE (Gao et al., 2019). Blue: Gβ1, brown: Gγt1, pink: Gαt1, green: rhodopsin, red: Gβ1 E12, yellow: Gβ1 D27. **(B)** The putative arginylation sites (capped), the peptides (underlined), and the surrounding regions are shown. The putative arginylation sites are on the N-terminal directly preceding the first β-sheet of the seven WD40 domains (Sondek et al., 1996). These sites are shared between Gβ1, Gβ3, and Gβ5.

and the Gβ5 isoform forms obligatory heterodimers with RGS6, RGS7, or RGS11. Arginylation of Gβ5 can affect all the G-protein signaling in the retina, predominately regulated by R7 family proteins.

### 3.4 Putative Arginylation Sites of RGS6 and RGS7

RGS6 is the closest family member to RGS7 and presumably shares many structural and functional properties with RGS7. We have previously found that the deletion of Arginyltransferase 1 (Ate1) in the retina leads to a prominent increase in the levels of RGS7 and its obligatory binding partner Gβ5 in the dendritic processes of ON-bipolar cells (Fina et al., 2021), but in that work we found no direct evidence of arginylation.

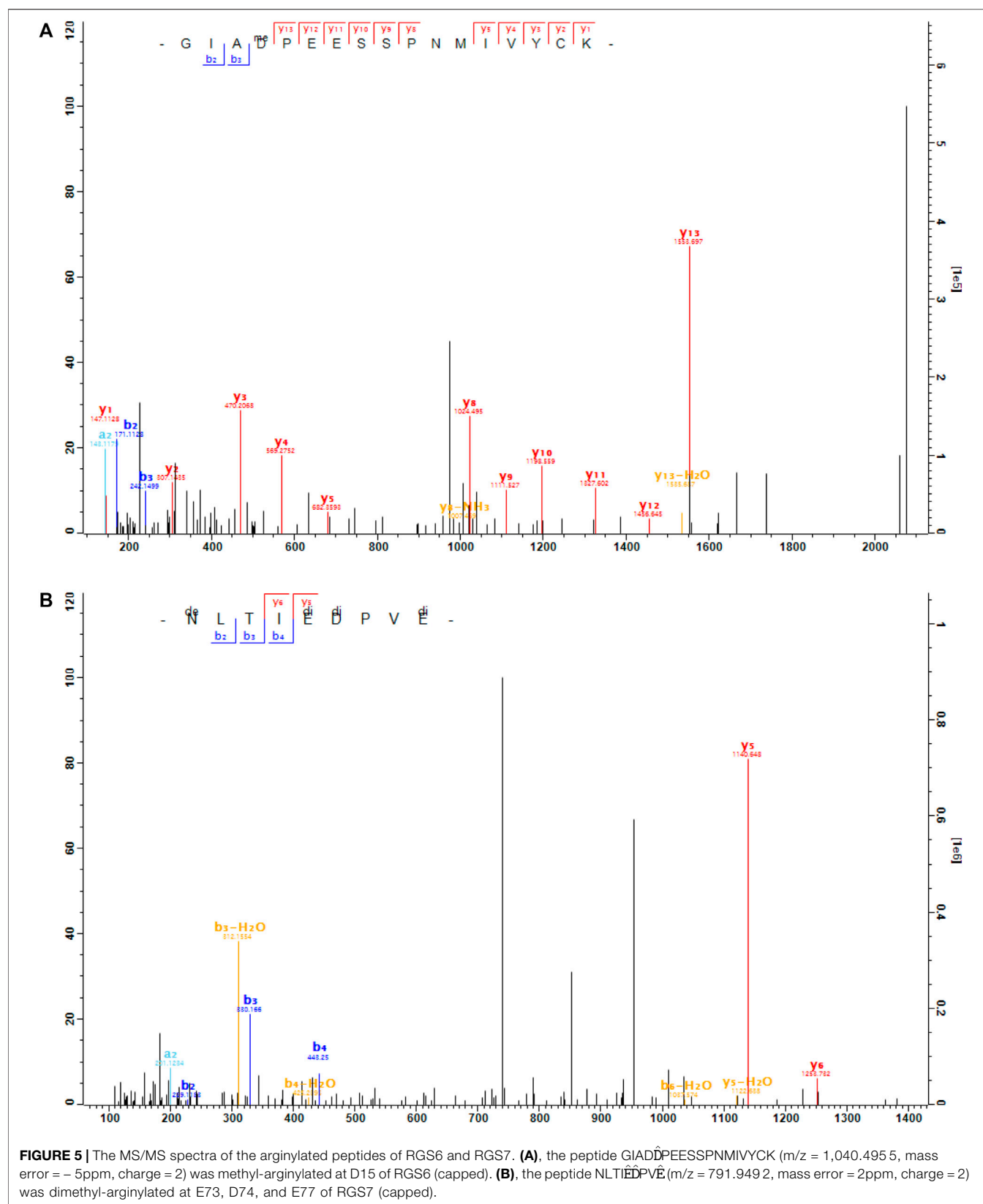
Here, we found that RGS6 was arginylated at the site of D15 and RGS7 was arginylated at three sites: E73, D74 and E77 (Figure 5). These sites are located in the N-terminal region which has the membrane targeting DEP domain. These sites are conserved between RGS6 and RGS7, and the surrounding

regions are highly homologous between RGS6 and RGS7 (Figure 6). Thus, it is likely that these sites are arginylated in both RGS6 and RGS7, and that this arginylation can directly contribute to an increase of their levels in synaptic processes of starburst amacrine cells and ON-bipolar cells, respectively.

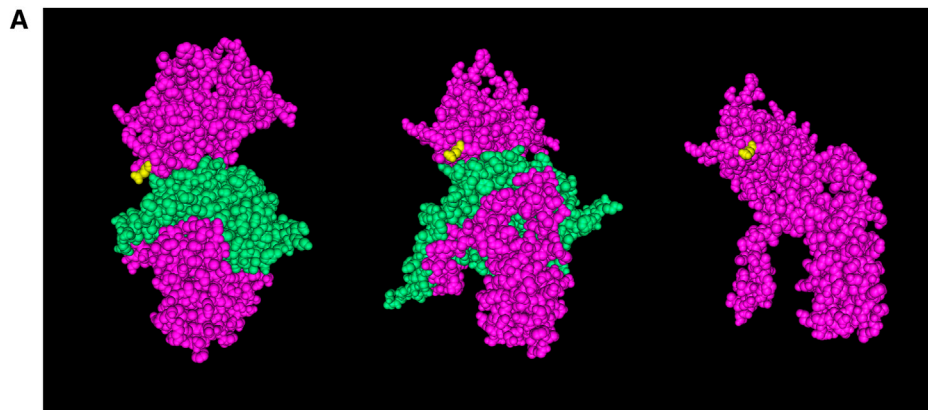
This is the first evidence that R7 family RGS proteins are arginylated on side chains, in contrast to the previous finding that R4 family RGS proteins are arginylated on N-termini (Lee et al., 2005).

### 3.5 RGS6 and RGS7 Proteins Are Enriched in the G-protein Signaling Complexes in the Absence of Arginylation

To test whether abolishment of arginylation affects the level of RGS6 and RGS7 proteins in the G-protein signaling complexes, we compared the RGS6 and RGS7 protein levels in retinal synaptic processes of the wild-type (WT) and the conditional Ate1 knockout (KO) mice. In the KO mice, Ate1 deletion is driven by neuron-specific Nestin promoter, occurring in the







**B**

Domains

RGS6 1 MAQGSG-DQRAVGIA<sup>Δ</sup>PEESSPNMIVYCKIEDIITKMQDDKTGGVPIRTVKSFLSKIPSV-

RGS7 1 MAQGNNGQTSNGVAD---ESPNNLVYRKMEDVIARMQDEKNG-IPRTVKSFLSKIPSV-

aaaaaaaaa aaaaaaaaaaaaaa bb bbb

VTGTDIVQWLMKNLSIEDPVEAIHLGSLIAAQGYIFPISDHVLTMKDDGTFYRFQAPYFWPSNCWE-

FSGSDIVQWLIK<sup>Δ</sup>NLTIE<sup>Δ</sup>DPV<sup>Δ</sup>EALHLGTLMAAHGYFFPISDHVLTCLKDDGTFYRFQTPYFWPSNCWE-

a:  $\alpha$ -helix b:  $\beta$ -sheet

**FIGURE 6 |** Putative arginylation sites of RGS6 and RGS7. **(A)** The 3D structure of RGS7 in the RGS7-G $\beta$ 5 heterodimer based on the structure data 6N9G (Patil et al., 2018). Pink: RGS7, green: G $\beta$ 5, yellow: RGS7 E73. **(B)** The putative arginylation sites (capped), the peptides (underlined), and the surrounding regions are shown with RGS6 and RGS7 alignment (Altschul et al., 1997). The putative arginylation sites are near/on the DEP domain, one in front of the 1st  $\alpha$ -helix and three between the 2nd and 3rd  $\alpha$ -helices in the secondary structures (Wong et al., 2000). These sites are shared between RGS6 and RGS7.

entire nervous system during embryogenesis (Wang et al., 2017a; Wang et al., 2017b). ATE1 protein level in these mice is greatly reduced in most retinal neurons (Fina et al., 2021).

RGS6 and RGS7 in the retina are prominently expressed in the synaptic processes of starburst amacrine cells in the inner plexiform layer (IPL) and ON-bipolar cells in the outer plexiform layer (OPL), separately (Song et al., 2007). In agreement with previous studies, our immunohistochemistry staining showed that RGS6 was prominently enriched in the starburst amacrine cell (SAC) processes, which are localized within two distinct bands in the IPL (**Figure 7A**). We used the total sum within the  $1.1\mu\text{m} \times 1.1\mu\text{m}$  window, centered and averaged along the SAC bands, to quantify the RGS6 protein level in the synaptic processes. The RGS6 protein level was significantly higher in KO than in WT (**Figure 7B**). Consistent with that, RGS6's obligatory binding partner G $\beta$ 5 was also enriched in the two distinct bands in the IPL (**Figure 7C**) and its level was significantly higher in KO than in WT (**Figure 7D**). In addition, in a separate study, we showed that RGS7 and G $\beta$ 5 proteins levels were significantly higher in KO

than in WT dendritic processes of both rod- and cone-OBCs in the OPL (Fina et al., 2021). These results are summarized in **Figures 8A,B**.

### 3.6 Post-Translational Changes of RGS6 and RGS7 Proteins

It is interesting to know if the observed increase of RGS6 and RGS7 proteins at the synaptic processes are associated with an overall increase of their levels in the retina. In our previous study, we used Western blots to show that in total retina extracts RGS7 levels increased in Ate1 knockout, but Gβ5 did not (Fina et al., 2021). Thus, since RGS6 is the dominant binding partner with Gβ5 in the retina (Shim et al., 2012) and they form an obligatory complex *in vivo*, it would be highly unlikely for the total RGS6 in the retina to increase significantly in the absence of arginylation without simultaneously causing Gβ5 to do the same.

We compared the mRNA levels of Rgs6, Rgs7, and Gnb5 of Ate1 KO and WT mice. There was no significant difference for any of them (**Figure 8C**). This indicates that the changes of the

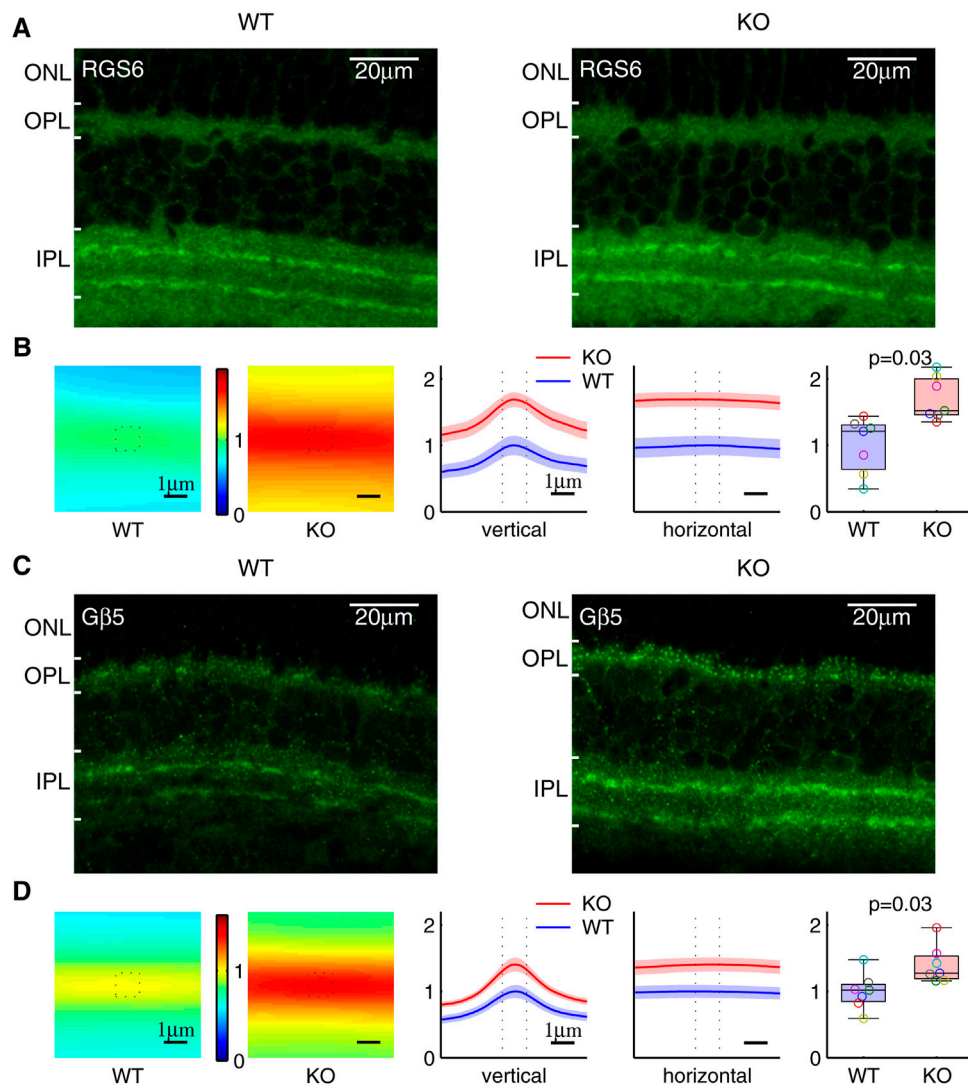


**FIGURE 7 |** Increased RGS6 and G $\beta$ 5 protein level in the synaptic processes of Ate1 knockout (KO) mouse. **(A)** Immunohistochemistry of retinas stained with anti-RGS6. Both the wild-type (WT) and KO retinas have clear staining of two distinct bands of synaptic processes in the inner plexiform layer (IPL). **(B)** The RGS6 staining intensities averaged along the bands are shown on the left. The values along the vertical and horizontal middle lines are plotted in the middle with the SEM in shaded colors. The dotted lines mark the central 1.1  $\mu$ m region surrounding the maxima. In the box plot on the right, the total sum at the central region shows a significant increase of RGS6 proteins in the synaptic processes of KO mice. **(C)** and **(D)** Immunohistochemistry of retina stained with anti-G $\beta$ 5 show the same pattern and the results as **(A)** and **(B)** for RGS6. Each pair of data points of the same color represents a WT/KO littermate pair ( $n = 7$ ). The p-values are from paired Wilcoxon  $t$ -test (signed-rank test for median). The maximum length of the whiskers are 1.5 times of the inter quartile range. Note: the anti-G $\beta$ 5 and anti-RGS6 also stained puncta in ON-bipolar dendrites in the outer plexiform layer (OPL)—the latter due to a cross interaction with RGS7; however, its staining in IPL represents RGS6 only since RGS7 is not present in IPL (Song et al., 2007). ONL: the outer nuclear layer.

corresponding protein levels and/or distributions are most likely post-translational.

It is conceivable that the overall increase of RGS7 protein level causes its increase at ON-bipolar dendritic processes. However, it cannot be the case for RGS6. Its redistribution to SAC synaptic processes upon arginylation could be due, e.g., to the fact that arginylation of RGS6 and/or other proteins in SAC could contribute to its targeting to the membrane and the synapses. It is known that light exposure leads to redistribution of G-proteins in the rods from the outer segments to the inner segments and the rod terminals (Whelan and McGinnis, 1988;

Sokolov et al., 2002). Our ongoing study also shows that RGS7 levels at the synapses change significantly depending on the synaptic activity. Since Ate1 knockout increases the activities of ON-bipolar cells and down-stream neurons (Fina et al., 2021), RGS6 can undergo activity-dependent redistribution. Similar mechanisms could also be at work with RGS7. One possibility is that Ate1 knockout changes ON-bipolar activities pre-synaptically through G $\beta$ 1.

G $\beta$ 1 plays an important role in the rods. In addition to the rising phase of light responses in the outer segments, it also facilitates the synaptic transmission to OBCs (Majumder et al.,

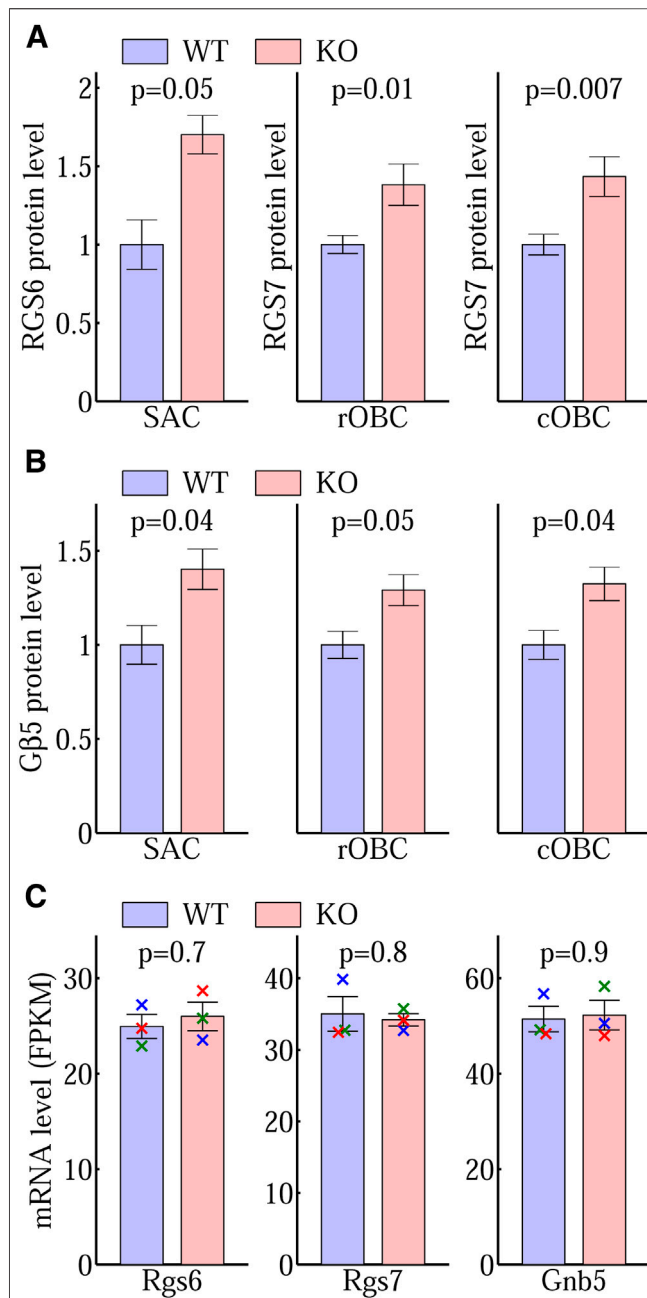


**FIGURE 8 |** Post-translational changes of RGS6, RGS7, and Gβ5.

Immunostaining quantification of **(A)** the protein levels of RGS6 in SAC and RGS7 in rOBC and cOBC synaptic processes and **(B)** the corresponding Gβ5 levels demonstrate a significantly higher level of these proteins in the Ate1 knockout (KO) than the wild-type (WT) mice. SAC: starburst amacrine cell. rOBC: rod ON-bipolar cell. cOBC: cone ON-bipolar cell. In **(A)** and **(B)**, the bar plots for SAC are based on the same data of the box plots of **Figure 7** and the bar plots for rOBC and cOBC are based on the data of Fina et al. (2021). The p-values are from paired Student's t-test and the error bars represent SEM. The differences between KO and WT were also evaluated with a non-parametric statistical hypothesis test (**Figure 7** for RGS6 and Gβ5 in SAC; Fina et al. (2021) for RGS7 and Gβ5 in rOBC and cOBC), which confirmed the conclusions in **(A)** and **(B)**. **(C)** The Rgs6, Rgs7, and Gnb5 (short) mRNA encoding RGS6, RGS7, and Gβ5 proteins in the mouse brains from WT and KO littermates, expressed in Fragments Per Kilobase of transcript per Million (Continued)

**FIGURE 8 |** mapped reads (FPKM) from RNA sequencing. There is no significant difference between WT and KO. Each pair of data points of the same color represents a WT/KO littermate pair ( $n = 3$ ). The p-values are from paired Student's t-test and the error bars represent SEM. The p-values from non-parametric statistical hypothesis test (paired Wilcoxon t-test) (0.8, 1, and 1, respectively) also shows no significant difference in **(C)**.

2013). Here, we presented evidence that Gβ1 is arginylated. However, we did not observe any significant change of the rising phase of the light responses of the rods after deletion of Ate1 (Fina et al., 2021). In our current ongoing project, we also did not see any obvious change in Gβ1 in the outer segments after Ate1 deletion (manuscript in preparation). It should be noted that lack of changes we have seen so far in Gβ1 does not exclude a possible effect of Gβ1 at the pre-synaptic terminals of photoreceptors, in contact with On-bipolar cell dendritic processes. It would be very interesting to address this possibility in a follow up study.

According to prior studies, RGS6 is not implicated in G-protein signaling in photoreceptors or ON-bipolar cells, where the major players are RGS9 (in the photoreceptors) and RGS7/RGS11 (in the ON-bipolar cells). In our experiments, the strongest RGS6 staining and the significant change due to Ate1 deletion, by far, was observed in the synaptic processes of starburst amacrine cells. This suggests that RGS6 likely plays an arginylation-dependent role in G-protein signaling in these cells. Elucidating this role is a very interesting future direction, and we hope our present findings will help future research to reveal the functional role of RGS6 in the retina.

## 4 SUMMARY

This work represents the first comprehensive analysis of arginylation of the components of G-protein signaling in the retina, including GPCR, G-proteins, and RGS proteins. We find putative arginylation sites on the aspartate and glutamate side chains of Gat1, Gβ1, RGS6, and RGS7, and no N-terminal arginylation among the proteins involved in the G-protein signaling in the retina. While, due to probabilistic nature of mass spectrometry analysis of post-translational modifications, as well as potential alteration of protein stability or intracellular localization of proteins after arginylation, it is still possible that other proteins in the retina are also arginylated, the targets identified here are likely more prominent and abundant.

Our results provide concrete evidence that arginylation targets proteins involved in G-protein signaling in the retina, and extend a mechanistic foundation to our previous findings that arginylation regulates retina responses in vision. We show here that abolishment of arginylation leads to an increase in RGS6 and RGS7 protein levels, suggesting that this mechanism can directly regulate the events downstream of RGS. Taken together, our findings demonstrate that arginylation regulates G-protein responses in the retina by directly targeting several key players in this signaling cascade.

## DATA AVAILABILITY STATEMENT

The datasets presented in this study can be found in online repositories. The names of the repository/repositories and accession number(s) can be found in the article/**Supplementary Material**.

## ETHICS STATEMENT

The animal study was reviewed and approved by University of Pennsylvania IACUC.

## AUTHOR CONTRIBUTIONS

AK provided the brain-specific Ate1 knockout mice; DD and MF designed and performed the immunohistochemistry experiments; DD, AK, JW, and PV prepared samples for RNA sequencing and mass spectrometry; H-YT performed mass spectrometry; DD conceptualized the study, analyzed the data, and wrote the first draft of the manuscript; DD and AK prepared the figures and wrote the manuscript. All authors reviewed the manuscript.

## REFERENCES

- Altschul, S., Madden, T. L., Schaffer, A. A., Zhang, J., Zhang, Z., Miller, W., et al. (1997). Gapped BLAST and PSI-BLAST: a New Generation of Protein Database Search Programs. *Nucleic Acids Res.* 25, 3389–3402. doi:10.1093/nar/25.17.3389
- Balzi, E., Choder, M., Chen, W. N., Varshavsky, A., and Goffeau, A. (1990). Cloning and Functional Analysis of the Arginyl-tRNA-Protein Transferase Gene ATE1 of *Saccharomyces cerevisiae*. *J. Biol. Chem.* 265, 7464–7471. doi:10.1016/s0021-9258(19)39136-7
- Bongiovanni, G., Fissolo, S., Barra, H. S., and Hallak, M. E. (1999). Posttranslational Arginylation of Soluble Rat Brain Proteins after Whole Body Hyperthermia. *J. Neurosci. Res.* 56, 85–92. doi:10.1002/(sici)1097-4547(19990401)56:1<85::aid-jnr11>3.0.co;2-t
- Cabrera, J. L., de Freitas, F., Satpaev, D. K., and Slepak, V. Z. (1998). Identification of the Gβ5-RGS7 Protein Complex in the Retina. *Biochem. Biophys. Res. Commun.* 249, 898–902. doi:10.1006/bbrc.1998.9218
- Cao, Y., Pahlberg, J., Sarria, I., Kamasawa, N., Sampath, A. P., and Martemyanov, K. A. (2012). Regulators of G Protein Signaling RGS7 and RGS11 Determine the Onset of the Light Response in ON Bipolar Neurons. *Proc. Natl. Acad. Sci.* 109, 7905–7910. doi:10.1073/pnas.1202332109
- Chen, F. S., Shim, H., Morhardt, D., Dallman, R., Krahn, E., McWhinney, L., et al. (2010). Functional Redundancy of R7 RGS Proteins in ON-Bipolar Cell Dendrites. *Invest. Ophthalmol. Vis. Sci.* 51, 686–693. doi:10.1167/iovs.09-4084
- Chen, K., Chen, C., Li, H., Yang, J., Xiang, M., Wang, H., et al. (2021). Widespread Translational Control Regulates Retinal Development in Mouse. *Nucleic Acids Res.* 49 (17), 9648–9664. doi:10.1093/nar/gkab749
- Ciechanover, A., Ferber, S., Ganoth, D., Elias, S., Hershko, A., and Arfin, S. (1988). Purification and Characterization of Arginyl-tRNA-Protein Transferase from Rabbit Reticulocytes. Its Involvement in post-translational Modification and Degradation of Acidic NH2 Termini Substrates of the Ubiquitin Pathway. *J. Biol. Chem.* 263, 11155–11167. doi:10.1016/s0021-9258(18)37936-5
- Cowan, C. W., Fariss, R. N., Sokal, I., Palczewski, K., and Wensel, T. G. (1998). High Expression Levels in Cones of RGS9, the Predominant GTPase Accelerating Protein of Rods. *Proc. Natl. Acad. Sci.* 95, 5351–5356. doi:10.1073/pnas.95.9.5351

## FUNDING

This work was supported by the NIH/NIGMS R35GM122505, NIH/NINDS R01NS102435, NIH/NEI P30EY001583, the Office of Dean at School of Veterinary Medicines and the Office of the Vice Provost for Research at the University of Pennsylvania.

## ACKNOWLEDGMENTS

We thank Drs. Noga Vardi, Catherine CL Wong, Shuaxin Gao, and Nan Zhang for helpful discussions. We thank Stephanie Sterling and Nicolae A Leu for help with mouse colony maintenance and breeding. We thank Drs. Jason CK Chen and Theodore G Wensel for donating antibodies used in this study.

## SUPPLEMENTARY MATERIAL

The Supplementary Material for this article can be found online at: <https://www.frontiersin.org/articles/10.3389/fcell.2021.807345/full#supplementary-material>

- Davydov, I. V., and Varshavsky, A. (2000). RGS4 Is Arginylated and Degraded by the N-End Rule Pathway *In Vitro*. *J. Biol. Chem.* 275 (30), 22931–22941. doi:10.1074/jbc.m001605200
- De Vries, L., Mousli, M., Wurmser, A., and Farquhar, M. G. (1995). GAIP, a Protein that Specifically Interacts with the Trimeric G Protein G Alpha I3, Is a Member of a Protein Family with a Highly Conserved Core Domain. *Proc. Natl. Acad. Sci.* 92 (25), 11916–11920. doi:10.1073/pnas.92.25.11916
- Decca, M. B., Carpio, M. A., Bosc, C., Galiano, M. R., Job, D., Andrieux, A., et al. (2007). Post-translational Arginylation of Calreticulin. *J. Biol. Chem.* 282 (11), 8237–8245. doi:10.1074/jbc.m608559200
- Dhingra, A., Ramakrishnan, H., Neinstein, A., Fina, M. E., Xu, Y., Li, J., et al. (2012). G 3 Is Required for Normal Light ON Responses and Synaptic Maintenance. *J. Neurosci.* 32, 11343–11355. doi:10.1523/jneurosci.1436-12.2012
- Dobin, A., Davis, C. A., Schlesinger, F., Drenkow, J., Zaleski, C., Jha, S., et al. (2013). STAR: Ultrafast Universal RNA-Seq Aligner. *Bioinformatics* 29 (1), 15–21. doi:10.1093/bioinformatics/bts635
- Dohlman, H. G., Apanieski, D., Chen, Y., Song, J., and Nusskern, D. (1995). Inhibition of G-Protein Signaling by Dominant Gain-Of-Function Mutations in Sst2p, a Pheromone Desensitization Factor in *Saccharomyces cerevisiae*. *Mol. Cell Biol.* 15 (7), 3635–3643. doi:10.1128/mcb.15.7.3635
- Druey, K. M., Blumer, K. J., Kang, V. H., and Kehrl, J. H. (1996). Inhibition of G-Protein-Mediated MAP Kinase Activation by a New Mammalian Gene Family. *Nature* 379 (6567), 742–746. doi:10.1038/379742a0
- Fina, M. E., Wang, J., Nikonov, S. S., Sterling, S., Vardi, N., Kashina, A., et al. (2021). Arginyltransferase (Ate1) Regulates the RGS7 Protein Level and the Sensitivity of Light-Evoked ON-Bipolar Responses. *Sci. Rep.* 11, 9376. doi:10.1038/s41598-021-88628-3
- Gao, Y., Hu, H., Ramachandran, S., Erickson, J. W., Cerione, R. A., and Skiniotis, G. (2019). Structures of the Rhodopsin-Transducin Complex: Insights into G-Protein Activation. *Mol. Cell* 75 (4), 781–790. doi:10.1016/j.molcel.2019.06.007
- Gao, Y., Eskici, G., Ramachandran, S., Poitevin, F., Seven, A. B., Panova, O., et al. (2020). Structure of the Visual Signaling Complex between Transducin and Phosphodiesterase 6. *Mol. Cell* 80 (2), 237–245.e4. doi:10.1016/j.molcel.2020.09.013



- Harman, J. C., Guidry, J. J., and Giddy, J. M. (2018). Comprehensive Characterization of the Adult ND4 Swiss Webster Mouse Retina: Using Discovery-Based Mass Spectrometry to Decipher the Total Proteome and Phosphoproteome. *Mol. Vis.* 24, 875–889.
- Haverkamp, S., and Wässle, H. (2000). Immunocytochemical Analysis of the Mouse Retina. *J. Comp. Neurol.* 424, 1–23. doi:10.1002/1096-9861(20000814)424:1<1:aid-cne1>3.0.co;2-v
- He, W., Cowan, C. W., and Wensel, T. G. (1998). RGS9, a GTPase Accelerator for Phototransduction. *Neuron* 20, 95–102. doi:10.1016/s0896-6273(00)80437-7
- Hu, R.-G., Sheng, J., Qi, X., Xu, Z., Takahashi, T. T., and Varshavsky, A. (2005). The N-End Rule Pathway as a Nitric Oxide Sensor Controlling the Levels of Multiple Regulators. *Nature* 437 (7061), 981–986. doi:10.1038/nature04027
- Hunt, T. W., Fields, T. A., Casey, P. J., and Peralta, E. G. (1996). RGS10 Is a Selective Activator of Gai GTPase Activity. *Nature* 383 (6596), 175–177. doi:10.1038/383175a0
- Jiang, Y., Lee, J., Lee, J. H., Lee, J. W., Kim, J. H., Choi, W. H., et al. (2016). The Arginylation branch of the N-End Rule Pathway Positively Regulates Cellular Autophagic Flux and Clearance of Proteotoxic Proteins. *Autophagy* 12 (11), 2197–2212. doi:10.1080/15548627.2016.1222991
- Karakozova, M., Kozak, M., Wong, C. C. L., Bailey, A. O., Yates, J. R., 3rd, Mogilner, A., et al. (2006). Arginylation of  $\beta$ -Actin Regulates Actin Cytoskeleton and Cell Motility. *Science* 313 (5784), 192–196. doi:10.1126/science.1129344
- Koelle, M. R., and Horvitz, H. R. (1996). EGL-10 Regulates G Protein Signaling in the *C. elegans* Nervous System and Shares a Conserved Domain with many Mammalian Proteins. *Cell* 84, 115–125. doi:10.1016/s0092-8674(00)80998-8
- Kurosaka, S., Leu, N. A., Zhang, F., Bunte, R., Saha, S., Wang, J., et al. (2010). Arginylation-dependent Neural Crest Cell Migration Is Essential for Mouse Development. *Plos Genet.* 6 (3), e1000878. doi:10.1371/journal.pgen.1000878
- Kwon, Y. T., Kashina, A. S., Davydov, I. V., Hu, R.-G., An, J. Y., Seo, J. W., et al. (2002). An Essential Role of N-Terminal Arginylation in Cardiovascular Development. *Science* 297 (5578), 96–99. doi:10.1126/science.1069531
- Lambright, D. G., Sondek, J., Bohm, A., Skiba, N. P., Hamm, H. E., and Sigler, P. B. (1996). The 2.0 Å Crystal Structure of a Heterotrimeric G Protein. *Nature* 379 (6563), 311–319. doi:10.1038/379311a0
- Lee, M. J., Tasaki, T., Moroi, K., An, J. Y., Kimura, S., Davydov, I. V., et al. (2005). RGS4 and RGS5 Are *In Vivo* Substrates of the N-End Rule Pathway. *Proc. Natl. Acad. Sci.* 102 (42), 15030–15035. doi:10.1073/pnas.0507533102
- Lee, M. J., Kim, D. E., Zakrzewska, A., Yoo, Y. D., Kim, S.-H., Kim, S. T., et al. (2012). Characterization of Arginylation branch of N-End Rule Pathway in G-Protein-Mediated Proliferation and Signaling of Cardiomyocytes. *J. Biol. Chem.* 287 (28), 24043–24052. doi:10.1074/jbc.m112.364117
- Leu, N. A., Kurosaka, S., and Kashina, A. (2009). Conditional Tek Promoter-Driven Deletion of Arginyltransferase in the Germ Line Causes Defects in Gametogenesis and Early Embryonic Lethality in Mice. *PLoS One* 4 (11), e7734. doi:10.1371/journal.pone.0007734
- Liang, J.-J., Chen, H. H. D., Jones, P. G., and Khawaja, X. Z. (2000). RGS7 Complex Formation and Colocalization with the Gbeta5 Subunit in the Adult Rat Brain and Influence on Gbeta5gamma2-mediated PLCbeta Signaling. *J. Neurosci. Res.* 60, 58–64. doi:10.1002/(sici)1097-4547(20000401)60:1<58:aid-jnr6>3.0.co;2-l
- Majumder, A., Pahlberg, J., Boyd, K. K., Kerov, V., Kolandaivelu, S., Ramamurthy, V., et al. (2013). Transducin Translocation Contributes to Rod Survival and Enhances Synaptic Transmission from Rods to Rod Bipolar Cells. *Proc. Natl. Acad. Sci. USA* 110, 12468–12473. doi:10.1073/pnas.1222666110
- Mojumder, D. K., Qian, Y., and Wensel, T. G. (2009). Two R7 Regulator of G-Protein Signaling Proteins Shape Retinal Bipolar Cell Signaling. *J. Neurosci.* 29, 7753–7765. doi:10.1523/jneurosci.1794-09.2009
- Patil, D. N., Rangarajan, E. S., Novick, S. J., Pascal, B. D., Kojetin, D. J., Griffin, P. R., et al. (2018). Structural Organization of a Major Neuronal G Protein Regulator, the RGS7-G $\beta$ 5-R7BP Complex. *eLife* 7, e42150. doi:10.7554/eLife.42150
- Peng, Y. W., Robshaw, J. D., Levine, M. A., and Yau, K. W. (1992). Retinal Rods and Cones Have Distinct G Protein Beta and Gamma Subunits. *Proc. Natl. Acad. Sci.* 89, 10882–10886. doi:10.1073/pnas.89.22.10882
- Rai, R., Wong, C. C. L., Xu, T., Leu, N. A., Dong, D. W., Guo, C., et al. (2008). Arginyltransferase Regulates Alpha Cardiac Actin Function, Myofibril Formation and Contractility during Heart Development. *Development* 135 (23), 3881–3889. doi:10.1242/dev.022723
- Ramakrishnan, H., Dhingra, A., Tummala, S. R., Fina, M. E., Li, J. J., Lyubarsky, A., et al. (2015). Differential Function of G $\gamma$ 13 in Rod Bipolar and On Cone Bipolar Cells. *J. Physiol.* 593, 1531–1550. doi:10.1113/jphysiol.2014.281196
- Saha, S., and Kashina, A. (2011). Posttranslational Arginylation as a Global Biological Regulator. *Dev. Biol.* 358 (1), 1–8. doi:10.1016/j.ydbio.2011.06.043
- Sarria, I., Pahlberg, J., Cao, Y., Kolesnikov, A. V., Kefalov, V. J., Sampath, A. P., et al. (2015). Sensitivity and Kinetics of Signal Transmission at the First Visual Synapse Differentially Impact Visually-Guided Behavior. *Elife* 4, e06358. doi:10.7554/eLife.06358
- Shim, H., Wang, C.-T., Chen, Y.-L., Chau, V. Q., Fu, K. G., Yang, J., et al. (2012). Defective Retinal Depolarizing Bipolar Cells in Regulators of G Protein Signaling (RGS) 7 and 11 Double Null Mice. *J. Biol. Chem.* 287, 14873–14879. doi:10.1074/jbc.m112.345751
- Sokolov, M., Lyubarsky, A. L., Strissel, K. J., Savchenko, A. B., Govardovskii, V. I., Pugh, E. N., Jr, et al. (2002). Massive Light-Driven Translocation of Transducin between the Two Major Compartments of Rod Cells. *Neuron* 34 (1), 95–106. doi:10.1016/s0896-6273(02)00636-0
- Sondek, J., Bohm, A., Lambright, D. G., Hamm, H. E., and Sigler, P. B. (1996). Crystal Structure of a GA Protein  $\beta\gamma$ dimer at 2.1 Å Resolution. *Nature* 379 (6563), 369–374. doi:10.1038/379369a0
- Song, J. H., Song, H., Wensel, T. G., Sokolov, M., and Martemyanov, K. A. (2007). Localization and Differential Interaction of R7 RGS Proteins with Their Membrane Anchors R7BP and R9AP in Neurons of Vertebrate Retina. *Mol. Cel. Neurosci.* 35, 311–319. doi:10.1016/j.mcn.2007.03.006
- Squires, K. E., Montañez-Miranda, C., Pandya, R. R., Torres, M. P., and Hepler, J. R. (2018). Genetic Analysis of Rare Human Variants of Regulators of G Protein Signaling Proteins and Their Role in Human Physiology and Disease. *Pharmacol. Rev.* 70 (3), 446–474. doi:10.1124/pr.117.015354
- Stewart, A., and Fisher, R. A. (2015). Introduction: G Protein-Coupled Receptors and RGS Proteins. *Prog. Mol. Biol. Transl. Sci.* 133, 1–11. doi:10.1016/bs.pmbts.2015.03.002
- Sze, Y. H., Zhao, Q., Cheung, J. K. W., Li, K. K., Tse, D. Y. Y., To, C. H., et al. (2021). High-pH Reversed-Phase Fractionated Neural Retina Proteome of normal Growing C57BL/6 Mouse. *Sci. Data* 8 (1), 27. doi:10.1038/s41597-021-00813-1
- Tummala, S. R., Dhingra, A., Fina, M. E., Li, J. J., Ramakrishnan, H., and Vardi, N. (2016). Lack of mGluR6-Related cascade Elements Leads to Retrograde Trans-synaptic Effects on Rod Photoreceptor Synapses via Matrix-Associated Proteins. *Eur. J. Neurosci.* 43 (11), 1509–1522. doi:10.1111/ejn.13243
- Tyanova, S., Temu, T., and Cox, J. (2016). The MaxQuant Computational Platform for Mass Spectrometry-Based Shotgun Proteomics. *Nat. Protoc.* 11 (12), 2301–2319. doi:10.1038/nprot.2016.136
- Varshavsky, A. (2011). The N-End Rule Pathway and Regulation by Proteolysis. *Protein Sci.* 20 (8), 1298–1345. doi:10.1002/pro.666
- Voigt, T. (1986). Cholinergic Amacrine Cells in the Rat Retina. *J. Comp. Neurol.* 248, 19–35. doi:10.1002/cne.902480103
- Wang, J., Han, X., Wong, C. C. L., Cheng, H., Aslanian, A., Xu, T., et al. (2014). Arginyltransferase ATE1 Catalyzes Midchain Arginylation of Proteins at Side Chain Carboxylates *In Vivo*. *Chem. Biol.* 21 (3), 331–337. doi:10.1016/j.chembiol.2013.12.017
- Wang, J., Han, X., Leu, N. A., Sterling, S., Kurosaka, S., Fina, M., et al. (2017a). Protein Arginylation Targets Alpha Synuclein, Facilitates normal Brain Health, and Prevents Neurodegeneration. *Sci. Rep.* 7 (1), 11323. doi:10.1038/s41598-017-11713-z
- Wang, J., Pavlyk, I., Vedula, P., Sterling, S., Leu, N. A., Dong, D. W., et al. (2017b). Arginyltransferase ATE1 Is Targeted to the Neuronal Growth Cones and Regulates Neurite Outgrowth during Brain Development. *Dev. Biol.* 430 (1), 41–51. doi:10.1016/j.ydbio.2017.08.027
- Watson, N., Linder, M. E., Druey, K. M., Kehrl, J. H., and Blumer, K. J. (1996). RGS Family Members: GTPase-Activating Proteins for Heterotrimeric G-Protein  $\alpha$ -subunits. *Nature* 383 (6596), 172–175. doi:10.1038/383172a0
- Whelan, J. P., and McGinnis, J. F. (1988). Light-dependent Subcellular Movement of Photoreceptor Proteins. *J. Neurosci. Res.* 20 (2), 263–270. doi:10.1002/jnr.490200216
- Witherow, D. S., Wang, Q., Levay, K., Cabrera, J. L., Chen, J., Willars, G. B., et al. (2000). Complexes of the G Protein Subunit G $\beta$ 5 with the Regulators of G Protein Signaling RGS7 and RGS9. *J. Biol. Chem.* 275, 24872–24880. doi:10.1074/jbc.m001535200

- Wong, H. C., Mao, J., Nguyen, J. T., Srinivas, S., Zhang, W., Liu, B., et al. (2000). Structural Basis of the Recognition of the Dishevelled DEP Domain in the Wnt Signaling Pathway. *Nat. Struct. Biol.* 7, 1178–1184. doi:10.1038/82047
- Zanakis, M. F., Chakraborty, G., Sturman, J. A., and Ingoglia, N. A. (1984). Posttranslational Protein Modification by Amino Acid Addition in Intact and Regenerating Axons of the Rat Sciatic Nerve. *J. Neurochem.* 43, 1286–1294. doi:10.1111/j.1471-4159.1984.tb05385.x
- Zhang, J.-H., and Simonds, W. F. (2000). Copurification of Brain G-Protein  $\beta 5$  with RGS6 and RGS7. *J. Neurosci.* 20 (3), RC59. doi:10.1523/jneurosci.20-03-j0004.2000
- Zhang, J., Jeffrey, B. G., Morgans, C. W., Burke, N. S., Haley, T. L., Duvoisin, R. M., et al. (2010). RGS7 and -11 Complexes Accelerate the ON-Bipolar Cell Light Response. *Invest. Ophthalmol. Vis. Sci.* 51, 1121–1129. doi:10.1167/iops.09-4163
- Zhao, L., Chen, Y., Bajaj, A. O., Eblimit, A., Xu, M., Soens, Z. T., et al. (2016). Integrative Subcellular Proteomic Analysis Allows Accurate Prediction of Human Disease-Causing Genes. *Genome Res.* 26, 660–669. doi:10.1101/gr.198911.115

**Conflict of Interest:** The authors declare that the research was conducted in the absence of any commercial or financial relationships that could be construed as a potential conflict of interest.

**Publisher's Note:** All claims expressed in this article are solely those of the authors and do not necessarily represent those of their affiliated organizations, or those of the publisher, the editors and the reviewers. Any product that may be evaluated in this article, or claim that may be made by its manufacturer, is not guaranteed or endorsed by the publisher.

Copyright © 2022 Fina, Wang, Vedula, Tang, Kashina and Dong. This is an open-access article distributed under the terms of the Creative Commons Attribution License (CC BY). The use, distribution or reproduction in other forums is permitted, provided the original author(s) and the copyright owner(s) are credited and that the original publication in this journal is cited, in accordance with accepted academic practice. No use, distribution or reproduction is permitted which does not comply with these terms.



# Protein Posttranslational Signatures Identified in COVID-19 Patient Plasma

Pavan Vedula<sup>1</sup>, Hsin-Yao Tang<sup>2</sup>, David W. Speicher<sup>2</sup> and Anna Kashina<sup>1\*</sup>  
The UPenn COVID Processing Unit

<sup>1</sup>Department of Biomedical Sciences, University of Pennsylvania School of Veterinary Medicine, Philadelphia, PA, United States,

<sup>2</sup>The Wistar Institute, Philadelphia, PA, United States

## OPEN ACCESS

### Edited by:

Fangliang Zhang,  
University of Miami, United States

### Reviewed by:

Vladimir N. Uversky,  
University of South Florida,  
United States  
Lianjun Zhang,  
Chinese Academy of Medical  
Sciences, China

### \*Correspondence:

Anna Kashina  
akashina@upenn.edu

### Specialty section:

This article was submitted to  
Cellular Biochemistry,  
a section of the journal  
Frontiers in Cell and Developmental  
Biology

**Received:** 01 November 2021

**Accepted:** 06 January 2022

**Published:** 11 February 2022

### Citation:

Vedula P, Tang H-Y, Speicher DW and  
Kashina A (2022) Protein  
Posttranslational Signatures Identified  
in COVID-19 Patient Plasma.  
Front. Cell Dev. Biol. 10:807149.  
doi: 10.3389/fcell.2022.807149

Severe acute respiratory syndrome coronavirus-2 (SARS-CoV-2) is a highly contagious virus of the coronavirus family that causes coronavirus disease-19 (COVID-19) in humans and a number of animal species. COVID-19 has rapidly propagated in the world in the past 2 years, causing a global pandemic. Here, we performed proteomic analysis of plasma samples from COVID-19 patients compared to healthy control donors in an exploratory study to gain insights into protein-level changes in the patients caused by SARS-CoV-2 infection and to identify potential proteomic and posttranslational signatures of this disease. Our results suggest a global change in protein processing and regulation that occurs in response to SARS-CoV-2, and the existence of a posttranslational COVID-19 signature that includes an elevation in threonine phosphorylation, a change in glycosylation, and a decrease in arginylation, an emerging posttranslational modification not previously implicated in infectious disease. This study provides a resource for COVID-19 researchers and, longer term, and will inform our understanding of this disease and its treatment.

**Keywords:** COVID-19, proteomics, peptidomics, posttranslational modifications, arginylation

## KEY POINTS

1. Plasma from COVID-19 patients exhibits prominent protein- and peptide-level changes
2. Proteins from COVID-19 patient plasma exhibit prominent changes in several key posttranslational modifications

## 1 INTRODUCTION

Severe acute respiratory syndrome coronavirus-2 (SARS-CoV-2) is a respiratory virus of the coronavirus family that causes coronavirus disease-19 (COVID-19) in humans and a number of animal species (Swelum et al., 2020). COVID-19 has rapidly propagated worldwide in the past 2 years, causing a global pandemic (see, e.g., (Novelli et al., 2021), for a recent review). This highly contagious disease causes respiratory symptoms that range from mild to severe, and is associated with a number of other serious health implications, including lung inflammation and damage, thrombosis, stroke, renal failure, neurological disorders, and others (Hanff et al., 2020; Schmulson et al., 2020; Troyer et al., 2020; Vakil-Gilani and O'Rourke, 2020; Harapan and Yoo, 2021; Ostergaard, 2021). This list continues to grow, and despite extensive research in the past year and a half, full understanding of COVID-19 mechanisms of action and health consequences has not yet been achieved.

While the initial route of SARS-CoV-2 infection involves the respiratory tract, some of the most prominent effects of COVID-19 can be detected in the blood plasma, which contains antibodies against SARS-CoV-2, and is a major site of immune response that builds the body's defense against the virus. It is of no coincidence that convalescent plasma from COVID-19 patients has been proposed as treatment for this disease, as well as a foundation for some of the diagnostic tests. Plasma is arguably one of the most rapidly changing environments upon SARS-CoV-2 infection. Thus, studies of the disease-related changes in the plasma appear highly promising as a tool that would enable better understanding of this disease progression.

Here, we performed proteomic analysis of plasma samples from COVID-19 patients with symptoms severe enough to require hospitalization compared to healthy control donors, in an attempt to gain insights into protein-level changes in the patients caused by SARS-CoV-2 infection and to identify potential proteomic and posttranslational signatures of this disease. Our analysis revealed a number of changes in protein and peptide composition of the COVID-19 patients' plasma samples. Furthermore, global analysis of posttranslational modifications (PTMs) in these samples showed a striking change in several key physiological PTMs, including phosphorylation, glycosylation, citrullination, and arginylation, which exhibited differential up- and down-regulation in COVID-19 patients compared to controls and, in the case of arginylation and phosphorylation, modified different repertoire of sites on a limited number of target proteins. These patterns suggest a global change in protein processing and regulation that occurs in response to SARS-CoV-2, and the existence of a posttranslational COVID-19 "code". Deciphering this code may advance our understanding of disease progression and long-term implications, as well as potentially inform novel strategies of COVID-19 diagnostics and treatment.

## 2 RESULTS AND DISCUSSION

### 2.1 COVID-19 Patients Exhibit Prominent Changes in Their Plasma Peptidomes

To address potential protein and peptide changes in the plasma associated with COVID-19, we obtained plasma samples from 6 COVID patients with severe disease that required hospitalization and 7 similarly drawn control samples from healthy donors collected independently within the same time frame (**Supplementary Table S1**).

To analyze plasma peptidomes, we used size exclusion under denaturing conditions followed by C18 reverse phase cleanup to isolate plasma peptides followed by LC-MS/MS without proteolysis treatment. LC-MS/MS data were searched against the human protein database using no-enzyme specificity so that peptides naturally occurring or produced by *in vivo* proteolysis could be identified. The final search results were filtered by *p*-value ( $<0.05$ ) and fold change (2-fold and above) to define 180 peptides that showed significant differences in abundance between patients and controls. The significantly changed peptides are shown in **Supplementary Table S2**, and the list of identified peptides that

did not meet these statistical criteria and were not used in the final analysis is shown in **Supplementary Table S3**.

No known regulatory peptides were identified, likely due to their lower abundance. All the significant peptides identified constituted proteolytic fragments predominantly from abundant plasma proteins, which were apparently produced by proteolytic events that accompany immune response, cell migration and adhesion, and other physiological processes (Arapidi et al., 2018). Interestingly, when the total number of identified peptides were compared (**Supplementary Tables S2, S3**), substantially fewer peptides were identified overall in the COVID-19 samples compared to control (**Supplementary Figure S1**), in seeming contrast to the fact that SARS-CoV-2 infection is associated with increased proteolysis (Anand et al., 2020; Ramos-Guzmán et al., 2020; Świderek and Moliner, 2020; Meyer et al., 2021; Tang et al., 2021).

To further analyze COVID-19-dependent peptidomics trends, we used our significantly changed peptide list (**Supplementary Table S2**) and grouped the identified peptides by their parent proteins. For each given protein we plotted combined intensities of all significantly changed peptides (**Supplementary Figure S2**), and separately plotted all the combined intensities grouped by protein for the most abundant hits showing overall increase in control (**Figure 1A**) and COVID-19 (**Figure 1B**).

Most of the combined peptide intensities for each protein were substantially higher in the control samples compared to COVID-19, consistent with the fact that control plasma contained more peptides overall (**Supplementary Figure S1**). However, peptides derived from a small group of proteins showed significant elevation in COVID-19 plasma (**Figure 1B**). The most abundant of these, Alpha-1-antitrypsin, C4a anaphylatoxin, and Serum amyloid A-2, have known functional association with disease pathology. Alpha-1-antitrypsin is a protease inhibitor, involved in regulation of plasma proteolysis (Stockley, 2014). C4 anaphylatoxin and Serum amyloid A-2 are involved in immune response (Gorski et al., 1979; Zheng et al., 2020). All of these processes are highly relevant to the COVID-19 disease (Katneni et al., 2020; Gómez-Mesa et al., 2021; Montenegro et al., 2021; Ostergaard, 2021), and thus increased abundance of significantly changed peptides for these proteins in COVID-19 patients may indicate a direct association between these proteins' proteolysis and SARS-CoV-2 infection. In contrast, peptide groups showing higher levels in control belong to normal proteins expected to be proteolyzed in the blood due to normal organismal functions, and their decrease in COVID-19 would likely lead to impairment of these functions because of SARS-CoV-2 infection.

An additional interesting observation concerns alpha-fibrinogen, which had the largest number of significantly changing peptides (**Supplementary Table S2**). Even though the combined intensities of significantly changed fibrinogen-derived peptides was much higher in control compared to COVID-19 (**Figure 1A**; **Supplementary Figure S2**), individual peptides derived from alpha-fibrinogen showed different trends, with some peptides elevated in COVID-19 rather than control samples (**Figure 2A**; **Supplementary Figure S2**). The peptides with the highest abundance were still more prevalent in control (**Figure 2A**, left), however out of the 17 peptides showing significant change, 8 were more



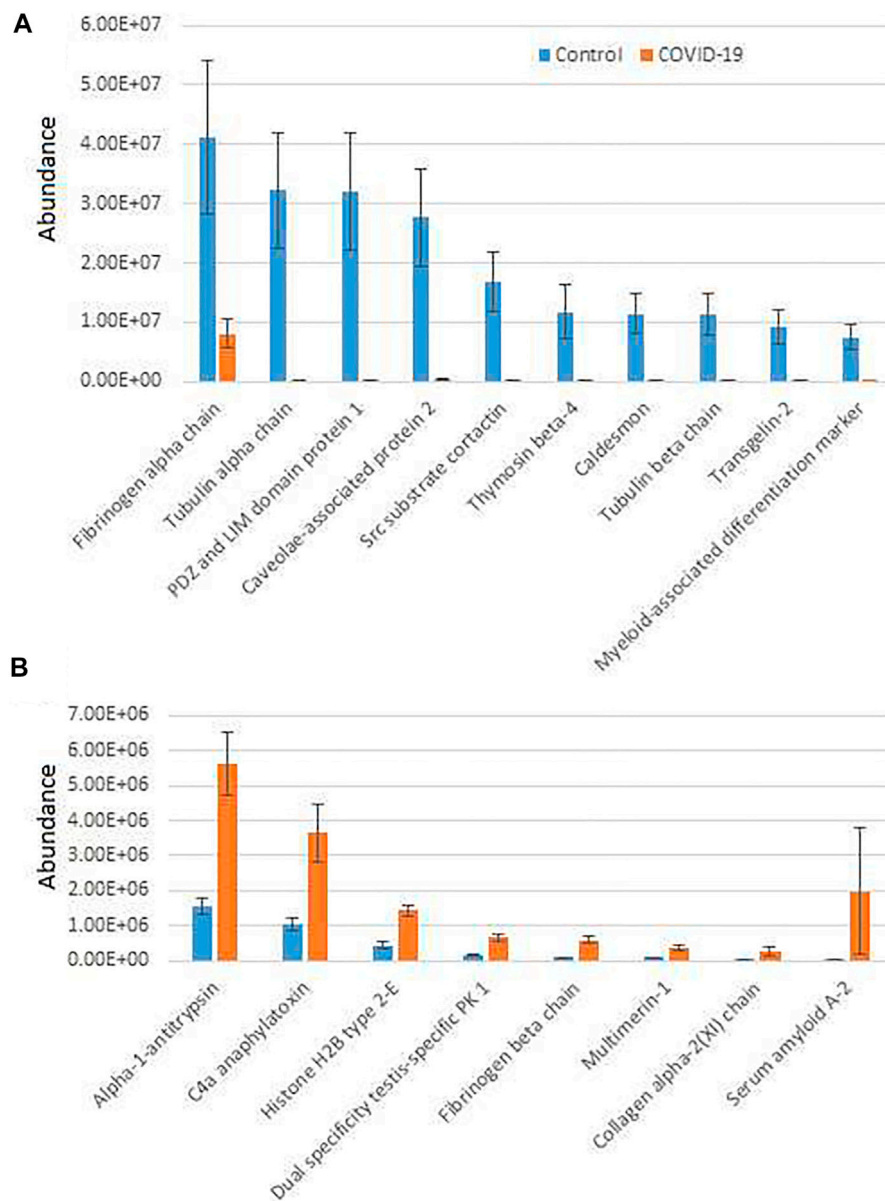


**FIGURE 1 |** Plasma peptides from COVID-19 patients exhibits prominent changes compared to control. Combined total intensities of all significantly changed peptides for each parent protein listed on the X axis. A and B show the most abundant peptide groups in control (**A**) and COVID-19 (**B**). See **Supplementary Figure S2** for the full list of proteins with significantly changed peptides. Error bars represent SEM ( $n = 7$  for control, 6 for COVID-19).

abundant in the COVID-19 samples (**Figure 2A**, right). A somewhat similar pattern was observed with serglycin: only two peptides were identified, but one of these was much more abundant in control, while the other showed the opposite trend (**Figure 2B**). While each change was significant, added together, the intensities of these peptides evened out and showed no change in the serglycin protein group shown in **Supplementary Figure S2**. This observation suggests that fibrinogen and serglycin undergo different proteolytic events in normal physiology and during SARS-CoV-2 infection. Fibrinogen plays a key role in blood clotting (May et al., 2021), a process shown to be impacted in

COVID-19 patients (Ahmed et al., 2020); serglycin is key to the biology of the blood cells (Scully et al., 2012). Altered proteolytic patterns of these proteins in COVID-19 may prove to be a potentially interesting biomarker in future studies.

## 2.2 COVID-19 Patient Plasma Exhibits Prominent Changes in the Global Proteome

Next, we analyzed plasma samples by shotgun proteomics. For this, IgG/albumin-depleted plasma samples were loaded onto SDS PAGE and run ~0.5 cm into the gel, followed by Coomassie Blue staining and excision of the entire protein-containing gel

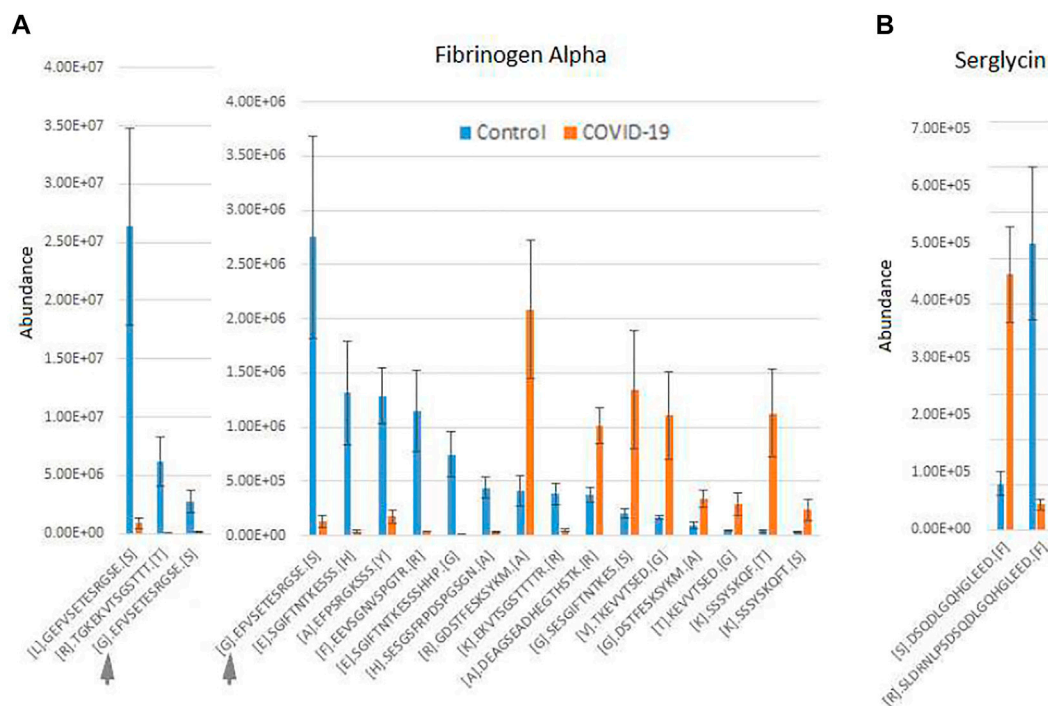


**FIGURE 2 |** Fibrinogen- and serglycin-derived peptides exhibit differential abundance changes between COVID-19 and control, suggesting different proteolytic patterns in response to Sars-CoV-2 infection. Normalized intensities of the most abundant individual peptides in control and COVID-19 plasma samples are shown for fibrinogen (A) and serglycin (B). Peptides in A are plotted in two charts on two different scales, including one overlapping peptide is shown in both charts for scale ([G]. EFVSETESRGSE[S] indicated with a gray arrow in both charts). Error bars represent SEM ( $n = 7$  for control, 6 for COVID-19).

zone, which was then subjected to in-gel digestion with trypsin and analyzed by LC-MS/MS. Differences between COVID-19 and control samples were considered as high confidence significant changes if they exhibited a greater than 2-fold increase or decrease and  $q$ -value less than 0.05. Proteins that passed these criteria and were used for further analysis are listed in **Supplementary Table S4**. The remaining identified proteins are listed in **Supplementary Table S5**.

Interestingly, only 12 proteins were significantly increased in COVID-19 plasma while 35 proteins were decreased in these samples compared with controls (**Figure 3**; **Supplementary Figure S3**). When total iBAQ was used as a rough metric of relative abundance across proteins, only three of the 8 most abundant proteins were increased in COVID-19 plasma (**Figure 3**). One of these proteins, serum amyloid A-2 also showed up in our peptidomics dataset (**Figure 1**), where peptides derived from this protein were elevated to a similar extent in COVID-19 compared to control. This suggests that serum amyloid A-2 is both upregulated and more heavily proteolyzed in COVID-19. The other two proteins increased in COVID-19 plasma were serum amyloid A-1 and C-reactive protein, which are known to be elevated in the plasma in response to inflammation, and thus their increased levels observed in our dataset is fully consistent with known COVID-19 effects. In contrast, proteins showing decreased levels in COVID-19 compared to control (**Figure 3**; **Supplementary Figure S3**; **Supplementary Table S4**) are

mostly related to normal physiological functions, including anti-inflammatory response (apolipoprotein A-IV and C-III) and overall protective functions (serum paraoxonase), hormone and vitamin transport (retinol-binding protein and transthyretin). It is possible that their elevated levels in control versus patient plasma reflect down-regulation or depletion of these normal proteins upon SARS-CoV-2 infection that ultimately contribute to disease pathology.

Thus, our data suggest that a limited set of proteins related to inflammation, immune response, and normal organismal homeostasis are prominently altered between COVID-19 and control, potentially as a direct consequence of SARS-CoV-2 infection.

## 2.3 COVID-19 Plasma Proteome Exhibits Altered Posttranslational Modification Patterns

To test whether COVID-19 is associated with any changes in PTMs, we analyzed our total proteomics run of plasma samples using pFIND, a software package that can simultaneously identify a large number of different PTMs, and chemical modifications based on mass shifts (Li et al., 2005; Wang et al., 2007). We manually added arginylation into the program (including addition of unmodified, mono- and dimethyl-Arg that have been all shown to occur *in vivo* through our previous work (Saha et al., 2011; Wang et al., 2014; Wang et al., 2019)). This

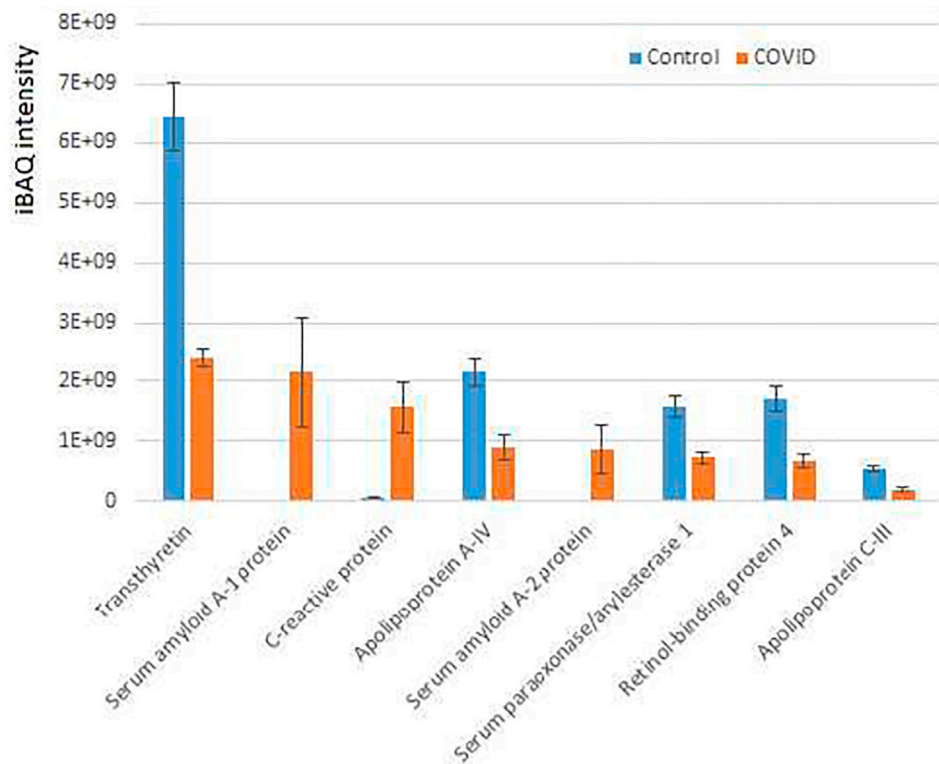


**FIGURE 3 |** Plasma proteins from COVID-19 patients exhibits prominent changes compared to control. iBAQ intensities of the most abundant proteins showing significant differences between COVID-19 and control. See **Supplementary Figure S4** for the full list of hits. Bars represent normalized intensity levels averaged for all samples in each group, error bars represent SEM ( $n = 7$  for control, 6 for COVID-19).

search identified a total of 2630 modifications in the samples. The results were filtered by precursor mass tolerance of 10 ppm, fragment ion tolerance of 20 ppm, and false discovery rate (FDR)  $< 1\%$  at peptide and protein level.

Total results from the pFIND search, including data in individual samples, is shown in **Supplementary Table S6**, and the 10 most abundant modifications from COVID-19 and control patient samples are plotted in **Supplementary Figure S4**. These results were used to calculate each modified peptide amount as spectra count normalized to the percent of the total peptides in the sample, and these numbers were then compared across samples between control and COVID-19 to calculate  $p$ -value and fold change.

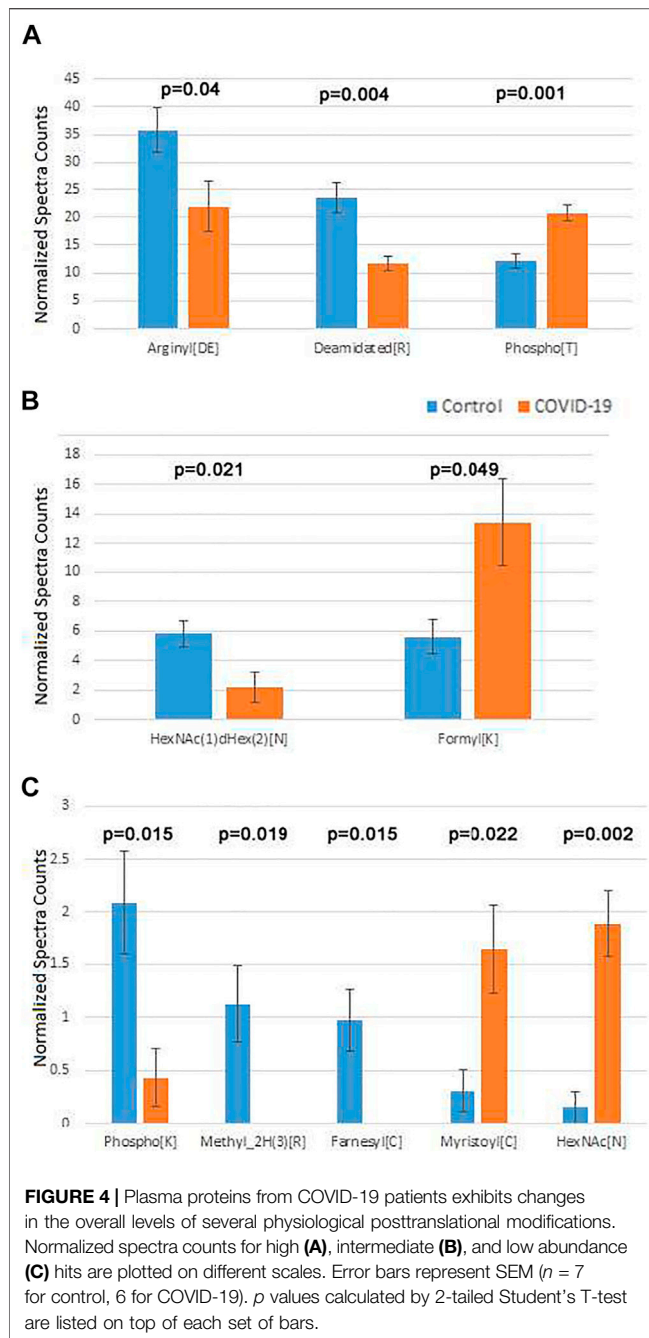
We defined putative significant differences as a greater than 1.5 fold change between control and COVID-19 peptides, with  $p$ -value less than 0.05. These hits are listed in **Supplementary Table S6**, and the modified sites identified in our search are listed in **Supplementary Table S7**.

A total of 82 PTMs showed statistically significant differences between COVID-19 and control. However, many of these modifications are apparently chemically induced and have not been described to happen under normal physiological conditions. Such modifications in the plasma can potentially occur in response to drugs and environmental factors; thus, it is unlikely that these modifications occur because of SARS-CoV-2 infection, even though they might be directly or indirectly

related to the patients' treatment or susceptibility to symptomatic COVID-19. Given this uncertainty, we excluded these PTMs, and manually selected only the known naturally occurring modifications for further analysis.

After this filtering, only a few physiological PTMs showed significant differences between COVID-19 and controls (**Figure 4**). These PTMs were plotted in three separate groups: high abundance (**Figure 4A**), intermediate abundance (**Figure 4B**), and low abundance (**Figure 4C**). Notably, only three of them were in the high abundance group, including phosphorylation on Thr, which showed a nearly 2-fold increase in COVID-19 patients, Arg deamidation, ~2-fold increased in control, and a  $>1.5$ -fold reduction in side chain arginylation of Asp and Glu residues in COVID-19 patients (**Figure 4A**). Arginylation is an emerging poorly characterized modification, which is still non-routine during proteomics analysis and normally requires manual data validation. While it was not feasible to manually validate all identified peptides, we validated a number of representative MS/MS spectra (Dataset 1) to confirm that arginylation on the identified sites is likely.

Both arginylation and Thr phosphorylation have been previously proposed to play a global regulatory role. Thus, we performed further analysis of these two modifications to dissect the likely functional consequences of their change in COVID-19. Mapping the identified sites for these two modifications on the target proteins identified in our sets (see **Supplementary Tables**



S8, S9 for arginylation and phosphorylation, respectively) revealed that in addition of the total level change for each of the PTMs, COVID-19 patients also exhibit a different repertoire of arginylation and phosphorylation sites compared to control. This points to a likely possibility that the target proteins affected by these altered regulatory PTMs, including components of the blood coagulation cascade and immune response, along with several other functions implicated in COVID-19 infection, may be differentially regulated by these two PTMs in healthy individuals versus those infected by SARS-CoV-2. While the effect of these PTMs is not yet understood, it is attractive to

suggest that arginylation/phosphorylation on these sites may underlie COVID-19 dependent protein regulation and disease progression.

The two less abundant lists included a number of additional PTMs that play important physiological roles. Among these were two types of N-linked glycosylation: HexNAc(1)dHex(2) [N] was up in control (Figure 4, middle), and HexNAc [N], was up in COVID-19 (Figure 4, bottom). Notably, changes in glycosylation were previously observed on the viral SARS-CoV-2 proteins during COVID-19 (Praisman and Wells, 2021; Reis et al., 2021; Shajahan et al., 2021; Zhong et al., 2021), even though such changes in the host organism, to the best of our knowledge, were not previously reported. Additional modifications on this list were detected at very low levels. Even though physiologically important, it is difficult to assess the biological role of their changes in the plasma of COVID-19 patients.

In addition to these PTMs, a substantial number of amino acid substitutions were significantly different between COVID-19 and control plasma (Supplementary Figure S5). Of those, Glu to Asp substitution was by far the most abundant (Supplementary Figure S5, bottom). These substitutions normally reflect single nucleotide polymorphisms (SNPs), and thus are not a result of SARS-CoV-2 infection. However, the presence of these SNPs potentially reflect genetic changes that might make the patients more vulnerable to COVID-19.

### 3 CONCLUSION

To our knowledge, the data presented in this manuscript represents the first global proteome and peptidome analysis of plasma from COVID-19 patients. Other studies have extensively analyzed the proteomics and posttranslational state of SARS-CoV-2 proteins during COVID-19 infection, but no one has as yet focused on the changes in the patient plasma proteome.

Our data suggests the existence of global protein-level trends in the patients' plasma that may inform our understanding of biology, prevention, diagnostics, and treatment of COVID-19. We find that plasma proteins in COVID-19 patients contain elevated levels of a limited number of proteins associated with inflammation and immune response, and some of these proteins, including fibrinogen, apparently undergo different proteolytic events compared to normal controls. Some of these changes may underlie the less understood clinical symptoms of COVID-19.

Our study shows that COVID-19 infection is accompanied by a prominent posttranslational signature, with differential increase and reduction in several key regulatory modifications, including glycosylation, citrullination, Thr phosphorylation, and arginylation. Decoding this signature may potentially inform our understanding of the biology, diagnostics, and treatment of COVID-19.

### 4 MATERIALS AND METHODS

#### 4.1 Biosafety

All human patient samples were handled under BSL-2 containment.



## 4.2 Human Patient Samples

Blood from 7 healthy controls and 6 COVID-19 patients was collected in lavender-top EDTA tubes from BD (cat no. 368661). These tubes come with 10.8 mg K2 EDTA spray dried inside the tube. Blood was drawn into the tube by clinical staff and handed off to the processing unit within 8 h, usually much less. Tubes were then spun down at 1,000 × g at room temperature for 15 min. Plasma supernatant was removed, aliquoted, snap frozen and stored on dry ice for ~1 h, then transferred to –80°C for storage.

## 4.3 Plasma Fractionation for Protein and Peptide Fractions

### 4.3.1 Plasma Clarification

Frozen plasma aliquots were thawed on ice and centrifuged at 13,000 g at 4°C for 30 min. The supernatant was used for peptide isolation or further depleted of IgG and albumin for analyzing the protein composition using mass spectrometry.

### 4.3.2 Peptide Isolation

50 µl of clarified plasma was mixed with 200 µl of Phosphate Buffered Saline. 1 ml of freshly prepared 100 mM Tris, 8 M urea, pH 7.5 at room temperature was used to denature the proteins and dissociate bound peptides from abundant plasma proteins. Denatured samples were loaded onto a pre-rinsed Amicon Ultra 30 kDa MWCO filter (Millipore) and centrifuged at 13,000 g at 4°C for 20 min. Formic acid was added to the flow-through containing primarily peptides to a final concentration of 0.1% (v/v). MacroSpin Vydac Silica C18 columns (the Nest Group, Inc., Part #SMM SS18V, Lot #060310) were pre-washed first with 500 µl of 100% acetonitrile and then with water followed by centrifugation at 100 g at 4°C for 1 min to remove the liquid after each wash. The same centrifugation condition was used for all subsequent steps. Briefly, columns were equilibrated with 300 µl 0.2% acetonitrile; the 30 kDa MWCO flow-through was applied; columns were washed three times with 400 µl of 0.1% formic acid, and peptides were then eluted using 300 µl of 0.1% formic acid, 50% acetonitrile, snap frozen in liquid nitrogen, and stored at –80°C until the analysis.

### 4.3.3 Albumin & IgG Depletion for Proteomics

The plasma samples were depleted of IgG and albumin using Albumin & IgG depletion SpinTrap columns (GE healthcare) according to manufacturer's instructions. Briefly, the column was resuspended, and the storage buffer was discarded by centrifugation at 100 g for 30 s. The column was then equilibrated with 400 µl of binding buffer (20 mM sodium phosphate, 150 mM sodium chloride, pH 7.4), which was discarded by centrifugation at 800 g for 30 s. Immediately after thawing an aliquot, the plasma sample was diluted 1:1 with binding buffer, applied to the column, mixed with the resin and incubated for 5 min at room temperature. The albumin and IgG depleted protein fraction was collected by centrifugation at 800 g for 30 s, the column was washed twice with 100 µl binding buffer flowed by centrifugation at 800 g for 30 s, and the flowthrough and washes were combined. The eluted proteins were precipitated by adding 9 volumes of –20°C ethanol and stored overnight at 4°C. Precipitated

protein was collected by centrifugation at 13000 g at 4°C for 30 min. The pellet was heat inactivated at 60°C for 20 min to denature any viral load that might have been present.

## 4.4 Peptidomics

### 4.4.1 Sample Preparation and LC-MS/MS Analysis

Total peptide fraction purified by C18 column from 13 COVID-19 patient and control plasma (7 controls and 6 diseased) were lyophilized and resuspended in 30 µl of 3% acetonitrile, 0.1% formic acid. The volume of plasma was kept constant between samples at each step to enable non-normalized comparison of abundances for each identified peptide. 5 µl of each sample was analyzed by LC-MS/MS on the Thermo Q Exactive HF mass spectrometer using a 2-h LC gradient (Su et al., 2021).

### 4.4.2 Data Analysis

MS/MS data were analyzed using Thermo Proteome Discoverer v2.4. Spectra were searched using no-enzyme specificity against the UniProt human proteome database (10/02/2020) and a common contaminant database using Sequest HT. Percolator target False Discovery Rate was set at 0.01 (Strict) and 0.05 (Relaxed). Only peptides identified with high confidence were retained. Common contaminants (primarily keratins) were removed. Peptide abundance values were determined from the peptide chromatographic peak areas. Ratio, *p*-value (t-test) and adjusted *q*-value (*p*-value adjusted to account for multiple testing using Benjamini-Hochberg FDR) were calculated using the non-normalized abundance values. Significant changing peptides are defined as peptides with a minimum absolute fold change of 2, adjusted *p*-value of 0.05, and identified in a minimum of 3 replicates in either group.

To produce the charts shown in the main and supplemental figures, we summed up total abundances of all peptides belonging to each protein that exhibited significant differences between groups and calculated the average of these sums between all control and all COVID-19 samples. For the chart showing differential proteolytic patterns of fibrinogen and serglycin (Figure 2), abundances of individual peptides were averaged across samples and plotted against each peptide sequence.

## 4.5 Proteomics

### 4.5.1 Sample Preparation and LC-MS/MS Analysis

The ethanol precipitated albumin and IgG depleted COVID-19 patient plasma (7 controls, denoted by 3-digit numbers starting with 0 in the supplemental tables, and 6 diseased, denoted by 3-digit numbers starting with 5 in the supplemental tables) fractions were dissolved in 50 µl of 1% SDS, 50 mM Tris-Cl pH 7.5. 10 µl of each was run into a NuPAGE 10% Bis-Tris gel (Thermo Scientific) for a short distance. The entire stained gel regions were excised, reduced with tris(2-carboxyethyl)phosphine (TCEP), alkylated with iodoacetamide, and digested with trypsin. Tryptic digests were analyzed using a single-shot extended 4 h LC gradient on the Thermo Q Exactive Plus mass spectrometer.

### 4.5.2 Data Analysis

Peptide sequences were identified using MaxQuant 1.6.17.0 (Cox and Mann, 2008). MS/MS spectra were searched against a UniProt human proteome database (10/02/2020) and a common

contaminants database using full tryptic specificity with up to two missed cleavages, static carboxamidomethylation of Cys, and variable Met oxidation, protein N-terminal acetylation and Asn deamidation. “Match between runs” feature was used to help transfer identifications across experiments to minimize missing values. Consensus identification lists were generated with false discovery rates set at 1% for protein and peptide identifications. Statistical analyses were performed using Perseus 1.6.15.0 (Tyanova et al., 2016). Protein fold changes were determined from the Intensity values. Missing values were imputed with a minimum Intensity value, and t-test *p*-values were adjusted to account for multiple testing using the permutation-based FDR function in Perseus. High confidence identification of proteins with significant change was determined based on the following criteria: minimum absolute fold change of 2, *q*-value <0.05, identified by a minimum of 2 razor + unique peptides, and detected in at least 3 of the replicates in one of the groups compared.

#### 4.6 Posttranslational Modifications Analysis

The “Proteomics” MS/MS data described above were analyzed using pFind 3.1.5 (Chi et al., 2018). Two separate pFind searches were performed: Control (containing all 7 control samples) and Disease (containing all 6 samples). Spectra were searched using partial tryptic specificity against the UniProt human proteome database (10/02/2020). The “Open Search” option was used to identify PTMs. Data were filtered using a precursor mass tolerance of 10 ppm, fragment ion tolerance of 20 ppm, and FDR <1% at peptide and protein level.

#### DATA AVAILABILITY STATEMENT

The data presented here has been deposited into the MassIVE public repository (<https://massive.ucsd.edu/ProteoSAFe/static/massive.jsp>) with the accession MSV000088382, and the ProteomeXchange repository (<http://www.proteomecentral.proteomexchange.org/cgi/>) with the accession PXD029756.

#### ETHICS STATEMENT

The studies involving human participants were reviewed and approved by the University of Pennsylvania Institutional Review Board. Written informed consent for participation was not

required for this study in accordance with the national legislation and the institutional requirements.

#### AUTHOR CONTRIBUTIONS

PV, AK, H-YT, and DS designed the research. PV and H-YT performed the experiments and analyzed data. AK and DS analyzed data and wrote the paper.

#### FUNDING

The Human Immunology Core is funded in part by NIH P30-AI0450080 and P30-CA016520. This work was supported by the NIH Grant R35GM122505 to AK and R50 CA221838 to H-YT.

#### ACKNOWLEDGMENTS

We are grateful to Dr. John Wherry and Penn Immune Health Initiative for support of this work and providing the plasma samples for this analysis. We thank the Human Immunology Core (HIC) facility for assistance with sample processing and provision of control samples for this study. The UPenn COVID Processing Unit is a unit of individuals from diverse laboratories at the University of Pennsylvania who volunteered time and effort to enable study of COVID-19 patients during the pandemic: Zahidul Alam, Mary M. Addison, Amy E. Baxter, Katelyn T. Byrne, Aditi Chandra, Kurt D’Andrea, Hélène C. Descamps, Jeanette Dougherty, Allison R. Greenplate, Nicholas Han, Yaroslav Kaminskiy, Justin Kim, Oliva Kuthuru, Jacob T. Hamilton, Julia Han Noll, Dalia K. Omran, Ajinkya Pattekar, Eric Perkey, Nils Wellhausen, Elizabeth M. Prager, Dana Pueschl, Jennifer B. Shah, Jake S. Shilan, and Ashley N. Vanderbeck.

#### SUPPLEMENTARY MATERIAL

The Supplementary Material for this article can be found online at: <https://www.frontiersin.org/articles/10.3389/fcell.2022.807149/full#supplementary-material>

#### REFERENCES

- Ahmed, S., Zimba, O., and Gasparyan, A. Y. (2020). Thrombosis in Coronavirus Disease 2019 (COVID-19) through the Prism of Virchow’s Triad. *Clin. Rheumatol.* 39 (9), 2529–2543. doi:10.1007/s10067-020-05275-1
- Anand, P., Puranik, A., Aravamudan, M., Venkatakrishnan, A., and Soundararajan, V. (2020). SARS-CoV-2 Strategically Mimics Proteolytic Activation of Human ENaC. *Elife* 9. doi:10.7554/eLife.58603
- Arapidi, G., Osetrova, M., Ivanova, O., Butenko, I., Saveleva, T., Pavlovich, P., et al. (2018). Peptidomics Dataset: Blood Plasma and Serum Samples of Healthy Donors Fractionated on a Set of Chromatography Sorbents. *Data in Brief* 18, 1204–1211. doi:10.1016/j.dib.2018.04.018
- Chi, H., Liu, C., Yang, H., Zeng, W.-F., Wu, L., Zhou, W.-J., et al. (2018). Comprehensive Identification of Peptides in Tandem Mass Spectra Using an Efficient Open Search Engine. *Nat. Biotechnol.* 36, 1059–1061. doi:10.1038/nbt.4236
- Cox, J., and Mann, M. (2008). MaxQuant Enables High Peptide Identification Rates, Individualized p.p.b.-Range Mass Accuracies and Proteome-Wide Protein Quantification. *Nat. Biotechnol.* 26 (12), 1367–72. doi:10.1038/nbt.1511
- Gómez-Mesa, J. E., Galindo-Coral, S., Montes, M. C., and Muñoz Martin, A. J. (2021). Thrombosis and Coagulopathy in COVID-19. *Curr. Probl. Cardiol.* 46 (3), 100742. doi:10.1016/j.cpcardiol.2020.100742
- Gorski, J. P., Hugli, T. E., and Muller-Eberhard, H. J. (1979). C4a: The Third Anaphylatoxin of the Human Complement System. *Proc. Natl. Acad. Sci.* 76 (10), 5299–5302. doi:10.1073/pnas.76.10.5299

- Hanff, T. C., Mohareb, A. M., Giri, J., Cohen, J. B., and Chirinos, J. A. (2020). Thrombosis in COVID-19. *Am. J. Hematol.* 95 (12), 1578–1589. doi:10.1002/ajh.25982
- Harapan, B. N., and Yoo, H. J. (2021). Neurological Symptoms, Manifestations, and Complications Associated with Severe Acute Respiratory Syndrome Coronavirus 2 (SARS-CoV-2) and Coronavirus Disease 19 (COVID-19). *J. Neurol.* 268 (9), 3059–3071. doi:10.1007/s00415-021-10406-y
- Katneni, U. K., Alexaki, A., Hunt, R. C., Schiller, T., DiCuccio, M., Buehler, P. W., et al. (2020). Coagulopathy and Thrombosis as a Result of Severe COVID-19 Infection: A Microvascular Focus. *Thromb. Haemost.* 120 (12), 1668–1679. doi:10.1055/s-0040-1715841
- Li, D., Fu, Y., Sun, R., Ling, C. X., Wei, Y., Zhou, H., et al. (2005). pFind: A Novel Database-Searching Software System for Automated Peptide and Protein Identification via Tandem Mass Spectrometry. *Bioinformatics* 21 (13), 3049–3050. doi:10.1093/bioinformatics/bti439
- May, J. E., Wolberg, A. S., and Lim, M. Y. (2021). Disorders of Fibrinogen and Fibrinolysis. *Hematology/Oncology Clin. North America* 35, 1197–1217. doi:10.1016/j.hoc.2021.07.011
- Meyer, B., Chiaravalli, J., Gellenoncourt, S., Brownridge, P., Bryne, D. P., Daly, L. A., et al. (2021). Characterising Proteolysis during SARS-CoV-2 Infection Identifies Viral Cleavage Sites and Cellular Targets with Therapeutic Potential. *Nat. Commun.* 12 (1), 5553. doi:10.1038/s41467-021-25796-w
- Montenegro, F., Unigarro, L., Paredes, G., Moya, T., Romero, A., Torres, L., et al. (2021). Acute Respiratory Distress Syndrome (ARDS) Caused by the Novel Coronavirus Disease (COVID-19): A Practical Comprehensive Literature Review. *Expert Rev. Respir. Med.* 15 (2), 183–195. doi:10.1080/17476348.2020.1820329
- Novelli, G., Biancolella, M., Mehrian-Shai, R., Colona, V. L., Brito, A. F., Grubaugh, N. D., et al. (2021). COVID-19 One Year into the Pandemic: From Genetics and Genomics to Therapy, Vaccination, and Policy. *Hum. Genomics* 15 (1), 27. doi:10.1186/s40246-021-00326-3
- Østergaard, L. (2021). SARS CoV-2 Related Microvascular Damage and Symptoms during and after COVID-19: Consequences of Capillary Transit-time Changes, Tissue Hypoxia and Inflammation. *Physiol. Rep.* 9 (3), e14726. doi:10.14814/phy2.14726
- Praissman, J. L., and Wells, L. (2021). Proteomics-Based Insights into the SARS-CoV-2-Mediated COVID-19 Pandemic: A Review of the First Year of Research. *Mol. Cell Proteomics* 20, 100103. doi:10.1016/j.mcpro.2021.100103
- Ramos-Guzmán, C. A., Ruiz-Pernía, J. J., and Tuñón, I. (2020). Unraveling the SARS-CoV-2 Main Protease Mechanism Using Multiscale Methods. *ACS Catal.* 10, 12544–12554. doi:10.1021/acscatal.0c03420
- Reis, C. A., Tauber, R., and Blanchard, V. (2021). Glycosylation Is a Key in SARS-CoV-2 Infection. *J. Mol. Med.* 99 (8), 1023–1031. doi:10.1007/s00109-021-02092-0
- Saha, S., Wong, C. C. L., Xu, T., Namgoong, S., Zebroski, H., Yates, J. R., et al. (2011). Arginylation and Methylation Double up to Regulate Nuclear Proteins and Nuclear Architecture *In Vivo*. *Chem. Biol.* 18 (11), 1369–1378. doi:10.1016/j.chembiol.2011.08.019
- Schmulson, M., Dávalos, M. F., and Berumen, J. (2020). Beware: Gastrointestinal Symptoms Can Be a Manifestation of COVID-19. *Revista de Gastroenterología de México (English Edition)* 85 (3), 282–287. doi:10.1016/j.rgmex.2020.04.001
- Scully, O. J., Chua, P.-J., Harve, K. S., Bay, B.-H., and Yip, G. W. (2012). Serglycin in Health and Diseases. *Anat. Rec.* 295 (9), 1415–1420. doi:10.1002/ar.22536
- Shajahan, A., Pepi, L. E., Rouhani, D. S., Heiss, C., and Azadi, P. (2021). Glycosylation of SARS-CoV-2: Structural and Functional Insights. *Anal. Bioanal. Chem.* 413, 7179–7193. doi:10.1007/s00216-021-03499-x
- Stockley, R. A. (2014). Alpha1-antitrypsin Review. *Clin. Chest Med.* 35 (1), 39–50. doi:10.1016/j.ccm.2013.10.001
- Su, C., Lu, F., Soldan, S. S., Lamontagne, R. J., Tang, H.-Y., Napoletani, G., et al. (2021). EBNA2 Driven Enhancer Switching at the CIITA-DEXI Locus Suppresses HLA Class II Gene Expression during EBV Infection of B-Lymphocytes. *Plos Pathog.* 17 (8), e1009834. doi:10.1371/journal.ppat.1009834
- Swelum, A. A., Shafi, M. E., Albaqami, N. M., El-Saadony, M. T., Elsify, A., Abdo, M., et al. (2020). COVID-19 in Human, Animal, and Environment: A Review. *Front. Vet. Sci.* 7, 578. doi:10.3389/fvets.2020.00578
- Świderek, K., and Moliner, V. (2020). Revealing the Molecular Mechanisms of Proteolysis of SARS-CoV-2 Mpro by QM/MM Computational Methods. *Chem. Sci.* 11 (39), 10626–10630. doi:10.1039/d0sc02823a
- Tang, T., Jaimes, J. A., Bidon, M. K., Straus, M. R., Daniel, S., and Whittaker, G. R. (2021). Proteolytic Activation of SARS-CoV-2 Spike at the S1/S2 Boundary: Potential Role of Proteases beyond Furin. *ACS Infect. Dis.* 7 (2), 264–272. doi:10.1021/acsinfectdis.0c00701
- Troyer, E. A., Kohn, J. N., and Hong, S. (2020). Are We Facing a Crashing Wave of Neuropsychiatric Sequelae of COVID-19? Neuropsychiatric Symptoms and Potential Immunologic Mechanisms. *Brain Behav. Immun.* 87, 34–39. doi:10.1016/j.bbi.2020.04.027
- Tyanova, S., Temu, T., Sinitcyn, P., Carlson, A., Hein, M. Y., Geiger, T., et al. (2016). The Perseus Computational Platform for Comprehensive Analysis of (Prote)omics Data. *Nat. Methods* 13 (9), 731–40. doi:10.1038/nmeth.3901
- Vakil-Gilani, K., and O'Rourke, K. (2020). Are Patients with Rheumatologic Diseases on Chronic Immunosuppressive Therapy at Lower Risk of Developing Severe Symptoms when Infected with COVID-19. *Clin. Rheumatol.* 39 (7), 2067–2068. doi:10.1007/s10067-020-05184-3
- Wang, J., Han, X., Wong, C. C. L., Cheng, H., Aslanian, A., Xu, T., et al. (2014). Arginyltransferase ATE1 Catalyzes Midchain Arginylation of Proteins at Side Chain Carboxylates *In Vivo*. *Chem. Biol.* 21 (3), 331–337. doi:10.1016/j.chembiol.2013.12.017
- Wang, J., Yates, J. R., 3rd, and Kashina, A. (2019). Biochemical Analysis of Protein Arginylation. *Methods Enzymol.* 626, 89–113. doi:10.1016/bs.mie.2019.07.028
- Wang, L.-h., Li, D.-Q., Fu, Y., Wang, H.-P., Zhang, J.-F., Yuan, Z.-F., et al. (2007). pFind 2.0: A Software Package for Peptide and Protein Identification via Tandem Mass Spectrometry. *Rapid Commun. Mass. Spectrom.* 21 (18), 2985–2991. doi:10.1002/rcm.3173
- Zheng, H., Li, H., Zhang, J., Fan, H., Jia, L., Ma, W., et al. (2020). Serum Amyloid A Exhibits pH Dependent Antibacterial Action and Contributes to Host Defense against *Staphylococcus aureus* Cutaneous Infection. *J. Biol. Chem.* 295 (9), 2570–2581. doi:10.1074/jbc.RA119.010626
- Zhong, L., Zhu, L., and Cai, Z.-W. (2021). Mass Spectrometry-Based Proteomics and Glycoproteomics in COVID-19 Biomarkers Identification: A Mini-Review. *J. Anal. Test.* 5, 298–313. doi:10.1007/s41664-021-00197-6

**Conflict of Interest:** The authors declare that the research was conducted in the absence of any commercial or financial relationships that could be construed as a potential conflict of interest.

**Publisher's Note:** All claims expressed in this article are solely those of the authors and do not necessarily represent those of their affiliated organizations, or those of the publisher, the editors and the reviewers. Any product that may be evaluated in this article, or claim that may be made by its manufacturer, is not guaranteed or endorsed by the publisher.

Copyright © 2022 Vedula, Tang, Speicher and Kashina. This is an open-access article distributed under the terms of the Creative Commons Attribution License (CC BY). The use, distribution or reproduction in other forums is permitted, provided the original author(s) and the copyright owner(s) are credited and that the original publication in this journal is cited, in accordance with accepted academic practice. No use, distribution or reproduction is permitted which does not comply with these terms.

# Advantages of publishing in Frontiers



## OPEN ACCESS

Articles are free to read  
for greatest visibility  
and readership



## FAST PUBLICATION

Around 90 days  
from submission  
to decision



## HIGH QUALITY PEER-REVIEW

Rigorous, collaborative,  
and constructive  
peer-review



## TRANSPARENT PEER-REVIEW

Editors and reviewers  
acknowledged by name  
on published articles

## Frontiers

Avenue du Tribunal-Fédéral 34  
1005 Lausanne | Switzerland

Visit us: [www.frontiersin.org](http://www.frontiersin.org)

Contact us: [frontiersin.org/about/contact](http://frontiersin.org/about/contact)



## REPRODUCIBILITY OF RESEARCH

Support open data  
and methods to enhance  
research reproducibility



## DIGITAL PUBLISHING

Articles designed  
for optimal readership  
across devices



## FOLLOW US

@frontiersin



## IMPACT METRICS

Advanced article metrics  
track visibility across  
digital media



## EXTENSIVE PROMOTION

Marketing  
and promotion  
of impactful research



## LOOP RESEARCH NETWORK

Our network  
increases your  
article's readership